ELECTRICAL MACHINES

1

A. IVANOV-SMOLENSKY

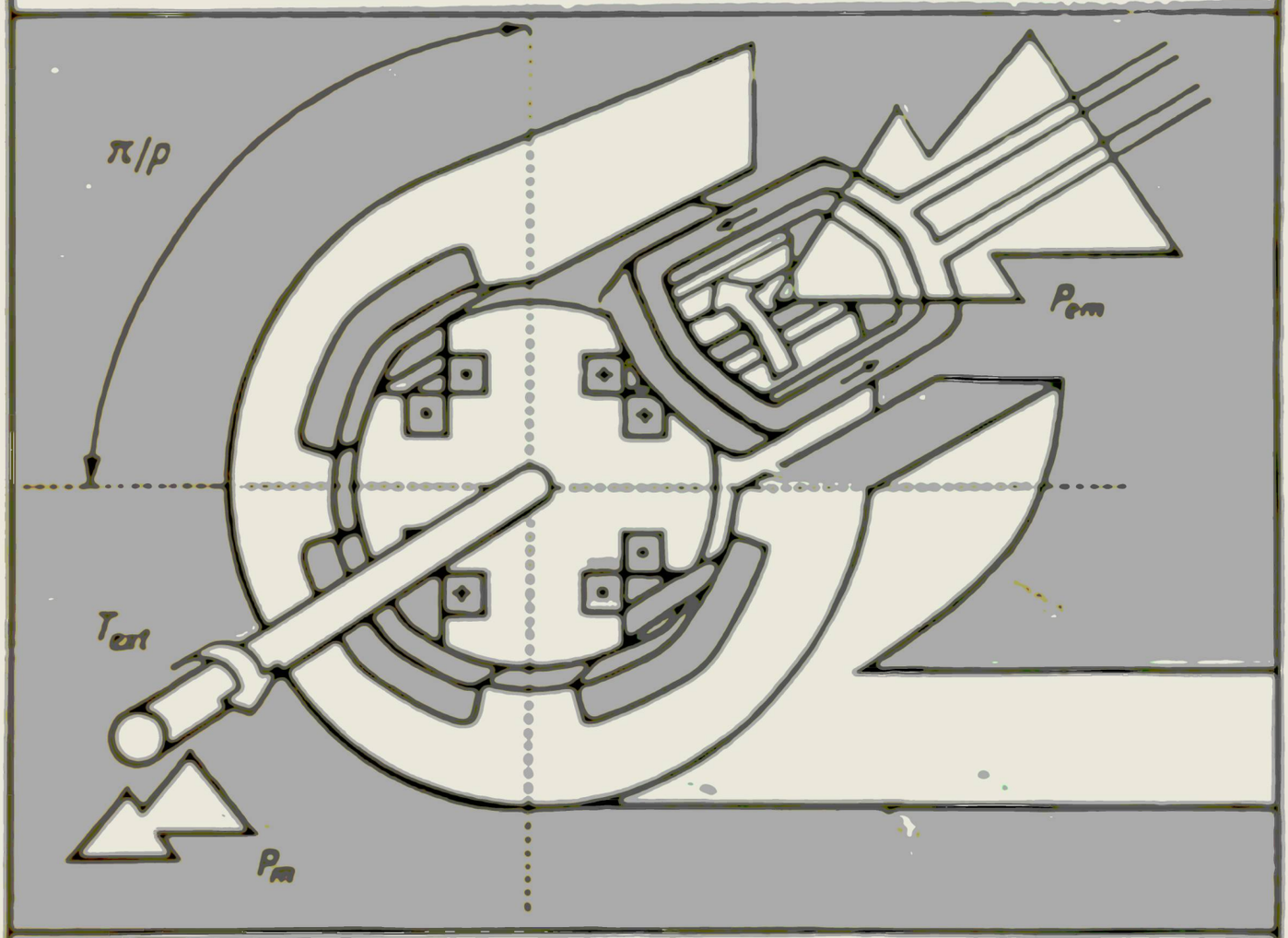

MIR Publishers Moscow

ABOUT THE BOOK

The book is in three volumes as follows.

Volume I:

Preface. Introduction. Transformers. A General Theory of Electrical Machines.

Volume II:

Classification of Electrical Machines. Mechanical, Hydraulic and Thermal Analysis and Design. Induction Machines. Synchronous Machines.

Volume III:

D.C. and Commutator Machines. Transients in Electrical Machines.

The book is intended for college and university students majoring in electrical-machine theory and design. It will also be useful to electrical power engineers.

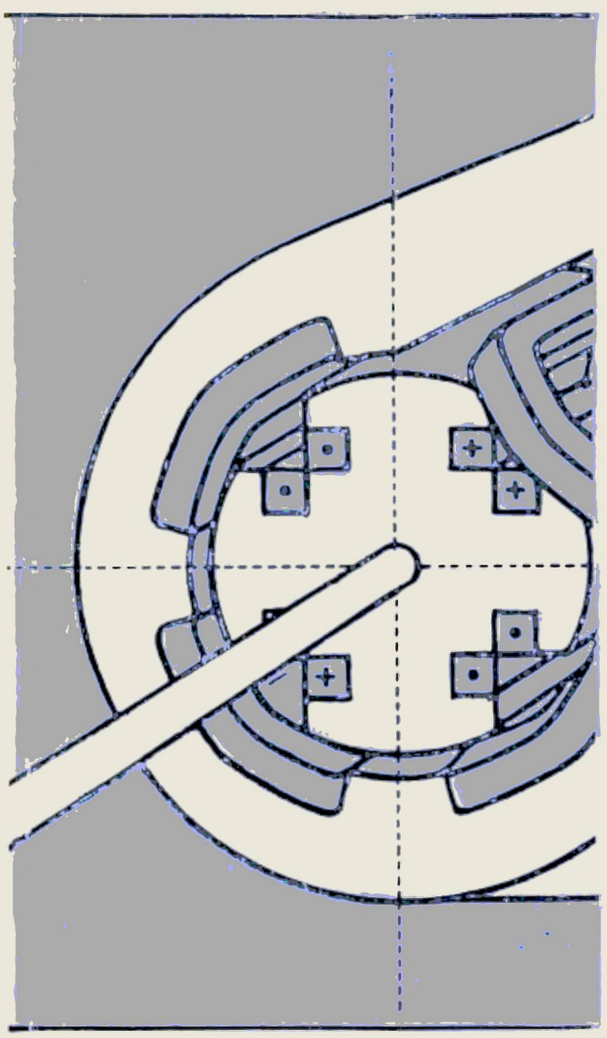

ABOUT THE AUTHOR

Professor Alexei V. IVANOV-SMOLENSKY, D. Sc. (Tech.), is a leading Soviet authority in his field. Currently, he is with the Moscow Power Institute. He has written (individually and as a coauthor) six books on electricity including the present one.

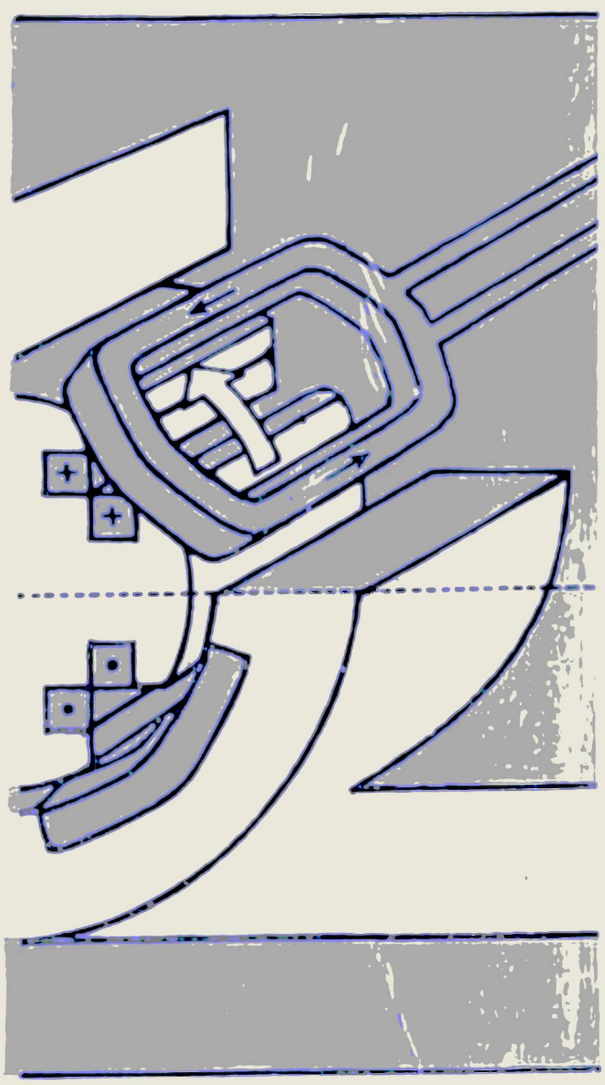

ELECTRICAL MACHINES vol. 1

A. IVANOV-SMOLENSKY

Mir Publishers Moscow

А. В. Иванов-Смоленский

ЭЛЕКТРИЧЕСКИЕ МАШИНЫ

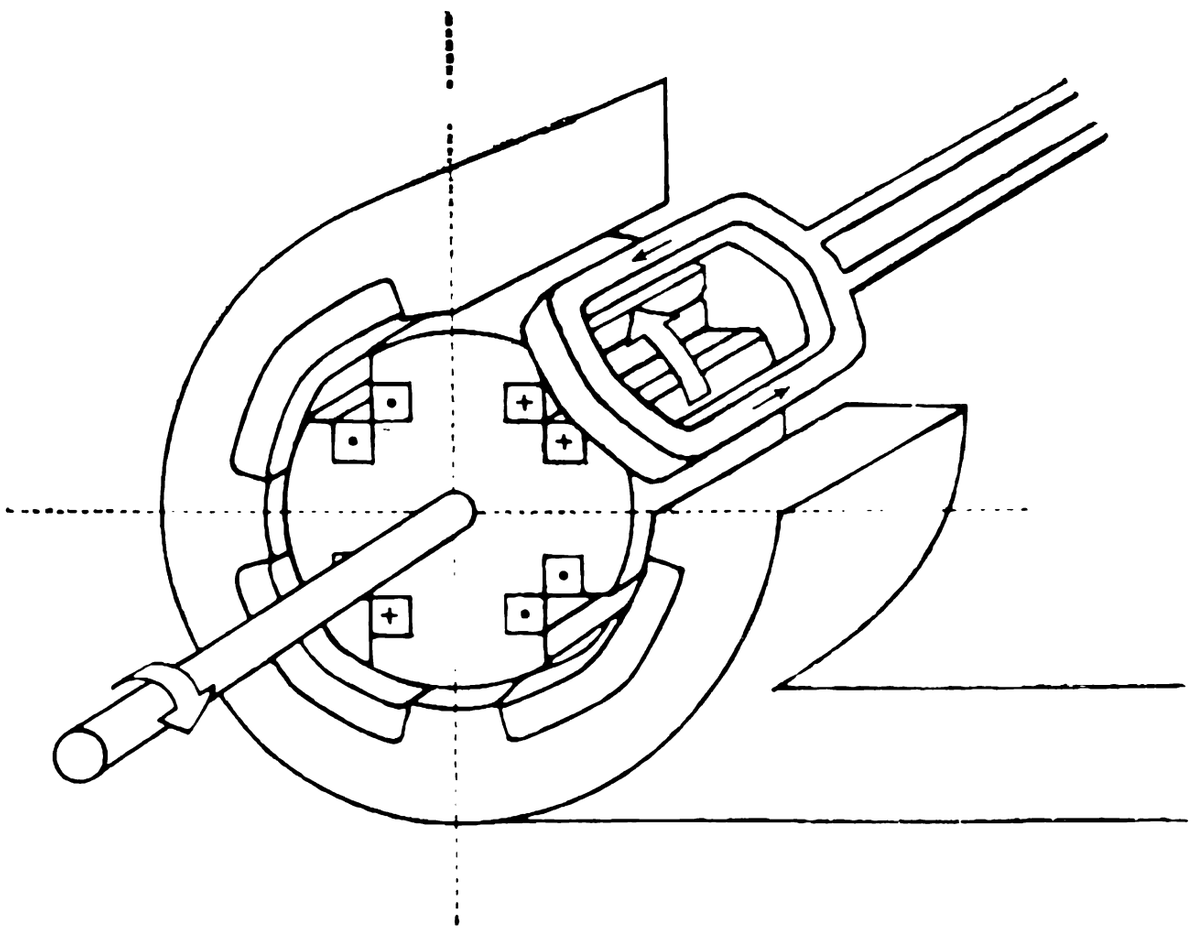

Москва Издательство «Энергия»

ELECTRICAL MACHINES

A. IVANOV-SMOLENSKY

Vol. 1

Translated from Russian
by Boris V. KUZNETSOV

MIR Publishers Moscow

First published 1982
Revised from the 1980 Russian edition

На английском языке

© Издательство «Энергия», 1980г.
© English translation, Mir Publishers, 1982

Contents

Preface 11

Introduction 13

I-1 Basic Definitions *13*
I-2 Conversion of Electric Energy by the Transformer *15*
I-3 Electromechanical Energy Conversion by an Electrical Machine *18*
I-4 Functional Classification of Electromagnetic Energy Converting Devices *24*

---

1 Transformers

Chapter 1 An Outline of Transformers 27

1-1 Purpose, Applications, Ratings *27*
1-2 Construction of a Transformer *31*

Chapter 2 Electromagnetic Processes in the Transformer at No-Load 43

2-1 The No-Load Condition *43*
2-2 Voltage Equations *45*
2-3 Variations in EMF with Time. An EMF Equation *46*
2-4 The Magnetization Curve of the Transformer *47*
2-5 The No-Load Current Waveform *49*
2-6 Transformer Equations at No-Load in Complex Form *50*
2-7 No-Load Losses *52*
2-8 The Effect of the Core Loss on the Transformer's Performance at No-Load *53*

Chapter 3 Electromagnetic Processes in the Transformer on Load 56

3-1 The Magnetic Field in a Transformer on Load. The MMF Equation. The Leakage Inductance of the Windings *56*
3-2 Voltage Equations of the Transformer Windings *60*
3-3 Transferring the Secondary Quantities to the Primary Side *62*

3-4 The Phasor Diagram of a Transformer *65*
3-5 The Equivalent Circuit of the Transformer *68*
3-6 The Per-Unit Notation *69*
3-7 The Effect of Load Variations on the Transformer *72*
3-8 Energy Conversion in a Loaded Transformer *75*

Chapter 4 Transformation of Three-Phase Currents and Voltages 79
4-1 Methods of Three-Phase Transformation. Winding Connections *79*
4-2 A Three-Phase Transformer on a Balanced Load *83*
4-3 Phase Displacement Reference Numbers *84*
4-4 The Behaviour of a Three-Phase Transformer During Magnetic Field Formation *89*

Chapter 5 Measurement of Transformer Quantities 99
5-1 The Open-Circuit (No-Load) Test *99*
5-2 The Short-Circuit Test *102*

Chapter 6 Transformer Performance on Load 106
6-1 Simplified Transformer Equations and Equivalent Circuit for $I_1 \gg I_0$ *106*
6-2 Transformer Voltage Regulation *107*
6-3 Variations in Transformer Efficiency on Load *111*

Chapter 7 Tap Changing 113
7-1 Off-Load Tap Changing *113*
7-2 On-Load Tap Changing *114*

Chapter 8 Calculation of Transformer Parameters 117
8-1 No-Load (Open-Circuit) Current and Mutual Impedance *117*
8-2 Short-Circuit Impedance *119*

Chapter 9 Relationship Between Transformer Quantities and Dimensions 121
9-1 Variations in the Voltage, Current, Power and Mass of a Transformer with Size *121*
9-2 Transformer Losses and Parameters as Functions of Size *123*

Chapter 10 Multiwinding Transformers. Autotransformers 125
10-1 Multiwinding Transformers *125*
10-2 Autotransformers *133*

Chapter 11 Transformers in Parallel 138
11-1 Use of Transformers in Parallel *138*
11-2 Procedure for Bringing Transformers in for Parallel Operation *139*
11-3 Circulating Currents due to a Difference in Transformation Ratio *141*
11-4 Load Sharing Between Transformers in Parallel *143*

Chapter 12 Three-Phase Transformers Under Unbalanced Load 145
12-1 Causes of Load Unbalance *145*
12-2 Transformation of Unbalanced Currents *146*
12-3 Magnetic Fluxes and EMFs under Unbalanced Load Conditions *151*
12-4 Dissymmetry of the Primary Phase Voltages under Unbalanced Load *154*
12-5 Dissymmetry of the Secondary Voltages under Unbalanced Load *156*
12-6 Measurement of the ZPS Secondary Impedance *160*
12-7 Single- and Two-Phase Unbalanced Loads *161*

Chapter 13 Transients in Transformers 164
13-1 Transients at Switch-On *164*
13-2 Transients on a Short-Circuit Across the Secondary Terminals *167*

Chapter 14 Overvoltage Transients in Transformers 171
14-1 Causes of Overvoltages *171*
14-2 The Differential Equation for the Initial Voltage Distribution in the Transformer Winding *172*
14-3 Voltage Distribution over the Winding and Its Equalization *175*

Chapter 15 Special-Purpose Transformers 177
15-1 General *177*
15-2 Three-Phase Transformation with Two Transformers *177*
15-3 Frequency-Conversion Transformers *178*
15-4 Variable-Voltage Transformers *179*
15-5 Arc Welding Transformers *180*
15-6 Insulation Testing Transformers *181*
15-7 Peaking Transformers *182*
15-8 Instrument Transformers *182*

Chapter 16 Heating and Cooling of Transformers 184
16-1 Temperature Limits for Transformer Parts under Steady-State and Transient Conditions *184*
16-2 Transformer Cooling Systems *186*

Chapter 17 Transformers of Soviet Manufacture 189
17-1 USSR State Standards Covering Transformers *189*
17-2 Type Designations of Soviet-made Transformers *190*
17-3 Some of Transformer Applications *191*

2 A general theory of electromechanical energy conversion by electrical machines

Chapter 18 Electromechanical Processes in Electrical Machines 192

18-1 Classification of Electrical Machines *192*
18-2 Mathematical Description of Electromechanical Energy Conversion by Electrical Machines *195*

Chapter 19 Production of a Periodically Varying Magnetic Field in Electrical Machines 201
19-1 A Necessary Condition for Electromechanical Energy Conversion *201*
19-2 The Cylindrical (Drum) Heteropolar Winding *202*
19-3 The Toroidal Heteropolar Winding *206*
19-4 The Ring Winding and a Claw-Shaped Core *206*
19-5 The Homopolar Ring Winding and a Toothed Core *206*

Chapter 20 Basic Machine Designs 207
20-1 Modifications in Design *207*
20-2 Machines with One Winding on the Stator and One Winding on the Rotor *211*
20-3 Machines with One Winding on the Stator and Toothed Rotor and Stator Cores (Reluctance Machines) *214*
20-4 Machines with Two Windings on the Stator and Toothed Cores for the Stator and Rotor (Inductor Machines) *218*

Chapter 21 Conditions for Unidirectional Energy Conversion by Electrical Machines 227
21-1 The Single-Winding Machine *227*
21-2 Two-Winding Machines *230*

Chapter 22 Windings for A. C. Machines 235
22-1 Introductory Notes *235*
22-2 The Structure of a Polyphase Two-Layer Winding *235*
22-3 Connection of Coils in a Lap Winding. The Number of Paths and Turns per Phase *240*
22-4 Coil Connection in the Wave Winding *244*
22-5 The Selection of a Winding Type and Winding Characteristics *246*
22-6 A Two-Pole Model of a Winding. Electrical Angles between Winding Elements *247*
22-7 Two-Layer, Fractional-Slot Windings *250*
22-8 Field Windings *255*

Chapter 23 Calculation of the Magnetic Field in an Electrical Machine 257
23-1 The Statement of the Problem *257*
23-2 Assumptions Made in Calculating the Magnetic Field *260*
23-3 The Spatial Pattern of the Magnetic Field Set Up by a Polyphase Winding *262*
23-4 Calculation of the Mutual Magnetic Field for a Polyphase Winding *264*
23-5 Effective Length of the Core *265*

Contents

Chapter 24 The Mutual Magnetic Field of a Phase Winding and Its Elements 267

24-1 The Magnetic Field and MMF due to a Basic Set of Currents *267*

24-2 The Effect of Core Saliency. The Carter Coefficient *270*

24-3 The MMF due to a Basic Coil Set *272*

24-4 Expansion of the Periodic MMF due to a Basic Coil Set into a Fourier Series. The Pitch Factor *276*

24-5 The Phase MMF. The Distribution Factor *280*

24-6 Pulsating Harmonics of the Phase MMF *287*

Chapter 25 The Mutual Magnetic Field of a Polyphase Winding 288

25-1 Presentation of the Pulsating Harmonics of the Phase MMF as the Sum of Rotating MMFs *288*

25-2 Presentation of Phase MMF Harmonics as Complex Time-Space Functions *291*

25-3 Time and Space-Time Complex Quantities and Functions of the Quantities Involved in Operation of a Polyphase Machine *294*

25-4 The MMF of a Polyphase Winding. Its Rotating Harmonics *297*

25-5 The Fundamental Component of the Magnetic Flux Density in a Polyphase Winding (the Rotating Field) *303*

25-6 Magnetic Flux Density Harmonics in the Rotating Magnetic Field of a Polyphase Winding *306*

Chapter 26 The Magnetic Field of a Rotating Field Winding 316

26-1 The Magnetic Field of a Concentrated Field Winding *316*

26-2 The Magnetic Field of a Distributed Field Winding *319*

26-3 The Rotating Harmonics of the Excitation Field *321*

Chapter 27 Flux Linkages of and EMFs Induced by Rotating Fields 323

27-1 Introductory Notes *323*

27-2 The Flux Linkage and EMF of a Coil *323*

27-3 The Flux Linkage and EMF of a Coil Group *328*

27-4 The Flux Linkage and EMF of a Phase *330*

27-5 The Flux Linkages and EMFs of a Polyphase Winding. A Space-Time Diagram of Flux Linkages and EMFs *333*

27-6 The Flux Linkages and EMFs due to the Harmonics of a Nonsinusoidal Rotating Magnetic Field *335*

Chapter 28 The Inductances of Polyphase Windings 341

28-1 The Useful Field and the Leakage Field *341*

28-2 The Main Self-Inductance of a Phase *342*

28-3 The Main Mutual Inductance Between the Phases *343*

28-4 The Main Mutual Inductance Between a Stator Phase and a Rotor Phase *344*

28-5 The Main Self-Inductance of the Complete Winding *345*
28-6 The Main Mutual Inductance between a Primary Phase and the Secondary Winding *347*
28-7 The Leakage Inductance of the Complete Winding *348*

Chapter 29 The Electromagnetic Torque 351
29-1 The Torque Expressed in Terms of Variations in the Energy of the Magnetic Field *351*
29-2 The Electromagnetic Torque Expressed in Terms of Electromagnetic Forces *358*
29-3 Electromagnetic Force Distribution in a Wound Slot *367*

Chapter 30 Energy Conversion by a Rotating Magnetic Field 372
30-1 Electromagnetic, Electric and Magnetic Power *372*
30-2 Energy Conversion in an Electrical Machine and Its Model *376*

Chapter 31 Energy Conversion Losses and Efficiency 379
31-1 Introductory Notes *379*
31-2 Electrical Losses *380*
31-3 Magnetic Losses *387*
31-4 Mechanical Losses *396*

Bibliography 397

Index 399

Preface

The subject matter in the text is presented in the sequence traditionally followed in the Soviet Union. It starts with transformers, passes on to induction and synchronous machines, d.c. machines, and concludes with a.c. commutator machines. Separate chapters are devoted to a general theory of electrical machines, machine design and engineering, and transients in electrical machinery.

The electromagnetic processes that take place in electrical machines are examined from the view-point of electromechanical and mechanoelectrical energy conversion. With such an approach, it has been possible to extend the mathematics used to both conventional and any other conceivable types of electrical machines.

In addition to electromagnetic processes, consideration is given to the thermal, aerodynamic, hydraulic and mechanical processes associated with electromechanical and mechanoelectric energy conversion.

In view of the importance attached to the above accompanying processes, the text discusses general aspects of machine design and engineering.

The chapters on transients are based on the theory of a generalized machine. The material includes the derivation of differential equations for induction and synchronous machines in terms of the d, q, 0 and the α, β, 0 axes, and their transformation to a form convenient for computer-assisted analysis and design.

The chapters dealing with specific types of machine (induction, synchronous, d.c.) are largely concerned with the conventional design. In each case, however, there is a short discourse on the operating principle and arrangement of the most commonly used special-purpose modifications.

The electromagnetic processes occurring in conventional a.c. machines are described in terms of the resultant complex functions of electric-circuit parameters or their projections on the axes of a complex plane. As far as practicable, a unified or generalized approach has been taken to deve-

loping equations for and describing the physical processes in the two basic types of machine—the induction machine and the synchronous machine. This concerns electromagnetic torque, electromagnetic active and reactive power, saturable magnetic circuits, machine inductances, etc.

More space is given to thyristor-controlled machines gaining an ever-wider ground, than to a.c. collector machines used on a limited scale.

In the light of new findings, the effect of core saliency on the harmonics of the airgap flux density has been treated in a more rigorous form. A novel approach has been taken towards the equations for mmfs, emfs, electromagnetic forces, electromagnetic torque, and machine characteristics. Among other things, the equations for the synchronous salient-pole machines are developed in terms of the d, q, 0 axes, the analysis of transients includes the short-circuit condition in the synchronous generator, the starting of the induction motor, and events in the single-phase motor.

The material marked with an asterisk (*) may be omitted on first reading, without disrupting the integrity of the exposition.

A. V. Ivanov-Smolensky

Introduction

I-1 Basic Definitions

The utilization of natural resources inevitably involves the conversion of energy from one form to another. Quite aptly, devices doing this job by performing some mechanical motion may be called energy converting machines. For example, heat engines convert the heat supplied by the combustion of a fuel into mechanical energy.

In fact, the same name goes for devices converting energy in one form into energy of the same form but differing in some parameters. An example is a hydraulic machine which converts the mechanical energy of a reciprocating fluid flow into mechanical energy further transmitted by a rotating shaft.

A sizeable proportion of the energy stored by nature in chemical compounds, the atoms and nuclei of substances, the flow of rivers, the tides of seas, the wind, and solar radiation is now being converted to electric energy. This form of conversion is attractive because electricity can in many cases be transmitted over long distances, distributed among consumers and converted back to mechanical, thermal, or chemical energy with minimal losses. However, at present thermal, chemical or nuclear energy is converted directly to electricity on a very limited scale, because this still involves heavy capital investments and is wasteful of power. Rather, any form of energy is first converted to mechanical by heat or water machines and then to electricity. The final step in this sequence—conversion of mechanical energy to electricity or back—is done by electrical machines.

From other electromechanical energy converting devices, electrical machines differ in that, with a few exceptions, they convert energy in one direction only and continuously.

An electrical machine converting mechanical energy to electricity is called a *generator*. An electrical machine performing the reverse conversion is called a *motor*. In fact, a generator can be made to operate as a motor, and a motor as a generator—they are reversible. If we apply mechanical energy to the movable member of an electrical

machine, it will operate as a generator; if we apply electricity, the movable member of the machine will perform mechanical work.

Basically, an electrical machine is an electromagnetic system consisting of a magnetic circuit and an electric circuit coupled with each other. The magnetic circuit is made up of a stationary and a rotating magnetic member and a nonmagnetic air gap to separate the two members. The electric circuit can be in the form of one or several windings which are arragned to move relative to each other together with the magnetic members carrying them.

For their operation, electrical machines depend on electromagnetic induction and utilize the electromotive forces (emfs) that are induced by periodic variations in the magnetic field as the windings or magnetic members are rotated.

For this reason, electrical machines may be called electromagnetic. This also applies to devices that convert electric energy at one value of current, voltage and/or frequency to electric energy at some other value of current, voltage and/or frequency. The simplest and most commonly used electromagnetic energy conversion device which converts alternating current at one voltage to alternating current at some other voltage is the *transformer*. Its coils and core remain stationary relative to each other, and periodic variations in the magnetic field essential for an emf to be induced in the coils are produced electrically rather than mechanically.

Electromagnetic energy converting devices with moving or, rather, rotating parts are more customarily called *rotary converters*. They do not differ from electrical machines in either design or the principle of operation. In fact, rotary converters can sometimes double as electric-to-mechanical (or mechanical-to-electric) energy converting machines. Therefore, we may extend the term "machine" to transformers and rotary converters as special kinds of electrical machine.

Apart from electromagnetic electrical machines, some special applications involve the use of electrostatic machines in which the electromechanical conversion of energy is based on electrostatic induction and utilizes periodic variations in the electric field of a capacitor in which the plates are free to move relative to one another. However, electrostatic machines are no match for electromagnetic machines in terms of size, weight and cost, and are not used in commercial or industrial applications.

As energy converters, electrical machines are important elements in any power-generating, power-consuming, or industrial installation. They are widely used as generators, motors, or rotary converters at electric power stations, factories, farms, railways, automobiles, and aircraft. They are finding an ever increasing use in automatic control systems.

Electrical machines are classed into alternating-current (a.c.) and direct-current (d.c.) machines, according as they operate into or from an a.c. or a d.c. supply line.

I-2 Conversion of Electric Energy by the Transformer

In sketch form, the arrangement of a simple single-phase two-winding transformer is shown in Fig. I-1. As is seen, it consists of two windings, *1* and *2*, with turns w_1 and w_2,

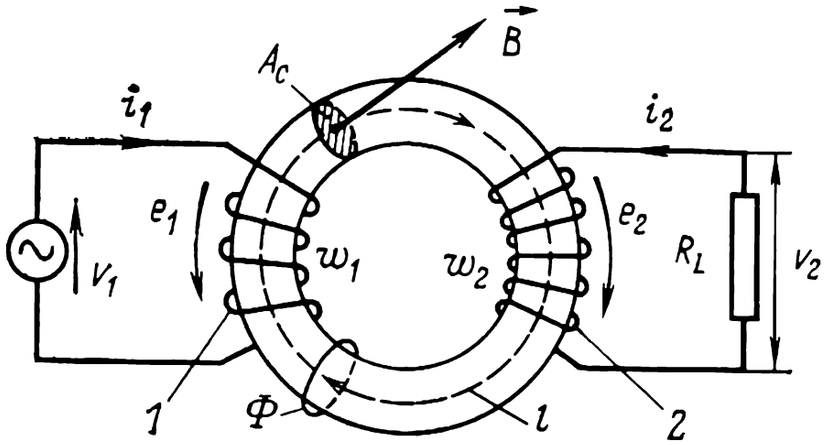

Fig. I-1 Electric and magnetic circuits of a transformer

which are wound on a magnetic core. For better coupling between the coils, the core is assembled from laminations punched in electric-sheet steel having a high relative permeability, μ_r, with no air gap left around the magnetic circuit. The laminations or punchings are made thin in order to reduce the effect of eddy currents on the magnetic field which alternates at an angular frequency ω. Let us open, say, coil *2* and connect coil *1* to a source of a sinusoidal alternating current of frequency $f = \omega/2\pi$ and of voltage $v_1 = \sqrt{2}\, V_1 \cos \omega t$, where V_1 is the rms value of voltage. This will give rise to an alternating current, $i_1 = i_0$, in the coil, which can be found from the voltage equation for the

circuit where it is flowing:

$$v_1 = -e_1 + R_1 i_0 \qquad \text{(I-1)}$$

where R_1 = resistance of winding *1*
$e_1 = -\mathrm{d}\Psi_{11}/\mathrm{d}t$ = emf of self-induction
$\Psi_{11} = w_1\Phi$ = flux linkage
$\Phi = BA_c$ = magnetic flux
B = magnetic induction (magnetic flux density)
A_c = cross-sectional area of the core.

On setting μ_r constant and applying Ampere's circuital law to the magnetic circuit

$$\oint H_l \, \mathrm{d}l = \oint (B/\mu_r\mu_0) \, \mathrm{d}l = \Phi/\Lambda_\mu = i_0 w_1 \qquad \text{(I-2)}$$

where $\Lambda_\mu = \mu_r\mu_0 A_c/l_c$ is the permeance of the core and l_c is the mean core length, it is an easy matter to find the inductance of winding *1*

$$L_{11} = w_1\Phi/i_0 = w_1^2\Lambda_\mu$$

and the mutual inductance

$$L_{12} = w_2\Phi/i_0 = w_1 w_2 \Lambda_\mu$$

and to express in their terms the flux linkage

$$\Psi_{11} = i_0 L_{11}, \qquad \Psi_{21} = i_0 L_{12}$$

and the emf

$$e_1 = -L_{11} \, \mathrm{d}i_0/\mathrm{d}t$$

Using Eq. (I-1) and neglecting $R_1 i_0$, we obtain the magnetizing current

$$i_0 = \sqrt{2} \, I_0 \cos(\omega t - \pi/2)$$

which produces an alternating magnetic flux

$$\Phi = i_0 w_1 \Lambda_\mu$$

Variations in the flux Φ linking coil *2* induce in the latter a sinusoidal emf of mutual induction

$$e_2 = -\mathrm{d}\Psi_{21}/\mathrm{d}t = -L_{12} \, \mathrm{d}i_0/\mathrm{d}t$$

Thus, coil *2* can be used as a source of an alternating current of the same frequency f, but at another voltage, $v_2 = e_2$.

As is seen, the ratio of the instantaneous and the rms emfs across windings *1* and *2* and of the respective rms vol-

tages, is equal to the turns, or transformation, ratio:

$$e_1/e_2 = E_1/E_2 = V_1/V_2 = w_1/w_2 \qquad \text{(I-3)}$$

If V_1 is specified in advance, we may use Eq. (I-3) to find the turns numbers w_1 and w_2 such that V_2 will always have the desired value. Winding *2* can be used as an a.c. source by connecting it across a load resistance, R_L. Then the emf e_2 will induce in it a sinusoidal alternating current

$$i_2 = e_2/(R_L + R_2)$$

which can be found from the voltage equation for the circuit thus formed*

$$e_2 = R_2 i_2 + v_2 \qquad \text{(I-4)}$$

where $v_2 = R_L i_2$.

The secondary current i_2 will bring about a proportionate change in the primary current i_1. The relationship between i_1 and i_2 can be established by again using Ampere's circuital law written by analogy with Eq. (I-2) and recalling that in a transformer under load both windings contribute to the magnetic flux

$$\oint H_l \, dl = \Phi/\Lambda_\mu = i_1 w_1 + i_2 w_2 \qquad \text{(I-5)}$$

Also, in writing the voltage equation for the circuit containing coil *1*

$$v_1 = -e_1 + R_1 i_1 \qquad \text{(I-6)}$$

and neglecting $R_1 i_1$ as in Eq. (I-1), we find that under load the emf e_1 remains about the same as when coil *2* is open-circuited. This implies that e_1 is induced by variations in the same flux Φ and in the same magnetizing current i_0 in coil *1*, as exist when coil *2* is open-circuited. If so, we may equate the right-hand sides of Eqs. (I-1) and (I-5) and argue that the sum of the magnetomotive forces in coils *1* and *2* is equal to the mmf due to the magnetizing current i_0 in coil *1*

$$i_1 w_1 + i_2 w_2 = i_0 w_1 \qquad \text{(I-7)}$$

In an adequately loaded transformer with a closed (no-airgap) core, $i_0 w_1$ is negligible

$$| i_0 w_1 | \ll | i_1 w_1 | \approx | i_2 w_2 |$$

* Here and in Eq. (I-6), the emfs induced by leakage fluxes are not included.

So, without introducing an appreciable error, we may set

$$i_0 w_1 = 0$$

On this assumption, the directions of currents in the windings are such that their mmfs balance each other:

$$i_2 = -i_1 w_1 / w_2 \tag{I-8}$$

It follows from Eq. (I-8) that the ratio of the absolute values, $| i |$, and of the rms values, I, of the currents in coils *1* and *2* are inversely proportional to their turns ratio

$$| i_1 | / | i_2 | = I_1 / I_2 = w_2 / w_1 \tag{I-9}$$

Using Eqs. (I-3), (I-4), (I-6), and (I-8) and neglecting the losses associated with the cyclic magnetization of the core and with variations in the energy of the magnetic field, let us consider the balance of the instantaneous powers in the transformer. The power delivered to coil *1* by the supply line is

$$p_1 = v_1 i_1 = -e_1 i_1 + i_1^2 R_1$$

Some part of this power, $i_1^2 R_1$, is dissipated as heat in coil *1*, and the remainder, $-e_1 i_1 = e_2 i_2$, is transferred by the electromagnetic field into coil *2*. The power supplied to coil *2*

$$e_2 i_2 = i_2^2 R_2 + v_2 i_2$$

is partly dissipated as heat ($i_2^2 R_2$), whereas the remainder, $v_2 i_2$, is delivered to the load.

I-3 Electromechanical Energy Conversion by an Electrical Machine

In sketch form, the arrangement of a simple rotating electrical machine is shown in Fig. I-2. As is seen, it consists of a stationary member called the *stator*, and a rotating member called the *rotor*. The stator core, *4*, is made fast to a base-plate, whereas the rotor core, *3*, is mounted on a shaft carried in bearings, so that it is free to rotate, remaining aligned with the axis of the stator. On its cylindrical surface, the rotor core *3* has slots which receive a single-coil rotor winding, *1*, with turns w_1. The stator core has similar slots which receive a single-coil stator winding with turns w_2.

The stator and rotor cores are assembled from ring-shaped laminations punched in electrical-sheet steel having a high permeability for better magnetic coupling between the windings. For the same purpose, the coils are sunk in slots rather than put on the outer surface of the

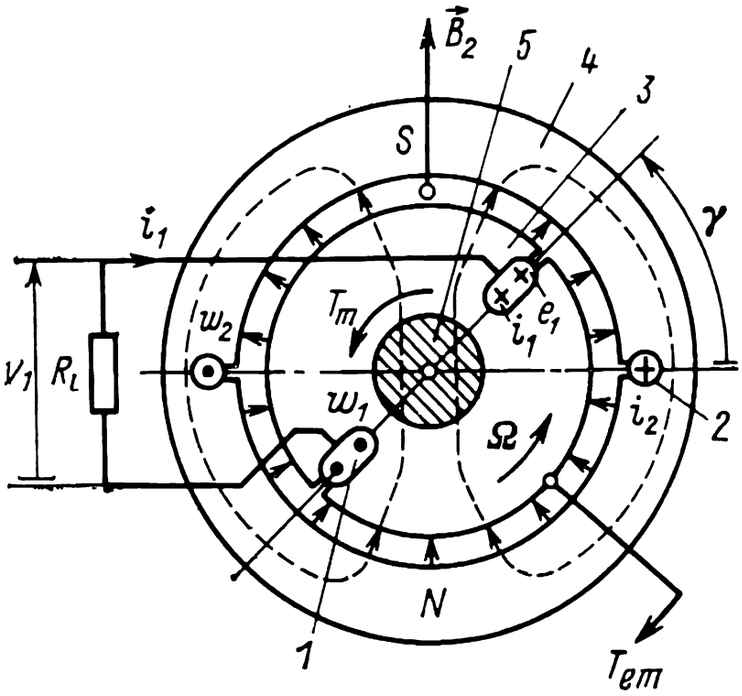

Fig. I-2 Electric and magnetic circuits of a simple electrical machine in the generating mode ($i_1 > 0$, $T_{em} < 0$)

cores. With this arrangement, the air gap between the stator and rotor may be made very small and the magnetic circuit presents a very low reluctance.

The shaft carrying the rotor couples it to another machine with which it exchanges mechanical energy (delivering it in motoring, and receiving it in operation as a generator). The stator and rotor windings are connected to lines with voltages v_2 and v_1, respectively. In motoring the lines (or one of them) deliver electric energy to the machine. In operation as a generator, the machine delivers electric energy to the lines (or one of them).

Electromechanical energy conversion by an electrical machine utilizes the emfs that are induced in the windings as a result of variations in their relative position in space. To begin with, suppose that winding *2* is energized with $i_2 =$ constant, and winding *1* is open-circuited, so that $i_1 = 0$. In the circumstances, a stationary magnetic field is set up, with its north pole, N, located in the bottom part, and the south pole, S, in the top part of the stator core.

Assuming that the permeability of the stator and rotor cores, $\mu_{a,c}$, is infinitely large in comparison with that of the air gap, μ_0 ($\mu_{a,c} \gg \mu_0$), we may neglect the magnetic potential difference across the core. Then, on writing Ampere's circuital law for any loop enclosing the current $i_1 w_2$ in coil *2* (for example, the loop shown by the dashed line in Fig. I-2),

$$\oint H_l \, dl = B_2 \cdot 2\delta/\mu_0 = i_2 w_2$$

we find the magnetic induction in the air gap due to coil *2* to be

$$B_2 = \mu_0 i_2 w_2 / 2\delta \qquad \text{(I-10)}$$

where δ is the radial air gap length.

The flux linkage Ψ_{12} of this field with winding *1* varies with the angle γ that it makes with winding *2*. When $\gamma = 0$, the flux linkage has a maximum positive value

$$\Psi_{12,m} = B_2 \tau l w_1 \qquad \text{(I-11)}$$

where l is the core length in the axial direction and $\tau = \pi R$ is the pole pitch.

As the rotor turns through an angle γ anywhere from zero to 180°, the flux linkage varies linearly as a function of the angle γ

$$\Psi_{12} = \Psi_{12,m} (1 - 2\gamma/\pi) \qquad \text{(I-12)}$$

When $\gamma = \pi/2$, the flux linkage is zero, $\Psi_{12} = 0$. When $\gamma = \pi$, it has a maximum negative value, $\Psi_{12} = -\Psi_{12,m}$. As the rotor keeps rotating, the flux linkage builds up linearly as a function of the angle γ

$$\Psi_{12} = -\Psi_{12,m} (3 - 2\gamma/\pi) \qquad \text{(I-13)}$$

and completes a period of variations when $\gamma = 2\pi$.

The mutual inductance between the windings, $L_{12} = \Psi_{12}/i_2$, varies in a similar way:

$$\begin{aligned} L_{12} &= L_{12,m} (1 - 2\gamma/\pi) && \text{for } 0 < \gamma < \pi \\ L_{12} &= -L_{12,m} (3 - 2\gamma/\pi) && \text{for } \pi < \gamma < 2\pi \end{aligned} \qquad \text{(I-14)}$$

where $L_{12,m} = \mu_0 w_1 w_2 l \tau / 2\delta$ is the maximum mutual inductance between the windings.

If the rotor is turning with an angular frequency Ω, the angle $\gamma = \Omega t$ increases linearly, so that the emf induced in winding *1* is given by

$$e_1 = -\mathrm{d}\Psi_{12}/\mathrm{d}t = -i_2\,\mathrm{d}L_{12}/\mathrm{d}t = -i_2\Omega\,\mathrm{d}L_{12}/\mathrm{d}\gamma \quad \text{(I-15)}$$

It is called the emf of rotation or the motional emf.

As is seen, the motional emf is proportional to the angular displacement, angular frequency and derivative of the mutual inductance with respect to the angular displacement of the rotor. From Eqs. (I-14) and (I-15) it follows that

$$e_1 = (2/\pi)\,L_{12,m}i_2\Omega \qquad \text{for} \quad 0 < \gamma < \pi$$

$$e_1 = -(2/\pi)\,L_{12,m}i_2\Omega \qquad \text{for} \quad \pi < \gamma < 2\pi$$

The "+" sign applies when the emf is in the positive direction of the current in coil *1*; the "—" sign applies when it is in the negative direction. The positive directions of currents in windings *1* and *2* are such that the magnetic fields are directed upwards as in Fig. I-2, with $\gamma = 0$.

Thus, with i_2 held constant, a square emf waveform is induced in winding *1* of the elementary machine. The flux linkage, mutual inductance and emf vary with a period $T = 2\pi/\Omega$. Hence, these quantities vary with a frequency given by

$$f = \Omega/2\pi \quad \text{(I-16)}$$

Using Eqs. (I-10) and (I-14), we can express the motional emf defined by Eq. (I-15) in terms of the magnetic induction B_2 in the air gap

$$e_1 = 2B_2luv_1 \qquad \text{for} \quad 0 < \gamma < \pi$$

where $u = r\Omega$ is the tangent velocity at the middle of the air gap. Therefore, the direction of e_1 can be determined not only from Eq. (I-15), using Lenz's rule, but also using the right-hand rule. Of course, both approaches give the same result (Fig. I-2).

If we, now, connect winding *1* having an internal resistance R_1 across a load resistance R_L, the circuit thus formed will carry an alternating current given by

$$i_1 = e_1/(R_L + R_1) \quad \text{(I-17)}$$

varying with the same frequency f as e_1 does. The power generated in winding *1* will then be

$$e_1 i_1 = -i_1 i_2 \Omega\,(\mathrm{d}L_{12}/\mathrm{d}\gamma) = (v_1 + i_1 R_1)\,i_1 \quad \text{(I-18)}$$

Some of this power, $i_1^2 R_1$, will be dissipated as heat in winding *1*; the remainder

$$p_1 = v_1 i_1 = i_1^2 R_L$$

will be delivered to load.

The voltage across winding *1*,

$$v_1 = i_1 R_L$$

which is the same as the load voltage, will likewise vary with frequency f.

On the assumption that i_2 is constant, winding *2* is energized from a source of d.c. voltage

$$v_2 = i_2 R_2$$

The power

$$p_2 = v_2 i_2$$

it receives does not undergo electromechanical conversion and is completely dissipated as heat.

The interaction of the magnetic fields set up by i_2 and i_1 produces an electromagnetic torque T_{em} acting on the rotor. In determining T_{em}, we may proceed from the fact that the work it performs as the rotor is turned through a small angle $d\gamma$ is equal to the change in the energy of the magnetic field, dW, caused by a change in the mutual inductance, dL_{12}, assuming that both i_1 and i_2 remain constant, or mathematically

$$T_{em}\, d\gamma = dW = i_1 i_2\, dL_{12}$$

Hence,

$$T_{em} = i_1 i_2\, dL_{12}/d\gamma \qquad \text{(I-19)}$$

If the angular displacement of the rotor, $d\gamma$, is in the direction of rotation, the torque in Eq. (I-19) acts likewise in the direction of rotation and is positive. If $d\gamma$ is in the opposite direction, the torque in Eq. (I-19) is in the opposite direction, too, and negative. In the generator mode of operation, the torque is, as is shown in Fig. I-2, negative, $T_{em} < 0$. Using Eqs. (I-10) and (I-14), we can express the electromagnetic torque in terms of the magnetic induction in the air gap, B_2, as well:

$$| T_{em} | = 2B_2 l i_1 w_1 r \qquad \text{(I-20)}$$

The direction of the tangential electromagnetic force, $F = 2B_2 l i_1 w_1$, and of the torque in Eq. (I-20) can be ascertained, using the left-hand rule, as is done in Fig. I-2 for the generator mode.

Under steady-state conditions, when the rotor is spinning at a constant frequency Ω, the electromagnetic torque T_{em} must be balanced by an external (mechanical or load) torque T_m

$$T_m = -T_{em} = -i_1 i_2 (dL_{12}/d\gamma) \qquad \text{(I-21)}$$

For this to happen, a mechanical power must be applied to the rotor via its shaft

$$T_m\Omega = -i_1 i_2 \Omega (dL_{12}/d\gamma) \qquad \text{(I-22)}$$

which is converted to an equal electric power, $e_1 i_1$, given by Eq. (I-18).

When γ is anywhere between zero and 180°, both i_2 and i_1 are positive and $dL_{12}/d\gamma < 0$. In contrast, when γ is anywhere between 180° and 360°, i_2 is positive, i_1 is negative, and $dL_{12}/d\gamma > 0$. Accordingly, the power in Eq. (I-22) is positive, $T_m\Omega > 0$, not only when the rotor takes up the position shown in Fig. I-2, but in any other angular position. This implies that an elementary electrical machine can perform electromechanical conversion of energy in one direction only (in our case, it can only operate as a generator).

The same elementary machine can operate as a motor, thereby converting electricity to mechanical energy. To this end, winding *1* must be connected to an a.c. supply line of voltage v_1 and frequency f, so that i_1 is always in opposition to e_1 (Fig. I-3). On writing the voltage equation for the circuit thus formed

$$v_1 = -e_1 + i_1 R_1$$

and multiplying it by i_1, we obtain the power delivered by the supply line to winding *1*:

$$v_1 i_1 = -e_1 i_1 + i_1^2 R_1$$

Some of this power, $i_1^2 R_1$, is dissipated as heat in winding *1* and the remainder

$$-e_1 i_1 = i_1 i_2 \Omega (dL_{12}/dt)$$

is converted to mechanical power

$$T_{em}\Omega = i_1 i_2 \Omega (dL_{12}/dt)$$

transmitted by the rotor to the shaft of the driven machine. Using the right- and left-hand rules, it is an easy matter to see that in motoring the torque is positive ($T_{em} > 0$) and is in the direction of rotation.

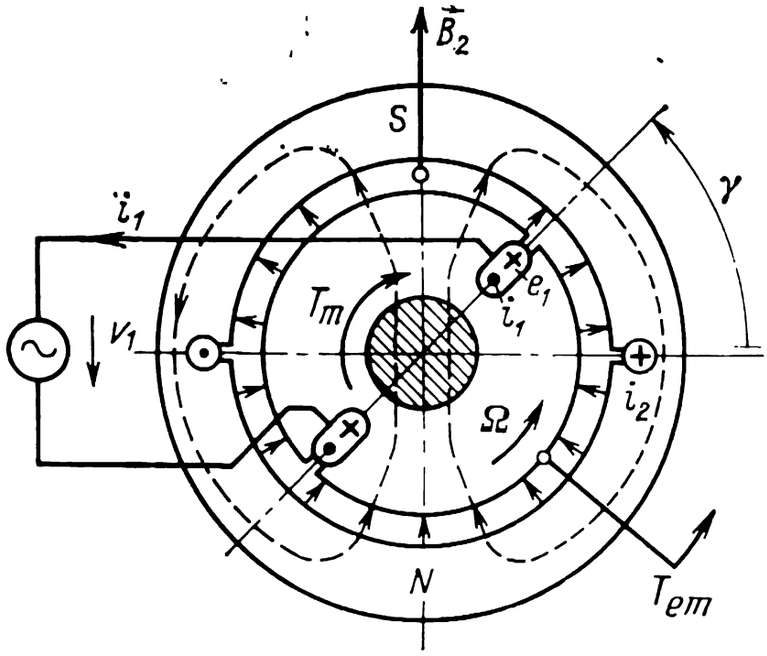

Fig. I-3 Electric and magnetic circuits of a simple electrical machine in the motoring mode ($i_1 < 0$, $T_{em} > 0$)

To sum up, the elementary electrical machine we have examined is reversible—it can operate as both a generator and a motor. This is in fact true of any electrical machine.

I-4 Functional Classification of Electromagnetic Energy Converting Devices

The analysis of simple electromagnetic energy converting devices set forth in Secs. I-2 and I-3 shows that transformers and elementary electrical machines can only operate from an a.c. supply line operating at frequency f.

If a transformer or an electrical machine is to convert d.c. energy, the d.c. supply must first be converted to an a.c. form by a suitable device. This may be a semiconductor device, or a mechanical one as in electrical machines (in the form of a commutator whose bars are connected to the respective coils of the rotating winding, and fixed brushes riding the commutator).

Table I-1 Functional Classification of Electromagnetic Energy Converting Devices

Description	Block diagram	Function(s) performed
Transformer	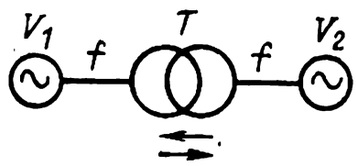	Conversion of alternating current at one voltage to alternating current at another voltage
A. C.-to-D.C. converter, D. C.-to-A. C. inverter	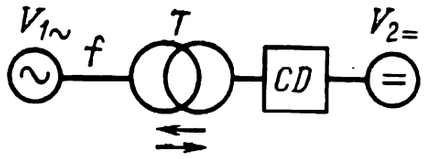	Conversion of a.c. to d.c., or back
D. C.-to-D. C. converter	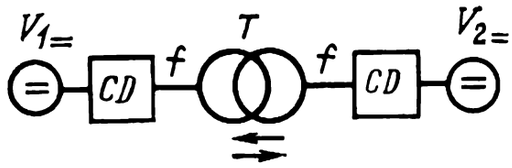	Conversion of d.c. at one voltage to d.c. at another voltage
A. C. electrical machine	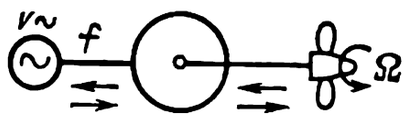	Conversion of a.c. to mechanical energy (or back)
D. C. electrical machine (commutator- or rectifier-type)	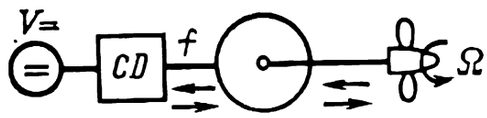	Conversion of d.c. to mechanical energy (or back)
A. C. rotary converter (A. C.-D. C. electrical machine)	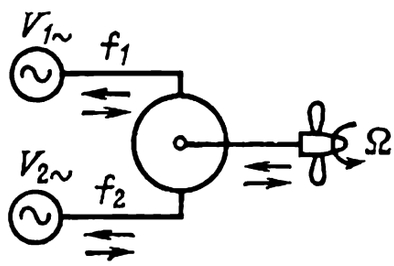	Conversion of a.c. at f_1 to a.c. at $f_2 \neq f_1$ and to mechanical energy (or in any other direction)
A. C.-to-D. C. rotary converter	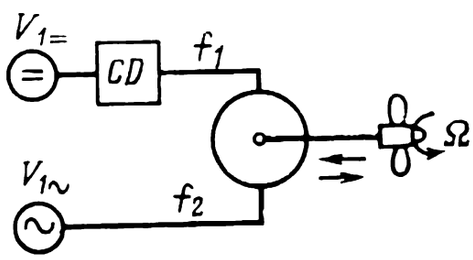	Conversion of a.c. at f_1 to d.c. or mechanical energy (or in any other direction)

Table I-1 (continued)

Description	Block diagram	Function(s) performed
D. C. rotary converter	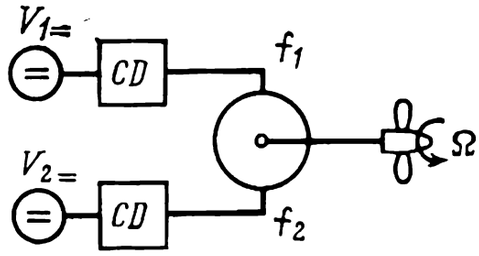	Conversion of d.c. at V_1 to d.c. at $V_2 \neq V_1$ and to mechanical energy (or in any other direction)

If we consider an electromagnetic energy converting device in combination with a rectifier as an entity performing a specific function, we shall obtain a functional classification as given in Table I-1.

Transformers

1

1 An Outline of Transformers

1-1 Purpose, Applications, Ratings

A transformer is an electromagnetic energy converting device which has no moving parts and two (or more) windings fixed relative to each other, intended to transfer electric energy between circuits or systems by virtue of electromagnetic induction.

Electric energy in the form of an alternating current taken from a supply line with m_1 phases at a phase voltage V_1 and frequency f_1 is impressed on the input, or *primary*, winding whence it is transferred by a magnetic field into the output, or *secondary*, winding with m_2 phases at voltage V_2 and frequency f_2. In most cases, transformers only change voltages, $V_1 \neq V_2$, or currents, $I_1 \neq I_2$, without affecting frequency or number of phases.

As a rule, there is no conductive connection between the primary and secondary windings, and energy transfer between them is only by induction ("transformer action").

A transformer having two single- or polyphase windings with no conductive connection between them is termed a *two-winding transformer* (Figs. 1-1*a* and 1-2, respectively). A transformer having three or more windings (Fig. 1-1*b*) with no conductive connection between them is called a *threewinding transformer* or a *multiwinding transformer* (see Sec. 10-1).

Standing apart from other transformers is the autotransformer in which some of the energy delivered by a supply line is transferred to the secondary winding conductively (see Sec. 10-2) owing to a connection between the primary and secondary sides.

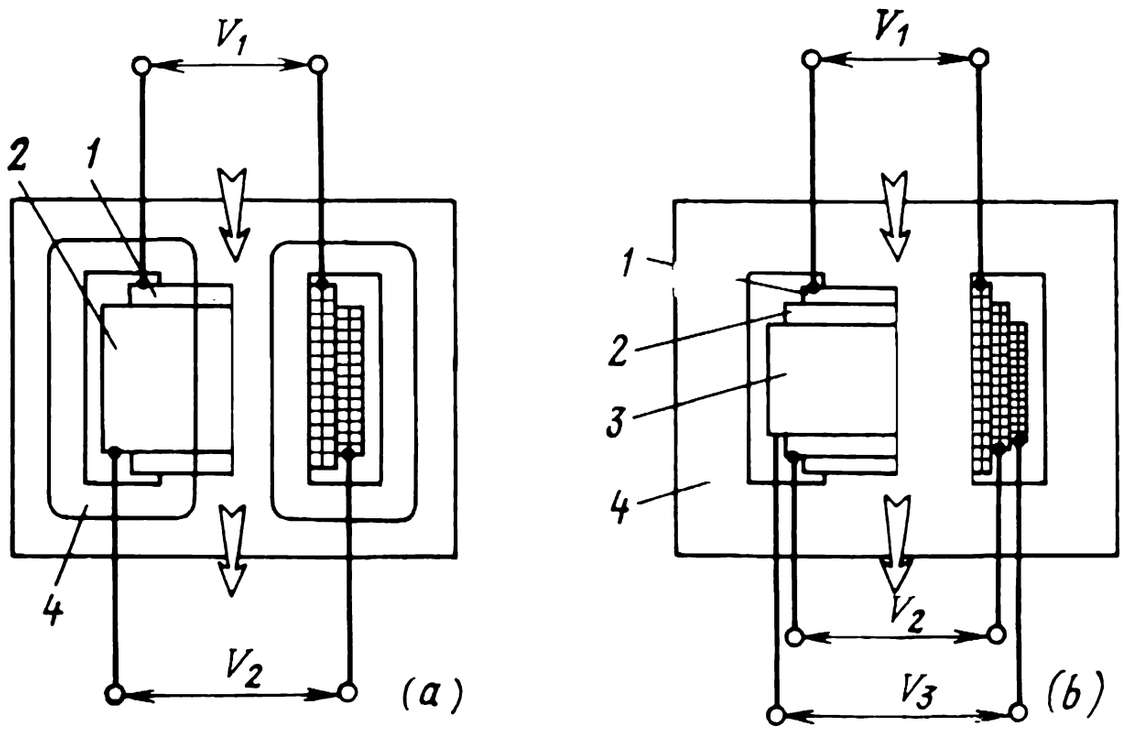

Fig. 1-1 Single-phase transformers: (*a*) two-winding and (*b*) three-winding:
1—primary winding; *2*—secondary winding; *3*—secondary winding; *4*—magnetic circuit (core)

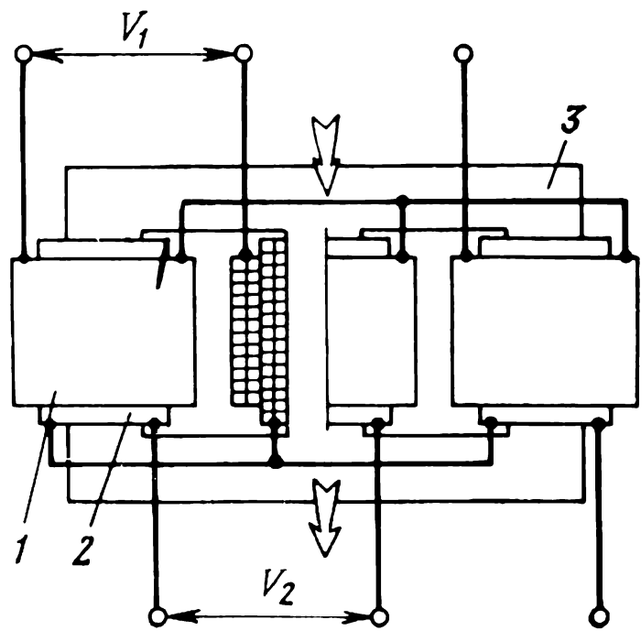

Fig. 1-2 Three-phase, two-winding transformer:
1—star-connected three-phase primary coils; *2*—star-connected three-phase secondary coils; *3*—magnetic circuit (core)

As already noted, energy supplied by a line is impressed on the primary winding which may be single- or polyphase. If energy conversion proceeds in the direction shown in Figs. 1-1 and 1-2, the primary windings are those which are labelled by the numeral "*1*". The secondary windings deliver power to a load line; in Fig. 1-1, windings *2* and *3* are the secondary windings, and in Fig. 1-2 it is winding *2*. As is seen, a multiwinding transformer may have several primary and secondary windings. For example, the transformer in Fig. 1-1*b* has two secondary windings, *2* and *3*.

Polyphase windings are formed by star- or delta-connecting the phase windings of which there are as many as are phases in the supply line. Each phase winding is a multiturn coil mounted on a separate limb (or leg) of the transformer core.

In terms of phases, there may be single-phase transformers (Fig. 1-1*a* and *b*), three-phase transformers (Fig. 1-2), and polyphase transformers.

As electric energy converters, transformers have found many uses. Among other things, they are involved in the transmission of power from electric stations to consumers. As often as not, this calls for the voltage to be stepped down or up more than once. Therefore, the overall installed capacity of transformers in present-day electric systems is five to seven times the installed capacity of generators.

Apart from transformers and autotransformers used in power transmission and distribution systems and referred to as power transformers, wide use is made of transformers intended to transform the number of phases and frequency. Also, special-purpose transformers are used in various industrial installations, communications, radio, television, automatic control, and measurements.

Commercially available transformers are made with power ratings from fractions of a volt-ampere to several hundred megavolt-amperes, for voltages from fractions of a volt to several hundred kilovolts, for currents up to tens of kiloamperes, and for frequencies up to several thousand hertz. Among special-purpose transformers are pulse transformers, variable-voltage transformers, stabilized-voltage transformers, etc. (see Chap. 15).

Transformers are manufactured to relevant specifications or standards and are designed to perform specific functions. Accordingly, they are rated in terms of frequency, current,

voltage, power, or some other values, all of which are called ratings or rated values. They are given on a nameplate attached to each transformer. In this text we shall denote them by the subscript "R".

The voltage rating, or rated voltage, is the line (or line-to-line) voltage as measured across the line terminals of a particular winding, and is designated (in Soviet practice) as $V_{1,\,\mathrm{R,\,line}}$ or $V_{2,\,\mathrm{R,\,line}}$.

The power rating, or rated power, of a transformer is its total power, which is

$$S_{1,\,\mathrm{R}} = V_{1,\,\mathrm{R}}\, I_{1,\,\mathrm{R}}$$

for a single-phase transformer, and

$$S_{1,\,\mathrm{R}} = \sqrt{3}\, V_{1,\,\mathrm{R,\,line}} I_{1,\,\mathrm{R,\,line}} = 3V_{1,\,\mathrm{R}} I_{1,\,\mathrm{R}}$$

for a three-phase transformer*.

In a two-winding transformer, the power rating, or rated power, of the primary winding, $S_{1,\,\mathrm{R}}$, is the same as that of the secondary winding, $S_{2,\,\mathrm{R}}$, and equal to the power rating of the transformer, $S_{1,\,\mathrm{R}} = S_{2,\,\mathrm{R}} = S$.

The rated frequency, f_{R}, of a harmonically varying quantity (current or voltage) for general-purpose transformers is 50 Hz in the USSR and 60 Hz in the USA and some other countries.

Rated currents are found from the power rating and the rated voltage of the respective winding:

$$I_{1,\mathrm{R}} = S_{\mathrm{R}}/V_{1,\mathrm{R}}$$

for single-phase transformers,

$$I_{1,\,\mathrm{R,\,line}} = S_{\mathrm{R}}/\sqrt{3}\, V_{1,\,\mathrm{R,\,line}}$$

for three-phase transformers (line current) and

$$I_{1,\mathrm{R}} = S_{\mathrm{R}}/3V_{1,\mathrm{R}}$$

for three-phase transformers (phase current).

The nameplate data are not to be understood as a prescription to operate the transformer only at its rated capability. Actually, its secondary current is allowed to vary

---

* Here and elsewhere in the text, the line quantities have the subscript "line", whereas the phase quantities have no subscript. For example, $V_{1,\,\mathrm{line}}$ is the primary line voltage and V_1 is the primary phase voltage.

from zero to $I_{2,R}$, with short-duration overcurrents [13]. Also, applicable standards permit slight variations in voltage and frequency.

It is to be noted that if we hold the primary voltage constant, the secondary voltage will vary with the magnitude and nature of load and may differ from its value at no-load (open-circuit voltage), when the secondary current is zero. It would seem that the rated secondary voltage should be taken equal to that at the rated power S_R. Unfortunately, this voltage depends on the phase relation between the secondary current and voltage. Therefore, to avoid ambiguity, the rated secondary voltage, $V_{2,R}$, is taken to be equal to the no-load (open-circuit) voltage, when the secondary current is zero.

Arbitrarily, the rated secondary current is taken to be equal to that computed from the rated power at the rated secondary voltage:

$$I_{2,R} = S_R/V_{2,R}$$

for single-phase transformers,

$$I_{2,\,R,\,line} = S_R/\sqrt{3}\,V_{2,\,R,\,line}$$

for the line current of a three-phase transformer, and

$$I_{2,R} = S_R/3V_{2,R}$$

for the phase current of a three-phase transformer.

A transformer can step up or down the applied voltage. In a *step-up transformer*, the primary winding is on the low-voltage (LV) side, and the secondary winding is on the high-voltage (HV) side. In a *step-down transformer*, they are arranged the other way around. For example, the transformer in Fig. 1-2 will be a step-up one if $V_{1,R}$ is lower than $V_{2,R}$, or a step-down one if $V_{1,R}$ is higher than $V_{2,R}$ (the arrows in the figure show the direction of power transfer).

1-2 Construction of a Transformer

(i) The Core and Coils

The actual energy conversion in a transformer takes place in its core and coils.

For better energy conversion, the coils are placed on, or enclosed in, a magnetic circuit fabricated from a ferromagnetic material having a high permeability, μ_a, which

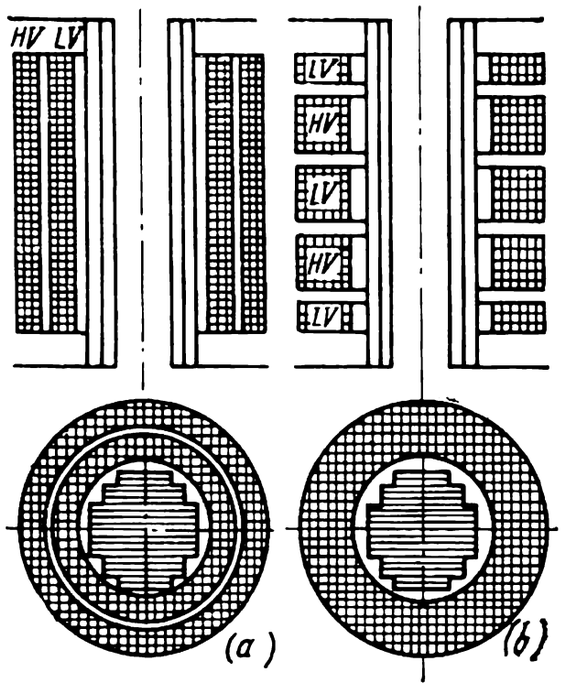

Fig. 1-3 Transformer windings: (*a*) coaxial and (*b*) interleaved sandwich

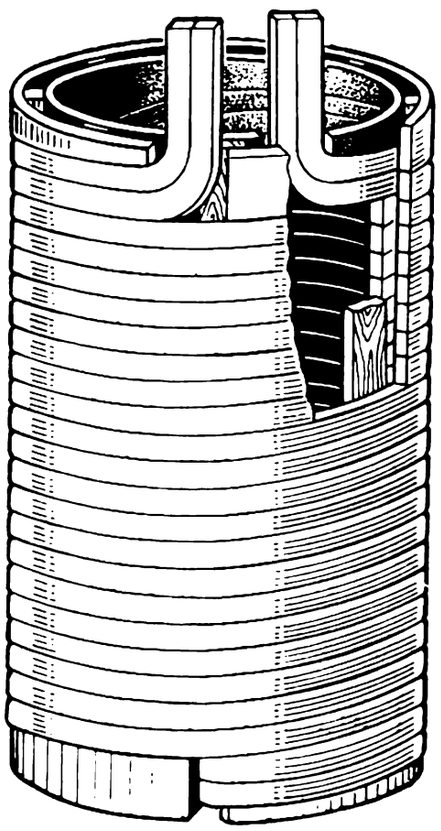

Fig. 1-4 Two-layer cylindrical strip-conductor winding

is hundreds of times that of free space, μ_0 (see Figs. 1-1 and 1-2). To have a high permeability, the magnetic circuit ought not to be excessively saturated, and its magnetic induction (magnetic flux density) at a maximum magnetic flux ought not to exceed 1.4 to 1.6 T*. The required reactive power can be reduced by minimizing the leakage fluxes each of which links with only the primary or only the secondary winding. One way to reduce leakage fluxes is to reduce the gap between the primary and secondary windings. To this end, the primary and secondary coils of a phase are put on the same leg or limb (see Figs. 1-1 and 1-2). The windings may be in the form of cylindrical coils taking up the whole length of, and arranged coaxially on, the limb (Fig. 1-3*a*) or as a series of pancake or disc coils with the primary and secondary sections alternating in an interleaved or sandwich arrangement (Fig. 1-3*b*). Of a large number of various coaxial windings, the cylindrical winding is the simplest (Fig. 1-4).

An important aspect in improving the efficiency of energy

---

* T stands for the tesla, the unit of magnetic flux density in the International System (SI).— *Translator's note.*

conversion is to reduce the amount of power lost as heat. To this end, the windings are made of a material with a low resistance and a large cross-sectional area, and with a minimum acceptable turn length.

The magnetic circuit is designed so as to keep eddy-current and hysteresis losses to a minimum. This is usually done by using magnetically soft, electrical-sheet steels which

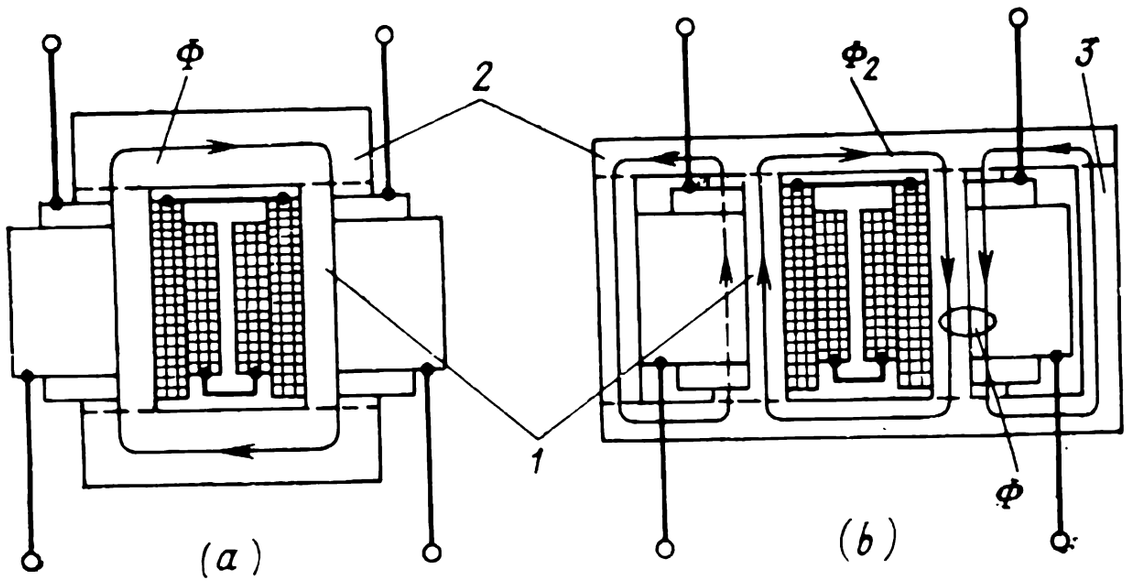

Fig. 1-5 Single-phase transformers: (*a*) core type and (*b*) core-and-shell (five-leg core) type:
1—limb (leg); *2*—yoke; *3*—outer limb (leg)

have a low hysteresis loss and high resistivity, and assembling the core from individually insulated laminations with a thickness chosen such that eddy currents would not affect the main magnetic field and would not lead to increased eddy-current loss. The lamination thickness d depends on the frequency f of the magnetizing current (see Sec. 31-3), and is taken as 0.35 mm or 0.5 mm for 50 Hz.

With a core fabricated as outlined above, the iron (or core) loss can be kept at a level comparable with the copper loss, and the demagnetizing effect of eddy currents can be reduced to a minimum.

Transformer cores mostly come in any one of two designs, the *core type* and the *shell type*. In a core-type single-phase transformer, the core consists of two vertical limbs around which the preformed circular windings are placed. The windings consist each of two coils which may be connected in series or parallel and are placed on different limbs. The top and bottom members, called the yokes, join the two limbs into a closed magnetic circuit (see Fig. 1-5*a*).

In *a core-type three-phase transformer*, a primary and a secondary winding of one phase are wound on each limb (see Fig. 1-2). The three equal limbs are joined by the two yokes into a closed magnetic path.

In *a single-phase shell-type transformer*, the core is divided so that parallel magnetic paths encircle the single group of coils on two sides as if by a shell (see Fig. 1-1). As is seen, the yokes are built up to a cross-sectional area half as large as that of the limb carrying the coils.

To reduce height and to facilitate transit by rail, high-power transformers have five-leg core-type circuits called

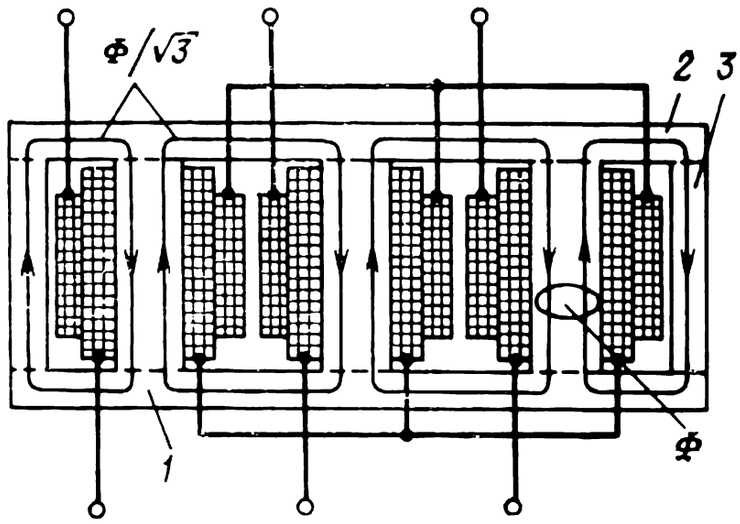

Fig. 1-6 Three-phase core-and-shell-type transformer:
1—limb; *2*—yoke; *3*—outer limb

the core-and-shell type in Soviet usage (Figs. 1-5*b* and 1-6). A *core-and-shell transformer* is lower in height because the yokes have to carry half as large a flux and may therefore have a lower height, too. As an illustration, Fig. 1-5 shows single-phase transformers of the core and the core-and-shell type of construction having the same power rating. The height can be reduced by about the same amount in a three-phase core-and-shell transformer (Fig. 1-6) where the yokes have to carry a flux which is $1/\sqrt{3}$ times that in the limbs. In core-type transformers, the yokes carry the same flux as the limbs do.

At the corners of a core, the yokes and limbs may be joined in any one of two manners. One gives *butt joints*; and the other, *interleaved* (or *imbricated*) *joints*.

With *butt joints*, the limbs and the yokes are stacked up separately, the coils are put on the limbs, and the top yoke

is then placed on (joined with) the limbs to form a closed magnetic circuit. The butt joints are filled by insulating spacers to avoid eddy currents at those places. The spacers form a virtual air gap which absorbs reactive power over and above that required by the iron itself. Because of this, butt joints are seldom used, although they simplify assembly and disassembly.

Interleaved (or *imbricated*) *joints* are used on a wider scale. In this case, the successive layers of laminations in the yokes and limbs are interleaved so as to give an overlap at the corners to reduce the joint reluctance (Fig. 1-7). Even so, the flux has to cross the insulation between the laminations at the overlapped portions, but the virtual air gap thus formed absorbs less reactive power than a core of the butt-joint type. A disadvantage of the interleaved type is that a core already assembled has to be disassembled (unbladed) at the top yoke so as to let the coils be put on the limbs. After that the top yoke is assembled (rebladed) again.

Modern electrical-sheet steels display directional (anisotropic) properties produced by cold rolling so that in the direction of rolling they have a reduced specific loss and an increased permeability [13]. However, there is an increase in loss and a reduction in magnetic intensity at the joints between the limbs and yokes, where the magnetic lines of force turn through 90° from the direction of rolling. This drawback can to a marked degree be minimized by using mitred joints or overlaps as shown in Fig. 1-8.

In low-power, low-voltage transformers, the coils may be wound on rectangular formers and the limbs may be given a rectangular cross-section. In high-power transformers, the coils are wound on a cylindrical mandrel, and the limbs are given multistep cruciform cross section approaching the area of the circumscribing circle so that the area within the coils has a more efficient iron-to-air ratio (Fig. 1-9). The yokes usually have a rectangular or a cruciform section with a limited number of steps.

Clamping and packing arrangements for transformers vary from size to size. In power transformers rated at under 1 MVA (per limb), this is done with wooden or plastic battens and bars which fill the space between the limb and the insulating sleeve carrying the LV winding which is placed next to the limb iron (Fig. 1-9*a*).

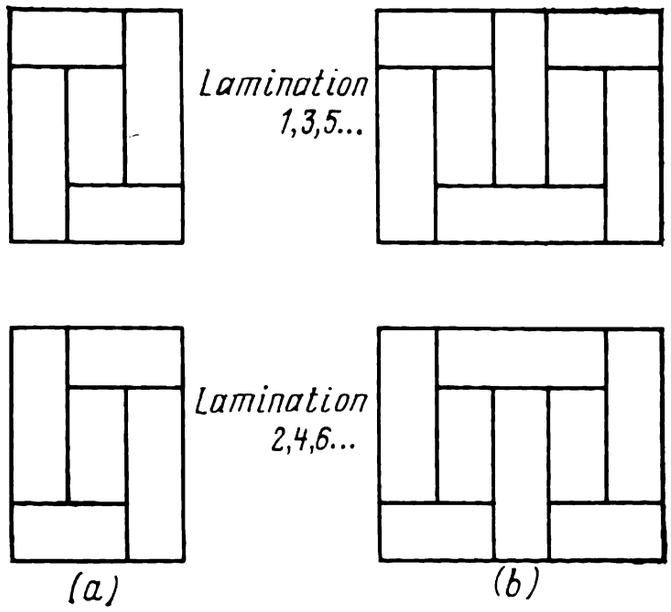

Fig. 1-7 Imbricated (interleaved) joints in a magnetic core:
(*a*) single-phase core-type transformer; (*b*) three-phase core-type transformer

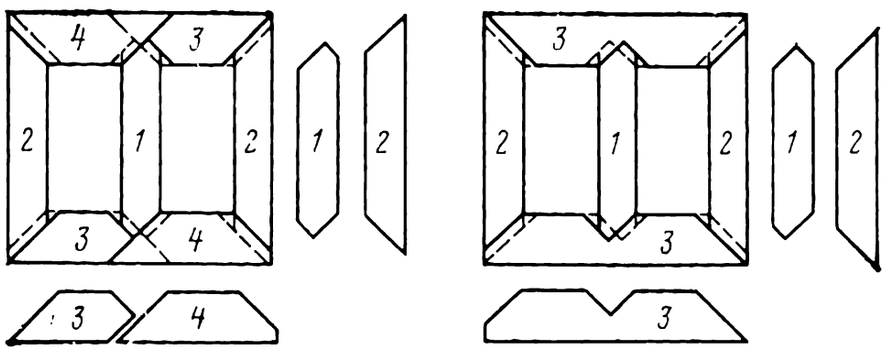

Fig. 1-8 Mitred joints for a three-phase core-type transformer using cold-rolled grain-oriented steel sheet laminations

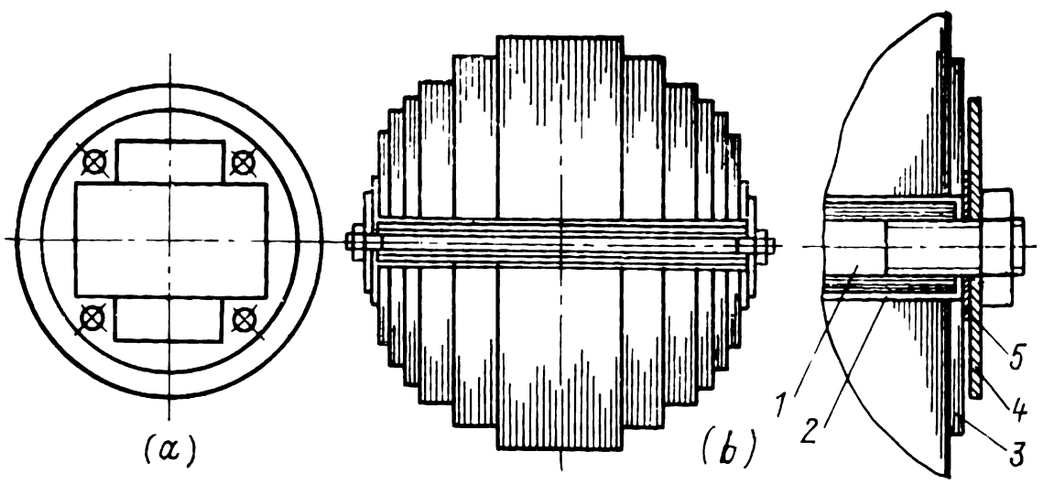

Fig. 1-9 Yoke clamping:
(*a*) by wooden battens; (*b*) by steel studs (*1*—steel stud; *2*—insulating tube; *3*—pressboard washer; *4*—steel washer; *5*—pressboard washer)

In high-power transformers, the limbs were at one time clamped by steel studs insulated from the iron by synthetic-resin-bonded paper cylinders (Fig. 1-9*b*), whereas the yokes were clamped with similar studs extending through wooden or steel yoke clamps (Fig. 1-10).

The more recent practice is to clamp together the laminations in transformer limbs and, often, yokes with circumfe-

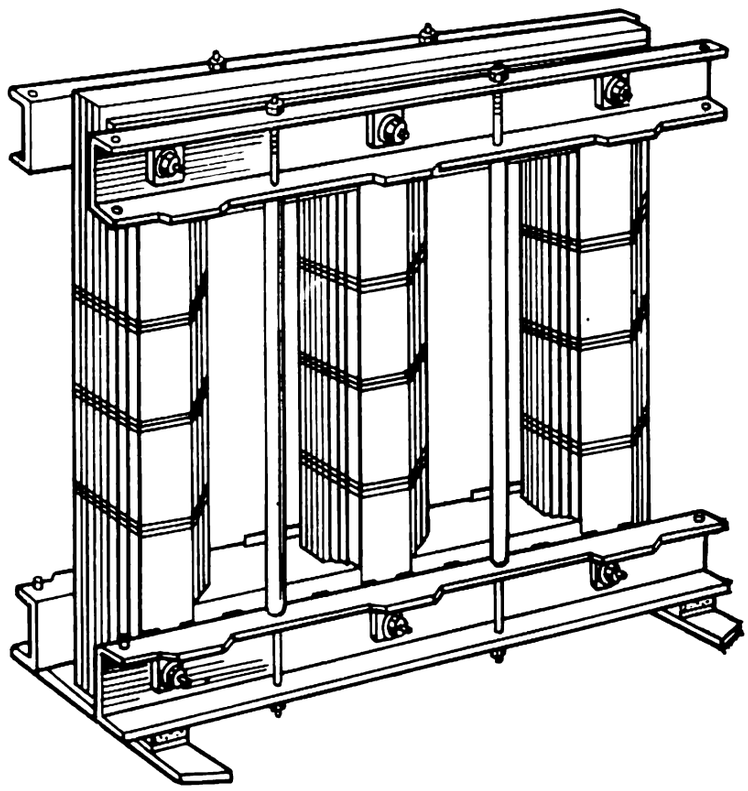

Fig. 1-10 Transformer frame

rential bands usually made of glass fibre bonded with thermo-setting epoxy compounds. (Such bands can be seen on the limbs in Fig. 1-10, and on the limbs and yokes in Fig. 13.) With epoxy-resin-bonded bands, one need not use clamping studs or punch holes in the core laminations (such holes reduce the reluctance of the core and add to no-load losses).

The core and the yoke clamps along with the other parts serving to hold the core and coils in place make up the frame of a transformer (Fig. 1-10).

Microtransformers rated for units to tens of volt-amperes use far simpler core designs. As often as not, their cores are assembled with one-piece punchings as shown in Fig. 1-11*a*, or two-piece laminations (one piece being E-shaped, and the other I-shaped) as shown in Fig. 1-11*b*.

In the lamination shown in Fig. 1-11*a*, the middle limb is cut through, so it can be bent away during assembly,

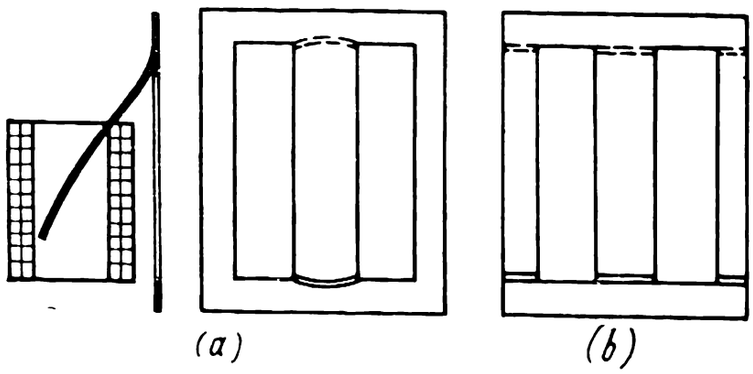

Fig. 1-11 Core assembly for microtransformers:
(*a*) ⊟-shaped laminations; (*b*) E- and I-shaped laminations

and coils can be put on it and inside the lamination. The next lamination is inserted from the opposite end of the

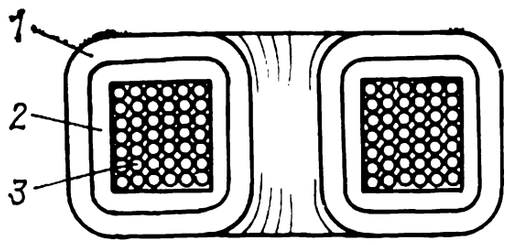

Fig. 1-12 Strip-wound transformer:
1—primary; *2*—secondary; *3*—core

coil. After assembly, the core is clamped tight by pressure end plates and studs.

Another popular core design is that using long strips or ribbons of transformer steel wound on a ring-shaped former, and the coils in turn wound on the core by a suitable machine (Fig. 1-12).

(ii) Structural Parts of a Transformer

The function of the structural parts in any transformer is to provide electrical insulation between the windings, to hold the core and coils in place, to cool the transformer, to provide connection between the transformer windings and the associated electric lines, and the like. Actually, the yoke clamps and the other clamping and packing-out parts may also be classed as structural parts.

Let us take a closer look at the structural parts, choosing an oil-immersed three-phase power transformer as an example. Its general arrangement is shown in Fig. 1-13.

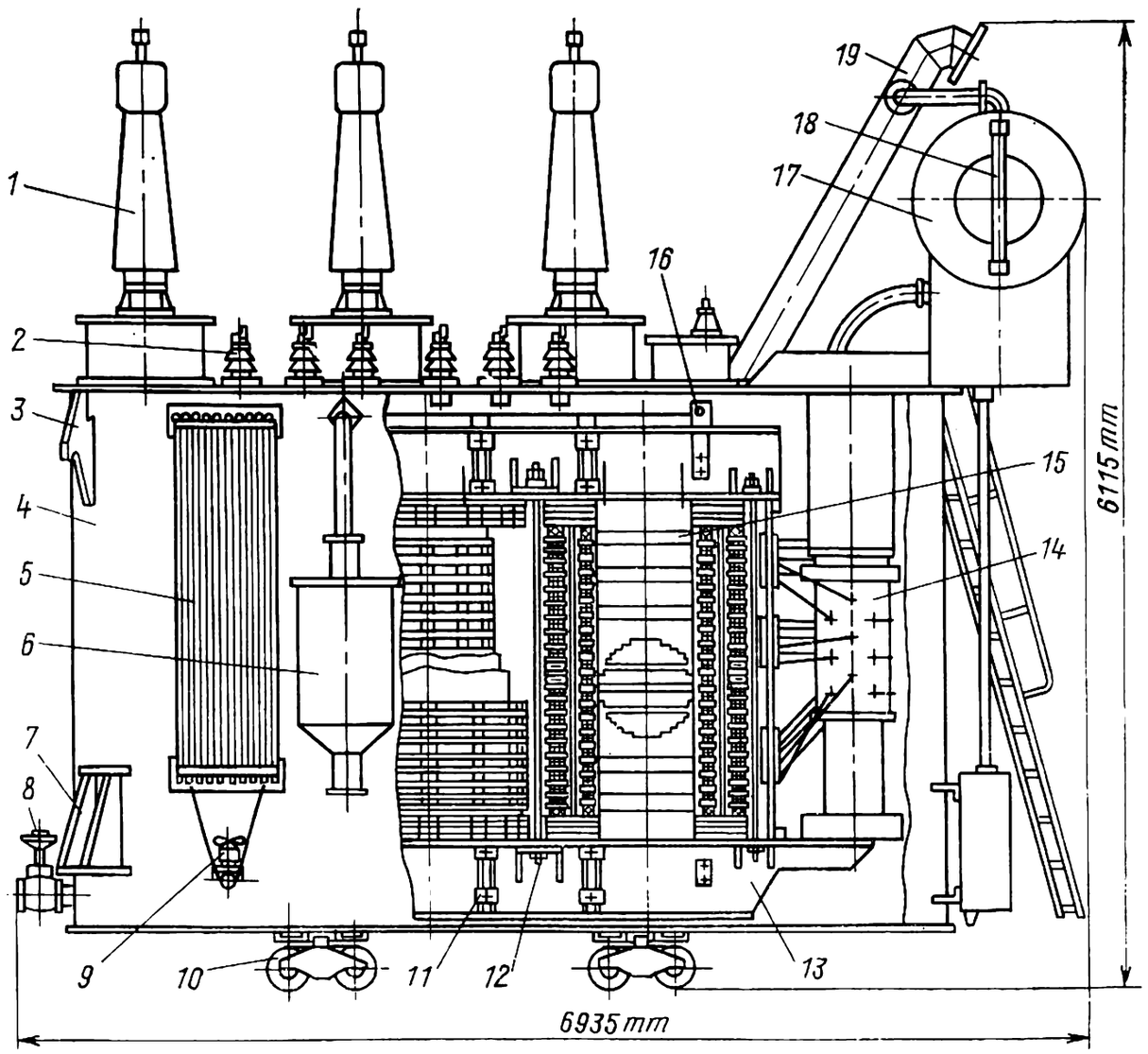

Fig. 1-13 Three-phase, two-winding, 40-MVA, 110-kV transformer with split LV windings and on-load tap-changing on the HV side: *1*—110-kV bushing; *2*—10-kV LV bushing; *3*—lifting lug; *4*—tank; *5*—tubular cooler; *6*—thermal siphon filter; *7*—jacking lug; *8*—oil drain cock; *9*—blower; *10*—castors; *11*—yoke bands; *12*—frame tie-rod; *13*—yoke clamp; *14*—HV tap-changer; *15*—limb bands; *16*—core-and-coil lifting lug; *17*—conservator; *18*—oil gauge; *19*—explosion stack

Winding insulation. The turns of a transformer winding must reliably be insulated from one another, from the turns of other windings, and from the transformer frame. In oil-immersed transformers for 10 kV and higher, this purpose is served by oil-paper barrier insulation. It is obtained by impregnating cable paper or electric-grade pressboard with transformer oil which is also used to fill

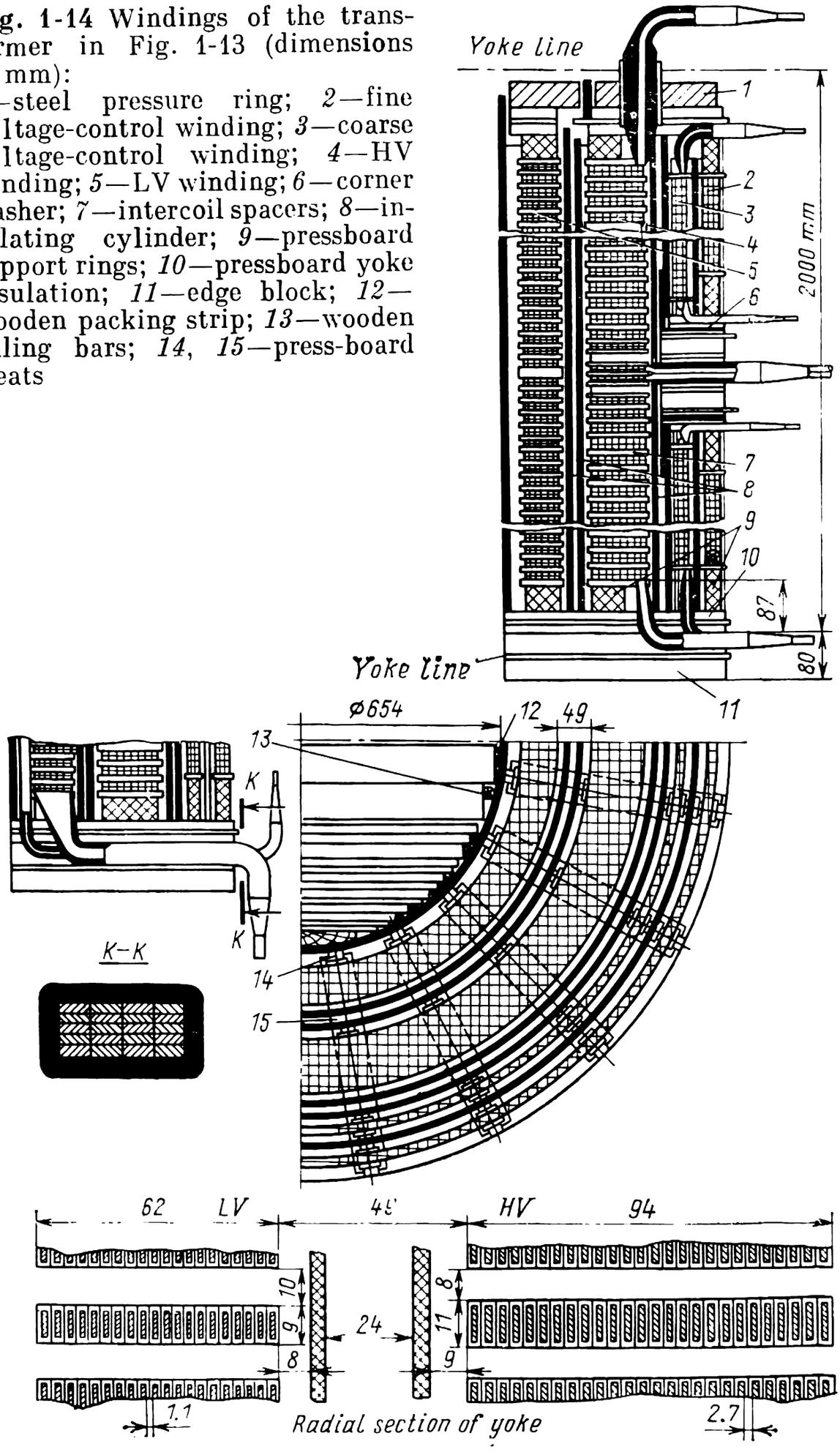

Fig. 1-14 Windings of the transformer in Fig. 1-13 (dimensions in mm):
1—steel pressure ring; *2*—fine voltage-control winding; *3*—coarse voltage-control winding; *4*—HV winding; *5*—LV winding; *6*—corner washer; *7*—intercoil spacers; *8*—insulating cylinder; *9*—pressboard support rings; *10*—pressboard yoke insulation; *11*—edge block; *12*—wooden packing strip; *13*—wooden filling bars; *14*, *15*—press-board cleats

the space between the coils and the frame. Apart from providing electrical insulation, the transformer oil filling the transformer tank also doubles as a coolant.

Interturn insulation is provided by the oil-impregnated insulation on the coil conductors (which may be round wire or strip conductors).

The arrangement of the major insulation separating the windings from each other, from the tank, and from the frame is shown in Fig. 1-14.

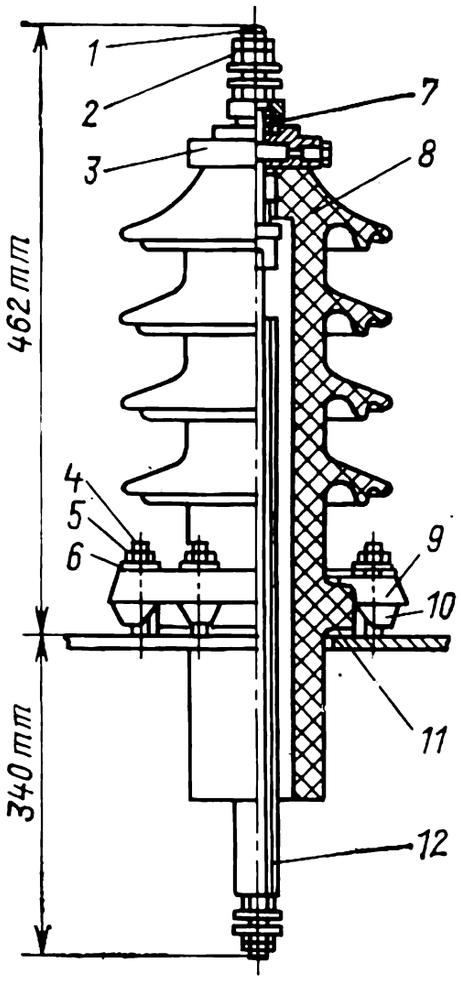

Fig. 1-15 Outdoor-service, 35 kV, 250 A bushing with central conductor connected to a lead:
1—copper terminal; *2*—brass nut; *3*—brass cap; *4*—steel stud; *5*—nut; *6*—washer; *7*—rubber grommet; *8*—porcelain insulator; *9*—steel flange; *10*—lug; *11*—rubber seal; *12*—central conductor inside insulating tube

Leads and terminal bushings. The L.V. and H. V. windings of a transformer are connected to external circuits by means of leads (insulated conductors mounted inside the transformer tank) and terminal bushings (devices consisting of a porcelain cylinder, a central current-carrying conductor, and a mounting flange).

The conductor of a terminal bushing must reliably be insulated from the grounded top cover on either ("oil" and "air") side (Fig. 1-15). The size and complexity of terminal bushings grow with the voltage rating of transformers. For 110 kV and higher, oil-filled terminal bushings are used.

Tank accessories and fittings. If the tank of an oil-immersed transformer were filled full with oil and completely sealed off, it would inevitably burst under the action of oil pressure building up in the tank with rising temperature. One way to prevent bursting is to keep the oil level in the tank some distance below the top cover and let the tank's insides communicate with the atmosphere. In such a case, however, the oil is exposed to air over the entire area under

the cover—a feature which speeds up oil ageing through oxidation and moisture pick-up, so the oil loses its valuable properties too soon. Another course of action is to fit a *conservator* (or expansion tank) to the tank—a cylindrical

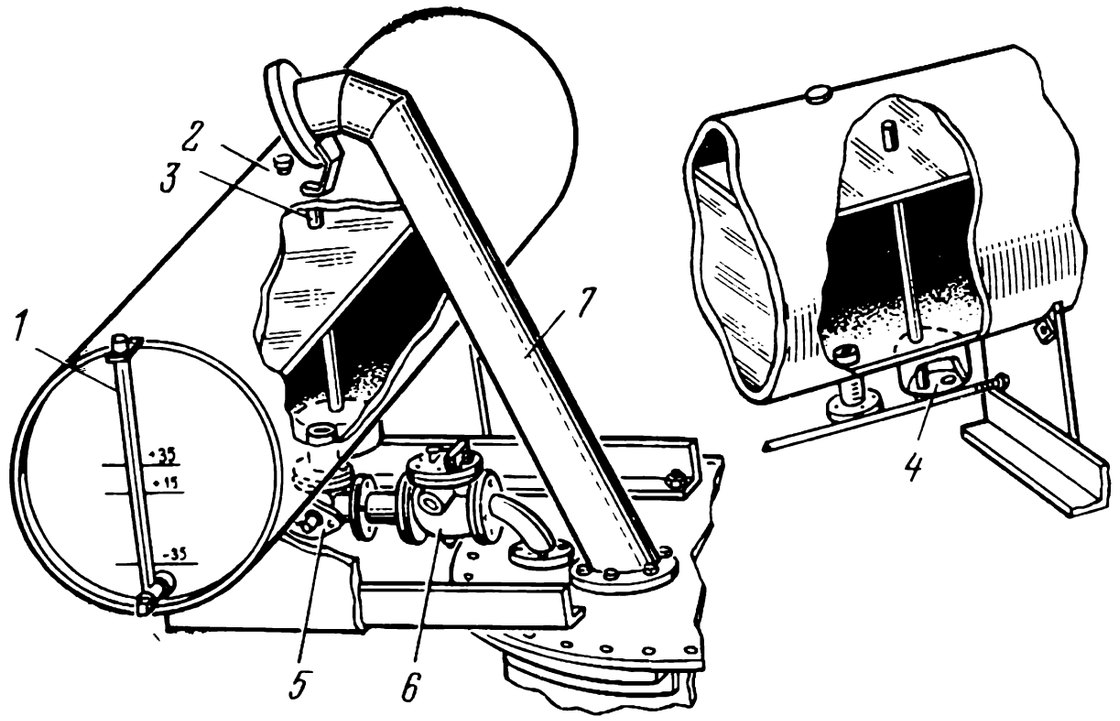

Fig. 1-16 Accessories of a transformer tank:
1—oil gauge; *2*—filler cap; *3*—breather; *4*—sludge sump; *5*—conservator shut-off cock; *6*—Buchholz relay; *7*—relief stack

vessel communicating with the tank and limiting oil exposure to air (Fig. 1-12). In a transformer with a conservator, the oil needs to be dried, purified and regenerated or changed far less often.

The conservator is usually fitted with an oil level gauge (see Fig. 1-16), and a sump to collect sludge and moisture. The space at the top of the conservator communicates with the atmosphere via a breather tube brought out to terminate under the conservator (so as to keep drops of moisture from finding their way into the conservator).

Any transformer generates a large amount of heat in operation, and this calls for a proper cooling arrangement. On large transformers, this is done by tubular radiators (see Fig. 1-13) which are attached to ports welded into the tank. The ports are fitted with cocks so that the radiators can be shut off and detached while keeping the tank filled. The temperature of oil is indicated by a thermometer mounted in the top part of the tank. On small and medium-size

transformers, mercury thermometers are used, whereas on large units a better choice is filled-system thermometers or remote-reading resistance thermometers with their indicators mounted at an instrument board.

Any fault which occurs inside a transformer in operation (insulation puncture, shorted turns, poor contact or sparking due to poor grounding) is generally accompanied by the evolution of gas as a result of the decomposition of oil or solid insulation. The gas bubbles rise to the surface and finally find their way to the conservator. On its way there, the gas is collected in what is known as the *Buchholz* or *gas-formation relay* (see Fig. 1-16) installed on a stub pipe between the tank and conservator.

The Buchholz relay has an upper and a lower float. As gas collects in the relay housing, it displaces oil out of it. The top float drops, and its mercury switch completes an alarm circuit. In the case of a more serious fault, such as an interturn short (or shorts) and the like, gas is usually liberated in an explosive fashion, and a large amount of oil is forced from the tank into the conservator. This causes the lower float to rise and close its mercury switch, thereby activating a tripping circuit which disconnects the transformer from the supply line and averts a major breakdown.

To avoid irrepairable damage to the tank in the case of a heavy gas evolution, a device known as the relief or explosion stack is installed on transformers (see Figs. 1-13 and 1-16). It is a long steel pipe communicating with the tank at one end and closed by a disc of thin glass at the other. When the pressure inside the tank rises dangerously, the disc bursts, so that excess oil and gas are expelled into the atmosphere before the tank has time to be deformed.

2 Electromagnetic Processes in the Transformer at No-Load

2-1 The No-Load Condition

On the primary side, transformers are excited by a harmonically varying voltage

$$v_1 = V_{1,m} \cos \omega t \qquad (2\text{-}1)$$

As the load varies, the peak value $V_{1,m}$ and the frequency f of the primary voltage change but little, so it is usually assumed that they are constant and equal to their rated values

$$V_{1,m} = V_{1,m\mathrm{R}} = \text{constant}$$

$$f = f_{\mathrm{R}} = \text{constant}$$

This also goes for the angular frequency

$$\omega = 2\pi f = \omega_{\mathrm{R}} = \text{constant}$$

The secondary current is inversely proportional to the impedance of the line to which it is connected

$$|Z| = \sqrt{R^2 + X^2}$$

At a certain definite value of this impedance, $Z = Z_{\mathrm{R}}$, the secondary winding carries its rated current

$$I_2 = I_{2,\mathrm{R}}$$

At $Z < Z_{\mathrm{R}}$, the secondary current exceeds its rated value

$$I_2 > I_{2,\mathrm{R}}$$

and the transformer is somewhat overloaded.

At $|Z| > |Z_{\mathrm{R}}|$

$$I_2 < I_{2,\mathrm{R}}$$

and the transformer is underloaded. When $|Z|$ is infinity, which occurs when the transformer is disconnected from the

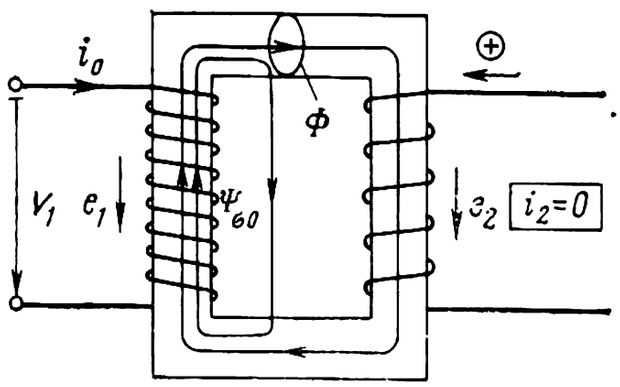

Fig. 2-1 Single-phase two-winding transformer on no-load

receiving line on the secondary side (the secondary is open-circuited), the secondary current falls to zero. In the circumstances, the transformer supplies no-load current, which is why this state is called the *no-load* (*open-circuit*) *condition*.

The electromagnetic processes occurring in a transformer at no load are far simpler than they are under load, with $I_2 > 0$, so their study can best be begun with the no-load condition.

Consider the electromagnetic processes at no-load in the single-phase two-winding transformer shown in sketch form in Fig. 2-1. This is a core-type transformer whose primary and secondary windings are shown for convenience located on different limbs. (The actual arrangement of the windings on a core-type transformer has been described in Sec. 1-3, see Fig. 1-5*a*.)

2-2 Voltage Equations

The supply voltage v_1 impressed on the primary winding gives rise in it to an alternating current i_0, called the *no-load current*. This current produces two fluxes, namely the *mutual* (*useful*) *magnetic flux* which has its path wholly within the core of a very high permeability, $\mu_r \gg 1$, and links all the turns w_1 and w_2 of the primary and secondary windings, and also the *leakage flux* which links only the primary turns.

If we find the mutual magnetic flux Φ at any section of the closed magnetic circuit, we shall be able to find the mutual flux linkage with the primary winding

$$\Psi_{011} = w_1\Phi$$

and with the secondary winding

$$\Psi_{021} = w_2\Phi$$

The leakage flux has its path completed through nonmagnetic materials (air gaps, insulation) with a permeability equal to that of free space, μ_0, and substantially smaller than that of the magnetic core. Therefore, the leakage flux linkage with the primary winding at no-load, $\Psi_{\sigma 0}$, is a small fraction of the mutual flux linkage with the primary, Ψ_{011} (Fig. 2-1).

The periodically varying mutual and leakage fluxes induce electromotive forces in the windings with which they link. For the positive directions of currents, voltages, emfs and magnetic lines of force shown in Fig. 2-1, the *primary emf of mutual induction* is

$$e_1 = -w_1 \, d\Phi/dt = -d\Psi_{011}/dt \qquad (2\text{-}2)$$

whereas the *secondary emf of mutual induction* is

$$e_2 = -w_2 \, d\Phi/dt = -d\Psi_{021}/dt \qquad (2\text{-}3)$$

and the *leakage primary emf* is

$$e_{\sigma 0} = -\mathrm{d}\Phi_{\sigma 0}/\mathrm{d}t \ll e_1 \qquad (2\text{-}4)$$

Interpreting v_1 as an emf impressed on the winding from the supply line, we may write Kirchhoff's voltage equation

$$v_1 + e_1 + e_{\sigma 0} = R_1 i_0 \qquad (2\text{-}5)$$

where R_1 is the resistance of the primary winding.

The no-load voltage across the secondary is the same as the emf induced in it

$$v_2 = e_2$$

2-3 Variations in EMF with Time. An EMF Equation

For all power transformers (and for most microtransformers), we may neglect in Eq. (2-5) both the voltage drop across R_1 and the leakage emf $e_{\sigma 0}$

$$|R_1 i_0| \ll |e_1|$$
$$|e_{\sigma 0}| \ll |e_1|$$

and deem, with sufficient accuracy, that the primary emf of mutual induction is in antiphase with the primary voltage (Fig. 2-2):

$$e_1 = -v_1 = -V_{1,m} \cos \omega t$$
$$= -E_{1,m} \cos \omega t \qquad (2\text{-}6)$$

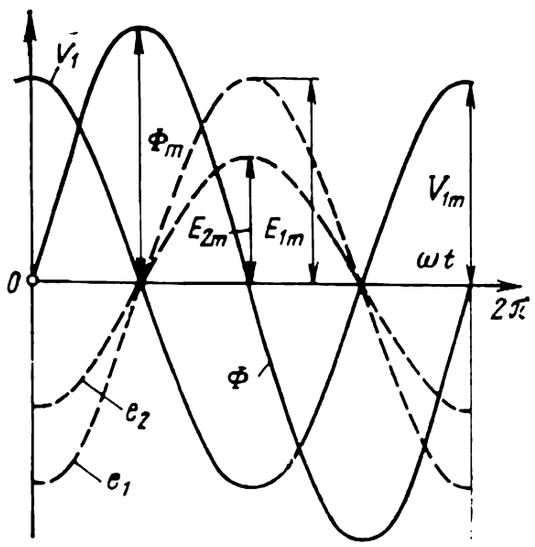

Fig. 2-2 Time variations in voltages, emfs and magnetic flux of a transformer

It follows from Eq. (2-6) that the emf of mutual induction varies with time harmonically, and its peak (rms) value does not differ from the peak (rms) value of the voltage

$$E_{1,m} = V_{1,m}, \quad (E_1 = V_1) \qquad (2\text{-}7)$$

From a comparison of Eqs. (2-2) and (2-3), we may conclude that the ratio of e_2 and e_1 is time-invariant. This ratio is called the *transformation*, or *turns*, *ratio*

$$e_2/e_1 = E_{2,m}/E_{1,m} = E_2/E_1 = w_2/w_1 = n_{21} \qquad (2\text{-}8)$$

On the basis of Eqs. (2-6) and (2-8), we may argue that e_2 varies likewise harmonically and is in phase with e_1.

We may express the magnetic flux Φ in terms of e_1 by integrating the differential equation (2-2) subject to Eq. (2-6):

$$\Phi = -\frac{1}{w_1}\int_0^t e_1\,dt = \frac{E_{1,m}}{w_1}\int_0^t \cos\omega t\,dt$$

$$= \Phi_m \sin\omega t \tag{2-9}$$

where

$$\Phi_m = E_{1,m}/w_1\omega \tag{2-10}$$

is the peak value of the magnetic flux.

Using Eq. (2-10), we can derive an equation giving the rms value of e_1 from the given peak magnetic flux or flux linkage

$$E_1 = E_{1,m}/\sqrt{2} = \omega w_1\Phi_m/\sqrt{2} = \omega\Psi_{011,m}/\sqrt{2}$$

or

$$E_1 = (2\pi/\sqrt{2})\,fw_1\Phi_m \tag{2-11}$$

Accordingly, the rms value of e_2 is

$$E_2 = \omega w_2\Phi_m/\sqrt{2} = \omega\Psi_{021,m}/\sqrt{2}$$

or

$$E_2 = (2\pi/\sqrt{2})\,fw_2\Phi_m \tag{2-12}$$

Referring to the plot of Fig. 2-2, the magnetic flux lags behind v_1 by 90° (it is said to be in quadrature lagging with the primary voltage), and leads e_1 and e_2 by 90° (it is said to be in quadrature leading with the two emfs).

2-4 The Magnetization Curve of the Transformer

The thickness and material of the laminations for a transformer core are always chosen according to the frequency of the magnetizing current, so as to keep eddy currents to a minimum. The instantaneous magnetic flux may then be determined from the instantaneous primary mmf, i_0w_1, at no-load. The resultant relationship between the instantaneous values of the two quantities, $\Phi = f(i_0)$, is identical

to that obtained with d.c., when eddy currents are nonexistent.

Graphically, the nonlinear relationship between the flux Φ in the core and the direct current i_0 in the primary winding is depicted by what is called the *d.c. magnetization curve* (or *characteristic*) of a transformer. It can be constructed on the basis of Ampere's circuital law in integral form. On aligning the loop enclosing the current in all the primary turns, $i_0 w_1$, with a line of force of the mutual magnetic flux in the core, Ampere's circuital law may be written

$$i_0 w_1 = \oint \mathbf{H}_l \, \mathrm{d}\mathbf{l}$$

The procedure yielding the circulation of the **H** vector is as follows:

(1) Assign a desired value to the magnetic flux in the core.

(2) Break up the core into n portions of length l_k each, such that within each portion the active iron cross-sectional area A_k and the permeability remain constant for the specified magnetic flux.

(3) Calculate the magnetic induction within each portion, $B_k = \Phi/A_k$.

(4) Using the d.c. magnetization curve for each portion, $B = f(H)$, determine H_k and $\mu_{ak} = B_k/H_k$.

(5) Adopt $\mu_{ak} = \mu_0 = 4\pi \times 10^{-7}$ H/m for the nonmagnetic gaps, and

(6) Replace the circulation $\oint \mathbf{H}_l \, \mathrm{d}\mathbf{l}$ with the sum of magnetic potential drops across the individual portions, spread over all the n portions:

$$i_0 w_1 = \oint \mathbf{H}_l \, \mathrm{d}\mathbf{l} = \sum_{k=1}^{n} H_k l_k = \sum_{k=1}^{n} (B_k/\mu_{ak}) \, l_k$$

$$= \Phi \sum_{k=1}^{n} l_k/\mu_{ak} A_k = \Phi/\Lambda_\mu \qquad (2\text{-}13)$$

where $\Lambda_\mu = 1/\sum_{k=1}^{n} l_k/\mu_{ak} A_k$ is the permeance of the core.

On solving Eq. (2-13) for several values of Φ and finding each time $i_0 = \Phi/w_1 \Lambda_\mu$, we can then plot the magnetiza-

tion curve $\Phi = f(i_0)$ for the transformer. An approximate shape of the magnetization curve is shown in Fig. 2-3 which also gives the $\Lambda_\mu = f(i_0)$ curve. As is seen, Λ_μ is a maximum near the knee on the magnetization curve. As i_0 and Φ keep increasing, the permeance decreases.

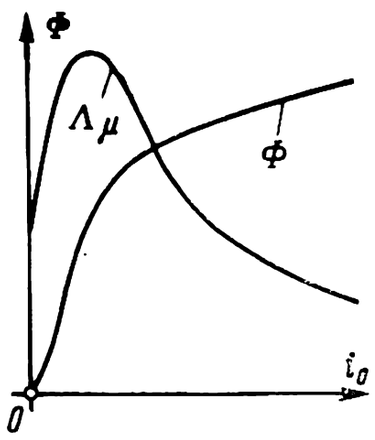

Fig. 2-3 Magnetization curve, $\Phi = f(i_0)$, of a transformer

2-5 The No-Load Current Waveform

As already noted, if we neglect the effect of eddy currents and the core losses, the relationship between the instantaneous flux and no-load current is the same as with direct current. Therefore, since the magnetic flux has been found to vary with time sinusoidally, as defined in Eq. (2-9), we can use the d.c. magnetization curve shown on the left of Fig. 2-4 in order to see how the no-load current varies

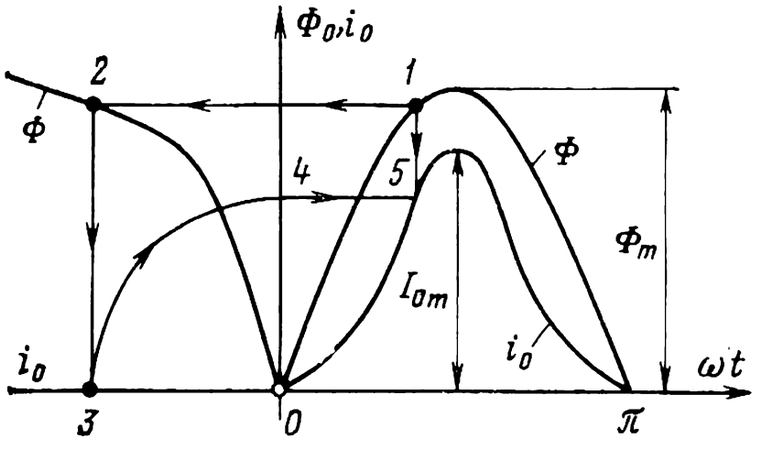

Fig. 2-4 No-load current waveform (ignoring core loss)

with time, $i_0 = f(t)$ or $f(\omega t)$. To do this, we should plot variations in the magnetic flux with time, $\Phi = \Phi_m \sin \omega t$ (on the right of Fig. 2-4) and determine the instantaneous values of no-load current for some selected values of the magnetic flux.

The relevant graphical procedure is indicated in the figure by arrows. Taking the value of Φ at point *1* and moving through points *2*, *3*, and *4*, we find the corresponding no-load current i_0 at the intersection, *5*, of the horizontal extending

from point *4* and the vertical extending from point *1*. With a sinusoidal magnetic flux, the no-load current as depicted by the $i_0 = f(\omega t)$ curve turns out to be nonsinusoidal. The no-load current grows increasingly more nonsinusoidal as the peak magnetic flux Φ_m raises the level of saturation in the core or, which is the same, as Φ_m exceeds increasingly more the fluxes corresponding to the linear portion of the magnetization curve where Φ is proportional to i_0.

2-6 Transformer Equations at No-Load in Complex Form

Complex notation is applicable to equations that connect sinusoidal currents, voltages and emfs. Therefore, before we may write the transformer equations at no-load in complex form, we must replace the nonsinusoidal no-load current i_0 by a sinusoidal current $i_{0r} = \sqrt{2}\, I_{0r} \sin \omega t$ (Fig. 2-5) equivalent in terms of the reactive power consumed. (Since the copper loss in the primary is low, the iron loss is likewise low, so we may take it that the active power and the resistive current are small in comparison with the reactive power and the reactive current.)

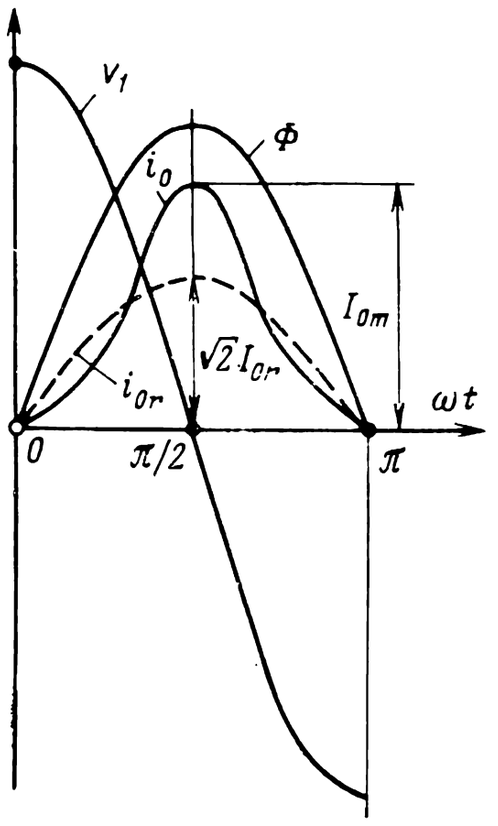

Fig. 2-5 Replacement of no-load current i_0 by an equivalent sinusoidal current i_{0r}

For this change not to affect the reactive power consumed, the rms value of the equivalent sinusoidal current, I_{0r}, must be equal to the rms value of the nonsinusoidal no-load current, that is

$$I_{0r} = \sqrt{\frac{1}{T}\int_0^T i_0^2\, dt} \qquad (2\text{-}14)$$

In our further discussion, we call this current the *reactive (magnetizing) component of the no-load current*. As is seen from Fig. 2-5, the current i_{0r} must be in quadrature lagging with v_1. (A transformer at no-load and free from iron loss

may be regarded with respect to the supply line as an inductor having a negligible ohmic resistance.)

As will be shown later, even if we include losses, the active component of the no-load current is very small in comparison with the reactive component, $I_{0a} \ll I_{0r}$. Therefore, it is legitimate to deem the rms value of the no-load current, I_0, equal to the rms value of the reactive current

$$I_0 = \sqrt{I_{0a}^2 + I_{0r}^2} \approx I_{0r}$$

It is important to note that the no-load primary current usually ranges anywhere from 0.1 to 0.005 of the rated primary current.

For each rms value of the primary voltage, V_1, we find I_{0r}, and compute the equivalent primary inductance related to the main or mutual magnetic flux or between the primary and secondary. This will be referred to as the *main* or *mutual primary inductance*. It is defined as the ratio of the peak flux linkage to the peak reactive component of the no-load current:

$$L'_{12} = \Psi_{011,m}/\sqrt{2}\, I_{0r} = w_1\Phi_m/\sqrt{2}\, I_{0r} \qquad (2\text{-}15)$$

If we express the magnetic flux in terms of the equivalent permeance Λ_{12} of the transformer

$$\Phi = \Lambda_{12}\,(w_1 i_{0r})$$

or

$$\Phi_m = \Lambda_{12}\,[w_1\,(\sqrt{2}\, I_{0r})]$$

this permeance and the mutual primary inductance may be connected by a relation of the form

$$L'_{12} = w_1^2\Lambda_{12} \qquad (2\text{-}16)$$

From this inductance, we can compute the *mutual inductive reactance* of the primary winding

$$X_{12} = \omega L'_{12} = \omega w_1^2\Lambda_{12} \qquad (2\text{-}17)$$

Now that we have introduced the necessary definitions, we may write complex relations connecting the emf and the sinusoidal reactive component of the no-load current.

As follows from Eqs. (2-2), (2-15), and (2-16),

$$e_1 = -\mathrm{d}\Psi_{011}/\mathrm{d}t = -L_{12}\,\mathrm{d}i_{0r}/\mathrm{d}t \qquad (2\text{-}18)$$

Now we shall express e_1 and i_{0r} as the real parts of the respective complex amplitudes multiplied by exp $(j\omega t)$*

$$e_1 = \mathrm{Re}\,[\sqrt{2}\,\dot{E}_1 \exp(j\omega t)] \tag{2-18a}$$

$$i_{0r} = \mathrm{Re}\,[\sqrt{2}\,\dot{I}_{0r} \exp(j\omega t)] \tag{2-18b}$$

On substituting the above expressions in Eq. (2-18) and differentiating, we obtain Eq. (2-18) re-written in complex notation:

$$\mathrm{Re}\,[\sqrt{2}\,\dot{E}_1 \exp(j\omega t)] = -L'_{12}\frac{\mathrm{d}}{\mathrm{d}t}\{\mathrm{Re}\,[\sqrt{2}\,\dot{I}_{0r} \exp(j\omega t)]\}$$

$$= \mathrm{Re}\left\{-L'_{12}\frac{\mathrm{d}}{\mathrm{d}t}[\sqrt{2}\,\dot{I}_{0r} \exp(j\omega t)]\right\}$$

$$= \mathrm{Re}\,\{-j\omega L'_{12}[\sqrt{2}\,\dot{I}_{0r} \exp(j\omega t)]\}$$

or

$$\dot{E}_1 = -j\omega L'_{12}\dot{I}_{0r} = -jX_{12}\dot{I}_{0r} \tag{2-19}$$

Graphically, Eq. (2-19) and also Eqs. (2-6), (2-9), (2-11), and (2-12), as written in complex notation

$$-\dot{V}_1 = \dot{E}_1 = -j\omega w_1 \dot{\Phi}_m/\sqrt{2}$$

$$\dot{V}_2 = \dot{E}_2 = -j\omega w_2 \dot{\Phi}_m/\sqrt{2} \tag{2-20}$$

can be depicted by a phasor diagram for a transformer at no-load, such as shown in Fig. 2-6.

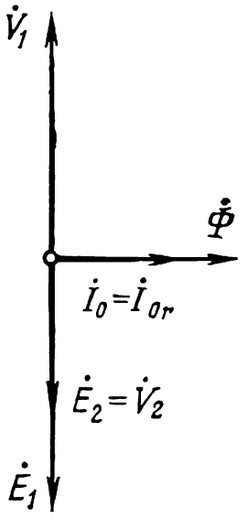

Fig. 2-6 Phasor diagram of a transformer on no load (ignoring losses and active current)

2-7 No-Load Losses

Although the core of a transformer is assembled from thin insulated electrical-sheet steel laminations, the iron (core) loss accounts for 0.1% to 0.2% of the transformer's power rating. For example, in a 100-MVA transformer, the core loss is up to 200 kW.

In microtransformers rated from 0.1 to 10^3 W, the core loss rises to from 2% to 20% of the power rating.

* The symbols with a dot above refer to complex quantities.

The core loss is the sum of the hysteresis loss P_h which is proportional to the frequency f and the square of the magnetic induction, B_k^2, and the eddy-current loss, P_e, which is proportional to the frequency squared, f^2, and the magnetic induction also squared, B_k^2.

In practical calculations, it is customary to find directly the total core loss, P_{core}, in the various core elements with an active iron cross-sectional area A_k, magnetic induction $B_k = \Phi_m/A_k$, and the iron mass m_k

$$P_{core} = P_h + P_e = \sum p_{1.0/50} B_k^2 (f/50)^{1.3} m_k \qquad (2\text{-}21)$$

where $p_{1.0/50}$ (in watts per kg) is the specific core loss at a frequency of 50 Hz and a magnetic induction of 1 T [13].

At no-load and the rated primary voltage, $V_{1,R}$, the core loss is about the same as at rated load. Therefore (as will be shown later), the magnetic flux and induction in the core at V_1 are nearly independent of the load condition. The copper loss in the primary at no-load, $P_{Cu,0} = R_1 I_0^2$, may be neglected, because the no-load current is small and this loss is a fraction of that at the rated primary current

$$P_{Cu,1R} = R_1 I_{1,R}^2$$

If we neglect the copper loss, the no-load loss of a transformer, P_0, may be deemed equal to its core loss:

$$P_0 \approx P_{core}$$

2-8 The Effect of the Core Loss on the Transformer's Performance at No-Load

A transformer with the core loss P_{core} draws from the supply line an active power given by $V_1 I_{0a}$. The rms value of the sinusoidal active current is

$$I_{0a} = P_{core}/V_1 \qquad (2\text{-}22)$$

This current is in phase with the applied voltage, so it may alternatively be expressed in terms of an equivalent resistance R_{12}

$$I_{0a} = V_1/R_{12} \qquad (2\text{-}23)$$

From a comparison of Eqs. (2-22) and (2-23), the equivalent resistance R_{12} may be expressed in terms of voltage

and core loss as follows*:

$$R_{12} = V_1^2/P_{\text{core}} \tag{2-24}$$

The current drawn by the primary winding at no-load is the sum of the active current I_{0a} and the reactive current I_{0r}:

$$\dot{I}_0 = \dot{I}_{0a} + \dot{I}_{0r} = \dot{V}_1/R_{12} + \dot{V}_1/jX_{12} = \dot{V}_1 Y_0 \tag{2-25}$$

The admittance

$$Y_0 = 1/R_{12} + 1/jX_{12} \tag{2-26}$$

is equivalent to R_{12} and jX_{12} connected in parallel.

Equation (2-25) describing the events occurring in a transformer at no-load, with allowance for the core loss, corresponds to the equivalent circuit shown in Fig. 2-7*a*. In practical calculations, however, it is more convenient to re-draw

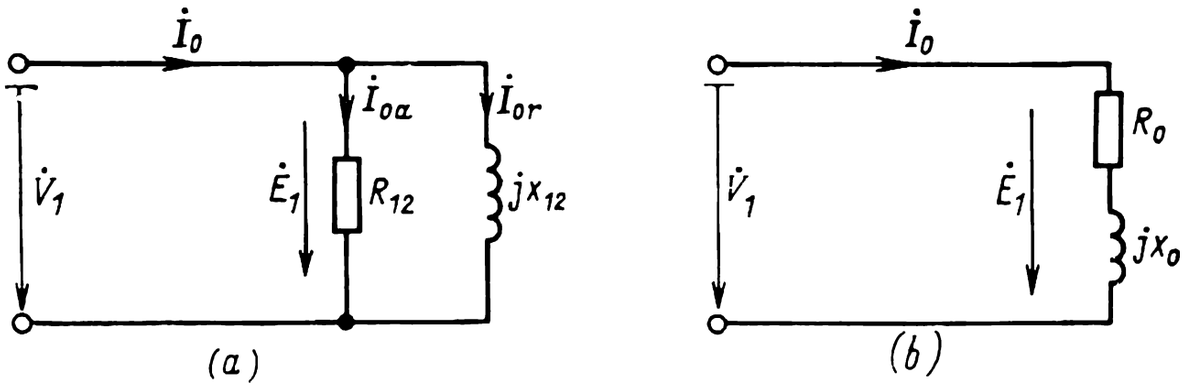

Fig. 2-7 Equivalent circuit of a transformer on no-load: (*a*) with R and X connected in parallel; (*b*) with R and X connected in series

the equivalent circuit as shown in Fig. 2-7*b* which includes the primary impedance at no-load

$$Z_0 = R_0 + jX_0 \tag{2-27}$$

On expressing Z_0 in terms of Y_0 in Eq. (2-26)

$$Z_0 = R_0 + jX_0 = 1/Y_0 = 1/(1/R_{12} + 1/jX_{12})$$

and equating the coefficients of the imaginary and real parts, we find that

$$\begin{aligned} R_0 &= R_{12}^2 X_{12}^2/(R_{12}^2 + X_{12}^2) \\ X_0 &= X_{12} R_{12}^2/(R_{12}^2 + X_{12}^2) \end{aligned} \tag{2-28}$$

* The loss across R_{12} at V_1 is equal to the core loss.

because when $I_{0a} \ll I_{0r}$, it is inevitable that $R_{12} \gg X_{12}$. Finally, we may write

$$R_0 = X_{12}^2/R_{12},\ X_0 = X_{12},\ R_0 \ll R_{12} \qquad (2\text{-}29)$$

The quantity X_0 retains the name of the mutual inductive reactance of the primary winding. R_0 is a fictitious resistance the loss across which at I_0 is equal to the core loss of the transformer

$$P_{\text{core}} = I_0^2 R_0$$

As is seen from the equivalent circuit in Fig. 2-7*b*, the products $R_0\dot{I}_0$ and $jX_0\dot{I}_0$ are, respectively, the active and reactive components of the primary voltage $\dot{V}_1$.

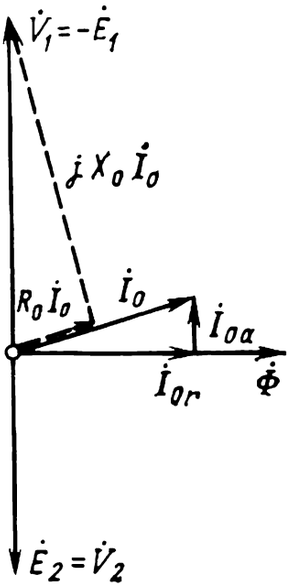

Fig. 2-8 Phasor diagram of a transformer on no-load

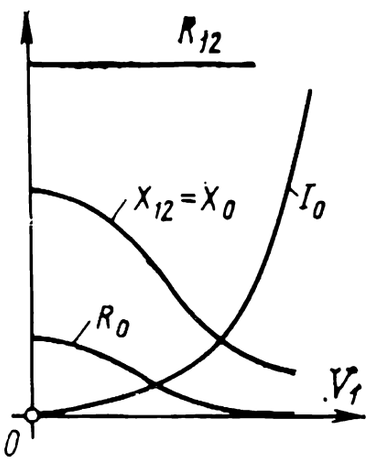

Fig. 2-9 Impedance of the equivalent circuit and no-load current I_0 as functions of V_1

The relation between the primary voltage V_1 and the no-load current $\dot{I}_0$

$$\dot{V}_1 = -\dot{E}_1 = Z_0\dot{I}_0 \qquad (2\text{-}30)$$

is illustrated by the phasor diagram in Fig. 2-8 which, with $P_{\text{core}} = 0$, $R_{12} = \infty$, and $I_{0a} = 0$, is the same as that shown in Fig. 2-6.

Because the magnetic circuit of a transformer is nonlinear, the no-load current I_0 rises at a faster rate than V_1, so R_0 and X_0 depend substantially on V_1 (Fig. 2-9):

$$X_0 = X_{12} \sim V_1/I_0$$

and

$$R_0 \sim (V_1/I_0)^2$$

In contrast, as the primary voltage is varied, R_{12} remains practically unchanged, because the core loss is proportional to the square of the magnetic induction, Eq. (2-21), or the primary voltage, Eq. (2-20).

3 Electromagnetic Processes in the Transformer on Load

3-1 The Magnetic Field in a Transformer on Load. The MMF Equation. The Leakage Inductance of the Windings

When a transformer is operating on load, its secondary is traversed by a current

$$\dot{I}_2 = \dot{V}_2/Z$$

The load current gives rise to a change in the primary current. Proportionate changes also occur in the magnetic flux and the secondary voltage, and there is an increase

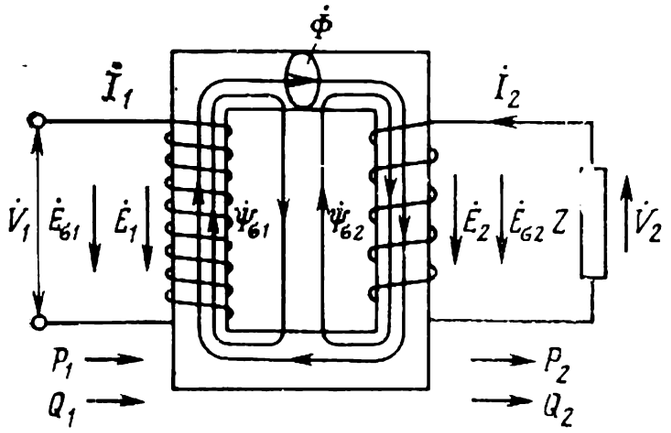

Fig. 3-1 Single-phase, two-winding transformer on load

in the power lost. For a proper estimate of these changes in a transformer on load, it is essential above all to examine its magnetic field and to develop voltage equations for its primary and secondary windings.

Figure 3-1 shows a single-phase, two-winding transformer whose secondary is connected across a load impedance Z. Assuming that all the relevant electric and magnetic quantities are varying harmonically, we may write them in complex notation. In doing so, it is important to remember that the instantaneous value of a harmonic quantity is to be construed as the real part of the respective complex amplitude multiplied by exp $(j\omega t)$

$$i = \mathrm{Re}\,[\sqrt{2}\,\dot{I}\exp(j\omega t)]$$

$$v = \mathrm{Re}\,[\sqrt{2}\,\dot{V}\exp(j\omega t)]$$

$$e = \mathrm{Re}\,[\sqrt{2}\,\dot{E}\exp(j\omega t)]$$

$$\Phi = \mathrm{Re}\,[\dot{\Phi}_m \exp(j\omega t)]$$

$$\Psi = \mathrm{Re}\,[\dot{\Psi}_m \exp(j\omega t)]$$

The adopted positive directions of the above quantities are shown in Fig. 3-1. Positive directions for I_1 and I_2 are chosen such that they set up a positive mutual magnetic flux. Positive directions for the voltages and emfs across the windings are the same as for the respective currents. Positive directions on load are chosen the same as for operation at no load.

When a transformer is operating on load, its magnetic flux is established by the primary current I_1 traversing the primary winding and by the secondary current I_2 traversing the secondary winding. To simplify the matters, this magnetic flux can be visualized as a superposition of two fluxes, namely the mutual (or magnetizing) flux and the leakage flux.

The greater proportion of the flux linking the windings is the mutual flux which has all of its path within the core and completely encloses the windings from both sides. The mutual flux Φ (Fig. 3-1) is the same at any section of the core; its linkage with the primary is $w_1\Phi_m$, and with the secondary, $w_2\Phi_m$. Under Ampere's circuital law, the magnetic intensity due to mutual induction is the sum of the primary and secondary mmfs

$$i_1 w_1 + i_2 w_2 = \oint H_l \, dl$$

Since the mutual magnetic induction and the mutual flux are connected to the field intensity in a well-defined manner (see Chap. 2), we may argue that the mutual flux Φ is established by the sum of the primary and secondary mmfs. This sum may be visualized as the mmf due to some current i_0 traversing the primary winding

$$i_1 w_1 + i_2 w_2 = i_0 w_1 \tag{3-1}$$

Therefore, the current given by

$$i_0 = (i_1 w_1 + i_2 w_2)/w_1$$

may be called the *magnetizing current*, and Eq. (3-1), an *mmf equation.*

The nonlinear effects taking place in the transformer core as it undergoes cycles of magnetization by the current i_0 may be accounted for as in the case of no-load operation. The nonsinusoidal current i_0 may be replaced by an equivalent sinusoidal magnetizing current the rms value of which is

$$I_0 = \sqrt{I_{0a}^2 + I_{0r}^2}$$

and whose active component I_{0a} is related to the core losses. Then we may write the mmf equation in complex notation as

$$\dot{I}_1 w_1 + \dot{I}_2 w_2 = \dot{I}_0 w_1 \tag{3-2}$$

In our further discussion, the term "magnetizing current" will refer to the equivalent sinusoidal magnetizing current $\dot{I}_0$.

Now we are in a position to present the primary mmf $i_1 w_1$ as a sum of $i_0 w_1$ and $(i_1 w_1 - i_0 w_1) = -i_2 w_2$ which balances the secondary mmf $i_2 w_2$, and the magnetic flux in operation on load as a sum of three fluxes, namely:

(a) the mutual magnetic flux Φ and the leakage flux with flux linkage $\Psi_{\sigma 0}$, set up by the primary mmf $i_0 w_1$ (Fig. 3-2*a*);

(b) the leakage flux established by the mutually balancing mmfs, namely $(i_1 w_1 - i_0 w_1) = -i_2 w_2$ on the primary side and $i_2 w_2$ on the secondary side (Fig. 3-2*b*).

Referring to Figure 3-2, it is seen that the lines of the leakage flux have their path completed through nonmagnetic (air, oil, etc.) gaps $a_1 b_1$ and $a_2 b_2$ comparable in length with the portions of the lines accommodated within the core ($b_1 a_1$ and $b_2 a_2$). These lines link either the primary turns ($\Psi_{\sigma 1}$ and $\Psi_{\sigma 0}$), or the secondary turns ($\Psi_{\sigma 2}$).

The lines of the leakage flux in a transformer may be divided into two groups—those linking only the primary turns and giving rise to the flux linkage $\Psi_{\sigma 0}$ due to i_0 and

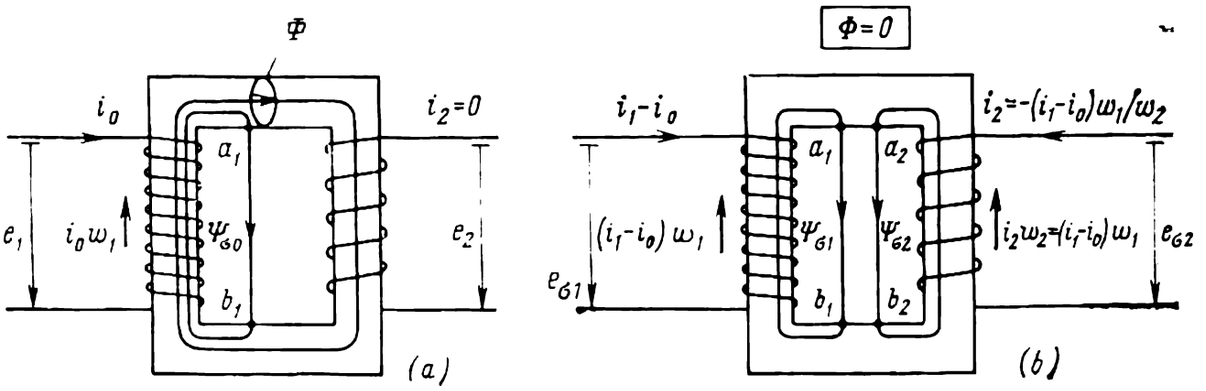

Fig. 3-2 Magnetic flux on load as the sum of (*a*) mutual flux and (*b*) leakage flux

$\Psi_{\sigma 1}$ due to $(i_1 - i_0)$, and those linking only the secondary turns and giving rise to the flux linkage $\Psi_{\sigma 2}$.

To appraise the relationship between the flux linkages and the currents in the windings, we shall develop an equation by Ampere's circuital law for, say, a closed line of the leakage flux linking the primary winding as shown in Fig. 3-2*b*:

$$\oint \mathbf{H}\,\mathrm{d}\mathbf{l} = \int_{a_1}^{b_1} \mathbf{H}_0\,\mathrm{d}\mathbf{l} + \int_{b_1}^{a_1} \mathbf{H}_{\mathrm{core}}\,\mathrm{d}\mathbf{l} = (i_1 - i_0)\,w_1$$

Let us write the magnetic field in the nonmagnetic region, H_0, and the magnetic field in the core, H_{core}, in terms of the respective induction and permeability:

$$H_0 = B_0/\mu_0$$

$$H_{\mathrm{core}} = B_{\mathrm{core}}/\mu_{a,\mathrm{core}}$$

$$\mu_{a,\mathrm{core}} = \mu_{r,\mathrm{core}}\,\mu_0$$

$$\mu_{r,\mathrm{core}} \gg 1$$

Therefore, the leakage field in the core is negligibly small

$$H_{\mathrm{core}} = B_{\mathrm{core}}/\mu_{a,\mathrm{core}} = 0$$

The total current is equal to the magnetic potential difference across the nonmagnetic gap

$$\int_{a_1}^{b_1} \mathbf{H}_0 \, \mathrm{d}\mathbf{l} = \frac{1}{\mu_0} \int_{0}^{b_1} \mathbf{B}_0 \, \mathrm{d}\mathbf{l} = (i_1 - i_0) w_1$$

It follows from the foregoing that $\Psi_{\sigma 1}$ is proportional to $(i_1 - i_0)$. The same holds for $\Psi_{\sigma 0}$ and $\Psi_{\sigma 2}$ and their respective currents i_0 and i_2. Therefore, the leakage inductances of the windings

$$\begin{aligned} L_{\sigma 1} &= \Psi_{\sigma 1}/(i_1 - i_0) \\ L_{\sigma 2} &= \Psi_{\sigma 2}/i_2 \\ L_{\sigma 0} &= \Psi_{\sigma 0}/i_0 \end{aligned} \tag{3-3}$$

are constant for a given transformer and solely depend on the width of nonmagnetic gaps and the number of turns in the windings (see Sec. 8-2).

With a high degree of accuracy, the total leakage flux linkage with the primary winding may be written

$$\Psi_{\sigma 1} = \Psi_{\sigma 0} + \Psi_{\sigma 10} = L_{\sigma 0} i_0 + L_{\sigma 1} (i_1 - i_0) \approx L_{\sigma 1} i_1 \tag{3-4}$$

because in operation on load $i_1 \gg i_0$, and we may neglect whatever difference there may be between $L_{\sigma 0}$ and $L_{\sigma 1}$ and deem that $L_{\sigma 0} \approx L_{\sigma 1}$. By analogy with the mutual inductance [see Eq. (2-16)], the leakage inductances may be expressed in terms of the respective permeances, $\Lambda_{\sigma 1}$ and $\Lambda_{\sigma 2}$:

$$L_{\sigma 1} = w_1^2 \Lambda_{\sigma 1}, \quad L_{\sigma 2} = w_2^2 \Lambda_{\sigma 2}$$

or in terms of permeance coefficients

$$\begin{aligned} L_{\sigma 1} &= \mu_0 w_1^2 \lambda_{\sigma 1} \\ L_{\sigma 2} &= \mu_0 w_2^2 \lambda_{\sigma 2} \end{aligned} \tag{3-5}$$

where

$$\begin{aligned} \lambda_{\sigma 1} &= \Lambda_{\sigma 1}/\mu_0 \\ \lambda_{\sigma 2} &= \Lambda_{\sigma 2}/\mu_0 \end{aligned} \tag{3-6}$$

3-2 Voltage Equations of the Transformer Windings

The emf induced in each of the transformer windings can conveniently be presented as the sum of the mutual emf E_1 (or E_2) and of the leakage emf $E_{\sigma 1}$ (or $E_{\sigma 2}$).

The mutual flux shown in Fig. 3-2*a* does not differ from that in a transformer on no-load (see Fig. 2-1). Therefore, the mutual emf may be expressed in terms of the mutual flux in precisely the same manner as at no-load.

Given a certain E_1, the magnetizing current i_0 must be the same as at no-load, provided that E_1 and Φ are the same in either case. Therefore, I_0 and E_1 can be connected by an equation of the form

$$-\dot{E}_1 = Z_0 \dot{I}_0 \tag{3-7}$$

where

$$Z_0 = R_0 + jX_0$$

Using the turns ratio, $n_{21} = w_2/w_1$, we can write the mutual emf on the secondary side as

$$-\dot{E}_2 = -n_{21}\dot{E}_1 = n_{21}Z_0\dot{I}_0 \tag{3-8}$$

The primary and secondary leakage emfs, $e_{\sigma 1}$ and $e_{\sigma 2}$, are induced by the leakage flux linkages $\Psi_{\sigma 1}$ and $\Psi_{\sigma 2}$, respectively, proportional to the primary and secondary currents:

$$\begin{aligned} e_{\sigma 1} &= -\mathrm{d}\Psi_{\sigma 1}/\mathrm{d}t = -L_{\sigma 1}\,\mathrm{d}i_1/\mathrm{d}t \\ e_{\sigma 2} &= -\mathrm{d}\Psi_{\sigma 2}/\mathrm{d}t = -L_{\sigma 2}\,\mathrm{d}i_2/\mathrm{d}t \end{aligned} \tag{3-9}$$

Using complex notation and differentiating by analogy with Eq. (2-19), we get

$$\dot{E}_{\sigma 1} = -j\omega L_{\sigma 1}\dot{I}_1 = -jX_1\dot{I}_1$$

and, similarly

$$\dot{E}_{\sigma 2} = -j\omega L_{\sigma 2}\dot{I}_2 = -jX_2\dot{I}_2 \tag{3-10}$$

Here,

$$X_1 = \omega L_{\sigma 1} \text{ and } X_2 = \omega L_{\sigma 2} \tag{3-11}$$

are called the leakage inductive reactance of the primary and secondary, respectively.

As is seen from Eq. (3-10), the leakage emfs are in quadrature lagging with the associated currents.

Now that we have defined the primary and secondary emfs of a loaded transformer and recalling that all the quantities involved vary harmonically*, we may write Kirchhoff's

* The nonsinusoidal magnetizing current is replaced by an equivalent sinusoidal current.

voltage equations for the primary and secondary windings in complex form as

$$\begin{aligned} \dot{V}_1 + \dot{E}_1 + \dot{E}_{\sigma 1} &= R_1 \dot{I}_1 \\ \dot{E}_2 + \dot{E}_{\sigma 2} &= R_2 \dot{I}_2 + \dot{V}_2 \end{aligned} \tag{3-12}$$

where R_1 and R_2 are the resistances of the primary and secondary windings, respectively, including additional losses due to alternating current (see Sec. 31-2).

In writing Eqs. (3-12), positive directions were chosen as shown in Fig. 3-1. The voltage V_1 is the supply emf impressed on the winding from an external source. The voltage $\dot{V}_2 = Z\dot{I}_2$ is the voltage drop across the load on the secondary side with an impedance of value $Z = R + jX$. Expressing the leakage emfs in (3-12) in terms of the respective leakage inductive reactances and currents (3-10), we may re-write the voltage equations as follows:

$$\begin{aligned} \dot{V}_1 &= -\dot{E}_1 + \dot{I}_1 Z_1 \\ \dot{V}_2 &= \dot{E}_2 - \dot{I}_2 Z_2 \end{aligned} \tag{3-13}$$

where $Z_1 = R_1 + jX_1$ and $Z_2 = R_2 + jX_2$ are the complex impedances of the primary and secondary windings, respectively.

3-3 Transferring the Secondary Quantities to the Primary Side

The performance analysis of a transformer can greatly be simplified, if we transfer the quantities associated with the secondary to the primary winding. This technique consists in that the real transformer having in the general case different numbers of primary and secondary turns, w_1 and w_2, is replaced by an equivalent transformer in which the secondary has the same number of turns as the primary, $w_2' = w_1$ (see Fig. 3-3). The quantities associated with the equivalent secondary having w_1 turns are said to be transferred (or referred) to the primary winding or side. They are expressed in terms of the original secondary quantities adjusted in value by a suitable factor so that transfer of secondary quantities to the primary side will leave the magnetic field, and the power fluxes P_1, Q_1, P_2, and Q_2 unaltered. The procedure is as follows.

(1) To leave the magnetic flux Φ unaltered, we must retain the secondary mmf unchanged, that is

$$\dot{I}'_2 w_1 = \dot{I}_2 w_2$$

whence

$$\dot{I}'_2 = \dot{I}_2 w_2 / w_1 \tag{3-14}$$

Here and elsewhere, the prime on a secondary quantity indicates that it has been transferred to the primary side.

(2) With Φ kept constant, the emf is proportional to the turns number. Therefore, the emf across the secondary

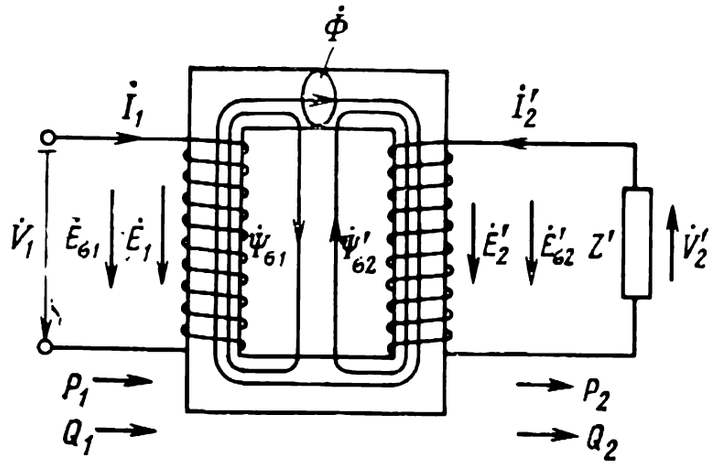

Fig. 3-3 Transformer of Fig. 3-1 with its secondary transferred to the primary, $w'_2 = w_1$

winding transferred to the primary side will increase w_1/w_2 times:

$$E'_2 = E_2 w_1 / w_2 \tag{3-15}$$

(3) To keep unchanged the values of P_2 and Q_2 drawn by the load on the secondary side, its R and X must be replaced by those transferred to the primary side:

$$P_2 = RI_2^2 = R'I_2'^2$$
$$Q_2 = XI_2^2 = X'I_2'^2$$

Using Eq. (3-14), we get

$$R' = R\,(w_1/w_2)^2$$
$$X' = X\,(w_1/w_2)^2$$

Therefore,

$$Z' = R' + jX' = Z\,(w_1/w_2)^2 \tag{3-16}$$

We can see that the secondary impedance can be transferred to the primary side, adjusted in value by the turns ratio squared.

The secondary voltage can likewise be transferred to the primary side, adjusted in value by the turns ratio

$$\dot{V}_2' = Z'\dot{I}_2' = Z\,(w_1/w_2)^2\,\dot{I}_2 w_2/w_1 = \dot{V}_2 w_1/w_2 \qquad (3\text{-}17)$$

The secondary impedance Z_2, its resistive component R_2 and its inductive component X_2 can be transferred to the primary side in about the same manner:

$$\begin{aligned} Z_2' &= R_2' + jX_2' = Z_2\,(w_1/w_2)^2 \\ R_2' &= R_2\,(w_1/w_2)^2 \\ X_2' &= X_2'\,(w_1/w_2)^2 \end{aligned} \qquad (3\text{-}18)$$

As a result, the secondary voltage equation takes the form

$$\dot{E}_2' = \dot{E}_2\,(w_1/w_2) = \dot{V}_2 w_1/w_2 + Z_2\,(w_1/w_2)^2\,\dot{I}_2 w_2/w_1$$

or

$$\dot{E}_2' = \dot{V}_2' + Z_2'\dot{I}_2' \qquad (3\text{-}19)$$

Because the primary and secondary windings have the same number of turns, the transferred (or referred) secondary emf is the same as the primary emf:

$$\dot{E}_2' = \dot{E}_2 w_1/w_2 = \dot{E}_1$$

The mmf equation for a transformer with its secondary parameters transferred to the primary side is extended to include the secondary mmf expressed in terms of the secondary current referred to the primary winding

$$\dot{I}_1 w_1 + \dot{I}_2' w_1 = \dot{I}_0 w_1$$

Dividing the above equation through by w_1 gives the equation of transformer currents

$$\dot{I}_1 + \dot{I}_2' = \dot{I}_0 \qquad (3\text{-}20)$$

which has the same physical meaning as the mmf equation (2-30). With a sufficiently heavy load, when the primary current markedly exceeds the magnetizing current, $I_1 \gg I_0$, the current equation can approximately be written as

$$\dot{I}_1 = -\dot{I}_2' = -\dot{I}_2 w_2/w_1$$

or

$$I_1/I_2 = w_2/w_1 \qquad (3\text{-}21)$$

As is seen, given a heavy load, the referred secondary current, I_2', does not differ from the primary current, I_1.

3-4 The Phasor Diagram of a Transformer

The voltage and current phasor diagram of a transformer is a graphical interpretation of the equations describing the performance of the transformer. These equations include —the winding voltage equations

$$\dot{V}_1 = -\dot{E}_1 + Z_1\dot{I}_1 \tag{3-22a}$$

$$-\dot{E}'_2 = -\dot{E}_1 = -\dot{V}'_2 + Z'_2\,(-\dot{I}'_2) \tag{3-22b}$$

—the load voltage equation

$$-\dot{V}'_2 = Z'\,(-\dot{I}'_2) \tag{3-22c}$$

—the mutual emf equation

$$-\dot{E}_1 = -\dot{E}'_2 = Z_0\dot{I}_0 \tag{3-22d}$$

—the current equation

$$\dot{I}_1 = \dot{I}_0 - \dot{I}'_2 \tag{3-22e}$$

Using a phasor diagram constructed to a certain definite scale, we can determine the voltages, emfs and currents of a transformer on load. The sequence in which a phasor diagram is constructed depends on which quantities are specified to define the operation of the transformer and which quantities are to be determined.

Suppose that we know the secondary current $\dot{I}_2$ and the load impedance $Z = R + jX$ (for an inductive load, $X > 0$; and for a capacitive load, $X < 0$). We set out to find the secondary voltage $\dot{V}_2$, the primary emf $\dot{E}_1$, the magnetizing current $\dot{I}_0$, the primary current $\dot{I}_1$, and the primary voltage $\dot{V}_1$. The phasor diagram is usually constructed for the transformer with its secondary quantities referred to the primary side. Therefore, the first step is to determine the secondary quantities referred to the primary side (that is, adjusted in value by the turns ratio or the turns ratio squared). The referred secondary current is

$$I'_2 = I_2\,(w_2/w_1)$$

and the referred impedances are

$$Z' = Z\,(w_1/w_2)^2 = R' + jX'$$

$$Z'_2 = Z_2\,(w_1/w_2)^2 = R'_2 + jX'_2$$

The phasor diagram is made more compact if the complex quantities referred to the primary side are taken with a minus sign, $-\dot{I}'_2$ and $-\dot{V}'_2$. The first to be plotted (see

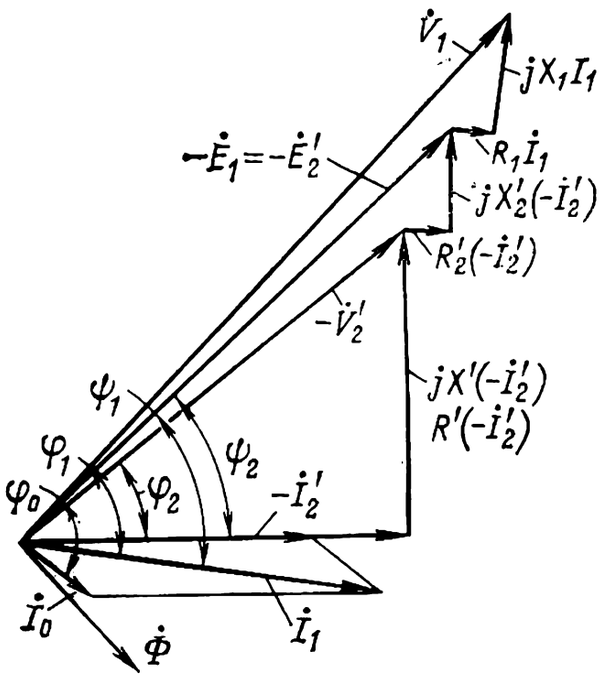

Fig. 3-4 Phasor diagram of a transformer operating into a resistive-inductive load ($\varphi_2 > 0$, $X > 0$)

Fig. 3-4) should be $-\dot{I}_2$ which may be drawn in an arbitrary direction, say along the positive axis of the complex time plane and on the scale adopted for currents. Then, using the load voltage equation, we find the referred secondary voltage, $-\dot{V}'_2$. This voltage has an active component, $R'\,(-\dot{I}'_2)$, and a reactive component, $jX'\,(-\dot{I}'_2)$, which are laid off to the adopted scale. The active component is laid off in the direction of $-\dot{I}'_2$, whereas the reactive component leads $-\dot{I}'_2$ by 90°, if the load is inductive and $X > 0$. The actual secondary voltage is found by Eq. (3-17):

$$V_2 = V'_2\,(w_2/w_1)$$

Then we find graphically the mutual emf $-\dot{E}_1 = -\dot{E}_2'$ and compute the magnetizing current

$$I_0 = E_1 / \sqrt{R_0^2 + X_0^2}$$

and the phase angle

$$\varphi_0 = \arctan (X_0/R_0)$$

Now $\dot{I}_0$ can be laid off on the phasor diagram. The mutual flux Φ can be found from Eq. (3-7) and laid off on a scale of its own (the flux is in quadrature lagging with $-\dot{E}_1$). The primary current $\dot{I}_1$ is deduced from the current equation.

The primary voltage $\dot{V}_1$ is found graphically in a similar way. The construction thus obtained also gives the phase

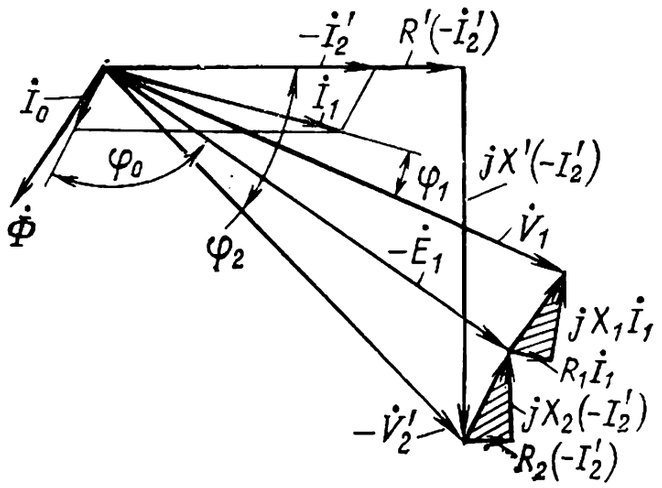

Fig. 3-5 Phasor diagram of a transformer operating into a resistive-capacitive load ($\varphi_2 < 0$, $X < 0$)

shift φ_2 between the secondary voltage and current, and the phase shift φ_1 between the corresponding primary quantities.

With a resistive-inductive load, both the primary and the secondary currents lag behind the respective voltages in phase, so φ_1 and φ_2 are taken to be positive: $\varphi_1 > 0$ and $\varphi_2 > 0$ (see Fig. 3-4).

The phasor diagram for a resistive-capacitive load is plotted in Fig. 3-5. As is seen, the secondary current leads the voltage by an angle φ_2 ($\varphi_2 < 0$). If the load is predominantly capacitive (see Fig. 3-5), the primary current like-

wise leads the voltage by an angle $\varphi_1 < 0$. If the capacitive component is less pronounced, the primary current may even lag behind the voltage.

3-5 The Equivalent Circuit of the Transformer

If we treat a single-phase, two-winding transformer as a two-port, the equivalent circuit stems from Eqs. (3-22*a*) through (3-22*d*), where the secondary quantities are transferred to the primary side.

Given $\dot{V}_1$, the circuit equivalent to a given transformer must draw from the supply line the same primary current $\dot{I}_1$ as the transformer itself. In order to identify the configuration of this equivalent circuit, we must express the primary voltage in terms of the primary current.

To begin with, we shall express $\dot{I}_1$ in terms of $\dot{E}_1$ and the circuit parameters

$$\dot{I}_1 = \dot{I}_0 - \dot{I}'_2 = -\dot{E}_1/Z_0 + \frac{-\dot{E}_1}{Z'_2 + Z}$$

Hence,

$$-\dot{E}_1 = \frac{\dot{I}_1}{1/Z_0 + 1/(Z'_2 + Z)}$$

Substituting the above expression into the voltage equation gives

$$\dot{V}_1 = \dot{I}_1 Z_1 - \dot{E}_1 = \dot{I}_1 \left[Z_1 + \frac{1}{1/Z_0 + 1/(Z'_2 + Z')} \right] = \dot{I}_1 Z_{eq} \quad (3\text{-}23)$$

It is seen from Eq. (3-23) that the transformer equivalent circuit drawing a primary current $\dot{I}_1$ must have an equivalent impedance given by

$$Z_{eq} = Z_1 + \frac{1}{1/Z_0 + 1/(Z'_2 + Z')}$$

This impedance is presented by the circuit in Fig. 3-6 where Z_1 is shown connected in series with a parallel combination of Z_0 and $(Z'_2 + Z')$.

A detailed analysis would show that the individual arms of the equivalent circuit carry the same currents as the

windings of the transformer in which the secondary quantities are transferred to the primary side. Also, the currents

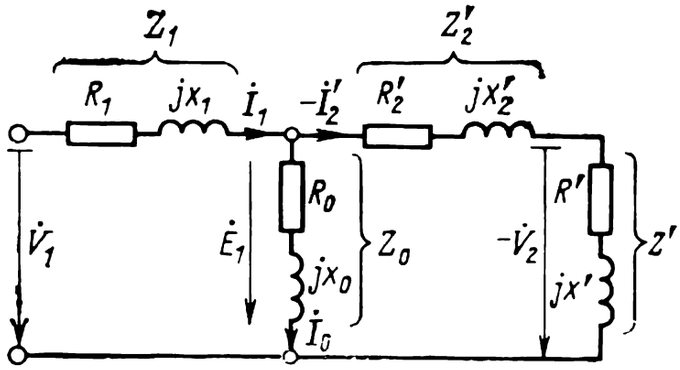

Fig. 3-6 Equivalent circuit of a transformer

entering the nodes of the circuit and its loop voltages satisfy the basic transformer equations.

3-6 The Per-Unit Notation

Electrical quantities (such as currents and voltages) and circuit parameters (reactances and resistances) can be expressed each as a fraction of an arbitrarily chosen base or reference quantity, thereby giving *per-unit quantities.*

The per-unit notation simplifies the equations describing transformer performance. It also simplifies a check on the design data and results, because the per-unit quantities of different transformers differ much less than the same quantities expressed in absolute units.

The base quantities usually chosen for the primary side of transformers are:

—the rated phase primary voltage, $V_{1,\,R}$

—the rated phase primary current, $I_{1,\,R}$

—the rated impedance presented by the transformer to the supply line,

$$|Z_{1,\,R}| = V_{1,\,R}/I_{1,\,R} \tag{3-24}$$

—the power rating of the transformer

$$S_{1,\,R} = V_{1,\,R}I_{1,\,R}$$

in the case of a single-phase transformer, and

$$S_{1,\,R} = 3V_{1,\,R}I_{1,\,R}$$

for a three-phase transformer.

The base quantities usually chosen for the secondary side are:

—the rated phase secondary voltage, $V_{2,\,R} = V_{1,\,R}\,(w_2/w_1)$;

—the rated phase secondary current, $I_{2\,,R} = I_{1,\,R}\,(w_1/w_2)$;

—the impedance presented to the line on the secondary side (at $V_{2,\,R}$ and $I_{2,\,R}$)

$$|Z_{2,\,R}| = V_{2,\,R}/I_{2,\,R} = |Z_{1,\,R}|\,(w_2/w_1)^2 \qquad (3\text{-}25)$$

—the base power on the primary side

$$S_{2,\,R} = S_{1,\,R}$$

To obtain a per-unit quantity on the primary side, its absolute value is divided by an appropriate base quantity taken in the same units

$$\begin{aligned} V_{*1} &= V_1/V_{1,\,R} \\ I_{*1} &= I_1/I_{1,\,R} \\ |Z_{*0}| &= |Z_0|/|Z_{1,\,R}| \\ |Z_{*1}| &= |Z_1|/|Z_{1,\,R}| \\ P_{*1} &= P_1/S_{1,\,R} = V_{*1}I_{*1}\cos\varphi_1 \end{aligned} \qquad (3\text{-}26)$$

where an asterisk stands for per unit. Sometimes, this index may be omitted, if the use of the per-unit notation is referred to in the text. The power equation in per-unit quantities is equally applicable to single- and three-phase transformers.

The quantities associated with the secondary winding of a transformer can be expressed as per-unit quantities in any one of two ways. For example, we may divide a given secondary quantity taken in absolute units by the corresponding secondary quantity taken as the base. Alternatively the secondary quantity may first be referred to the primary side by adjusting it in value by the turns ratio or the turns ratio squared, as the case may be, and the result may then be divided by the adopted base quantity associated with the primary side:

$$\begin{aligned} V_{*2} &= V_2/V_{2,\,R} = V_2'/V_{1,\,R} \\ I_{*2} &= I_2/I_{2,\,R} = I_2'/I_{1,\,R} \\ |Z_{*2}| &= |Z_2|/|Z_{2,\,R}| = |Z_2'|/|Z_{1,\,R}| \\ P_{*2} &= P_2/S_{2,\,R} = P_2'/S_{1,\,R} = V_{*2}I_{*2}\cos\varphi_2 \end{aligned} \qquad (3\text{-}27)$$

For obvious reasons, the secondary quantities expressed on the per-unit basis carry no referring index.

Any one transformer equation may be written in per-unit notation. To this end, it must be divided through by the corresponding base quantity. As an example, let us do this for Eq. (3-13) which gives the primary voltage

$$\dot{V}_{*1} = \dot{V}_1/\dot{V}_{1,\,R} = -\dot{E}_1/V_{1,\,R} + Z_1 \frac{I_{1,\,R}}{V_{1,\,R}} \frac{\dot{I}_1}{I_{1,\,R}}$$

or

$$\dot{V}_{*1} = -\dot{E}_{*1} + Z_{*1}\dot{I}_{*1} \tag{3-28}$$

For the current equation, we obtain

$$\dot{I}_1/I_{1,\,R} + \dot{I}'_2/I_{1,\,R} = \dot{I}_0/I_{1,\,R}$$

or

$$\dot{I}_{*1} + \dot{I}_{*2} = \dot{I}_{*0} \tag{3-29}$$

As is seen, the per-unit equations are written in about the same way as those in absolute quantities, except that they have no indexes to show transferring to the primary side.

Per-unit quantities are also helpful in expressing the parameters and quantities involved in equivalent circuits, and in constructing phasor diagrams. The per-unit parameters and losses of a transformer vary within a ralatively narrow range of values and depend mainly on its power rating. Let us establish the relations between some of the per-unit quantities. Among other things, we will find that the mutual inductive reactance varies inversely as the no-load current:

$$\begin{aligned} X_{*0} &= |Z_{*0}| = |Z_0|/|Z_{1,\,R}| \\ &= (V_{1,\,R}/I_0)\,(I_{1,\,R}/V_{1,\,R}) \\ &= I_{1,\,R}/I_0 \end{aligned} \tag{3-30}$$

The resistance during magnetization can be expressed in terms of the no-load current and the core losses (the no-load or open-circuit losses) as

$$\begin{aligned} R_{*0} &= R_0/|Z_{1,\,R}| = P_{\text{core}} I_{1,\,R}/3I_0^2 V_{1,\,R} \\ &= (P_{\text{core}}/3V_{1,\,R}I_{1,\,R})\,(I_{1,\,R}/I_0)^2 \\ &= P_{*,\,\text{core}}/I_{*0}^2 \end{aligned} \tag{3-31}$$

Finally, the winding resistances are equal to the copper losses

$$\begin{aligned} R_{*1} &= R_1/|Z_{1,\,R}| = 3R_1I_{1,\,R}^2/3V_{1,\,R}I_{1,\,R} \\ &= P_{Cu,\,1}/S_{1,\,R} = P_{*Cu,\,1} \\ R_{*2} &= R_2'/|Z_{1,\,R}| = 3R_2'I_{1,\,R}^2/3V_{1,\,R}I_{1,\,R} \\ &= P_{Cu,\,2}/S_{1,\,R} = P_{*Cu,\,2} \end{aligned} \tag{3-32}$$

Using the above relations and data sheet values, the range of values for the basic per-unit quantities of three-phase power transformers rated from 25 to 500 000 kVA can readily be defined. Transformers with higher ratings have lower resistances and higher inductive reactances:

$$\begin{aligned} I_{*0} &= 0.03 \text{ to } 0.003 \\ P_{*,\,core} &= P_{*0} = 0.005 \text{ to } 0.000\,6 \\ P_{*1,\,Cu} + P_{*2,\,Cu} &= P_{*,\,Cu} = 0.025 \text{ to } 0.002\,5 \\ X_{*1} &= X_{*2} = 0.03 \text{ to } 0.07 \\ |Z_{*0}| &= X_{*0} = 33 \text{ to } 330 \\ R_{*1} &= R_{*2} = 0.012\,5 \text{ to } 0.001\,25 \\ R_{*0} &= 5.5 \text{ to } 65 \end{aligned} \tag{3-33}$$

As is seen from the above figures, as the power is changed by a factor of 20 000, the per-unit quantities change not more than ten-fold (in fact, X_{*1} and X_{*2} only change by a factor of 2). As can readily be checked, the same parameters expressed in absolute units will change by a factor of many hundred thousand.

3-7 The Effect of Load Variations on the Transformer

In a transformer, the primary and secondary windings are coupled by a mutual flux. Therefore, any change in load impedance (the impedance on the secondary side), with the primary voltage held constant, leads not only to a change in the secondary current, but also to a change in the magnetic flux, the magnetizing current, the primary current, and the secondary voltage. After the transients associated with a load change die out, the transformer settles down to a new steady state in which the electric and magnetic circuits are at equilibrium. In other words, the currents in the windings and the magnetic flux in the core take on values which again

satisfy the conditions of equilibrium for its electric circuits defined by the voltage equations, (3-13) or (3-19), and for its magnetic circuit defined by the current equation (3-20) supplemented by the emf equations (3-7) and (3-8).

A change in the secondary current immediately brings about a change in the peak magnetic flux Φ_m and the primary emf E_1 it induces. The state of equilibrium that existed on the primary side prior to that change and with which was associated a certain definite primary current is upset, and a current is induced in the primary in accord with Eq. (3-13)

$$\dot{I}_1 = [\dot{V}_1 - (-\dot{E}_1)]/Z_1$$

The primary emf and the primary current keep varying until the magnetizing current (with the new value of I_2) and the corresponding emf, $-\dot{E}_1 = Z_0\dot{I}_0$, build up enough for a steady-state current to appear in the primary winding.

Considering together the equations written earlier, the primary current (Fig. 3-7) may be written

$$\begin{aligned}\dot{I}_1 &= \dot{V}_{1,\,\mathrm{R}}/(Z_0 + Z_1) - \dot{I}'_2 Z_0/(Z_0 + Z_1)\\ &= \dot{I}_{0,\,\mathrm{NL}} - \dot{I}'_2 Z_0/(Z_0 + Z_1)\end{aligned} \qquad (3\text{-}34)$$

where

$$\dot{I}_{0,\,\mathrm{NL}} = \dot{V}_{1,\,\mathrm{R}}/(Z_0 + Z_1)$$

is the magnetizing current at no-load.

Because $Z_1 \ll Z_0$, with a sufficiently large load we have

$$I_{0,\,\mathrm{NL}} \ll 1 \quad \text{and} \quad \dot{I}_1 = -\dot{I}'_2$$

The magnetic flux varies directly with E_1 which is in turn a function of the magnitude and phase of the primary current

$$-\dot{E}_1 = \dot{V}_{1,\,\mathrm{R}} - Z_1\dot{I}_1$$

or, in per-unit

$$-\dot{E}_{*1} = \dot{V}_{*1,\,\mathrm{R}} - Z_{*1}\dot{I}_{*1} \qquad (3\text{-}35)$$

At no-load, when $I_1 = I_{0,\,\mathrm{NL}} \approx 0$, the emf and the flux are equal to the primary voltage taken as unity

$$E_{*1} = \Phi_{*1} = \Phi_1/\Phi_{1,\,\mathrm{R}} = V_{*1,\,\mathrm{R}} = 1$$

At rated load ($I_{*1} = I_{*1,\,R} = 1$), the emf and flux change insignificantly in comparison with their no-load values. Even when the phase of $\dot{I}_{1,\,R}$ is such that $Z_1\dot{I}_1$ is in the same or opposite direction with $\dot{V}_{1,\,R}$, the emf is

$$E_{*1,\,R} = V_{*1,\,R} \pm Z_{*1}I_{*1,\,R} = 1 \pm Z_{*1}$$

where Z_{*1} = 0.03 to 0.07 (see Eqs. 3-33).

Thus, even in the worst loading case, with the load rising from zero to its full value (see Fig. 3-7), the emf and flux change by as little as

$$Z_{*1} \times 100 = 3\% \text{ to } 7\%$$

Given other phases for I_1 and I_2, the changes in the emf and flux are still more insignificant. Referring to Figs. 3-4 and 3-5, the emf decreases in the case of a resistive-inductive load and may increase if the load is resistive-capacitive and the phase shift is close to $-\pi/2$. The effect of load variations on the magnetizing current is likewise insignificant. It can be evaluated by Eq. (3-20):

$$\begin{aligned}\dot{I}_0 &= -\dot{E}_1/Z_0 \\ &= (\dot{V}_1 - Z_1\dot{I}_1)/Z_0 \\ &= \dot{I}_{0,\,NL} - \dot{I}_1Z_1/Z_0 \end{aligned} \quad (3\text{-}36)$$

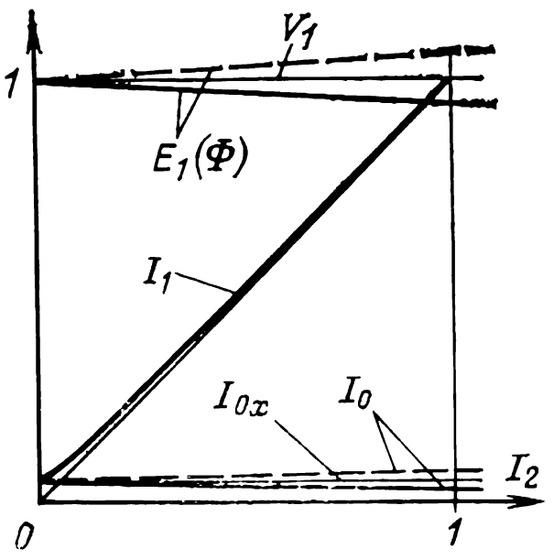

Fig. 3-7 Flux, primary emf, magnetizing current and primary current as functions of secondary current: solid line, resistive-inductive load, $\varphi_2 > 0$; dashed line, resistive-capacitive load, $\varphi_2 < 0$; $I_{0x} = I_{0,NL}$

In a linear approximation, this current varies in the same manner as the primary emf. If we include the nonlinear behaviour of the magnetic circuit which causes Z_0 to vary as well, this change becomes more pronounced. The effect of nonlinearity may be accounted for by using the magnetization curve, $\Phi = f(I_0)$, shown in Fig. 2-9.

Plots of I_1, E_1, Φ, and I_0 as functions of I_2 for inductive and capacitive loads are shown in Fig. 3-7.

3-8 Energy Conversion in a Loaded Transformer

The energy fed into the primary winding of a transformer from a supply line is customarily treated as the sum of two parts.

One part is delivered to load and is partly lost in the transformer itself. The average time rate of this unidirectional flow of energy is called the *active power* drawn by the primary winding from the supply line. For a single-phase transformer, it is given by

$$P_1 = V_1 I_1 \cos \varphi_1 = V_1 I_{1a} = V_{1a} I_1 \qquad (3\text{-}37)$$

where $I_{1a} = I_1 \cos \varphi_1$ is the active current
$V_{1a} = V_1 \cos \varphi_1$ is the active voltage

The active power is taken as positive, $P_1 > 0$, if φ_1 lies anywhere between $-90°$ and $+90°$ (electrical).

The other part of input energy is spent to establish magnetic fields in the transformer itself* and also electric and magnetic fields in the load. The direction of this energy is changed twice every cycle, so the respective power averaged over a cycle is zero.

The transfer of energy between the supply line and a field (electric or magnetic) is described in terms of the peak instantaneous power, called the *reactive power*. The reactive power drawn by the primary winding of a single-phase transformer from the supply line is given by

$$Q_1 = V_1 I_1 \sin \varphi_1 = V_1 I_{1r} = V_{1r} I_1 \qquad (3\text{-}38)$$

where $I_{1r} = I_1 \sin \varphi_1$ is the rms value of reactive current
$V_{1r} = V_1 \sin \varphi_1$ is the rms value of reactive voltage

The reactive power is assumed to be positive, $Q_1 > 0$, if the reactive current is lagging behind the voltage, $0 < \varphi_1 < \pi$, which corresponds to a resistive-inductive load. The reactive power is taken to be negative, $Q_1 < 0$, if the reactive current is leading the voltage, $0 > \varphi_1 > -\pi$, which corresponds to a resistive-capacitive load.

Consider the conversion of active power in a transformer. Let us write the active component of the primary voltage, $V_{1a} = V_1 \cos \varphi_1$, as the sum of projections of E_1 and the

---

* The energy associated with the electric field within the transformer is usually neglected.

voltage drop R_1I_1 (see the phasor diagram in Fig. 3-8*a*)

$$V_{1a} = V_1 \cos \varphi_1 = E_1 \cos \psi_1 + R_1I_1$$

and the active power P_1 supplied to the primary winding by a supply line (its direction is shown in Fig. 3-9 by an arrow) as the sum of two components

$$P_1 = (V_1 \cos \varphi_1)\, I_1 = (E_1 \cos \psi_1)\, I_1 + (R_1I_1)\, I_1 \qquad (3\text{-}39)$$

The term $I_1^2R_1 = P_{\text{Cu},1}$ is the copper loss in the primary winding, that is, the power lost as heat dissipated in the primary turns (see the arrows in Fig. 3-9).

Referring to Fig. 3-8*b*, the active component of the primary current, $I_1 \cos \psi_1$, is shown as the sum of the active components of the magnetizing current $I_0 \cos \varphi_0$ and of the secondary current $I_2' \cos \psi_2$. Therefore, the term $(E_1 \cos \psi_1)\, I_1$ may likewise be written as the sum of two components:

$$\begin{aligned} E_1I_1 \cos \psi_1 &= E_2I_2' \cos \psi_2 + E_1I_0 \cos \varphi_0 \\ &= P_{\text{em}} + P_{\text{core}} \end{aligned} \qquad (3\text{-}40)$$

The term $P_{\text{em}} = E_1I_2' \cos \psi_2$ is called *electromagnetic power*. It is transferred inductively from the primary to the secondary winding. The flow of electromagnetic power crosses the channel between the two windings (Fig. 3.9).

The term $E_1I_0 \cos \varphi_0 = E_1I_{0a} = P_{\text{core}}$ represents core loss in the transformer.

Referring to Fig. 3-8*c*, the active component of the primary emf, $E_1 \cos \psi_2$, can be expressed in terms of the active component of the secondary voltage, $V_2' \cos \varphi_2$, and resistive voltage drop, $R_2'I_2'$. Hence, we may write

$$\begin{aligned} P_{\text{em}} &= (E_1 \cos \psi_2)\, I_2' = (V_2' \cos \varphi_2)\, I_2' + (R_2'I_2')\, I_2' \\ &= P_2 + P_{\text{Cu},2} \end{aligned} \qquad (3\text{-}41)$$

Some of the electromagnetic power is expended to make up for the copper loss in the secondary winding,

$$P_{\text{Cu},2} = I_2'^2R_2'$$

The remainder,

$$P_2 = V_2'I_2' \cos \varphi_2$$

is transferred to the load conductively (see Fig. 3-9).

The active power input to a transformer is

$$\begin{aligned} P_1 &= P_{\text{Cu},1} + P_{\text{core}} + P_{\text{em}} \\ P_{\text{em}} &= P_{\text{Cu},2} + P_2 \end{aligned} \qquad (3\text{-}42)$$

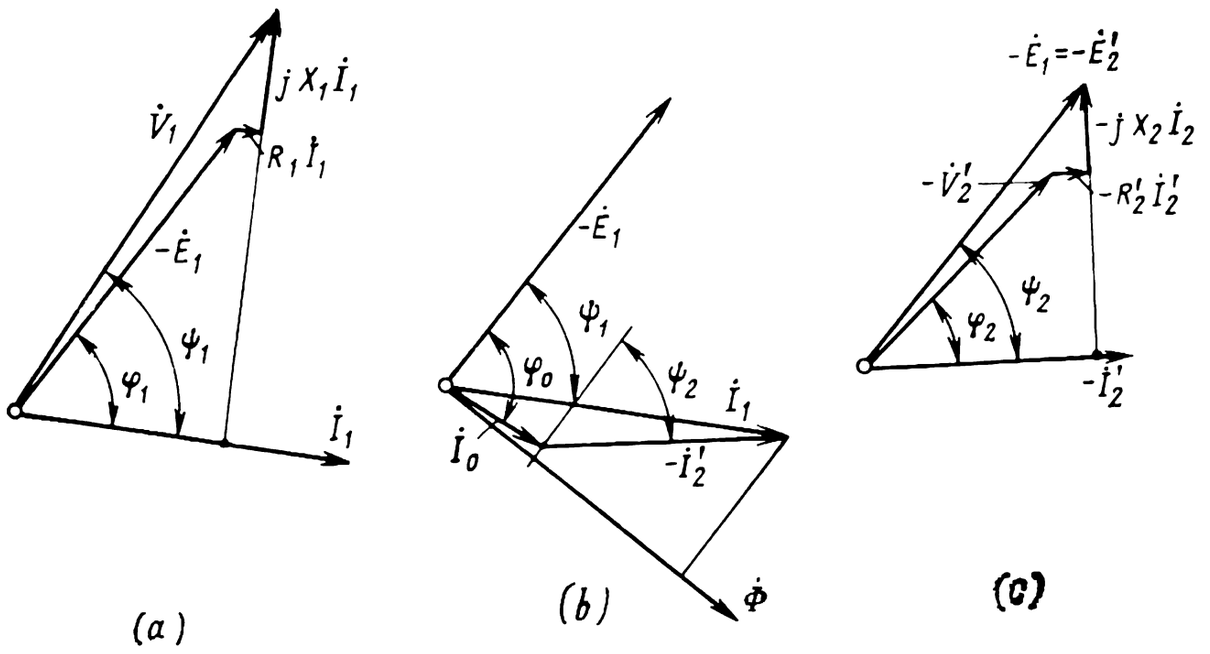

Fig. 3-8 Phasor diagrams of a transformer operating into a resistive-inductive load (see Fig. 3-4)

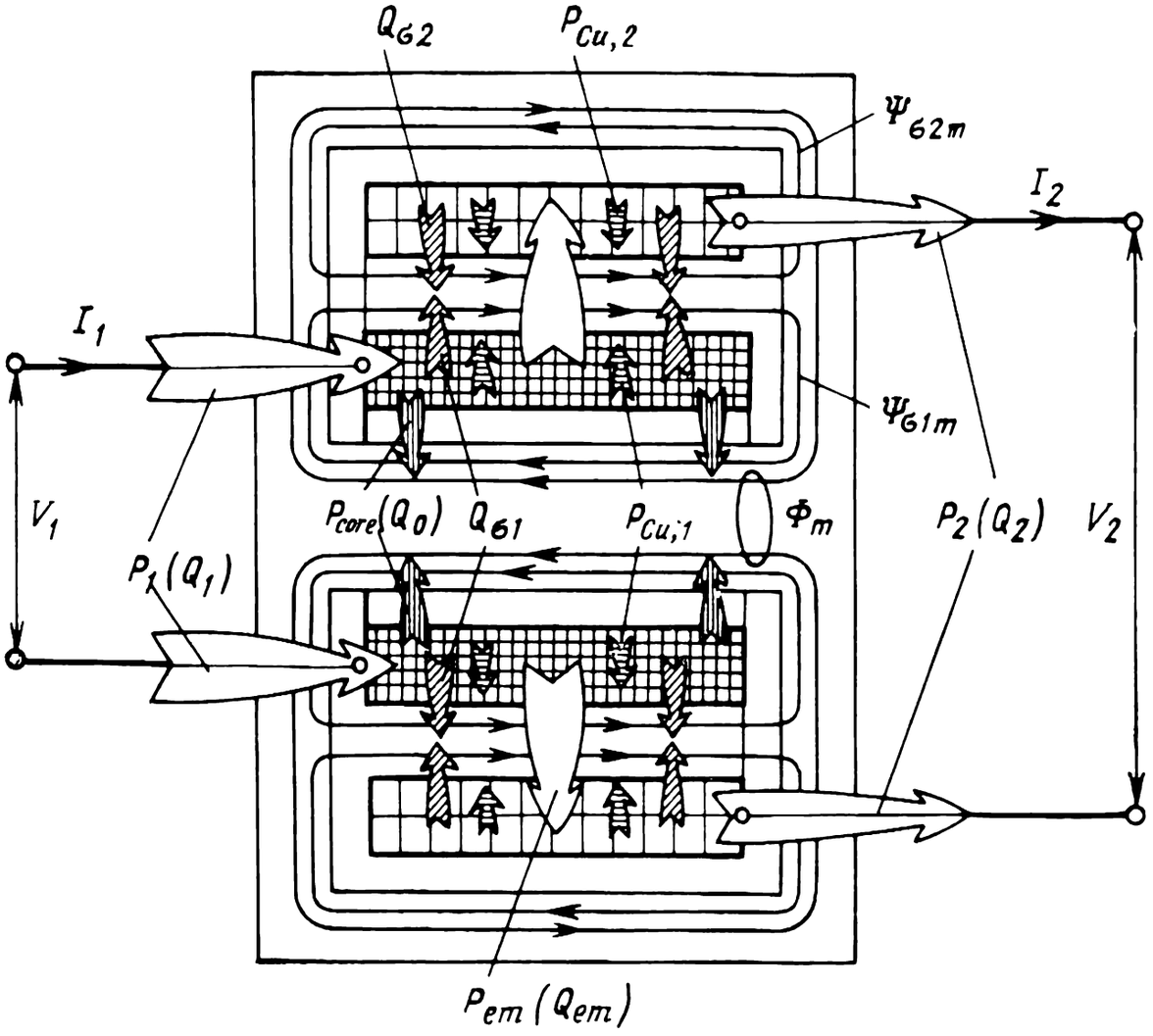

Fig. 3-9 Flows of active and reactive power in a loaded transformer

or

$$P_1 = P_2 + \sum P_{\text{loss}}$$

where

$$\sum P_{\text{loss}} = P_{\text{Cu},1} + P_{\text{Cu},2} + P_{\text{core}}$$

The conversion of reactive power in a transformer may be treated in a similar way, likewise referring to the phasor diagram in Fig. 3-8.

The primary reactive power can be treated as the sum of the following components:

$$\begin{aligned} Q_1 &= (V_1 \sin \varphi_1) I_1 = (E_1 \sin \psi_1) I_1 + (X_1 I_1) I_1 \\ &= (E_1 \sin \psi_1) I_1 + Q_{\sigma 1} \end{aligned} \tag{3-43}$$

where

$$\begin{aligned} E_1 (I_1 \sin \psi_1) &= E_1 (I_2' \sin \psi_2) + E_1 (I_0 \sin \varphi_0) \\ &= Q_{\text{em}} + Q_0 \end{aligned}$$

$$\begin{aligned} Q_{\text{em}} &= (E_1 \sin \psi_2) I_2' = (V_2' \sin \varphi_2) I_2' + (X_2' I_2') I_2' \\ &= Q_2 + Q_{\sigma 2} \end{aligned}$$

The physical meaning of the reactive components is as follows:

$Q_{\text{em}} = E_1 (I_2' \sin \psi_2)$ is the reactive power transferred inductively from the primary to the secondary winding

$Q_0 = E_1 (I_0 \sin \varphi_0) = E_1 I_{0r}$ is the reactive power required to establish the magnetizing (mutual) flux

$Q_{\sigma 1} = X_1 I_1^2$ is the reactive power expended in setting up the leakage flux on the primary side

$Q_{\sigma 2} = X_2' I_2'^2$ is the reactive power expended in setting up the leakage flux on the secondary side

$Q_2 = V_2' I_2' \sin \varphi_2$ is the reactive power drawn by the load

The directions of these power components are shown in Fig. 3-9.

4 Transformation of Three-Phase Currents and Voltages

4-1 Methods of Three-Phase Transformation. Winding Connections

Three-phase currents and voltages may be transformed either by a bank of three single-phase two-winding transformers (Fig. 4-1) or by a three-phase, two-winding transformer whose windings are put on a common magnetic circuit of the core or the shell-and-core (five-leg core) construction (Fig. 4-2).

The magnetic circuit of a core-type three-phase transformer can be formed from those of three single-phase transformers combined together. Arranging the single-phase transformers as shown in Fig. 4-3*a* and combining the limbs that do not carry any windings (Fig. 4-3*b*), it can be noted that with a symmetrical set of voltages (Fig. 4-1), the flux in the combined limb, equal to the sum of the phase fluxes, vanishes

$$\dot{\Phi}_A + \dot{\Phi}_B + \dot{\Phi}_C = 0$$

Therefore, we are free to remove the combined limb altogether (Fig. 4-3*b*). The magnetic circuit thus derived is sometimes used in practice and is known as a spatial three-phase core. In such a transformer, the instantaneous fluxes in limbs A and C have their paths completed through limb B, because

$$\dot{\Phi}_B = -\dot{\Phi}_A - \dot{\Phi}_C$$

Most frequently, however, the magnetic circuit of a three-phase transformer is built as a flat (or planar) core-type structure (Fig. 4-3*c*), with the limbs arranged to lie in a common plane. It differs from a spatial core in that the phase B core has no yokes and the axes of all the phase legs and yokes lie in a common plane.

A flat core shows a degree of asymmetry which results in an asymmetry of the magnetizing currents. However, this is of minor importance because these currents are small.

The shell-and-core (five-leg core) form of the magnetic circuit is employed in high-power transformers (Fig. 4-2*b*) so as to reduce the yoke height. This is achieved owing

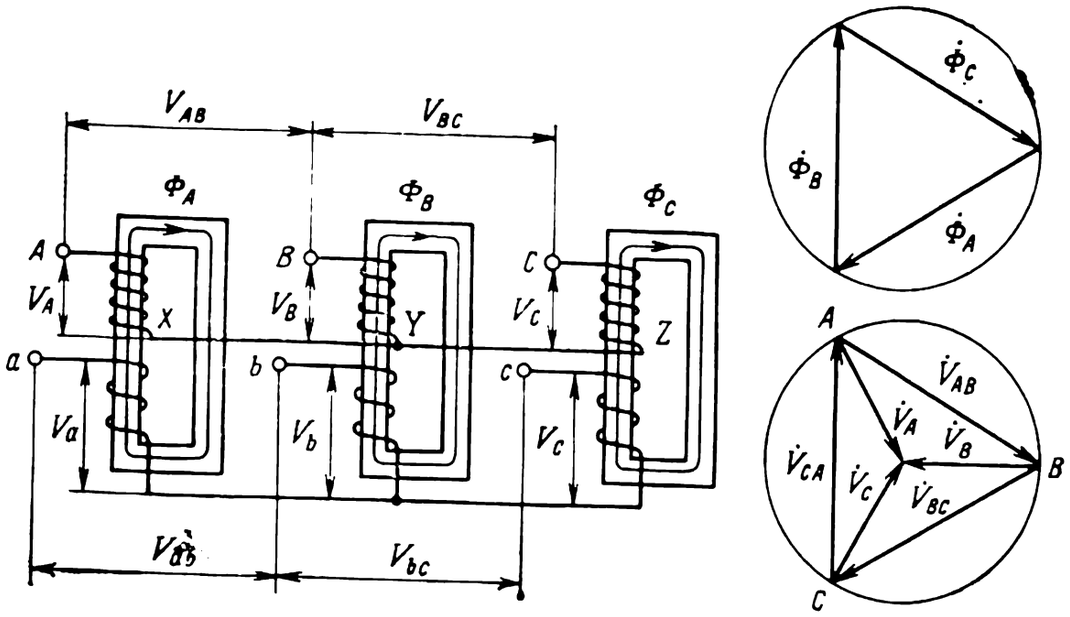

Fig. 4-1 Three-phase transformation by a bank of single-phase transformers

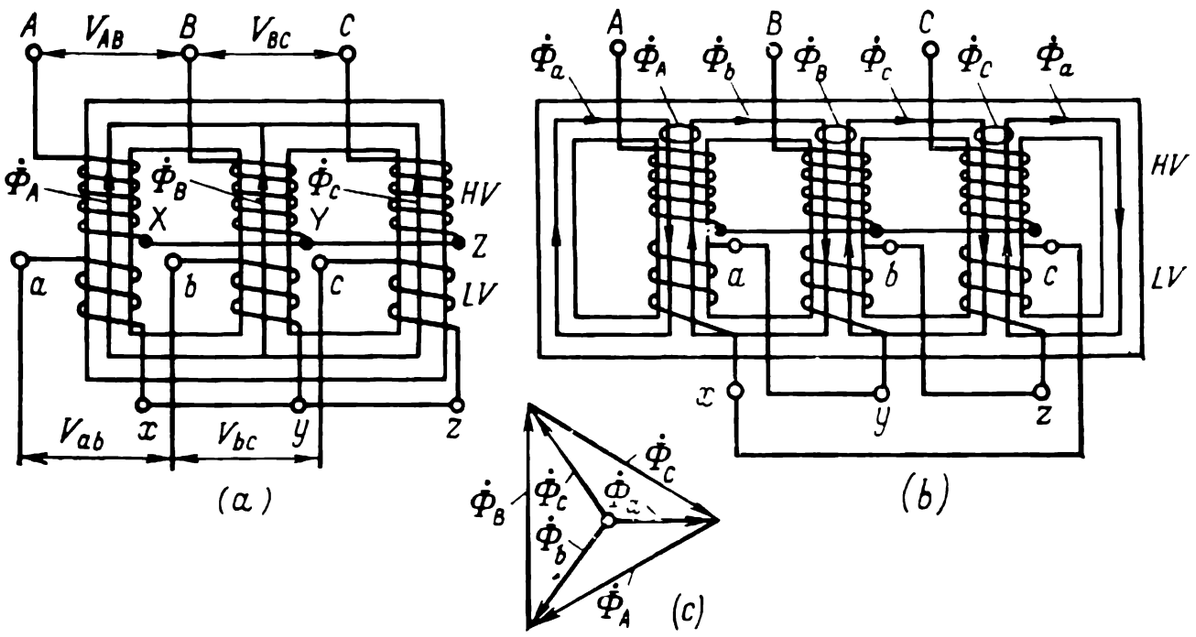

Fig. 4-2 Three-phase transformers: (*a*) core-type; (*b*) shell-and-core (five-leg core) type

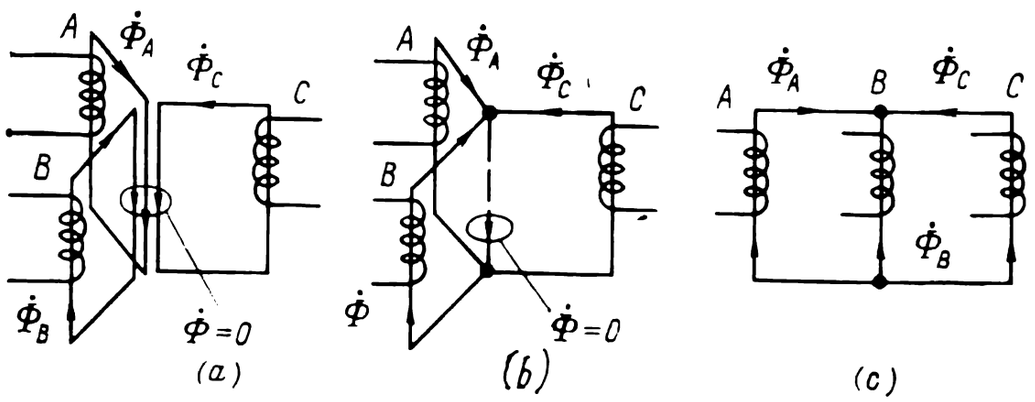

Fig. 4-3 Three single-phase magnetic circuits transformed into (*a*) and (*b*) a "spatial" core and (*c*) a planar core

to the formation of extra closed paths (through the side limbs) for the magnetic fluxes. In a shell-and-core magnetic circuit, the phase fluxes $\dot{\Phi}_A$, $\dot{\Phi}_B$, and $\dot{\Phi}_C$ may be visualized as composed of the individual loop fluxes $\dot{\Phi}_a$, $\dot{\Phi}_b$, and $\dot{\Phi}_c$ (Fig. 4-2*b*), such that $\dot{\Phi}_A = \dot{\Phi}_b - \dot{\Phi}_a$, $\dot{\Phi}_B = \dot{\Phi}_c - \dot{\Phi}_b$, and $\dot{\Phi}_C = \dot{\Phi}_a - \dot{\Phi}_c$. As follows from the flux phasor diagram in Fig. 4-2*c*, constructed on the basis of design data for

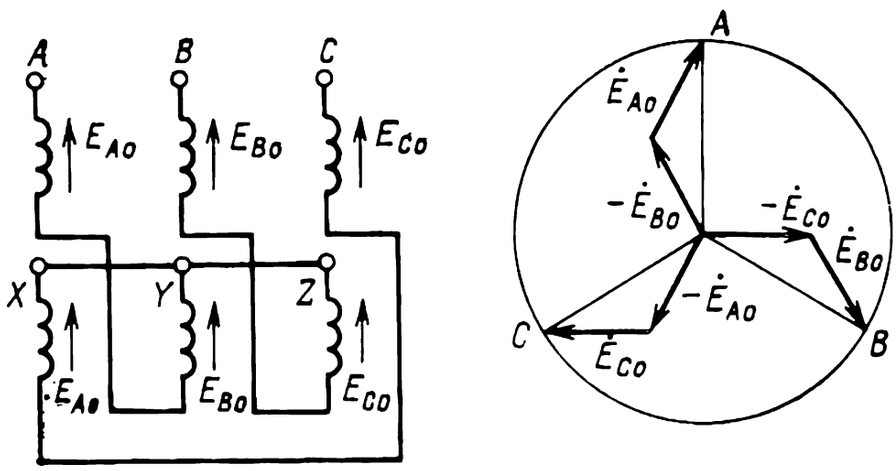

Fig. 4-4 Zigzag-star connection

the core, the fluxes in the yoke loops form a nearly symmetrical star (Φ_a is somewhat smaller than $\Phi_b = \Phi_c$), and the fluxes in yokes *b* and *c* are $1/\sqrt{3}$ times the fluxes in the phase limbs. (It is to be recalled that in the core-form transformer of Fig. 4-2*a* the yoke fluxes do not differ from those in the phase limbs.)

A three-phase transformer is far more economical, so banks of single-phase transformers are only used where a single three-phase transformer of the same power rating would have a prohibitively large weight or size.

The phase windings may be connected in a *star* (Figs. 4-1 and 4-2*a*), a *delta* (the LV winding in Fig. 4-2*b*) and, though seldom, a *zigzag* (Fig. 4-4). In a star connection,

$$V_{\text{line}} = V_{AB} = V_{BC} = V_{CA} = \sqrt{3}\, V_{\text{ph}}$$

where

$$V_{\text{ph}} = V_A = V_B = V_C$$

and

$$I_{\text{line}} = I_{\text{ph}}$$

In a delta connection,

$$V_{\text{line}} = V_{\text{ph}} = V_a = V_b = V_c = V_{ab} = V_{bc} = V_{ac}$$

and

$$I_{\text{line}} = \sqrt{3}\, I_{\text{ph}}$$

In a zigzag (or interconnected-star) connection, the voltage and current relations are the same as in a star connection, but in order to obtain the same phase voltage the number of turns per phase must be increased $2/\sqrt{3} = 1.16$ times. This leads to a higher cost which is to some degree offset by an improvement in performance (as regards the waveform of phase emfs and fluxes).

The star connection is designated by a "$\curlyvee$" sign or the letter Y (sometimes spelled in full as "a wye connection"). The delta connection is designated by the Greek letter Δ or the Roman letter D. The zigzag connection is designated by the letter Z.

A winding carrying the highest rated (line) voltage is referred to as a high-voltage (HV) winding. A winding carrying the lowest rated (line) voltage is referred to as a low-voltage (LV) winding.

In the Soviet Union, the manner in which the windings of a two-winding transformer are connected is designated by a fraction, with the form of connection of the HV winding placed in the numerator and that of the LV winding in the denominator. For example, the form of connection for the transformer in Fig. 4-2*a* will be designated Y/Y, and for that in Fig. 4-2, Y/Д. Outside the Soviet Union, the same forms of connections may alternatively be designated as Y-Y (or wye-wye) and Y-Δ (or wye-delta).

Under a relevant USSR standard, the start and finish of the HV winding in a single-phase transformer are marked as A and X, and those of the LV winding, as a and x. The starts and finishes of the HV winding in a three-phase transformer will be designated as A, B, C and X, Y, Z, and those of the LV winding, as a, b, c and x, y, z. The neutral wire is designated as N, and the centre (or zero) point of a star connection is marked O on the HV side and o on the LV side.

4-2 A Three-Phase Transformer on a Balanced Load

The performance of a three-phase transformer on a balanced load may be described in terms of the theory developed for single-phase transformers. In fact, all the relations derived for a single-phase transformer fully apply to any phase formed by a primary and a secondary on a common limb. Some adjustment needs only to be made for the magnetization of the core in a three-phase transformer (see Sec. 4-4) and the calculation of the magnetizing current (see Sec. 8-1). However, the magnetizing currents are negligible in comparison with the load currents, and the unbalance in these currents related to the dissymmetry of a flat (planar) three-phase magnetic circuit is of minor importance. Therefore, the actual calculations are based on an equivalent balanced set of averaged magnetizing currents to which correspond the averaged mutual impedances ($Z_{0A} = Z_{0B} = Z_{0C}$) accounting for the magnetic coupling between the various phase windings.

Because the leakage fluxes are concentrated in the space taken up by the windings themselves (see Sec. 8-2), the leakage fluxes of the individual phases may be considered independently of one another, whereas the leakage impedances of the phase windings equal in size may be deemed identical ($X_{1A} = X_{1B} = X_{1C}$, $X_{2A} = X_{2B} = X_{2C}$). This also goes for the phase resistances (R_1 and R_2).

Therefore, with balanced primary line voltages and balanced load impedances, the phase currents and voltages are likewise balanced. In the circumstances, the line and phase quantities are connected by simple relations:

$$I_{\text{ph}} = I_{\text{line}}$$
$$V_{\text{ph}} = V_{\text{line}} / \sqrt{3}$$

in the case of a star connection, and

$$V_{\text{ph}} = V_{\text{line}}$$
$$I_{\text{ph}} = I_{\text{line}} / \sqrt{3}$$

in the case of a delta connection, and we may describe the performance of any of the phases, using the equations, equivalent circuit, and phasor diagram developed for a single-

phase transformer (see Chap. 3), extended to include the phase voltages, currents and impedances, and also the transformation ratio in terms of phase voltages or turns:

$$n_{21} = V_{2,\,R(ph)}/V_{1,\,R(ph)} = w_2/w_1$$

4-3 Phase Displacement Reference Numbers

For proper use of transformers in power systems, it is important to know the phase displacement between the emfs on the HV and LV sides, as measured across like terminals. For example, on the HV side the emf must be measured across terminals A and B, and on the LV side, across terminals a and b.

In single-phase transformers, the phase displacement between the emfs on the HV and LV sides may be 0° or 180°. The line emfs on the HV and LV sides in three-phase transformers can only be displaced in phase through an angle which is a multiple of 30°. Transformers having the same phase displacement between their HV and LV emfs fall in the same phase displacement (or reference phasor) group, each group being assigned a distinct reference number.

Since an angle of 30° is exactly the angle between adjacent hour markings on a clock dial, a convention adopted internationally is to indicate phase displacement as a clock figure representing the hour read by a clock when the minute hand takes the place of the line emf phasor on the primary side and is set at 12 o'clock, and the hour hand represents the line emf phasor on the secondary side. The "time" thus read is the reference number assigned. An example of this convention for phase displacement group 11 is shown in Fig. 4-5. The positive directions adopted are from A to B and from a to b.

In the designation of a transformer, the reference number follows the symbol for the winding connection (for example, Y/Y-0 or Y/Δ-11).

If the phase windings on the HV and LV sides are wound in the same direction, the LV leads may be marked in any one of two ways, shown in Fig. 4-6. Because the windings link the same flux, the emfs labelled by the same letters will be in phase in case (a), and in anti-phase in case (b). (As the flux decreases, the HV and LV emfs will be directed

from X to A and from x to a in case (a), and the LV emf will be directed from a to x in case (b).)

As already noted, single-phase transformers can only have zero or 180° phase displacement. Consequently, they may bear only reference number 0 (12) or 6, respectively. For brevity, they are designated by the symbols I/I-0 (see Fig. 4-6a) and I/I-6 (Fig. 4-6b). A change from group 0 (12) to group 6 calls for no connection changes in the transformer itself; it will suffice to remark lead a as x, and lead x as a. In the USSR, single-phase transformers are manufactured with a I/I-0 winding connection.

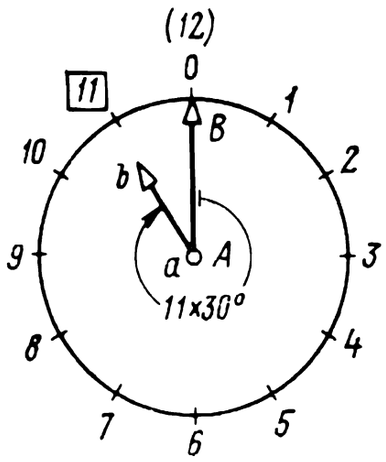

Fig. 4-5 Clock-hour convention to designate phase displacement groups

Extending the foregoing to the HV and LV phase windings of a three-phase transformer and referring to the phasor diagram, it can be seen that a Y/Y three-phase transformer with the leads marked as shown in Fig. 4-7a falls in phase

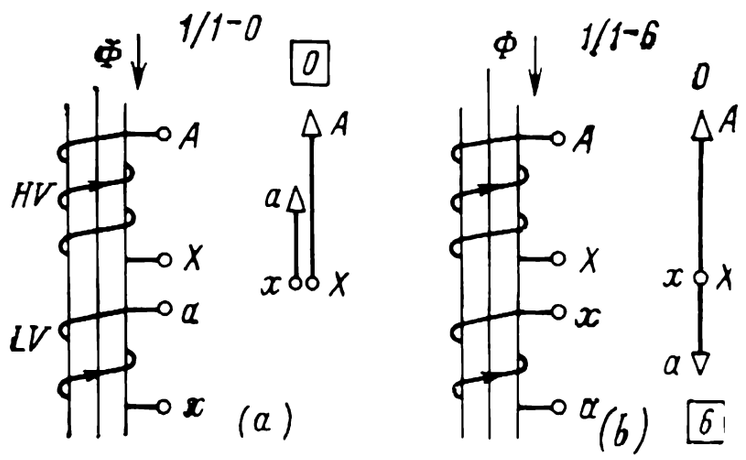

Fig. 4-6 Lead markings and phase displacement group numbers for single-phase transformers

displacement group 0, so its designation is Y/Y-0. (The phase emf ax is in the direction of the phase emf AX; the phase emf by is in the direction of the phase emf BY, $cz \rightarrow CZ$, and the line emf ab is in the direction of the line emf AB.) If we re-label the leads, going all the way round the circle, we can convert a group 0 transformer to a group 4 or group 8 transformer without actually shifting any connections inside the transformer. With the leads marked as

shown in the parentheses, (*a*), (*b*) and (*c*), the line emf (*a*) (*b*) is in the direction of the line emf *BC* (because these emfs are measured across the windings put on the same limbs), and the transformer is converted to one in phase displacement group (4). With the leads labelled as shown in the

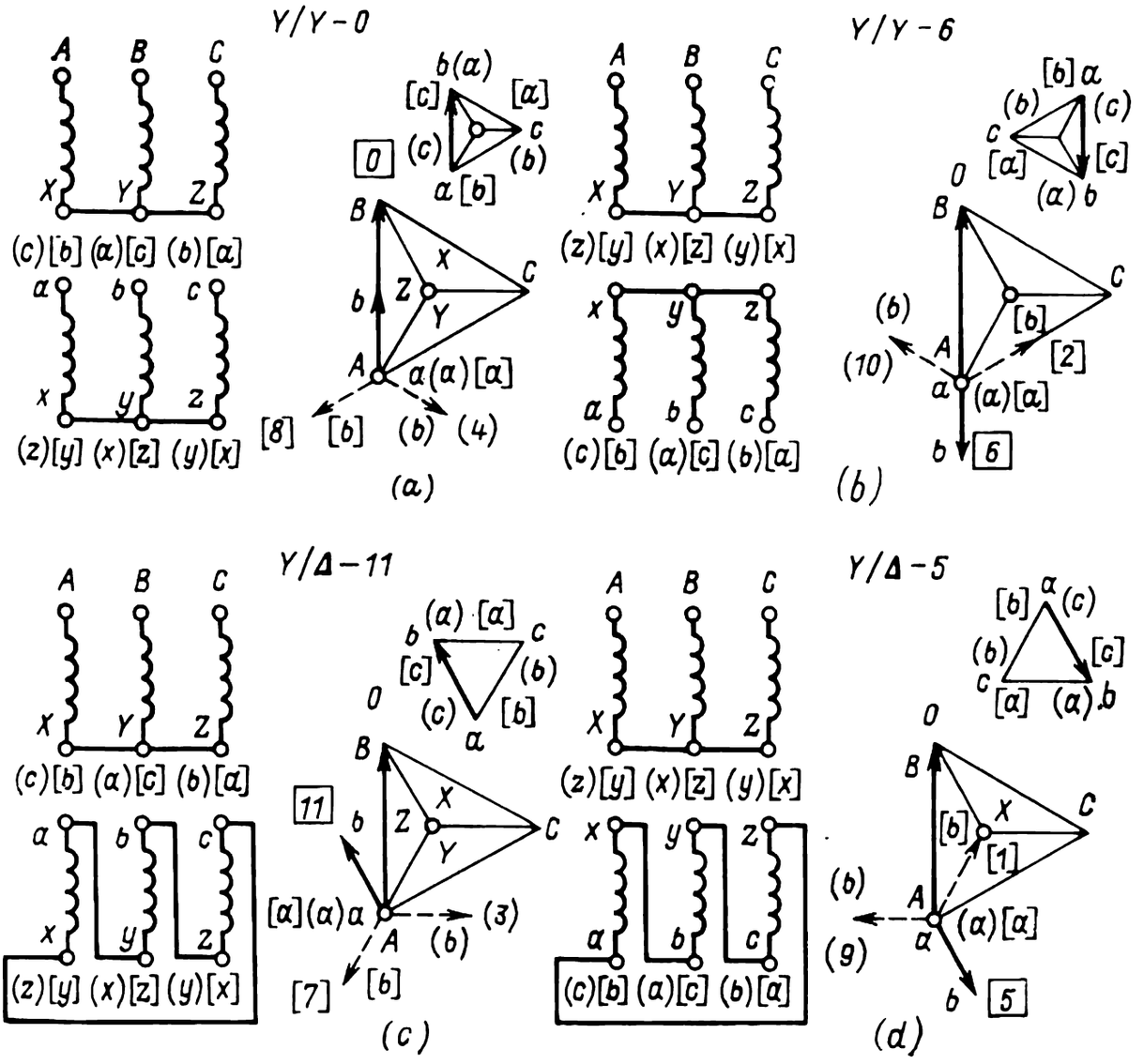

Fig. 4-7 Lead markings and phase displacement group numbers for three-phase transformers

brackets, the emf [*a*] [*b*] is in the direction of emf *CA*, and the transformer is converted to one falling in phase displacement group [8]. If we wish to obtain a Y/Y-6 transformer (Fig. 4-7*b*), we must shift the neutral jumper that reverses the phase of all the emfs (the emf *ab* is in anti-phase with the e mf *AB*). If we re-label the leads all the way round the circle, a group 6 transformer will be converted to a group (10) or a group [2] transformer. (The respective markings are given in Fig. 4-7*b* in parentheses and brackets, respect-

ively.) This exhausts all the likely even reference numbers that can be derived for a Y/Y connection.

Odd phase displacement clock numbers are obtained for a Y/Δ connection. With the leads marked without parentheses or brackets (*a*, *b*, *c*, *x*, *y*, and *z* in Fig. 4-7*c*), the line emf *ab* which is at the same time the phase emf *yb* is in the direction of the emf *YB*, and the transformer falls in phase displacement group 11.

If we re-label the leads all the way round the circle as shown in the parentheses and brackets in Fig. 4-7*c*, we shall obtain group (3) and group [7]. (Each time we re-label the leads, a particular emf is turned through an angle 120° $= 4 \times 30°$ and the reference number is incremented by 4.)

If we interchange the starts and finishes of the phase windings, a group 11 transformer will become a group 5 transformer (the respective markings are given without parentheses in Fig. 4-7*d*). Finally, if we re-label the leads all the way round the circle as shown in Fig. 4-7*d*, we shall obtain group (9) and group [1].

Of all the likely phase displacement groups, three-phase two-winding transformers of Soviet manufacture are only available in group 0 and group 11, with the (neutral) lead of the star available for connection where necessary (Y/Y_n-0, Y/Δ-11, Y_n/Δ-11). Additionally, some transformers may have their HV windings connected in Δ/Y_n-11. As is seen from Fig. 4-8, the delta connection in this case is obtained differently than in a Y/Δ-11 transformer. (*A* is connected to *Z*, whereas in a delta on the LV side *a* was connected to *y*.) If the delta on the HV side were connected in the same manner as the delta on the LV side in a Y/Δ-11 connection in Fig. 4-8*c*, the Δ/Y connection would fall in phase displacement group 1, rather than 11.

It is of interest to see how, in the general case, the phase displacement number will change if we make the LV winding an HV one and the HV winding an LV one, while retaining their connection and markings.

Obviously, the phase displacement between the HV and LV line emfs *AB* and *ab* will be the same as before, being $30° \times N$ (Fig. 4-9). However, the emf *ab* in the diagram shown by dashed lines will now lead the emf *AB* by the same angle $30° \times N$ by which it lags behind in the diagram shown by solid lines. Therefore, if we count the phase displacement from emf *AB* to emf *ab* always clockwise, the

angle 30° × N' in the second case will complement the original 30° × N angle to 360°

$$30° \times N' + 30° \times N = 360°$$

Thus, after the above manipulation, the phase displacement reference number N' can be found as

$$N' = 12 - N$$

where N is the original clock figure. For $N = 11$, $N' = 12 - 11 = 1$.

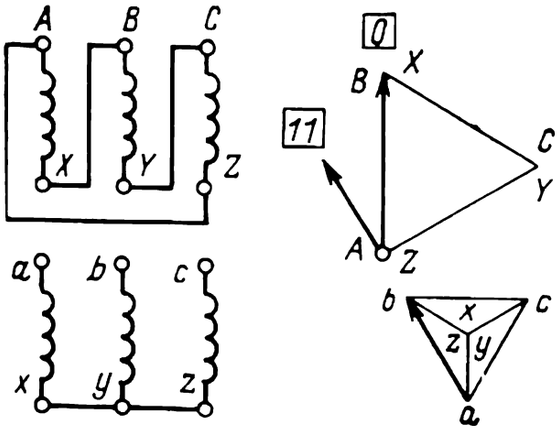

Fig. 4-8 Δ/Y-11 transformer

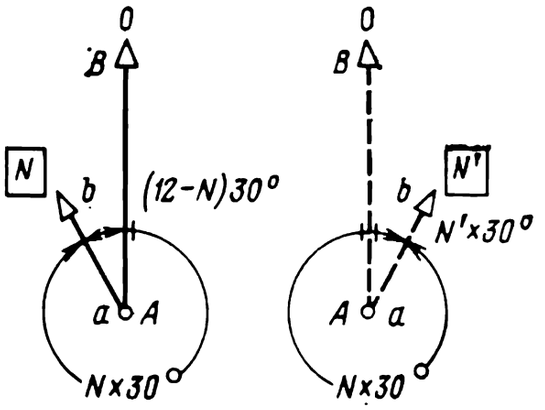

Fig. 4-9 Using the clock figure and lead markings of the LV (HV) winding to derive the clock figure and lead markings for the HV (LV) winding

The Δ/Y_n-11 connection ($N' = 11$) can be derived from the Y_n/Δ-1 connection ($N = 12 - N' = 1$) which is in turn derived from the Y_n/Δ-11 connection by modifying the delta connection (see below).

Which phase displacement group a transformer will fall in depends not only on the sequence of marking the starts and finishes of its LV winding, but also on how the phase windings are connected in a delta. Under a relevant USSR standard, the delta on the LV side must be formed by connecting lead a to lead y, lead b to lead z, and lead c to lead x, as shown in Fig. 4-7 or 4-10 by solid lines. If, instead, we form a delta by connecting terminal a to terminal z, terminal b to terminal x, and terminal c to terminal y (as shown in Fig. 4-10 by dashed lines), the LV emf, say ab, will be turned through 180 — 120 = 2 × 30° clockwise, and the clock figure will be incremented by 2. (With the leads marked as shown in Fig. 4-10, group 3 will change to group 3 + 2 = 5.) With the connection shown by solid lines, the line emf ab, which is at the same time the phase emf yb, is in the direction of the emf ZC. With the connection shown by dashed lines,

the line emf *ab* which is now the phase emf *ax* is in the direction of the emf *BY*. That is, it is turned from its original direction through 2 × 30°.

This rule extends to any other odd phase displacement groups. So, when the delta is formed in any other way than recommended, reference number N will become reference number $N' = N + 2$. More specifically, instead of group 11

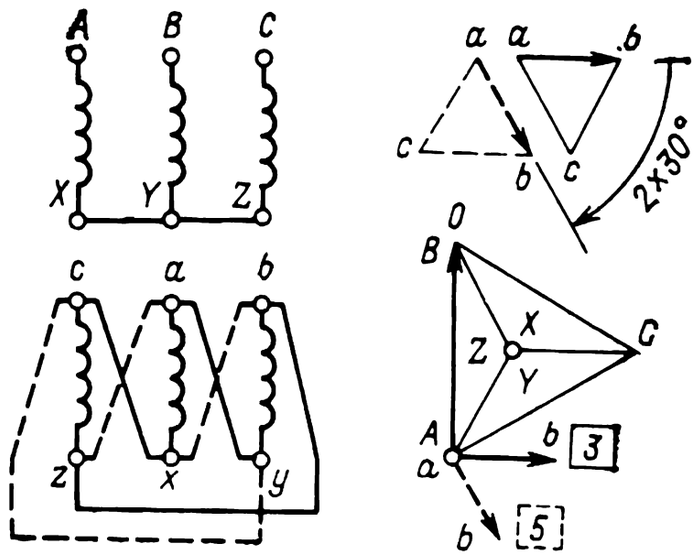

Fig. 4-10 Phase displacement group resulting from the manner of delta connection

there will be group 1; instead of group 3 there will be group 5; instead of group 7 there will be group 9; instead of group 1 there will be group 3; instead of group 5 there will be group 7; and instead of group 9 there will be group 11.

A relevant USSR standard recommends that the zigzag connection should solely be used on the LV side, and prescribes only one group, namely Y/Z_n-11, that is, one with the neutral line at the zigzag available for connection.

4-4 The Behaviour of a Three-Phase Transformer During Magnetic Field Formation

In discussing single-phase transformer in Sec. 2-5, we have seen that when the magnetic flux is sinusoidal, $\Phi = \Phi_m \sin \omega t$, the magnetizing current i_0 is nonsinusoidal. In addition to the fundamental component, $I_{01,m} \sin \omega t$, varying with an angular frequency ω, the magnetizing

current i_0 contains odd harmonics*, $I_{0k,m} \sin k\omega t$, varying with an angular frequency $k\omega$, where k stands for the integers 3, 5, 7, 11, 13, and so on,

$$i_0 = I_{01,m} \sin \omega t + \sum_k I_{0k,m} \sin k\omega t$$

Distortion in the waveform of i_0 increases (the odd harmonics grow in amplitude) as the magnetization characteristic $\Phi = f(i_0)$ becomes progressively more nonlinear.

In three-phase transformers, the nonlinearity of the magnetization characteristic leads to far more complex effects,

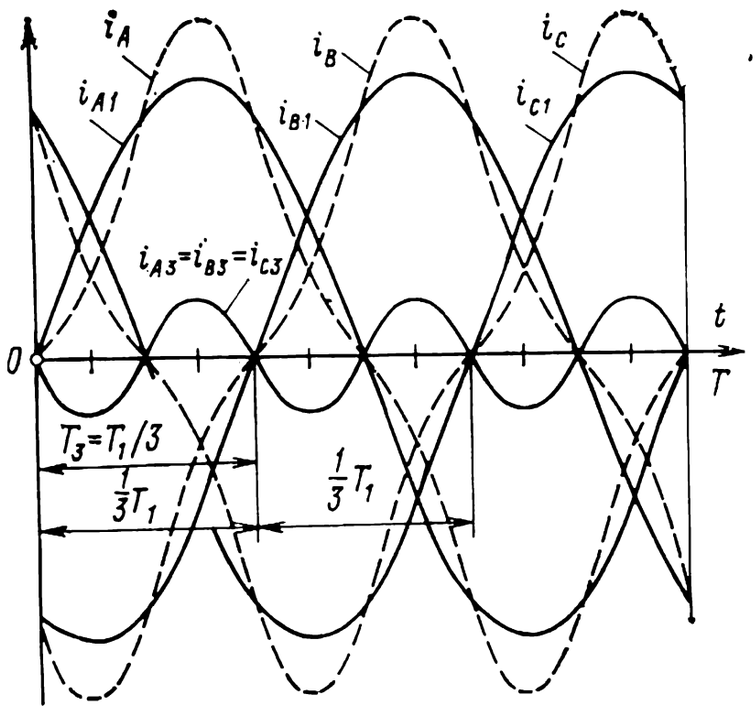

Fig. 4-11 Harmonic components of a symmetrical set of three-phase currents

and the manner in which they manifest themselves depends on the type of winding connection and the core design. Three-phase transformation may be accompanied by distortion in the sinusoidal waveshape not only of the magnetizing currents, but also of the magnetic fluxes and phase voltages.

Before going any further, it appears worth while recalling some features of the harmonic components in symmetrical three-phase systems of emfs, voltages, currents and fluxes.

---

* Here and elsewhere, only the reactive components of the no-load current are considered.

A symmetrical three-phase system has three sets of nonsinusoidal phase quantities (currents, voltages, and fluxes) that, at any instant, are equal in magnitude, waveform and fundamental frequency, but are separated in time-phase by one-third of a period $T_1 = 2\pi/\omega$. A symmetrical three-phase system of nonsinusoidal currents i_A, i_B, and i_C is shown in Fig. 4-11.

The fundamental terms of the phase quantities (say, currents) are likewise separated in time-phase by a third of a cycle and form a symmetrical system that has a *positive phase sequence*, PPS (Fig. 4-11)

$$i_{A1} = \sqrt{2}\, I_{A1} \sin \omega t$$

$$i_{B1} = \sqrt{2}\, I_{A1} \sin (\omega t - 2\pi/3)$$

$$i_{C1} = \sqrt{2}\, I_{A1} \sin (\omega t + 2\pi/3)$$

The sum of phase quantities (say, currents) in the case of the positive phase sequence is always zero

$$i_{A1} + i_{B1} + i_{C1} = 0 \qquad (4\text{-}1)$$

This can readily be proved if we write the phase quantities (say, currents) as a symmetrical set of complex quantities

$$\dot{I}_{A1}, \quad \dot{I}_{B1} = \dot{I}_{A1} \exp (-j2\pi/3),$$

$$\dot{I}_{C1} = \dot{I}_{A1} \exp (j2\pi/3)$$

Similar symmetrical systems with a positive or negative phase sequence are formed by all harmonics whose order k is not a multiple of three (that is, other than *triplen* harmonics*)

$$k = 6c \pm 1 \qquad (4\text{-}2)$$

where $c = 0, 1, 2, 3, \ldots$.

Thus,

$$i_{Ak} = \sqrt{2}\, I_{Ak} \sin k\omega t$$

$$i_{Bk} = \sqrt{2}\, I_{Ak} \sin k(\omega t - 2\pi/3) = \sqrt{2}\, I_{Ak} \sin (k\omega t \mp 2\pi/3)$$

$$i_{Ck} = \sqrt{2}\, I_{Ak} \sin k(\omega t + 2\pi/3) = \sqrt{2}\, I_{Ak} \sin (k\omega t \pm 2\pi/3)$$

---

* Triplen harmonics refer to all harmonics which are multiples of three.

When $k = 6c + 1$, in which case the upper signs in the arguments of the sines apply, a positive phase sequence of quantities (say, currents) is formed. When $k = 6c - 1$, in which case the lower signs in the arguments of the sines apply, a *negative phase sequence* (NPS) of quantities (say, currents) is formed. The sum of the kth harmonics of the phase quantities is likewise equal to zero

$$i_{Ak} + i_{Bk} + i_{Ck} = 0 \tag{4-3}$$

The harmonics of phase quantities, whose order is an integral multiple of three (triplen harmonics),

$$k = 6c + 3 \tag{4-4}$$

where $c = 0, 1, 2, 3, \ldots$, form a *zero phase sequence system* (ZPS). The triplen-harmonic terms are all in phase

$$\begin{aligned} i_{Bk} &= \sqrt{2}\, I_{Ak} \sin k(\omega t \mp 2\pi/3) \\ (Ck) \\ &= \sqrt{2}\, I_{Ak} \sin (k\omega t) = i_{Ak} \\ i_{Ak} &= i_{Bk} = i_{Ck} \end{aligned} \tag{4-5}$$

For the third-harmonic terms, this rule is illustrated in Fig. 4-11.

Now we shall see what restraints are imposed on nonsinusoidal currents by the various winding connection types. All harmonic terms other than triplen, that is, the 1st, 5th, 7th, 11th, 13th, etc. harmonics, form a *positive* or *negative phase sequence* (PPS or NPS) system and exist in the phase windings connected in any manner. In the neutral wire, these harmonics do not exist, because their sum is always zero. The line currents of these harmonic terms, with the windings connected in a delta, are $\sqrt{3}$ times the phase currents, for example

$$I_{AB1} = I_{BC1} = I_{CA1} = \sqrt{3}\, I_{A1} \tag{4-6}$$

where $\dot{I}_{AB1} = \dot{I}_{A1} - \dot{I}_{B1}$.

All triplen harmonics, that is, those harmonics whose order is an integer multiple of three, that is 3, 9, 15, etc., cannot exist in a wye-connection without a neutral wire (Fig. 4-12). In a three-phase star-connected system with the neutral wire, Y_n, available for connection, the neutral

wire carries a current equal to three times the phase current. For example

$$i_{A3} + i_{B3} + i_{C3} = 3i_{A3} \qquad (4\text{-}7)$$

In a three-phase delta-connected system, the third-harmonic phase currents circulate within the closed path formed by the delta, and are not present in the line wires.

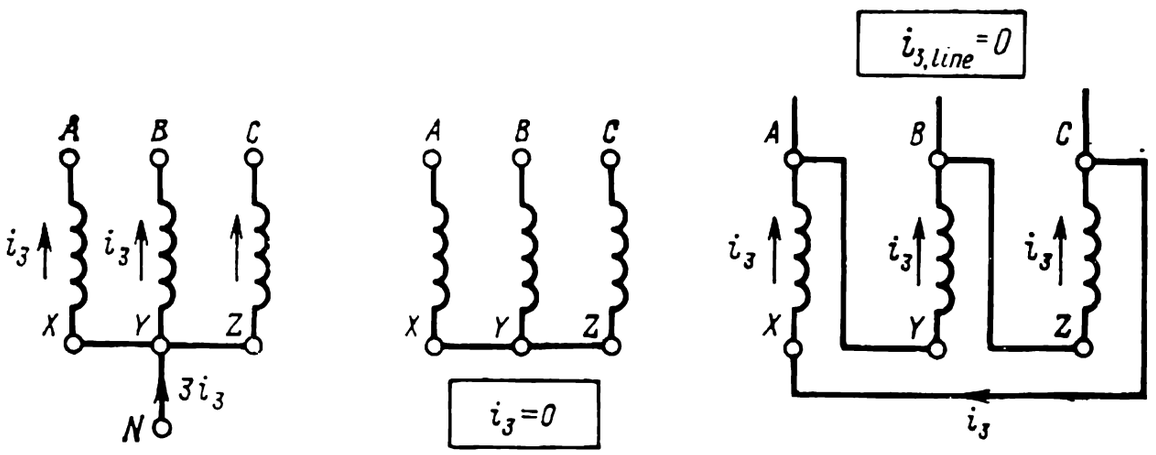

Fig. 4-12 Third-harmonic currents in various forms of winding connections

A similar situation exists for nonsinusoidal fluxes in the various core designs.*

In a three-phase bank of single-phase transformers, such as shown in Fig. 4-13*a*, the third-harmonic phase fluxes $\Phi_{A3} = \Phi_{B3} = \Phi_{C3} = \Phi_3$ have their path completed within the core in the same manner as the fundamental terms. The dependence of $\Phi \approx \Phi_1 + \Phi_3$ on i_0 is representable by the magnetization curve $\Phi = f(i_0)$ (see Fig. 4-13*a*).

In a shell-and-core (five-leg core-type) transformer, the outer limbs play the same part as the neutral wire in a star-connected winding. They form a split "neutral" core which provides a closed path for the third-harmonic fluxes. In each outer limb, the third-harmonic flux is $3\Phi_3/2$.

The outer limbs also provide a closed path for the fundamental fluxes Φ_{A1}, Φ_{B1}, and Φ_{C1}. Therefore, the dependence of the nonsinusoidal flux $\Phi \approx \Phi_1 + \Phi_2$ on i_0 may, to a first approximation, be deemed similar to the magnetization characteristic of a shell-and-core transformer with a sinusoidal flux (see Fig. 4-13*a*).

* In our further discussion, we shall only be concerned with the fundamental and third-harmonic terms.

In a three-phase core-type transformer which has no "neutral" core in the form of outer limbs, the third-harmonic phase fluxes (Fig. 4-13*b*) have their path completed through the tank walls and run into the appreciable opposition presented by nonmagnetic gaps. Because of this, the reluctance seen by the third-harmonic fluxes is tens of times

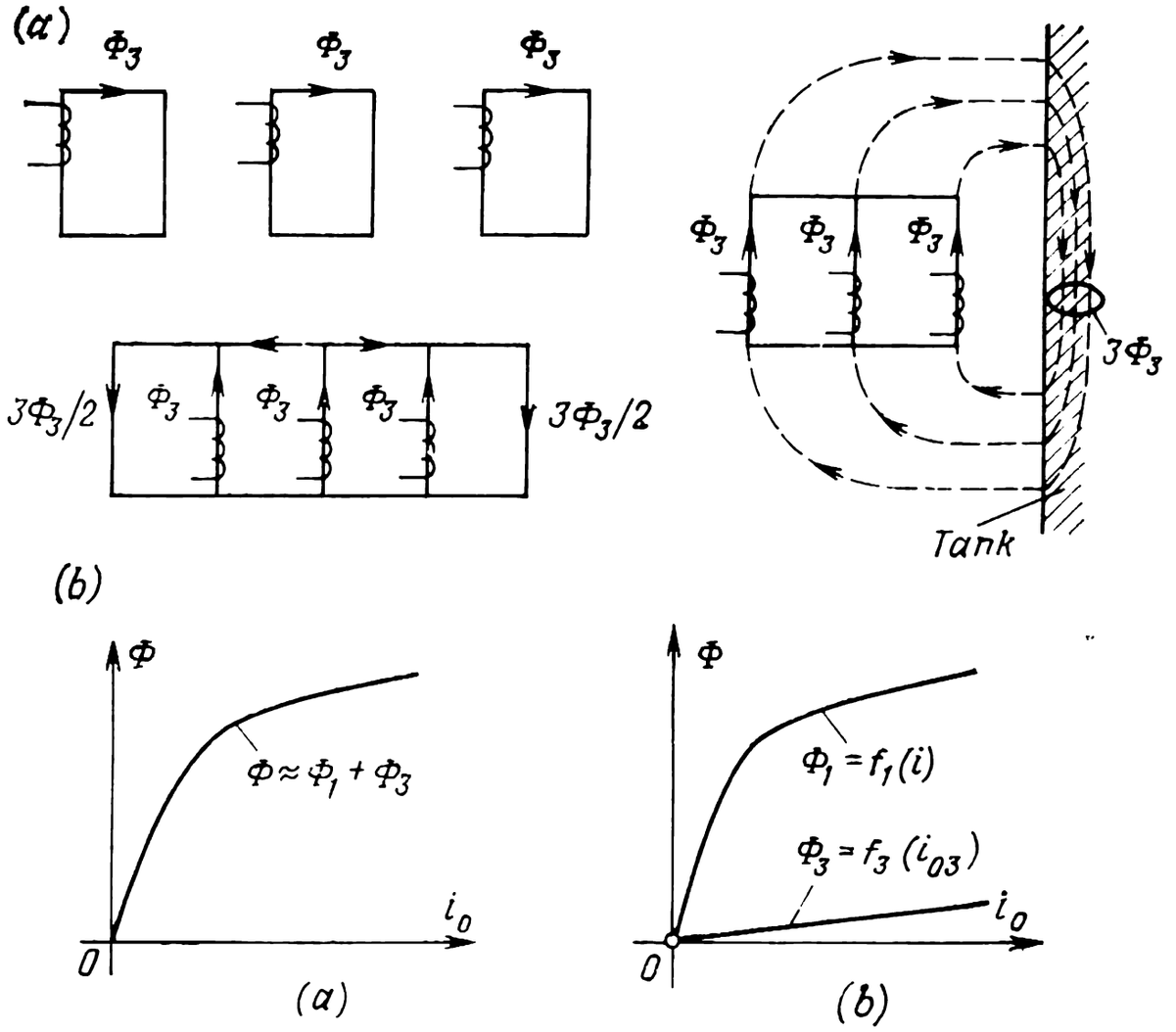

Fig. 4-13 Third-harmonic fluxes in various core designs

higher than that seen by the fundamental fluxes traversing a closed path within the core. In determining the fundamental and third-harmonic terms, we have to invoke different magnetization characteristics. For the third-harmonic flux, this is the linear magnetizing characteristic, $\Phi_3 = f_3(i_3)$. For the fundamental flux, this is the nonlinear magnetization characteristic, $\Phi_1 = f_1(i_0)$, derived for the sinusoidal flux upon replacing i_0 with $(i_0 - i_3)$ which gives rise to the mmf associated with the fundamental flux (Fig. 4.13*b*)*.

---

* This is true, if we consider the fundamental and third-harmonic terms only.

Now we shall examine the waveforms of magnetizing currents, fluxes and voltages associated with the various winding connections and core designs, assuming that at no-load the transformer is energized from the HV side.

1. A three-phase bank of single-phase transformers. Δ/Y connection. With the supply voltage impressed on the delta-connected HV side, the phase voltage is the same as the sinusoidal line voltage. Therefore, all the single-phase transformers in the bank are connected to carry a sinusoidal voltage, and they are magnetized in the same manner as an individual single-phase transformer is magnetized with a sinusoidal voltage (see Sec. 2-5). In other words, the flux varies sinusoidally and the magnetizing phase current, nonsinusoidally. The magnetizing current has the waveshape shown in Fig. 2-4.

The line conductors carry harmonic currents whose order is not a multiple of three (especially, the fundamental term $i_{01,\text{line}}$). Their rms values are $\sqrt{3}$ times the rms values of the phase quantities

$$I_{01,\text{line}} = \sqrt{3}\, I_{01}$$

[see Eq. (4-6)]. The triplen harmonics (especially i_{03}) traverse a closed path within the delta, and are not present in the line conductors (see Fig. 4-12). Because the phase fluxes contain solely the fundamental terms (Φ_{A1}, Φ_{B1}, and Φ_{C1}), the foregoing fully applies to delta-wye-connected three-phase transformers of both the shell-and-core and the core type.

2. A three-phase bank of single-phase transformers. Y-Y and Y-Δ connections. If the HV side is energized with sinusoidal line voltages, the phase voltages may contain both the fundamental terms and triplen harmonics, whereas any other odd harmonics (say, the 5th, 7th, etc.) cannot be present in the phase voltages, because they would then be present in the line voltages as well.

The magnetizing currents in a wye connection with the neutral isolated (see Fig. 4-12) may contain all harmonics except the third. If we neglect all harmonics except the fundamental term, we may, with a sufficient degree of accuracy, deem that the magnetizing current is a sinusoidal one, $i_0 \approx i_{01}$ (Fig. 4-14). The magnetic fluxes in a bank of single-phase transformers (see Fig. 4-13) contain only the

fundamental flux and the third-harmonic flux, $\Phi \approx \Phi_1 + \Phi_3$ (if we recall that they will not induce the 5th and 7th harmonic phase voltages).

The waveform of the magnetic flux is determined graphically, using the magnetization curve $\Phi = f(i_0)$ for a sinusoidal magnetizing current, $i_0 \approx i_{01}$. (Actually, this current

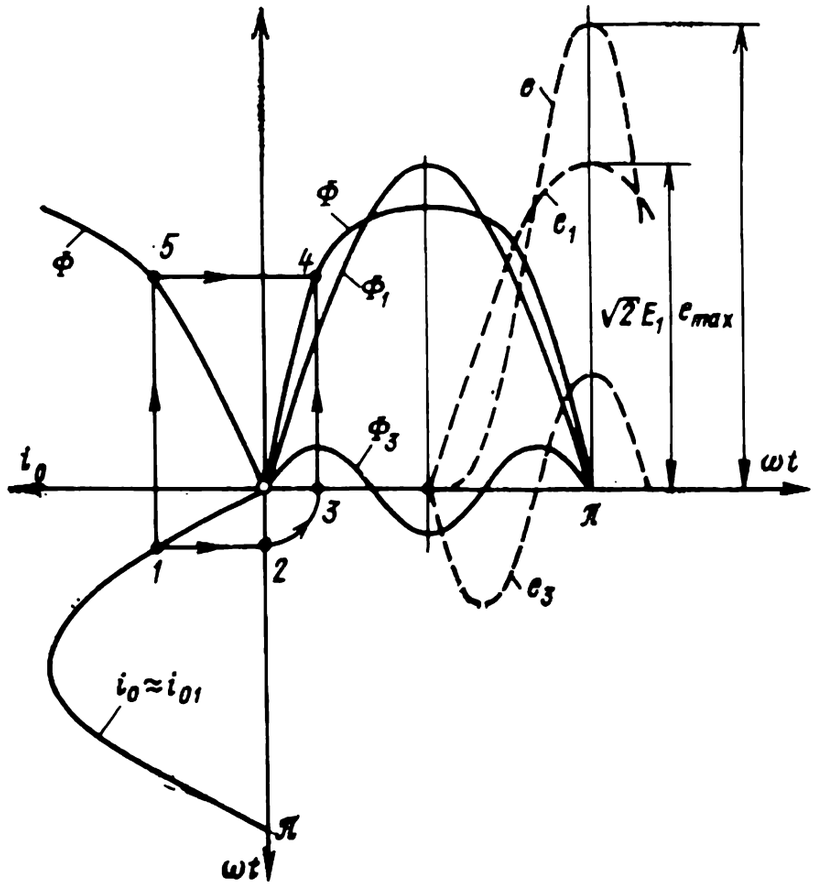

Fig. 4-14 Harmonic components of current, flux and phase emf in a bank of Y/Y single-phase transformers

contains the 5th and 7th harmonics, because these terms are not present in the flux.)

The phase flux in Fig. 4-14 is determined to within the third harmonic. As is seen, the flux waveform is heavily flattened. This leads to a distortion in the sinusoidal waveform of the phase emfs and voltages. With a flattened flux waveform, the phase emf has a well-defined peak (see Fig. 4-14) which may exceed the fundamental peak by as much as 60% to 90%. Accordingly, the transformer insulation must be designed for this peak, and this leads to a more expensive transformer. This is the reason why the Y/Y connection is not used for banks of transformers or where the magnetic circuit is of the shell-and-core form.

From this point of view, it is preferable to use the Δ/Y or Y/Δ connection. If such a transformer is energized on the star-connected HV side, the departure of the fluxes and phase emfs from the sinusoidal waveshape will be negligible. With this form of connection and with any core design, the third-harmonic fluxes are reduced by the third-harmonic currents for which the path is closed within the delta-connected LV winding. The third-harmonic fluxes (Fig. 4-15)

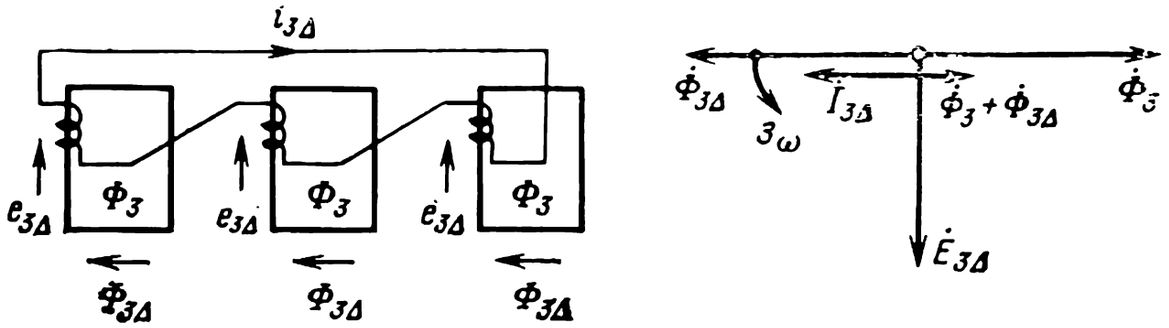

Fig. 4-15 Damping of third-harmonic currents by the currents circulating around a closed delta

induce in the phases of the delta-connected winding the third-harmonic emfs $e_{3\Delta}$ which give rise to third-harmonic currents $i_{3\Delta}$. Because the delta presents a low (practically inductive) impedance. the currents lag behind the emfs by an angle close to $\pi/2$ and set up third-harmonic fluxes $\Phi_{3\Delta}$ which balance out the fluxes Φ_3 almost completely.

3. A three-phase, Y/Y, Y/Y$_n$, Y/Δ, or Y$_n$/Δ-connected core-type transformer. With a Y/Y connection, the HV winding energized by a sinusoidal voltage may carry sinusoidal harmonic currents whose order is not a multiple of three (see Fig. 4-12). Neglecting all the current harmonics, except the fundamental term, the current traversing the HV winding may be treated as sinusoidal, $i_0 \approx i_{01}$.

In a core-type transformer, the harmonic fluxes whose order is a multiple of three have their path completed through large air gaps (see Fig. 4-13*b*). Therefore, given the same mmfs. they are substantially smaller than in a bank of single-phase transformers or in a shell-and-core transformer (see Fig. 4-13*a*). Because Φ_3 is small in comparison with Φ_1 (all the other harmonic fluxes are neglected), it is legitimate to take it that Φ_1 and Φ_3 traversing different closed paths do not affect each other and are set up independently by i_0 and i_{03}, respectively (see Fig. 4-13*b*).

Assigning some value to Φ_1 and using the $\Phi_1 = f_1(i_0)$ curve, we can determine the waveform of i_0. (Plotting point *4* for the i_0 curve is shown in Fig. 4-16.) As is seen, i_0 must contain both i_{01} and i'_{03}:

$$i_0 = i_{01} + i'_{03}$$

However, a star-connected winding can only carry i_{01} which may be construed as the sum of i_0 and i''_{03} equal to $-i'_{03}$, that is

$$i_{01} = i_0 - i'_{03}$$

The current i_0 sets up Φ_1, and $i''_{03} = -i'_{03}$, which balances out the third harmonic of i_0, establishes $\Phi_3 = f_3(i''_{03})$.

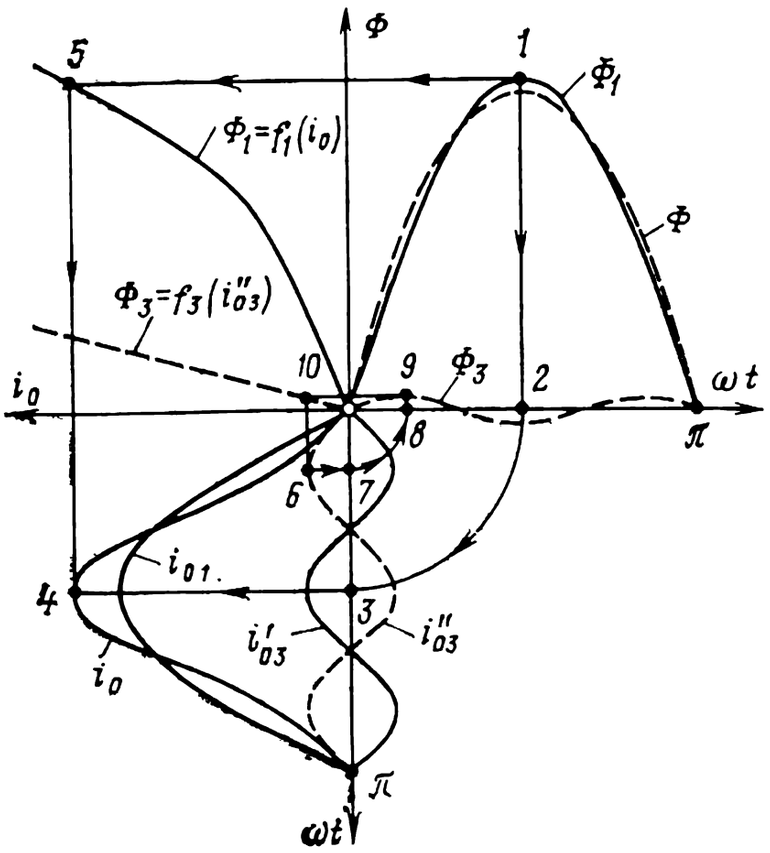

Fig. 4-16 Harmonic components of current and flux in a Y/Y three-phase core-type transformer

As is seen from the plot of Φ_3, this flux has a small peak (point 9), so the flux $\Phi = \Phi_1 + \Phi_3$ is distorted in shape only slightly. Unfortunately, the third-harmonic fluxes in a Y-Y transformer complete their path through the structural parts and tank walls—a fact which might substantially raise the no-load losses.

One way to reduce these extra no-load losses and to improve the waveform of phase voltages, the windings in core-

type transformers are preferably connected Y/Y_n, Y/Δ, or Y_n/Δ. Then the third-harmonic fluxes are reduced still more by the third-harmonic currents traversing a closed path around the delta or in the neutral wire, Y_n. The winding losses due to these currents are smaller than those due to the third-harmonic fluxes in the structural parts and tank walls.

In a delta-connected winding with its neutral wire available for connection, the third-harmonic currents flow in the line wires and have their path completed through the transmission-line capacitances and the neutral wire. They interfere with the operation of nearby communication lines and produce extra losses in the cable sheath because, as follows from Ampere's circuital law, their external magnetic field is non-zero.

For this reason, the Y/Y_n-0 connection is only used in small transformers supplying local loads. In all other cases, a relevant standard recommends to use the Y/Δ-11 or Y_n/Δ-11 connection. The Y/Y connection is not considered in this standard at all.

5 Measurement of Transformer Quantities

5-1 The Open-Circuit (No-Load) Test

The transformer quantities, including losses, can conveniently be measured by an *open-circuit* (*no-load*) *test* and a *short-circuit test.*

The performance of a transformer at no-load has already been examined in Chap. 2. The equations for a transformer at no-load, with allowance for the primary impedance Z_1, can be derived from the general equations (3-8), (3-13), (3-19), and (3-20), if we set the load impedance, Z, tending to infinity and the secondary current equal to zero

$$\begin{aligned} \dot{V}_1 &= -\dot{E}_1 + Z_1\dot{I}_1 = \dot{I}_1 (Z_1 + Z_0) \\ -\dot{V}_2' &= -\dot{E}_2' = -\dot{E}_1 = Z_0\dot{I}_0 \\ \dot{I}_1 &= \dot{I}_0 \end{aligned} \qquad (5\text{-}1)$$

On open circuit, the load impedance in the equivalent circuit of Fig. 3-6 must be set to infinity, $Z' = \infty$. Recalling [see Eq. (3-33)] that $Z_1 \ll Z_0$, it is legitimate to take it that $Z_1 = 0$ and $\dot{V}_1 = -\dot{E}_1 = Z_0\dot{I}_0$*.

The open-circuit test does not call for expensive equipment which would be necessary if the transformer quantities were measured by tests under load. As its name implies, the open-circuit test is carried out with the secondary open-circuited, and with the test gear arranged as shown in the

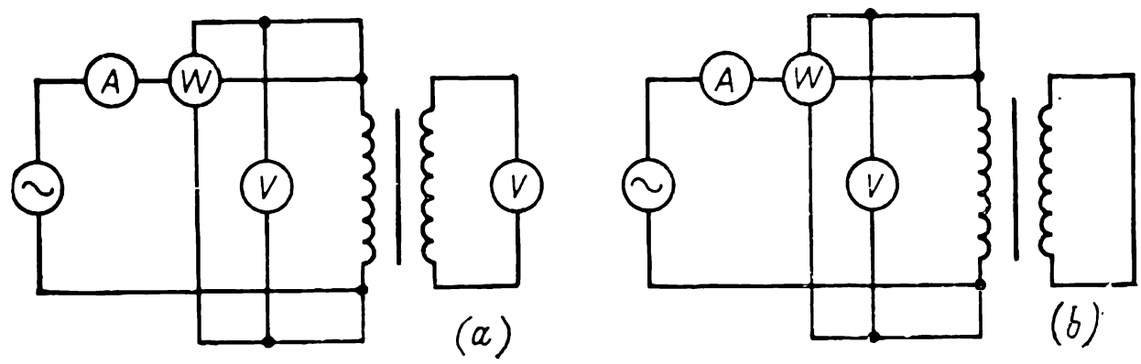

Fig. 5-1 Measuring the parameters of a single-phase transformer by (*a*) an open-circuit test and (*b*) short-circuit test

test set-up in Fig. 5-1*a*. The power rating of the variable-voltage source which energizes the primary may be as low as a few per cent of that of the transformer under test.

During a test, V_1 is gradually raised from zero to 10% above its rated value. Holding the frequency at its rated value, too, the experimenter measures $I_1 = I_0$ (doing this for each phase of a three-phase transformer) and the power P_0 drawn by the transformer under test. Using the data thus obtained, he plots the no-load phase current I_0, the power P_0, and the power factor $\cos\varphi = P_0/V_1I_0$ as functions of the phase voltage V_1. In the case of a three-phase transformer, the plots are constructed for the average phase current

$$I_0 = (I_{0A} + I_{0B} + I_{0C})/3$$

and the average phase voltage

$$V_1 = (V_A + V_B + V_C)/3$$

* We assumed that $Z_1 = 0$ already in Chap. 2, because Z_1 is no more than one-thousandth of Z_0.

Using the values of I_0 and V_1 thus found, the experimenter finds the power factor at no-load, $\cos \varphi_0$.

The following transformer quantities are found by an open-circuit test at the rated voltage.

1. The transformation ratio defined as the ratio of the secondary to the primary voltage at no-load

$$n_{21} = w_2/w_1 = E_{2,R}/E_{1,R} \approx V_{2,R}/V_{1,R}$$

2. The no-load current, found either on a per-unit basis (as a fraction)

$$I_{0,oc} = I_{0,oc}/I_{1,R}$$

or as a percentage

$$I_0 = (I_{0,oc}/I_{1,R}) \times 100\%$$

The no-load current must lie within the limits given in Eq. (3-33).

3. The mutual impedance, defined for $Z_1 \approx 0$ from Eq. (5-1),

$$| Z_0 | \approx V_{1,R}/I_{0,oc} = | Z_{oc} |$$

its resistive component being

$$R_0 = P_{0,oc}/3I_{0,oc}^2 = | Z_0 | \cos \varphi_0$$

and its reactive component being

$$X_0 \approx \sqrt{Z_0^2 - R_0^2} \approx | Z_0 | \sin \varphi_0 \approx | Z_0 |$$

4. The no-load loss. At $V_1 = V_{1,R}$ it does not practically differ from the no-load core loss, $P_{core,\,oc}$, because the primary copper loss under these conditions, $P_{Cu,\,1,\,oc} = 3I_{0,oc}^2 R_1$, is a small fraction of the core loss, $I_{0,\,oc}$ being very small.

As has been shown in Chap. 3, the magnetic flux at rated load remains about the same as it is at no-load (provided V_1 is held unchanged). Therefore, given the rated applied voltage, the core loss at rated load, P_{core}, is approximately equal to the core loss at no-load, $P_{core,\,oc}$, and the total no-load loss, $P_{0,\,oc}$

$$P_{core} = P_{core,\,oc} = P_0 \qquad (5\text{-}2)$$

5-2 The Short-Circuit Test

In this test, the secondary is short-circuited, so that the load impedance is $Z_0 = 0$, and the secondary voltage, V_2, is likewise zero. (In a three-phase transformer, it is presumed that the secondary leads are all commoned so as to give

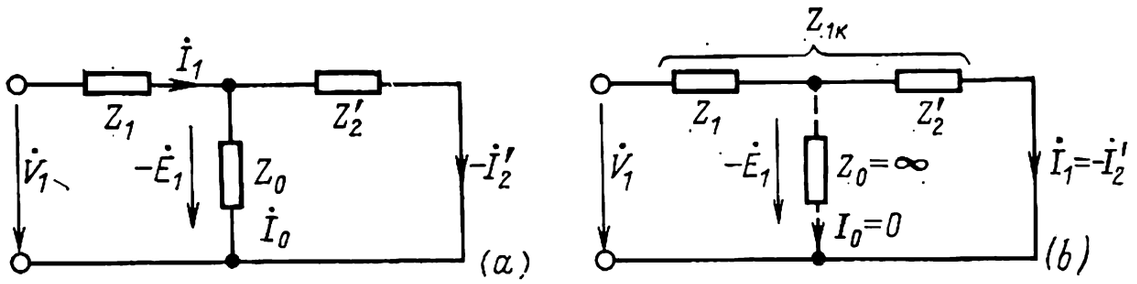

Fig. 5-2 Equivalent circuit of a transformer on a short circuit: (*a*) complete; (*b*) simplified

a balanced short-circuit.) The transformer equations for a short-circuit test can be derived from the general equations (3-8), (3-13), (3-19), and (3-20)

$$\begin{aligned} \dot{V}_1 &= -\dot{E}_1 + Z_1\dot{I}_1 \\ -\dot{E}_1 &= -\dot{E}_2' = -Z_2'\dot{I}_2' = Z_0\dot{I}_0 \\ \dot{I}_1 &= \dot{I}_0 - \dot{I}_2' \end{aligned} \tag{5-3}$$

Using the above equations or the equivalent circuit in Fig. 5-2*a* drawn for the short-circuit test, we can find the primary and secondary currents, the magnetizing current, and mutual emf on short-circuit

$$\begin{aligned} \dot{I}_1 &= \frac{\dot{V}_1}{Z + Z_2'Z_0/(Z_2' + Z_0)} = \dot{V}_1/Z_{sc} \approx \dot{V}_1/(Z_1 + Z_2') \\ -\dot{I}_2' &= \dot{I}_1 Z_0/(Z_2' + Z_0) \approx \dot{I}_1 \\ \dot{I}_0 &= \dot{I}_1 Z_2'/(Z_2' + Z_0) \approx (\dot{V}_1/Z_0)(Z_2'/Z_{sc}) \\ &= \dot{I}_{0,oc} Z_2'/Z_{sc} \\ -\dot{E}_1 &= Z_0\dot{I}_0 \approx Z_0\dot{I}_{0,\,oc} Z_2'/Z_{sc} = \dot{V}_1 Z_2'/Z_{sc} \end{aligned} \tag{5-4}$$

where

$$\begin{aligned} Z_{sc} &= Z_1 + Z_2' Z_0/(Z_2' + Z_0) \approx Z_1 + Z_2' \\ &= R_{sc} + jX_{sc} \\ R_{sc} &\approx R_1 + R_2' \\ X_{sc} &\approx X_1 + X_2' \end{aligned} \tag{5-5}$$

is the short-circuit impedance, resistance and reactance of the transformer (that is, the impedance of a transformer with its secondary short-circuited, as seen by the supply line).

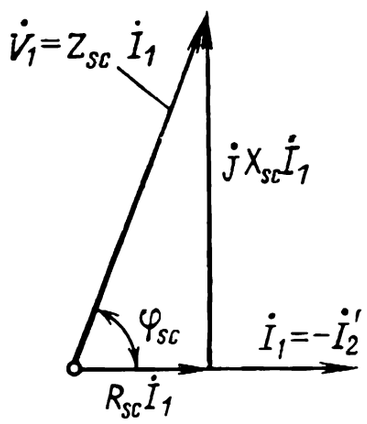

Fig. 5-3 Phasor diagram of a transformer with its secondary short-circuited ($I_0 \approx 0$)

The approximate expressions for I_1, I_2', I_0 and E_1 have been derived for $I_0 \ll I_1$, $|Z_1| \ll |Z_0|$, and $|Z_2'| \ll |Z_0|$ [see Eq. (3-33)], and are fairly accurate. The corresponding equivalent circuit is shown in Fig. 5-2*b*, and the corresponding phasor diagram in Fig. 5-3. As is seen from the phasor diagram, the short-circuit voltage $\dot{V}_1 = Z_{sc}\,\dot{I}_1$ is the hypothenuse of a triangle whose legs are the active voltage $R_{sc}\dot{I}_1$ and the reactive voltage $jX_{sc}\,\dot{I}_1$.

The right-angled voltage (or impedance) triangle drawn for the short-circuit condition is referred to as the *short-circuit triangle*, and the angle

$$\varphi_{sc} = \arctan\,(X_{sc}/R_{sc})$$

is called the *short-circuit angle*. On setting also [see Eq. (3-33)]

$$Z_1 \approx Z_2' = Z_{sc}/2 \tag{5-6}$$

we will obtain still simpler expressions for the magnetizing current and emf

$$\begin{aligned} \dot{I}_1 &= -\dot{I}_2' = \dot{V}_1/Z_{sc} \\ \dot{I}_0 &= \dot{V}_1/2Z_0 = \dot{I}_{0,oc}/2 \\ -\dot{E}_1 &= Z_0\dot{I}_{0,oc}/2 = \dot{V}_1/2 \end{aligned} \tag{5-7}$$

Hence it follows that the referred secondary current on short circuit does not differ from the primary current, which is also true of the rated-load condition; the magnetizing current is about half as large as the no-load (open-circuit) current with the same primary voltage applied; the mutual emf is about half as large as the open-circuit primary voltage or emf.

If the secondary is short-circuited with the rated primary voltage applied, $V_1 = V_{1,R}$, then the transients (to be discussed in Sec. 13-2) will give rise to short-circuit primary and secondary currents [see Eqs. (5-6) and (5-7)] dangerous to the transformer. On a per-unit basis [see Eq. (3-33)] these currents are

$$I_{*2} = I_{*1} = V_{*1,R}/|Z_{*,sc}| = 7 \text{ to } 16 \qquad (5.8)$$

that is, they are 7 to 16 times as heavy as the rated currents in the windings.

If such currents were allowed to exist for a long time, the resultant temperature rise would impair the electrical and mechanical strength of the insulation. For this reason, a short-circuit test is conducted at a reduced primary voltage whose value is chosen such that the currents in the windings could not exceed their rated values.

On a per-unit basis, this voltage should not exceed

$$V_{*1} < V_{*1,sc} = |Z_{*sc}| I_{*1,R} = |Z_{*,sc}| = 0.06 \text{ to } 0.14$$

A likely set-up for a short-circuit test is shown in Fig. 5-1*b*. As in the open-circuit test, it does not require any bulky load resistors or a large test voltage source. (With the short-circuit current adjusted to the rated value, the power rating of the test source is not over 0.06 to 0.14 of the power rating of the transformer under test.) The voltage is gradually raised from zero to anywhere from 0.06 to 0.14 of the rated primary voltage. While holding the frequency at its rated value, $f = f_{rated}$, readings are taken of the same quantities as in the open-circuit test, namely the primary current I_1 and the power drawn by the transformer, P_{sc}.

Using these readings, I_1, P_{sc} and $\cos \varphi_{sc}$ are plotted as functions of the phase voltage V_1, and the plots thus obtained are used to determine graphically $V_{1,sc}$, P_{sc} and $\cos \varphi_{sc}$ at the rated primary current, $I_1 = I_{1,R}$. For a three-phase transformer, the plots are constructed for the average phase current I_1 and the average phase voltage V_1, and the power

factor is found from the average values of I_1 and V_1 as

$$\cos \varphi_{sc} = P_{sc}/3V_1I_1$$

With the current maintained at its rated value, the short-circuit test yields the following transformer quantities.

1. The short-circuit impedance from Eq. (5-7) as

$$| Z_{sc} | = V_{1.\,sc}/I_{1,R}$$

its resistive component

$$R_{sc} = P_{sc}/3I_{1,R}^2 = | Z_{sc} | \cos \varphi_{sc}$$

and its reactive component

$$X_{sc} = \sqrt{| Z_{sc}^2 | - R_{sc}^2} = | Z_{sc} | \sin \varphi_{sc}$$

The resistive component is the sum of the winding resistances, $R_{sc} = R_1 + R_2'$. During a short-circuit test, it is important to note the winding temperature θ at which R_{sc} is measured. The measured value of R_{sc} is then adjusted to a temperature of 75°C:

$$R_{sc,\,75} = R_{sc}\,[1 + 0.004\,(75 - \theta)]$$

The reactive component of the short-circuit impedance is the sum of the leakage inductances, $X_{sc} = X_1 + X_2'$, which, as has been explained in Chap. 3, are independent of the currents traversing the respective windings. For the same reason, X_{sc} is independent of the current at which it is measured.

The short-circuit impedance and power factor are likewise adjusted to a temperature of 75°C:

$$| Z_{sc,\,75} | = \sqrt{R_{sc,\,75}^2 + X_{sc}^2}$$

$$\cos \varphi_{sc,\,75} = R_{sc,\,75}/| Z_{sc,\,75} |$$

2. The short-circuit loss P_{sc}. At $I_1 = I_{1,R}$, it does not practically differ from the copper losses in the primary and secondary windings carrying rated currents

$$P_{Cu,R} = P_{Cu,\,1,R} + P_{Cu,\,2,R} = 3R_1I_{1,R}^2 + 3R_2I_{2,R}^2$$
$$= 3R_1I_{1,R}^2 + 3R_2'I_{2,R}'^2 = 3R_{sc}I_{1,R}^2$$

because the copper loss is many times the short-circuit core loss, $P_{core,\,sc}$.

With $V_{1,\,sc}$ equal to 0.06 to 0.14 of $V_{1,\,R}$, the short-circuit primary emf is

$$E_{1,\,sc} = V_{1,\,sc}/2 = 0.03V_{1,\,R} \text{ to } 0.07V_{1,\,R}$$

The short-circuit flux and induction in the core, which are proportional to $E_{1,\,sc}$, amount to anywhere between 0.03 and 0.07 of their open-circuit values. The short-circuit core loss, which is proportional to the magnetic flux density squared, ranges between 0.9×10^{-3} and 5×10^{-3} of the core loss under rated conditions, and between 2×10^{-4} and 12×10^{-4} of the copper loss also under rated conditions.

3. The impedance voltage. It is defined as the voltage that must be applied to one of the windings, with the other short-circuited, so as to circulate rated current at a temperature of 75°C, with the windings connected as for rated voltage operation. If this voltage is applied to the primary winding, the impedance voltage expressed in absolute units is

$$V_{1,\,sc} = |Z_{sc,\,75}| I_{1,\,R}$$

Usually, the impedance voltage is expressed in per unit or percent of the rated voltage of the winding in which the voltage is measured

$$v_{sc} = V_{*1,\,sc} = V_{1,\,sc}/V_{1,\,R} = Z_{*,\,sc}$$

or (5-9)

$$v_{sc} = (V_{1,\,sc}/V_{1,\,R}) \times 100\%$$

Similarly, the resistive component of the impedance voltage is given by

$$v_a = R_{sc,\,75} I_{1,\,R}/V_{1,\,R} = R_{*,\,sc} = v_{sc} \cos \varphi_{sc}$$

and its reactive component is given by

$$v_r = X_{sc} I_{1,\,R}/V_{1,\,R} = X_{*,\,sc} = v_{sc} \sin \varphi_{sc} \quad (5\text{-}10)$$

(see the phasor diagram in Fig. 5-3).

6 Transformer Performance on Load

6-1 Simplified Transformer Equations and Equivalent Circuit for $I_1 \gg I_0$

In service, the load on a transformer is varying all the time. As a result of variations in the load impedance Z, the secondary current may vary from zero to its rated value, and its phase relative to the secondary voltage also varies.

As has been explained in Sec. 3-7, variations in the secondary current are accompanied by nearly proportionate variations in the primary current, and this leads to slight variations in the magnetic flux. This chapter will deal with the effects that variations in the secondary current may have on the secondary voltage and efficiency of a transformer. Analysis will be carried out for the most frequently encountered load conditions, namely $V_{1,R}$ = constant and $I_1 \gg I_0$.

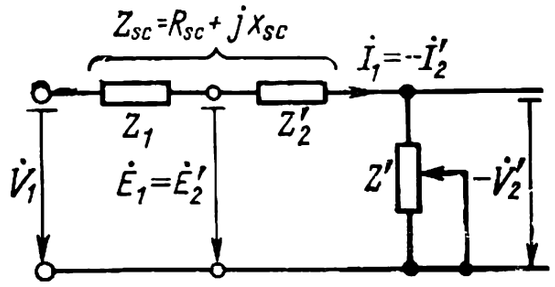

Fig. 6-1 Simplified equivalent circuit of a transformer with $I_1 \gg I_0$

When $I_1 \gg I_0$, we may, as in the case of a short-circuit, set $I_0 = 0$ and $|Z_0| = \infty$. On this assumption, the primary current [see Eq. (3-20)] does not differ from the secondary current referred to the primary $\dot{I}_1 = -\dot{I}_2'$, and the voltage equations for the primary and secondary windings, Eqs. (3-13) and (3-19), may be combined into a single equation

$$\dot{V}_1 = -\dot{V}_2' + Z_{sc}\dot{I}_1 \qquad (6\text{-}1)$$

where $Z_{sc} = Z_1 + Z_2' = R_{sc} + jX_{sc}$ is the short-circuit impedance of the transformer. Therefore, the equivalent circuit in Fig. 3-6 may be simplified by removing the arm carrying the magnetizing current, and the sum of impedances $Z_1 + Z_2'$ may be replaced by Z_{sc}. The simplified equivalent circuit answering Eq. (6-1) appears in Fig. 6-1.

6-2 Transformer Voltage Regulation

Graphically, the dependence of V_2 on I_2, with the power factor $\cos \varphi_2$ and $V_{1,R}$ held constant, can be shown by an *external characteristic*. Plotted in arbitrary units, it takes the form shown in Fig. 6-2. The manner in which V_2 varies with I_2 depends on the character of load. If the load is resistive-inductive ($\varphi_2 > 0$), V_2 decreases as I_2 increases. If the load is predominantly capacitive ($\varphi_2 \approx -\pi/2$), the on-load secondary voltage may exceed its rated no-load value.

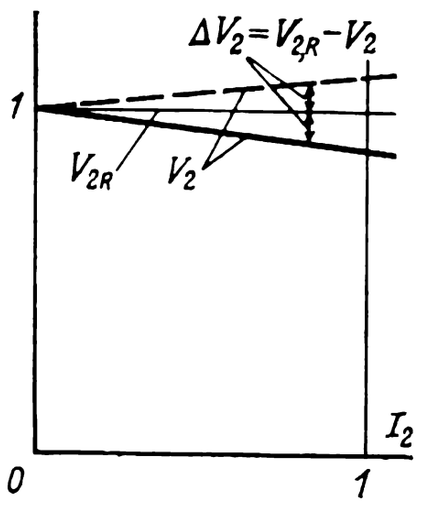

Fig. 6-2 External characteristics, $V_2 = f(I_2)$, of a transformer with V_1 held constant: solid line, resistive-inductive load, $\varphi_2 = \text{const} > 0$; dashed line, resistive-capacitive load, $\varphi_2 = \text{const} < 0$

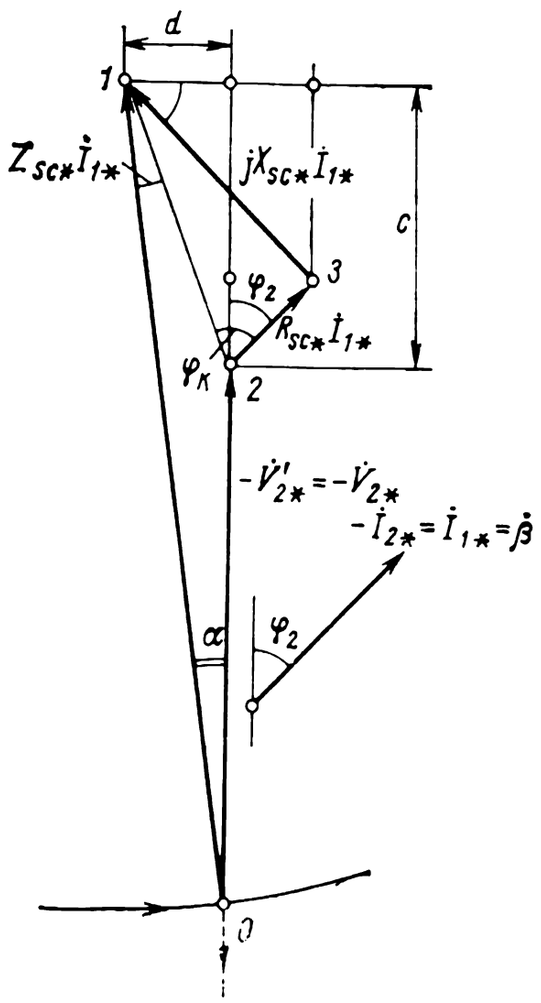

Fig. 6-3 Simplified phasor diagram of transformer voltage regulation, with $I_1 \gg I_0$

A measure of how much changes in I_2 will cause V_2 to change is given by *voltage change* defined as

$$\Delta V_2 = V_{2,R} - V_2$$

with $V_1 = V_{1,R}$ held constant. It is usually expressed in per-unit and known as *voltage regulation*

$$\begin{aligned}\Delta v &= \Delta V_2 / V_{2,R} = \Delta V' / V_{1,R} \\ &= (V'_{2,R} - V'_2)/V_{1,R} \\ &= (V_{1,R} - V'_2)/V_{1,R}\end{aligned}$$

or

$$\begin{aligned}\Delta v &= V_{*1,R} - V_{*2} \\ &= 1 - V_{*2}\end{aligned} \qquad (6\text{-}2)$$

If the per-unit voltage regulation is known, the per-unit secondary voltage can be found from

$$V_{*2} = 1 - \Delta v$$

The voltage regulation equation can be derived from the voltage regulation diagram in Fig. 6-3. (For convenience, the voltage drop phasors $R_{*.sc}I_1$ and $X_{*.sc}I_1$ are shown on an exaggerated scale.)

Construction of the voltage regulation diagram begins at point *2* which is the tip of the $-\dot{V}'_2$ phasor. The $-V'_2$ phasor is drawn through this point in an arbitrary direction, and $\dot{I}_1 = \dot{I}'_2$ is then drawn to make an angle φ_2 with the

$-\dot{V}'_2$ phasor. Now point *2* is used as the origin for the phasor representing the resistive voltage drop $R_{sc}\dot{I}_1$ and the reactive voltage drop $jX_{sc}\dot{I}_1$. Point *1* occurs at the tip of the $\dot{V}_1$ phasor. The value of $-\dot{V}'_2$ is found at the intersection of the $-\dot{V}'_2$ phasor and the circle with point *1* as centre and with $V_{1,R}$ as radius. At the same time, the direction of $\dot{V}_1$ and the angle α between $\dot{V}_1$ and $-\dot{V}'_2$ are found.

The diagram in Fig. 6-3 has been plotted in per-unit and its components are given [see Eq. (5-10)] by the following equations:

$$\begin{aligned}
V_{*1,R} &= V_{1,R}/V_{1,R} = 1\\
I_{*1} &= I_1/I_{1,R} = I_{*2} = I_2/I_{2,R} = I'_2/I_{1,R} = \beta\\
V'_{*2} &= V'_2/V_{1,R}\\
R_{*,sc}I_{*1} &= R_{sc}\,(I_{1,R}/V_{1,R})\,I_{*1} = v_a\beta\\
X_{*,sc}I_{*1} &= X_{sc}\,(I_{1,R}/V_{1,R})\,I_{*1} = v_r\beta
\end{aligned}$$

Let us write the voltage regulation as the difference between $V_{*1,R}$ and V_{*2}:

$$\Delta v = V_{*1,R} - V_{*2} = 1 - V_{*2}$$

Referring to the voltage regulation diagram

$$V_{*2} = V'_{*2} = V_{*1,R}\cos\alpha - c = \cos\alpha - c$$

In turn, because the angle α is negligibly small

$$\cos\alpha = \sqrt{1-\sin^2\alpha} \approx 1 - (\sin^2\alpha)/2 = 1 - d^2/2$$

On expressing the segments c and d as the sum and difference of projections of $R_{*,sc}I_{*1}$ and $X_{*,sc}I_{*1}$ on the V'_{*2} direction and on a direction at right angles to it

$$\begin{aligned}
c &= (R_{*,sc}\cos\varphi_2 + X_{*,sc}\sin\varphi_2)\,I_{*1}\\
&= (v_a\cos\varphi_2 + v_r\sin\varphi_2)\,\beta\\
d &= (X_{*,sc}\cos\varphi_2 - R_{*,sc}\sin\varphi_2)\,I_{*1}\\
&= (v_r\cos\varphi_2 - v_a\sin\varphi_2)\,\beta
\end{aligned}$$

we obtain an expression for the voltage regulation

$$\Delta v = c + d^2/2 = (v_a\cos\varphi_2 + v_r\sin\varphi_2)\,\beta + \frac{(v_r\cos\varphi_2 - v_a\sin\varphi_2)^2\,\beta^2}{2} \qquad (6\text{-}3)$$

As is seen, the secondary voltage regulation depends substantially on the load phase angle φ_2. A plot of Δv as a function of φ_2 with $\beta = 1$ for a transformer with $v_{sc} = 0.1$, $v_a = 0.04$ and $v_r = 0.0918$ is shown in Fig. 6-4. The dashed line gives the same dependence on neglecting the second

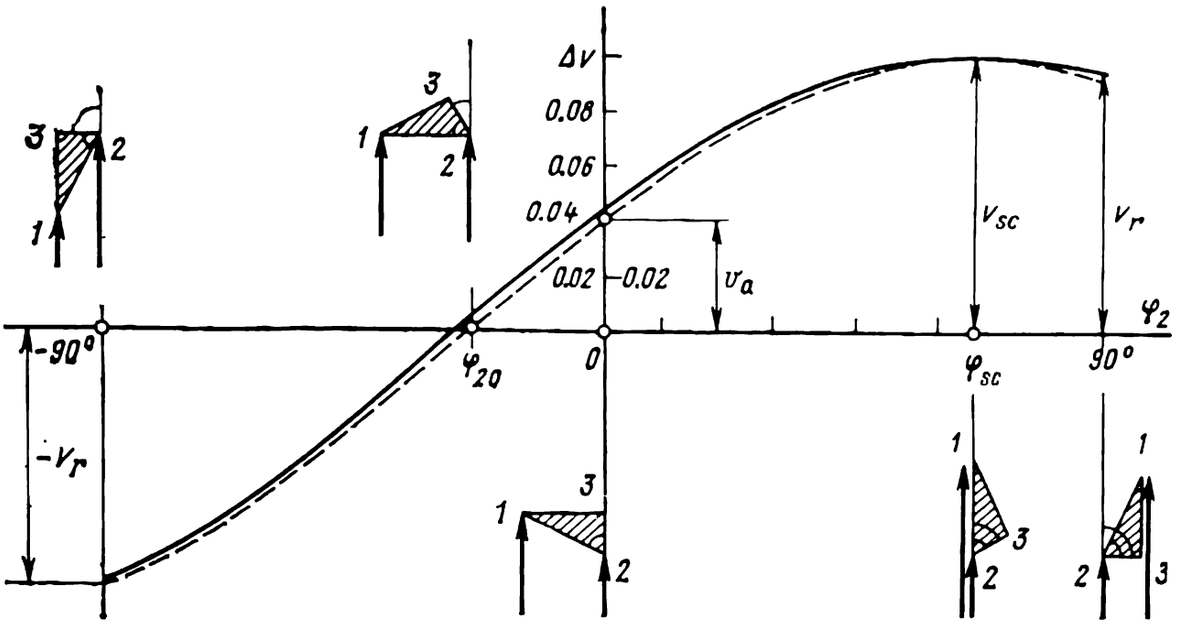

Fig. 6-4 Voltage regulation, Δv, as a function of φ_2, with $I_2 = I_{2,R}$ and $\beta = 1$:
solid line, by Eq. (6-3); and dashed line, with the second term in the equation ignored

term in the equation. Because the inclusion of the second term affects the final result but little, an approximate equation, convenient for analysis,

$$\begin{aligned} \Delta v &= (v_a \cos \varphi_2 + v_r \sin \varphi_2)\, \beta \\ &= \beta v_{sc} \cos (\varphi_{sc} - \varphi_2) \end{aligned} \qquad (6\text{-}4)$$

is used in many cases (especially where v_{sc} is low).

As follows from Eq. (6-4) the voltage regulation is a maximum, $\Delta v = v_{sc}$, when $\varphi_2 = \varphi_{sc}$, because $\cos (\varphi_{sc} - \varphi_2) = 1$. Conversely, the voltage regulation is a minimum, $\Delta v = 0$, when $\varphi_{sc} - \varphi_{2,0} = 90°$ and $\varphi_{2,0} = -(90° - \varphi_{sc})$, because then $\cos (\varphi_{sc} - \varphi_{2,0}) = 0$ (see Fig. 6-4). With some other load phase angles, the short-circuit triangle takes up the characteristic positions shown in Fig. 6-4, such that

$$\Delta v = v_a \quad \text{for} \quad \varphi_2 = 0$$
$$\Delta v = \pm v_r \quad \text{for} \quad \varphi_2 = \pm 90°$$

Because the second term in Eq. (6-3) is small, the dependence of voltage regulation on the relative secondary current β, with φ_2 held constant, is practically linear.

6-3 Variations in Transformer Efficiency on Load

Electric energy should preferably be transformed with as low relative losses as practicable or, which is the same, with as high an efficiency as can be achieved. Here, the efficiency of a transformer is defined as the ratio between the active power delivered to the line on the secondary side and the active power drawn from the supply line on the primary side

$$\eta = P_2/P_1 = m_2 V_2 I_2 \cos \varphi_2 / m_1 V_1 I_1 \cos \varphi_1 \qquad (6\text{-}5)$$

The primary active power may be written

$$P_1 = P_2 + P_{\text{core}} + P_{\text{Cu, 1}} + P_{\text{Cu, 2}}$$

We shall limit ourselves to the operation of a loaded transformer with the rated primary voltage, $V_{1,\text{R}}$, held constant. We shall make the same assumptions as in Sec. 6-2. That is, we shall deem $I_1 \gg I_0$, $I_2 = I_2'$, and $|Z_0| = \infty$. We will also neglect the difference in core loss between operation on load and at no-load and assume that

$$P_{\text{core}} = P_{\text{core, oc}} = P_0$$

where P_0 is the no-load loss with the rated primary voltage applied. Then the copper losses may be expressed in terms of the short-circuit loss P_{sc} at the rated primary current:

$$\begin{aligned} P_{\text{Cu, 1}} + P_{\text{Cu, 2}} &= I_1^2 R_1 + I_2'^2 R_2' = I_1^2 R_{\text{sc}} \\ &= I_{1,\text{R}}^2 R_{\text{sc}} (I_1/I_{1,\text{R}})^2 = P_{\text{sc}} \beta^2 \end{aligned}$$

The secondary active power is given by*

$$\begin{aligned} P_2 &= m_2 V_2 I_2 \cos \varphi_2 = m_1 V_{1,\text{R}} I_2' \cos \varphi_2 \\ &= m_1 V_{1,\text{R}} I_{1,\text{R}} (I_2'/I_{1,\text{R}}) \cos \varphi_2 = S_{\text{R}} \beta \cos \varphi_2 \end{aligned}$$

---

* In setting $V_2' = V_{1,\text{R}}$, we neglect the effect of voltage regulation on the secondary active power.

Substituting the above expressions in Eq. (6-5) gives us the dependence of the efficiency on β:

$$\eta = \frac{P_1 - (P_{core} + P_{Cu.\,1} + P_{Cu.\,2})}{P_1}$$
$$= 1 - \frac{P_0 + \beta^2 P_{sc}}{\beta S_R \cos \varphi_2 + P_0 + \beta^2 P_{sc}} \qquad (6\text{-}6)$$

The effect of the secondary current on the secondary voltage may be accounted for as follows:

$$V_2' = V_{1,R} (1 - \Delta v)$$

and its effect on the iron loss thus:

$$P_{core} = P_0 (E_1/V_{1,R})^2 = P_0 (1 - \Delta v)$$

where, with sufficient accuracy,

$$E_1 = V_{1,R} (1 - \Delta v/2)$$

Accordingly, the equation for the secondary active power may be re-written as

$$P_2 = m_2 V_2 I_2 \cos \varphi_2 = m_1 V_2' I_2' \cos \varphi_2$$
$$= S_R \beta (1 - \Delta v) \cos \varphi_2$$

Then, the efficiency equation may be refined as

$$\eta = 1 - \frac{P_0 (1 - \Delta v) + \beta^2 P_{sc}}{\beta (1 - \Delta v) S_R \cos \varphi_2 + P_0 (1 - \Delta v) + \beta^2 P_{sc}} \qquad (6\text{-}7)$$

Equation (6-7) holds for the entire range of changes in secondary currents. On both open- and short-circuit

$$P_2 = \beta (1 - \Delta v) S_R \cos \varphi_2 = 0$$

and the efficiency reduces to zero. This can be proved formally from Eq. (6-7), recalling that at no-load $\beta = 0$, whereas on short-circuit, $\Delta v = 1 - V_{2*} = 1$, because $V_{2*} = 0$.

Although approximate, Eq. (6-6) derived for $\Delta v = 0$ is sufficiently accurate for the relative secondary current varying from $\beta = 0$ to $\beta \approx 1$. Let us find the value of β at which the efficiency is a maximum. Equating the derivative $d\eta/d\beta$ to zero and simplifying the equation, we obtain

$$P_0 = \beta_{max}^2 P_{sc} = P_{Cu,\,1} + P_{Cu.\,2}$$

or

$$\beta_{max} = \sqrt{P_0/P_{sc}} \qquad (6\text{-}8)$$

This implies that the efficiency of a transformer is a maximum when the load is such that the no-load core loss at rated primary voltage, P_0, is equal to the copper loss, $P_{Cu,\,1} + P_{Cu,\,2}$.

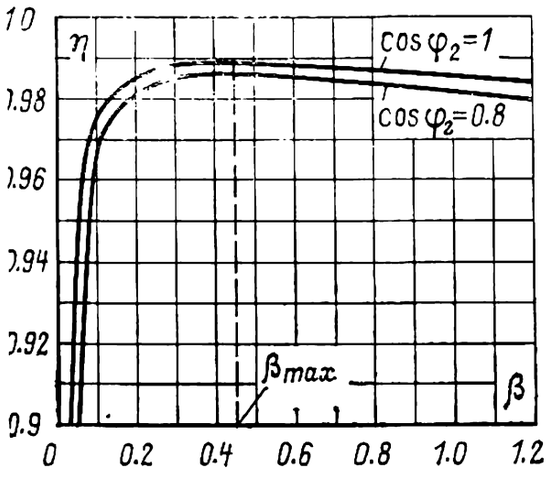

Fig. 6-5 Efficiency, η, as a function of the relative load current

In present-day power transformers, P_0/P_{sc} ranges from 0.2 to 0.25, and the efficiency is a maximum at $\beta = 0.45$ to 0.5.

Efficiency curves for a 1-MVA three-phase transformer for $\cos \varphi_2 = 1$ and $\cos \varphi_2 = 0.8$ are shown in Fig. 6-5. As is seen, $P_0 = 2.45$ kW and $P_{sc} = 12.2$ kW. The efficiency is a maximum at

$$\beta_{max} = \sqrt{2.45/12.2} = 0.45$$

In the range from $0.4\beta_{max}$ to $2.5\beta_{max}$, the efficiency falls off insignificantly. Such variations in efficiency are typical of all power transformers.

7 Tap Changing

7-1 Off-Load Tap Changing

As follows from the analysis given in Sec. 6-2, in the worst case (when the load phase angle φ_2 is equal to the phase angle on a short circuit, φ_{sc}), the per-unit voltage regulation may be anywhere between 0.06 and 0.14. This is far more than is permitted by relevant service codes. To maintain the secondary voltage constant against such variations, tappings on the coils are brought out to terminals so that the number of turns can be changed.

This tap-changing can be effected on either the primary or the secondary side. In transformers operating at a fixed primary voltage, this is done by changing the number of turns on the secondary side, while holding the primary turns unchanged. With this arrangement, the magnetic flux, the core loss, and the magnetizing current (which is a function of the ratio V_1/w_1) remain practically constant.

In transformers operated at constant load (or, which is the same, at a constant secondary current) and a varying primary voltage, V_1, it is preferable to change taps on the primary side so as to maintain the ratio V_1/w_1 nearly constant.

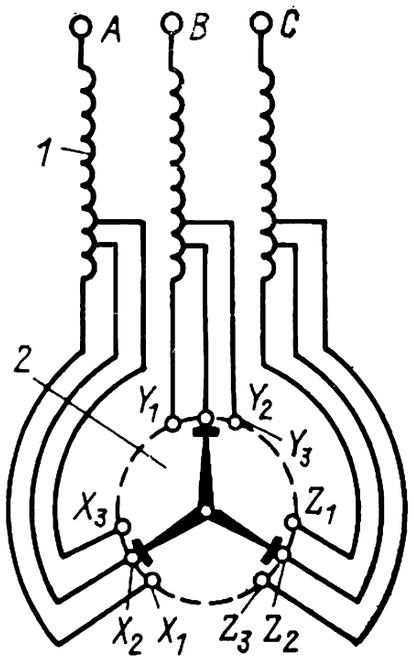

Fig. 7-1 Tap-changing by a switch:
1—transformer winding; *2*—tap-changing switch

All power transformers have tappings on the primary or secondary coils which permit voltage adjustment within ±5%. Low- and medium-power transformers (Fig. 7-1) usually have three taps per phase (+5%, 0, and —5% variations in the turns ratio), whereas transformers of higher power ratings have five taps (+5%, +2.5%, 0, —2.5%, and —5% variations in the turns ratio). Tap stepping operations are performed by contact switches, usually called *tap changers*. Tap changers can be made simple and inexpensive if taps are stepped with the transformer out of circuit and the taps are made at the neutral point of a three-phase star-connected winding (see Fig. 7-1). This avoids a short circuit between adjacent taps or breaking a live circuit during a transition. The operating handle of the tap-changer is passed outside through the tank side.

7-2 On-Load Tap Changing

Voltage adjustment can be made far more accurate and automated if tap changing is done with the transformer left on load, without breaking the circuit. This, of course, calls for a more sophisticated tap-changing arrangement, notably one incorporating what is known as a transition impedance. Impedance in the form of either resistors or iron-core inductors is introduced to limit the circulating current between the two tappings.

Most frequently, resistor transition is used for on-load tap changers. The arrangement of such a tap changer for

one phase is shown in Fig. 7-2. This is seen to be a combination of a fast-acting diverter switch DS, an even tap selector TS_1, and an odd tap selector TS_2. The diverter switch and the transition resistors, R_1 and R_2, are usually installed in a separate oil-filled tank. The diverter switch is designed to carry the current usually developed when the two taps are bridged. The tap selectors may be moved from tap to tap only when their circuits are de-energized. Figure 7-2 shows the diverter switch and the even tap selector in the position when the T_2 tap is brought in circuit. To move to the next, T_3, tap, the odd tap selector should first be moved to that tap, and the diverter switch may then be rotated clockwise. The ensuing sequence of events is as follows: contacts *1* and *2* break, contacts *1* and *3* make, contacts *1* and *3* break, and contacts *3* and *4* make. When fully automated, a tap stepping operation is completed in a matter of a split second.

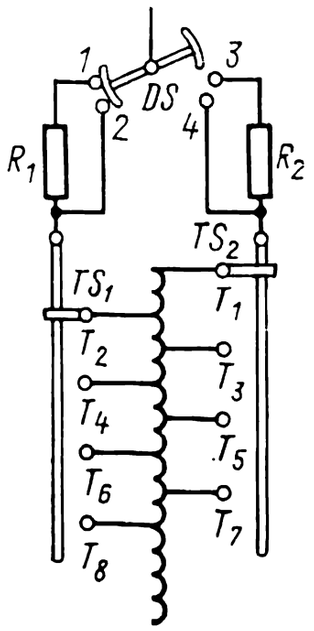

Fig. 7-2 On-load tap changer with current-limiting resistors

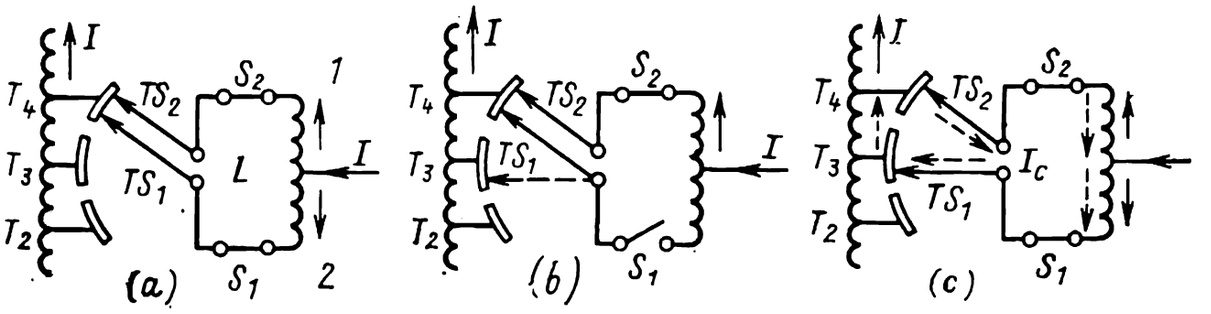

Fig. 7-3 On-load tap-changer with a transition inductor

The arrangement of a tap changer (for one phase) which uses the transition impedance in the form of an iron-cored inductor is shown in Fig. 7-3. In addition to a transition centre-tap inductor (or reactor), L, which is wound in two halves, *1* and *2*, put on a common no-gap core, the arrangement includes two tap selectors, TS_1 and TS_2, which can

move from tap to tap after their circuits have been de-energized, and two on-off switches, S_1 and S_2, to de-energize the respective tap-selector circuits.

The tap selectors and the centre-tap inductor are located in the transformer tank, and the on-off switches are enclosed in a separate tank mounted on the transformer. In Fig. 7-3*a*, the load current is shown passing from tap T_4 through the halves of the inductor in opposition, and hence noninductively (without magnetizing the inductor core). Therefore, the inductor presents to the load current only a small resistance, while its reactance may be ignored. Transition from tap T_4 o, say, tap T_3 may be visualized as consisting of a sequence of seven steps listed in Table 7-1. The most significant steps

Table 7.1 Tap-to-Tap Transition Steps

Step	Position				Figure No.
	TS_1	TS_2	S_1	S_2	
1	T_4	T_4	ON	ON	7-3*a*
2	T_4	T_4	OFF	ON	7-3*b*
3	T_3	T_4	OFF	ON	7-3*b* (dashed)
4	T_3	T_4	ON	ON	7-3*c*
5	T_3	T_4	ON	OFF	
6	T_3	T_3	ON	OFF	
7	T_3	T_3	ON	ON	

are illustrated in Fig. 7-3. In Fig. 7-3*b*, one of the two tap selectors has opened, and the load current is carried through one half of the inductor inductively (setting up a magnetic flux around it). However, the inductor is designed so that the instantaneous reactive voltage drop during this step has but an insignificant effect on the secondary terminal voltage of the transformer. In Fig. 7-3*c* the inductor is shown bridging the two adjacent tappings, T_4 and T_3. The load current is shared equally between the two tappings and passes noninductively in opposition through the halves of the inductor. The tap step voltage is applied to the whole of the inductor winding and the circulating current, I_c, is limited by the total impedance of the inductor whose field is now directed aiding to the mmf due to the circulating current (shown by the dashed lines in the figure).

8 Calculation of Transformer Parameters

8-1 No-Load (Open-Circuit) Current and Mutual Impedance

In Sec. 2-6 it has been shown that the reactive component of the no-load current, I_{0r}, can be deduced from the parameters of the magnetic circuit. It is, however, simpler and more convenient to determine it from the reactive power required to magnetize the transformer. The reactive power may be expressed in terms of either the mutual emf and the reactive component of the no-load current

$$Q_0 = E_1 I_{0r}$$

(for a single-phase transformer) or the core flux. Let us do this with reference to Fig. 8-1.

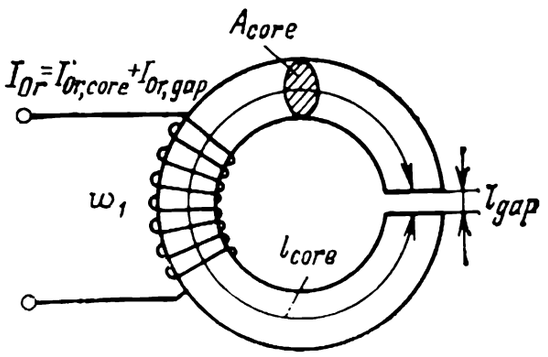

Fig. 8-1 To calculation of reactive currents required to magnetize the core, $I_{0r\ \mathrm{core}}$, and the gaps, $I_{0r,\ \mathrm{gap}}$

In terms of the peak flux, E_1 is given by

$$E_1 = 2\pi f w_1 \Phi_m / \sqrt{2}$$

where

$$\Phi_m = A_{\mathrm{core}} B_m$$

In accord with Eqs. (2-13) and (2-14), the reactive component of no-load current can be written as

$$I_{0r} = I_{0r,\ \mathrm{core}} + I_{0r,\ \mathrm{gap}}$$

The first term on the right-hand side sustains the magnetic potential drop in the core

$$I_{0r,\ \mathrm{core}} = H_m l_{\mathrm{core}} / \sqrt{2}\, w_1$$

and the second term sustains the magnetic potential drop in the air gap

$$I_{0r,\ \mathrm{gap}} = B_m l_{\mathrm{gap}} / \sqrt{2}\, w_1 \mu_0$$

The total reactive power is the sum of the reactive powers required to set up the flux in the core and the gap

$$\begin{aligned} Q_0 = E_1 I_{0r} &= E_1 I_{0r,\ \mathrm{core}} + E_1 I_{0r,\ \mathrm{gap}} \\ &= m_{\mathrm{core}} q_{\mathrm{core}} + A_{\mathrm{core}} q_{\mathrm{gap}} \end{aligned}$$

where $q_{\text{core}} = E_1 I_{0r,\,\text{core}}/m_{\text{core}} = \pi f B_m H_m/\gamma$ is the specific magnetizing power of the core

$q_{\text{gap}} = \pi f B_m^2 l_{\text{gap}}/\mu_0$ is the specific magnetizing power of the air gap

m_{core} = mass of the core

A_{core} = cross-sectional area of the core

γ = density of the core material

The values of the specific magnetizing power as a function of induction (magnetic flux density) for imbricated-joint cores are given in [13]. The reactive power required to magnetize a core of any design is given by

$$Q_0 = q_{\text{leg}} m_{\text{leg}} + q_{\text{yoke}} m_{\text{yoke}} + n_{\text{gap, leg}} q_{\text{gap, leg}} A_{\text{leg}} + n_{\text{gap, yoke}} q_{\text{gap, yoke}} A_{\text{yoke}} \tag{8-1}$$

where m_{leg} and m_{yoke} are the mass of the legs and yokes, A_{leg} and A_{yoke} are the cross-sectional areas of the leg and yoke, and q_{leg}, q_{yoke}, $q_{\text{gap, leg}}$ and $q_{\text{gap, yoke}}$ are the specific magnetizing powers of the legs, yokes, leg gaps, and yoke gaps.

In a single-phase core-type magnetic circuit, $n_{\text{gap, leg}} = 2$ and $n_{\text{gap, yoke}} = 2$. In a three-phase core-type magnetic circuit, $n_{\text{gap, leg}} = 3$, and $n_{\text{gap, yoke}} = 4$.

The active power, equal to the core or no-load loss, is deduced from the specific loss for legs, p_{leg}, and yokes, p_{yoke}, which are given in [13]

$$P_0 = p_{\text{leg}} m_{\text{leg}} + p_{\text{yoke}} m_{\text{yoke}} \tag{8-2}$$

This power is ordinarily calculated for the rated primary voltage, $V_{1,\text{R}} = E_{1,\text{R}}$, only. Once it is found, it is an easy matter to determine the no-load current components (see Sec. 2-8):

$$I_{0r} = Q_0/mV_{1,\text{R}}, \quad I_{0a} = P_0/mV_{1,\text{R}}$$

the no-load current

$$I_0 = \sqrt{I_{0a}^2 + I_{0r}^2}$$

and the components of the mutual impedance

$$Z_0 = V_{1,\text{R}}/I_0, \quad R_0 = P_0/mI_0^2, \quad X_0 = \sqrt{Z_0^2 - R_0^2}$$

✳ 8-2 Short-Circuit Impedance

On a short circuit (see Sec. 5-2), the primary mmf, i_1w_1, and the secondary mmf i_2w_2, balance each other almost completely. Therefore, without running into a serious error, we may deem that $i_1w_1 = -i_2w_2$, and that, on a short circuit, only the leakage flux exists, whereas the mutual flux is non-existent, because

$$i_0w_1 = i_1w_1 + i_2w_2 = 0$$

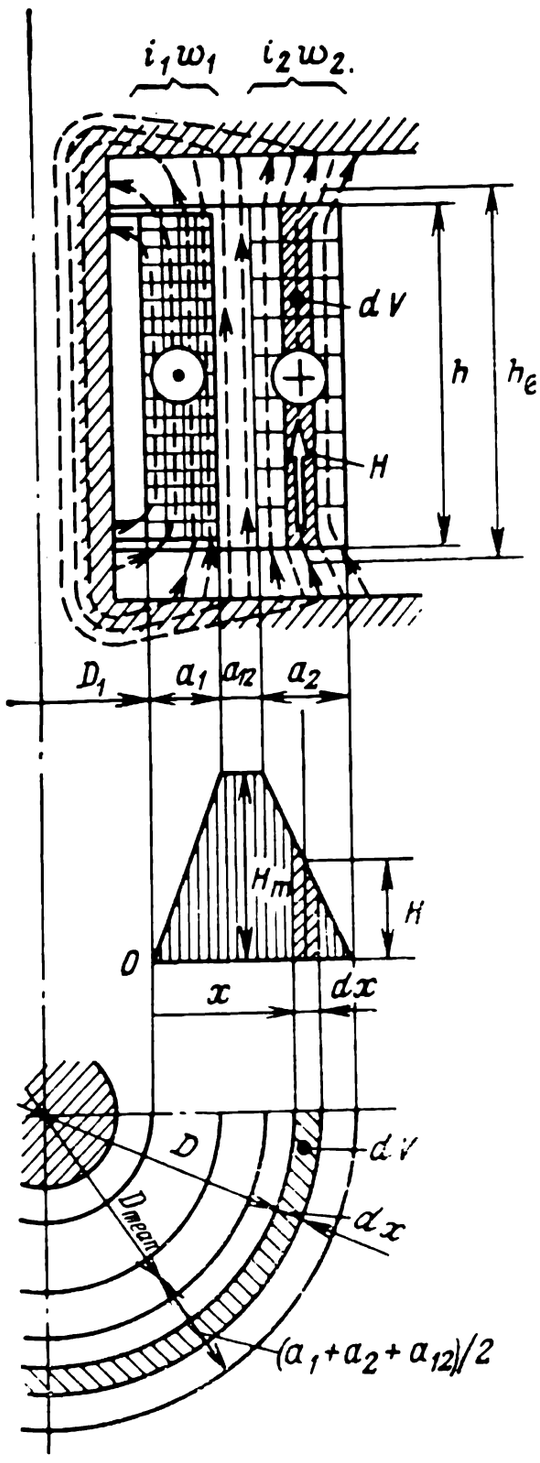

Fig. 8-2 Leakage flux in a transformer on a short-circuit ($i_1w_1 = -i_2w_2$)

The flux pattern applicable to this case, with the windings arranged coaxially, is shown in Fig. 8-2. The magnetic field intensity H within and between the windings acts along the leg axis. With sufficient accuracy, the magnetic field may be taken as being symmetrical about the leg axis. Therefore, the value of H remains practically the same within a distance $D/2$ of the leg axis and along the coil height h. The magnetic intensity distribution along the radial coordinate x reckoned from the inside surface of the coil area is shown in the same figure.

By Ampere's circuital law, the magnetic field intensity is a maximum between the windings ($a_1 < x < a_1 + a_{12}$), where the magnetic lines of force link all of the primary current:

$$H = H_m \approx i_1w_1/h$$

In a first approximation, the magnetic potential drop in a core material with $m_{r,\,\mathrm{core}} = \infty$ and $H_{\mathrm{core}} = 0$ may be

neglected. Within the windings, the magnetic field intensity varies linearly from zero to H_m. For example, when x is anywhere from zero to a_1, the magnetic lines of force link with a current $i_1 w_1 x/a_1$, and the magnetic field intensity is

$$H = i_1 w_1 x/h a_1 = H_m x/a_1$$

The energy associated with the leakage flux established by two magnetically coupled windings may be expressed in terms of the inductances of those windings

$$W = L_1 i_1^2/2 + L_2' i_2'^2/2 + i_1 i_2' L_{12}'$$

Recalling that

$$L_1 = L_{1\sigma} + L_{12}'$$
$$L_2' = L_{2\sigma}' + L_{12}'$$
$$i_1 = -i_2'$$

and

$$L_{1\sigma} + L_{2\sigma}' = L_{sc}$$

we obtain

$$W = (L_{1\sigma} + L_{2\sigma}')\, i_1^2/2 = L_{sc} i_1^2/2 \qquad (8\text{-}3)$$

where L_{sc} is the short-circuit inductance.

The same energy may be expressed in terms of the specific energy of the magnetic field

$$w = HB/2 = \mu_0 H^2/2$$

In determining the energy, the integral may only be taken over the volume $V = \pi D_{mean} (a_1 + a_{12} + a_2)\, h$, occupied by the windings, which encloses the bulk of the leakage energy

$$W = \int_V w\, dV = (\mu_0/2) \int_V H^2\, dV$$

Because H remains the same all the way round the circle with the diameter $D = D_1 + x$ and along the height h, the elementary volume is

$$dV = \pi D h\, dx = \pi\, (D_1 + x) h\, dx$$

With an accuracy sufficient for engineering purposes, the diameter $D = D_1 + x$ may be replaced with a mean diameter

$$D_{mean} = D_1 + (a_1 + a_{12} + a_2)/2$$

After this simplification,

$$W = (\mu_0 h \pi D_{mean}/2) \int_0^{a_1+a_{12}+a_2} H^2 \, dx = (\mu_0/2)\, \pi D_{mean} h a_\sigma H_m^2 \tag{8-4}$$

where $a_\sigma = a_{12} + (a_1 + a_2)/3$.

Equating (8-3) and (8-4) yields an expression which connects the short-circuit inductance to the size and winding data of a transformer

$$L_{sc} = \pi \mu_0 D_{mean} w_1^2 a_\sigma k_R / h \tag{8-5}$$

where

$$k_R = 1 - (a_1 + a_{12} + a_2)/\pi h$$

is the Rogovsky coefficient (after its originator). It minimizes the error in calculations due to the assumptions made.

The short-circuit inductive reactance is given by

$$X_{sc} = (2\pi^2 f \mu_0 D_{mean} a_\sigma w_1^2)\, k_R / h \tag{8-6}$$

The resistive component of the short-circuit impedance is calculated as the sum of the referred resistances of the windings

$$R_{sc} = R_1 + R_2' = R_1 + R_2 (w_1/w_2)^2 \tag{8-7}$$

where $R_1 = \rho_{75} \pi D_{mean} w_1 k_s / A_{w1}$ is the resistance of the primary

$R_2 = \rho_{75} \pi D_{mean} w_2 k_s / A_{w2}$ is the resistance of the secondary

A_{w1}, A_{w2} = cross-sectional area of the primary or secondary turns, respectively

ρ_{75} = resistivity of the wire at 75°C after [13]

k_s = 1.05 to 1.15 is the series-loss coefficient.

9 Relationship Between Transformer Quantities and Dimensions

9-1 Variations in the Voltage, Current, Power and Mass of a Transformer with Size

Suppose we have a range of geometrically similar transformers. Two transformers out of this hypothetical range are shown in Fig. 9-1. Any dimension of any transformer

in this range differs by a factor of k from the like dimension of any other transformer in the range.

Taking any linear dimension, say, the height, l, of the core as the base or reference dimension, we may deem that all the other dimensions of the transformers in a given range are proportional to it. For example, the mean turn diameter, D_{mean}, is about equal to l. The cross-sectional area of any element of a transformer is proportional to the square of the base dimension, $A \sim l^2$. By the same token, the volume of any element is proportional to the base dimension cubed, $V \sim l^3$.

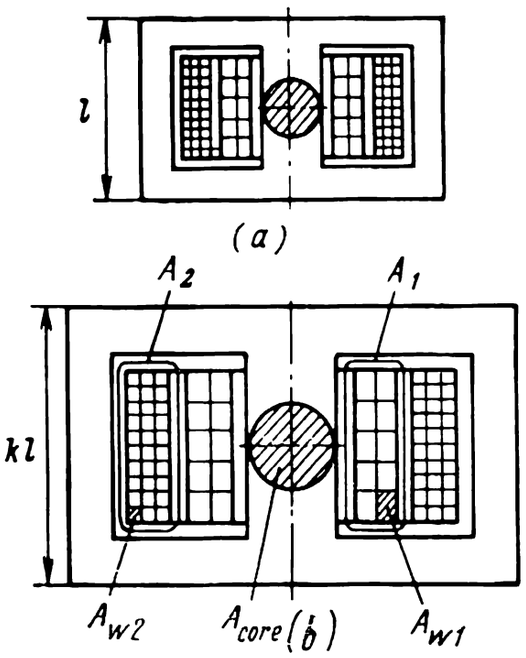

Fig. 9-1 Geometrically similar single-phase transformers

Now let us see how the rated electromagnetic quantities of a transformer are related to its size. Suppose that all the transformers in a given range are fabricated of the same materials and that the magnetic flux density B in the core, the current density J in the windings, and frequency remain always constant.

1. Neglecting the difference between terminal voltage and generated emf, we get

$$V_{1,R} \approx E_{1,R} = (2\pi/\sqrt{2})\, f w_1 B A_{leg} \sim w_1 A_{leg} \sim w_1 l^2 \qquad (9\text{-}1)$$

That is, the primary voltage is proportional to the number of turns in the primary winding and the square of the base dimension.

2. Assuming that as l is varied, the total cross-sectional area of conductors in a winding remains proportional to l^2, we get

$$I_{1,R} = A_1 J/w_1 \sim i^2/w_1 \qquad (9\text{-}2)$$

That is, the primary current is proportional to the square of the base dimension. (Here, A_1 is the total cross-sectional area of the conductors in the winding.)

3. The total (or apparent) power of a transformer

$$S = S_R = V_{1,R} I_{1,R} \sim l^2 w_1 (l^2/w_1) = l^4 \qquad (9\text{-}3)$$

is proportional to the base dimension raised to the fourth power. Importantly, on the assumptions made, the power of the transformer is independent of the number of turns.

4. The mass of the transformers in a range fabricated of the same materials

$$m = \sum \gamma V \sim l^3$$

is proportional to the base dimension cubed.

The mass per unit power

$$m/S \sim l^3/l^4 \sim 1/l \ (\sim 1/S^{1/4})$$

is inversely proportional to the base dimension. (The mass per unit power decreases as power rating goes up.)

9-2 Transformer Losses and Parameters as Functions of Size

1. The total loss of power in a transformer is the sum of the core loss and the copper loss.

The core loss

$$P_{\text{core}} = \sum p_{\text{core}} m_{\text{core}} \sim l^3$$

is proportional to the mass of the core elements, m_{core}, because the specific core loss in similar elements remains unchanged as the physical dimensions are varied.

The copper loss may be expressed in terms of the winding volume

$$V_1 = \pi D_{\text{mean}} A_1$$

and

$$V_2 = \pi D_{\text{mean}} A_2$$

and also the current density J and the resistivity ρ

$$P_{\text{Cu}} = P_{\text{Cu, 1}} + P_{\text{Cu. 2}} = \rho J^2 V_1 + \rho J^2 V_2$$

If the materials remain the same and the current density is held constant, the copper loss is proportional to the base dimension cubed

$$P_{\text{Cu}} = \rho J^2 (V_1 + V_2) \sim l^3$$

Thus, the transformer loss

$$P_{\text{core}} + P_{\text{Cu}} \sim l^3 \qquad (9\text{-}5)$$

is proportional to the base linear dimension cubed.

The specific loss (the total loss divided by total power)

$$(P_{Cu} + P_{core})/S \sim l^3/l^4 \sim 1/l \sim 1/S^{1/4} \qquad (9\text{-}6)$$

is inversely proportional to the base linear dimension or the fourth-power root of the total power. (In high-power transformers, the specific loss is lower.)

The loss per unit of cooling area, A_{cool}

$$(P_{Cu} + P_{core})/A_{cool} \sim l^3/l^2 = l$$

is proportional to the base linear dimension and increases with increasing power rating. This is the reason why high-power transformers must be provided with a well-developed cooling area in the form of ducts in the core and windings.

2. The short-circuit inductive reactance (see Sec. 8-2)

$$X_{sc} \sim w_1^2 D_{mean} a_\sigma / h \sim w_1^2 l \qquad (9\text{-}7)$$

is proportional to the number of turns squared and the base linear dimensions.

The short-circuit resistance

$$R_{sc} = P_{Cu}/I_{1,R}^2 \sim l^3/(l^2/w_1)^2 \sim w_1^2/l \qquad (9\text{-}8)$$

is proportional to the number of turns squared and inversely proportional to the base linear dimension.

The reactive and resistive components of the impedance (short-circuit) voltage are given by

$$X_{*sc} = v_r = X_{sc} I_{1,R}/V_{1,R} \sim (w_1^2 l/w_1 l^2)\,(l^2/w_1) \sim l$$
$$R_{*sc} = v_a = R_{sc} I_{1,R}/V_{1,R} \sim (w_1^2/l)\,(l^2/w_1)\,(1/w_1 l^2) \sim 1/l$$

The short-circuit tangent is

$$\tan \varphi_{sc} = X_{*sc}/R_{*sc} = v_r/v_a \sim 1/l^2 \qquad (9\text{-}9)$$

In other words, as a transformer grows in size, its v_r rises and its v_a falls. This checks well with practice.

3. The reactive and active components of the no-load current (see Sec. 2-6)

$$I_{0r} \sim \oint H_l \, dl/w_1 \sim l/w_1$$
$$I_{0a} = P_{core}/V_{1,R} \sim l^3/w_1 l^2 \sim 1/w_1 \qquad (9\text{-}10)$$

are proportional to the base linear dimension and inversely proportional to the number of turns.

The relative no-load current (or the relative magnetizing power)

$$Q_0/S = I_0 V_{1,R}/I_{1,R} V_{1,R} = I_0/I_{1,R} \sim (l/w_1)(w_1/l_2) = 1/l \qquad (9\text{-}11)$$

is inversely proportional to the base linear dimension.

In commercially available transformers, geometric similarity is never complete, nor can B and J be held constant. Nevertheless, the relationships set forth above are true, at least qualitatively.

As follows from the foregoing, it is advantageous to use transformers with higher power ratings, because they take less materials per unit power, need lower reactive power, and dissipate less heat.

10 Multiwinding Transformers. Autotransformers

10-1 Multiwinding Transformers

(i) Three-Winding Transformers

In a multiwinding transformer, the core carries more than two electrically isolated windings.

Power systems mostly use three-winding transformers to couple electric systems or networks operating at three different voltages, V_1, V_2, and V_3. Three-winding transformers may be single-phase (Fig. 10-1) and three-phase, with their windings connected $Y_n/Y_n/\Delta$-0-11 (Fig. 10-2) and $Y_n/\Delta/\Delta$-11-11.

A three-winding transformer may have either one primary (*1*) and two secondaries (*2* and *3*), or two primaries (*1* and *2*) and one secondary (*3*). Our discussion will be limited to transformers having one primary and two secondaries.

A three-winding transformer does the job of two two-winding transformers one of which connects network (or system) *1* to network *2*, and the other, network *1* to network *3*. Economically, a three-winding transformer is more attractive than two two-winding units. Among other things,

it is less expensive to make and takes up less space at a substation It can transfer power not only from the primary

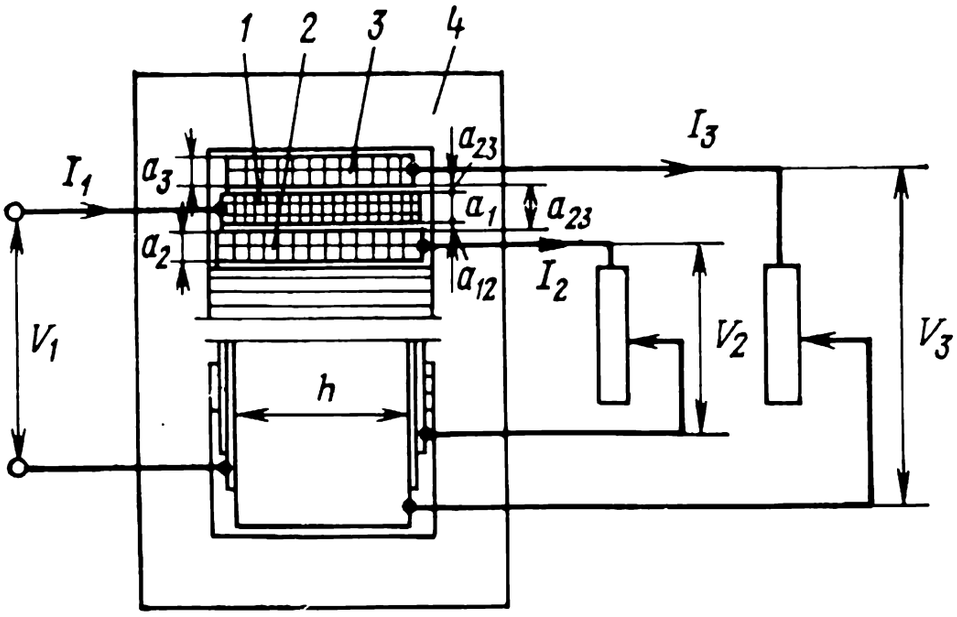

Fig. 10-1 Single-phase, three-winding transformer:
1—primary winding; *2*—secondary winding; *3*—tertiary winding; *4*—shell-and-core-type magnetic circuit

network (*1*) to any of the secondary networks (*2* or *3*), but also directly (by a single transformation step) from one of

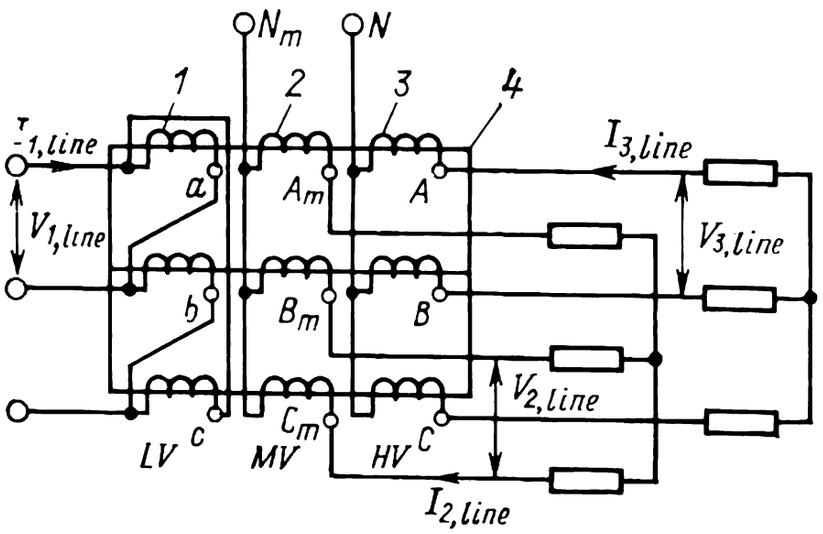

Fig. 10-2 $Y_n/Y_n/\Delta$-0-11 three-phase, three-winding transformer:
1—LV three-phase winding; *2*—MV three-phase winding; *3*—HV three-phase winding; *4*—core-type magnetic circuit

the secondary networks to the other (say, from network *2* to network *3*). With two two-winding transformers, such power transfer necessitates two transformation steps—first from network *2* to network *1*, then from network *1*

to network *3*. Accordingly, the losses are about twice as heavy.

On the demerit side, a three-winding transformer is less reliable. Should any of its windings be damaged, the entire unit must be removed from service. With two two-winding transformers, damage to any of them leaves the other unaffected.

The electromagnetic processes in a three-winding transformer may be described by analogy with a two-winding unit (see Chapters 2 and 3). As a preliminary step, however, its secondary and tertiary quantities must be referred to the primary side, with their values multiplied by the respective turns ratio or its square:

$$\begin{aligned} I'_2 &= I_2 \times (w_2/w_1) \\ I'_3 &= I_3 \times (w_3/w_1) \\ V'_2 &= V_2 \times (w_1/w_2) \\ V'_3 &= V_3 \times (w_1/w_3) \\ |Z'_2| &= |Z_2| \times (w_1/w_2)^2 \\ |Z'_3| &= |Z_3| \times (w_1/w_3)^2 \end{aligned}$$

The mutual flux is set up by a magnetizing current $\dot{I}_0$ which is given by the current equation

$$\dot{I}_1 + \dot{I}'_2 + \dot{I}'_3 = \dot{I}_0 \qquad (10\text{-}1)$$

and the mutual emf is given by

$$-\dot{E}_1 = -\dot{E}'_2 = -\dot{E}'_3 = Z_0\dot{I}_0 \qquad (10\text{-}2)$$

where $Z_0 = R_0 + jX_0$ is the mutual impedance.

The leakage flux is established by a balanced (or symmetrical) set of currents, $\dot{I}'_1$, $\dot{I}'_2$, and $\dot{I}'_3$, where $\dot{I}'_1 = \dot{I}'_1 - \dot{I}_0$.

The leakage emf in each winding is

$$\begin{aligned} \dot{E}_{\sigma 1} &= -jX_1\dot{I}'_1 \approx -jX_1\dot{I}_1 \\ \dot{E}'_{\sigma 2} &= -jX'_2\dot{I}'_2 \\ \dot{E}'_{\sigma 3} &= -jX'_3\dot{I}'_3 \end{aligned}$$

where X_1, X'_2, and X'_3 are the equivalent leakage reactances of the windings, found with allowance for the effect of currents in the other windings.

Formally, the voltage equations for the three windings are written as for a two-winding transformer [see Eqs. (3-13) and (3-19)]:

$$\begin{aligned}
\dot{V}_1 &= -\dot{E}_1 - \dot{E}_{\sigma 1} + R_1\dot{I}_1 = -\dot{E}_1 + Z_1\dot{I}_1 \\
-\dot{E}'_2 &= -\dot{V}'_2 + \dot{E}'_{\sigma 2} - R'_2\dot{I}'_2 = -\dot{V}'_2 + Z'_2(-\dot{I}'_2) \\
-\dot{E}'_3 &= -\dot{V}'_3 + \dot{E}'_{\sigma 3} - R'_3\dot{I}'_3 = -\dot{V}'_3 + Z'_3(-\dot{I}'_3)
\end{aligned} \qquad (10\text{-}3)$$

where

$$\begin{aligned}
Z_1 &= R_1 + jX_1 \\
Z'_2 &= R'_2 + jX'_2 \\
Z'_3 &= R'_3 + jX'_3
\end{aligned}$$

Equations (10-1) through (10-3) apply to the equivalent circuit in Fig. 10-3.

The mutual impedance Z_0 is found by calculation or experiment in exactly the same way as for a two-winding transformer (see Secs. 5-1 and 8-1). The impedances Z_1, Z'_2 and

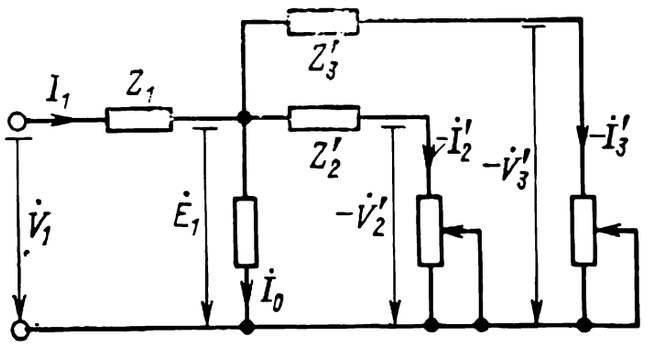

Fig. 10-3 Equivalent circuit of a three-winding transformer

Z'_3 are expressed in terms of the short-circuit impedances Z_{sc12}, Z_{sc13} and Z_{sc23}, as determined by a short-circuit test, using the test set-up shown in Fig. 10-4. $Z_{sc12} = R_{sc12} + jX_{sc12}$ is found with the tertiary winding open-circuited. $Z_{sc13} = R_{sc13} + jX_{sc13}$ is found with the secondary winding open-circuited. Finally $Z_{sc23} = R_{sc23} + jX_{sc23}$ is found with the secondary energized and the primary open-circuited, and is referred to the primary by the equation

$$Z'_{sc23} = Z_{sc23}(w_1/w_2)^2$$

It is to be noted that

$$Z_{sc12} = Z_1 + Z'_2, \quad Z_{sc23} = Z_1 + Z'_3, \quad Z'_{sc23} = Z'_2 + Z'_3$$

Solving the above equations for Z_1, Z_2', and Z_3', we get

$$\begin{aligned} Z_1 &= (Z_{sc12} + Z_{sc13} - Z'_{sc23})/2 \\ Z_2' &= (Z_{sc12} + Z'_{sc23} - Z_{sc13})/2 \\ Z_3' &= (Z_{sc13} + Z'_{sc23} - Z_{sc12})/2 \end{aligned} \tag{10-4}$$

The resistive components of the above impedances are the resistances R_1, R_2' and R_3' of the respective windings (see

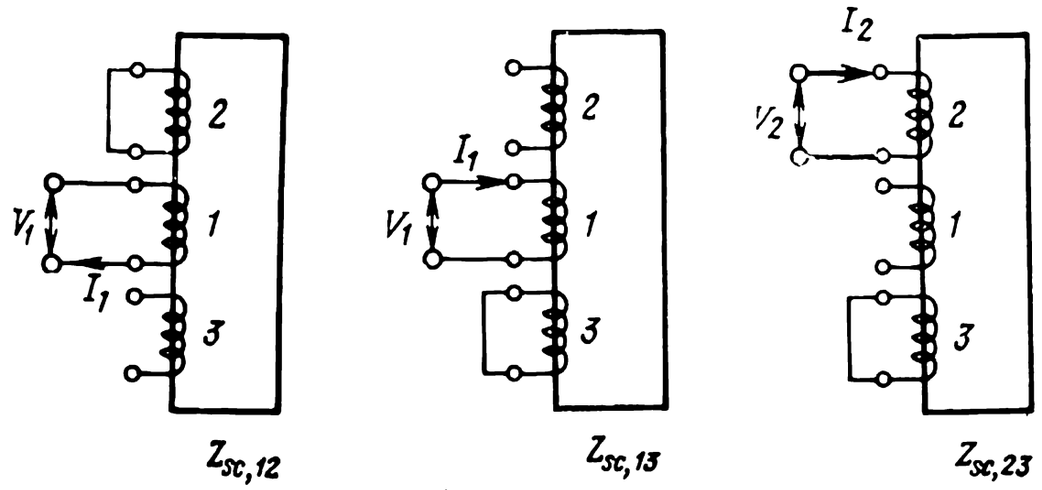

Fig. 10-4 Short-circuit test on a single-phase, three-winding transformer

Sec. 8-2), whereas their reactive components have the meaning of the equivalent leakage inductive reactances of the windings:

$$\begin{aligned} X_1 &= (X_{sc12} + X_{sc13} - X'_{sc23})/2 \\ X_2' &= (X_{sc12} + X'_{sc23} - X_{sc13})/2 \\ X_3' &= (X_{sc13} + X'_{sc23} - X_{sc12})/2 \end{aligned}$$

The secondary and tertiary voltages of a loaded three-winding transformer may be found analytically, using Eqs. (10-1) and (10-3), or graphically, using the phasor diagram shown in Fig. 10-5. On assuming $I_0 \ll I_1$ and deeming $\dot{V}_{1,R}$, $\dot{I}_2$ and $\dot{I}_3$ known in advance, we can find $\dot{E}_1$, V_2' and V_3', and determine the per-unit voltage regulation for the secondary and tertiary windings:

$$\begin{aligned} \Delta v_2 &= (V_2' - V_{1,R})/V_{1,R} \\ \Delta v_3 &= (V_3' - V_{1,R})/V_{1,R} \end{aligned}$$

From the equivalent circuit or the phasor diagram, it is seen that when $Z_1 \neq 0$, the referred secondary voltage de-

pends not only on the referred secondary current, but also on the referred tertiary current (by the same token, V_3' depends not only on I_3' but also on I_2')—a feature undesirable from the consumer's point of view. This effect can be minimized by reducing Z_1 at the expense of its reactive component, X_1. Practically, this can be done by placing the primary winding between the secondary and tertiary windings, as shown in Fig. 10-1. If we express the short-circuit inductive reactances in terms of the winding dimensions (see Sec. 8-2):

$$X_{sc12} \sim (a_1 + a_2)/3 + a_{12}$$
$$X_{sc13} \sim (a_1 + a_3)/3 + a_{13}$$
$$X'_{sc23} \sim (a_2 + a_3)/3 + a_{23}$$

where $a_{23} = a_1 + a_{13} + a_{12}$, we can see that with this arrangement X_1 becomes negative (as in the phasor diagram of Fig. 10-5) and very small in absolute value

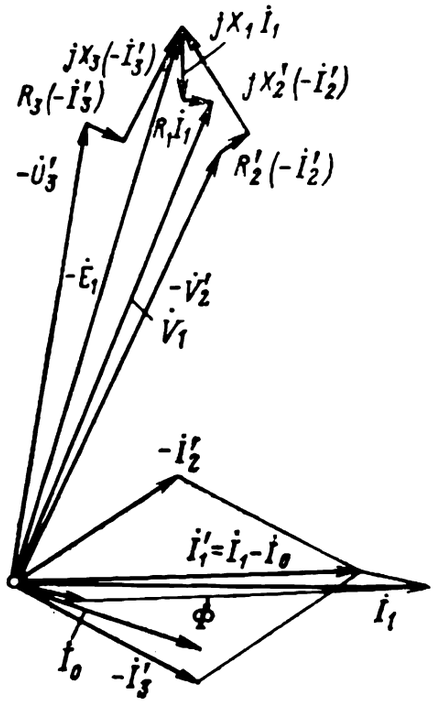

Fig. 10-5 Phasor diagram of a three-winding transformer

$$X_1 = (X_{sc12} + X_{sc13} - X'_{sc23})/2$$
$$\sim 2a_1/3 + a_{12} + a_{13} - a_{23} = -a_1/3 < 0$$

Three-winding transformers are built with their windings differing in power ratings. A relevant Soviet standard stipulates the following ratios (as fractions of the primary power):

$S_{1,R}/S_{1,R}$	$S_{2,R}/S_{1,R}$	$S_{3,R}/S_{1,R}$
1	1	1
1	1	2/3
1	2/3	2/3

The power ratios must be the same as the ratios between the respective referred currents. It is also required that $\dot{I}_1 = -\dot{I}_2' - \dot{I}_3'$ (see Fig. 10-5). However, the sum of the secondary and tertiary currents may exceed the primary current

$$I_2' + I_3' \geqslant I_1$$

and the sum of the secondary and tertiary powers mayexceed the primary power

$$V_1 I_2' + V_1 I_3' \geqslant V_1 I_1$$

or

$$S_2 + S_3 \geqslant S_1$$

The same Soviet standard requires also that for the first power ratio

$$S_2 + S_3 \leqslant 2S_1$$

for the second,

$$S_2 + S_3 \leqslant 1^{2/3} S_1$$

and for the third

$$S_2 + S_3 \leqslant 1^{1/3} S_1$$

With any power ratio, however, a three-winding transformer must satisfy the active and reactive power balances

$$P_1 = P_2 + P_3 + \sum P$$

$$Q_1 = Q_2 + Q_3 + \sum Q$$

where $\sum P$ and $\sum Q$ are the active and reactive power losses in the transformer itself (see Sec. 3-8).

(ii) Split-Primary (Split-Secondary) Two-Winding Transformers

A split primary (or split secondary) consists of two electrically isolated parts, so, in effect, such a transformer is a three-winding transformer. From a three-winding unit proper, it differs in that energy need not be transferred between the halves of the split winding.

The arrangement of a transformer having one primary (*1*) and a split secondary (*2* and *3*) is shown in Fig. 10-6. The magnetic circuit is of the core-and-shell (five-leg core) form, as shown in Fig. 1.5*b*. The halves of the split secondary are on the low-voltage side and are wound on different legs. The primary winding, which is on the HV side, has two parallel paths likewise wound on different legs.

With this arrangement, magnetic coupling between the halves of the split secondary is very loose, and transfer of energy from network *2* to network *3* by virtue of a magnetic field is negligible. Because of this, such a transformer

may be looked upon as a combination of two separate transformers, one coupling network *1* to network *2*, and the other coupling network *1* to network *3*. If only one half of the LV secondary, say, LV2, is loaded, on the HV side only one of the parallel paths, wound on the same leg will likewise be loaded. Of course, such a transformer can transfer energy in the reverse direction as well. Then it will have two primaries, LV2 and LV3, each supplied from a separate source, and one secondary, HV1.

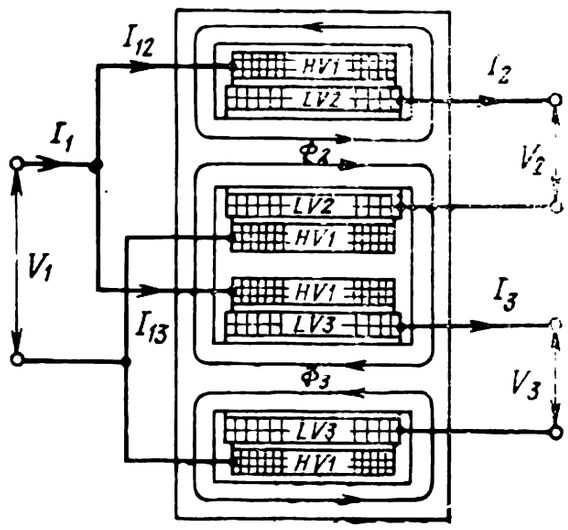

Fig. 10-6 Single-phase, two-winding transformer with a split LV winding

The values of V_3 and V_2 may be the same or different. The values of Φ_2 and Φ_3 and of the refferred currents I'_2 and I'_3 depend on the relative magnitudes of V_1 and the referred secondary and tertiary voltages, V'_2 and V'_3. If

$$\dot{V}'_2 = \dot{V}'_3$$

then

$$\dot{I}'_2 = \dot{I}'_3, \text{ and } \dot{\Phi}_2 = \dot{\Phi}_3$$

and, as a consequence, the fluxes in the outer (unwound) limbs of a five-leg core-type magnetic circuit are non-existent.

In the general case, when the voltages in networks *2* and *3* are such that $\dot{V}_2 \neq \dot{V}'_3$, the referred currents and fluxes are likewise different

$$\dot{I}'_2 \neq \dot{I}'_3 \text{ and } \dot{\Phi}_2 \neq \dot{\Phi}_3$$

and the difference flux, $\dot{\Phi}_2 - \dot{\Phi}_3$, has its path completed via the outer legs. If the transformer had a two-limb core, then, with $\dot{V}'_2 \neq \dot{V}'_3$, the difference flux between the upper and lower yokes would run outside the magnetic circuit, and appreciable eddy currents would be produced within the sides of the oil tank and other substantial structural parts, leading to increased eddy-current losses. This

is the reason why it is preferable to use the core form of magnetic circuit for split-winding transformers.

As compared with conventional two-winding transformers having one HV primary winding and one LV winding, split-winding units offer an unfailing advantage in that should a short-circuit occur across the secondary terminals, it will draw half as heavy a current from the supply line. This is because in a conventional two-winding transformer windings *2* and *3* are connected in parallel and its short-circuit impedance $Z_{sc\,123}$ is half the short-circuit impedance of windings *1* and *2* (or *1* and *3*) in a split-winding transformer, $Z_{sc\,12} = Z_{sc\,13}$. Understandingly, split-winding transformers have gained marked popularity.

10-2 Autotransformers

In an autotransformer, the primary and secondary windings are coupled both inductively and conductively. In fact, it

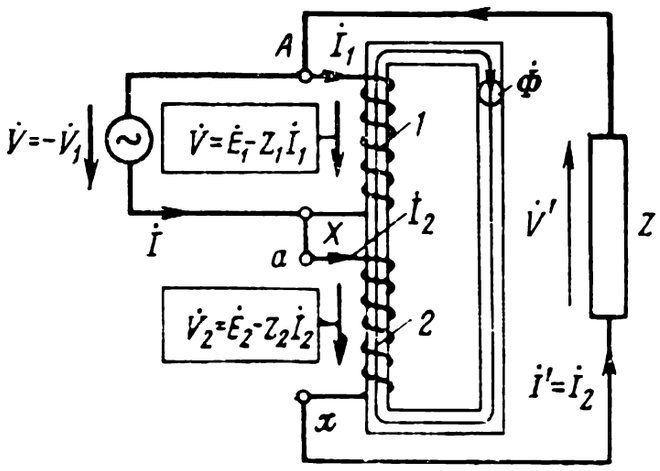

Fig. 10-7 Autotransformer connection

has a single tapped winding which serves both primary and secondary functions.

The auto-connection used to transfer energy from an input network at voltage V to an output network at voltage $V' > V$ is shown in Fig. 10-7. The figure shows two windings, *1* and *2*, wound on the same core and enclosing each other (see Fig. 1-1*a*). The primary is on the LV side, V, and the secondary is connected between terminal a (X) on the input network and terminal x on the output network in such a way that its voltage V_2 is added to V to give V'.

The secondary of an auto-transformer must be designed for V or V', whichever is the higher (in the circuit of Fig. 10-7, this is V'), rather than for V_2, as in an ordinary transformer.

The transformation ratio n of an autotransformer is the ratio V/V' at no-load ($I' = 0$). For the circuit in Fig. 10-7,

$$n = V/V' = E_1/(E_1 + E_2) = 1/(1 + n_{21})$$

where $n_{21} = E_2/E_1 = w_2/w_1$.

Electromagnetic processes in an autotransformer can be described, using the usual transformer equations

$$\begin{aligned} -\dot{V}_1 &= \dot{E}_1 - Z_1\dot{I}_1 \\ \dot{V}_2 &= \dot{E}_2 - Z_2\dot{I}_2 \\ \dot{I}_1 + \dot{I}_2 n_{21} &= \dot{I}_0 \\ \dot{E}_1 &= \dot{E}_2/n_{21} = -Z_0\dot{I}_0 \end{aligned} \qquad (10\text{-}5)$$

To them are added equations describing the circuit itself, with the positive directions assumed as shown in Fig. 10-7:

$$\begin{aligned} \dot{V}' &= \dot{V} + \dot{V}_2 \\ \dot{V} &= -\dot{V}_1 \\ \dot{I}' &= \dot{I}_2 \\ \dot{I} &= -\dot{I}_1 + \dot{I}_2 \end{aligned} \qquad (10\text{-}6)$$

A phasor diagram for an autotransformer is shown in Fig. 10-8.

For insight into the basic energy processes in an autotransformer, we shall neglect I_0 and the voltage drops in the windings which enter Eqs. (10-5) and (10-6) by assuming $I_0 = 0$, $|Z_1| = 0$, and $|Z_2| = 0$. Then,

$$\begin{aligned} I_1/I_2 &= V_2/V_1 = n_{21} \\ V &= V_1 \\ V' &= V + V_2 = V_1(1 + n_{21}) = V/n \\ I &= I_1 + I_2 = I_2(1 + n_{21}) = I'/n \end{aligned} \qquad (10\text{-}7)$$

With the above simplifications and the active and reactive power losses neglected, the total power of an autotrans-

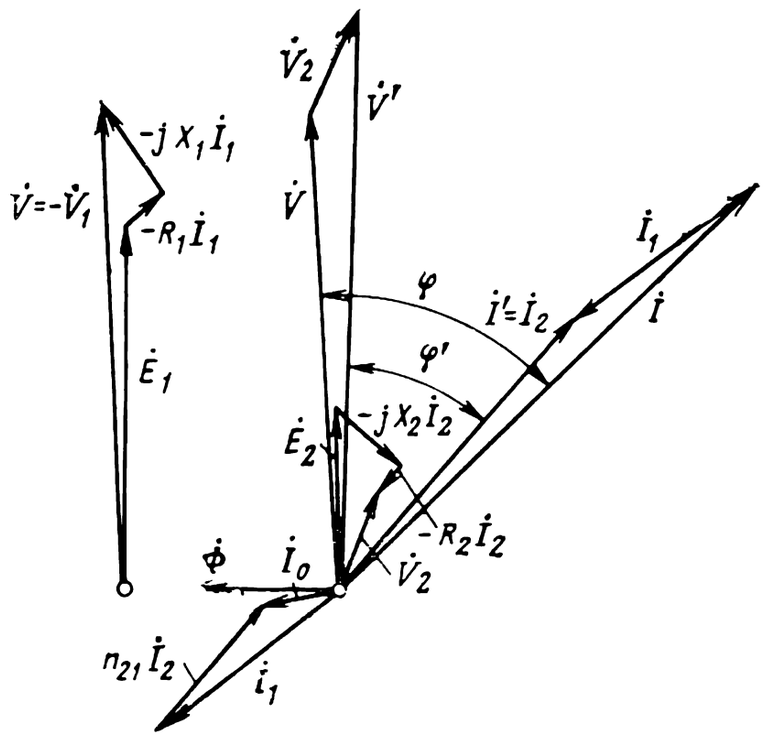

Fig. 10-8 Phasor diagram of an autotransformer in the case of a resistive-inductive load; $\varphi' > 1$, $n_{21} = 0.5$, $n = 1/(1 + 0.5) = 2/3$

former may be written as the sum of two components

$$\begin{aligned} S &= VI = V_1I_1 + V_1I_2 = V_2I_2 + V_1I_2 \\ &= S_{T(a)} + S_C \\ &= (V_1 + V_2)\, I_2 = V'I' = S' \end{aligned} \tag{10-8}$$

where

$$S_{T(a)} = V_1I_1 = V_2I_2$$

is the power transferred inductively (the transformed power), and

$$S_C = V_1I_2$$

is the power transferred from the primary to the secondary network conductively (the conducted power). This is why an autotransformer needs to be designed to withstand only the $S_{T(a)}$ term which accounts for only a fraction of the total power, S, called the auto fraction

$$S_{T(a)}/S = V_2I_2/V'I_2 = (V' - V)/V' = 1 - n \tag{10-9}$$

where $n < 1$.

In an autotransformer as in a conventional transformer, the transformer size is solely determined by the transformed power S_T. As has been shown in Sec. 9-1, the transformer size is proportional to $S^{1/4}$. For an ordinary transformer, $S_T = S$. For an autotransformer, $S_T = S_{T(a)} = (1 - n) S$. Accordingly, given the same power rating, an autotransformer will be smaller in size and less expensive to make.

An autotransformer becomes more attractive as its transformation ratio n differs progressively less from unity. For example, when $n = 0.9$, the transformed power decreases ten-fold, whereas when $n = 0.1$, it is about the same as that of an ordinary transformer. This is the reason why it is common practice to make autotransformers with n ranging between 0.5 and 1. In such cases, the relatively more expensive insulation on the secondary is more than offset by the reduction in the weight of, and the losses in, the autotransformer.

Autotransformers are widely used to power domestic appliances and control-system units and come in sizes from 10 to under 1 000 VA. In the Soviet Union, they are common in high-voltage power transmission lines where they are used to tie networks operating at closely spaced voltages, namely 110 and 220 kV, 220 and 500 kV, and 330 and 750 kV. The overall capacity of such autotransformers runs into hundreds of megavolt-amperes.

Autotransformers may be used to both step up and step down the applied voltage. For example, the autotransformer in Fig. 10-7 will step down the applied voltage, if the load is connected to receive V, and power input comes from a network at V'.

Apart from single-phase, two-winding autotransformers (Fig. 10-9*a*), power systems often employ three-phase, two-winding autotransformers (Fig. 10-9*c*), and also single-phase (Fig. 10-9*b*) and three-phase (Fig. 10-9*d*) three-winding autotransformers. The standard winding connections and phase displacement groups used in the Soviet Union for autotransformers are listed in Fig. 10-9. Auto-connected single-phase windings are denoted by I_{auto}, whereas star-connected three-phase autowindings, with the neutral available for connection, are denoted by $Y_{n, auto}$.

Autotransformers may constitute an electric hazard, especially when $1/n \gg 1$, because of direct connection between the HV network at V' and the LV network at

$V \ll V'$. In the absence of grounding, the voltage between the LV conductors and ground is $V'/2$, which appears owing to capacitive coupling between the HV wires and ground.

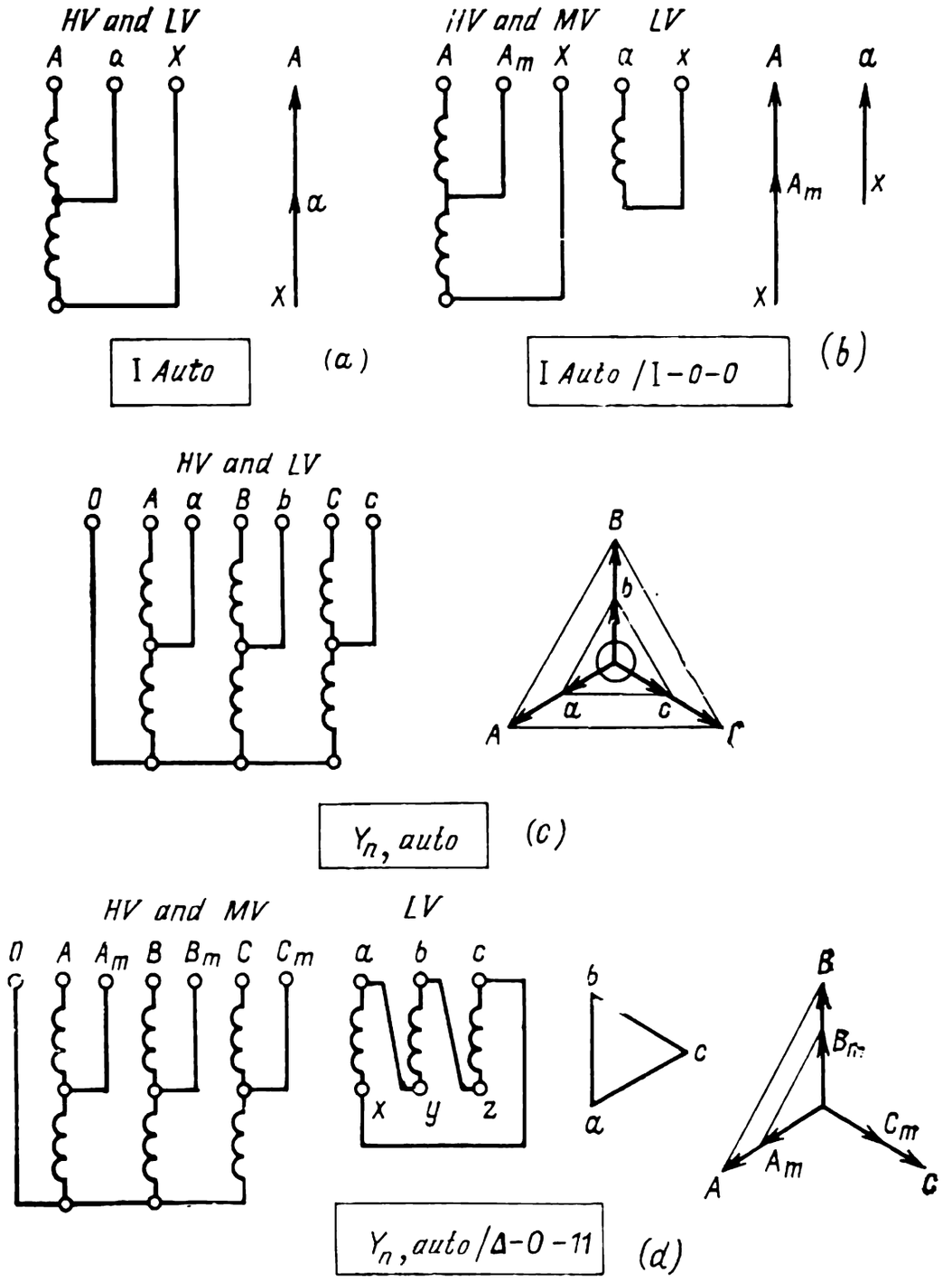

Fig. 10-9 Winding connections and phase displacement groups for autotransformers

For example, if an autotransformer were used to step down from 3 kV to 220 V, the voltage between the 220-V wires and ground would be 3/2 = 1.5 kV. This is why applicable safety codes guard against using autotransformers with $1/n > 2$.

The use of autotransformers with $n \approx 1$ runs into certain difficulties because fairly heavy short-circuit currents are likely to develop. If an autotransformer is energized with V' on the HV side (Fig. 10-7) and a short-circuit occurs on the LV side, V would reduce to zero, and winding *1* of the autotransformer would be short-circuited. At the same time, the voltage across winding *2* would rise from V_2 to V', and this would lead to a further increase in the short-circuit currents. On setting $V = -V_1 = 0$ in Eqs. (10-5) and (10-6), let us determine the steady-state short-circuit current in winding *2*:

$$I_{sc2} = V'/Z_{sc21} = (V_2/Z_{sc21})\,(V'/V_2) = I_{sc2,\,T}/(1-n) \quad (10\text{-}10)$$

where

Z_{sc21} = short-circuit impedance with winding *1* short-circuited and with the supply voltage applied to winding *2*

$I_{sc2,\,T} = V_2/Z_{sc21}$ is the short-circuit current in winding *2* with V_2 impressed on winding *2*.

It is seen from Eq. (10-10) that the short-circuit current in winding *2* of an autotransformer is $V'/V_2 = 1/(1-n)$ times the short-circuit current of a conventional transformer used to transfer energy from a network at V_2 into a network at V_1. The closer is n to unity, the larger the short-circuit currents, I_{sc2} and $I_{sc1} = n_{21}I_{sc2}$, and the more dangerous are their consequences.

II Transformers in Parallel

11-1 Use of Transformers in Parallel

Parallel connection of several transformers is widely used in electrical systems. In many cases, it is the only way to convey large blocks of power over large distances. Several transformers operating in parallel at a major substation cannot be replaced by a single unit of the same total power rating, because it would be prohibitively large and unwieldy both to manufacture and move it to its permanent location.

Even at not so large substations, the use of several transformers operating in parallel offers a more convenient way to tackle the problems of reliability and plant expansion.

Should any unit fail, the remaining ones will still be operable and take up the load previously carried by the faulty transformer. In the meantime, the failing transformer can be replaced by a standby unit whose cost will undoubtedly be small in comparison with that of all the installed transformers. Also, if a substation has a sufficiently large number of transformers, it is always possible to combine in parallel as many of them as may be necessary for optimal load sharing and energy conversion at a minimal loss (see Sec. 6-3).

The choice of a number of transformers to be operated in parallel is both an engineering and an economic problem in optimization. In this problem, the variables to be optimized are the total cost of manufacture and operation of the installed transformers. An important point to bear in mind is that the cost of the energy lost and the cost of manufacture decrease with the increase in per unit rating, whereas the redundancy cost increases.

11-2 Procedure for Bringing Transformers in for Parallel Operation

To avoid likely errors, the transformers to be operated in parallel must be interconnected at identically marked terminals. An example of two transformers connected for parallel

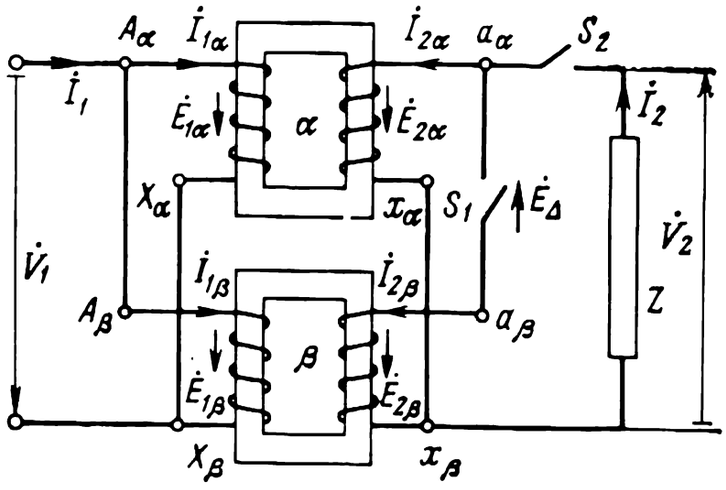

Fig. 11-1 Parallel operation of two 1/1-0 single-phase, two-winding transformers

operation is shown in Fig. 11-1. As is seen, the identically marked terminals of transformers α and β (A_α and A_β, X_α and X_β, a_α and a_β, x_α and x_β) are respectively connected to the same bus.

Let us formulate the rules for paralleling two transformers, with their load Z disconnected (that is, with switch S_2 open). Obviously, the primary terminals of the two transformers, namely A_α, A_β, X_α, and X_β, may be connected in the above way to the input network without having to meet any additional requirements. After the primaries are connected for $V_1 = V_{1\alpha} = V_{2\beta}$, the voltages existing between the disconnected secondary terminals $a_\alpha x_\alpha$ and $a_\beta x_\beta$ will be as follows:

$$V_{2\alpha} = E_{2\alpha} = V_{1\alpha}/n_{12\alpha} = E_{1\alpha}/n_{12\alpha}$$

and

$$V_{2\beta} = E_{2\beta} = V_{1\beta}/n_{12\beta} = E_{1\beta}/n_{12\beta}$$

Terminals x_α and x_β may be commoned without running any risk. However, commoning terminals a_α and a_β may give rise to an emf across switch S_1

$$\dot{E}_\Delta = \dot{E}_{2\alpha} - \dot{E}_{2\beta} \qquad (11\text{-}1)$$

Commoning terminals a_α and a_β will not give rise to any circulating currents in the windings only if

$$\dot{E}_\Delta = \dot{E}_{2\alpha} - \dot{E}_{2\beta} = 0$$

or when the secondary emfs are the same

$$\dot{E}_{2\alpha} = \dot{E}_{2\beta}$$

For this to happen, the transformers to be brought in for parallel operation must meet the following requirements:

1. *Have the same transformation ratio.* If $n_{12\alpha} = n_{12\beta}$ and $V_{1\alpha} = V_{1\beta}$, the secondary emfs will be the same, $E_{2\alpha} = E_{2\beta}$.

2. *Fall in the same phase displacement (clock figure) group.* If so, $N_\alpha = N_\beta = N$, the secondary emfs, $\dot{E}_{2\alpha}$ and $\dot{E}_{2\beta}$, will be turned through the same phase angle relative to the identical primary emfs, $\dot{E}_{1\alpha} = \dot{E}_{1\beta} = -\dot{V}_1$, and will therefore be in phase

$$\dot{E}_{2\alpha} = (\dot{E}_{1\alpha}/n_{12\alpha}) \exp(j\theta_N)$$
$$= (\dot{E}_{1\beta}/n_{12\beta}) \exp(j\theta_N) = \dot{E}_{2\beta}$$

The above requirements are also applicable to three-phase transformers. When they are brought in for parallel operation, connections must be made between the identically

marked line and neutral terminals (A_α and A_β, B_α and B_β, C_α and C_β, a_α and a_β, b_α and b_β, c_α and c_β, O_α and O_β). If this condition is met, the secondary line emfs will be identical in both magnitude and phase.

11-3 Circulating Currents Due to a Difference in Transformation Ratio

Consider two 1/1-0 single-phase transformers α and β. If their transformation ratios are not the same, $n_{12\alpha} \neq n_{12\beta}$, and $\dot{E}_\Delta \neq 0$, the circulating currents $I_{1\alpha}$, $I_{1\beta}$, $I_{2\alpha}$, and $I_{2\beta}$ which will appear in the windings upon closure of switch S_1, can be estimated on neglecting the magnetizing currents ($\dot{I}_{0\alpha} = \dot{I}_{0\beta}$) and writing the equations for transformers α and β (see Sec. 3-3) for the positive directions shown in Fig. 11-1:

$$\dot{V}_{1\alpha} = -\dot{E}_{1\alpha} + \dot{I}_{1\alpha}Z_{1\alpha}, \quad \dot{V}_{2\alpha} = \dot{E}_{2\alpha} - \dot{I}_{2\alpha}Z_{2\alpha} \qquad (11\text{-}2)$$

$$\dot{V}_{1\beta} = -\dot{E}_{1\beta} + \dot{I}_{1\beta}Z_{1\beta}, \quad \dot{V}_{2\beta} = \dot{E}_{2\beta} - \dot{I}_{2\beta}Z_{2\beta}$$

where

$$\dot{E}_{1\alpha} = \dot{E}_{2\alpha}n_{12\alpha}, \quad \dot{E}_{1\beta} = \dot{E}_{2\beta}n_{12\beta}$$

$$\dot{I}_{2\alpha} = -\dot{I}_{1\alpha}n_{12\alpha}, \quad \dot{I}_{2\beta} = -\dot{I}_{1\beta}n_{12\beta}$$

Also, we must consider what happens when the two transformers are brought in parallel while the load is disconnected (switch S_2 is open and $I_2 = 0$):

$$\dot{V}_1 = \dot{V}_{1\beta} = \dot{V}_{1\alpha}, \quad \dot{V}_2 = \dot{V}_{2\alpha} = \dot{V}_{2\beta} \qquad (11\text{-}3)$$

$$\dot{I}_1 = \dot{I}_{1\alpha} + \dot{I}_{1\beta}, \quad \dot{I}_{2\alpha} + \dot{I}_{2\beta} = \dot{I}_2 = 0$$

Solving Eqs. (11-2) and (11-3) for the secondary circulating current $\dot{I}_{2\alpha} = -\dot{I}_{2\beta}$ gives

$$\dot{I}_{2\alpha} = -\dot{I}_{2\beta} = \frac{\dot{V}_2(n_{12\beta} - n_{12\alpha})}{n_{12\beta}Z'_{sc\,\beta} + n_{12\alpha}Z'_{sc\,\alpha}} \qquad (11\text{-}4)$$

where $Z'_{sc\,\beta} = Z_{2\beta} + Z_{1\beta}/n^2_{12\beta}$ and $Z'_{sc\,\alpha} = Z_{2\alpha} + Z_{1\alpha}/n^2_{12\alpha}$ are the short-circuit impedances of the two transformers, when the functions of the windings are reversed.

Using Eqs. (11-4) and (11-2), we can readily establish the relationship between the voltages $\dot{V}_2 = \dot{V}_{2\alpha} = \dot{V}_{2\beta}$ and $\dot{V}_1$ that exist after switch S_1 is closed

$$\dot{V}_1 = -\dot{V}_2 \frac{Z'_{sc\,\alpha} + Z'_{sc\,\beta}}{Z_{sc\,\alpha} n_{21\beta} + Z'_{sc\beta} n_{21\beta}} \tag{11-5}$$

where $n_{21\beta} = 1/n_{12\beta}$, $n_{21\alpha} = 1/n_{12\alpha}$, and for $Z'_{sc\alpha} = Z'_{sc\beta}$

$$\dot{V}_1 = -\dot{V}_2/n_{21} \tag{11-6}$$

where $n_{21} = (n_{21\alpha} + n_{21\beta})/2$ is the mean transformation ratio.

If the difference in transformation ratio between the two transformers is small ($n_{12\alpha}/n_{12\beta} \approx 1$),

$$\dot{I}_{2\alpha} = -\dot{I}_{2\beta} \approx \dot{E}_\Delta/(Z'_{sc\beta} + Z'_{sc\alpha})$$

where

$$\dot{E}_\Delta = \dot{E}_{2\alpha} - \dot{E}_{2\beta} = \dot{E}_1 (1/n_{12\alpha} - 1/n_{12\beta}) \approx \dot{V}_2 (\Delta n) \tag{11-7}$$

is the difference between the secondary emfs given by Eq. (11-1), Δn is the per-unit difference in transformation ratio, and n_{12} is the mean transformation ratio.

The circulating currents defined by Eq. (11-4) and appearing at the rated primary voltage, $V_1 = V_{1,R}$, when $V_2 \approx V_{2,R}$, can conveniently be expressed in per-unit, taking the rated current of, say, transformer α as the base quantity:

$$\begin{aligned} I_{*c\alpha} &\approx I_{2\alpha}/I_{2\alpha,R} = I_{1\alpha}/I_{1\alpha,R} \\ &\approx \Delta n/(v_{sc,\alpha} + v_{sc\beta} S_{\alpha,R}/S_{\beta,R}) \end{aligned} \tag{11-8}$$

where

$$\begin{aligned} v_{sc\alpha} &= I_{2\alpha,R} Z'_{sc\alpha}/V_{2\alpha,R} \\ v_{sc\beta} &= I_{2\beta,R} Z'_{sc\beta}/V_{2\beta,R} \end{aligned}$$

are the impedance voltages of the two transformers, and

$$\begin{aligned} S_{\alpha,R} &= I_{2\alpha,R} V_{2\alpha,R} \\ S_{\beta,R} &= I_{2\beta,R} V_{2\beta,R} \end{aligned}$$

are the power ratings (rated powers) of the two transformers.

It follows from Eq. (11-8) that even with a small difference in the transformation ratio, the circulating currents may be comparable in magnitude with the rated currents of

the paralleled transformers. For example, when $S_{\alpha,R}/S_{\beta,R} = 1$, $v_{sc\alpha} = v_{sc\beta} = 0.05$, and $\Delta n = 0.05$, the circulating current will be

$$I_{*,c} = I_2/I_{2R} = 0.05/(2 \times 0.05) = 0.5 \text{ per-unit}$$

To avoid hazardous circulating currents, the transformers to be paralleled may differ in their transformation ratios by not more than 0.005.

11-4 Load Sharing Between Transformers in Parallel

If paralleled transformers meet all the requirements, no circulating currents will be flowing in their windings when the load is disconnected.

Let us load the paralleled transformers by closing switch S_2 (see Fig. 11-1) and see how the load current will be

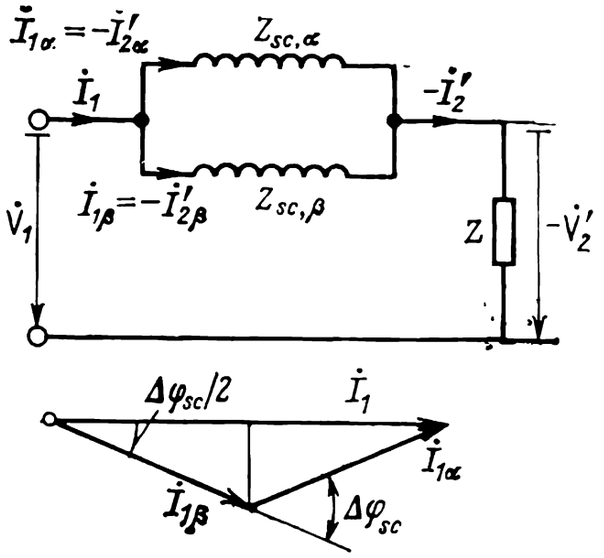

Fig. 11-2 Equivalent circuit of two transformers in parallel operation

shared. This can be done by reference to the equivalent circuit in Fig. 11-2. In fact, it is a combination of the equivalent circuits for transformers α and β, as given in Fig. 6-1.

The currents in the parallel branches formed by the short-circuit impedances of the transformers

$$Z_{sc\alpha} = Z_{1\alpha} + n_{12}^2 Z_{2\alpha} = Z_{sc\alpha} \exp(j\varphi_{sc\alpha})$$
$$Z_{sc\beta} = Z_{1\beta} + n_{12}^2 Z_{2\beta} = Z_{sc\beta} \exp(j\varphi_{sc\beta})$$

are inversely proportional to the impedances

$$\dot{I}_{1\alpha}/\dot{I}_{1\beta} = Z_{sc\beta}/Z_{sc\alpha} = (Z_{sc\beta}/Z_{sc\alpha}) \exp(j\Delta\varphi_{sc}) \qquad (11\text{-}9)$$

The sum of the currents gives the load current

$$\dot{I} = \dot{I}_{1\alpha} + \dot{I}_{1\beta}$$

If the paralleled transformers are fully identical and their short-circuit impedances are the same in magnitude, $Z_{sc\alpha} = Z_{sc\beta}$, and in phase angle, $\varphi_{sc\alpha} = \varphi_{sc\beta}$, then each transformer will carry half the total current

$$I_{1\alpha} = I_1\beta = I_1/2$$

If the short-circuit impedances are the same in magnitude, but differ in phase angle, $\varphi_{sc\alpha} < \varphi_{sc\beta}$, then

$$\dot{I}_{1\alpha} = \dot{I}_{1\beta} \exp(j\Delta\varphi_{sc})$$

and the current phasor diagram looks like one shown in Fig. 11-2. Each transformer carries a current given by

$$I_{1\alpha} = I_{1\beta} = I_1/2 \cos(\Delta\varphi_{sc}/2)$$

which is $1/\cos(\Delta\varphi_{sc}/2)$ times the current $I_1/2$ existing when the load is shared equally. Fortunately, even with the largest possible value of $\varphi_{sc\beta}$ (about 90°) and the least possible value of $\varphi_{sc\alpha}$ (about 60°), their difference is about 30°, and the resultant overload does not exceed

$$1/\cos(\Delta\varphi_{sc}/2) \leqslant 1/\cos(30°/2) = 1.03$$

Therefore, the overload due to a difference in φ_{sc} may be neglected, and consideration should only be given to the difference in magnitude between the short-circuit impedances. It follows from Eq. (11-9) that the current magnitudes are inversely proportional to the magnitudes of the short-circuit impedances

$$I_{1\alpha}/I_{1\beta} = Z_{sc\beta}/Z_{sc\alpha}$$

Simple manipulations give

$$(I_{1\alpha}/I_{1\beta})(V_{1,R}/V_{1,R}) = \frac{Z_{sc\,\beta}I_{1\beta,R}}{V_{1,R}} \frac{V_{1,R}}{Z_{sc,\,\alpha}I_{1\alpha,\,R}} \frac{I_{1\alpha,R}V_{1,R}}{I_{1\beta,R}V_{1,\,R}}$$

Noting that

$$\frac{I_{1\alpha}V_{1,R}}{I_{1\alpha,R}V_{1,R}} = S_\alpha/S_{\alpha,R} = S_{*\alpha} = I_{*\alpha}$$

and

$$Z_{sc\alpha}I_{1\alpha,R}/V_{1,\,R} = v_{sc\alpha}$$

we can readily find that per-unit loads on the paralleled transformers, $S_{*\alpha}$ and $S_{*\beta}$, are inversely proportional to the impedance voltages, $v_{sc\alpha}$ and $v_{sc\beta}$:

$$S_{*\alpha}/S_{*\beta} = v_{sc\beta}/v_{sc\alpha} \qquad (11\text{-}10)$$

If $v_{sc\beta} = v_{sc\alpha}$, the per-unit load is about the same on either of the paralleled transformers, and each is being utilized to full advantage. If one carries its rated per-unit load, $S_{*\alpha} = 1$, the other, too, will carry its rated per-unit load, $S_{*\beta} = 1$.

If, say, $v_{sc\beta} > v_{sc\alpha}$, transformer β will be under-loaded, although transformer α is carrying its rated load

$$S_{*\beta} = (v_{sc\alpha}/v_{sc\beta})\, S_{*\alpha} < 1$$

Conversely, if transformer β is carrying its rated load, transformer α will be overloaded

$$S_{*\alpha} = (v_{sc\beta}/v_{sc\alpha})\, S_{*\beta} > 1$$

This is the reason why the transformers to be paralleled must have identical relative impedance voltages. (In practice, the maximum difference is allowed to be as high as 10%.)

12 Three-Phase Transformers Under Unbalanced Load

12-1 Causes of Load Unbalance

In the preceding sections, we discussed three-phase transformers operated in networks with symmetrical voltages and balanced loads. Unfortunately, an ideally balanced load is practically nonexistent in power systems, and there is always some degree of unbalance present. This unbalance increases with increasing power rating of single-phase loads drawing their power from three-phase systems, and is especially pronounced under abnormal conditions, such as two- and single-phase faults to ground, failure of one of the phases, and the like.

To form a reliable estimate of the unbalance that may be tolerated in an operating system, we need a mathematical description of what happens in a transformer in the case of an unbalanced load.

In the most general case, a transformer may be not only carrying unbalanced secondary line currents $\dot{I}_{a,\text{line}}$, $\dot{I}_{b,\text{line}}$ and $\dot{I}_{c,\text{line}}$, but also operating from a network with unbalanced line voltages $\dot{V}_{AB}$, $\dot{V}_{BC}$, and $\dot{V}_{CA}$. To obtain a complete picture of the events taking place in such a case, we must determine the phase secondary currents $\dot{I}_a$, $\dot{I}_b$, and $\dot{I}_c$ (if the secondary is delta-connected), phase and line primary currents $\dot{I}_A$, $\dot{I}_B$, $\dot{I}_C$ and $\dot{I}_{A,\text{line}}$, $\dot{I}_{B,\text{line}}$, $\dot{I}_{C,\text{line}}$ (the latter only if the primary is delta-connected), primary phase voltages $\dot{V}_A$, $\dot{V}_B$, and $\dot{V}_C$ (the primary is star-connected), secondary phase and line voltages $\dot{V}_a$, $\dot{V}_b$, $\dot{V}_c$ and $\dot{V}_{ab}$, $\dot{V}_{bc}$, $\dot{V}_{ca}$ (the latter only if the secondary is star-connected).

Most commonly, these quantities are found by the method of symmetrical (phase-sequence) components. By this method, an unsymmetrical (unbalanced) set of phase voltages, currents or fluxes is resolved into symmetrical systems equal in number to the number of phases and formed by the respective components in the positive, negative and zero phase sequences.

An important point to bear in mind is that the phase sequence in the supply network has no bearing on what happens in a transformer under balanced load contitions. This implies that its winding impedances for the negative-phase-sequence (NPS) currents do not differ from those for the positive-phase-sequence (PPS) currents, Z_1, Z_2 and Z_0 (see Chap. 8). Special treatment is only needed for zero-phase-sequence (ZPS) currents.

12-2 Transformation of Unbalanced Currents

(i) Star-Connected Secondary

With the secondary star-connected, the specified unbalanced line currents $\dot{I}_{a,\text{ line}}$, $\dot{I}_{b,\text{ line}}$, and $\dot{I}_{c,\text{ line}}$ are, at the same time, phase currents

$$\dot{I}_a = \dot{I}_{a,\text{ line}}, \quad \dot{I}_b = \dot{I}_{b,\text{line}}, \quad \dot{I}_c = \dot{I}_{c,\text{line}}$$

The phase secondary currents may be represented as sums of symmetrical current components, namely, PPS currents

$$\begin{aligned} \dot{I}_{a1} &= (\dot{I}_a + a^2\dot{I}_b + a\dot{I}_c)/3 \\ \dot{I}_{b1} &= \dot{I}_{a1}a^2 \\ \dot{I}_{c1} &= \dot{I}_{a1}a \end{aligned} \qquad (12\text{-}1)$$

NPS currents

$$\begin{aligned} \dot{I}_{a2} &= (\dot{I}_a + a^2\dot{I}_b + a\dot{I}_c)/3 \\ \dot{I}_{b2} &= \dot{I}_{a2}a \\ \dot{I}_{c2} &= \dot{I}_{a1}a^2 \end{aligned} \qquad (12\text{-}2)$$

where $a = \exp(j2\pi/3)$, and ZPS currents

$$\dot{I}_{a0} = \dot{I}_{b0} = \dot{I}_{c0} = (\dot{I}_a + \dot{I}_b + \dot{I}_c)/3 \qquad (12\text{-}3)$$

How a set of phase currents is resolved into symmetrical components is illustrated in Fig. 12-1.

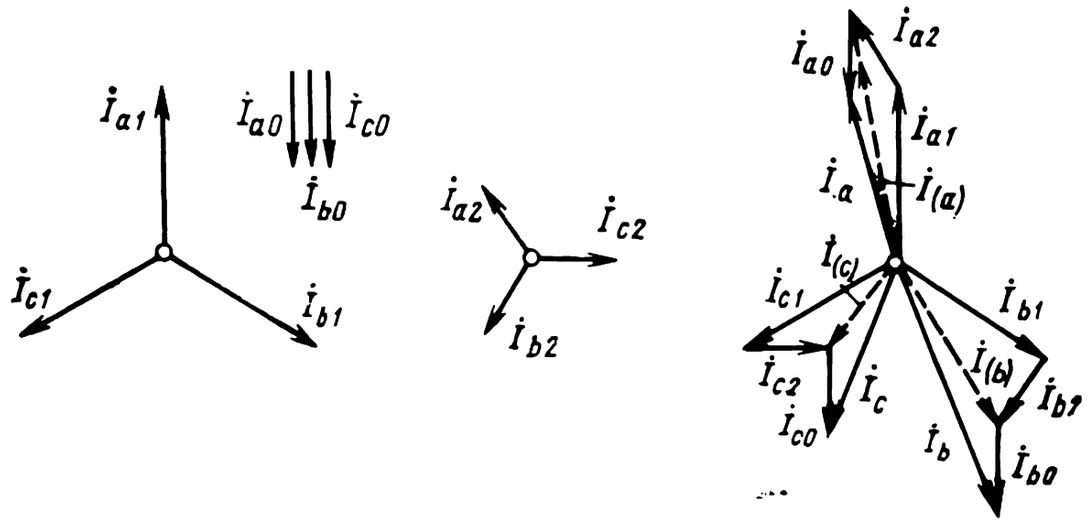

Fig. 12-1 Resolution of an unbalanced system of currents into symmetrical components

The neutral wire of a Y_n-connected winding carries a current

$$\dot{I}_n = \dot{I}_a + \dot{I}_b + \dot{I}_c = 3\dot{I}_{a0} \qquad (12\text{-}4)$$

As is seen, this current is three times the ZPS current.

Assuming that the system (network) is linear and neglecting the magnetizing currents in comparison with the load currents, we may deal with the transformation of each of the symmetrical systems individually.

The relationship between the PPS primary and secondary currents has been established in Sec. 3-7. It has been shown that whatever the connection of the secondary and primary windings,

$$\dot{I}_1 = -\dot{I}'_2 + \dot{I}_0 \approx -\dot{I}'_2$$

This equation may be written for any of the three phases, using the notation adopted for an unbalanced load:

$$\dot{I}_{A1} = -\dot{I}'_{a_1},\ \dot{I}_{B1} = -\dot{I}'_{b_1},\ \dot{I}_{C1} = -\dot{I}'_{c_1} \qquad (12\text{-}5)$$

where $\dot{I}'_{a_1}$, $\dot{I}'_{b_1}$, and $\dot{I}'_{c_1}$ are the secondary currents referred to the primary side.*

Because the phase sequence in a transformer is of no importance, the relationship between the NPS secondary and primary currents will be the same

$$\dot{I}_{A2} = -\dot{I}'_{a_2},\ \dot{I}_{B2} = -\dot{I}'_{b_2},\ \dot{I}_{C2} = -\dot{I}'_{c_2} \qquad (12\text{-}6)$$

This relation may be extended to ZPS currents in cases where they can flow in the primary winding, that is, when the primary is star-connected, with the neutral brought out, or delta-connected:

$$\dot{I}_{A0} = -\dot{I}'_{a0} = \dot{I}_{B0} = -\dot{I}'_{b0} = \dot{I}_{C0} = -\dot{I}'_{c0} \qquad (12\text{-}7)$$

Thus, when the primary is connected in a Y_n or Δ, its phase currents are equal to the corresponding secondary phase currents:

$$\begin{aligned} \dot{I}_A &= \dot{I}_{A1} + \dot{I}_{A2} + \dot{I}_{A0} = -(\dot{I}'_{a_1} + \dot{I}'_{a_2} + \dot{I}'_{a0}) = -\dot{I}'_a \\ \dot{I}_B &= -\dot{I}'_b \\ \dot{I}_C &= -\dot{I}'_c \end{aligned} \qquad (12\text{-}8)$$

When the primary is connected in a Y_n, its line currents do not differ from its phase currents

$$\dot{I}_{A,\text{line}} = \dot{I}_A,\ \dot{I}_{B,\text{line}} = \dot{I}_B,\ \dot{I}_{C,\text{line}} = \dot{I}_C$$

---

* Equation (12-4) and all the other equations in this section are written for the winding connections where the identically marked phase windings (A and a, B and b, C and c) are wound on the same leg.

and the current in the neutral wire

$$\dot{I}_N = 3\dot{I}_{A0} = -3\dot{I}_{a0} = -\dot{I}'_n$$

is equal to the referred current in the neutral wire on the secondary side.

In a delta-connected primary, the line currents do not contain ZPS components

$$\begin{aligned}\dot{I}_{A,\text{line}} &= \dot{I}_A - \dot{I}_B = (\dot{I}_{A1} + \dot{I}_{A2} + \dot{I}_{A0}) \\ &\quad - (\dot{I}_{B1} + \dot{I}_{B2} + \dot{I}_{B0}) \\ &= (\dot{I}_{A1} + \dot{I}_{A2}) - (\dot{I}_{B1} + \dot{I}_{B2}) \\ &= -(\dot{I}'_{a1} + \dot{I}'_{a2}) + (\dot{I}'_{b1} + \dot{I}'_{b2}) \qquad (12\text{-}9)\end{aligned}$$

The ZPS current I_{A0} has its path completely around the delta and does not appear in the line wires (Fig. 12-2).

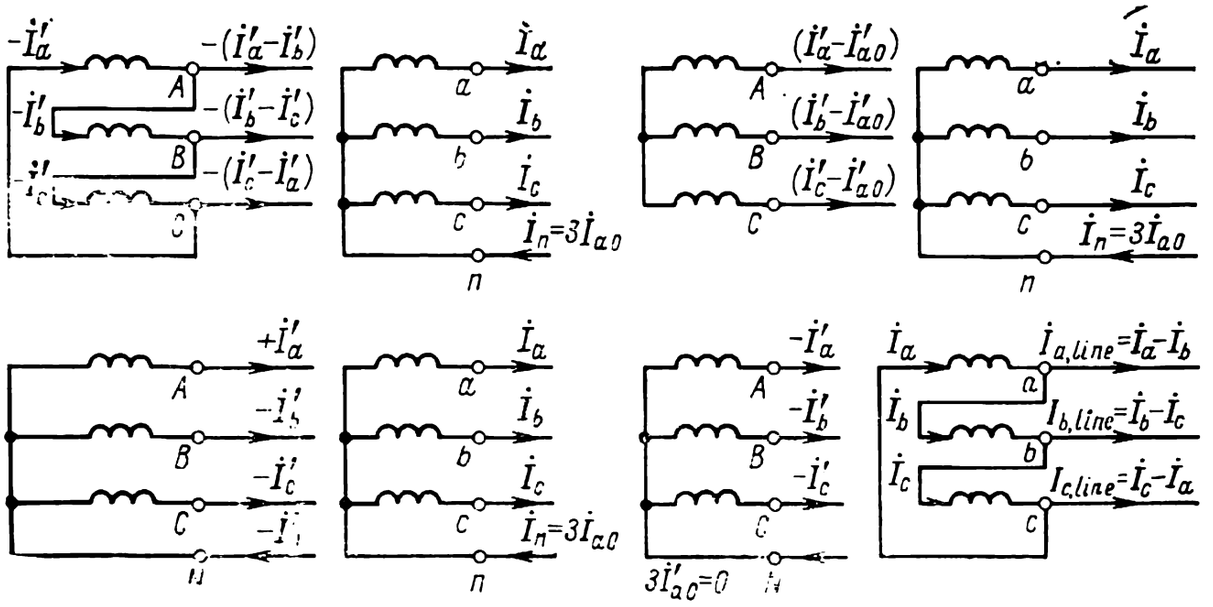

Fig. 12-2 Transformation of unbalanced currents by various winding connections

In a star-connected primary, there is no neutral wire that might carry ZPS currents. Therefore, no ZPS currents are induced into the primary

$$\dot{I}_{A0} = \dot{I}_N/3 = (\dot{I}_A + \dot{I}_B + \dot{I}_C)/3 = 0$$

and the phases of this winding only carry PPS and NPS currents

$$\begin{aligned}\dot{I}_A &= \dot{I}_{(A)} = \dot{I}_{A1} + \dot{I}_{A2} = -\dot{I}'_{a_1} - \dot{I}'_{a_2} = -\dot{I}'_{(a)} \\ &= -(\dot{I}'_a - \dot{I}'_{a0}) \\ \dot{I}_B &= \dot{I}_{(B)} = \dot{I}_{B1} + \dot{I}_{B2} = -\dot{I}'_{b_1} - I'_{b_2} \\ &= -\dot{I}'_{(b)} = -(\dot{I}'_b - \dot{I}'_{a0})\end{aligned} \tag{12-10}$$

As follows from the foregoing, whatever the form of connection, the PPS and NPS currents are transformed identically. Therefore, it appears reasonable to treat separately only the ZPS phase currents, and to lump together the PPS and NPS currents

$$\dot{I}_a = \dot{I}_{(a)} + \dot{I}_{a0}$$

where $\dot{I}_{(a)} = \dot{I}_{a1} + \dot{I}_{a2}$ is the PPS and NPS currents in phase a, shown by the dashed line in Fig. 12-1.

(ii) Delta-Connected Secondary

When the secondary is connected in a delta, the specified line currents always sum to zero

$$\dot{I}_{a,\text{line}} + \dot{I}_{b,\text{line}} + \dot{I}_{c,\text{line}} = 0$$

Because the line currents are the differences of phase currents

$$\dot{I}_{a,\text{line}} = \dot{I}_a - \dot{I}_b, \quad \dot{I}_{b,\text{line}} = \dot{I}_b - \dot{I}_c, \quad \dot{I}_{c,\text{line}} = \dot{I}_c - \dot{I}_a \tag{12-11}$$

and the phase currents do not contain ZPS components and sum to zero

$$\dot{I}_a + \dot{I}_b + \dot{I}_c = 3\dot{I}_{a0} = 0 \tag{12-12}$$

we may write the phase currents in terms of the line currents

$$\begin{aligned}\dot{I}_a &= (\dot{I}_{a,\text{line}} - \dot{I}_{c,\text{line}})/3 \\ \dot{I}_b &= (\dot{I}_{b,\text{line}} - \dot{I}_{a,\text{line}})/3 \\ \dot{I}_c &= (\dot{I}_{c,\text{line}} - \dot{I}_{b,\text{line}})/3\end{aligned} \tag{12-13}$$

Graphically, the phase currents are defined by the centroid of a line-current triangle, lying at the intersection of its medians. As will be recalled from school mathematics, the

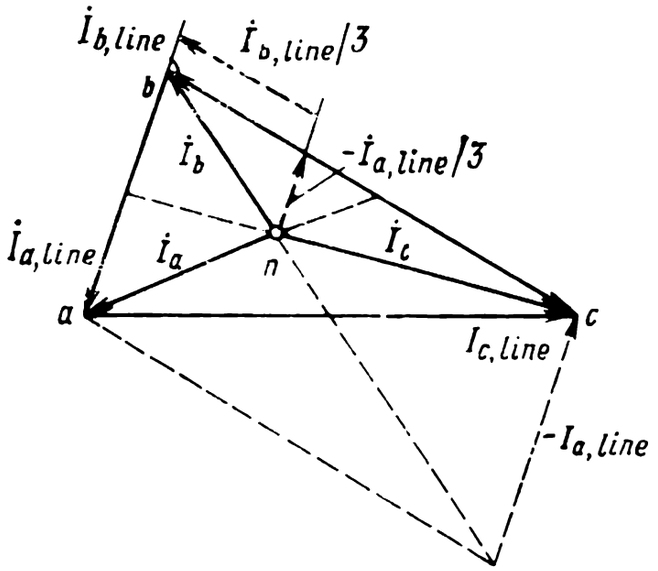

Fig. 12-3 Determining the phase currents in a delta-connected windnig

intersection of the medians in a triangle lies two-thirds of the way from its apexes (see Fig. 12-3).

Because the secondary phase currents do not contain any ZPS currents, they are fully transformed into the primary, no matter how it is connected (see Fig. 12-2):

$$\dot{I}_A = -\dot{I}'_a,\ \dot{I}_B = -\dot{I}'_b,\ \dot{I}_C = -\dot{I}'_c$$

When the primary is star-connected with its neutral brought out,

$$\dot{I}_N = 3\dot{I}_{A0} = -3\dot{I}'_{a0} = 0$$

12-3 Magnetic Fluxes and EMFs under Unbalanced Load Conditions

Under unbalanced load conditions, the total magnetic flux may, in a linear approximation, be visualized as the superposition of the fluxes set up by PPS, NPS and ZPS currents (Fig. 12-4).

The balance between the PPS primary currents ($\dot{I}_{A1}$, $\dot{I}_{B1}$, $\dot{I}_{C1}$) and the PPS secondary currents ($\dot{I}_{a1}$, $\dot{I}_{b1}$, $\dot{I}_{c1}$) is never complete. The unbalanced fractions of the PPS primary currents, which are the magnetizing currents $\dot{I}_{A1}$

$+ \dot{I}'_{a1}$, $\dot{I}_{B1} + \dot{I}'_{b1}$, $\dot{I}_{C1} + \dot{I}_{c1}$, give rise to a balanced set of PPS fluxes $\dot{\Phi}_{A1}$, $\dot{\Phi}_{B1}$, and $\dot{\Phi}_{C1}$ (see Fig. 12-4). This system of fluxes has all the properties of fluxes in three-phase

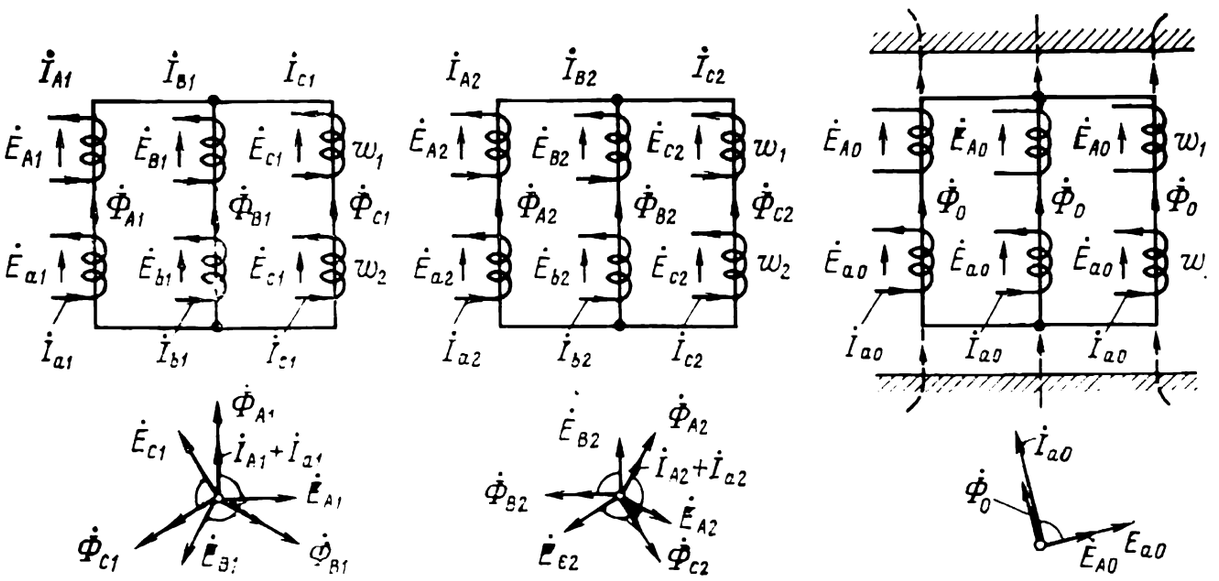

Fig. 12-4 Balanced components of magnetic fluxes and emfs under an unbalanced load

transformers under a balanced load (see Sec. 4-1). What is especially important is that these fluxes sum to zero.

$$\dot{\Phi}_{A1} + \dot{\Phi}_{B1} + \dot{\Phi}_{C1} = 0$$

So, they are free to traverse a closed path in any form of magnetic circuit.

The same goes for the systems of NPS currents in the primary winding (I_{A2}, I_{B2}, I_{C2}) and in the secondary winding (I_{a2}, I_{b2}, I_{c2}). They, too, are not completely balanced and form a symmetrical set of NPS fluxes (see Fig. 12-4)

$$\dot{\Phi}_{A2} + \dot{\Phi}_{B2} + \dot{\Phi}_{C2} = 0$$

In contrast, the ZPS fluxes established by the ZPS currents and their paths substantially depend on how the windings are connected and the form of the magnetic circuit.

As has already been explained in Sec. 7-3, the ZPS fluxes have their paths completed within the magnetic circuit only in the core-and-shell (five-leg core) type of transformer and also in a three-phase bank of single-phase transformers. In a core-type transformer (see Fig. 12-4), the in-phase

ZPS fluxes

$$\dot{\Phi}_{A0} = \dot{\Phi}_{B0} = \dot{\Phi}_{C0} = \dot{\Phi}_0$$

have their paths outside the magnetic circuit and within the nonmagnetic gaps, tank sides, and ferromagnetic structural parts.

Because the gaps offer a high opposition, the ZPS fluxes in a core-type transformer are markedly smaller than they are in a five-leg core-type transformer or in a bank of transformers (with the same mmf, $\dot{I}_{a0}w_2$).

The ZPS fluxes are especially strong when the ZPS currents flowing in a star-connected secondary with its neutral brought out are not balanced by the currents in the primary, which usually happens when the latter is star-connected with no neutral wire available (see Fig. 12-4).

As with PPS and NPS currents, it appears reasonable to lump together the PPS and NPS fluxes and to treat separately only the ZPS fluxes:

$$\dot{\Phi}_A = \dot{\Phi}_{(A)} + \dot{\Phi}_0, \quad \dot{\Phi}_B = \dot{\Phi}_{(B)} + \dot{\Phi}_0, \quad \dot{\Phi}_C = \dot{\Phi}_{(C)} + \dot{\Phi}_0$$

where $\dot{\Phi}_{(A)} = \dot{\Phi}_{A1} + \dot{\Phi}_{A2}$, $\dot{\Phi}_{(B)} = \dot{\Phi}_{B1} + \dot{\Phi}_{B2}$, and $\dot{\Phi}_{(C)} = \dot{\Phi}_{C1} + \dot{\Phi}_{C2}$ are the sums of the PPS and NPS fluxes.

Sinusoidal PPS and NPS fluxes induce in the primary phases the mutual emfs of positive and negative phase sequences [see Eq. (3-7)]:

$$\begin{aligned} \dot{E}_{(A)} &= \dot{E}_{A1} + \dot{E}_{A2} = -j\,(\omega/\sqrt{2})\,w_1\dot{\Phi}_{(A)} = \dot{E}'_{(a)} \\ \dot{E}_{(B)} &= \dot{E}_{B1} + \dot{E}_{B2} = -j\,(\omega/\sqrt{2})\,w_1\dot{\Phi}_{(B)} = E'_{(b)} \end{aligned} \qquad (12\text{-}14)$$

where $\dot{E}'_{(a)} = \dot{E}_{(a)}w_1/w_2$ is the PPS and NPS mutual emf of phase a referred to the primary side.

Sinusoidal ZPS fluxes induce in the primary phases mutual emfs of zero phase sequence (see Fig. 12-4):

$$\dot{E}_{A0} = -j\,(\omega/\sqrt{2})\,w_1\dot{\Phi}_0 = \dot{E}'_{a0} \qquad (12\text{-}15)$$

where $\dot{E}'_{a0} = \dot{E}_{a0}w_1/w_2$ is the ZPS mutual secondary emf referred to the primary side.

The ZPS mutual emf may be expressed in terms of the ZPS currents $\dot{I}_{a0}$ setting up the ZPS flux $\dot{\Phi}_0$ (the ZPS flux

needs to be treated separately only when the primary is star-connected and it carries no ZPS current, as in Fig. 12-4)

$$\dot{E}_{A0} = -Z'_{00}\dot{I}'_{a0} \tag{12-16}$$

where

$Z'_{00} = R'_{00} + jX'_{00}$ is the mutual impedance to ZPS currents

$X'_{00} = \omega w_1^2 \Lambda_{00}$ is the ZPS mutual reactance proportional to the permeance for the ZPS flux

R'_{00} = resistive component of the mutual impedance, due the hysteresis and eddy-current losses in the ferromagnetic structural parts, associated with the sinusoidal ZPS fluxes.

Because $\dot{I}_{a0}$ is the magnetizing current for the ZPS fluxes, Eq. (12-16) is written by analogy with Eq. (3-7) defining the relation between $\dot{I}_0$ and $\dot{E}_1$.

12-4 Dissymmetry of the Primary Phase Voltages under Unbalanced Load

The equations defining the primary phase voltages under unbalanced load are written by analogy with those for the balanced load conditions, Eqs. (3-13). The mutual emf $\dot{E}_1$ is replaced by the mutual phase emf which is the sum of the PPS and NPS emfs, and the ZPS emf, $\dot{E}_{A0} = \dot{E}_{B0} = \dot{E}_{C0}$:

$$\begin{aligned} \dot{V}_A &= -\dot{E}_{(A)} - \dot{E}_{A0} + Z_1\dot{I}_A \\ \dot{V}_B &= -\dot{E}_{(B)} - \dot{E}_{A0} + Z_1\dot{I}_B \\ \dot{V}_C &= -\dot{E}_{(C)} - \dot{E}_{A0} + Z_1\dot{I}_C \end{aligned} \tag{12-17}$$

The primary line voltages $\dot{V}_{AB}$, $\dot{V}_{BC}$ and $\dot{V}_{CA}$, which are in the general case unbalanced, are specified in advance.

When the primary is delta-connected, the primary phase voltages are the same as the specified line voltages and need not be determined. Also, the ZPS current I_{A0} around the delta balances the secondary ZPS currents, and $\dot{E}_{A0}$ in Eq. (12-17) vanishes.

When the line voltages are symmetrical, the phase voltages in a delta-connected primary are likewise symmetrical.

When the primary is star-connected with its neutral wire isolated, the specified line voltages are the differences of the respective primary phase voltages

$$\dot{V}_{AB} = \dot{V}_B - \dot{V}_A \qquad (12\text{-}18)$$
$$\dot{V}_{BC} = \dot{V}_C - \dot{V}_B$$

Also, adding together the right- and left-hand sides of Eqs. (12-17) and recalling that the emfs and currents containing no ZPS currents sum to zero

$$\dot{E}_{(A)} + \dot{E}_{(B)} + \dot{E}_{(C)} = (\dot{E}_{A1} + \dot{E}_{B1} + \dot{E}_{C1}) + (\dot{E}_{A2} + \dot{E}_{B2} + \dot{E}_{C2}) = 0$$
$$\dot{I}_{(A)} + \dot{I}_{(B)} + \dot{I}_{(C)} = (\dot{I}_{A1} + \dot{I}_{B1} + \dot{I}_{C1}) + (\dot{I}_{A2} + \dot{I}_{B2} + \dot{I}_{C2}) = 0$$

we obtain an important equation

$$\dot{V}_A + \dot{V}_B + \dot{V}_C = -3\dot{E}_{A0} = 3\dot{I}'_{a0}Z'_{00} \qquad (12\text{-}19)$$

Subtracting the second line in Eqs. (12-18) from the first and recalling Eq. (12-19), we get

$$\dot{V}_{AB} - \dot{V}_{BC} = -(\dot{V}_A + \dot{V}_B + \dot{V}_C) + 3\dot{V}_B = 3(\dot{E}_{A0} + \dot{V}_B)$$
$$\dot{V}_B = (\dot{V}_{AB} - \dot{V}_{BC})/3 - \dot{E}_{A0} = \dot{V}_{(B)} - \dot{E}_{A0}$$

and by analogy,

$$\dot{V}_C = (\dot{V}_{BC} - \dot{V}_{CA})/3 - \dot{E}_{A0} = \dot{V}_{(C)} - \dot{E}_{A0}, \text{ etc.} \qquad (12\text{-}20)$$

Here, $\dot{V}_{(B)}$ and $\dot{V}_{(C)}$ are the phase voltages with no ZPS current flowing in the secondary, that is, when $\dot{I}_{a0} = 0$ and

$$\dot{E}_{A0} = -Z_{00}\dot{I}'_{A0} = 0$$

As is seen from Fig. 12-5, the phase voltages $\dot{V}_{(A)}$, $\dot{V}_{(B)}$, and $\dot{V}_{(C)}$ are directed away from the centroid of the line-voltage triangle, N, towards its apexes [see also Eq. (12-13) and Fig. 12-3 for phase currents].

When the line voltages form a symmetrical set, $\dot{V}_{AB} = \dot{V}_{BC} = \dot{V}_{CA}$, and there is no ZPS current flowing in the secondary, $\dot{I}_{a0} = 0$, the primary phase voltages are likewise symmetrical

$$V_{(A)} = V_{(B)} = V_{(C)} = V_A = V_B = V_C$$

The appearance of ZPS currents ($\dot{I}_{a0} \neq 0$) causes the centroid of the line-voltage triangle to shift by a distance $\dot{E}_0$ (from point N to point N_0) and upsets the balance of the phase voltages. Now, even if the primary line voltages are balanced the phase voltages will be unbalanced, $V_A \neq V_B \neq V_C$.

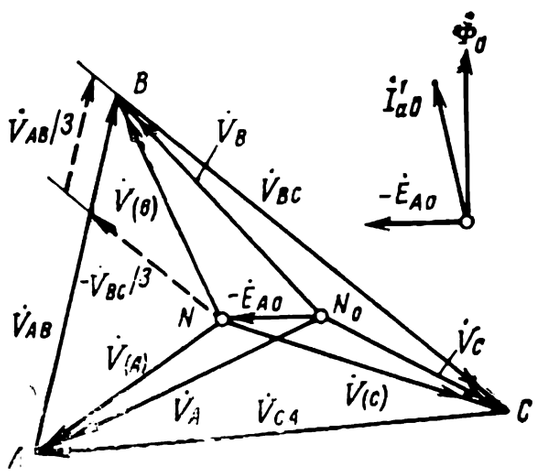

Fig. 12-5 Phasor diagram for primary voltages under an unbalanced load

In core-type transformers, the primary phase voltages are distorted considerably less, because the reluctance to the ZPS fluxes is many times that existing in a five-leg core (shell-and-core) type or in banks of single-phase transformers.

It follows from Eq. (12-20) that the unbalance of the phase voltages may arise from the dissymmetry of the line voltages even though there are no ZPS currents flowing. As regards the symmetry of phase voltages, it is preferable to connect the primary in a delta, because, given symmetrical line voltages, the phase voltages will not be distorted even when the secondary carries a ZPS current.

12-5 Dissymmetry of the Secondary Voltages under Unbalanced Load

The equations defining the secondary voltages may be written by analogy with Eq. (3-19) applicable to balanced load. The referred mutual emf $\dot{E}'_2 = \dot{E}_1$ is replaced by $\dot{E}'_{(a)} = \dot{E}'_{(A)}$

or $\dot{E}_{(B)}$, and $\dot{E}_{(C)}$, and also $\dot{E}'_{a0} = \dot{E}_{A0}$:

$$\begin{aligned} -\dot{V}'_a &= -\dot{E}_{(A)} - \dot{E}_{A0} + Z'_2\dot{I}'_a \\ -V'_b &= -\dot{E}_{(B)} - \dot{E}_{A0} + Z'_2\dot{I}'_b, \text{ etc.} \end{aligned} \tag{12-21}$$

Eliminating the emfs between the above equations by invoking Eq. (12-17), we can express the secondary phase voltages directly in terms of the primary phase voltages:

$$\begin{aligned} -\dot{V}'_a &= \dot{V}_A - Z_1\dot{I}_A + Z'_2\dot{I}'_a \\ -\dot{V}'_b &= V_B - Z_1\dot{I}_B + Z'_2\dot{I}'_b, \text{ etc.} \end{aligned} \tag{12-22}$$

It may be added that Eqs. (12-22) are applicable to any form of primary and secondary winding connection.

If the primary is delta-connected and the secondary is star-connected with its neutral brought out, the ZPS secondary current $\dot{I}_{a0}$ is balanced, from a magnetic point of view, by the primary ZPS current $\dot{I}_{A0}$ flowing around the delta, there is no ZPS flux, and the primary currents are equal to the respective secondary currents referred to the primary side:

$$\dot{I}_A = \dot{I}_{A1} + \dot{I}_{A2} + \dot{I}_{A0} = -\dot{I}'_{a1} - \dot{I}'_{a2} - \dot{I}'_{a0} = -\dot{I}'_a$$

$$\dot{I}_B = -\dot{I}'_b$$

$$\dot{I}_C = -\dot{I}'_c$$

Now the referred secondary phase voltage differs from the primary phase voltage by a relatively small voltage drop across the short-circuit impedance (as under balanced-load conditions)

$$\begin{aligned} -\dot{V}'_a &= \dot{V}_A + Z_{sc}\dot{I}'_a \\ -\dot{V}'_b &= \dot{V}_B + Z_{sc}\dot{I}'_b \end{aligned} \tag{12-23}$$

where $Z_{sc} = Z_1 + Z'_2$ is the short-circuit impedance.

When the specified primary line voltages are symmetrical, the primary phase voltages are, as already noted, likewise symmetrical, and the dissymmetry in the secondary phase voltages due to a dissymmetry in the currents is relatively small.

Equations (12-23) may be used to determine the secondary voltages also when the primary is star-connected, and the secondary is delta-connected (a Y/Δ transformer), because then the secondary and primary currents contain no ZPS currents ($I_{A0} = I_{a0} = 0$). In the circumstances, the primary and secondary currents balance themselves as well

$$\dot{I}_A = \dot{I}_{A1} + \dot{I}_{A2} = -\dot{I}'_{a1} - \dot{I}'_{a2} = -\dot{I}'_a$$
$$\dot{I}_B = -\dot{I}'_b$$
$$\dot{I}_C = -\dot{I}'_c$$

whereas the ZPS flux and the ZPS emf reduce to zero. Therefore, [see Eq. (12-20)] the primary phase voltages are determined by the position of the centroid of the line-voltage triangle

$$\dot{V}_A = \dot{V}_{(A)},\ \dot{V}_B = \dot{V}_{(B)},\ \dot{V}_C = \dot{V}_{(C)}$$

and, given symmetrical line voltages, are themselves symmetrical, and Eq. (12-22) reduces to Eq. (12-23).

The ZPS currents I_{a0} may cause a more noticeable dissymmetry in the primary and secondary phase voltages when the primary is star-connected and the secondary is star-connected with its neutral brought out, and there is no ZPS current flowing in the primary [see Eq. (12-10)]:

$$\dot{I}_A = \dot{I}_{(A)} = \dot{I}_{A1} + \dot{I}_{A2} = -\dot{I}'_{a_1} - \dot{I}'_{a_2} = -\dot{I}'_{(a)}$$
$$\dot{I}'_a = \dot{I}'_{a_1} + \dot{I}'_{a_2} + \dot{I}'_{a0} = \dot{I}'_{(a)} + \dot{I}'_{a0}$$

In view of Eqs. (12-10) and (12-20), we may re-write Eqs. (12-22) as

$$\begin{aligned} -\dot{V}'_a &= (\dot{V}_{(A)} + \dot{I}'_{a_1}Z_{sc}) + \dot{I}'_{a_2}Z_{sc} + \dot{I}'_{a0}Z'_n \\ -\dot{V}'_b &= (\dot{V}_{(B)} + \dot{I}'_{b_1}Z_{sc}) + \dot{I}'_{b_2}Z_{sc} + \dot{I}'_{a0}Z'_n, \text{ etc.} \end{aligned} \qquad (12\text{-}24)$$

where $Z'_n = Z'_{00} + Z'_2$ is the ZPS impedance of the secondary referred to the primary side.

When the primary line voltages are symmetrical, $\dot{V}_{(A)}$, $\dot{V}_{(B)}$ and $\dot{V}_{(C)}$ are likewise symmetrical, and the dissymmetry is related to the voltage drops due to the ZPS currents ($\dot{I}_{a2}Z_{sc}$, $\dot{I}_{b2}Z_{sc}$, $\dot{I}_{c2}Z_{sc}$) and the ZPS currents, $\dot{I}'_{a0}Z'_n$.

As is seen from Fig. 12-6, the voltage drops due to the PPS currents ($\dot{I}'_{a1}Z_{sc}$, $\dot{I}'_{b1}Z_{sc}$, $\dot{I}'_{c1}Z_{sc}$) do not lead to a voltage unbalance.

It is to be noted, however, that even in a core-type transformer in which the ZPS impedance is relatively small (Z'_{*n} = 0.3 to 1.0) and only several times the per-unit short-circuit impedance (Z_{*sc} = 0.05 to 0.13), the unbalance o-

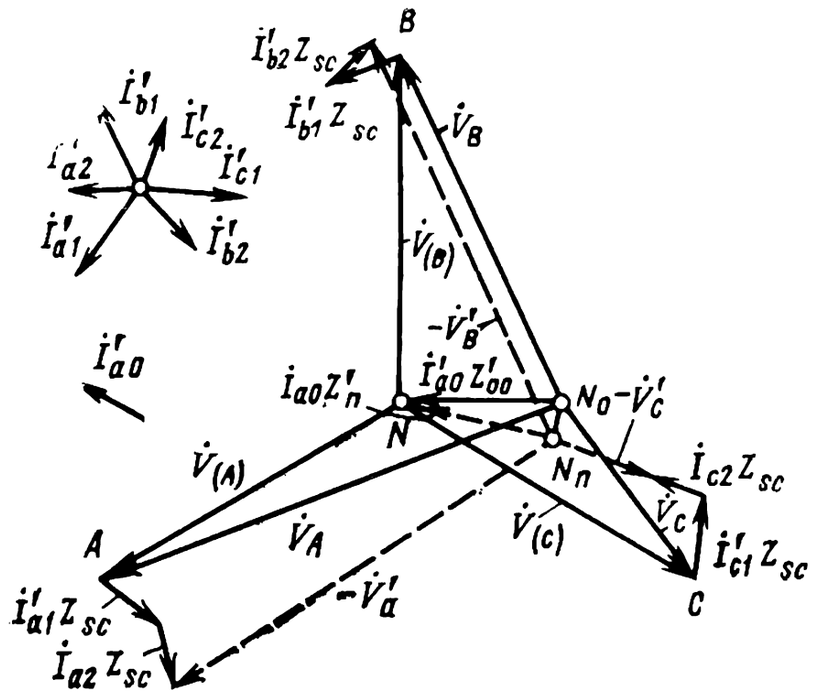

Fig. 12-6. Phasor diagram of a Y/Y_n transformer under an unbalanced load (the primary line voltages are balanced)

phase voltages is more noticeable due to ZPS currents than to NPS currents of the same magnitude. The effect of ZPS currents is especially troublesome in shell-and-core (five-leg core) transformers and in banks of Y/Y_n transformers. This is because the ZPS fluxes have their paths within the magnetic circuit in the same manner as the PPS fluxes. In such transformers, $Z'_{*n} = Z_{*0}$ = 10 to 100, so even small ZPS currents give rise to a prohibitive dissymmetry of phase voltages. This is why the Y/Y_n connection ought not to be used in shell-and-core (five-leg core) transformers and in banks of transformers. In core-type transformers using the Y/Y_n connection, it is important to limit the ZPS currents.

Subtracting the second line in Eqs. (12-24) from the first, we will find that the dissymmetry in the secondary line

voltages is solely related to the NPS currents

$$\dot{V}_{ab} = \dot{V}_b - \dot{V}_a$$
$$= \dot{V}_{(A)} - \dot{V}_{(B)} + (\dot{I}'_{a_1} - \dot{I}'_{b_1}) Z_{sc} + (\dot{I}'_{a_2} - \dot{I}'_{b_2}) Z_{sc},$$
etc.

The dissymmetry of phase voltages due to ZPS currents in shell-and-core transformers, banks of transformers, and large core-type transformers using the Y/Y_n connection can be minimized by providing an additional compensating delta-connected winding. The ZPS currents induced in the delta will damp out ZPS fluxes, thereby substantially reducing the unbalance of phase voltages in the main windings. Sometimes, this delta-connected winding is used as a tertiary winding and connected to the network. In such a case, the delta-connected winding is designed not only to balance out ZPS currents, but also to transform some power into the network to which it is connected.

* 12-6 Measurement of the ZPS Secondary Impedance

The secondary impedance to ZPS currents is measured by producing ZPS currents, $I_{a0} = I$, in the secondary phases. The simplest way to do this is by series-connecting the secondary windings into an pen delta (Fig. 12-7*a*).

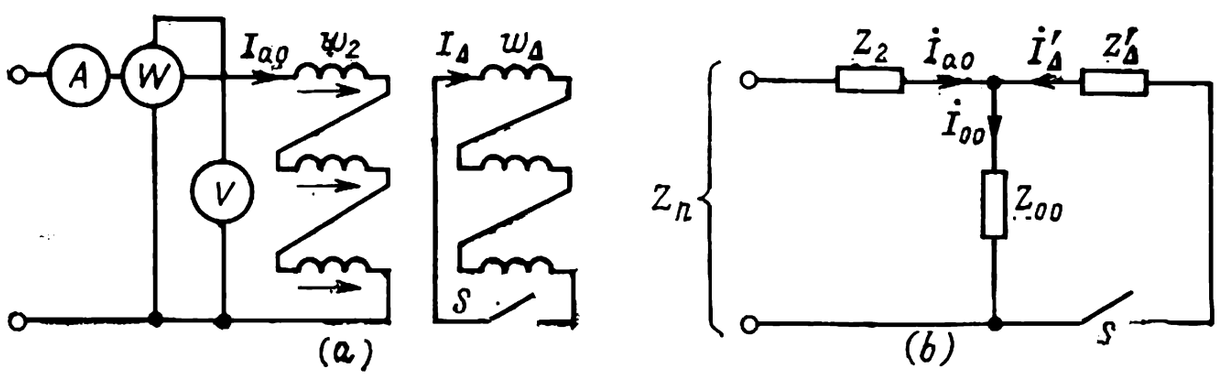

Fig. 12-7 Measurement of ZPS impedance:
(*a*) test set-up; (*b*) equivalent circuit for ZPS current

Once the voltage, current and active power are measured by the instruments connected as shown in the diagram, we can readily find the phase impedance to ZPS currents

$$Z_n = V/3I, \quad R_n = P/3I^2, \quad X_n = \sqrt{Z_n^2 - R_n^2}$$

The reactive component, X_n, is the sum of the ZPS mutual inductive reactance, X_{00}, and the leakage inductive reactance, X_2, of the secondary:

$$X_n = X_{00} + X_2 = \omega\Lambda_{00}w_2^2 + \omega\Lambda_{\sigma 2}w_2^2$$

where Λ_{00} and $\Lambda_{\sigma 2}$ are the permeances to the ZPS mutual flux and the leakage flux, respectively.

The resistive component of the ZPS mutual impedance, R_n, is the sum of the ZPS mutual resistance R_{00} and the secondary resistance R_2:

$$R_n = R_{00} + R_2$$

If, in addition to Y/Y_n-connected windings, a transformer has one more winding delta-connected, then, relative to the ZPS emf, it may be considered short-circuited. The ZPS current appearing in the delta, I_Δ, markedly reduces the ZPS fluxes and impedance (see Fig. 12-7*a*). In such a case, the ZPS impedance should be measured, with switch S closed (see Fig. 12-7*b*).

When the delta is open, the ZPS impedance of the secondary winding (see the equivalent circuit) is

$$Z_n = Z_2 + Z_{00}$$

When the delta is closed, it is substantially reduced to

$$Z_{n\Delta} = Z_2 + \frac{Z'_\Delta Z_{00}}{Z'_\Delta + Z_{00}} \approx Z_2 + Z'_\Delta \ll Z_n$$

because $Z'_\Delta \ll Z_{00}$.

∗12-7 Single- and Two-Phase Unbalanced Loads

Single-phase load, Y/Y_0 or $Y/\Delta/Y_n$ connection (Fig. 12-8*a*). The quantities specified in advance are the primary line voltages $V_{AB} = V_{BC} = V_{CA} = V_{1,\text{line}}$, and the load impedance Z.

Phase a carries a current $\dot{I}_a$ which has its path through the load impedance Z. The other phases carry no currents:

$$\dot{I}_b = \dot{I}_c = 0$$

The ZPS current is found to be

$$\dot{I}_{a0} = (\dot{I}_a + \dot{I}_b + \dot{I}_c)/3 = \dot{I}_a/3$$

The sum of the PPS and NPS currents in phase a is

$$\dot{I}_{(a)} = \dot{I}_{a1} + \dot{I}_{a2} = \dot{I}_a - \dot{I}_{a0} = 2\dot{I}_a/3$$

The currents in the primary winding [see Eq. (12-10)] are

$$\dot{I}_A = -\dot{I}'_{(a)} = -2\dot{I}'_a/3$$

$$\dot{I}_B = -\dot{I}'_{(b)} = \dot{I}'_b - \dot{I}'_{a0} = -\dot{I}'_a/3 = \dot{I}_C$$

The voltage across the load impedance Z and the phase a

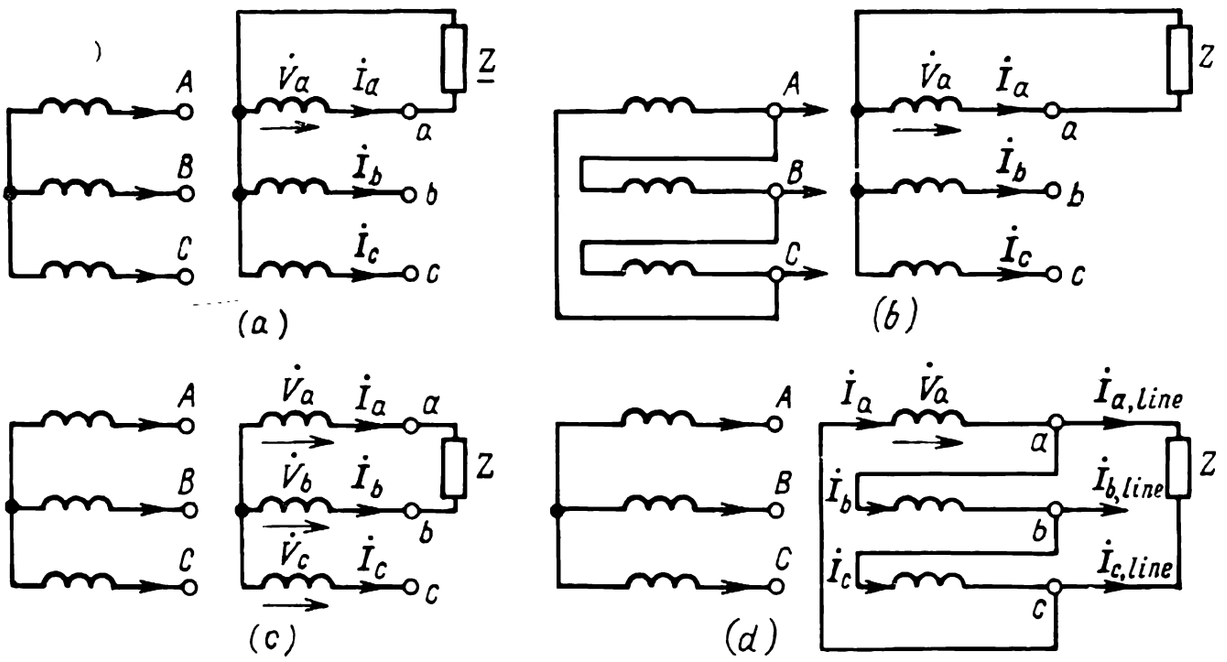

Fig. 12-8 Single- and two-phase loads in various types of connection

[see Eq. (12-24)] is

$$-\dot{V}'_a = \dot{V}_A + (\dot{I}'_{a_1} + \dot{I}'_{a_2})\, Z_{sc} + \dot{I}'_{a0} Z'_n = -Z'\dot{I}'_a$$

where $\dot{V}_A = \dot{V}_{line}/3$.

Recalling the relations between currents, the load current is found to be

$$\dot{I}'_a = -3\dot{V}_A/(2Z_{sc} + Z'_n + 3Z')$$

or

$$I'_a = \sqrt{3}\, V_{line}/|2Z_{sc} + Z'_n + 3Z'| \qquad (12\text{-}25)$$

On setting $Z' = 0$ in Eq. (12-25), we obtain an equation for a single-phase short-circuit current.

Single-phase load, Δ/Y_n connection (Fig. 12-8*b*). The quantities specified in advance are the primary phase vol-

tages which are the same as the phase voltages, $V_A = V_{CA} = V_B = V_{AB} = V_C = V_{BC} = V_{\text{line}}$, and the load impedance, $|Z|$.

The primary currents are given by Eq. (12-10):

$$\dot{I}_A = -\dot{I}'_a, \quad \dot{I}_B = \dot{I}_C = 0$$

The load voltage is equal to the phase a voltage [see Eq. (12-23)]

$$-\dot{V}'_a = \dot{V}_A + Z_{sc}\dot{I}'_a = -Z'\dot{I}'_a$$

The load current is found to be

$$\dot{I}'_a = \dot{V}_A/(Z_{sc} + Z')$$

or

$$I'_a = V_{1,\text{line}}/|Z_{sc} + Z'| \qquad (12\text{-}26)$$

On setting $Z' = 0$ in Eq. (12-26), we obtain an equation for a single-phase short-circuit current (which, in our example, does not differ from the current flowing in the case of a balanced three-phase short-circuit).

Two-phase load, Y/Y connection (Fig. 12-8*c*). The quantities specified in advance are the line voltages $V_{AB} = V_{BC} = V_{CA} = V_{\text{line}}$, and the load impedance Z. Phases a and b carry a load current $\dot{I}_b = -\dot{I}_a$, whereas phase c carries no current, $\dot{I}_c = 0$. The primary phase currents defined in Eqs. (12-10) are $\dot{I}_A = -\dot{I}'_a = \dot{I}'_b$, $\dot{I}_B = -\dot{I}'_b$, $\dot{I}_C = 0$.

The load voltage is equal to the line voltage V_{ab} [see Eq. (12-23)]:

$$\dot{V}'_{ab} = \dot{V}'_b - \dot{V}'_a = \dot{V}_A - \dot{V}_B + Z_{sc}(\dot{I}'_a - \dot{I}'_b) = Z\dot{I}'_b$$

The load current is given by

$$\dot{I}'_b = (\dot{V}_A - \dot{V}_B)/(2Z_{sc} + Z') = -\dot{V}_{AB}/(2Z_{sc} + Z')$$

or

$$I'_b = V_{1,\text{line}}/|2Z_{sc} + Z'| \qquad (12\text{-}27)$$

On putting $Z' = 0$ in Eq. (12-27), we obtain an equation for a two-phase short-circuit current.

Two-phase load, Δ/Y connection. If the primary is delta-connected and the load is arranged as shown in Fig. 12-8*c*,

the load current may be found from Eq. (12-27).

Noting that in a delta-connected winding $V_A = V_B = V_{1,\text{line}}$ and $|\dot{V}_A - \dot{V}_B| = \sqrt{3}V_{1,\text{line}}$, the magnitude of load current is found to be

$$I'_b = \sqrt{3}V_{1,\text{line}}/|2Z_{sc} + Z'| \qquad (12\text{-}28)$$

On putting $Z' = 0$ in Eq. (12-27), we obtain an equation for a two-phase short-circuit current.

Two-phase load, Y/Δ connection (Fig. 12-8*d*). The line load current is $\dot{I}_{a,\text{line}} = \dot{I}_{c,\text{line}}$, whereas the line current in phase *b* is zero. According to Eq. (12-13), the secondary phase currents are

$$\dot{I}_a = (\dot{I}_{a,\text{line}} - \dot{I}_{c,\text{line}})/3 = 2\dot{I}_{a,\text{line}}/3$$

$$\dot{I}_b = -\dot{I}_{a,\text{line}}/3$$

$$\dot{I}_c = -\dot{I}_{a,\text{line}}/3$$

The load voltage is equal to the phase *a* voltage, Eq. (12-23), or the line voltage $\dot{V}_{ca}$:

$$-\dot{V}'_a = -\dot{V}'_{ca} = \dot{V}_A + Z_{sc}\dot{I}'_a = -\dot{I}_{a,\text{line}}Z'$$

The load current is given by

$$\dot{I}_{a,\text{line}} = -\dot{V}_A/(2Z_{sc}/3 + Z')$$

or

$$I_{a,\text{line}} = V_{1,\text{line}}/(\sqrt{3}\,|2Z_{sc}/3 + Z'|) \qquad (12\text{-}29)$$

On setting $Z' = 0$ in Eq. (12-29), we obtain an equation for a two-phase short-circuit current.

13 Transients in Transformers

13-1 Transients at Switch-On

Each time a change occurs in the load or the primary voltage, a transformer does not reach a new steady state until all transients die out. Sometimes, the currents accompanying the transients may exceed their steady-state values many-fold. The winding temperature and the emfs, all of which are current-dependent, rise substantially and may even

exceed the maximum safe values. Obviously, if the designer fails to take a proper account of the transients that are likely to occur in a transformer, he will not be able to choose the correct dimensions, service conditions, and the extent of protection needed.

To begin with, let us consider the transients that occur when a transformer is just switched on.

Suppose that the secondary winding is open-circuited ($i_2 = 0$). At time $t = 0$, the primary is switched into a supply network (or system) with a phase voltage

$$v_1 = V_{1m} \cos(\omega t + \psi)$$

The transients in the primary circuit of a transformer can be described by a nonlinear differential voltage equation

$$i_0 R_1 + w_1 \, d\Phi/dt = v_1 \qquad (13\text{-}1)$$

where i_0 is the transient no-load current, $\Phi = f(i_0)$ is the mutual flux which is a nonlinear function of i_0 (see Fig. 2-3).

Since $i_0 R_1 \ll w_1 \, d\Phi/dt$, we may, without committing a serious error, write i_0 in terms of Φ as

$$i_0 = w_1 \Phi / L_0$$

where $L_0 = \text{const}$ is the mean primary inductance

$$d\Phi/dt = \Phi R_1 / L_0 = v_1 / w_1 \qquad (13\text{-}2)$$

The solution of a linear differential equation with constant coefficients is the sum of two terms, a free (or transient) term and a forced (or steady-state) term. In our case,

$$\Phi = \Phi_t + \Phi_{ss}$$

The transient term

$$\Phi_t = C \exp(-\alpha_0 t)$$

is the general solution of a homogeneous equation

$$d\Phi/dt + \Phi R_1 / L_0 = 0$$

where $-R_1/L_0 = \alpha_0$ is a root of the characteristic equation.

The steady-state term

$$\Phi_{ss} = \Phi_m \sin(\omega t + \psi), \quad \text{where} \quad \Phi_m = V_{1m}/\omega w_1$$

is the mutual flux Φ [see Eq. (2-9)] which is established in the transformer core at no-load and $v_1 = V_{1m} \cos(\omega t + \psi)$. The constant C is determined from initial conditions.

If we neglect the residual flux, $\Phi_{res} = 0$, then at $t = 0$ the flux in the core is zero:

$$\Phi_{t=0} = \Phi_t + \Phi_{ss} = C + \Phi_m \sin \psi = 0$$

Hence,

$$C = -\Phi_m \sin \psi$$

and

$$\Phi = -\Phi_m \sin \psi \exp(-\alpha_0 t) + \Phi_m \sin(\omega t + \psi) \quad (13\text{-}3)$$

The worst case at switch-on occurs when $\psi = \pm\pi/2$, because at $t = 0$, $v_1 = 0$. In the circumstances, the initial

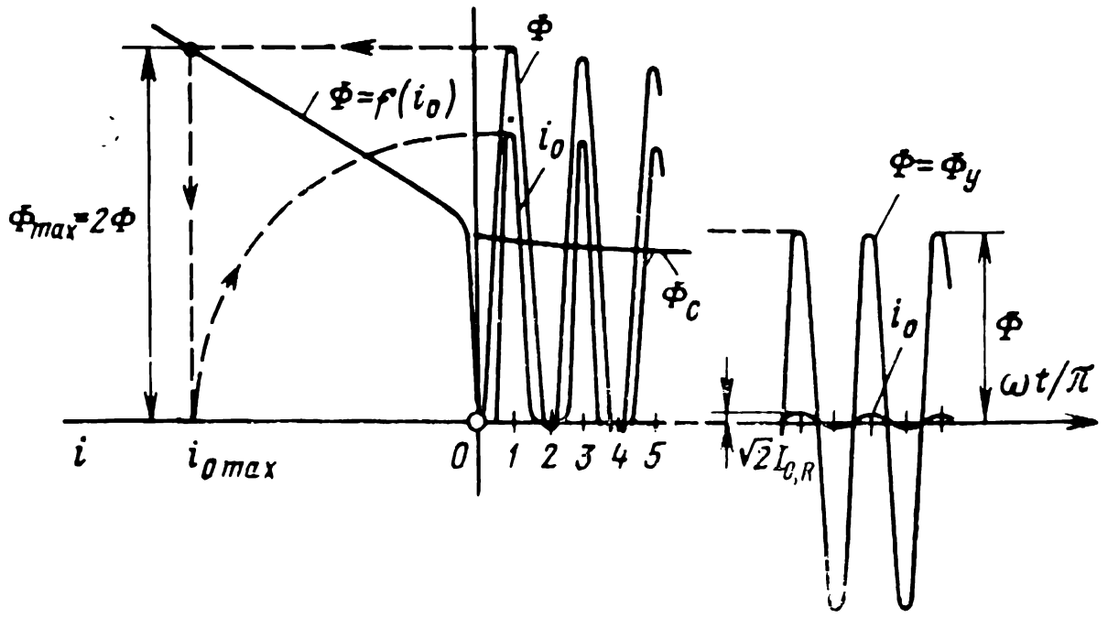

Fig. 13-1 Variations in the flux and magnetizing current of a transformer at switch-on; $\psi = -\pi/2$, $\Phi_{core} = \Phi \exp(-\alpha_0 t)$

value of the transient flux is equal to the peak value of the steady-state flux, $C = \mp\Phi_m$, and, as is seen from Fig. 13-1, a half-cycle after switch-on the flux in the core rises to a maximum value equal to twice the peak value, $\Phi_{max} \approx 2\Phi_m$. (By this instant, the transient term subsides very little, $\exp(-\alpha_0\pi/\omega) \approx 1$.)

The current in the winding following switch-on can be found graphically from Fig. 13-1, using the magnetization curve in Fig. 2-3.*

The maximum switch-on current $i_{0,max}$ observed a half-cycle after the onset of the transients may exceed the peak

* The replacement of the nonlinear magnetization curve by a linear one results in an error in the value of α_0 and the damping of the transient flux.

value of the rated load current

$$i_{0,\,\max} \gtrsim \sqrt{2}\, I_{1,R} \gtrsim \sqrt{2}\, I_{0,R}$$

This point must be borne in mind when adjusting the setting of the protective relays and carrying out an open-circuit test.

13-2 Transients on a Short-Circuit Across the Secondary Terminals

We shall limit ourselves to a balanced (three-phase) short-circuit across the secondary terminals of a transformer. Suppose that prior to a short-circuit, that is, at $t < 0$, the primary was energized with

$$v_1 = V_{1,m} \cos(\omega t + \psi)$$

and the secondary was open-circuited.

If we ignore the magnetizing current and deem $i_1 = -i_2'$, the transients on a short-circuit may be solved, using an equivalent circuit for a short-circuited transformer.

Referring to Fig. 5-2*b*, the equivalent circuit of a short-circuited transformer contains a resistive component,

$$R_{sc} = R_1 + R_2'$$

and an inductive component

$$X_{sc} = X_1 + X_2'$$

such that

$$X_{sc}/\omega = L_{sc} = L_1 + L_2'$$

The transients in such a circuit can be described by a linear differential equation with constant coefficients, R_{sc} = constant, and L_{sc} = constant:

$$R_{sc} i_1 + L_{sc}\, di_1/dt = v_1 \qquad (13\text{-}4)$$

whose solution is

$$i_1 = i_{1,t} + i_{1,ss}$$

The transient term

$$i_{t,1} = C \exp(-\alpha_{sc} t)$$

is the solution of a homogeneous equation

$$di_1/dt + R_{sc} i_1/L_{sc} = 0$$

where $-R_{sc}/L_{sc} = \alpha_{sc}$ is a root of the characteristic equation.

The steady-state term

$$i_{1,ss} = \sqrt{2}\, I_{sc} \cos(\omega t + \varphi - \varphi_{sc})$$

is the particular solution of Eq. (13-4) at $t = \infty$, or the steady-state short-circuit current. The amplitude and phase of this current can be ascertained from a short-circuit equivalent circuit (see Fig. 5-2*b*):

$$\sqrt{2}\, I_{sc} = V_{1m}/\sqrt{R_{sc}^2 + (\omega L_{sc})^2} = V_{1m}/|Z_{sc}|$$

$$\varphi_{sc} = \arctan(\omega L_{sc}/R_{sc})$$

The constant C may be defined from initial conditions. Prior to the short-circuit, the transformer was running at no-load, so (neglecting the no-load current) we may deem that at $t = 0$,

$$i_{1,\,t=0} = -i'_{2,\,t=0} = i_{1,\,t} + i_{1,\,ss}$$

$$= C + \sqrt{2}\, I_{sc} \cos(\psi - \varphi_{sc}) = 0$$

Hence,

$$C = -\sqrt{2}\, I_{sc} \cos(\psi - \varphi_{sc})$$

and the transient current is

$$i_1 = -i'_2 = -\sqrt{2}\, I_{sc} \cos(\psi - \varphi_{sc}) \exp(-\alpha_{sc} t)$$

$$+ \sqrt{2}\, I_{sc} \cos(\omega t + \varphi - \varphi_{sc}) \qquad (13\text{-}5)$$

The transient time is in fact the time required for the transient current $i_{1,t}$ to die out. In time $t = 1/\alpha_{sc}$ after the onset of the transients, the transient current falls to $1/e$ of its original value. In time $3/\alpha_{sc}$, it falls to $1/e^3$, or one-twentieth of its original value and is practically non-existent.

The time required for the transient component to reduce to $1/e$ of its original value is called the transient time or decay modulus, $\tau = 1/\alpha$.

For power transformers (see Sec. 3-6),

$$\tau_{sc} = 1/\alpha_{sc} = X_{sc}/\omega R_{sc} = 0.01 \text{ to } 0.2 \text{ s}$$

that is, the decay modulus increases as the power rating of transformers goes up.

An increase in the initial value of the free (transient) component leads to an increase in the short-circuit current.

A short-circuit is most severe if it occurs when $\psi = \varphi_{sc}$ or $\psi = \varphi_{sc} + \pi$. In such cases, the initial value of the free component is equal to the peak value of the forced component

$$-\sqrt{2}\, I_{sc} \cos(\psi - \varphi_{sc}) = \mp \sqrt{2}\, I_{sc}$$

The waveforms of short-circuit currents when $\psi = \varphi_{sc} + \pi$ are shown in Fig. 13-2. The currents in the windings attain

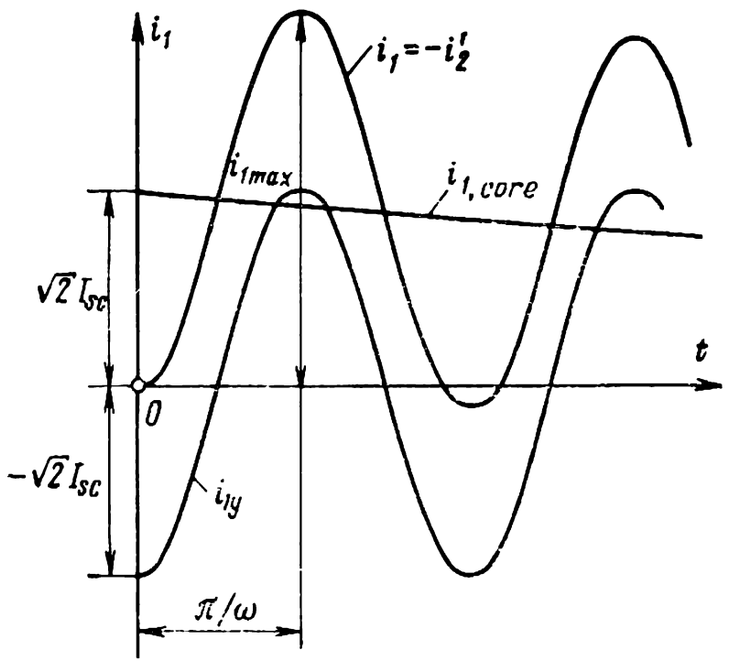

Fig. 13-2 Variations in transformer current during transients following a short-circuit on the secondary side ($\psi = \varphi_{sc} + \pi$)

their maximum values a half-cycle after the onset of the transients

$$i_{1,\,max} = |\, i_2' \,|_{max} = \sqrt{2}\, I_{sc} [1 + \exp(-\pi/\omega\tau_{sc})]$$

Dividing this current by the peak rated current and assuming that the primary voltage is at its rated value, we get

$$\begin{aligned} i_{1,\,max}/\sqrt{2}\, I_{1,\,R} &= (I_{sc}/I_R)[1 + \exp(-\pi/\omega\tau_{sc})] \\ &= (1/v_{sc})[1 + \exp(-\pi/\omega\tau_{sc})] \end{aligned} \qquad (13\text{-}6)$$

where v_{sc} is the per-unit short-circuit current.

In power transformers, the maximum short-circuit current may be as high as

$$i_{1,\,max}/\sqrt{2}\, I_R = 25 \text{ to } 15 \text{ per unit} \qquad (13\text{-}7)$$

(The larger values apply to transformers of lower power ratings.)

A transformer must be designed so that a short-circuit would not put it out of service or cut down its service life.

In choosing the winding design and clamping arrangement, preference should be given to those preventing the damage that the electromagnetic forces might do to the windings during a short-circuit. The point is that the primary and secondary windings of a transformer carry currents flowing in opposite directions. On a short-circuit, $i_{1,\,max}$ and $i_{2,\,max}$ are many times the rated values. The electromagnetic forces arising from the interaction of the oppositely directed currents in the primary and secondary tend to compress the turns in the inner winding and to expand the turns in the outer winding. The electromagnetic forces arising from the interaction of currents flowing in the same direction in the turns of each of the windings tend to compress the windings in height.

During a short-circuit, the electromagnetic forces, which are proportional to the current product, $i_{1,\,max} i_{2,\,max}$, or the square of each current, $i^2_{1,max}$ or $i^2_{2,\,max}$, increase 225 to 625 times. These forces are pulsating at a frequency $2f = 2 \times 50 = 100$ Hz without reversing their direction. The windings will not be damaged if the accompanying mechanical stresses do not exceed 50 to 60 N mm^{-2}.

No less dangerous is the heat effect of short-circuit currents, because the copper losses (proportional to the current squared) increase many-fold, and the temperature of the windings abruptly rises. Since the free component of the short-circuit current decays in $3\tau_{sc} = 0.03$ to 0.6 s, the rate of temperature rise may be evaluated from the steady-state short-circuit current. This current causes the copper loss to grow 49 to 225 times.

The current density in the windings builds up appreciably and may be as high as 20 to 40 A mm^{-2}. If the windings are assumed to be heated adiabatically (that is, the heat liberated within the windings is not transferred to the surroundings), the temperature of the windings will rise at the rate given by

$$J^2/170 \approx 2.4 \text{ to } 9.5 \text{ °C s}^{-1}$$

Prior to a short-circuit, the maximum safe temperature of the windings may be as high as 105°C (see Sec. 16-1). The short-time maximum safe temperature of the windings, at which their insulation still remains intact, is set at 250°C.

If we know the rate of temperature rise, we can readily find the time, t_{sc}, during which the winding temperature will go up from 105°C to 250°C:

$$t_{sc} \approx 2.5\,(100v_{sc}/J_R)^2 = 5 \text{ to } 25 \text{ s}$$

As a rule, the protective relay(s) will disconnect a transformer from its supply much earlier, and the winding temperature will not rise to its limit.

14 Overvoltage Transients in Transformers

14-1 Causes of Overvoltages

In service, transformers are often subjected to overvoltages. For example, an overvoltage may develop when an element (or elements) of an electric system is turned on or

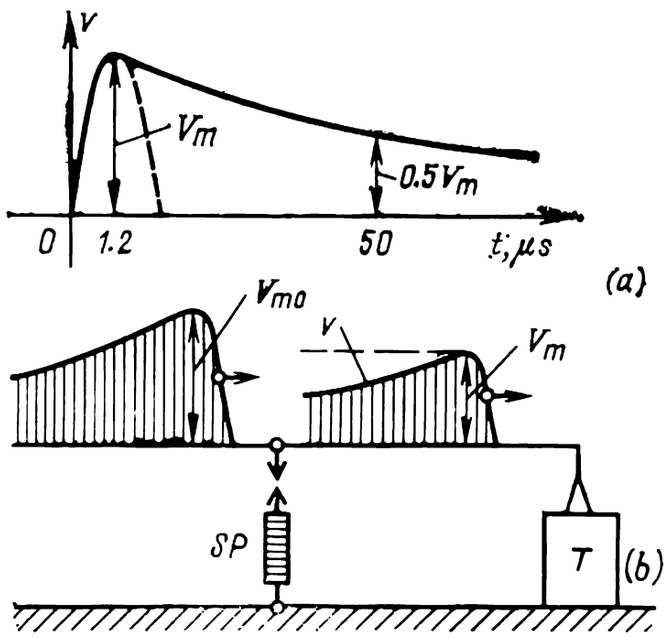

Fig. 14-1 Overvoltage waves

off (switching voltage surges), but this contingency is usually provided for in transformer design.

More dangerous to transformer insulation are overvoltages produced by lightenings which strike line conductors and induce high-voltage waves in them (lightening voltage surges).

An overvoltage wave propagates both ways from the point of occurrence at a velocity very close to that of light. An overvoltage wave has the shape of an overdamped pulse with a steep leading edge (Fig. 14-1*a*). The rise time of this wave is usually a split microsecond or millisecond; the pulse duration equal to the wave length runs into tens of microseconds. Figure 14-1*a* shows a standard total overvoltage wave used in testing transformers for pulse strength. Its length, in terms of the fall or decay time to half its peak value, is 50×10^{-6} s.

To minimize overvoltages (see Fig. 14-1*b*), it is usual to equip transformers with a spark-gap, SP, which will break down at V_m. Ahead of a spark-gap, the overvoltage wave may have a very large peak value, V_{m0}. Past the spark-gap, its peak value, V_m, ought not to exceed the voltage used in testing the insulation for pulse strength (see Table 14-1)*.

Table 14-1 Pulse Test Voltages for Transformer Insulation used in the USSR

Winding voltage class, kV	3	6	10	15	35	110	115	220	330	500
Peak value of test voltage (total wave), kV	44	60	80	108	200	480	550	750	1050	1550

The transients that take place in a transformer when the incident wave has a fast rise time, t_r (a few microseconds) are of a very complex character.

14-2 The Differential Equation for the Initial Voltage Distribution in the Transformer Winding

The transients occurring in a transformer as the applied voltage is raised from zero to V_m during the rise time t_r may be likened to what happens when the same transformer is energized with an alternating voltage having the same peak value, V_m, and a period $T_t = 4t_r$ (see the dashed line

* The wave reflected from the input capacitance of the transformer is combined with the incident wave, but the total wave does not raise the voltage above V_m at which the spark-gap breaks down.

in Fig. 14-1*a*). This alternating voltage has a fairly high frequency. For the standard test wave, this frequency is

$$f_t = \omega_t/2\pi = 1/T_t = 1/4t_r$$
$$= 1/(4 \times 1.2 \times 10^{-6})$$
$$= 2.08 \times 10^5 \text{ Hz}$$

At such a frequency, we may no longer ignore the capacitive coupling existing between the winding elements, C'_d, and between the winding elements and the grounded parts of the

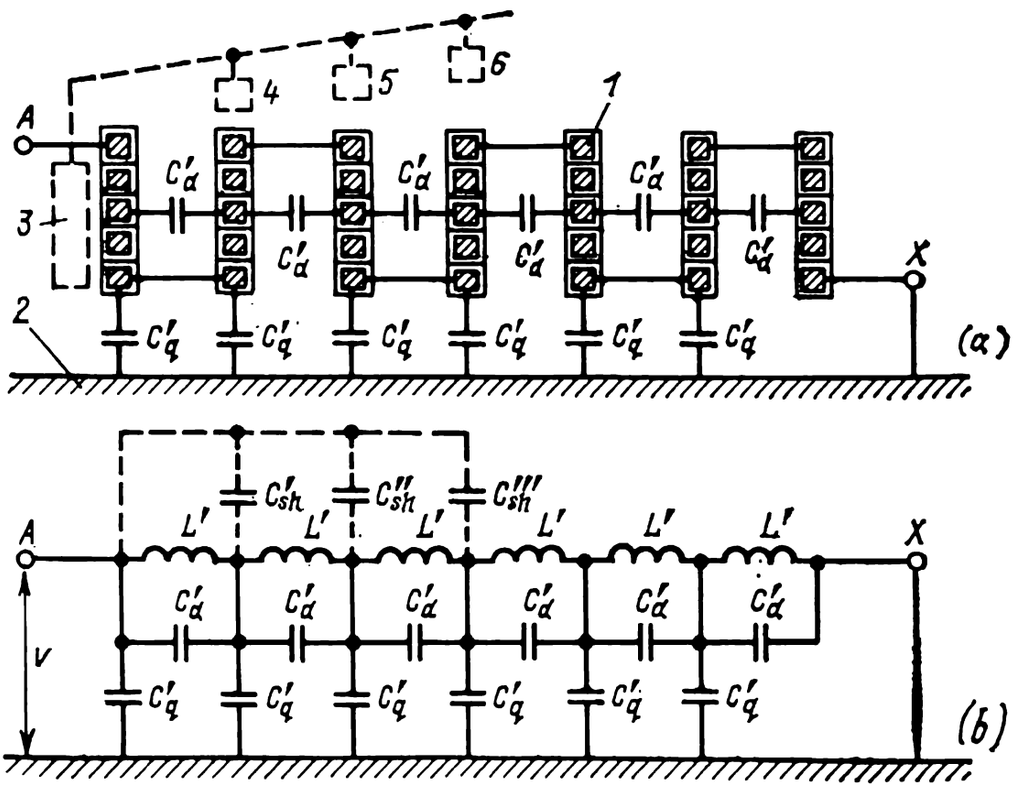

Fig. 14-2 Overvoltage in a winding: (*a*) cross-sectional view; (*b*) equivalent circuit:
1—winding conductors; *2*—grounded parts; *3*—through *6*—electrostatic shields around the coils next to the winding start; C'_d—capacitance between coils; C'_q—capacitance of coil to ground; C'_{sh}, C''_{sh}, C'''_{sh}—capacitances between shields and winding

transformer, C'_q (Fig. 14-2*a*). Nor may we use the usual equivalent circuit which only considers inductive coupling and is applicable to operation at the rated frequency (which is 50 Hz for power transformers in the Soviet Union).

Now we must use an equivalent circuit which includes both the inductances of the various winding elements, L', and the capacitances between them, C'_d, and their capacitances to the grounded parts, C'_q. Such an equivalent circuit, with the terminal X grounded, is shown in Fig. 14-2*b*.

If we are only interested in the initial voltage distribution, when the voltage at the winding start is V_m, then, because f_t is very high, we may deem that no currents can flow in the turns because their inductive reactance $\omega_t L'$ is very high. Rather, they flow in the series capacitive reactances, $1/\omega C'_d$, and the shunt capacitive reactances, $1/\omega C'_q$. Therefore, we put $\omega_t L'$ equal to infinity and assume that the voltage distribution is solely dependent on the capacitances included in the equivalent circuit in Fig. 14-2*b* (for the time being, we ignore the part of the circuit shown by dashed lines).

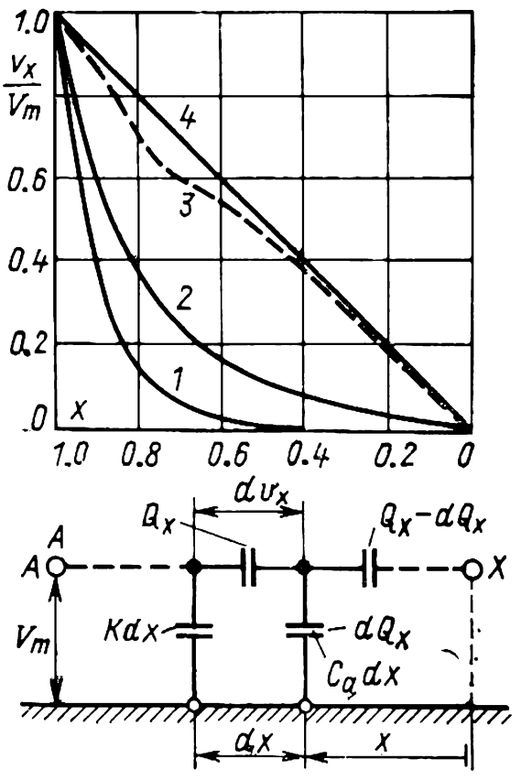

Fig. 14-3 Voltage distribution in the capacitive circuit of a winding with its finish grounded:
1—initial distribution at $\alpha = 10$; *2*—initial distribution at $\alpha = 5$; *3*—initial distribution in a transformer with electrostatic shields; *4*—initial distribution at $\alpha = 0$ and final distribution at any value of α

Let us replace the lumped-capacitance circuit in Fig. 14-2*b*, composed of n elements, by a distributed-capacitance circuit shown in Fig. 14-3. Then the total series capacitance will be

$$C_d = 1/\sum (1/C'_d) = C'_d/n$$

and the total shunt capacitance will be

$$C_q = \sum C'_q = nC'_q$$

Taking the winding length as unity, we may, for a winding element of length dx, find its shunt capacitance $C_q\,dx$ and the shunt differential parameter $K\,dx$, where $K = 1/C_d$.

With V_m at the start of the winding held constant, the voltage v_x within a distance x of the grounded terminal X can be found by solving a set of differential equations for the shunt charge on the element $K\,dx$, equal to

$$Q_x = dv_x/K\,dx \qquad (14\text{-}1)$$

and the voltage across the capacitance $C_q\,dx$, equal to

$$v_x = dQ_x/C_q\,dx \qquad (14\text{-}2)$$

On finding the derivative dQ_x/dx from Eq. (14-1) and substituting it in Eq. (14-2), we obtain a linear differential equation with constant coefficients for v_x:

$$d^2v_x/dx^2 - (C_q/C_d)\, v_x = 0 \qquad (14\text{-}3)$$

14-3 Voltage Distribution over the Winding and Its Equalization

The solution of Eq. (14-3) has the form

$$v_x = D_1 \exp(\alpha x) + D_2 \exp(-\alpha x)$$

where $\alpha = \sqrt{C_q/C_d}$ and $-\alpha$ are the roots of the characteristic equation. Applying the boundary conditions that exist when the winding terminal is grounded

(1) $v_x = D_1 \exp(\alpha) + D_2 \exp(-\alpha) = V_m$ for $x = 1$

(2) $v_x = D_1 + D_2 = 0$ for $x = 0$

we can find the constants D_1 and D_2, and the initial voltage distribution will be

$$v_x = V_m \sinh \alpha x/\sinh \alpha \qquad (14\text{-}4)$$

As is seen from Fig. 14-3, for the values of α most frequently found in practice, $\alpha = 5$ to 10 (curves *1* and *2*), the initial voltage distribution is rather nonuniform, and becomes the more so as α increases (that is, with an increase in the shunt capacitance or a decrease in the series capacitance).

When the initial voltage distribution is ideally uniform (curve *4*) corresponding to $\alpha \approx 0$, and

$$v_x = V_m \sinh \alpha x/\sinh \alpha \approx V_m \alpha x/\alpha = V_m x,$$

the voltage existing across the element Δx nearest to the start of the winding is

$$\Delta v = V_m\, \Delta x$$

In a real winding ($\alpha \geqslant 3$), the voltage existing across the winding element Δx nearest to the start [see Eq. (14-4)] will be

$$\Delta v = (dv_x/dx)_{x=1}\, \Delta x = (V_m \alpha \coth \alpha)\, \Delta x$$
$$= V_m \alpha\, \Delta x$$

which is α times the voltage in the case of a uniform distribution.

The further propagation of the overvoltage wave along the transformer winding can conveniently be examined, if we assume that the wave is rectangular in shape, as shown by the dashed line at the bottom of Fig. 14-1. In this case, V_m at the winding start, appearing at $t_r \approx 0$, remains unchanged, and soon all points on the winding come by a steady-state voltage. This is the final voltage distribution. With the winding terminal grounded, this will be a linear distribution

$$v_x = V_m x$$

(curve *4* in Fig. 14-3).

The propagation of an overvoltage wave along the winding is in effect a transition from the initial voltage distribution at $t = t_r \approx 0$ to the final voltage distribution at $t = \infty$.

Because the equivalent circuit of the winding is composed of capacitances and inductances which form, between them, a cascade of resonant circuits, the transition from the initial to the final voltage distribution at each point is oscillatory. Owing to the losses in the resistances, these oscillations gradually decay. The swing of oscillations and the associated overvoltage increase with increasing difference between the initial and final voltage distributions.

To minimize the hazards associated with such oscillations, the value of α must be kept as small as practicable. Also, a decrease in α leads to a decrease in the initial voltages existing across the elements close to the start of the winding. Unfortunately, an ample spacing between the winding and the grounded parts cannot be obtained without a marked increase in the size and cost of the transformer.

The best way to equalize the initial voltage distribution and to make it comparable with the final distribution is to use electrostatic shields in the form of open metal rings (labelled *3* through *6* and shown dashed in Fig. 14-2*a*). When such shields are connected to the start of the winding, the capacitive coupling of the first coils to the winding start (via capacitances C'_{sh}, C''_{sh}, and C'''_{sh} in Fig. 14-2*b*) is substantially increased, and the initial voltage distribution becomes more uniform and close to the final one (curve *3* in Fig. 14-3).

In Soviet-made transformers, the use of shields around the windings guarantees the required pulse strength of insulation in transformers for 110 kV and higher (see Table 14-1).

15 Special-Purpose Transformers

15-1 General

This chapter discusses special-purpose transformers which either transform or convert some parameter(s) of electric energy (frequency, number of phases, or voltage waveform) or serve some special purposes (continuous voltage adjustment, supply of high voltages, isolation of the secondary current from the load impedance, supply of secondary current or voltage proportional to the primary one, etc.).

15-2 Three-Phase Transformation with Two Transformers

There are ways to transform three-phase with only two transformers. One of the most commonly used connections for this purpose, known as the Scott transformer or the T-connection, is shown in Fig. 15-1.

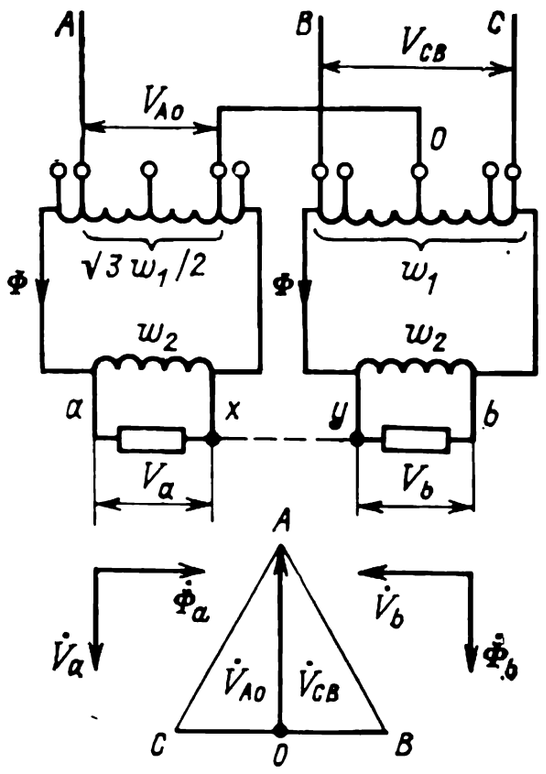

Fig. 15-1 Three/two-phase conversion

In the T-connection, one transformer, b, has its primary connected directly across two lines; this is the "main" transformer having w_1 turns and a primary voltage equal to the line voltage $V_{CB} = V_{1,\,line}$. The voltages V_{C0} and V_{0B} are equal, because the emfs in the two halves of the BC winding are induced by the same magnetic flux Φ_b. The other transformer, a, is called the *teaser*. Its primary has $\sqrt{3}\,w_1/2$ turns and is connected between terminals A and 0 of the main transformer, so that its primary voltage is $\sqrt{3}V_{1,\,line}/2$. The secondary voltages V_a and V_b form a balanced two-phase system, because they are equal in

magnitude

$$V_b = V_{CB}\,(w_2/w_1) = V_{1,\,line}\,(w_2/w_1)$$
$$V_a = V_{A0}\,(2w_2/\sqrt{3}\,w_1) = V_{1,\,line}\,(w_2/w_1)$$

and are shifted in phase by the same angle as V_{A0} and V_{CB}, that is, $\pi/2$.

15-3 Frequency-Conversion Transformers

(a) Frequency trebling. This purpose can be served by a bank of three single-phase transformers whose primaries are star-connected and energized from a three-phase supply at freq ncy f_1. As has been shown in Sec. 7-3, the fluxes of

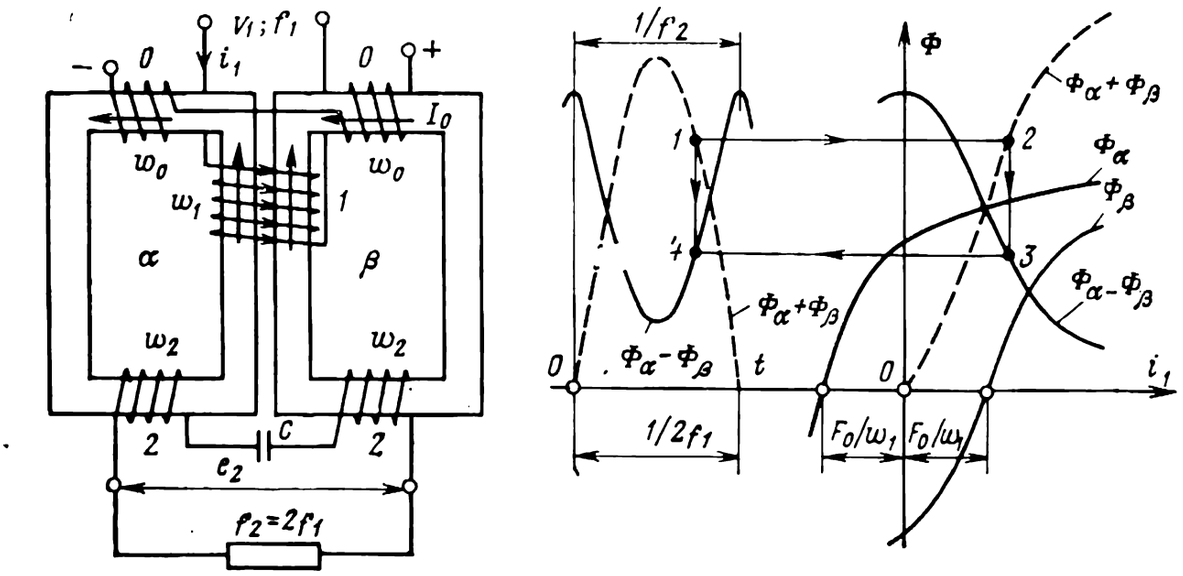

Fig. 15-2 Frequency doubling

such a transformer contain a sizeable proportion of the third harmonics for which $f_3 = 3f_1$. The third-harmonic emfs, E_3, induced into the secondary are in phase, so when the output winding is a combination of three single-phase secondaries connected in series aiding, the output will only contain $3E_3$ at $3f_1$, but no emf at the fundamental frequency, because in a balanced system the fundamental emfs sum to zero.

(b) Frequency doubling. This purpose can be served by a transformer having two independent magnetic circuits (at α and β in Fig. 15-2). The primary energized from a supply at f_1 encloses both magnetic circuits, so the emf induced in it is due to the sum of two fluxes, Φ_α and Φ_β.

The secondary in which the emf is induced at twice the fundamental frequency, $f_2 = 2f_1$, has w_2 turns contributed by two halves which are wound on different cores and are connected in opposition. With this arrangement, the flux linkage of the secondary is proportional to the difference flux, $\Phi_\alpha - \Phi_\beta$. As is seen from the plot in Fig. 15-2, as the sum flux $\Phi_\alpha + \Phi_\beta$ alternates at frequency f_1, the difference flux $\Phi_\alpha - \Phi_\beta$ alternates at twice that frequency, $f_2 = 2f_1$, if the two cores are biased in opposite senses by winding 0 energized with direct current I_0 and establishing an mmf $F_0 = w_0 I_0$ in each core.

15-4 Variable-Voltage Transformers

Stepwise voltage adjustment by tap changing has been examined in Chap. 6. Because of an added complexity in transformer design and tap-changers, only several steps of adjustment can be provided, and the overall range of adjustment does not exceed ±5%.

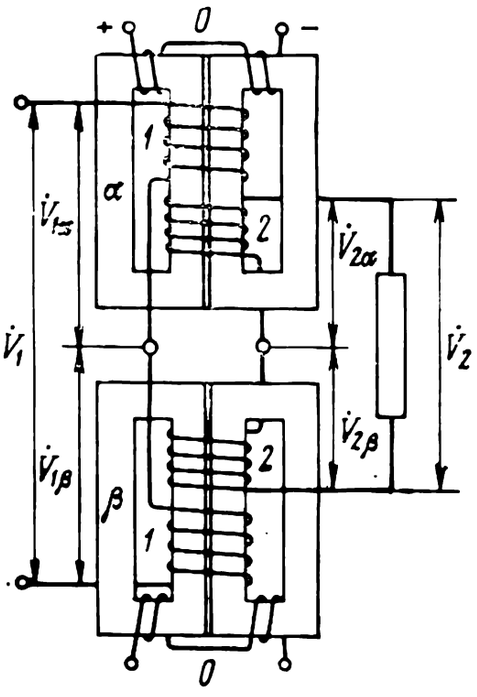

Fig. 15-3 Variable transformer with a d.c.-biased core

A more continuous voltage adjustment in low-voltage transformers and low-power autotransformers can be obtained with brushes or sliding contacts that can be moved across a skinned portion of the transformer winding. This form of adjustment changes the transformer voltage in small steps equal to the voltage across one turn; the range of adjustment can be extended considerably. This arrangement is utilized, for example, in *dimmer-control* transformers for auditoriums and theatre stages. In a 250 kVA unit, the output voltage can be varied from zero to 220/380 V.

In high-power or high-voltage transformers, continuous voltage adjustment can be obtained by biasing the core with direct current. A likely arrangement utilizing d.c. bias is shown in Fig. 15-3. It is a combination of two single-phase transformers differing in the transformation ratio, $n_{21\alpha}$

$\neq n_{21\beta}$. Each transformer has a split core biased with d.c. in the same manner as in the case of frequency doubling. (When the core halves are biased in opposite senses, the biasing current is nearly sinusoidal.)

The primaries with voltages $\dot{V}_{1\alpha}$ and $\dot{V}_{1\beta}$ are series-connected for a supply voltage $\dot{V}_1 = \dot{V}_{1\alpha} + \dot{V}_{1\beta}$. The secondaries with voltages $-\dot{V}_{2\alpha} = n_{21\alpha}\dot{V}_{1\alpha}$ and $-\dot{V}_{2\beta} = n_{21\beta}\dot{V}_{1\beta}$ are likewise series-connected and loaded into an impedance the voltage across which is

$$\dot{V}_2 = \dot{V}_{2\alpha} + \dot{V}_{2\beta}$$

When the cores of transformers α and β are biased separately, it is possible to vary the ratio between the resistances of the primary windings traversed by a common current I_1, and the voltage ratio

$$\xi = \dot{V}_{1\beta}/\dot{V}_{1\alpha}$$

For example, if we increase the bias on transformer β, the voltage ratio will decrease. A change in ξ brings about a proportionate change in the output voltage

$$-\dot{V}_2 = -\dot{V}_{2\alpha} - \dot{V}_{2\beta} = \dot{V}_1 \frac{n_{21\alpha} + \xi n_{21\beta}}{1 + \xi}$$

When $\xi = 0$, $-\dot{V}_2 = \dot{V}_1 n_{21\alpha}$; when $\xi = \infty$, $-\dot{V}_2 = \dot{V}_1 n_{21\beta}$. In practice, the output voltage can be varied within narrower, but sufficiently broad limits.

15-5 Arc Welding Transformers

Arc welding transformers have to operate intermittently, with frequent transitions from no-load to an arc often accompanied by instantaneous short-circuits.

It is usually required that the short-circuit current of a welding transformer be not more than two or three times its rated voltage. Another requirement is that variations in the circuit (load) impedance ought not to produce marked variations in output voltage. To meet these requirements, the short-circuit impedance of a welding transformer must be many times that existing in ordinary transformers. As a rule, the short-circuit impedance of welding transformers is raised at the expense of the inductive reactance. To this end,

the windings are placed on different sections of the core and are series-connected. A further increase in short-circuit inductance can be obtained by placing adjustable reactors in the secondary circuit.

15-6 Insulation Testing Transformers

Insulation testing uses voltages from 1 MV upwards. Such voltages can only be supplied by a cascade of series-connected transformers (Fig. 15-4). The total output voltage V is the

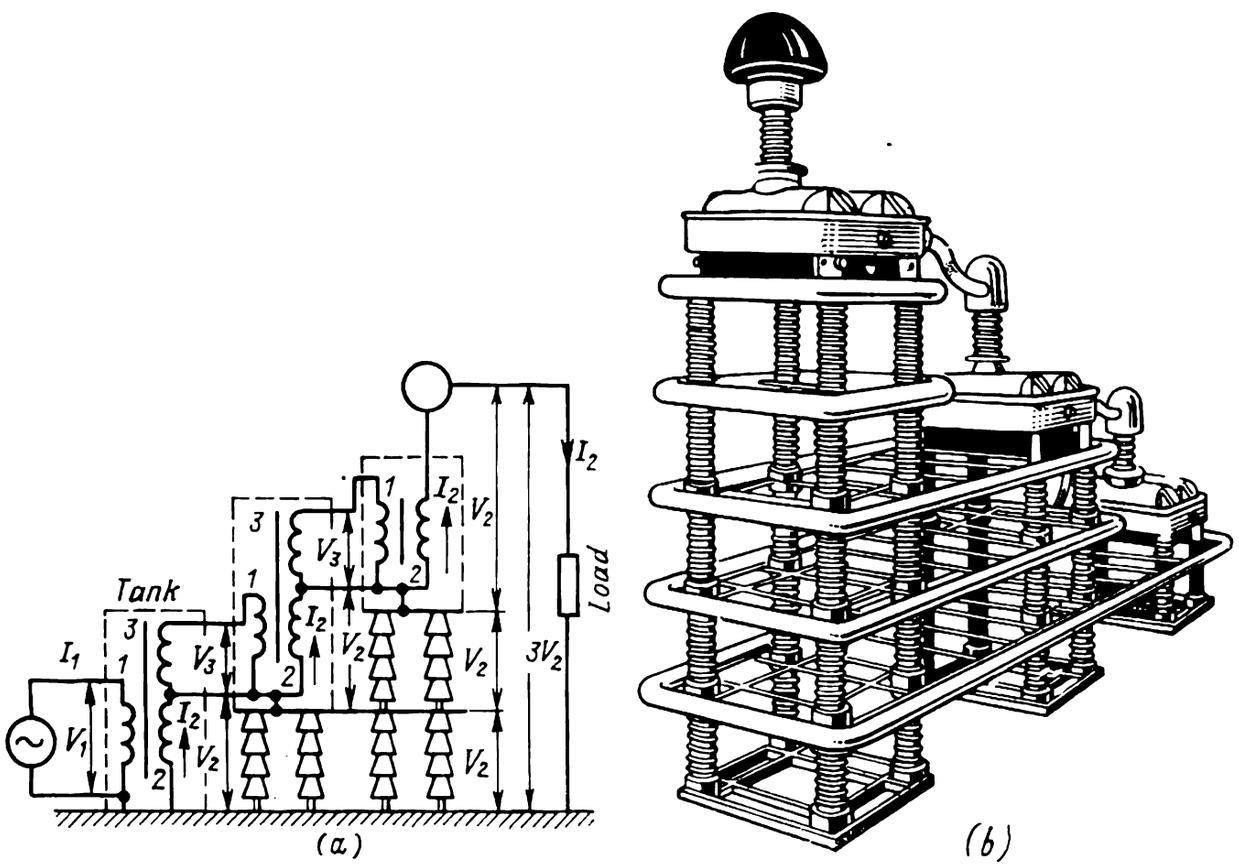

Fig. 15-4 Three-stage cascaded laboratory transformer:
(*a*) circuit diagram; (*b*) external appearance of a 1.5-MV, 1.5 MVA cascaded transformer (in contrast to the arrangement in (*a*), the transformer tank in the first stage is isolated from ground)

sum of the secondary voltages, V_2, supplied by each stage in a cascade. In a three-stage cascade, it is $V = 3V_2$. Each transformer in the cascade is installed in a separate tank and has three windings, namely winding *1* energized from the previous stage, and windings *2* and *3* which are autoconnected (the last unit in the cascade has only winding *1* and *2*). The tanks of the second and third stages stand on pedestal insulators and are at a voltage of V_2 and $2V_2$ relative to the ground, respectively. The tank of the first

stage is grounded. Accordingly, the winding insulation of the first and second transformers is designed for $V_2 + V_3$, and that of the third, for V_2.

15-7 Peaking Transformers

Peaking transformers are employed in electronics as sources of recurring peaked voltage pulses which have a short duration in comparison with the pulse period. Such a voltage can be produced across the secondary of a transformer with a heavily saturated core, if the primary is connected to a source of sinusoidal voltage, $v_1 = V_{1m} \sin \omega t$, via a high-value resistance R or a linear inductive reactance. Then the primary current i_1 will be sinusoidal, the flux waveform will be flattened, and the emf will be peaked. A similar effect, although less pronounced, can be obtained with a star-star three-phase transformer (see Sec. 4-4 and Fig. 4-14).

15-8 Instrument Transformers

Most power systems operate at voltages and currents too high to be measured by ordinary instruments directly. Instead, instruments must be connected to an H.V. network via instrument (or measuring) transformers which may be designed for voltage or current measurements. Instrument transformers are also used to energize control and safety relays and other automatic control devices. Instrument load on the secondary of a measuring transformer is called its burden and is expressed in volt-amperes at a certain power factor.

Voltage transformers. Instrument transformers in this group are designed to step down the primary voltage to around 100 V. The burden should be no less than some specified value, Z_R, and the transformer must be designed so that its referred secondary voltage changes little as the load is varied from zero to its full (rated) value.

In Sec. 5-1 it has been shown that

$$\dot{V}_2' \approx -\dot{V}_1 Z'/(Z_{sc} + Z')$$

Therefore, if $Z' \gg Z_{sc}$, then $\dot{V}_2' \approx -\dot{V}_1$. When this condition is met, the primary to secondary voltage ratio will always

be the same, and

$$\dot{V}_2 = -\dot{V}_1 w_2/w_1 = -\dot{V}_1 n_{21}$$

For all measures taken, Z_{sc} will always be greater than zero, and therefore a voltage transformer introduces two kinds of error in the measurements being made: the *ratio error* and the *phase-angle error*. The ratio error is given by

$$f_v = \frac{V_2 w_1/w_2 - V_1}{V_1} \times 100\%$$

and the phase-angle error δ_v refers to the phase angle between $\dot{V}_1$ and $-\dot{V}_2'$(see Fig. 15-5*a*). These errors increase with increasing Z and ought not to exceed certain limits specified in appropriate standards. The limits of error define the "accuracy class" of a transformer and are stated for the rated burden $Z = Z_R$ and the rated primary voltage. The error limits for three accuracy classes adopted in the USSR are given below.

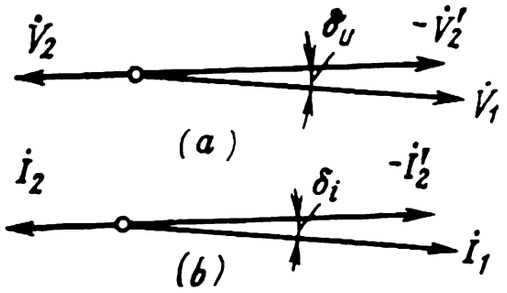

Fig. 15-5 Ratio and phase-angle errors of voltage and current instrument transformers

Accuracy class 1: $f_v = \pm 0.5\%$, $\delta_v = \pm 20'$

Accuracy class 2: $f_v = \pm 1.0\%$, $\delta_v = \pm 40'$

Accuracy class 3: $f_v = \pm 3.0\%$, $\delta_v =$ no limit

Current transformers. Instrument transformers in this group are intended to change currents in power networks to values acceptable to meters, usually down to 5 A.

As already noted, the secondary of a current transformer is connected to an ammeter, a wattmeter, or an automatic-control device. If several instruments are powered by the same current transformer, they are series-connected.

For proper operation, a current transformer must be held in a state close to a short-circuit (Fig. 15-5*b*). Its burden Z ought not to exceed a certain rated value, Z_R. As follows from the basic equations and equivalent circuits of transformers (see Sec. 3-5), the secondary current is related to the primary current by the following equation:

$$\dot{I}_2' = \dot{I}_2 w_2/w_1 = -\dot{I}_1 Z_0/(Z_0 + Z_2' + Z')$$

It is an easy matter to see that the ratio error and the phase-angle error will progressively decrease as the sum $Z_2' + Z'$ decreases in comparison with Z_0. This is why the designer makes every effort to turn out a current transformer having the highest possible value of Z_0, the lowest possible value of Z_2', and with $Z < Z_R$.

At the rated burden, the current ratio errors

$$f_i = \frac{I_2 w_2/w_1 - I_1}{I_1} \times 100\%$$

and the phase-angle error δ_i (see Fig. 15-5*b*) should not exceed the limits stated in applicable standards. In the Soviet Union, the following error limits and accuracy classes are adopted for current transformers.

Accuracy class 0.2: $f_v = 0.2\%$, $\delta_i = 10'$

Accuracy class 0.5: $f_v = 0.5\%$, $\delta_i = 40'$

Accuracy class 1: $f_v = 1.0\%$, $\delta_i = 80'$

Accuracy class 3: $f_v = 3.0\%$, $\delta_i =$ no limit

Accuracy class 10: $f_v = 10\%$, $\delta_i =$ no limit

16 Heating and Cooling of Transformers

16-1 Temperature Limits for Transformer Parts under Steady-State and Transient Conditions

Energy conversion by transformers involves a loss of power. The magnitude of power loss varies with the conditions under which a transformer is operating (see Sec. 6-3). The bulk of the power lost is dissipated as heat in the core and coils. The core loss may with sufficient accuracy be deemed proportional to the primary voltage squared, and the copper loss to the primary and secondary currents squared. A change in load mostly affects the copper loss, whereas the core loss, given a constant primary voltage, remains nearly unaffected.

Some of the power loss is dissipated also in the structural parts (the tank, clamping arrangement, etc.) lying within the magnetic field of the transformer.

The heat dissipates in the transformer parts, and they rise in temperature above the surroundings. As the transformer keeps rising in temperature, a progressively larger amount of heat is transferred to the surroundings, because the heat flux is proportional to the temperature rise (the degrees above the ambient temperature). Given a sufficiently long time (theoretically, an infinitely long time), the temperature will cease rising, because all of the heat dissipated will be transferred to the surroundings. (In more detail, heating and cooling is discussed in Sec. 35-3.)

The steady-state temperature of the transformer parts depends on the cooling arrangement used.

A transformer and its cooling system must be designed so that the temperature rise does not exceed the limit specified in each particular case. The limits given in relevant standards most apply to the parts coming in contact with the insulation, oil or any other dielectric liquid that may be used.

The reason for this is that elevated temperatures lead to an accelerated ageing of insulating materials with the resultant loss of electrical and mechanical strength. Experiments have shown that an increase of 8 degrees C in temperature will halve the service life of an oil-immersed transformer.

A transformer will serve reliably for 15 to 20 years, provided the temperature rise of its parts does not exceed the limits stated below (the figures are taken from an applicable Soviet standard).

Oil-Immersed Transformers	
Windings	65 deg. C
Exterior surfaces of core and structural work	75 deg. C
Top layer of oil:	
in totally enclosed units	60 deg. C
in other types of enclosure	55 deg. C
Dry Transformers	
Windings and core surfaces in contact with insulation according to insulation class:	
Class Y	50 deg. C
Class A	65 deg. C
Class E	80 deg. C
Class B	90 deg. C
Class F	115 deg. C
Class H	140 deg. C

The limits of temperature rise stated above are fixed, assuming that the ambient temperature is 40°C. In the case of water-cooled transformers, the inlet temperature of cooling water is assumed to be 25°C, and the respective limits of temperature rise may be raised by 15 deg. C.

The design temperatures of transformer parts are assumed to ensure a service life of 15 to 20 years, in view of the observed daily and yearly variations in ambient temperature and transformer load under actual service conditions. Most of the time, the load is less than rated and the ambient temperature is lower than 40°C, so the transformer insulation reaches its design temperature but seldom, and this extends the service life of transformers.

The limits established for the winding temperature under steady-state short-circuit conditions are as follows.

Oil-Immersed Transformers	
Copper windings	250°C
Aluminium windings	250°C
Dry Transformers	
Copper windings and insulation of the classes listed below:	
Class A	180°C
Class E	250°C
Classes B, F, H	350°C
Aluminium windings and insulation of the classes listed below:	
Class A	180°C
Classes E, B, F, H	200°C

The short-circuit duration (see Sec. 13-2) must be limited so that the temperature limits stated above could not be exceeded. In Soviet practice, it is under 5 s.

16-2 Transformer Cooling Systems

Small transformers are air-cooled and insulated, which is why they are usually referred to as *dry transformers.* For units of larger rating and higher voltage, oil cooling is more economical.

Oil cooling may be natural or forced. In the former case, transformers are referred to as oil-immersed air-cooled. The core and coil assembly of such a transformer is enclosed in a tank filled with transformer oil. Heat dissipated by the coils and core is transferred to the filling oil. The hot oil

is lighter than the cold oil next to the tank sides, and this difference gives rise to a natural circulation of oil in the tank. On picking up heat from the hot parts, it rises; near the tank sides, it gives up its heat and sinks. The heat transferred to the tank sides is then rejected to the surrounding air (Fig. 16-1).

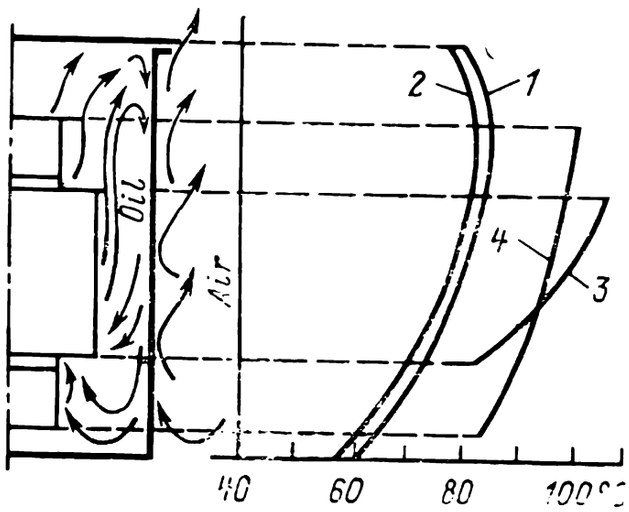

Fig. 16-1 Variations in temperature with height of a transformer:
1—oil temperature; *2*—tank side temperature; *3*—winding temperature; *4*—core temperature

Under steady-state conditions, the temperature distribution in each horizontal layer is such (Fig. 16-2) that the temperature rise of the core and coils relative to the oil, on the one hand, and the temperature rise of the oil relative to the surrounding air, on the other, is sufficient for all the heat dissipated by the core and coils to be transferred by convection to the oil and from the oil to the tank sides, and by convection and radiation to the ambient air. As is seen from the figure, the temperature within the core, coils and tank side changes but little because they are fabricated of metals having a high thermal conductivity. The temperature change is more marked in the coil insulation and also when heat is transferred from the core and the outer surfaces of coil insulation to oil and from oil to the tank sides. The temperature gradient is especially pronounced between the outer surface of the tank and the ambient air.

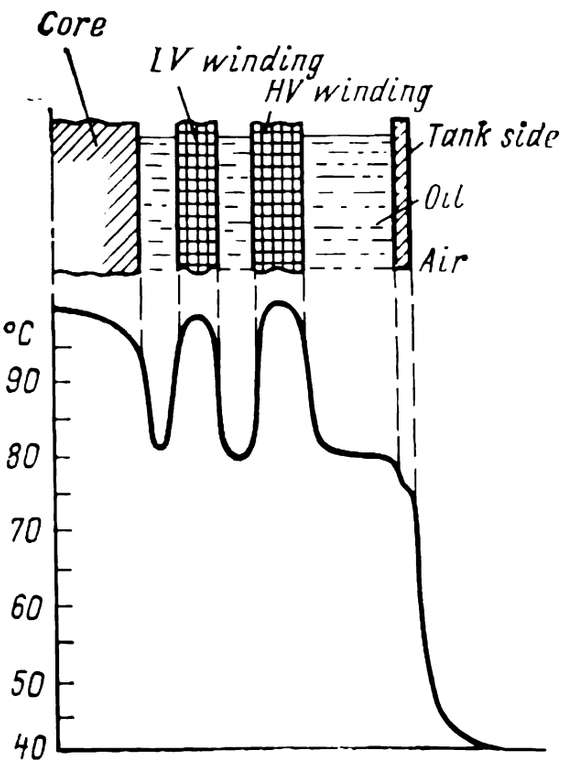

Fig. 16-2 Horizontal temperature distribution in an oil-immersed, natural air-cooled transformer

In transformers of high power ratings, the withdrawal of heat from the tank sides is a problem calling for special

treatment. The point is that the heat dissipated in a transformer per unit area increases in proportion to the linear dimension. In simpler words, an increased cooling surface is necessary. This extra surface may be obtained by making ducts in the core and coils, providing fins and corrugations on the tank sides or, which is the most common method, using a tubular radiator (Fig. 16-3). In oil-immersed, air-cooled transformers, oil circulates through the radiator (s) naturally, by convection.

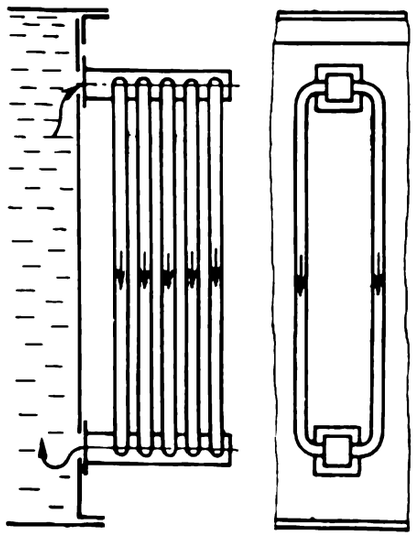

Fig. 16-3 Radiator

In air-insulated, natural-air-cooled transformers, the core and coil assembly is in direct contact with the ambient air and heat is abstracted by convection; some heat is withdrawn by radiation.

Large transformers use natural oil circulation and air blast. In them, by directing an air blast onto an ordinary

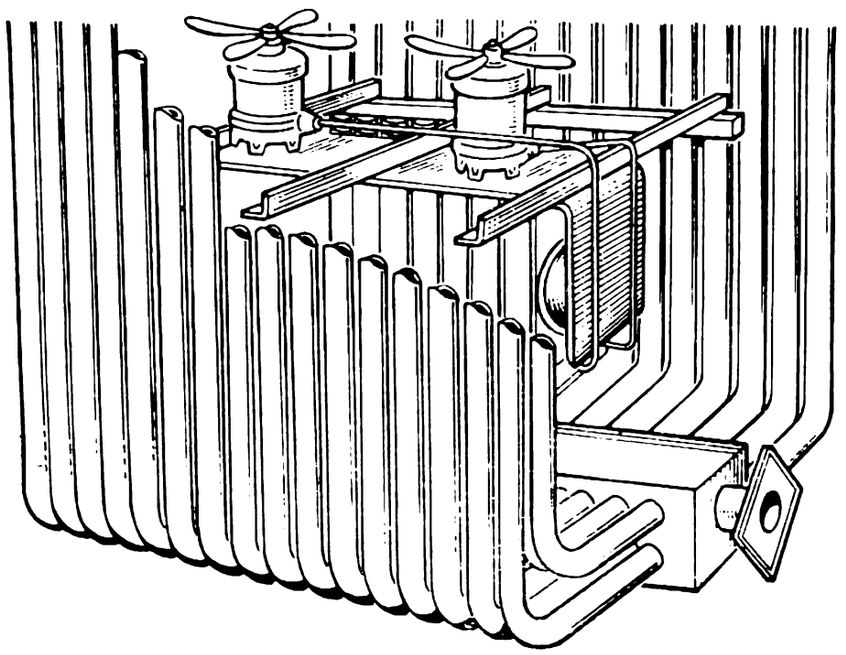

Fig. 16-4 Radiator blowers

tubular tank or onto separate radiators, the rate of heat dissipation can be increased several-fold (Fig. 16-4).

Better heat withdrawal is obtained by a combination of forced oil circulation and air blast. A still better arrange-

ment, especially for very large transformers, is to combine oil immersion and water cooling. In fact, two arrangements are possible in this case, namely natural oil circulation and water, and forced oil circulation and water. In the former case, an internal cooler is employed, whereas in the latter, the oil/water heat exchangers are external to the transformers. Oil-immersed, water-cooled transformers require large amounts of running water, so they are mostly installed at hydraulic power stations.

17 Transformers of Soviet Manufacture

17-1 USSR State Standards Covering Transformers

In his studies or work, the reader may run into transformers of Soviet manufacture. If so, it will be useful, as we believe, for him to know which USSR state standards, GOSTs, are applicable to various transformers.

GOST 16110-70. Power transformers. Terms and definitions (see also CMEA* Standard 1103-78).

GOST 11677-75. Power transformers. General specifications (see also CMEA Standard 1102-78).

GOST 721-77, GOST 21128-75. Rated phase-to-phase voltages.

GOST 18619-73. Power transformers, three-phase, natural air cooled, general-purpose, 10 to 160 kVA, up to 660 V.

GOST 14074-76. Power transformers, dry, protected, general-purpose, 160 to 1.6 MVA, 6 to 15.75 kV inclusive.

GOST 12022-76. Power transformers, three-phase, oil-immersed, general-purpose, 25 to 630 kVA, 35 kV inclusive.

GOST 12965-74. Power transformers, three-phase, oil-immersed, general-purpose, 110 kV.

GOST 17546-72. Transformers (and autotransformers), three-phase, power, oil-immersed, general-purpose, 150 kV.

GOST 15957-70. Transformers (and autotransformers), power, oil-immersed, general-purpose, 220 kV.

GOST 17545-72. Transformers (and autotransformers), power, oil-immersed, general-purpose, 330 kV.

* CMEA stands for the Council of Mutual Economic Assistance of which the USSR is a member.—Translator's note.

GOST 17544-72. Transformers (and autotransformers), power, oil-immersed, general-purpose, 500 kV.

GOST 3484-77. Power transformers. Test procedures.

GOST 1516.1-76. A.C. electrical equipment for 3 to 500 kV. Insulation strength requirements.

GOST 1516.2-76. A.C. electrical equipment and installation for 3 kV and higher. General procedures for insulation testing.

GOST 14209-69. Transformers (and autotransformers), power, oil-immersed. Load capacity.

17-2 Type Designations of Soviet-made Transformers

The type designation of a transformer consists of letters and numerals. The letters are used as follows.

A stands for an autotransformer.

T stands for three-phase. A second T, for three-winding.

O stands for single-phase.

P stands for a split LV winding (see Sec. 10-1).

H stands for on-load tap changing. (If there is no H in the type designation, the transformer is designed for off-load tap changing or has no tap changer at all.)

The numerals in the numerator, following the letter(s), give the power rating in kVA, and the numerals in the denominator, its kV class on the HV side.

The designations used for the various cooling arrangements are listed in the table that follows.

Table 17-1 Designation of Cooling Arrangements

Dry transformers	Designation
Natural air cooled, open	С
Same, protected	СЗ
Same, sealed	СГ
Air-blast cooled	СД
Oil-Immersed Transformers	
Oil natural	М
Oil-natural, air-blast	Д
Forced-oil, air-blast	ДЦ
Oil-natural, water	МВ
Forced-oil, water	Ц

17-3 Some of Transformer Applications

Dry transformers are mainly intended for installation in dry indoor locations with a relative humidity of not over 80% and in the absence of corrosive substances and current-conducting dust. They are fire-safe and are gaining popularity in residential buildings, in laboratories, etc. A dry transformer may be built into an enclosure so as to keep foreign objects from finding their way into the core and coil assembly, but to give free access for cooling air.

Low-power transformers (under 4 kVA for single-phase units and under 5 kVA for three-phase units) find use in radio, electronics, automatic control, communications, industrial drive, domestic appliances, and to energize hand-held power tools.

All transformers are designed for moderate climates, for tropical climates (tropicalized), and for cold climates.

A General Theory of Electromechanical Energy Conversion by Electrical Machines

2

18 Electromechanical Processes in Electrical Machines*

18-1 Classification of Electrical Machines

An electrical machine operating by electromagnetic induction consists essentially of a stationary member and a movable member (Figs. 18-1-18-5).

The stationary part is made up of a suitably shaped core, one or more windings, and structural parts intended to hold the stator in its designated position.

The movable part consists of a core, one or more windings, and structural parts enabling the movable part to move relative to the stationary part and to transmit mechanical energy to or from the machine.

The movable and stationary windings may be connected to external lines directly or through a suitable device. Connection to the movable windings is by sliding contacts. As a rule, the movable part of an electrical machine has one degree of freedom (motion in any other directions is prevented by bearings or supports which may be of one of several designs).

In most electrical machines, the movable member rotates relative to the stationary member. Quite aptly, they are called *rotating machines*, and their movable member is called the *rotor*, and the stationary member the *stator*.

---

* The author refers primarily to the motor mode of operation. By the reversibility principle, however, the reader may readily extend the reasoning to the generating mode where necessary.—Translator's note.

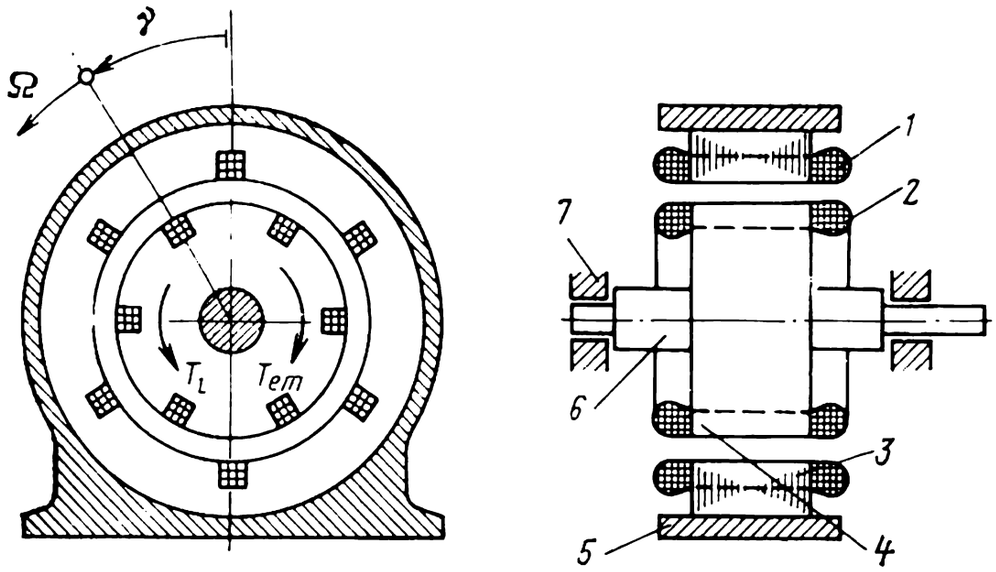

Fig. 18-1 Rotating cylindrical machine:
1—stator windings; *2*—rotor windings; *3*—stator core; *4*—rotor core; *5*—stator structural parts; *6*—rotor shaft; *7*—axial-radial bearings (supports)

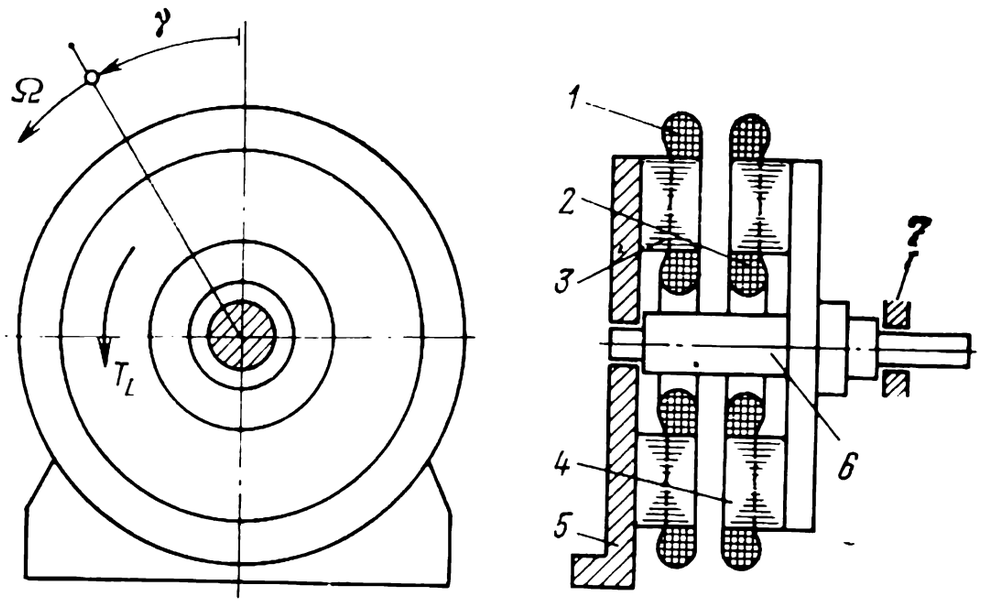

Fig. 18-2 Rotating disc-type machine (the notation is the same as in Fig. 18-1)

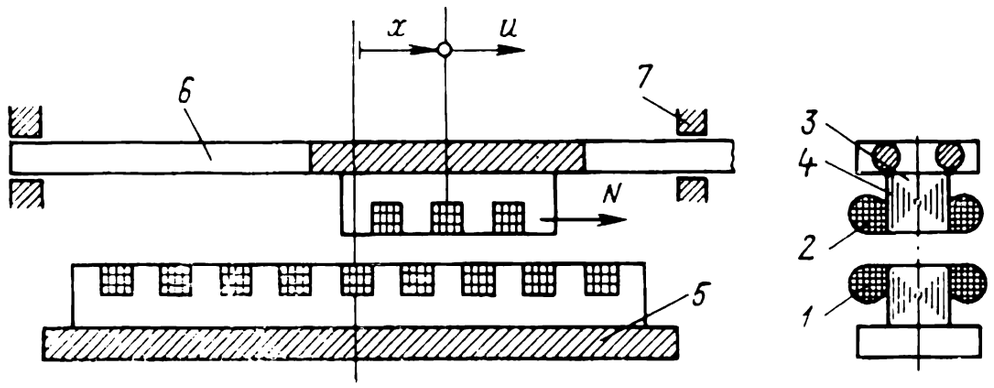

Fig. 18-3 Flat linear machine:
1—stator windings; *2*—movable-member windings; *3*—stator core; *4*—movable-member core; *5*—stator structural parts; *6*—movable-member connecting-rod; *7*—supports

Most frequently, the rotor is a cylinder rotating inside the stator which is likewise a cylinder but a hollow one (see Fig. 18-1). Sometimes, to increase the moment of inertia of the rotating parts, the rotor is made in the form of a ring enclosing the stator.

As an alternative, a rotating machine can be built so that the stator and the rotor are discs facing each other (Fig. 18-2).

A less frequent variety of electrical machines is one in which the movable part reciprocates relative to the stator

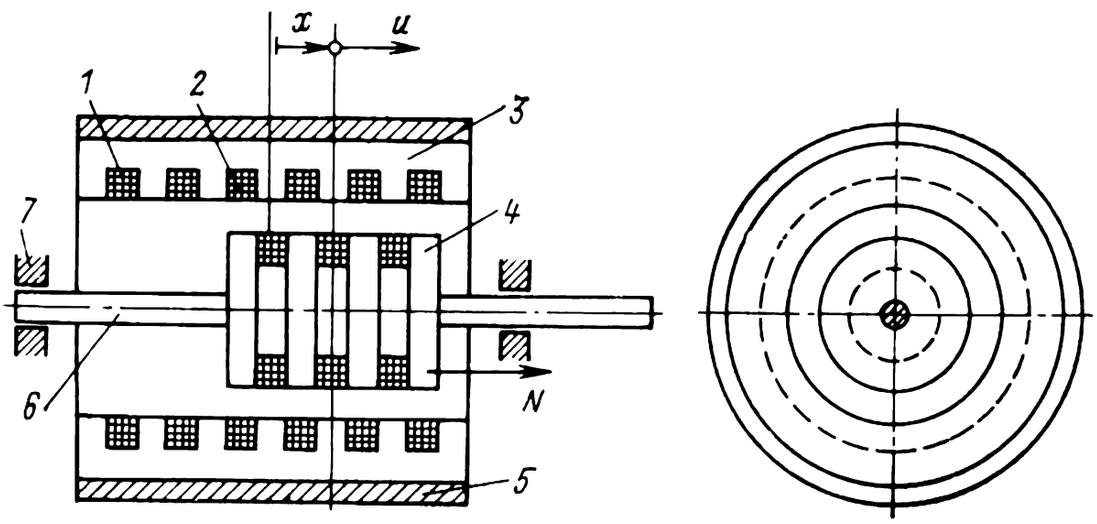

Fig. 18-4. Tubular linear machine (the notation as in Fig. 18.3)

in a linear fashion. Quite aptly, such machines are called *linear*. They may be *flat* and *tubular*.

In a flat linear machine, the movable and the stationary cores are each the shape of a parallelepiped, with their broad sides facing each other (Fig. 18-3). In a tubular linear machine, the movable cylindrical core is free to move axially inside the stationary annular core (for example, a plunger moving inside a solenoid), as in Fig. 18-4. Flat linear machines can serve as, say, drives for electric-powered rail-riding vehicles, especially where high speeds (over 200 or 300 kmph) are involved or desired. Tubular linear machines can be used to actuate the reciprocating parts of various mechanisms.

Both rotating and linear machines can be built for restricted to-and-fro motion. Restricted rotary motion may be utilized to operate, for example, the balance wheel of an electric clock, and restricted linear motion may serve to actuate an electric pick.

Sometimes, it may be necessary to link an electrical machine to a source (or sink) of mechanical energy so as to transform some parameter(s) of the mechanical energy being converted. This is done by what may be called *mechanical*

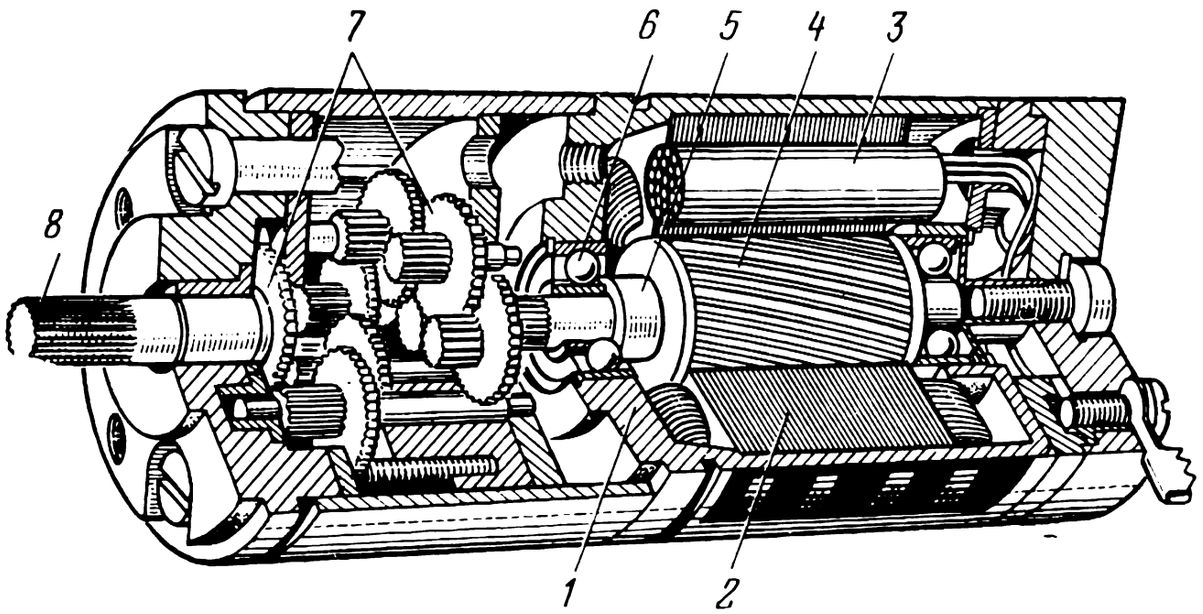

Fig. 18-5 Geared rotating electrical machine:
1—frame; *2*—stator core; *3*—stator winding; *4*—rotor; *5*—rotor shaft; *6*—ball bearing; *7*—gear train; *8*—gear-train shaft

converters. A mechanical converter is often made integral with the associated electrical machine. The most commonly used form of mechanical converter is a step-up or a step-down gear box (Fig. 18-5).

Rotating motion can be transformed to reciprocating motion by gears, a worm and gear combination, or friction transmission. Oscillatory motion can be transformed into rotating or translational motion by a variety of ratchets and pawls.

Most frequently, however, electrical machines are built without any mechanical converters.

18-2 Mathematical Description of Electromechanical Energy Conversion by Electrical Machines

Let us consider a rotating electrical machine in which the windings have an arbitrary number s of parallel paths (or circuits) embedded in slots or on the outer surface of the stator and rotor. Each path may consist of many coils connected in some particular manner. The cores, too, may be

of any configuration. As an example, Fig. 18-6 shows a rotating electrical machine with $s = 5$ parallel paths of which two (labelled "1" and "2") are located on the stator, and three (labelled "3", "4", and "5"), on the rotor.

The electromagnetic processes taking place in an electrical machine can be described by Kirchhoff's mesh (or loop)

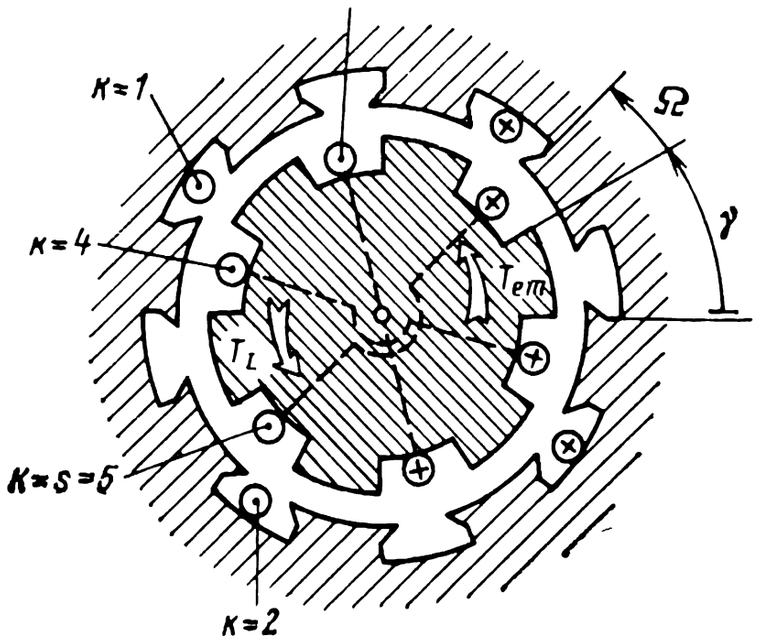

Fig. 18-6 Multiwinding rotating electrical machine

equations and the equations of motion for the rotor. In a linear approximation (that is, assuming that the core material has an infinitely large permeability), the flux linkage of, say, the kth path (where k may take on any value from 1 to s) can be expressed in terms of the winding currents i_n, the self-inductance of the kth winding, L_{kk}, and the mutual inductances between the kth winding and all the other windings, L_{kn}, where n can take on any value from $n = 1$ to $n = s$, except $n = k$

$$\Psi_k = \sum_{n=1}^{s} \Psi_{kn} = \sum_{n=1}^{s} i_n L_{kn}$$

In many cases, the mutual and self inductances of the windings are markedly affected by whether or not the cores have saliencies. With saliencies, rotation of the rotor causes variations not only in the mutual inductance between the paths on the stator and rotor, but also in the mutual inductances between the paths on only the stator and on only the rotor, and in the self-inductance of each path.

In the general case, all the self-inductances L_{kk} and all the mutual inductances L_{kn} are functions of the coil and core size and of the angular position of the rotor, $L_{kn} = f(\gamma)$.

Using Kirchhoff's voltage law, we may write a set of s voltage equations, each describing one of the parallel paths. For the kth path, such an equation takes the form

$$v_k = R_k i_k + \mathrm{d}\Psi_k/\mathrm{d}t$$

$$= R_k i_k + \sum_{n=1}^{s} (L_{kn}\, \mathrm{d}i_n/\mathrm{d}t + i_n \Omega\, \mathrm{d}L_{kn}/\mathrm{d}\gamma) \qquad (18\text{-}1)$$

where

$L_{kn}\, \mathrm{d}i_n/\mathrm{d}t$ = the transformer emf related to variations in the current in the nth path

$i_n\, \mathrm{d}L_{kn}/\mathrm{d}t$ = the rotational emf related to variations in the mutual inductance with the nth path (when $n \neq k$) or to variations in the self-inductance of the kth path (when $n = k$)

Thus, as follows from Eq. (18-1), the emfs induced in the kth loop are the sum of *transformer emfs* related to variations in coil currents when the mutual or self inductances remain unchanged,

$$-\sum_{n=1}^{s} L_{kn}\, \mathrm{d}i_n/\mathrm{d}t$$

and *rotational emfs* related to variations in the mutual or self-inductances, with the currents held constant

$$-\Omega \sum_{n=1}^{s} i_n\, \mathrm{d}L_{kn}/\mathrm{d}\gamma$$

The term "transformer emf" refers to the fact that a similar emf is induced in transformers where the primary and secondary are stationary relative to each other. The term "rotational emf" refers to the fact that it can only be generated when the rotor is moving at some angular velocity

$$\Omega = \mathrm{d}\gamma/\mathrm{d}t$$

For the loops connected to an external circuit, v_k in Eq. (18-1) can be interpreted as the emf of the circuit. For short-circuited loops, $v_k = 0$.

The mechanical power derived by an electrical machine from electrical energy can be expressed in terms of the associated circuit parameters, proceeding from the law of conservation of energy. To begin with, let us determine the

instantaneous electric power that the kth loop draws from the associated supply line

$$p_k = v_k i_k = R_k i_k^2 + i_k \sum_{n=1}^{s} L_{kn} \frac{\mathrm{d}i_n}{\mathrm{d}t} + \Omega i_k \sum_{n=1}^{s} i_n \frac{\mathrm{d}L_{kn}}{\mathrm{d}\gamma}$$

The total instantaneous electric power drawn by all the loops can be found by adding together the powers of all the loops:

$$\sum_{k=1}^{s} p_k = \sum_{k=1}^{s} R_k i_k^2 + \sum_{k=1}^{s} i_k \sum_{n=1}^{s} L_{kn} \frac{\mathrm{d}i_n}{\mathrm{d}t} + \Omega \sum_{k=1}^{s} i_k \sum_{n=1}^{s} i_n \frac{\mathrm{d}L_{kn}}{\mathrm{d}\gamma} \qquad (18\text{-}2)$$

The term $\sum_{k=1}^{s} R_k i_k^2$ is the power dissipated as heat in the loop resistances R_k and gives the power lost on conversion. The remainder of the input power goes to sustain variations in the field energy owing to variations in the loop currents and inductances. Because the magnetic field energy is

$$W' = \frac{1}{2} \sum_{k=1}^{s} i_k \sum_{n=1}^{s} i_n L_{kn} \qquad (18\text{-}3)$$

its total change over a time $\mathrm{d}t$ during which i_k, i_n, and L_{kn} change by $\mathrm{d}i_k$, $\mathrm{d}i_n$, and $\mathrm{d}L_{kn}$, is given by

$$\mathrm{d}W = (\partial W/\partial i_k)\,\mathrm{d}i_k + (\partial W/\partial i_n)\,\mathrm{d}i_n + (\partial W/\partial L_{kn})\,\mathrm{d}L_{kn}$$

$$= \sum_{k=1}^{s} i_k \sum_{n=1}^{s} L_{kn}\,\mathrm{d}i_n + \frac{1}{2} \sum_{k=1}^{s} i_k \cdot \sum_{n=1}^{s} i_n\,\mathrm{d}L_{kn}$$

Therefore, the power spent to sustain variations in the magnetic field energy is

$$p_W = \frac{\mathrm{d}W}{\mathrm{d}t} = \sum_{k=1}^{s} i_k \sum_{n=1}^{s} L_{kn} \frac{\mathrm{d}i_n}{\mathrm{d}t} + (\Omega/2) \sum_{k=1}^{s} i_k \sum_{n=1}^{s} i_n \frac{\mathrm{d}L_{kn}}{\mathrm{d}\gamma} \qquad (18\text{-}4)$$

It corresponds to the second and half the third term in Eq. (18-2). In other words, the power spent to sustain variations in the energy of the magnetic field is all of the sum of the powers defined as the products of the loop currents by the

transformer emf, and half the sum of the powers defined as the products of the loop currents by the rotational emf.

The remainder is the mechanical power transmitted by the shaft to the driven machine (in motoring) or from a prime mover (in generating)

$$p_{\text{mech}} = \sum_{k=1}^{s} p_k - p_e - p_W = \frac{\Omega}{2} \sum_{k=1}^{s} i_k \sum_{n=1}^{s} i_n \frac{dL_{kn}}{d\gamma} \qquad (18\text{-}5)$$

As follows from Eqs. (18-1), (18-2) and (18-5), the mechanical power is equal to half the sum of the powers defined as the products of loop currents and the rotational emf. Hence, we may conclude that electromechanical energy conversion involves only the rotational emf, whereas the transformer emf does not contribute to this conversion. It is to be noted that the power spent to sustain variations in the magnetic field energy is not wasted irrevocably, but sums on the average to zero. This is because in a rotating electrical machine all quantities (currents, self-inductances, mutual inductances, etc.) vary periodically. At the end of a cycle of alternation, all quantities, including the magnetic field energy, take on the same value they had at the beginning of the cycle, i.e., $W_{(t)} = W_{(t+T)}$. This implies that variations in the energy of the magnetic field over a cycle, or period, sum to zero, that is,

$$\int_{t}^{t+T} dW = W_{(t+T)} - W_{(t)} = 0$$

During that part of a cycle when the magnetic field energy builds up ($dW > 0$), the power p_W given by Eq. (18-4) is positive ($p_W > 0$), and the energy required to set up the magnetic field is taken by the loops from the line. During the remaining part of a period, $p_W < 0$, and the energy stored by the magnetic field is again returned to the line.

This exchange of energy between the machine and the line goes on in such a manner that the energy drawn from the line averages over a period to zero. A measure of this exchange is what is called the reactive (or magnetizing) power. In the case of a single-phase supply and sinusoidal variations, this is the maximum instantaneous power drawn from the line to set up the magnetic field in the machine:

$$Q = |\, dW/dt \,|_{\max}$$

Recalling that the electromagnetic torque, T_{em}, acting on the rotor at a given instant can be expressed in terms of p_{mech} defined in Eq. (18-5), and comparing the resultant expression with Eq. (18-3), we get

$$T_{em} = \frac{p_{mech}}{\Omega} = \frac{1}{2} \sum_{k=1}^{s} i_k \sum_{n=1}^{s} i_n \frac{dL_{kn}}{d\gamma} = \frac{dW}{d\gamma} \quad (i_k = \text{constant}) \tag{18-6}$$

Thus, in a machine with a linear magnetic circuit the electromagnetic torque is the partial derivative of the magnetic field energy W with respect to the angular position γ of the rotor, with the loop currents held constant (i_k = = constant, and i_n = constant). If this derivative is positive, the torque acts in the direction of rotation (or in the direction of increasing γ), and electric energy is converted to mechanical. If the derivative is negative, reverse conversion takes place.

Equation (18-6) may be extended to machines with nonlinear magnetic circuits, if variations in the magnetic field energy, dW, as the rotor turns through an angle $d\gamma$ can be found not only for i_k = constant, but also for μ_{aj} = constant. In each jth element of the magnetic circuit μ_{aj} must be found for i_k = constant and the angular position γ of the rotor.

If the terminal coil voltages v_k, the angular velocity Ω of the rotor, and the relation $L_{kn} = f(\gamma)$ are known or specified in advance, the currents can be found from Eqs. (18-1). Then the electromagnetic torque can be found by Eq. (18-6) where $\gamma = \Omega t$.

If the angular velocity is not known, but the external torque T_{ext} is specified in advance, then Eqs. (18-1) and (18-6) must be solved simultaneously with the equations of motion (18-7)

$$T_{em} - T_{ext} = J \, d\Omega/dt$$

$$\Omega = \Omega_{init} + \int_0^t (d\Omega/dt) \, dt \tag{18-7}$$

$$\gamma = \gamma_{init} + \int_0^t \Omega \, dt$$

The mathematical description derived above for a multi-loop (multipath) rotating machine can be extended to a linear machine whose movable member reciprocates relative to the stator.

The equations for a linear machine differ from the above equations only in that the angular displacement γ is replaced by a linear displacement x, the electromagnetic torque T_{em} is replaced by an electromagnetic force N acting in the direction of displacement, the angular velocity Ω by a linear velocity u, the angular acceleration $d\Omega/dt$ by a linear acceleration du/dt, the external torque T_{ext} by an external force N_{ext}, and the moment of inertia of the rotor J by the mass of the movable member, m.

19 Production of a Periodically Varying Magnetic Field in Electrical Machines

19-1 A Necessary Condition for Electromechanical Energy Conversion

From inspection of Eq. (18-6), we may conclude that a necessary condition for an electrical machine to perform electromechanical energy conversion is a change in the self or mutual inductances of the coils as the rotor turns through an angle. An electrical machine will perform its function if the derivative of at least one quantity with respect to the angular position of the rotor is non-zero

$$dL_{kn}/d\gamma \neq 0$$

because it is only then that $T_{em} \neq 0$ and $P_{mech} \neq 0$.

This is a necessary, but not a sufficient condition for a continuous, unidirectional electromechanical (or mechano-electrical) conversion of energy. It is also required that the currents in coils k and n should vary in such a manner that not only the instantaneous, but also the average values of T_{em} and P_{mech} be sufficiently large.

Because in technically feasible designs the magnetic fields, flux linkages, self and mutual inductances cannot be monotonically rising functions of currents and the angular position of the rotor, the only possible case is when these quantities

vary periodically as functions of γ, when the derivative $dL_{kn}/d\gamma$ likewise varies periodically.

For L_{kn} to be a periodic function of γ, it is essential that the current traversing coil n sets up a magnetic field periodically varying in space (tangentially to the air gap).

Some of the coil and core designs capable of producing a periodically varying magnetic field are discussed in the sections that follow.

19-2 The Cylindrical (Drum) Heteropolar Winding

The conductors of a drum winding are laid in slots on the side surface of the core which may be in the form of a *toothed* (or *salient-pole*) cylinder or toroid*.

As is seen from Fig. 19-1*a*, the current in the conductors on the core surface facing the air gap alternates in direction periodically. This gives rise to a magnetic field which varies periodically in space—the core is magnetized heteropolarly—in going round the circumference, an N pole is followed by an S pole, and an S pole is followed by an N pole.

The spacing between zones A and X occupied by conductors carrying currents which alternate in the direction of flow varies from design to design. Accordingly, a drum winding can set up a magnetic field with a varying number of periods, cycles of alternations per revolution, or, as more commonly stated, a varying *number of pole pairs*, (Fig. 19-2).

This spacing is measured along the periphery of the air-gap with a mean radius R and is called the *pole pitch*. If we designate the pole pitch as τ (see Fig. 19-1*a* and Fig. 19-2), then the number of pole pairs (or cycles of alternation per revolution) will be given by

$$p = \pi D/2\tau = \pi R/\tau \qquad (19\text{-}1)$$

The simplest of all drum windings is the two-pole winding for which $p = 1$, and the magnetic field completes one cycle of alternation per revolution. Those with $p > 1$, are called multipole windings.

---

* In machines with smooth cores (those having no slots), the coil conductors are bounded to the outer surface of the core.

In a drum winding, the conductors lying on the surface of the air gap may be interconnected in any one of several

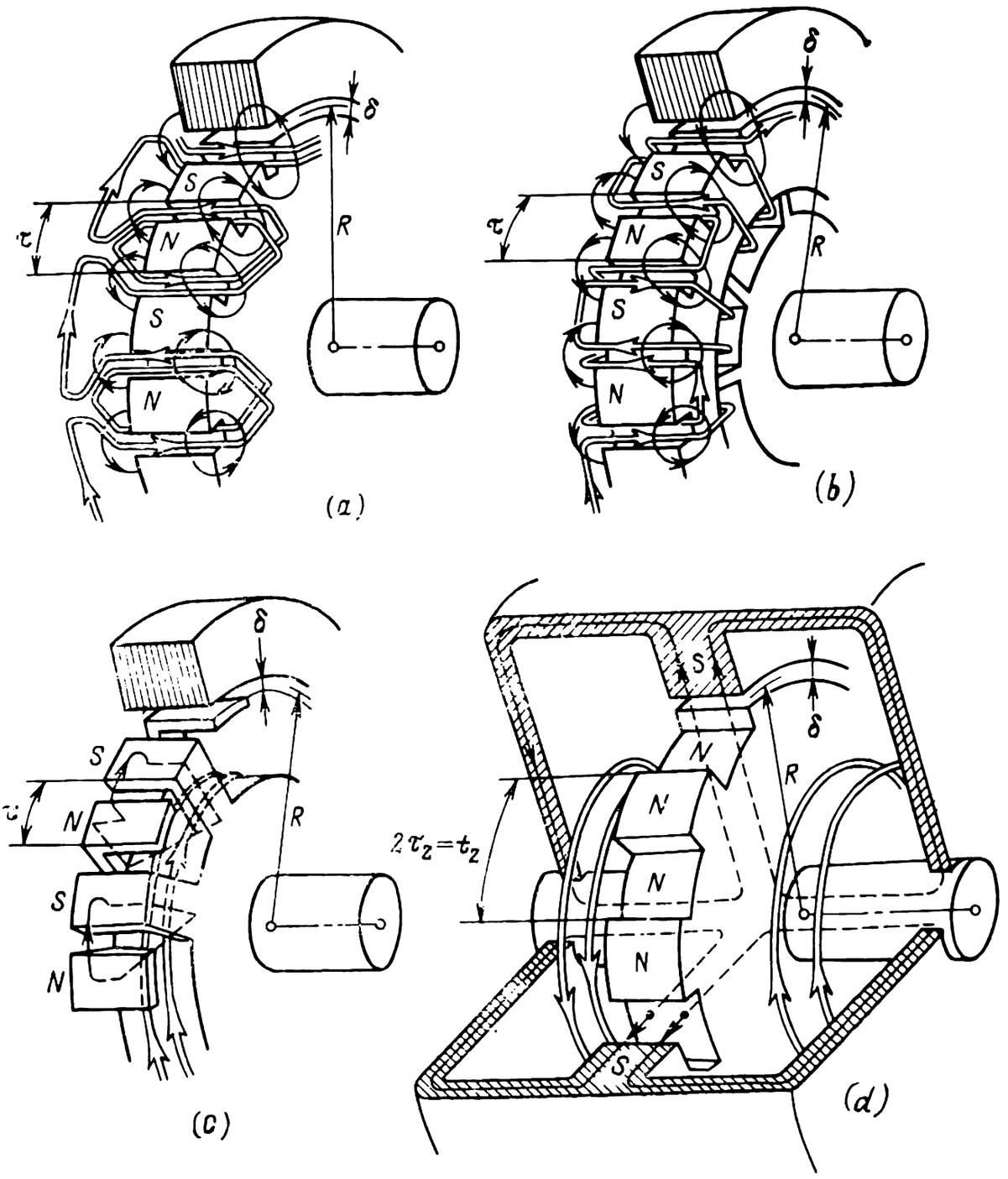

Fig. 19-1 Production of a periodically varying magnetic field in rotating electrical machines:
(*a*) cylindrical (drum) heteropolar winding; (*b*) toroidal heteropolar winding; (*c*) ring winding and claw-shaped core; (*d*) ring homopolar winding and toothed core

ways. Whatever the form of connection, however, the coil-ends will never encircle the yoke of the core.

Each coil may be wound with one or two turns. Each slot may contain one side (Figs. 19-1*a* and 19-2*a*) or two sides

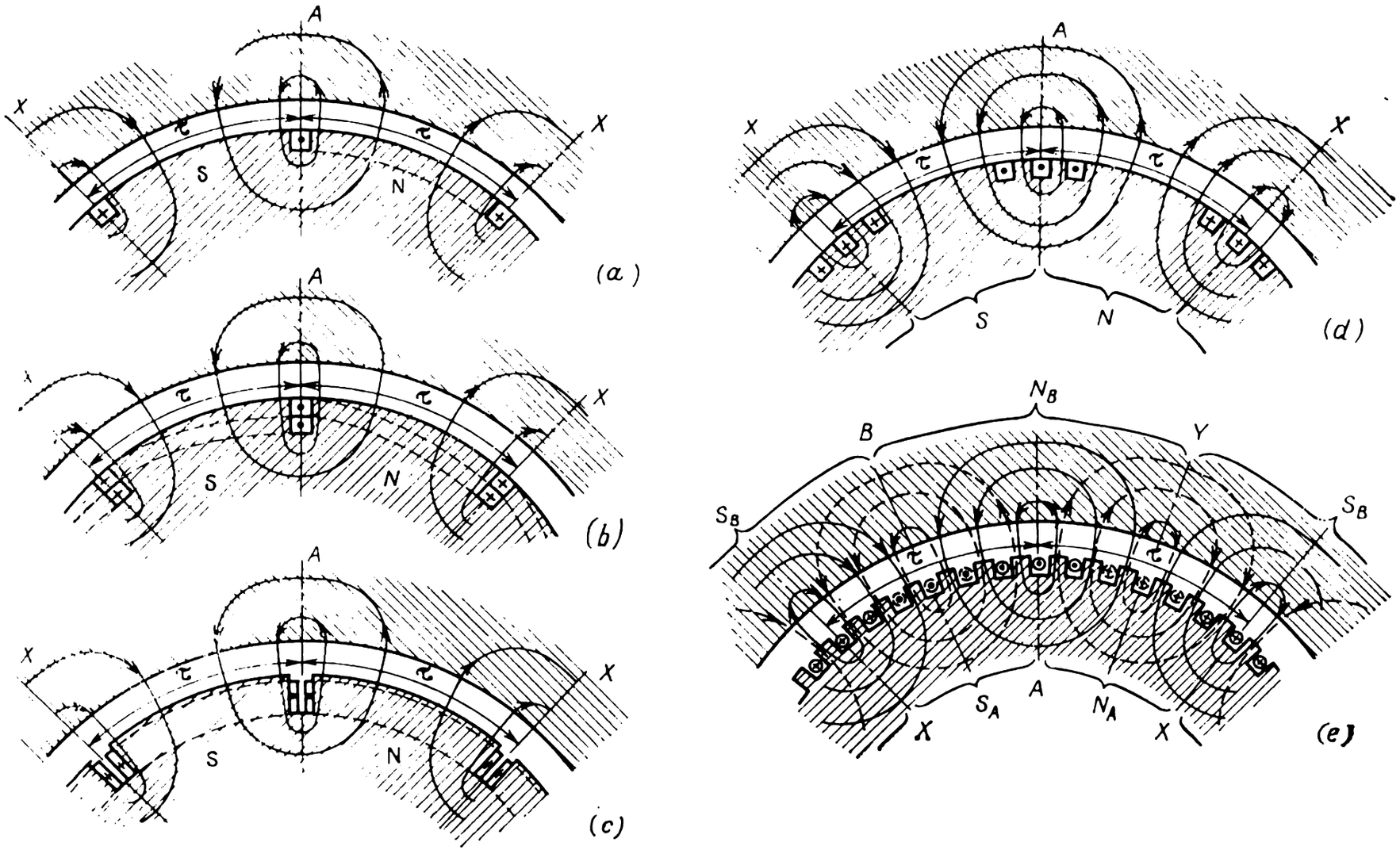

Fig. 19-2 Heteropolar cylindrical (drum) windings:
(*a*) single-layer, single-phase concentrated winding; (*b*) two-layer, single-phase concentrated winding; (*c*) two-row, single-phase concentrated winding; (*d*) single-layer, single-phase distributed winding ($q = 3$); (*e*) single-layer, two-phase distributed winding ($q = 3$)

(Fig. 19-2*b* and *c*) of a coil. In the former case, we have a *single-layer winding*, and in the latter, a *double-layer winding* if a given coil has one of its sides at the bottom of a slot and the other side at the top of the same slot (Fig. 19-2*b*). If the sides occupying the same slot lie in the same plane, we have a *double-row winding* (Fig. 19-2*c*).

Frequently, it is convenient to place conductors carrying currents flowing in the same direction in several, say three, slots (Fig. 19-2*d*) rather than in one. The number of slots occupied by a phase belt (that is, by a belt of phase conductors carrying currents flowing in the same direction) in a single-layer winding is called the *number of slots per pole*, denoted by q.

When $q = 1$, the winding is called *concentrated.* When $q > 1$, we have a *distributed* winding.

The slots of the same core may carry several identical heteropolar windings producing between them fields with the same number of cycles of change, p, and energized from (or supplying power to) a polyphase line. This structure is called a *polyphase* winding. As is seen from Fig. 19-2*e* which shows a two-phase winding, each phase is a distributed heteropolar winding with $q = 3$ (see Fig. 19-2*d*). Phase A consists of belts with conductors carrying the current flowing in the forward direction (A) and belts with conductors carrying the current flowing in the reverse direction (X), and the spacing between the adjacent belts is equal to the pole pitch τ. Phase B consists of belts with conductors carrying the current in the forward direction (B) and belts with conductors carrying the current in the reverse direction (Y). The belts of phase B are laid between the belts of phase A and are displaced from the phase A belts through a quarter of a cycle, or a half pole pitch, $\tau/2$.

A similar arrangement is applicable to a polyphase winding with m phases. In such a case, the number of slots per pole per phase, q, is given by

$$q = Z/2pm \tag{19-2}$$

where Z is the total number of slots on the core. The adjacent belts in a given phase are displaced from one another by a pole pitch τ, and the belts in the adjacent phases by a distance equal to τ/m.

19-3 The Toroidal Heteropolar Winding

A toroidal winding (see Fig. 19-1*b*) differs from a cylindrical in that the connections between its conductors carrying currents in the same direction, that is, the coil ends or overhangs, are wound around the toroidal core. If the conductors on the surface facing the air gap are arranged in the same manner as in a cylindrical coil, a toroidal coil does not differ from the latter as regards the production of a magnetic field periodically varying in space. In fact, it comes in the same modifications as the cylindrical winding. It offers some advantages in the manufacture of small electrical machines.

19-4 The Ring Winding and a Claw-shaped Core

So far we have dealt with forms of winding in which a periodic heteropolar magnetic field was produced by an alternation in the direction of current flow in the conductors. In a ring-shaped winding (see Fig. 19-1*c*), a periodic field is obtained due to an alternation in the direction in which the claw-shaped teeth of the core enclose the energized ring-shaped winding. As regards the production of a periodic field, this arrangement is equally efficient as the previous designs.

A limitation of this design is an increased magnetic leakage between the claw-shaped polepieces. An advantage is simplicity in manufacture. Its application is mainly in small machines and also in special-purpose medium-power units.

19-5 The Homopolar Ring Winding and a Toothed Core

A ring winding whose coils enclose the shaft of an electrical machine produces a homopolar field in the air gap. For the direction of current flow shown in Fig. 19-1*d*, the surface of the inner core is in N polarity, and that of the outer, in S polarity.

Periodic variations in the magnetic flux density within the air gap occur owing to the saliencies made on the core surface facing the air gap. If the surface of the other core is smooth or has a slight salience, then within the low areas (slots) the specific permeance will be smaller than it is within the saliences (teeth). Accordingly, the magnetic

flux density within a salience (tooth) will be higher than it is within a low area (slot).

The magnetic flux density in the air gap will vary with a space period equal to the tooth pitch, or spacing between adjacent teeth, t_Z. The number of pole pairs will be

$$p = \pi D/t_Z = Z \qquad (19\text{-}3)$$

where Z is the number of teeth in the core.

An advantage of this design is that the resultant magnetic field undergoes a larger number of alternations per revolution than with any other design because the coil conductors need not be laid in slots (the ring winding is external to the core), and there is no limit to slot size—in fact, they may be however small.

20 Basic Machine Designs

20-1 Modifications in Design

In the previous chapter, we discussed the ways and means of producing a periodic magnetic field in an electrical machine. Now we shall see how an electrical machine must be arranged for the self and mutual inductances of its windings to be functions of the angular position of the rotor and to vary periodically as the rotor rotates.

This effect can be obtained in any one of three basic machine designs, namely:

(1) in a machine with one winding on the stator and one winding on the rotor;

(2) in a machine with one winding on the stator and a toothed rotor;

(3) in a machine with two windings on the stator and a toothed rotor.

Each design may come in several modifications. As is explained in Chap. 19, the magnetic field in the air gap of an electrical machine may be either heteropolar or homopolar. Respectively, one uses two varieties of windings, *heteropolar* and *homopolar*. Heteropolar windings may be single-phase and polyphase. Homopolar windings may only be single-phase, and they may operate on a.c. or d.c. Instead of a single-phase heteropolar winding, use is sometimes made of a ring winding in a claw-shaped core.

Table 20-1. Conceivable

Winding 2		Rotor core	Winding 1 on Hetero A: Toothed stator core
Heteropolar on the rotor	1	Toothed rotor core	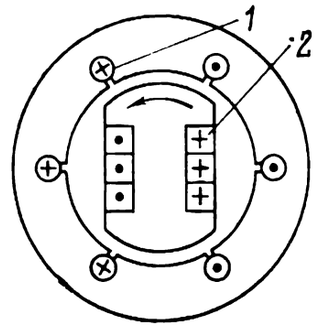
	2	Smooth rotor core	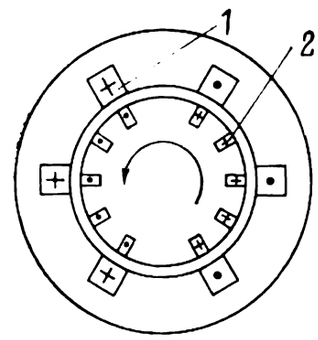
Heteropolar on the stator	3	Toothed rotor core	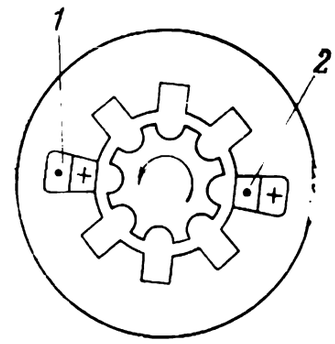
	4	Smooth rotor core	Uncapable of
Homopolar on the stator	5	Toothed rotor core	Similar to C3
	6	Smooth rotor core	Uncapable of

Designs of Electrical Machines

the stator

polar		Homopolar			
B	Smooth stator core	C	Toothed stator core	D	Smooth stator core
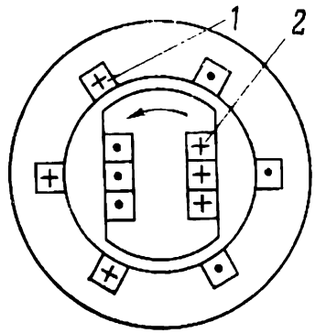		Similar to C3 (but needs external leads)		Uncapable of energy conversion in either direction	
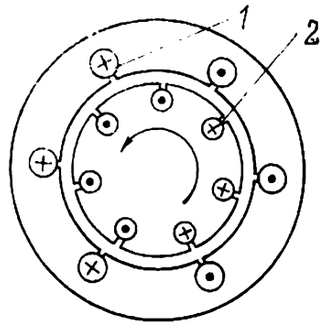		Similar to D3 (but needs external leads)			
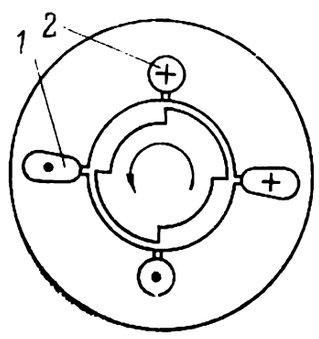		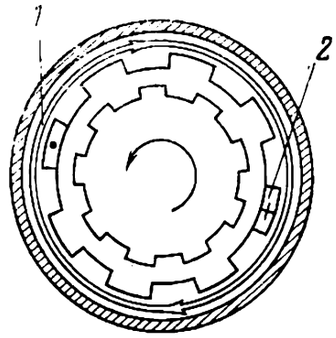		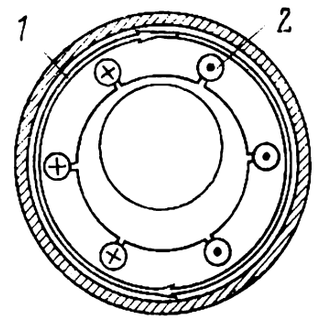	
energy conversion in either direction					
Similar to D3		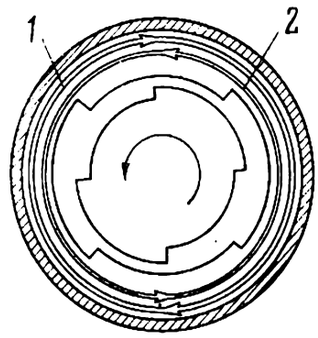		Uncapable of electromechanical or mechanoelectrical conversion	
energy conversion in either direction					

Winding 2		Rotor core	Winding 1 on Hetero	
			A	Toothed stator core
None	7	Toothed rotor core	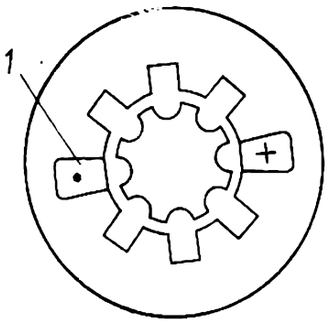	
	8	Smooth rotor core		Uncapable of

Note. Heteropolar winding *1* may be single- or polyphase. Homopo

The core surface facing the air gap may be smooth or toothed. Accordingly, there may be smooth cores and toothed cores. In toothed cores, the opening and, sometimes, the shape of slots and teeth have a direct bearing on the permeance of the air gap. In fact, the teeth can be suitably shaped to control the permeance of the air gap. In smooth cores, the slots have a limited opening (as compared with the air gap), and the air gap between the face of a tooth and the mating core remains constant as the rotor rotates. In such cores, the opening of slots has a negligible effect on the permeance of the air gap.

Toothed cores are used in electrical machines in which energy conversion is based on periodic variations in the permeance of the air gap. In some cases, the teeth of such cores are dimensioned so as to obtain a desired shape for the field in the air gap (this is true of the salient-pole rotors of synchronous machines and the salient-pole stators of d.c. machines). Also, cores in which the slots are made open for ease of coil placement behave like toothed cores. The use of open instead of semi-closed slots leads to increased pulsational losses and is justified only inasmuch as the manufacture is simplified. Wherever one may use slots with a small opening, a round core will be preferable, as it will keep the additional losses to a minimum.

Table 20-1 (continued)

the stator					
polar		Homopolar			
	B	Smooth stator core	C	Toothed stator core	D	Smooth stator core
	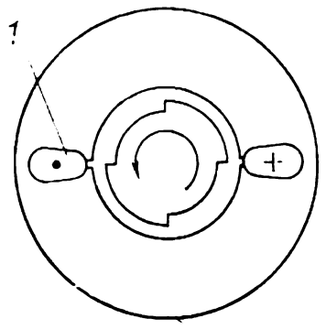		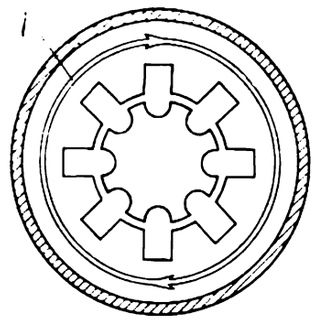		Uncapable of energy conversion in either direction
energy conversion in either direction					

lar winding *1* can only be single-phase.

Some of the conceivable machine designs are listed in Table 20-1. It gives combinations of heteropolar and homopolar windings and toothed and smooth cores for the stator and rotor. Combinations using ring windings and claw-shaped cores are not included because such machines are identical to those using a single-phase heteropolar winding. For the same reason, there has been no need to include cylindrical and toroidal heteropolar windings. The most important of the modifications listed in Table 20-1 are examined in the pages that follow.

20-2 Machines with One Winding on the Stator and One Winding on the Rotor

In a machine carrying one winding on the stator and one winding on the rotor, electromechanical energy conversion occurs mainly owing to variations in the relative position of, and in the mutual inductance between, the windings as the rotor rotates. Variations in the self and mutual inductance of the windings due to the saliency of the cores are of secondary importance.

In the arrangement considered, only heteropolar windings are used on the stator and rotor. The rotor core may be

toothed (notably, with salient poles) and smooth (round or cylindrical). The stator core may likewise be toothed or smooth. This gives a total of four combinations labelled as A1, A2, B1, and B2 in Table 20-1. Figure 20-1 shows a four-pole machine with single-phase heteropolar windings on the stator and rotor, and smooth stator and rotor cores (modification B2 in Table 20-1).

The winding currents i_1 or i_2 set up a four-pole ($p = 2$) magnetic field (the figure only shows the magnetic lines of

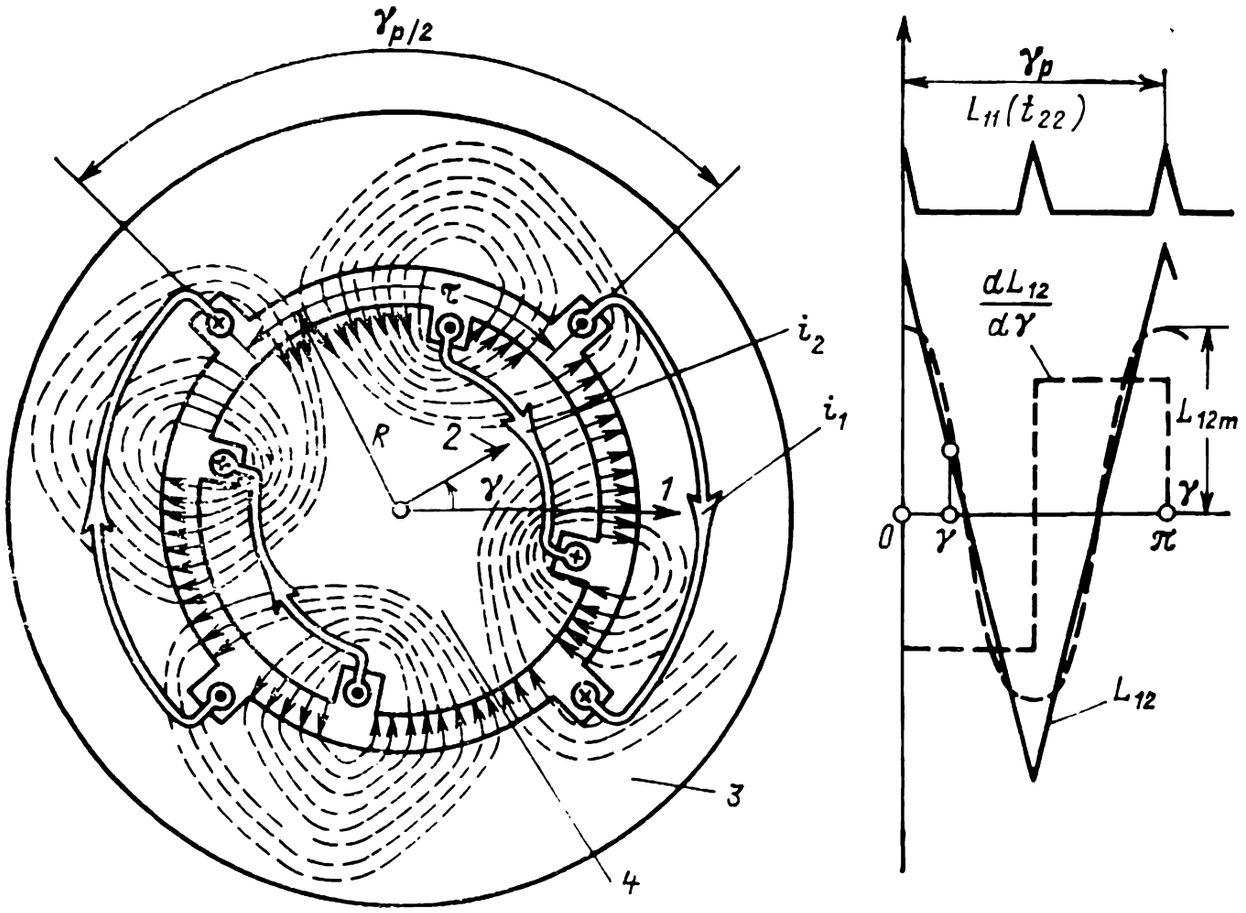

Fig. 20-1 Machine with one stator winding (*1*) and one rotor winding (*2*) ($p_1 = p_2 = 2$)

force due to i_2). A plot of L_{12} and L_{11} (L_{22}) as functions of the angle γ between the axes of the two windings is shown in the same figure. As is seen, the mutual inductance, proportional to the flux linkage of the magnetic field due to i_2 with the turns of winding *1* is a maximum when $\gamma = 0$, that is, when the axes of the coils run in the same direction. When the axis of coil *2* makes with the axis of coil *1* an angle $\gamma = \pi/4$, which corresponds to a linear displacement along the periphery of the air gap through $\tau/2$, or a quarter-cycle of change in the field, the flux linkage with coil *1* and the mutual

inductance will be zero. A cycle of change in the mutual inductance is completed as the rotor moves through 2τ or through a pole pitch angle $\gamma_p = \pi$. In the general case, when the windings set up a p-cycle field, the mutual inductance undergoes a complete cycle of change as the rotor moves through 2τ or the pole pitch angle given by

$$\gamma_p = (2\pi/2\pi R)\, 2\tau = 2\pi/p \tag{20-1}$$

If the rotor is rotating at angular velocity Ω, the mutual inductance will alternate with a period given by

$$T = \gamma_p/\Omega = 2\pi/p\Omega \tag{20-2}$$

Accordingly, the frequency of change in the mutual inductance, f, and the angular frequency of change in the mutual inductance, ω, are given by

$$f = 1/T = p\Omega/2\pi \tag{20-3}$$

$$\omega = 2\pi f = p\Omega \tag{20-4}$$

The shape of the plots for L_{12}, L_{11}, and L_{22} is typical of round (cylindrical) cores with $q = 1$: a half-cycle of change in L_{12} is triangular in shape, L_{11} and L_{22} are nearly constant; it is only when the slots in the stator and rotor are aligned that the self-inductances show slight variations, but these may safely be ignored. As the number of slots per pole per phase, q, increases, the pattern of change in L_{12} takes on a shape close to sinusoidal, which has a wholesome effect on the performance of the machine. Thus, by increasing the number of slots on a round rotor core carrying a single-phase winding the L_{12} pattern can be made nearly sinusoidal in the round-core synchronous machine shown as an example of modification A2 (see Table 20-1).

A practically sinusoidal pattern of change in L_{12} can be obtained with $q = 1$ as well, if the rotor core is so shaped that the air gap at the tooth axis is two-thirds to one-half of the gap at its tips (or edges).

This type of rotor (a salient-pole rotor) with a single-phase winding is used in modifications A1 and B1.

Most frequently, electrical machines are built with single- or polyphase heteropolar windings (see Sec. 19-2) having the same number of pole pairs. This is true of induction machines and conventional synchronous machines (see Parts 4, 5 and 6 of this text).

20-3 Machines with One Winding on the Stator and Toothed Rotor and Stator Cores (Reluctance Machines)

In a machine with one winding on the stator and toothed rotor and stator cores, electromechanical energy conversion is based on the variations caused in the self-inductance of the winding by the teeth on the cores. Figure 20-2 shows such a machine with a single-phase concentrated heteropolar

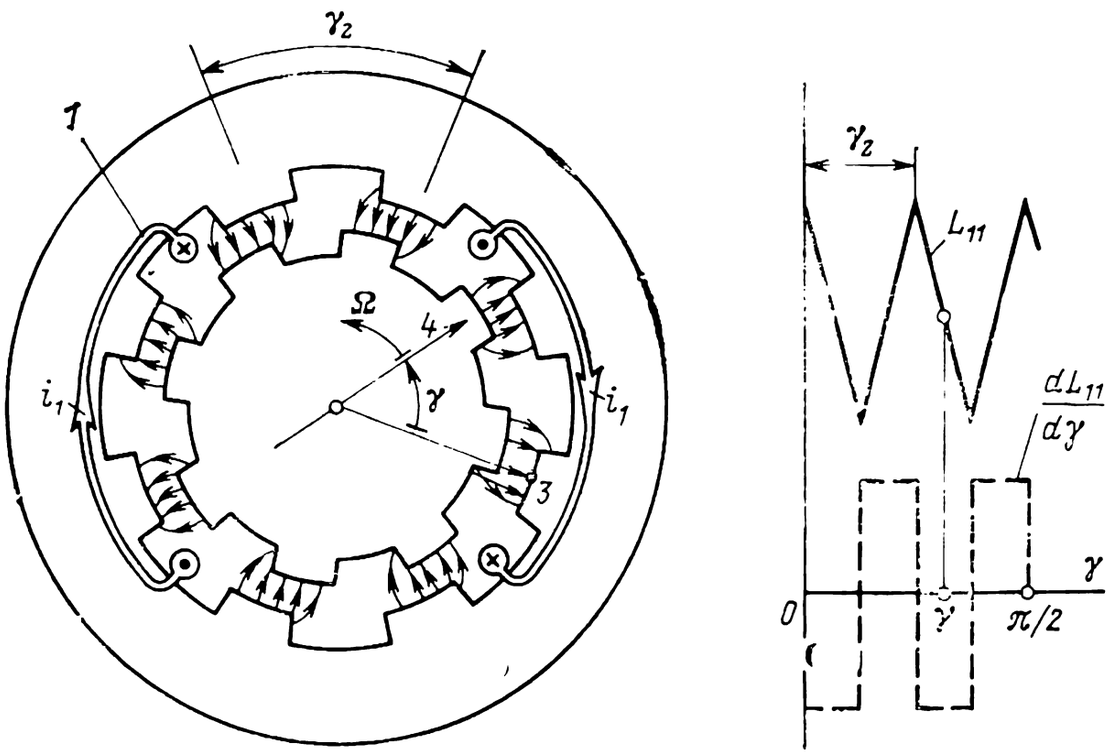

Fig. 20-2 Machine with concentrated heteropolar stator winding (*1*) ($p_1 = 2$, $q_1 = 1$) and toothed stator (*3*) and rotor (*4*) cores with an equal number of teeth ($Z_3 = Z_4 = 8$)

winding on the stator, and the rotor and stator cores having the same number of teeth, $Z_3 = Z_4 = Z$ (modification A7 in Table 20-1). The tooth pitch angle of the rotor, $\gamma_{Z4} = 2\pi/Z_4$, is the same as that of the stator, $\gamma_{Z3} = 2\pi/Z_3$.

As is seen from the curves in Fig. 20-2, when $Z_3 = Z_4$, variations in L_{11} are sufficiently large for an effective energy conversion to take place. To avoid some undesirable effects in operation, it will be well-advised to choose the number of teeth on the stator and rotor such that

$$Z_4 - Z_3' = \pm 2p_1 \qquad (20\text{-}5)$$

The rationale of such a choice will be explained later.

An example of a machine satisfying the condition in Eq. (20-5) is shown in Fig. 20-3. The rotor has Z_4 teeth,

whereas the salient-pole stator has $2p_1 = 4$ poles. The coils of the concentrated single-phase stator winding are wound around the pole-pieces and laid out in major slots between them. On the surface of the poles are made minor stator teeth displaced from one another by a tooth angle $\gamma_{Z3} = 2\pi/Z_3'$, where Z_3' is the number of tooth angles that can

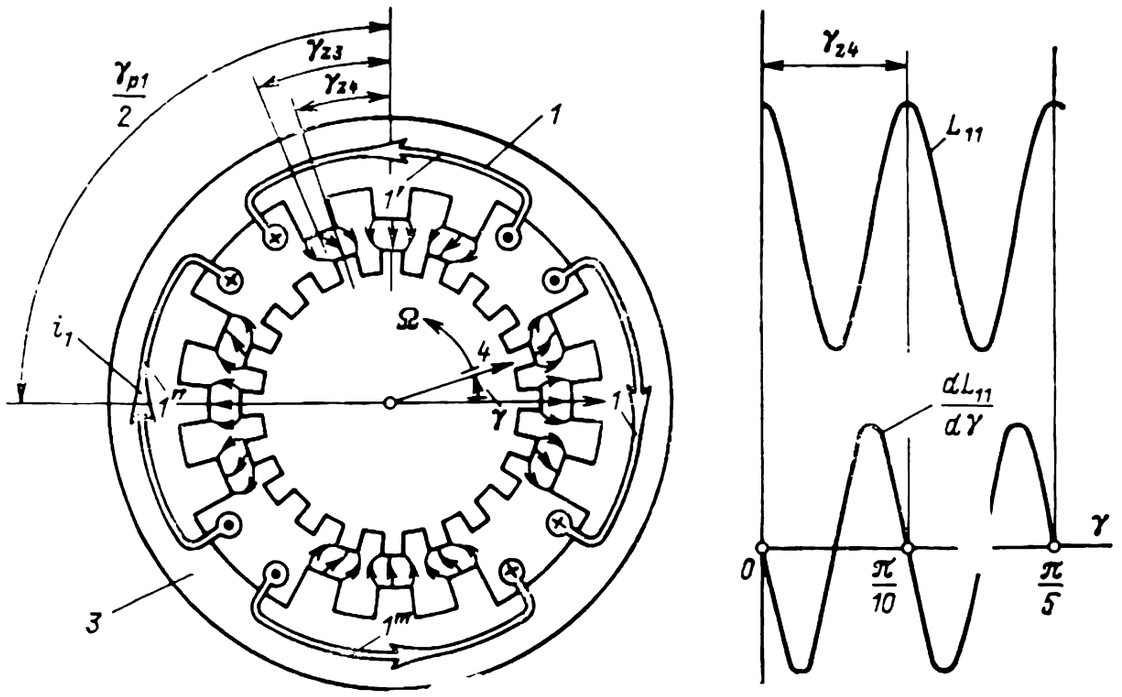

Fig. 20-3 Machine with concentrated heteropolar stator winding (*1*) ($p_1 = 2$, $q_1 = 1$) and toothed stator (*3*) and rotor (*4*) cores with different numbers of teeth ($Z_3 = 12$, $Z_3' = 16$, $Z_4 = 20$)

be accommodated round the core. The number Z_3' must satisfy the condition defined by Eq. (20-5) and be, of course, a multiple of $2p_1$, that is $Z_3' = 2p_1$ (an integer). This in turn requires that the rotor should have a number of teeth which is a multiple of the number of poles, that is, $Z_4 = 2p_1$ (an integer). In our case,

$$Z_4 = 2 \times 2 \times 5 = 20$$

$$Z_3' = 20 - 2 \times 2 = 16$$

For the machine to operate normally, it is essential that each pole should span 2/3 to 3/4 of a pole pitch, the remainder being taken up by the major slots between them. Accordingly, each pole must carry an odd number, N_3, of minor teeth. This number must lie within the limits given above

$$N_3 = \text{two-thirds to three-fourths of } Z_3'/2p \quad (20\text{-}6)$$

where $Z_3'/2p$ is the number of minor tooth angles per pole pitch. In our case,

$$N_3 = (2/3 \text{ to } 3/4) \times 16/4 = 3$$

The self-inductance of the stator winding, $L_{11} = \Psi_1/i_1$, varies with the relative position of the stator and rotor teeth. For the machine in Fig. 20-2 (with $Z_3 = Z_4$), it is a maximum when the stator and rotor teeth are aligned, for example when $\gamma = 0, \pi/4, \pi/2$, etc. It is a minimum when a slot is opposite a tooth, which happens when $\gamma = \pi/8, 3\pi/8, 5\pi/8$, etc., and the permeance of the air gap and the flux linkage Ψ_1 for a given i_1 are minimal.

For the machine in Fig. 20-3, the self-inductance of the winding is a maximum when the rotor teeth are aligned with the stator teeth lying on the axes of the winding poles (*1*, *1'*, *1''*, *1'''*). This happens when $\gamma = 0, \pi/10, \pi/5$, etc. In this position, all minor teeth on the poles are approximately opposite the rotor teeth, and the flux linkage of the winding for a given conductor current is a maximum. Conversely, the self-inductance of the winding is a minimum when the rotor slots are aligned with the stator teeth lying on the axes of the winding poles, which happens when, say, $\gamma = \pi/20, 3\pi/20$, etc.

The self-inductance undergoes a complete cycle of change as the rotor moves through one tooth pitch, or one tooth angle $\gamma_Z = \gamma_{Z4}$. (The pole pitch angle of the winding, $\gamma_{p1} = 2\pi/p_1$, and the tooth angle of the stator, γ_{Z3}', have no effect on the period of change in the self-inductance.) If the rotor is rotating at an angular velocity Ω, the time period of change in self-inductance, its frequency and angular frequency are given by

$$T = \gamma_{Z4}/\Omega = 2\pi/Z_4\Omega \tag{20-7}$$

$$f = Z_4\Omega/2\pi \tag{20-8}$$

$$\omega = Z_4\Omega$$

From comparison of Eqs. (20-8) and (20-3), it is seen that in synchronous reluctance machines, the frequency is Z_4/p times that of conventional two-winding machines with the same rotational frequency.

The rationale of choosing the number of teeth subject to Eq. (20-5), may be explained as follows. For variations in the self-inductance of the winding to be substantial, the

rotor and stator teeth must take up the same relative position at every pole of the winding (this is true, for example, of the case in Fig. 20-3 where the rotor and stator teeth are shown aligned at all the poles). Let one of the rotor teeth (say, tooth No. 1) be aligned with a stator tooth at pole *1'*. Then the next adjacent rotor tooth will be displaced from the next adjacent stator tooth through an angle $\gamma_{Z3} - \gamma_{Z4}$; the rotor tooth following it will be displaced from the corresponding stator tooth by an angle $2(\gamma_{Z3} - \gamma_{Z4})$, etc. As a result, the rotor tooth in alignment with the stator tooth at pole *1"* will be separated from the first by an angle $\gamma_{p1}/2$ or $\gamma_{p1}/2\gamma_{Z4}$ tooth pitches of the rotor. With the respect to the next adjacent stator tooth, this rotor tooth will be displaced through an angle $\gamma_{p1}(\gamma_{Z3} - \gamma_{Z4})/2\gamma_{Z4}$ which must be equal to the tooth angle of the stator, that is

$$\gamma_{p1}(\gamma_{Z3} - \gamma_{Z4})/2\gamma_{Z3} = \pm\gamma_{Z3}$$

Hence, on recalling that

$$\gamma_{p1} = 2\pi/p_1$$

we obtain the condition defined in Eq. (20-5).

If stator winding *1* (Fig. 20-4) is a distributed one, and the conductors carrying currents in the same direction are laid at each pole among several (q) slots (in Fig. 20-4, $q = 3$), the stator core *3* need not be a toothed one (modification B7 in Table 20-1). In the modification using a distributed winding, variations in the self-inductance of the winding can be produced by the teeth on the unwound core, *4*. The slots in core *3* carrying the winding may have a limited opening. In the circumstances, core *3* may be treated as a smooth one.

Variations in the self-inductance will be a maximum when the rotor has the same number of teeth, Z_4, as there are poles on winding *1* (in Fig. 20-4, $2p_1 = 4$ and $Z_4 = 4$). This design may be regarded as a special case of a machine with the number of teeth meeting the condition defined in Eq. (20-5) for a smooth stator, when $Z_3 = 0$, and Eq. (20-5) reduces to $Z_4 = 2p_1$.

In such a machine, the high-permeance zones lie opposite the rotor teeth, and the low-permeance zones lie opposite the rotor slots. If it has $Z_4 = 2p_1$ teeth, such a rotor is called *salient-pole*. The time period, frequency and angular frequency of variations in self-inductance are given by Eq. (20-8).

Apart from a heteropolar winding, the design in question may use a single-phase homopolar winding (modification

C7 in Table 20-1). In this design, variations in the self-inductance of the winding are obtained by using a toothed core for both the stator and rotor, the effect being a maximum when $Z_3 = Z_4$. In performance, such a machine is not unlike a single-phase heteropolar machine with $Z_3 = Z_4$.

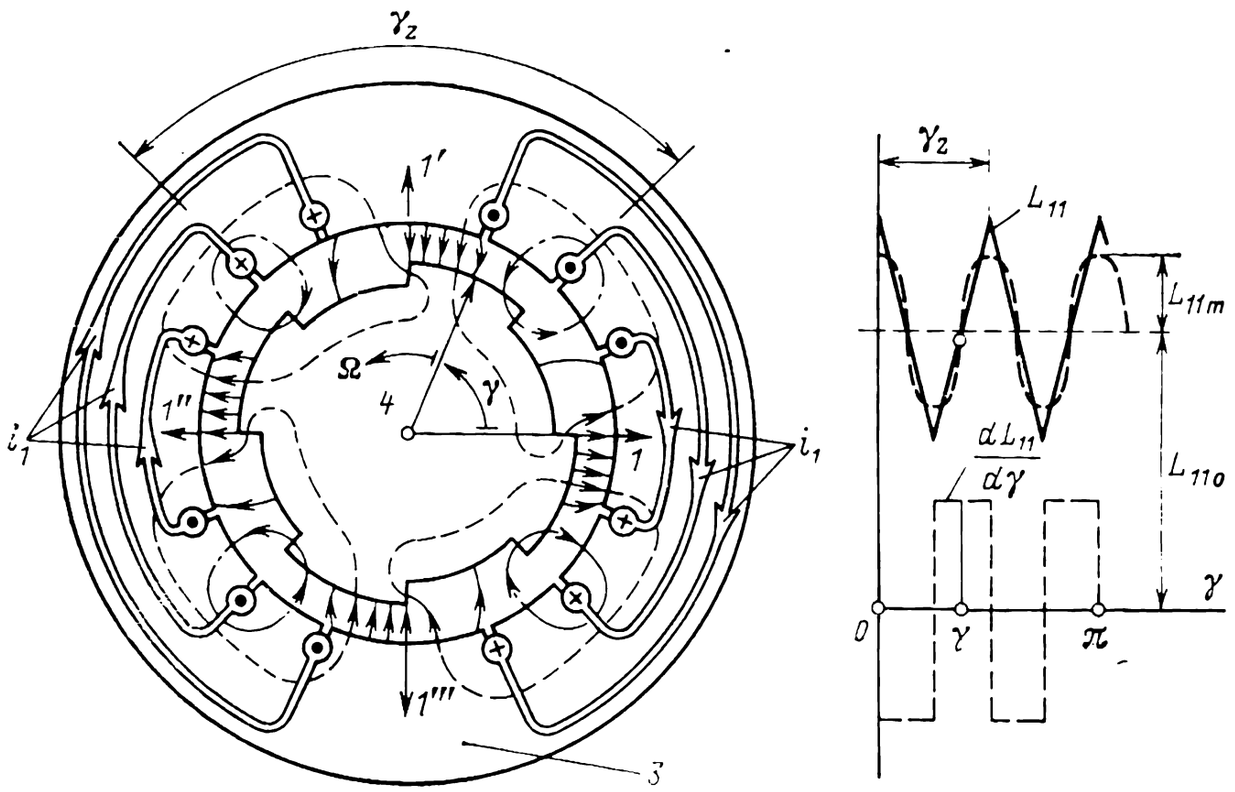

Fig. 20-4 Machine with distributed heteropolar stator (*1*) winding ($p_1 = 2$, $q_1 = 3$) and a toothed (salient-pole) rotor (*4*) core ($Z_4 = 2p_1 = 3$)

The time period, frequency and angular frequency of variations in the self-inductance of a homopolar winding are found by Eq. (20-8).

The design examined in this section is utilized in reluctance synchronous machines. It offers advantages of simple construction and freedom from sliding contacts in the electric circuit of the winding.

20-4 Machines with Two Winding on the Stator and Toothed Cores for the Stator and Rotor (Inductor Machines)

In this case, electromechanical (or mechanoelectric) energy conversion occurs mainly owing to variations in the mutual inductance between the stator windings as a toothed rotor core moves relative to them.

The windings may be heteropolar and have the same number of pole pairs ($p_1 = p_2$) or a different number of pole pairs, or they may be homopolar. It is also possible to combine a heteropolar and a homopolar winding. The stator may be built with either a toothed or a smooth core. This leaves

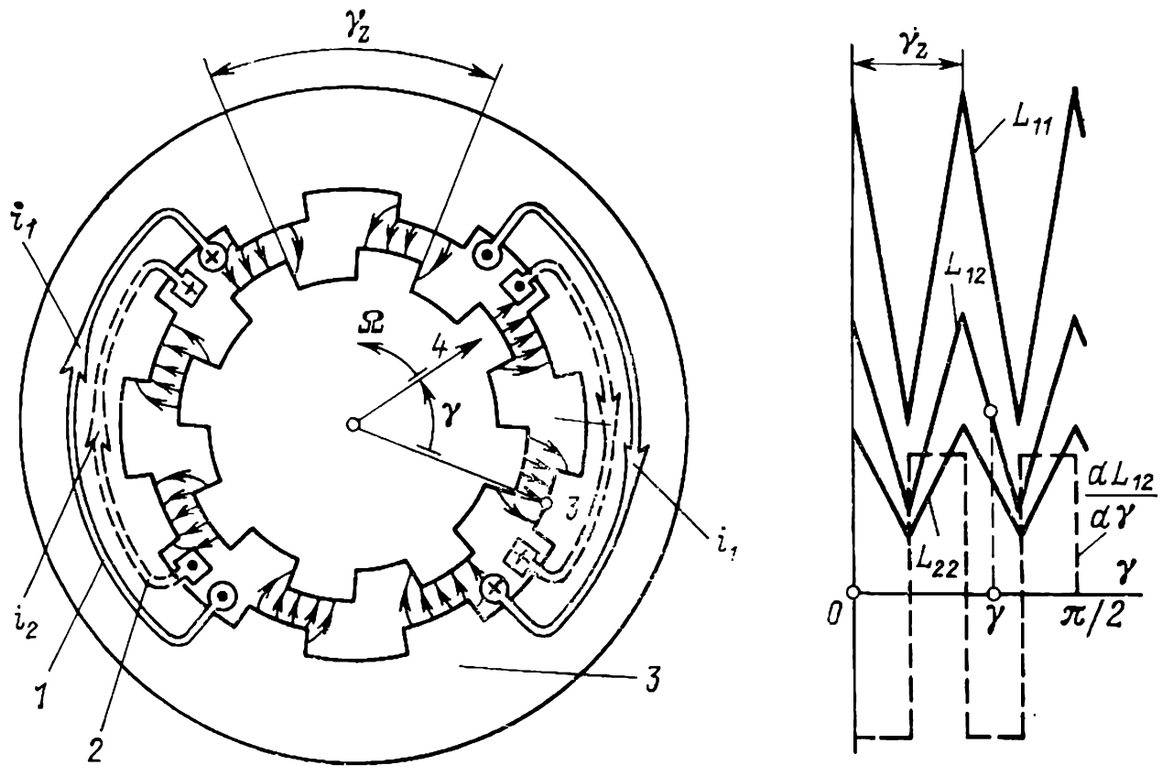

Fig. 20-5 Machine with two heteropolar stator windings, *1* and *2* ($p_1 = p_2 = 2$) and toothed cores for the stator (*3*) and rotor (*4*), with the same number of teeth ($Z_3 = Z_4 = 8$)

us with five likely modifications (A3, B3, C3, D3, and C5, see Table 20-1). One cycle of change in the mutual inductance is completed as the rotor (at *4* in Fig. 20-5) moves through a tooth pitch t_{Z4} or a tooth angle, $\gamma_{Z4} = \gamma_Z$.

If the rotor is rotating at an angular velocity Ω, the time period and angular frequency of the mutual inductance can be found by Eq. (20-8), assuming that the rotor core has a number $Z = Z_4$ of teeth. According to the manner in which the mutual inductance between the windings is made to vary, the machine can be built in one of four modifications.

(i) The mutual inductance between the windings varies owing to changes in the mean permeance of the air gap with the rotation of the toothed rotor core relative to the toothed stator core, both having the same number of teeth (modifications A3 and C5 in Table 20-1). In this arrangement, the mutual inductance has the same sign in any position of the

rotor relative to the stator. As the rotor rotates, it oscillates about its mean value, being a maximum when the stator teeth are aligned with the rotor teeth, and a minimum when the stator teeth are aligned with the rotor slots (and, of course, when the stator slots are aligned with the rotor teeth).

The number of teeth

$$Z = Z_3 = Z_4 \tag{20-9}$$

is chosen to give the requisite frequency of change in the mutual inductance, from Eq. (20-8).

Similar variations in the mutual inductance with $Z_3 = Z_4$ can be obtained with modification C5 which uses two homopolar windings. It is equivalent in performance to modification A3 when the latter uses single-phase windings with $p_1 = p_2$.

(ii) The mutual inductance between the two heteropolar windings on the stator is made to vary owing to the rotation of a toothed rotor core (modification B3 in Table 20-1). In this arrangement, the saliency of the stator is of minor significance. For variations in the mutual inductance to be as large as possible, the number of poles p_1 and p_2 and the number of teeth Z_4 must be chosen such that

$$Z_4 = p_2 \pm p_1 \tag{20-10}$$

For example, in the machine of Fig. 20-6 with a two-pole stator winding *1* ($p_1 = 1$) and a four-pole stator winding *2* ($p_2 = 2$), the condition defined by Eq. (20-10) will be satisfied if the rotor has three teeth ($Z_4 = p_1 + p_2 = 3$).

In such a machine, the permeance will be a maximum in zones B_1, B_2, and B_3 which are aligned with the rotor teeth. It is an easy matter to prove that the mutual inductance between the stator windings is a function of the position that zones B_1, B_2, and B_3 take up relative to these windings.

When the rotor takes up the position shown in the figure (the angle γ between winding *1* and the rotor teeth is $\pi/6$), the mutual inductance L_{12} is a positive maximum (the magnetic field due to the current i_2 produces a maximum positive flux linkage with winding *1*). If we rotate the rotor through $\pi/3$, its teeth will move into the position previously occupied by the slots and, as can readily be shown, the flux linkage and the mutual inductance will change sign and take each a maximum negative value equal to the positive

maximum value in magnitude. With $p_1 = 1$ and $p_2 = 2$, the average mutual inductance will be zero. It will likewise be zero if p_2/p_1 is an even number, that is, if the windings are such that given smooth cores, the mutual inductance

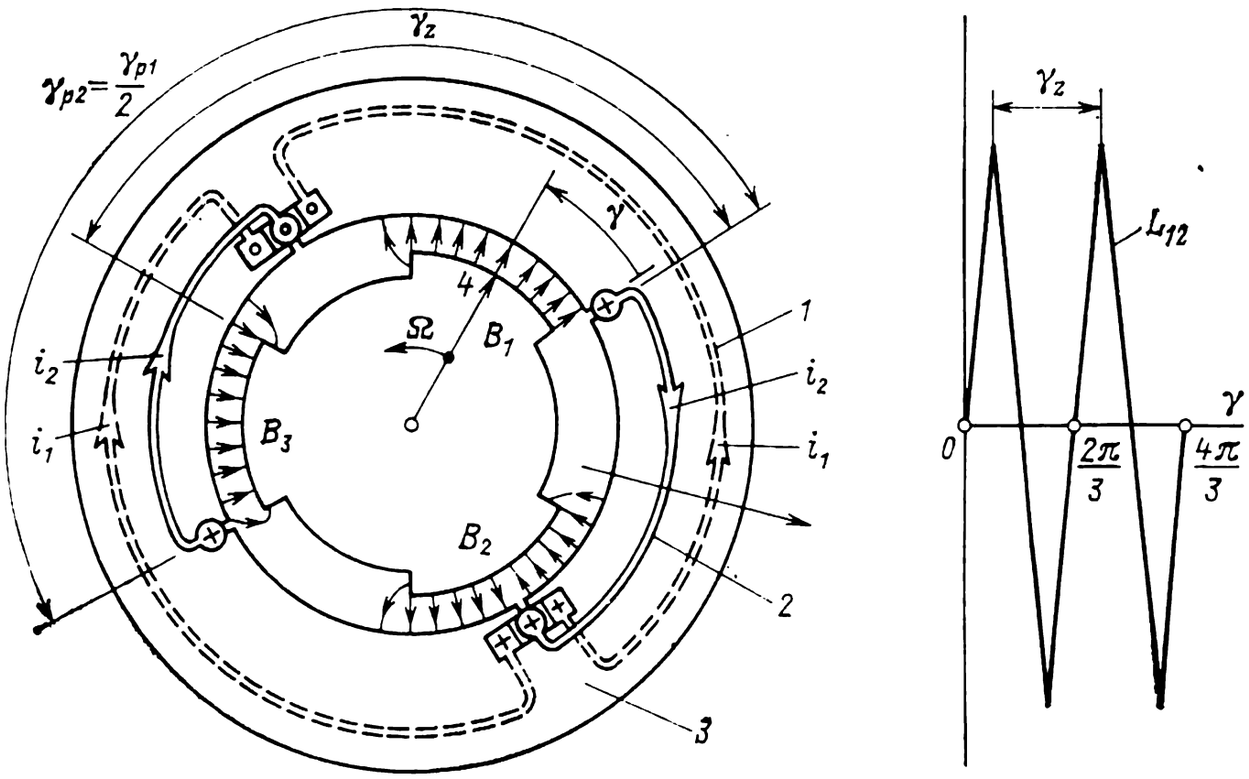

Fig. 20-6 Machine with two heteropolar stator windings, *1* and *2*, with a different number of pole pairs ($p_1 = 1$, $p_2 = 2$), a smooth stator core (*3*), and a toothed rotor core (*4*). $Z_4 = p_1 + p_2 = 3$

between them is zero. If p_2/p_1 is an odd number, the average mutual inductance will be non-zero, and the mutual inductance will be pulsating about its mean value.

The number of rotor teeth Z_4 is uniquely fixed by the specified frequency and angular frequency. As a rule Z_4 is fairly large, and in order to satisfy Eq. (20-10), winding *1* must be made with a moderate number of pole pairs ($p_1 = 1, 2, 3$) and winding *2* with a large number of pole pairs, close to that of rotor teeth, $p_2 = Z_4 - p_1$. This introduces some difficulties in the manufacture of winding *2*. In fact, if Z_4 is very large, one has to use the modification described in (iii) below. Winding *2* is laid in the minor slots shaped so that their effect on the permeance of the air-gap may be neglected. Winding *1* is laid in the major slots which can be formed by enlarging the cross-section of some minor slots without increasing their total number (Fig. 20-6), or they

may replace a group of several minor slots and teeth by removing one or several coils from winding *2*. When $Z_4 = 2p_1$, the two windings have the same number of pole pairs,

$$p_2 = Z_4 - p_1 = 2p_1 - p_1 = p_1$$

If, however, this arrangement is to permit variations in the mutual inductance, one of the windings must be distributed or, if both windings are left concentrated, they must be displaced from each other by a quarter of a cycle, as shown in the cross-sectional view of modification B3.

(iii) The mutual inductance between the two heteropolar windings on the stator is made to vary owing to changes in the position of a toothed stator core relative to a toothed rotor core, both having the same number of teeth. In this arrangement, the number of teeth on the stator and rotor must be chosen such that there are as many high-permeance zones as in a machine with a smooth stator core in (ii) (Fig. 20-6), that is, $p_2 \pm p_1$ (when $p = 1$ and $p_2 = 2$, the number of such zones will be $2 \pm 1 = 3$ or 1).

To obtain this number, it is essential that the difference in the number of teeth between the stator and rotor be $p_2 \pm p_1$,

$$Z_4 - Z_3 = p_2 \pm p_1 \qquad (20\text{-}11)$$

To prove, at the centre of a high-permeance zone, say, B_1 in Fig. 20-7, a rotor tooth is opposite a stator tooth (or, which is the same, a rotor slot is opposite a stator slot). An adjacent rotor tooth is displaced from an adjacent stator tooth by an angle $\gamma_{Z3} - \gamma_{Z4}$; the next adjacent rotor tooth is displaced from the next adjacent stator tooth by an angle $2(\gamma_{Z3} - \gamma_{Z4})$, and so on. To arrive at the centre of the next high-permeance, say, B_2 the displacement must be $2\pi/(p_2 \pm p_1)$ or $Z_4/(p_2 \pm p_1)$ rotor teeth. Then, because at the centre of zone B_2 the rotor tooth must again be opposite the stator tooth, the displacement of this rotor tooth from the corresponding stator tooth

$$Z_4(\gamma_{Z3} - \gamma_{Z4})/(p_2 \pm p_1)$$

must be equal to the tooth angle of the stator, that is,

$$Z_4(\gamma_{Z3} - \gamma_{Z4})/(p_2 \pm p_1) = \gamma_{Z3}$$

Hence, the number of teeth on the stator and rotor must satisfy the condition defined by Eq. (20-11).

Also, for windings *1* and *2* to be able to form balanced circuits, Z_3 must be equal to $2p_2$ (an integer), if $p_2 \geqslant p_1$.

As an example, Fig. 20-7 shows a machine having $p_2 = 2$ and $p_1 = 1$, as does the machine in Fig. 20-6. In view of the desired frequency,

$$Z_3 = 2 \times 2 \times 5 = 20$$
$$Z_4 = 20 + 2 + 1 = 23$$

The pattern of changes in L_{12} with the angular position of the rotor is qualitatively the same as for the machine in

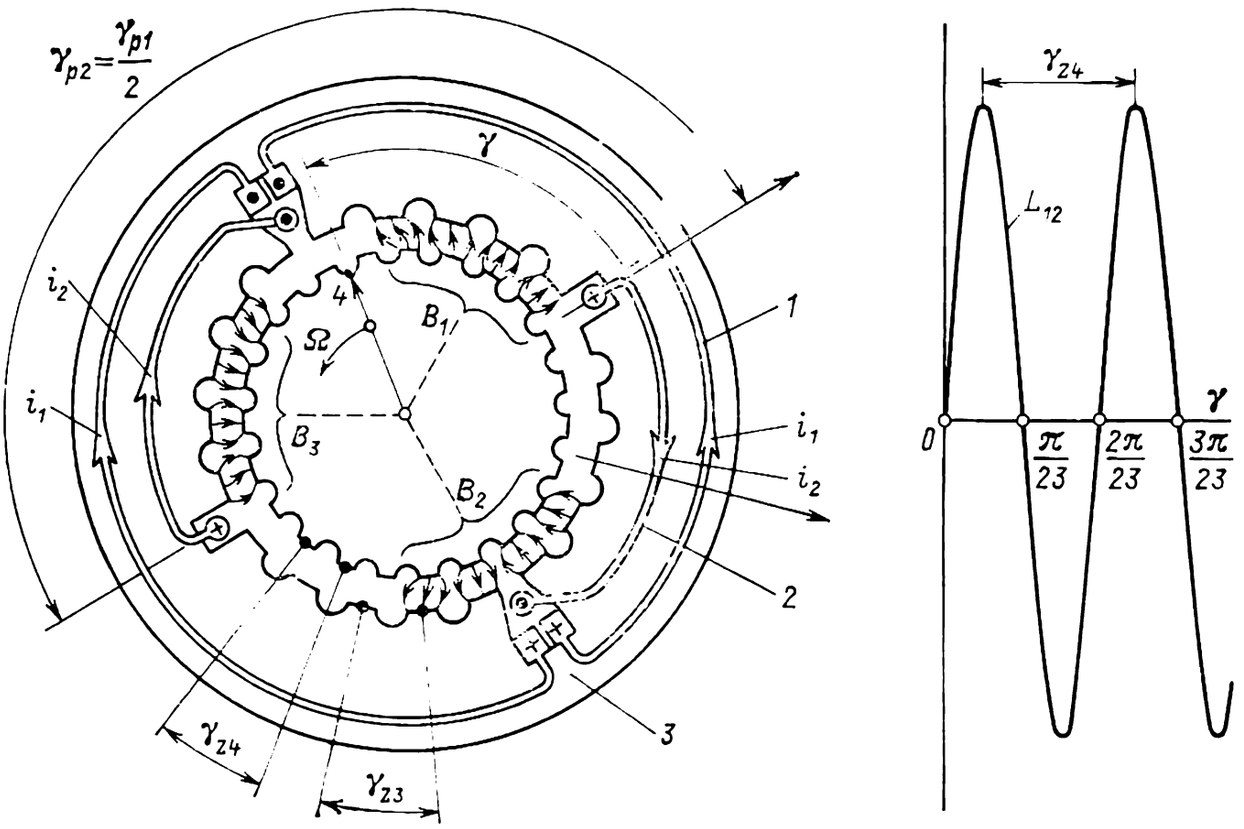

Fig. 20-7 Machine with two heteropolar stator windings, *1* and *2*, differing in the number of pole pairs ($p_1 = 1$, $p_2 = 2$). The stator and rotor are built with toothed cores differing in the number of teeth:

$Z_4 = Z_3 + p_1 + p_2 = 20 + 1 + 2 = 23$

Fig. 20-6. But the self-inductance varies nearly sinusoidally, and it completes a cycle of change in one tooth angle, γ_{Z4}. It is to be noted that as the rotor moves through one tooth pitch or through γ_{Z4}, the axis of a high-permeance zone moves through an angle $2\pi/(p_2 \pm p_1)$, so that zone B_1 takes up the place of B_2, zone B_2 takes up the position of B_3, and so on. As is seen, the high-permeance zones rotate at a higher speed

than the rotor by a factor of

$$2\pi/\gamma_{Z4}\,(p_2 \pm p_1) = Z_4/(p_2 \pm p_1)$$

The time period and frequency of variations in the self-inductance can be found from Eq. (20-8).

(iv) The mutual inductance between a heteropolar and a homopolar winding is made to vary by the rotation of

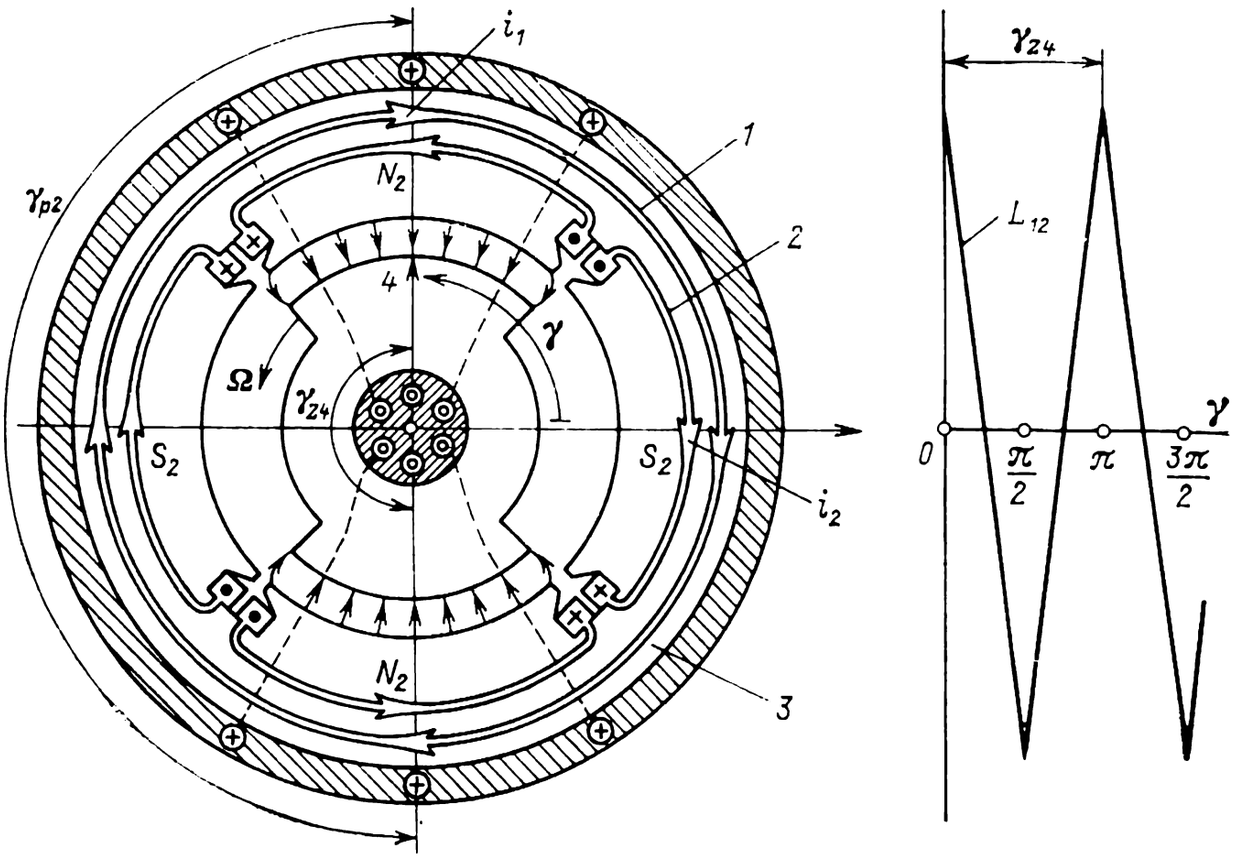

Fig. 20-8 Machine with a heteropolar (*2*) and a homopolar (*1*) stator windings, with a smooth stator core (*3*) and a toothed rotor core (*4*). $Z_4 = p_2 = 2$

a toothed rotor core relative to a smooth stator core (modification D3 in Table 20-1). As is seen from Fig. 20-8, the heteropolar winding is laid out in the stator slots (in the figure, $p_2 = 2$). The homopolar winding is wound as a ring around the rotor shaft. The figure shows the positive directions of the currents in the windings and the magnetic field set up by i_2.

If the stator and rotor cores were smooth, the magnetic field established by winding *2* would be periodic (as shown in Fig. 20-1). Its lines would close via the yokes and link the current i_2 in the slots without linking with winding *1*. To make variations in L_{12} as large as practicable, the rotor core

is made with teeth, and the number of teeth is taken equal to the number of pole pairs for winding *2*, that is,

$$Z_4 = p_2 \tag{20-12}$$

As an example, the condition defined by Eq. (20-12) will be satisfied by the machine shown in Fig. 20-8 ($p_2 = 2$) when $Z_4 = 2$. When the rotor is in the position shown in the figure (the angle between the axis of the S pole on winding *2* and the axis of a rotor tooth is $\gamma = \gamma_{Z4}/2 = \pi/2$), the mutual inductance L_{12} between windings *1* and *2* has a maximum negative value. In this position, the high-permeance zones aligned with the rotor teeth lie opposite the N poles on winding *2*. Conversely, the zones lying opposite the S poles have the lowest permeance, so the periodic magnetic field whose lines close around the currents in the slots, along the yokes, and across the gaps is insignificant.

In contrast, the homopolar field whose lines close around the coil ends on the N poles of winding *2*, across the gap zones having a maximum permeance, across the yokes, through the shaft, end-shields, and frame (see Fig. 19-1*d*) is substantial (it is shown by dashed lines in Fig. 20-8). As is seen, the lines of this homopolar field link with homopolar winding *1*, and the resultant flux linkage is negative. If we turn the rotor through $\gamma_{Z4}/2 = \pi/2$, the axes of the rotor teeth will line up with the axes of the S_2 poles on winding *2*, the high-permeance zones will lie opposite the S_2 poles on winding *2*, and the resultant homopolar field will produce a positive flux linkage with winding *1*. It should be noted that in Fig. 20-8 we have chosen small values for Z_4 and p_2 only to simplify the illustration. In practical machines, the relationship between f and Ω is usually such that $Z_4 = p_2$ must be fairly high. As already noted, winding *2* with a large number of poles is difficult to make. In fact, if $Z_4 = p_2$ turns out to be too large, the modification being discussed has to be replaced by that examined in(v)below.

(v) The mutual inductance between a heteropolar and a homopolar winding is made to vary by the rotation of a toothed rotor relative to a toothed stator, having different numbers of teeth (modification C3 in Table 20-1).

As follows from Fig. 20-9, this modification differs from that in (iv) only in that the stator core has teeth. To make variations in L_{12} as large as practicable, the number of teeth on the stator (Z_3) and the rotor (Z_4) must be chosen such

that the number of high-permeance zones formed around the periphery of the air gap be equal to p_2, as in the machine shown in Fig. 20-8. As has been proved in (iii), the number of high-permeance zones for a toothed stator and a toothed

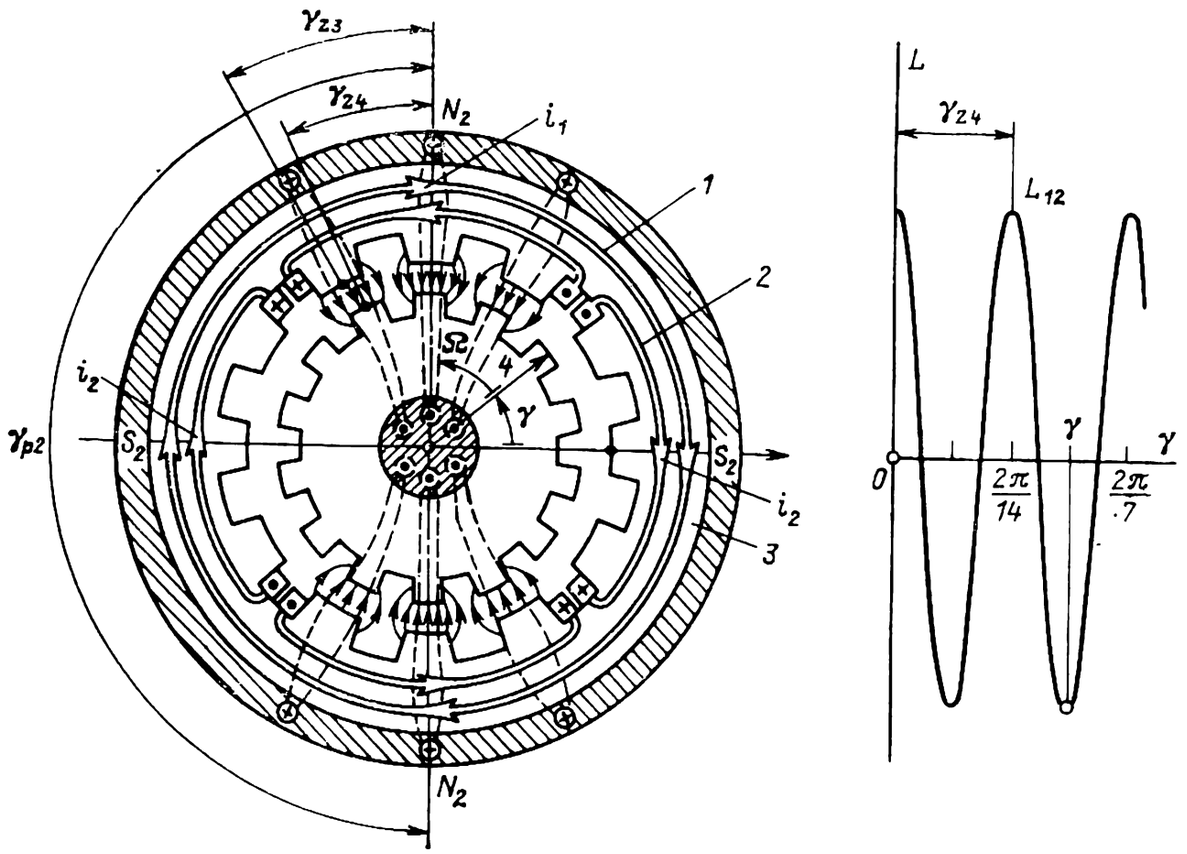

Fig. 20-9 Machine with a heteropolar (*2*) and a homopolar (*1*) winding on the stator and toothed stator (*3*) and rotor (*4*) cores having a different number of teeth ($Z_4 = Z_3 + p_2 = 12 + 2 = 14$)

rotor is equal to the difference in the number of teeth between the stator and rotor. Therefore, Z_3 and Z_4 must be chosen such that

$$Z_4 - Z_3 = p_2 \qquad (20\text{-}13)$$

As an example, for the machine in Fig. 20-9, which uses winding *2* with two pairs of poles ($p_2 = 2$) and stator *3* with $Z_3 = 12$ teeth, the condition defined in Eq. (20-13) will be satisfied when

$$Z_4 = Z_3 + p_2 = 12 + 2 = 14$$

When the rotor takes up the position shown in the figure (the angle between the axes of the stator and rotor teeth is $\gamma = 3\gamma_{Z4}/2 = 3\pi/14$), the mutual inductance between windings *1* and *2* has a maximum negative value. In this position, the high-permeance zones in the air gap, where the

stator teeth lie opposite the rotor teeth, are aligned with the N_2 poles of winding *2*. In contrast, the zones lying opposite the S poles have the lowest permeance. If we turn the rotor through an angle $\gamma_{Z_4}/2 = \pi/14$, the axes of the rotor teeth will align themselves with those of the stator teeth on the axes of the S poles. The high-permeance zones will then lie opposite the S_2 poles on winding *2* and produce a homopolar magnetic field which links with winding *1*.

The design with two windings on the stator is frequently used in special-purpose machines. Among its advantages are the relatively high frequency of variations in the self or mutual inductances at a relatively low rotational speed, and also freedom from sliding contacts in the electric circuits of the windings (for which reason such machines are called brushless or contactless).

In the generator mode of operation, such machines generate voltages at a high frequency, although the rotor is rotating at a medium velocity (inductor generators). In the motor mode of operation, their rotors rotate at a substantially lower speed than the machines having windings on both the stator and rotor. Because in such motors the rotor speed is reduced electromagnetically (without any gearing), they may be called electromagnetically down-geared motors.

21 Conditions for Unidirectional Energy Conversion by Electrical Machines

21-1 The Single-Winding Machine

In this chapter, we shall discuss what currents the windings of a machine must carry for undirectional energy conversion to take place. The discussion will be concerned with the same machine designs as are listed in Sec. 20-1.

To begin with, we shall turn to the equation of electromagnetic torque, Eq. (18-6), for a single- or a two-winding machine. In this equation, the self-inductance of one winding, L_{11}, or the mutual inductance L_{12} between two windings is a periodic function of the angular position of the rotor or time. For unidirectional energy conversion, the currents in the windings must vary so that the mean electromagnetic torque is nonzero.

Because all the events involved recur periodically, it will suffice to determine the torque averaged over a period

$$T_0 = \frac{1}{T}\int_0^T T\,dt$$

and to define the conditions for currents under which electric energy is converted to mechanical ($T_0 > 0$) or back ($T_0 < 0$).

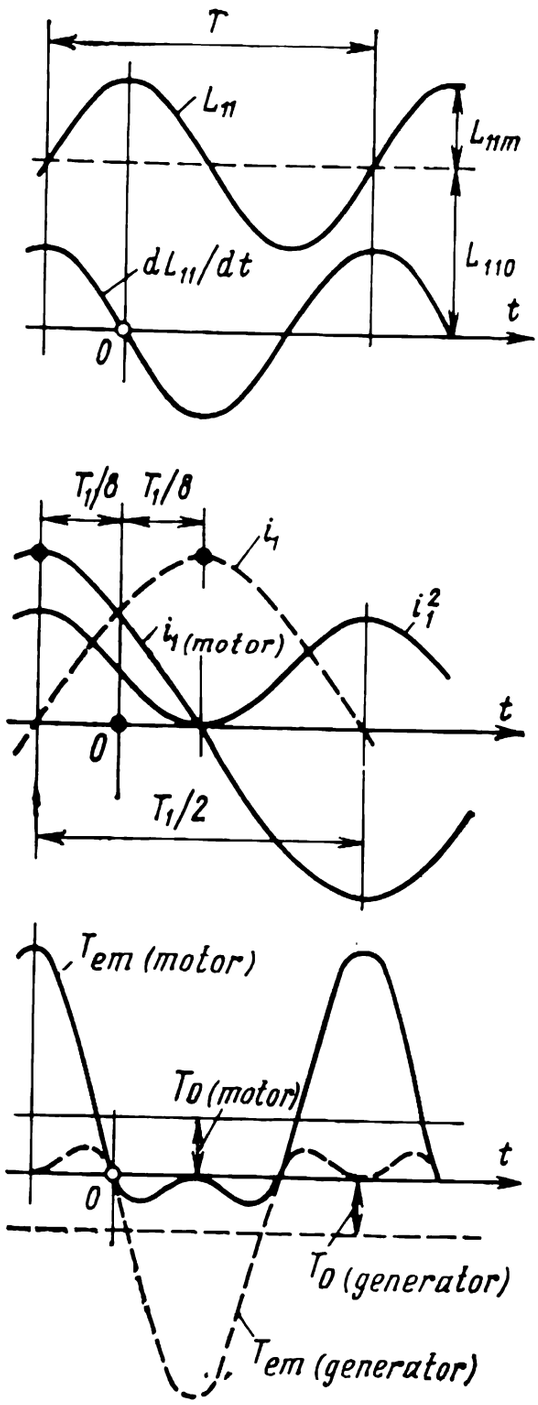

Fig. 21-1 Conditions for unidirectional energy conversion in a single-winding machine

Let us consider a single-winding machine first (see Sec. 20-3). As follows from Eq. (18-6), when $n = 1$ and $k = 1$, the electromagnetic torque developed by a machine with one winding *1* carrying a current i_1 (see Figs. 20-2 through 20-4) is given by

$$T = \frac{1}{2} i_1^2 \frac{dL_{11}}{d\gamma} \qquad (21\text{-}2)$$

No matter where the winding is wound (on the stator or rotor) and how it is arranged, variations in L_{11} will be qualitatively the same, with an angular period (tooth angle) γ_Z or a time period $T = -2\pi/p_Z\Omega = 2\pi/\omega$ [see Eq. (20-8)], about some mean self-inductance, L_{110}. Expanding into a Fourier series and retaining the zeroth and first terms, variations in the self-inductance with time may be described by an equation of the form

$$L_{11} \approx L_{110} + L_{11m}\cos\omega t \qquad (21\text{-}3)$$

where $\omega = \Omega p_Z = 2\pi/T$ is the angular frequency of variations in the self-inductance (see Fig. 21-1).

The derivative of the self-inductance with respect to the angular position of the rotor is

$$dL_{11}/d\gamma = (dL_{11}/dt)\,(dt/d\gamma) = -p_Z L_{11m} \sin \omega t \qquad (21\text{-}4)$$

where $\gamma = \Omega t$, and $dt/d\gamma = 1/\Omega$.

As we have already learned, the current in the only winding of a machine must be an alternating one. Using Eq. (21-1), it is an easy matter to see that if the winding carried a constant current, the mean torque T_0 would be zero.

Let us limit ourselves to the fundamental component of current, responsible for the largest mean electromagnetic torque. Then,

$$i_1 \approx I_{1m} \cos(\omega_1 t + \varphi) \qquad (21\text{-}5)$$

Now the question is: What should ω_1 and φ be for T_0 to be a maximum, with all other conditions being equal?

Since the mean torque is given by

$$T_0 = -\frac{p_Z I_{1m}^2 L_{11m}}{2T} \int_0^T \cos^2(\omega_1 t + \varphi) \sin \omega t \, dt$$

its evaluation reduces to evaluating its integral. Upon trigonometric manipulations in the integrand, we get

$$\int_0^T \cos^2(\omega_1 t + \varphi) \sin \omega t \, dt$$

$$= \frac{1}{2} \int_0^T \sin \omega t \, dt + \frac{1}{2} \int_0^T \cos(2\omega_1 t + 2\varphi) \sin \omega t \, dt$$

The first term on the right-hand side is equal to zero. The second term may be re-written as

$$\frac{1}{4} \int_0^T \sin[(\omega + 2\omega_1) t + 2\varphi] \, dt$$

$$+ \frac{1}{4} \int_0^T \sin[(\omega - 2\omega_1) t - 2\varphi] \, dt$$

When the angular frequency of the current is

$$\omega_1 = \omega/2 \qquad (21\text{-}6)$$

the time period of the current, $T_1 = 2T$, is twice the time period of the self-inductance, and the period of the current

squared, $T_1/2$, is equal to the time period of the self-inductance (see Fig. 21-1). Then the mean electromagnetic torque is

$$T_0 = (p_Z I^2_{1m} L_{11m}/8) \sin 2\varphi \qquad (21\text{-}7)$$

When $\varphi = \pi/4$, the mean torque is a maximum in the generator mode of operation. When $\varphi = -\pi/4$, it is a maximum in the motor mode of operation. Also, the periodic component of the current squared is in phase with the self-inductance in the former case, and in anti-phase in the latter case.

The respective plots of currents and torques appear in Fig. 21-1. The angle $\varphi = \pi/4$ corresponds to a time lead of $t = \varphi/\omega_1 = T_1/8$.

To sum up, it may be argued that for unidirectional energy conversion, a single-winding machine must carry a current at angular frequency ω_1 equal to half the angular frequency of variations in the self-inductance:

$$\omega_1 = \omega/2 = p_Z\Omega/2$$

The direction of energy conversion depends on the phase angle between the current and the self-inductance. When $\varphi = \pi/4$, the machine will be operating as a motor. When $\varphi = -\pi/4$, it will be operating as a generator.

The angular velocity of the machine is proportional to the angular frequency of the current in the winding connected to the electrical system

$$\Omega = 2\omega_1/p_Z \qquad (21\text{-}8)$$

A machine whose angular velocity is proportional to the angular frequency of the electrical system will be called a *synchronous machine*. A machine whose angular velocity does not satisfy this relation will be called an *asynchronous* one.

From Eq. (21-8) it follows then that all single-winding a.c. machines are synchronous machines.

21-2 Two-Winding Machines

The electromagnetic torque developed by a two-winding machine is given by

$$T = i_1 i_2 \, \mathrm{d}L_{12}/\mathrm{d}\gamma + \frac{1}{2} i_1^2 \, \mathrm{d}L_{11}/\mathrm{d}\gamma + \frac{1}{2} i_2^2 \, \mathrm{d}L_{22}/\mathrm{d}\gamma \qquad (21\text{-}9)$$

irrespective of the winding arrangement.

A major contribution to the electromagnetic torque comes from variations in the mutual inductance between the windings and is represented by the first term in Eq. (21-9)*. Therefore, we may limit our analysis to the first term.

As in the previous case, we may limit ourselves to the periodic component of the self-inductance with an angular period γ_p (or γ_Z) and a time period

$$T = 2\pi/p_0\Omega = 2\pi/\omega$$

where $p_0 = p$ is the number of pole pairs on the heteropolar windings of the stator and rotor [see Eqs. (20-2) through (20-4)]

$p_Z = Z$ is the number of teeth per pole on the rotor of a machine with two stator windings [see Eq. (20-8)]

As in the previous case, the mutual inductance varies with time as

$$L_{12} = L_{120} + L_{12m} \cos \omega t \qquad (21\text{-}10)$$

where $\omega = \Omega p_0 = 2\pi/T$.

The derivative of the mutual inductance with respect to the angular position of the rotor is

$$dL_{12}/d\gamma = (dL_{12}/dt)\,(dt/d\gamma) = -p_0 L_{12m} \sin \omega t \qquad (21\text{-}11)$$

In the general case, the windings carry alternating currents**. Limiting ourselves to the fundamental components as contributing most to the electromagnetic torque, we may write

$$\begin{aligned} i_1 &= I_{1m} \cos (\omega_1 t + \varphi_1) \\ i_2 &= I_{2m} \cos (\omega_2 t + \varphi_2) \end{aligned} \qquad (21\text{-}12)$$

In Fig. 21-2, $\omega_1 = 4\omega$, $\omega_2 = 3\omega$, $\varphi_1 = 0$, and $\varphi_2 = -\pi/2$.

Now let us find the values of ω_1, ω_2, φ_1, and φ_2 that will lead to a maximum mean electromagnetic torque in Eq. (21-1), with all other conditions being equal.

---

* The other components of the mean torque can be found as for a single-winding machine. As follows from Eq. (21-6), the mean torque of this kind may be non-zero at $\omega_1 = \omega/2$ or $\omega_2 = \omega/2$. Then it will be a maximum at $\varphi_1 = \pm\pi/4$ or $\varphi_2 = \pm\pi/4$.

** A machine with, say, the second winding carrying d.c. is a special case for which $\omega_2 = 0$ and $i_2 = \text{const}$.

The mean torque is given by

$$T_0 = -(p_0 I_{1m} I_{2m} L_{12m}/T) \int_0^T \cos(\omega_1 t + \varphi_1) \cos(\omega_2 t + \varphi_2) \sin \omega t \, dt$$

The products of the cosines in the integrand may be rewritten

$$\frac{1}{2} \cos[(\omega_1 + \omega_2) t + \varphi_1 + \varphi_2] + \frac{1}{2} \cos[(\omega_1 - \omega_2) t + \varphi_1 - \varphi_2]$$

where the first term varies with a frequency $\omega_1 + \omega_2$, and the second term with a frequency $\omega_1 - \omega_2$.

If one of these frequencies is the same as the frequency of variations in the mutual inductance, that is,

$$\omega_1 + \omega_2 = \omega \quad \text{or} \quad \omega_1 - \omega_2 = \omega \qquad (21\text{-}13)$$

then the mean torque will be nonzero. To demonstrate, on replacing the products

$$\frac{1}{2} \cos[(\omega_1 + \omega_2) t + \varphi_1 + \varphi_2] \sin \omega t$$

and

$$\frac{1}{2} \cos[(\omega_1 - \omega_2) t + \varphi_1 - \varphi_2] \sin \omega t$$

by a sum of four trigonometric functions, we get

$$T_0 = (p_0 I_{1m} I_{2m} L_{12m}/4T) \int_0^T \sin[(\omega_1 \pm \omega_2 - \omega) t + \varphi_1 \pm \varphi_2] \, dt$$

Hence, on satisfying the condition defined by Eq. (21-13), we obtain

$$T_0 = (p_0 I_{1m} I_{2m} L_{12m}/4) \sin(\varphi_1 \pm \varphi_2) \qquad (21\text{-}14)$$

where the "+" sign applies when $\omega_1 + \omega_2 = \omega$, and the "—" sign applies when $\omega_1 - \omega_2 = \omega$.

The integrals of the remaining three terms of the sum, varying at frequencies

$$\omega_1 + \omega_2 + \omega \neq 0$$
$$\omega_1 - \omega_2 + \omega \neq 0$$
$$\omega_1 \mp \omega_2 - \omega \neq 0$$

are equal to zero.

As is seen from Eq. (21-14), in the motor mode of operation ($T_0 > 0$), the mean torque is a maximum when $\varphi_1 \pm \varphi_2 = \pi/2$; in the generator mode of operation ($T_0 < 0$), this happens when $\varphi_1 \pm \varphi_2 = -\pi/2$.

Unidirectional energy conversion by a two-winding machine is illustrated in Fig. 21-2. With the frequencies and phase adopted in the figure,

$$\omega_1 - \omega_2 = \omega$$

and

$$\varphi_1 - \varphi_2 = \pi/2$$

so the resultant torque is nonzero.

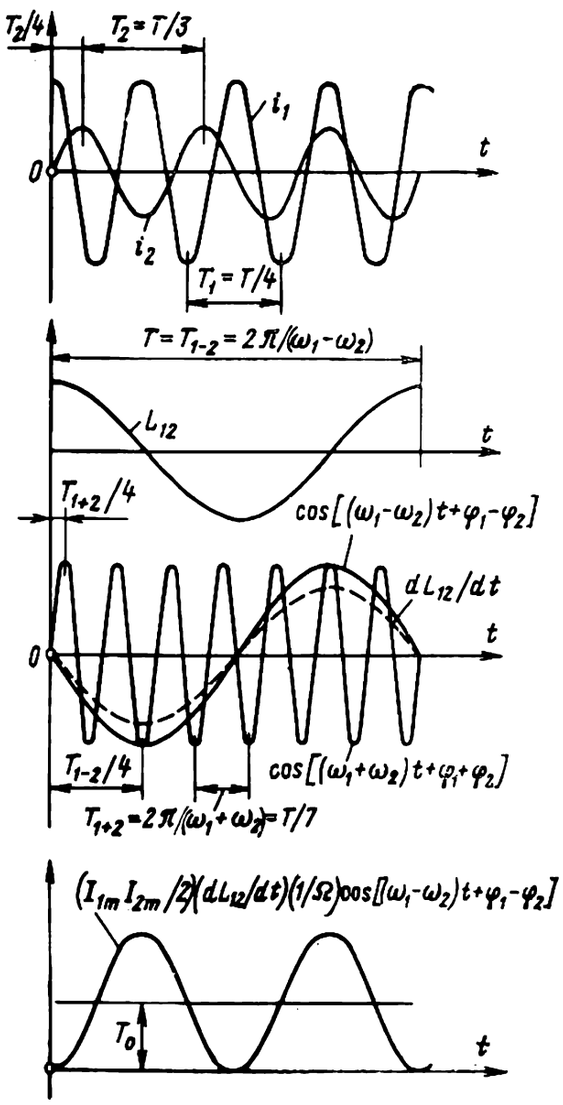

Fig. 21-2 Conditions for unidirectional energy conversion in a two-winding machine

To sum up, for unidirectional energy conversion by a two-winding a.c. machine, it is essential that the sum or the difference of the angular frequencies of the currents in the windings be equal to the angular frequency of variations in the mutual inductance between the windings. The direction of energy conversion is determined by the magnitude of the sum or difference of the phase angles of currents with respect to the mutual inductance. When $0 < (\varphi_1 \pm \varphi_2) < \pi/2$, electric energy is converted to mechanical; when $-\pi/2 < (\varphi_1 \pm \varphi_2) < 0$, mechanical energy is converted to electric.

According as the rotational frequency of the rotor does or does not change with variations in the external torque, there may be *asynchronous machines* and *synchronous machines.*

In a synchronous machine, both windings carry currents whose angular frequencies are fixed in advance. In the general case, the machine converts the electric energy fed into two windings. Therefore, such units are also called *double-fed machines.* With ω_1 and ω_2 held constant, the angular velocity of the rotor in a synchronous machine remains con-

stant, irrespective of the torque on its shaft*

$$\Omega = \frac{\omega}{p_0} \frac{\omega_1 \pm \omega_2}{p_0} = \text{constant}$$

Most frequently, synchronous machines are built with a three-phase heteropolar winding on the stator and a single-phase heteropolar winding on the rotor. If we put $\omega_2 = 0$ and $\varphi_2 = 0$, all the relations derived above will fully apply to such a machine.

If not otherwise qualified, the term "synchronous" refers exactly to the above type of machine.

In an asynchronous machine (primarily, a motor) only one winding, say *1*, is connected to a line whose frequency, say ω_1 is fixed in advance. The other winding is either short-circuited or connected across an impedance, and the current i_2 in this winding is produced by electromagnetic induction. Accordingly, asynchronous machines are more frequently called *induction machines*. The mutual emf is given by

$$e_{12} = -\mathrm{d}\Psi_{12}/\mathrm{d}t = -\frac{1}{2} i_{1m} L_{12m} (\omega_1 - \omega) \sin [(\omega_1 - \omega) t + \varphi_1]$$

$$+ \frac{1}{2} i_{1m} L_{12m} (\omega_1 + \omega) \sin [(\omega_1 + \omega) t + \varphi_1]$$

where

$$\Psi_{12} = i_1 L_{12} = i_{1m} \cos (\omega_1 t + \varphi_1) L_{12m} \cos \omega t$$

is the mutual flux linkage.

The frequency $\omega_2 = \omega_1 - \omega$ of i_2 is a function of the angular velocity of the rotor ($\omega_2 = \omega_1 - \Omega p_0$) and satisfies the condition for unidirectional energy conversion defined in Eq. (21-13).

Most frequently, asynchronous (induction) machines are built with a three-phase heteropolar a.c. winding on the stator, and a three-phase (or poly-phase) heteropolar short-circuited winding on the rotor.

If not otherwise qualified, the term "induction machine" refers to the above type of machine.

---

* Variations in the load on the shaft bring about only changes in the amplitude and phase of i_1 and i_2.

22 Windings for A.C. Machines

22-1 Introductory Notes

Our discussion will be limited to heteropolar cylindrical windings since they are used most frequently in electrical machines.

The coils of such windings are usually laid out in slots on the stator or rotor.

The arrangement of single-layer (Fig. 22-1*a*) and two-layer (Fig. 22-1*b*) heteropolar windings along with that of a simple polyphase single-layer winding has been explained in Sec. 19-2. Therefore, our discussion here will only be concerned with polyphase two-layer windings with $m \gg 1$ phases, since they are used most frequently in a.c. machines.

22-2 The Structure of a Polyphase Two-Layer Winding

A two-layer m-phase winding is designed for connection to an m-phase balanced a.c. line or system. In the case of a three-phase system, they can be connected in a star or a delta (Fig. 22-2*a* and *b*).

For the phase currents $\dot{I}_A$, $\dot{I}_B$, and $\dot{I}_C$ to form a balanced set, it is essential that the phase windings should have the same inductive reactances. This requirement will be satisfied if the axes of the phase windings are displaced from one another through an angle equal to $1/m$ of the angular period of the field (the pole pitch angle)*

$$\gamma_p/m = 2\pi/pm$$

The core of a three-phase, two-layer winding ($m = 3$) is shown in Fig. 22-3. Each phase winding consists of several coils (Fig. 22-4*a*), one coil side lying in the top half of a slot, and the other in the bottom half of another slot about one pole pitch away.[1] Each coil may have one turn ($w_c = 1$) or several turns ($w_c > 1$) insulated from

---

* This equation applies when $m > 2$. When $m = 2$, the phases are displaced through $\gamma_p/4$.

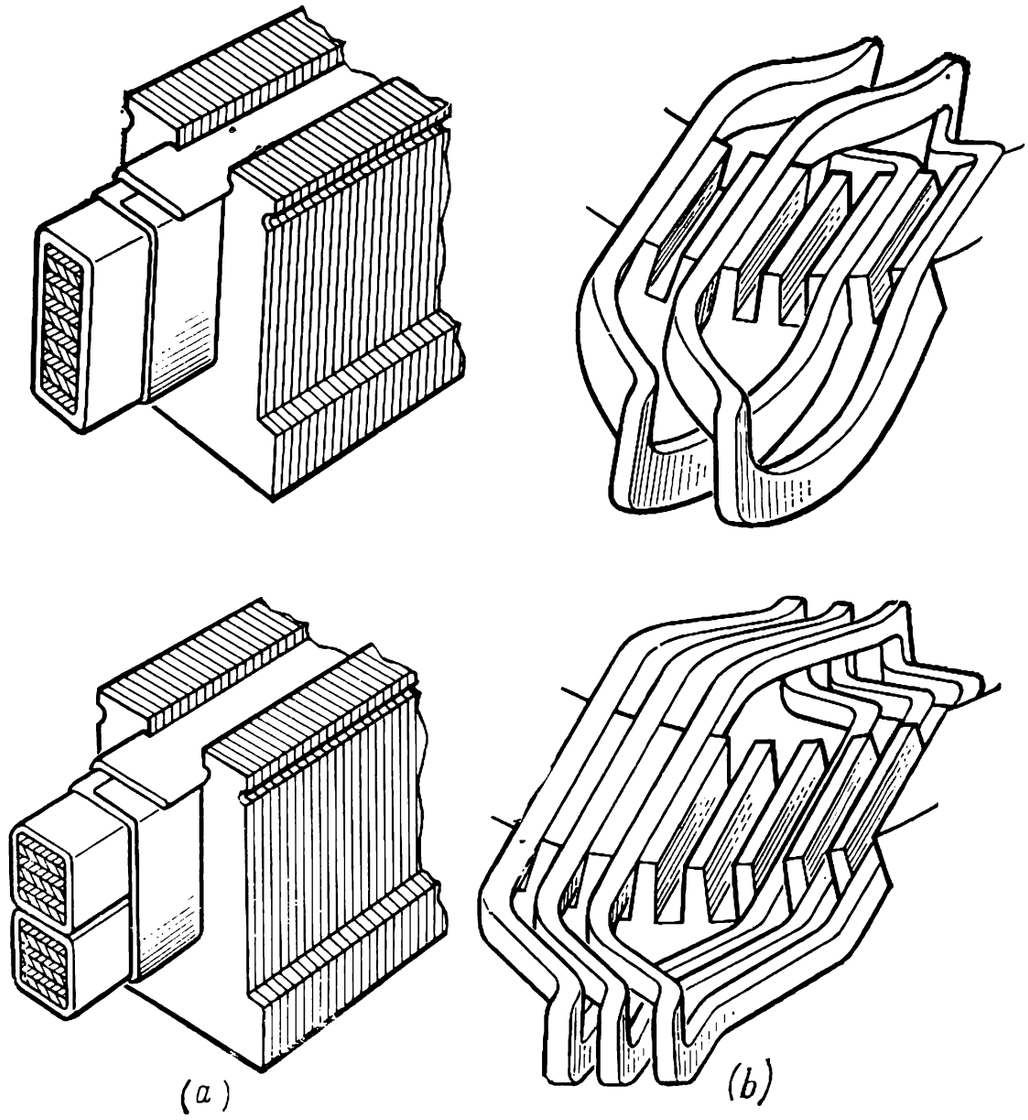

Fig. 22-1 Windings: (*a*) single-layer and (*b*) double-layer

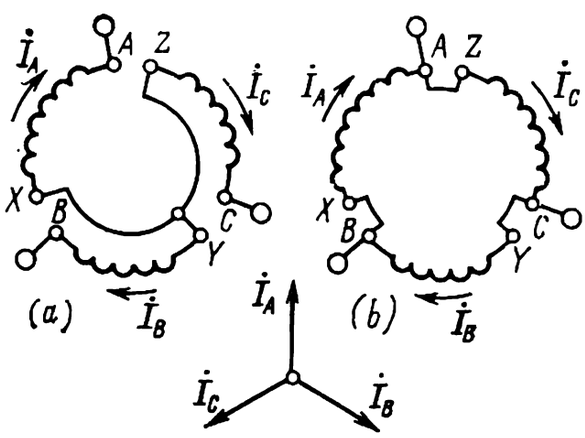

Fig. 22-2 Three-phase winding: (*a*) star-connected and (*b*) delta-connected

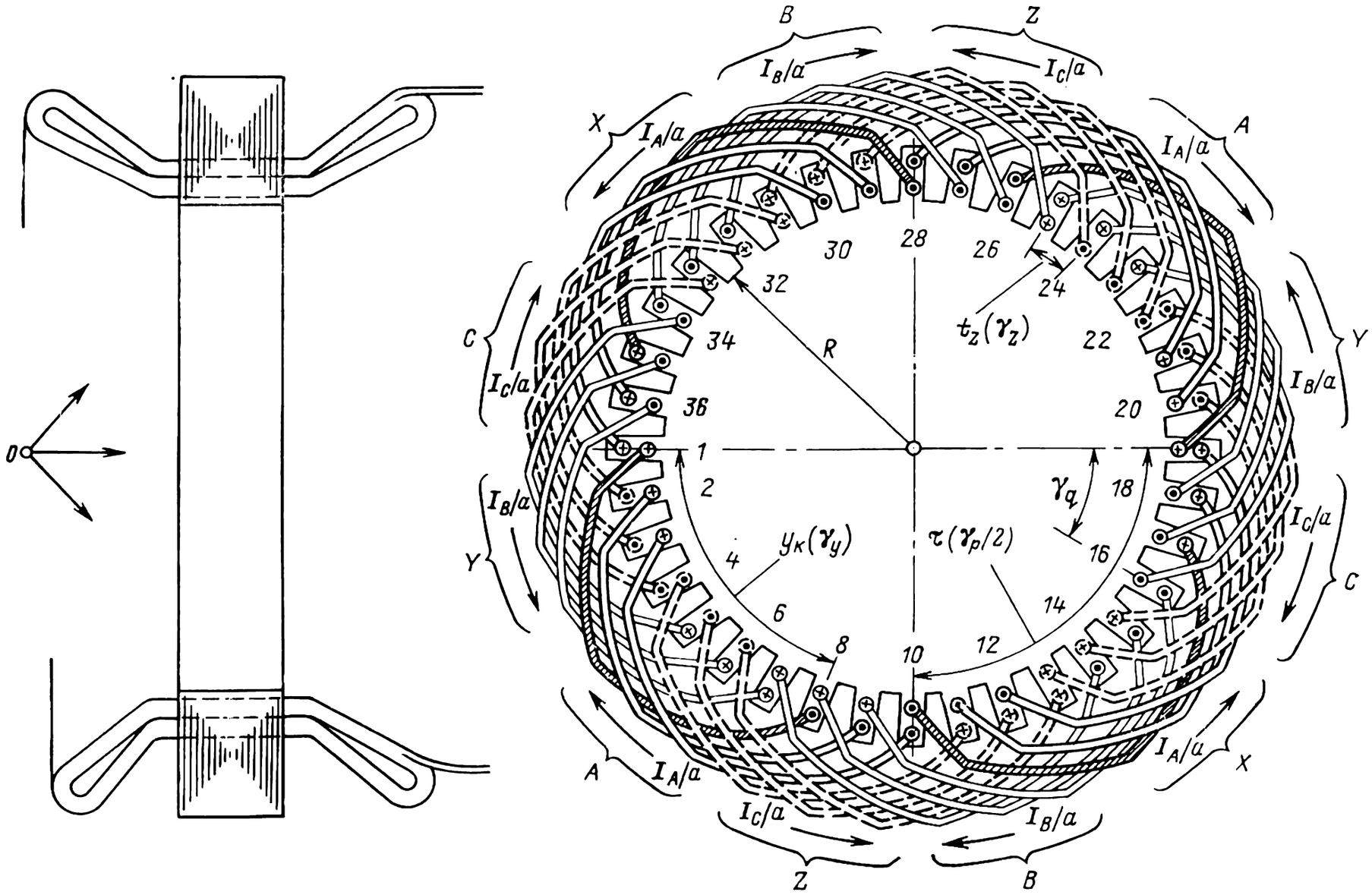

Fig. 22-3 Coil structure of a double-layer winding ($Z = 36$, $p = 2$, $m = 3$, $y = 7$, $\tau = 9$)

one another and from the slot sides (the coil in Fig. 22-4*a* has two turns). The coils may be *lap-wound* or *wave-wound*. In a lap winding, each coil is connected to the next adjacent coil in series. In a wave winding, each coil is connected to a coil two pole pitches farther away than the next adjacent coil.

Each coil has two leads. Let the lead on the upper coil side be the start (S) of the coil. Then the lead on its lower side will be its finish (F). As a rule, the leads of a coil are

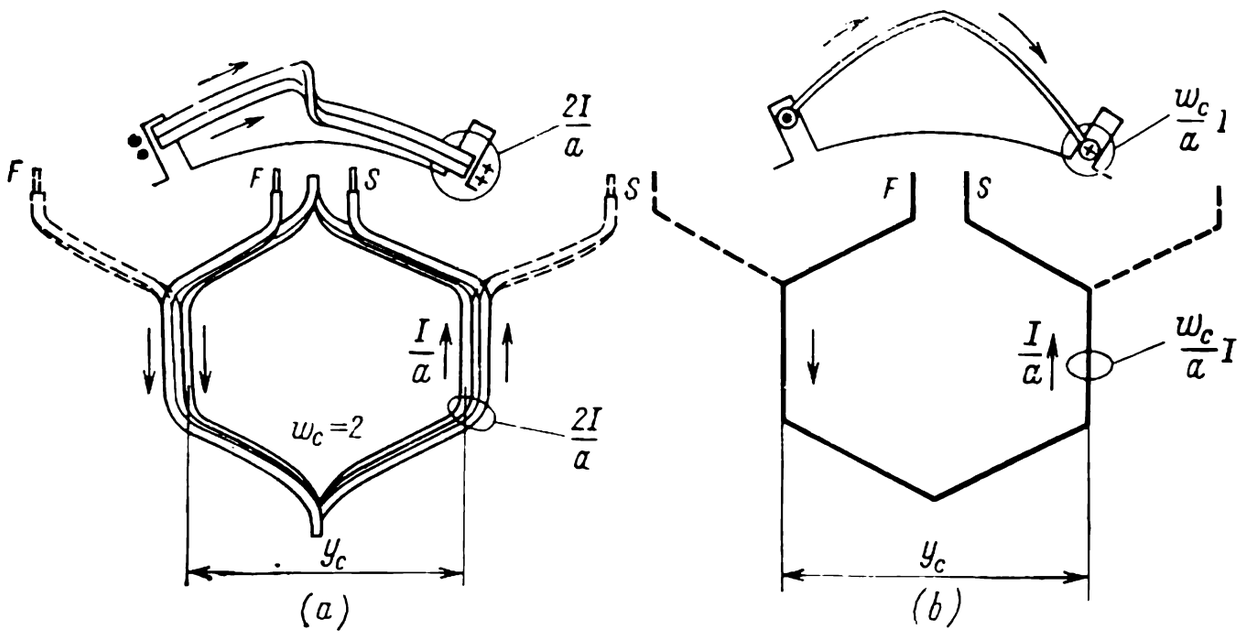

Fig. 22-4 Coils of a double-layer lap winding (solid lines) and a double-layer wave winding (dashed lines): (*a*) actual arrangement; (*b*) sketch

made long enough for direct connection to another coil. According to the manner in which the coils are interconnected within a phase, the leads may be differently shaped and proportioned.

In diagrams, coils are usually shown as single-turn loops. As is seen in Fig. 22-4*b*, a wave-wound coil differs from a lap-wound coil only in that the leads are shaped differently (the leads of a wave winding are shown by the dashed lines). The coil pitch y equal to the distance between the coil sides, may be equal to a pole pitch ($y = \tau$), or it may be somewhat shorter than one pole pitch, or chorded (usually, $y = 0.8\tau$). Accordingly, there may be a *full-pitched* or a *short-pitched* (or *chorded*) *winding*.

The pole pitch and the coil pitch may be measured in terms of the distance along the periphery of the air gap or in

tooth pitches

$$\tau = Z/2p \text{ (tooth pitches)} \qquad (22\text{-}1)$$

$$y = y_c/t_z \text{ (tooth pitches)} \qquad (22\text{-}2)$$

where y_c = coil (or slot) span (see Fig. 22-4)
$t_z = 2\pi R/Z$ = tooth pitch
Z = number of teeth (slots) on the core

Taking as an example a three-phase, four-pole, short-pitched (chorded) winding with $y = 7$ and $Z = 36$, Fig. 22-3 shows how the coils should be distributed among the phases, the coil sides laid out in slots, and the positive currents directed in the coil conductors of polyphase, two-layer windings.

The total number of coils in the winding is equal to the number of slots. So each phase contains

$$Z/m = 36/3 = 12 \text{ coils}$$

To establish a four-pole field, the coils in each phase should be divided into $2p = 4$ groups uniformly distributed all the way around the circumference (one group per pole pitch). Each group contains $q = Z/2pm$ adjacent coils. The number q is equal to the number of slots per pole per phase,

$$q = Z/2pm = 36 \div (2 \times 2 \times 3) = 3 \qquad (22\text{-}3)$$

Let us designate coils by the Nos. of the slots in which their top sides are laid. Then phase A will include the following coil groups: (*1*, *2*, *3*), (*10*, *11*, *12*), (*19*, *20*, *21*), and (*28*, *29*, *30*).

Adjacent groups in a phase are displaced from one another by one pole pitch

$$\tau = Z/2p = 36/4 = 9 \text{ slots}$$

For the resultant field to be periodically varying, all the coils in each phase must carry identical currents reversing in direction as they pass from one pole pitch to the next. Assuming that the current in phase A (see Fig. 22-2) is in the positive direction, the currents in the top sides of coil group (*1*, *2*, *3*) will be flowing "inwards" (away from the reader), the currents in the top conductors of coil group (*10*, *11*, *12*) will be flowing "outwards" (towards the reader), etc. To facilitate design work, the coil groups in which the

top conductors carry currents flowing away from the reader are assigned the index of the start of a given phase, A, and the coil groups in which the top conductors carry currents flowing towards the reader are assigned the index of the finish of the same phase, X.

Given the same positive directions of currents, the patterns of coils and currents in the remaining phases will be the same as in phase A. The only difference will be that phase B will be displaced from phase A counter-clockwise by an angle

$$\gamma_p/m = 2\pi/pm = \pi/3 \qquad (22\text{-}4)$$

that is, through $2\tau/m = 18/3 = 6$ slots. In turn, phase C will be displaced through the same angle from phase B.

If the coils of a phase are divided into a identical parallel paths (circuits) within each of which they are connected in series, then each parallel path will carry a current equal to I/a.

Referring to Fig. 22-3, it is seen that the currents in both the top and bottom conductors of a phase set up patterns repeated every four poles, that is with a period $p = 2$, so that in a short-pitched winding the currents in the bottom layer are replicas of the currents in the top layer, displaced by $\tau - y = 9 - 7 = 2$ slots clockwise. If the winding were full-pitched ($y = \tau$), the layers would not be displaced from each other, the currents in the top and bottom conductors in all the slots would be in the same direction and the conductors of a given phase would take up q slots per phase.

In short-pitched (chorded) windings (see Fig. 22-3), the phase conductors are laid out in $q + (\tau - y) = 3 + 9 - 7 = 5$ slots per pole. Chording results in an expanded belt occupied by the phase conductors within each pole pitch and, as will be explained in Sec. 24-5, makes the air gap field more sinusoidal.

22-3 Connection of Coils in a Lap Winding. The Number of Paths and Turns per Phase

As already noted, the coils of a winding may be lap-wound or wave-wound. In a lap winding, each of the q coils within a given pole pitch is connected to the next adjacent coil in

series aiding to form a coil group. For example, connecting the finish of coil *1* to the start of coil *2*, and the finish of coil *2* to the start of coil *3* (Fig. 22-5) produces a phase *A*

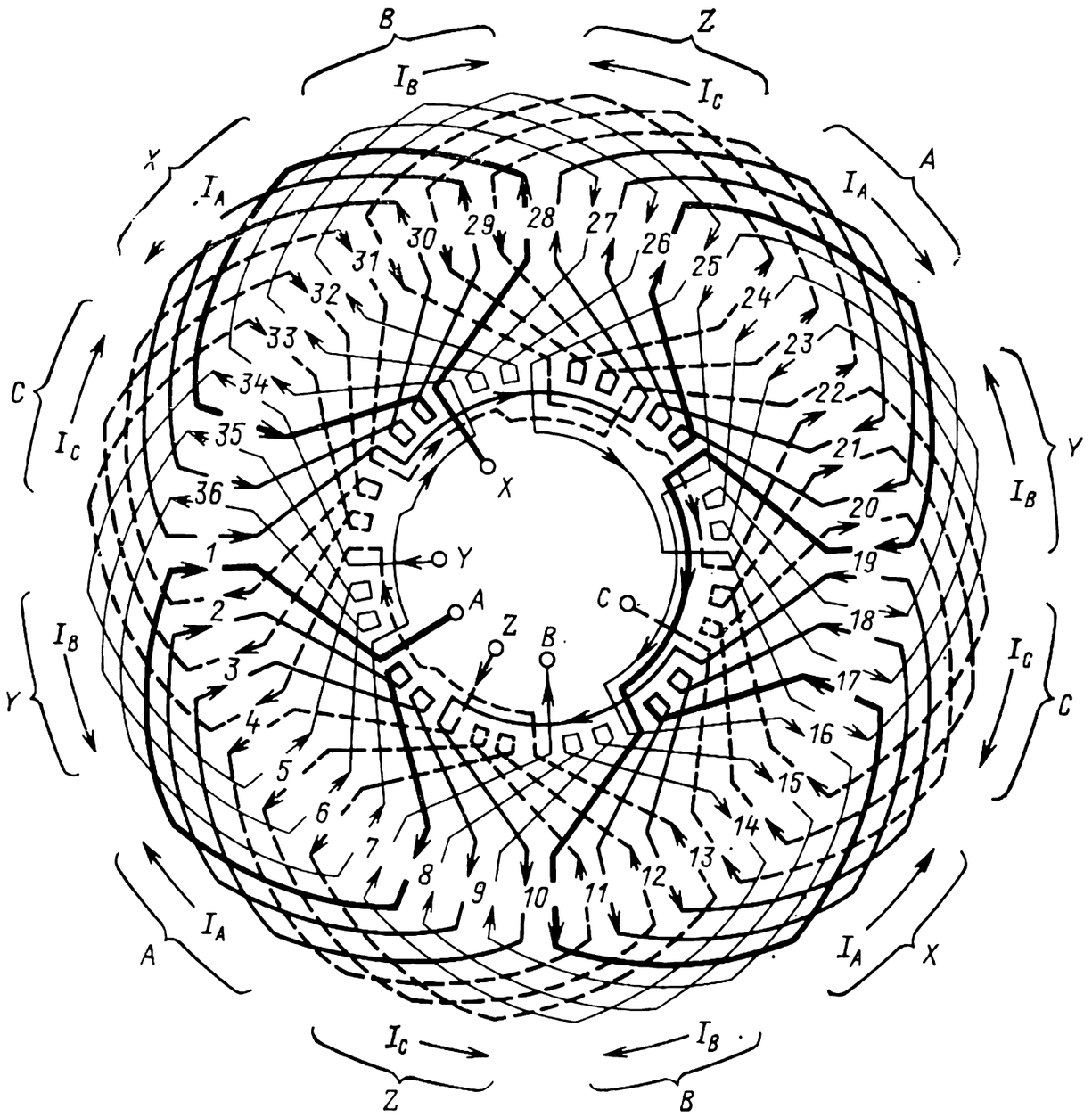

Fig. 22-5 Coil connection in a lap winding ($Z = 36$, $p = 2$, $m = 3$, $q = 3$, $\tau = 9$, $y = 7$, $a = 1$)

coil group consisting of coils *1*, *2* and *3*. The other coil groups in phase *A*, (*10*, *11*, *12*), (*19*, *20*, *21*), and (*28*, *29*, *30*), are formed in a similar manner.

The start of a coil group is the start of the lowest-numbered coil, and the finish of this coil group is the finish of the highest-numbered coil. For example, the starts of the coil groups listed just above are the starts of coils *1*, *10*, *19*, and *28*, whereas the finishes of the coil groups are the finishes of coils *3*, *12*, *21*, and *30*.

The term "lap" refers to the fact that, in going around from the start of a coil group towards its finish, the previous coil overlaps, as it were, the next adjacent one (see Fig. 22-5). The leads of the coils in a lap winding provided for connection to the next adjacent coils are shown in Fig. 22-4. In the simplest case, when there is only one path (or circuit) per phase ($a = 1$), the coil groups in a lap winding are connected in series. This arrangement is shown in Fig. 22-5. For this winding, the numbers of coils, phases and pole pairs have been chosen the same as for the winding in Fig. 22-3. For better presentation, the top coil sides are shown displaced counter-clockwise from the bottom coil sides laid in the same slots. (The coil No. is the same as that of the slot where the top side is laid.)

For proper periodic variations in the currents carried by the coil sides of the phase, coil group (*1*, *2*, *3*), bearing the index *A*, is connected in series opposition with coil group (*10*, *11*, *12*), bearing the index *X*. The finish of group *A* is connected to the finish of group *X*. The start of group (*10*, *11*, *12*), bearing the index *X*, is connected to the start of group (*19*, *20*, *21*) bearing the index *A*, and so on.

If the positive directions of currents in the coils are chosen in advance (see Fig. 22-3), it is an easy matter to establish the sequence of connection for the coils.

In the other phases, the coils are interconnected in the same manner as in phase *A*.

The coil groups in the lap winding of Fig. 22-5 can be interconnected in a simpler way. Referring to Fig. 22-6, the coil groups are shown as sectors spanning an angle $\gamma_p/2m$ subtended by the top coil sides. The numbering of the coil groups is given within the sectors. Each group has two leads. The start of a coil group is the lead of the lowest-numbered coil in the group.

When $a = 1$, the coil groups in Fig. 22-6*a* are connected in the same manner as in Fig. 22-5. The arrangement in Fig. 22-6*b* differs in that the same coil groups within each phase form the largest possible number of paths, $a = 2p = 4$. Each path in a phase is formed only by one coil group. The positive directions of current in the coil groups are indicated by arrows at the currents I_A/a, I_B/a, and I_C/a (pointing away from the finish towards the start of the forward groups *A*, *B* and *C*, and from the start towards the finish in the backward groups *X*, *Y*, and *Z*).

To obtain the desired positive directions for the coil currents the starts of groups A, B, and C must be connected to the starts of the respective phases (A, B, and C), their finishes to the finishes of phases X, Y, and Z, respectively.

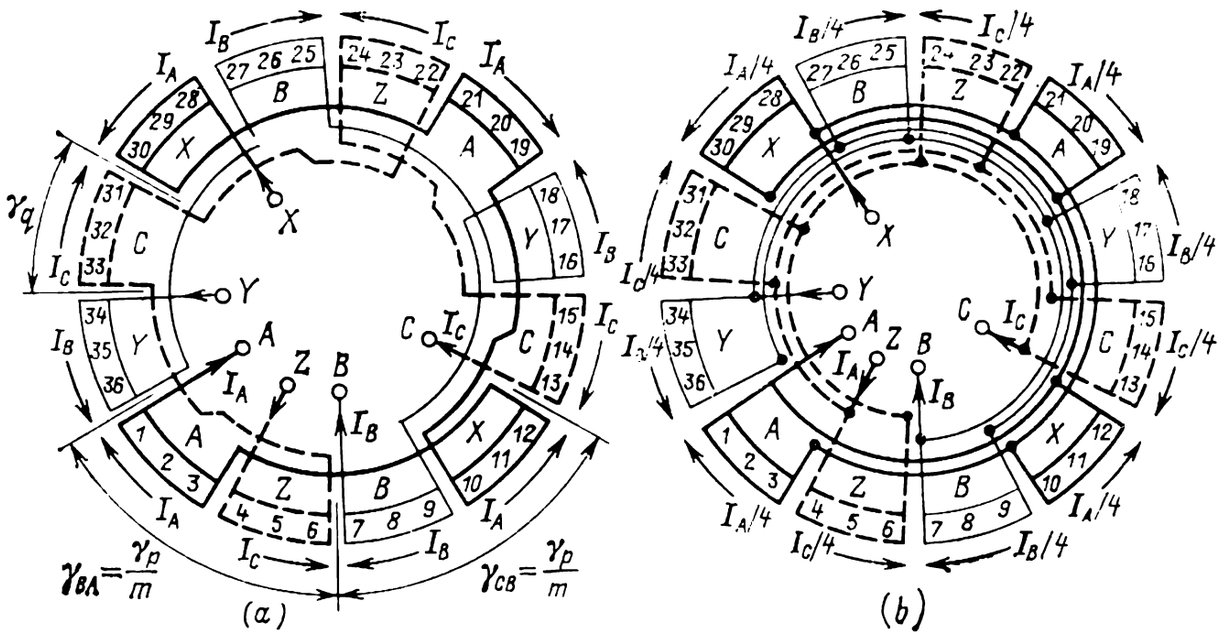

Fig. 22-6 Coil group connection in the lap winding of Fig. 22-3 for various numbers of paths: (*a*) for $a = 1$, (*b*) for $a = 2p = 4$

Conversely, the starts of groups X, Y and Z must be connected to the finishes of the respective phases, X, Y and Z, whereas the finishes of these groups to the starts of phases A, B and C.

There is also a way of connecting the coils in a winding where a ranges between $2p$ and unity. Now, the coils are connected in series-parallel. For example, in the arrangement of Fig. 22-3, with $a = 2$, each path will contain two coil groups. Generally, the number of coil groups per path is $2p/a$. This number must always be an integer. For the current to be equally shared among the paths, the latter must be completely identical (that is, present the same resistance and inductive reactance). This requirement is satisfied, if the paths are assembled from the same number of properly interconnected coil groups and have the same number of series-connected turns

$$w = (2p/a)\, qw_c \qquad (22\text{-}5)$$

where w_c = number of turns per coil
qw_c = number of turns per coil group
$2p/a$ = number of series-connected coil groups per path.

22-4 Coil Connection in the Wave Winding

The distribution of coils among the phases and the choice of positive directions for the currents in the coils are independent of whether the coils are connected in a lap or in a wave winding. Therefore, with given Z, p, y, and m, the coil structure (say, the one shown in Fig. 22-3) is equally

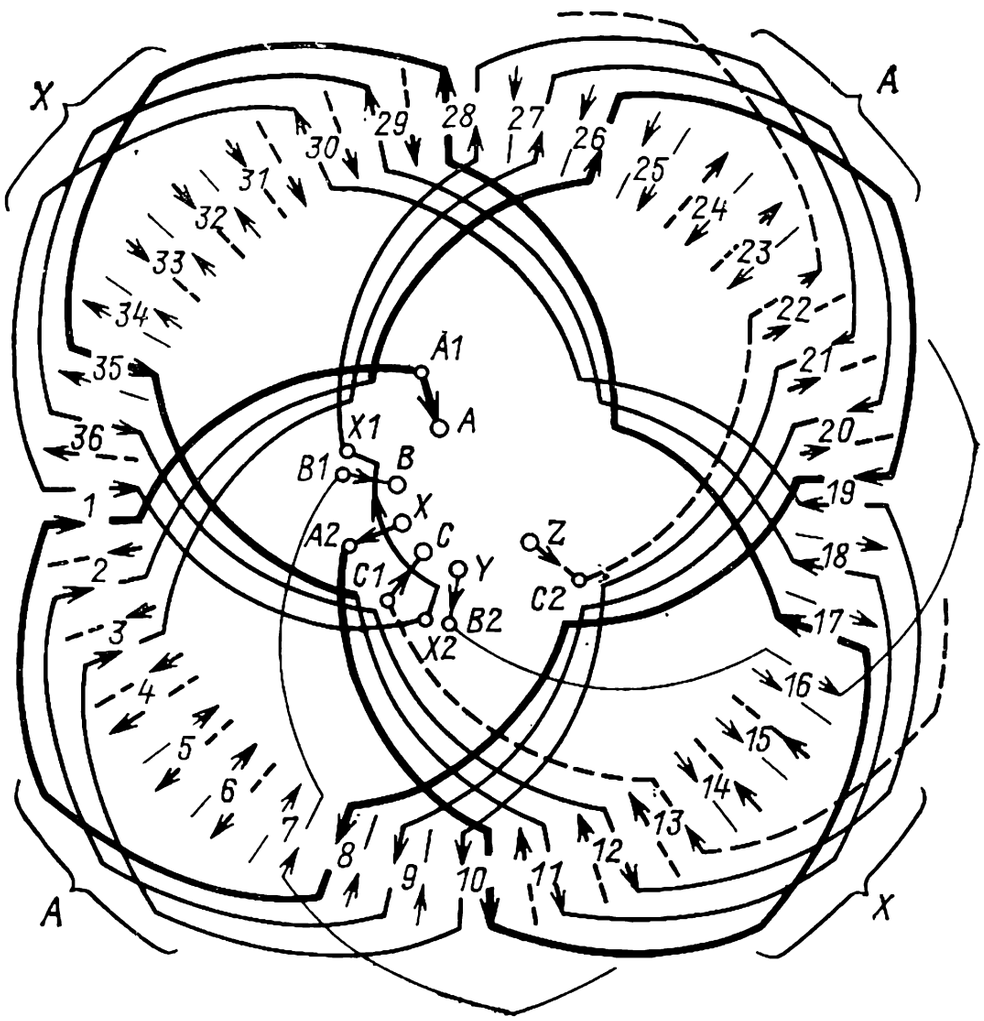

Fig. 22-7 Coil connection in a wave winding ($Z = 36$, $p = 2$, $m = 3$, $q = 3$, $\tau = 9$, $y = 7$)

applicable to both a lap and a wave winding. In a wave winding, however, the phase coils are interconnected differently. Here, the winding progresses around the core by passing successively under each pole before again approaching the starting point as shown in Fig. 22-7.

The coils in Fig. 22-7 differ from those in a lap winding only in the shape of the leads. The diagram shows all the connections between the coils of phase A. In forming this phase, let us start at coil *1*. During the first tour, the finish of coil *1* is connected to the start of coil *19* which is

displaced from coil *1* by $2\tau = 2 \times 9 = 18$ slots or an angle $\gamma_p = 2\pi/p = 180°$. One complete passage round the core will encompass p coils. Thus, within one tour, a given phase contains p coils connected series-aiding. In our case, one tour encompases two coils.

The first tour or wave must be followed by the second, third, etc., to give a total of q waves in the same direction. For the winding not to close upon itself at the end of the passage, the spacing between the last coil in a previous wave (say, coil *19* in the first wave) and the first coil of the next wave (say, coil *2* of the second wave) must be $2\tau + 1$, rather than 2τ. For the arrangement in Fig. 22-7, this spacing is

$$2\tau + 1 = 2 \times 9 + 1 = 19$$

On completing q waves, we shall have obtained the first part of the winding, *A1* — *X1*, containing in our example $q = 3$ waves (the first wave consists of coils *1* and *19*, the second of coils *2* and *20*, and the third of coils *3* and *21*).

The second part of the winding is formed in a similar manner, starting at coil *10* which is displaced from coil *1* by $\tau = 9$ slots or on angle $\gamma_p/2 = 90°$. The start *A2* of the second part of the winding will be the start of coil *10*, and its finish *X2* will be that of coil *30*.

The two parts of the winding are perfectly identical, because they have the same number of coils connected in series aiding (each part contains pq coils). Therefore, they may be connected not only in series, but in parallel as well. When connected in series, they form a winding with one path (or circuit) per phase ($a = 1$). When connected in parallel, they form a winding with two paths ($a = 2$).

When $a = 1$ (see Fig. 22-7), for the currents to flow in the chosen positive directions, the two parts of the winding must be connected in opposition, that is, the finish *X1* of the first part must be connected to the finish *X2* of the second part by a jumper. The start *A1* of the first part is the phase start *A*, and the start *A2* of the second part is the phase finish *X*.

When $a = 2$, the two parts are connected in parallel. The phase start *A* is connected to the start *A1* of the first part and the finish *X2* of the second part; the phase finish *X* is connected to the finish *X1* of the first part and the start *A2* of the second part.

The other two phases (Fig. 22-7 shows only the first and last coils) are formed in a similar way. The number of turns per path is found, as before, from Eq. (22-5).

22-5 The Selection of a Winding Type and Winding Characteristics

If a lap winding and a wave winding have the same number of coils (wound with wires of the same cross-sectional area, with the same number of turns per coil w_c and with the same coil span y), the same number of phases m and the same number of paths (or circuits) a, and intended to generate a magnetic field with the same number of pole pairs p, they will be fully identical electromagnetically, because, given the same current, the phases set up identical magnetic fields. They only differ in the total length of wire required to make coils and coil connections. With a large number of turns per coil and a large number of slots per pole per phase, the effect of coil ends is insignificant, and the total length of wire is practically the same in either case. With a small number of slots per pole per phase, $q \approx 2$ or 3, a large number of pole pairs, and a small number of turns per coil, especially when $w_c = 1$, a wave winding is more attractive. Then the saving in conductor material may be as high as 5% to 10%. The larger figure applies to machines with a relative core length equal to $l/\tau \approx 1.5$, and the smaller figure to machines with a relative core length equal to about 3.0. With a small number of pole pairs (say, $p = 1$ or 2), where the length of jumpers between the two parts of a phase winding (*A1-X1* and *A2-X2*) is large in comparison with the total length of coil ends, the use of a wave winding offers no advantages.

Practically, a single-turn coil is made by soldering, brazing or welding together two halves, called *bars*.

Windings in which all the coil sides carry the same current

$$Iw_c/a \quad \text{the same}$$

are equal as regards the production of a magnetic field. At the same time, they may have a different number of turns per coil, w_c, and a different number of paths (or circuits) per phase, a. As an example, Fig. 22-8 shows the coil sides of three windings identical in terms of the magnetic field produced. (It is assumed that in all other respects these windings

do not differ from one another. Notably, they have the same number of slots, the same number of pole pairs, the same number of phases, the same coil span, and the same current density in the conductors.)

When the current per coil side is the same, the number of circuits and the number of turns are chosen to suit the reliability requirements and to simplify the manufacture. If

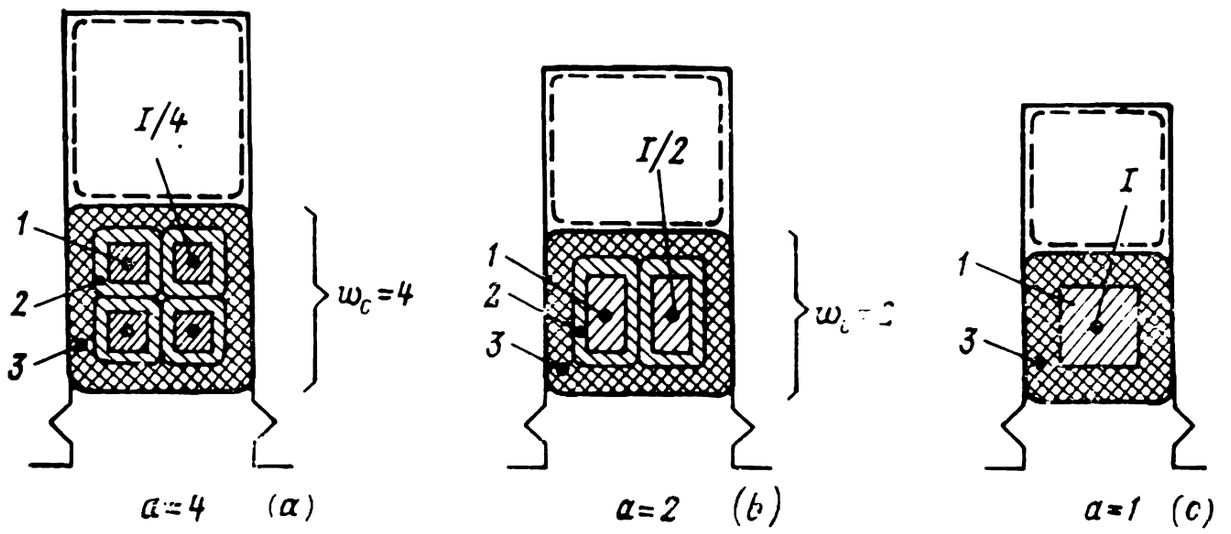

Fig. 22-8 Windings with the same current per coil side, Iw_c/a: *1*—active conductor carrying I/a; *2*—turn insulation between active conductors; *3*—ground insulation

the number of circuits can be chosen such that the resultant coil will be a single-turn one, $w_c = 1$, it is usual to pick the arrangement shown in Fig. 22-8*c*, because in a single-turn, two-layer coil (usually made of bars soldered, brazed or welded together), the ground insulation also doubles as the turn insulation. As a result, its manufacture requires a smaller quantity of insulating materials, and the coil takes up a smaller space in the slot, whereas the overall reliability is markedly improved. For a comparison of the quantity of insulation required, see Figs. 22-8*a* and *b*.

22-6 A Two-Pole Model of a Winding. Electrical Angles between Winding Elements

If we go round the periphery of a multipole, polyphase winding, we shall see that its structure is a repetition of some basic pattern and this repetition occurs in an angular distance equal to a pole pitch. For example, the pat-

tern that the winding in Fig. 22-3 has between slots *1* and *18* is fully repeated between slots *19* and *36* (in going counter-clockwise from pole to pole). In such a winding, the currents in the slots displaced from one another by a whole number k of pole pairs and numbered $N + 2\tau k$ are

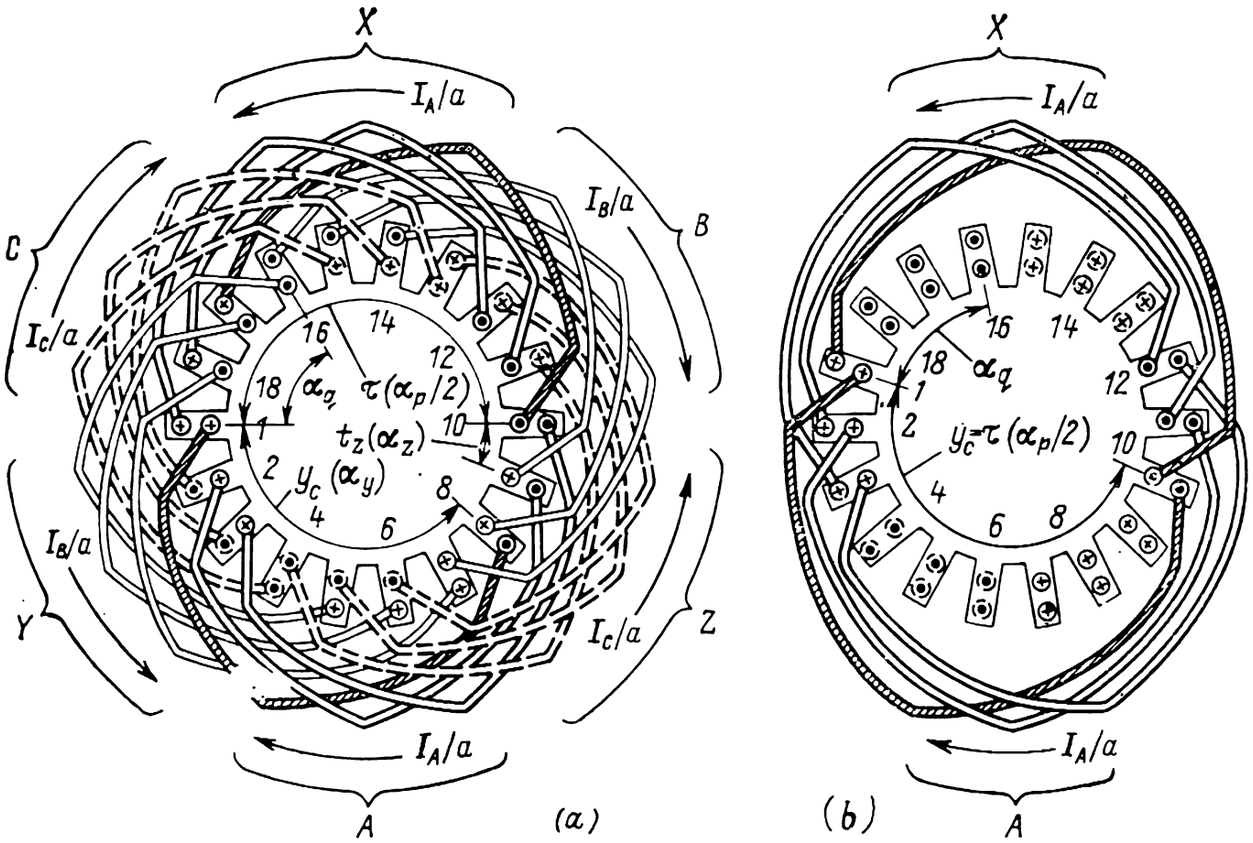

Fig. 22-9 Two-pole models of double-layer windings (*a*) for the winding in Fig. 22-3 ($\tau = 9$, $y = 7$, $q = 3$, $m = 3$); (*b*) for a winding with $\tau = y = 9$, $q = 3$, $m = 3$

always the same. For example, in slots $N = 6$ and $N + 2\tau k = 6 + 2 \times 9 \times 1 = 24$, the currents of phases *C* and *B* are of the same magnitude and flowing in the same direction.

To form a complete idea about the winding structure, it suffices to consider its pattern between any pair of adjacent poles. Consideration of its structure between other pairs of adjacent poles will add nothing new to our knowledge.

A two-pole model of a multipole winding is the winding of a two-pole machine having the same number m of phases, the same number q of poles per pole per phase, the same pole pitch τ, the same coil span y, and the same number of turns per coil, w_c.

A two-pole model of the winding in Fig. 22-3 appears in Fig. 22-9. It is an easy matter to see that it has the same

structure as the winding shown in Fig. 22-3 between any pair of adjacent poles. (The currents in slot N of the model are the same as the currents in slot $N + 2\tau k$ of the prototype winding, where $k = 0$ or 1, and $\tau = 9$.) The model equally applies to any pair of adjacent poles (that is, between slots *1* and *18*, or between slots *19* and *36*).

From a comparison of the prototype winding shown in Fig. 22-3, with its model shown in Fig. 22-9*a*, it can be seen that the angular period of the model, $\alpha_p = 2\pi$, is p times as great as that of the prototype winding given by

$$\gamma_p = 2\pi/p$$

Hence,

$$\alpha_p = p\gamma_p = 2\pi$$

The angles between the winding elements in the model increase by the same factor as compared with the corresponding angles in the prototype

$$\alpha = p\gamma \qquad (22\text{-}6)$$

where γ = angle between some elements of the prototype
α = angle between the same elements in the model.

In the theory of electrical machines, the angle γ between some elements in the prototype is referred to as the *mechanical angle**, whereas the angle $\alpha = p\gamma$ between the corresponding elements in the two-pole model is called the *electrical angle.*

The electrical angles between the characteristic elements of a winding (the angles in the model) determine the fundamental properties of the winding (irrespective of the number of pole pairs on it). The angular period of a $2p$-pole winding corresponds to an electrical angle

$$\alpha_p = 2\pi$$

The tooth (or slot) pitch in a model spans an angle

$$\alpha_Z = 2\pi/2mq = \pi/mq \qquad (22\text{-}7)$$

In a multipole winding, one tooth pitch spans an angle

$$\gamma_Z = 2\pi/Z = 2\pi/2pmq = \pi/pmq$$

---

* In this text, it is referred to simply as the angle.—*Translator's note.*

In the model, the phase belt occupied by the phase conductors (in one layer) within each pole pitch spans an angle

$$\alpha_q = q\alpha_Z = \pi/m \tag{22-8}$$

that is, $1/m$ part of a pole pitch. (In a multipole winding, this belt spans an angle $\gamma_q = q\gamma_Z = \pi/pm$.)

The coil in a model spans an angle

$$\alpha_y = (y_c/\tau)\pi \tag{22-9}$$

In a multipole winding, the coil spans an angle

$$\gamma_y = (y/\tau)\,(\gamma_p/2) = (y/\tau)\,(\pi/p)$$

The procedure for developing a two-pole winding model does not differ from that set forth above for a multipole winding. As an example, Fig. 22-9*b* shows a model winding which differs from that in Fig. 22-3 only in having a full pitch, that is, $y = \tau$. As is seen, when $y = \tau$, the top and bottom layers of the winding are not displaced from each other, so that all the phase conductors within a given pole pitch are only laid in q slots (in our case, $q = 3$). Compare this with Fig. 22-9*a*, where $y = 7$, $\tau = 9$, and the phase conductors within a pole pitch are laid in $q + (\tau - y) = 3 + 9 - 7 = 5$ slots.

22-7 Two-Layer, Fractional-Slot Windings

The two-layer windings examined above are *integral-slot windings*. This means that they have an integral number q of slots per pole per phase, and the number q of coils in each phase remains the same from pole pitch to pole pitch (in Figs. 22-3, 22-5, and 22-7, $q = 3$ coils in each phase). This is the most commonly used variety of two-layer winding. Another is what is called the *fractional-slot two-layer winding*. In such a winding, the poles of, say, the rotor are designed to occupy only a part (fraction) of the stator sector that bounds three slots (in the case of three-phase machines) of the stator winding, or less than one slot per phase per pole. That is why they are called fractional-slot windings. With a small number of slots per pole per phase ($q < 3$) and a large number of pole pairs, such windings offer a number of advantages over integral-slot windings.

To obtain a fractional-slot winding, it is necessary that there be one coil more in some phase coil groups than in others. Those with one coil more (the larger or major phase groups) will then have $(b + 1)$ coils each, and the others (the smaller or minor phase groups) will have b coils each.

Because of this, the winding does not repeat itself every pole pitch, but does so in a basic pole or coil pattern frequently called the repeatable (pole or coil) group. Denoting the number of major phase groups in one basic pattern as c and the number of major and minor phase groups (or poles) in one basic pattern as d, the number of slots per pole per phase for fractional-slot winding may be written

$$q = b + c/d$$

As a rule, use is made of fractional-slot windings with $b \geqslant 1$. In them, each phase has $2p$ coil groups (one group per pole). Of this number, the major groups will be under $n = 2p/(c/d)$ poles, and the minor groups under $(2p - n)$ poles. Then the number of slots per pole per phase for a fractional-slot winding may be written

$$q = \frac{n(b+1) + (2p-n)b}{2p} = b + c/d$$

As already noted, the denominator of the fraction is the number of pole pitches in one basic pattern. In a complete winding, there may be $2\,p/d$ such basic patterns. For a winding to be feasible, $2\,p/d$ must be an integer. A further requirements is that in a symmetrical polyphase winding the denominator should not be a multiple of the number of phases. Since the winding must produce a periodic field, it must have an even number of poles. Therefore, the repeatable group in a fractional-slot winding takes up d pole pitches when d is even and $2d$ pole pitches when d is odd.

When d is even, the winding has $2\,p/d$ basic patterns; when d is odd, it has $2p/2d$ basic patterns.

To sum up, a fractional-slot winding has "minor" phase groups of b coils each and "major" phase groups of $b + 1$ coils each. These groups alternate in a sequence which depends on the magnitude of the fractional part of the number q. The denominator is the number of all phase coil groups in which the sequence of major and minor groups is repeated. One sequence made up of d coil groups contains $d - c$

minor groups and c major groups. Each pole pitch corresponds to one phase group (with $q > 1$). In a three-phase winding the total number of phase groups is $6p$, so the sequence repeats itself 6 p/d times. When $b = 0$, the winding will consist solely of major groups, with one coil each.

The maximum number of circuits (paths) in a phase winding is $a_{max} = 2p/d$. The lowest possible number of circuits is such that $2p/ad$ is an integer.

A simple procedure to construct a fractional-slot, two-layer lap winding is as follows.

1. Determine the number of coils in a minor group, b, and in a major group, $b + 1$.

2. Write a series of c numbers: d/c, $2d/c$, $3d/c$, . . ., $cd/c = d$.

Replace each fractional number by the nearest integer number so as to obtain a series of c numbers: N_1, N_2, N_3, . . ., d. These are the Nos. of major coil groups arranged in the same sequence as the coil groups of all the phases are arranged around the core periphery for one repeatable group.

3. Assign numbers 1, 2, . . ., $N_1 - 1$ to the minor coil groups of b coils each. The next N_1th coil group, a major one, consists of $b + 1$ coils. In a similar way, form the other coil groups, assigning numbers N_2, N_3, . . ., d to major groups; the remaining groups will be minor ones. Follow the same sequence in forming the remaining $6p/d - 1$ repeatable groups (a three-phase winding is meant).

4. Distribute the coil groups among the phases. Each of the phases takes every third coil group.

Choose the positive directions of currents so that in adjacent coil groups (belonging to different phases) they are in opposite senses. Connect in series opposition the adjacent coil groups in each phase.

5. One path (or circuit) can be formed from d series-connected phase coil groups.

6. Once the coils of phase A have been connected (the phase start can conveniently be combined with that of the first coil group in the first repeatable group), the leads and connections between the paths in phases B and C may be chosen in any one of several ways, namely:

(i) all connections between the coil groups in phase B may be made similar to those in phase A, with a displacement equal to two coil groups. Then the connections in

phase C will repeat those in phase A, with a displacement equal to four coil groups;

(ii) all connections between the coil groups in phase B (C) are displaced from the connections in phase A by one basic pattern (that is, by d coil groups) if d is even, or by two basic patterns (that is, by $2d$ coil groups) if d is odd. In phase C (B), the connections should be displaced from those in phase B (C) again by as many coil groups.

In case (i), the phases are identical only as regards the production of the magnetic field; the sequence in which the minor and major coil groups are connected in the phases is different. In case (ii), the phases are nearly identical in regard to both the generation of the magnetic field and the sequence of coil groups. (Phase B can be formed by turning phase A through an appropriate angle.)

Example 22-1. Given: $Z = 42$, $2p = 8$, $m = 3$, $q = 1^3/_4$ ($b = 1$, $c = 3$, $d = 4$), $y = 4$, $a = 1$.

The number of coil groups in the basic pattern is

$$3d = 3 \times 4 = 12$$

The number of coil groups in the basic pattern per phase is $d = 4$.

Each minor group has $b = 1$ coil. Each major group has $b + 1 = 2$ coils.

The major coil groups in one basic pattern are numbered

$$d/c = 4/3 = 1^1/_3,\ 2d/c = 2^2/_3,\ 3d/c = 4$$

Rounding them off to the nearest integers, we get: 2, 3, 4.

The number of alternations in the entire winding is

$$6p/d = 6 \times 4 \div 4 = 6$$

The manner in which the coil groups are distributed along the core periphery is as follows (the numeral indicates the number of coils in a coil group; the vertical spaces separate the basic patterns):

1 2 2 2 1 2 2 2 1 2 2 2 1 2 2 2 1 2 2 2 1 2 2 2

$\underline{\underline{A}}$ $\underline{Z}$ B X $\underline{C}$ $\underline{Y}$ A Z $\underline{B}$ $\underline{X}$ C Y $\underline{\underline{A}}$ $\underline{Z}$ B X $\underline{\underline{C}}$ $\underline{Y}$ A Z $\underline{\underline{B}}$ $\underline{X}$ C Y

The letters A, B and C mark the forward coil groups, and the letters X, Y, and Z, the backward coil groups in the respec-

tive phases. The starts and finishes of the first basic phase patterns, labelled as advised in (ii) above, are underscored once; the starts and finishes of the second basic phase patterns are underscored twice (the start of a basic pattern

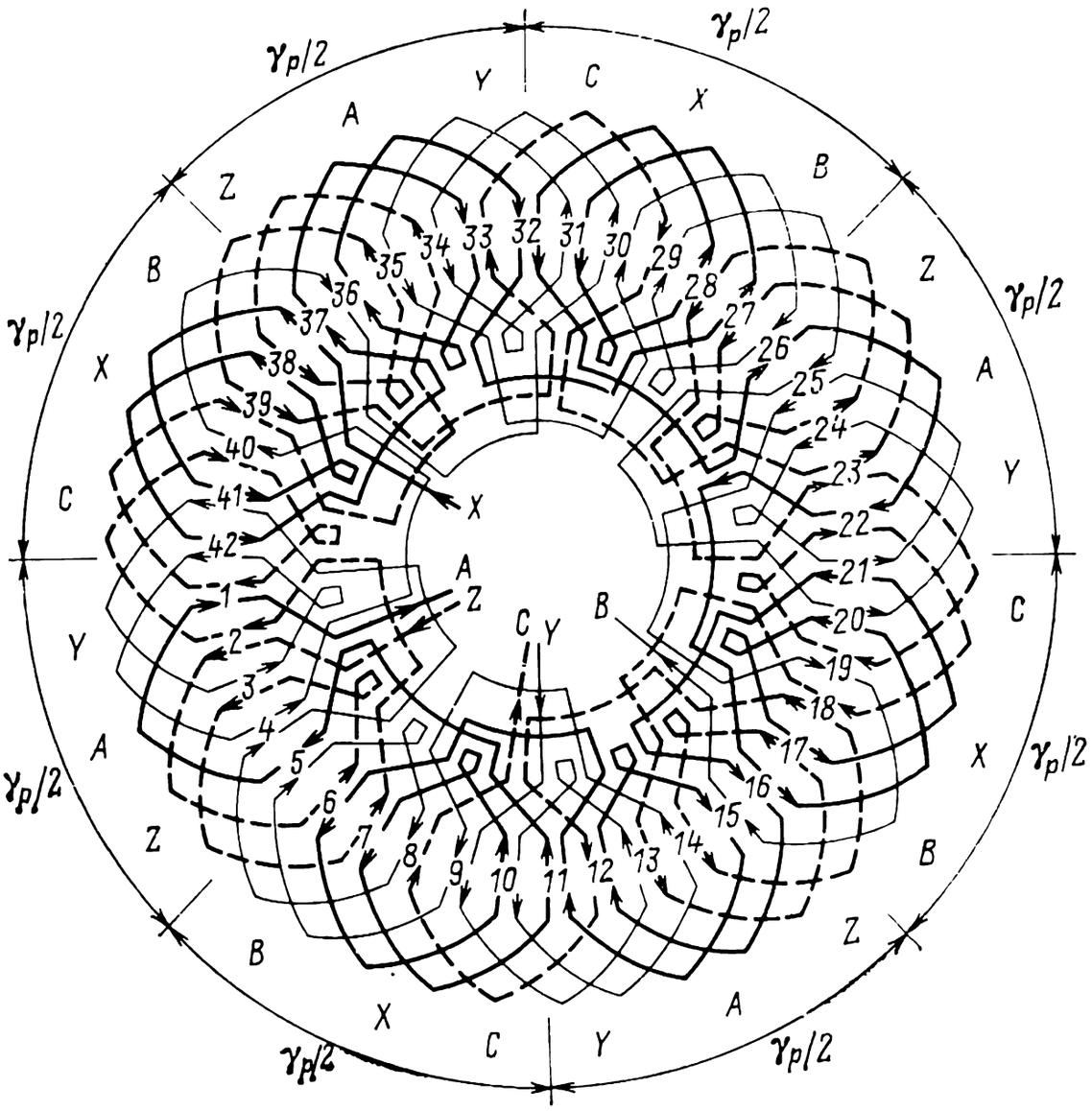

Fig. 22-10 Fractional-slot, double-layer lap winding ($Z = 42$, $p = 4$, $m = 3$, $y = 4$, $a = 1$, $q = 1\ ^3/_4$)

is the start of a forward coil group, and the finish of a basic pattern is the finish of a backward coil group).

Schematically, the resultant winding is shown in Fig. 22-10. As is seen, the pattern of the winding (and that of the field established by the currents) periodically repeats itself, its "period" being equal to the length of the basic pattern which spans $2p/k$ pole pitches or an angle $2\pi/k$, where k is the greatest common divisor for Z and p. In our example, $Z = 42$, $p = 4$, and $k = 2$. Therefore, the

repeatable group repeats itself every $2p/k = 2 \times 4/2 = 4$ pole pitches, $2p\tau/k = 2pmq/k = 2 \times 4 \times 3 \times 1^3/_4 \div 2 = 21$ slot pitches, or every $2\pi/k = 180°$. In Fig. 22-10, the pattern of currents and coils in the belt extending from slot *1* to slot *22* is fully repeated in the belt extending from slot *22* to slot *42*.

In a fractional-slot winding, the pattern of currents (and of the resultant field) is especially clearly seen to be recurring about every two pole pitches, 2τ, or in an angle equal to $\gamma_p = 2\pi/p$. For example, in phase *A* the groups of coil sides carrying currents flowing in alternate directions recur in about an angle $\gamma_p/2 = (2\pi/p)/2 = (2\pi/4)/2 = 45°$, as is shown in the figure. The group of coil sides carrying currents flowing in the same direction recur in the angle γ_p. As is seen, these groups do not contain an exactly same number of coil sides (three sides are laid in slots *41*, *42*, and *1*, three sides in slots *5*, *6*, and *7*, four sides in slots *10*, *11*, *12*, four sides in slots *15*, *16*, and *17*, etc. (In the general case, the number of sides is either $2(b + 1)$ or $2b + 1$.) Yet, the pattern of currents is periodic enough for the production of a magnetic field with the desired number of pole pairs p.

No two-pole model can be built for a fractional-slot winding. A model representing a complete cycle of change in the pattern must contain $2p' = 2p/k$ pole pitches, that is, as many as is occupied by the basic pattern.

22-8 Field Windings

The function of a field winding is to set up a heteropolar exciting magnetic field. It is a single-phase, heteropolar winding energized by direct current.

The two basic designs for this winding have been examined in Sec. 19-2. Figure 19-2*c* shows the arrangement of a concentrated field winding used on salient-pole cores. It is fabricated in the same manner as a single-phase, two-layer winding, but has only one coil per group, so that the number of coils per pole per phase is $q = 1$. Also, this is a full-pitch winding ($y_c = \tau$), and its coil sides are laid in slots next to each other, taking up a half slot width each (see Fig. 19-2*c*). The arrangement of a concentrated, two-layer field winding laid in slots *1* through *8* between poles is shown

in Fig. 22-11. The construction of a rotor carrying this type of winding is discussed in Sec. 51-3.

In a concentrated single-circuit field winding the number of series-connected turns is $w = 2pw_c$, where w_c is the number of turns per coil.

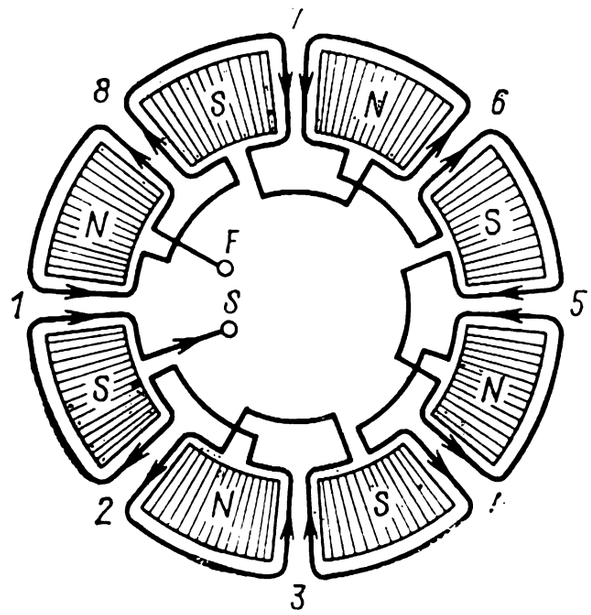

Fig. 22-11 Concentrated field winding ($p = 4$, $\tau = y$, $q = 2$)

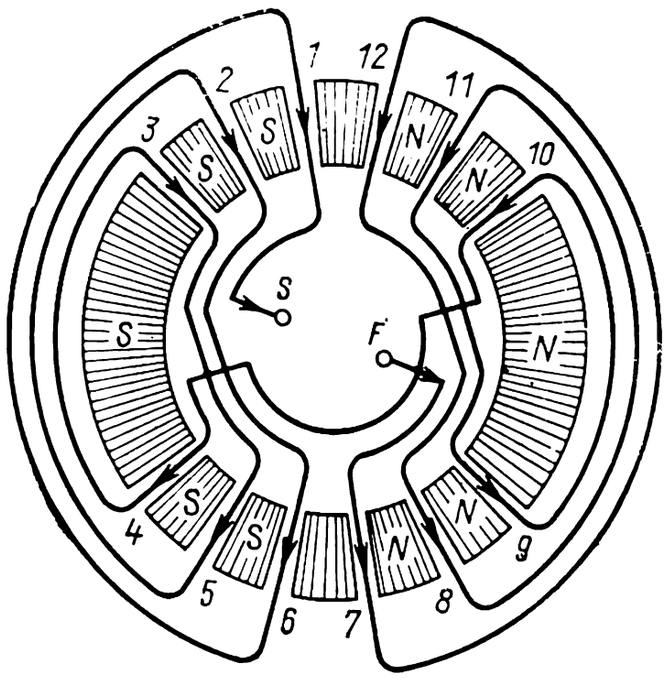

Fig. 22-12 Distributed single-layer field winding ($p = 1$, $q = 6$)

An alternate design of the field winding is shown in Fig. 19-2*d*. This is a distributed field winding, and it is used on round (cylindrical) cores. In contrast to a concentrated field winding which takes up only one slot within each pole pitch ($q = 1$), this winding is laid in $q > 1$ slots per

pole, and each slot receives only one coil side. Therefore, it may be treated as a single-layer winding.

As a rule, the winding has q slots per pole per phase. Accordingly, within each pole pitch there are $q/2$ concentrically arranged coils. As is seen from Fig. 22-12, the coils of a distributed field winding differ in pitch. For design purposes the coil pitch in such a winding is equal to the pole pitch, $y_c = \tau$. To make the magnetic field set up by the winding as nearly sinusoidal as practicable, the slots carrying conductors occupy 2/3 of a pole pitch. For example, the winding in Fig. 22-12 is laid out in 12 slots. The construction of the rotor carrying a distributed field winding is examined in Sec. 51-4.

In a single-circuit, single-layer distributed field winding, the number of series-connected turns is $w = pqw_c$, where w_c is the turns per coil.

23 Calculation of the Magnetic Field in an Electrical Machine

23-1 The Statement of the Problem

Energy conversion in an electrical machine operating by electromagnetic induction is based on its magnetic field. Therefore, the calculation of the magnetic field established by the currents flowing in the machine's windings is a major problem in the theory of electrical machines.

In the general case, the problem reduces to finding the magnetic induction (magnetic flux density) **B** from the specified density current **J** in the windings of the machine (Fig. 23-1), and it can be solved by the theory of the electromagnetic field.

The magnetic field strength (magnetic intensity) vector must satisfy Maxwell's first equation

$$\text{curl } \mathbf{H} = \mathbf{J} \tag{23-1}$$

the equation connecting the magnetic induction and the magnetic field strength

$$\mathbf{B} = \mu_a \mathbf{H} \tag{23-2}$$

where μ_a is the absolute permeability of the medium, and the continuity equation

$$\text{div } \mathbf{B} = 0 \qquad (23\text{-}3)$$

implying that the lines of magnetic flux are always closed.

In most cases, the current density vector **J** is uniformly distributed over the cross-sectional area Q of a conductor

$$J = I/Q$$

and points along the axis of the conductor in the direction where the current I is flowing (see Fig. 23-1).

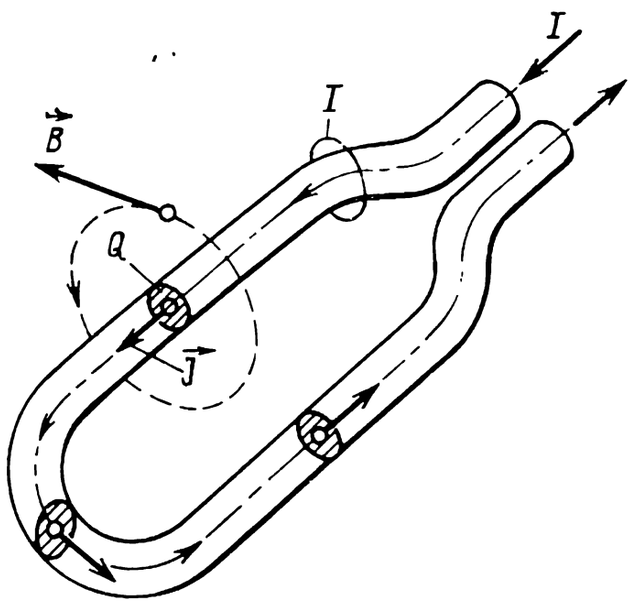

Fig. 23-1 Production of the magnetic field

Ordinarily, the winding conductors are laid in slots on the stator and rotor cores, and the magnetic field exists in a space taken up by the two cores, in the nonmagnetic gap separating them, and around the coil ends (or overhangs) (Fig. 23-2). In many cases, this field even threads the magnetic and conducting structural parts of the machine (the shaft, frame, end-shields, and so on).

To be able to calculate the magnetic field, the general field equations (23-1) through (23-3) should be extended to include the equations

$$f_{ik}(x, y, z) = 0 \qquad (23\text{-}4)$$

describing the surfaces separating the media i and k differing in relative permeability, $\mu_{r,i} \neq \mu_{r,k}$ (above all, the

equations describing the surfaces bounding the cores), and also boundary conditions for the tangential and normal components of the magnetic field vectors at the surfaces

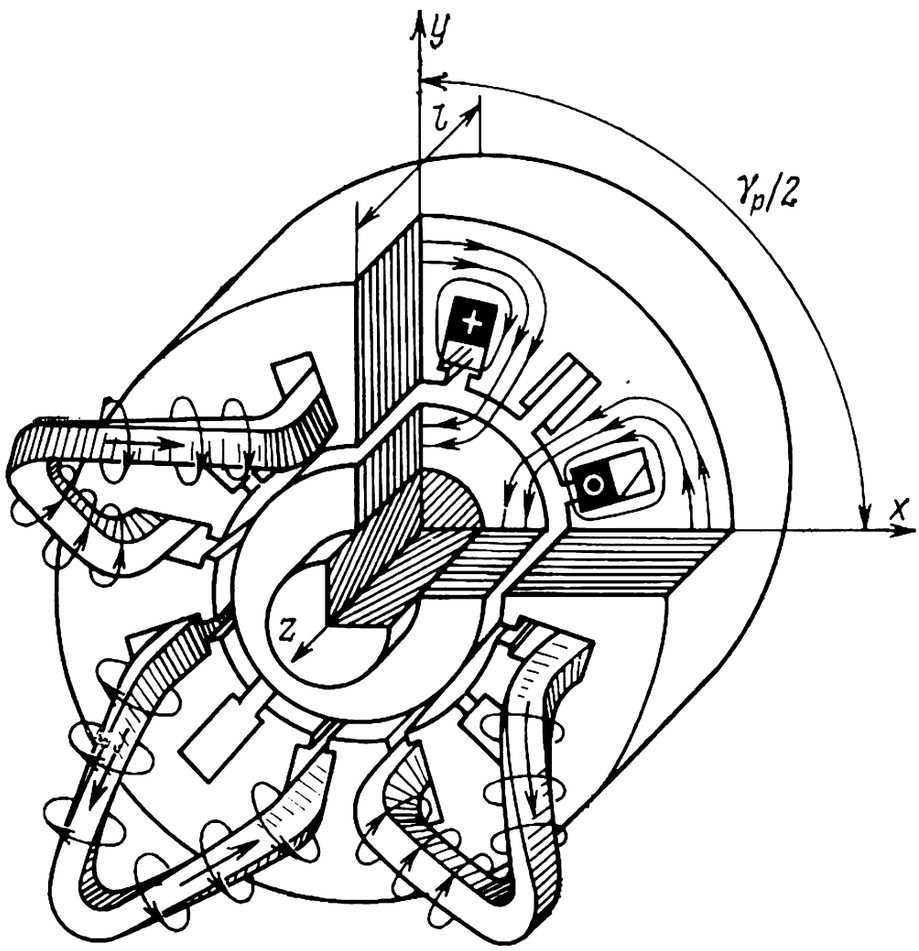

Fig. 23-2 Magnetic field set up by a basic coil set

separating the ith medium from the kth medium

$$H_{t,i} = H_{t,k} \tag{23-5}$$

$$B_{n,i} = \mu_{r,i} H_{n,i} = \mu_{r,k} H_{n,k} = B_{n,k}$$

where $H_{t,i}$, $H_{t,k}$ = tangential components of the magnetic field strength on the boundary

$B_{n,i}$, $B_{n,k}$ = normal components of the magnetic flux density at the same points on the boundary.

In cases where the permeability of the cores, $\mu_{r,c}$, cannot be deemed infinitely large in comparison with that of the areas taken up by air, insulating materials, and winding conductors, it is essential to take into account the nonlinear magnetic properties of the ferromagnetic materials, that is, the dependence of the relative permeability on the magne-

tic field strength

$$\mu_{r,c} = f(H) \tag{23-6}$$

Equations (23-1) through (23-6) uniquely describe the magnetic field in a machine, but they cannot in most cases be solved analytically by electromagnetic field theory. This is, above all, because the surfaces bounding the cores and current-carrying conductors are intricate in shape and also because one would have to consider the nonlinear magnetic properties of the ferromagnetic materials. Further difficulties arise because the relative position of the cores and current-carrying conductors is changing all the time, and the solution would have to be sought for all the likely positions.

23-2 Assumptions Made in Calculating the Magnetic Field

In the theory of electrical machines, several simplifying assumptions are made so that the magnetic field of a machine and the relevant winding characteristics could be determined analytically.

1. Because the current pattern in the windings repeats itself periodically (see Sec. 22-2), the field pattern is likewise repeated periodically every two poles. Therefore, in calculating the magnetic field of a machine, it will suffice to consider its variations over a pole-pitch angle γ_p or even over a half of the pole-pitch angle, $\gamma_p/2$. On an enlarged scale, Fig. 23-3 shows the magnetic field over a half of a pole pitch in the machine shown in Fig. 23-2.

2. It is assumed that the ferromagnetic cores have an infinitely large permeability, $\mu_{r,c}$, in comparison with that of free space. Because at a magnetic induction of 1.5 to 2.0 T the relative permeability of the core is several tens or hundreds, this assumption does not introduce any appreciable error in the calculation of the field. Also, one may allow for the finite value of $\mu_{a,c}$ and of the reluctance of the ferromagnetic parts of the magnetic circuit at a later stage, in practical calculations.

3. Once the assumption in (2) above is made, we may use the principle of superposition and treat the magnetic field of the machine as the sum of the fields set up by each of its windings. In turn, the field due to a winding may be treated

as the sum of the fields established by basic or repeatable coil sets*.

The term "basic coil set" refers to a set of $2p$ coils uniformly distributed all the way round the circle, displaced from one another by a half pole pitch, and interconnected so as to form a periodic current pattern with p pole-pairs.

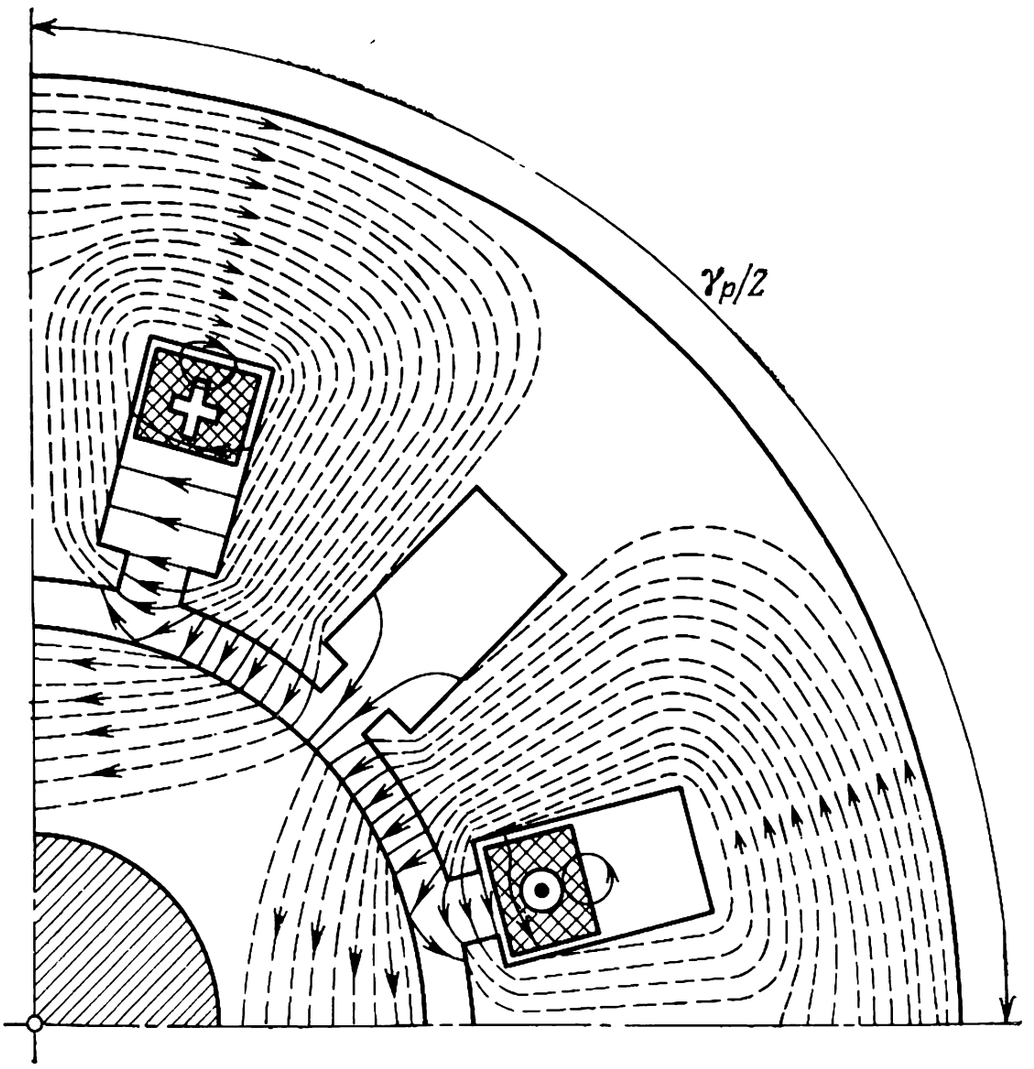

Fig. 23-3 Magnetic field from Fig. 23-2 shown enlarged within a pole pitch

In Figs. 22-3, 22-5, and 22-7, such a basic coil set is shown by heavy lines. In these figures, the top coil sides are laid in slots *1*, *10*, *19*, and *28*. Referring to these figures, it is an easy matter to see that any winding may be decomposed into a multiplicity of basic coil sets. A winding phase is formed by q basic coil sets displaced from one another in space by one tooth pitch. The entire winding has mq such basic coil sets.

---

* We consider only integral-slot windings (see Sec. 22-2).

To determine the total field, it will suffice to calculate the magnetic field due to one basic coil set carrying a unit current, $I = 1$, to find the fields of all the basic coil sets by scaling up the field due to a unit current, and to combine these fields subject to their relative position in space.

In this way, the problem of finding the magnetic field set up by the currents in all the windings of a machine reduces to calculating the magnetic field established by a basic coil set repeated periodically in the winding structure, assuming that the cores have a relative permeability of infinity.

23-3 The Spatial Pattern of the Magnetic Field Set Up by a Polyphase Winding

An idea about the spatial pattern of the magnetic field established by a polyphase winding can be gleaned from reference to the field established by the basic coil set (see Fig. 23-2). This is a four-pole field. Each two-pole interval contains one short-pitched coil. In moving through a half the pole-pitch angle, $\gamma_p/2$, the field pattern repeats itself, but with the signs reversed. Assuming that the permeability of the cores is infinitely large, the magnetic field within the cores need not be considered because its energy is zero (in Fig. 23-3 it is shown by dashed lines). In the nonmagnetic areas, the magnetic field may be decomposed into three components, namely:

(i) the field in the air gap
(ii) the field in the wound slots
(iii) the field around the coil ends (overhangs).

In machine design, the most important factor is the air gap field, that is, the field in the clearance between the cores. In terms of energy, this field exceeds the other flux by a wide margin, which is why we shall give it most of the treatment in our further discussion. In Fig. 23-3, the flux lines in the air gap are shown by solid and heavier lines. The distinctions of this field may be summed up as follows. Firstly, within the core length l its lines lie in planes at right angles to the z-axis, and the flux pattern repeats itself in each of these planes, so we may call it a *planar* (or two-dimensional) field. Secondly, all flux lines cross the air gap and determine the flux linkage and mutual inductance between the winding in question and the windings laid on the other core, for which reason we may call it a *mutual field.*

Thirdly, no distributed currents exist within the region taken up by this field, so in calculating it we may invoke the concept of a scalar magnetic potential (see Sec. 23-4).

On an enlarged scale, the field in a wound slot, that is, one enclosing current-carrying conductors, is shown in Fig. 23-4. Its lines link only with the conductors of the winding in question. They never cross the air gap, nor do they link with the windings laid on the other core. Such fields are called *leakage fields*. The region taken up by the slot leakage field is separated from that occupied by the mutual air-gap field by characteristic field lines *01* and *04* which pass through point *0* on the surface of the other core.

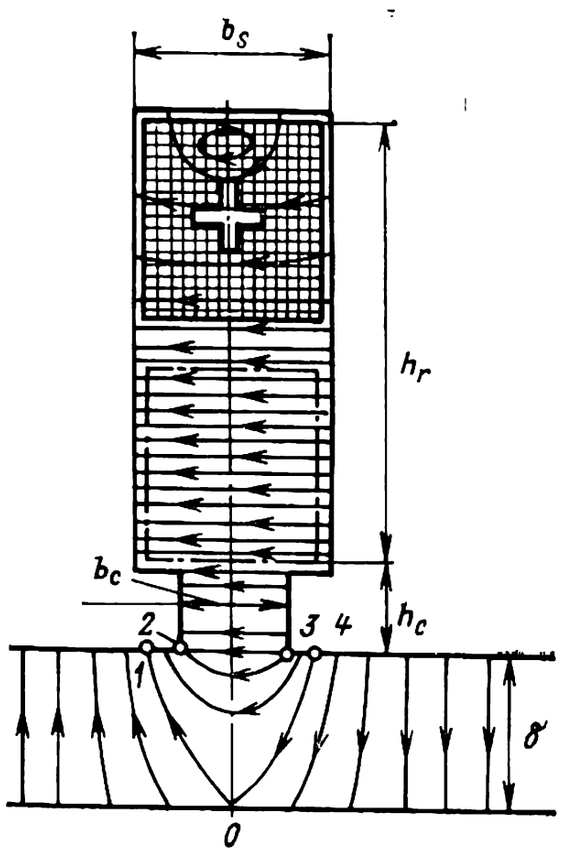

Fig. 23-4 Enlarged element of the magnetic field in Fig. 23-2, around a current-carrying slots

On a closer examination, the slot leakage field is seen to be the sum of a leakage field in the slot (that is, one existing inside the slot as far as line *23*), and a leakage field in the tooth, whose lines extend into the air gap and exist within the region *012340*.

Within the core length, the slot leakage field is planar. Its pattern repeats itself at any section of the machine and its lines lie in the section planes. The slot leakage field is more difficult to calculate than the air gap field, because of the distributed current existing in the slot region. (The current density J within the cross-section of a coil may be taken constant and directed along the z-axis of the machine.) In the general case, the slot leakage field can be found, using a general description of a magnetostatic field [see Eqs. (23-1) through (23-5)]. Still, although the field calculation is materially simplified because the field is two-dimensional, an analytical solution can only be obtained for some particular cases (say, for rectangular or circular slots). Even then the analytical solution is too unwieldy, and

practical calculations for slots of any shape are based on the approximate solutions deduced by idealizing the field pattern. Such an approximate solution will be considered in connection with the slot leakage inductance (see Sec. 28-7).

The *coil-end* (*overhang*) *field* refers to that around the coil-end connections and outside the cores. Its lines are closed around the coil ends and form a complex spatial pattern. For the coil-end field to be determined accurately, one would have to use a complete description of the magnetostatic field such as set forth at the beginning of this section. The solution of the problem is complicated by the fact that the field is three-dimensional and the coil overhangs are very complex in shape. Also, the field may to some extent be affected by the ferromagnetic parts of the machine, such as the end shields, frame, shaft, etc. On the other hand, we are free to neglect the angular position of the rotor relative to the stator.

The coil-end field is very low in energy. Therefore, the accuracy in calculating the coil-end field and inductance (see Sec. 8-7) need not be very exacting. It is important to note that some lines of the coil-end field link with the coil ends of the windings on the other core and contribute to the mutual inductance between the windings. Therefore, the coil-end field proper refers only to a fraction of the total coil-end field. The contribution of the coil-end field to the mutual inductance between the windings on different cores is very small (in comparison with the effect produced by the mutual air-gap field) and may be safely ignored.

23-4 Calculation of the Mutual Magnetic Field for a Polyphase Winding

On the assumption made in Sec. 23-2, the mutual field of a polyphase winding is planar (two-dimensional), and its energy is concentrated in the air gap where distributed currents are non-existent. Its strength **H** may be expressed as the gradient of a scalar magnetic potential, $\varphi_m = \varphi$

$$\mathbf{H} = -\operatorname{grad} \varphi \tag{23-7}$$

On substituting Eq. (23-7) into Eqs. (23-2) and (23-3), we can readily obtain for the scalar magnetic potential a second-order partial differential equation, known as the Laplace

equation:

$$\nabla^2\varphi = \partial^2\varphi/\partial x^2 + \partial^2\varphi/\partial y^2 = 0 \qquad (23\text{-}8)$$

To determine φ at any point (x, y) in the air gap, we must solve Eq. (23-8) subject to the boundary conditions corresponding to the instantaneous currents in the winding phases and existing on the ferromagnetic surfaces. The boundary conditions are specified by giving the distribution of the potential φ on the surfaces. The determination of this distribution is a problem in its own right, and it can be solved unambiguously, if we know the winding circuit and the instantaneous currents in the phases. Obviously, the solution becomes progressively more difficult to obtain as the winding grows more complicated in arrangement. Therefore, it is advantageous to solve the problem first for the currents in one basic coil set, and then to find the potential distribution for a polyphase winding by adding together the potentials of all the basic coil sets.

With φ found by solving Eq. (23-8), the components of the air gap field are found by Eq. (23-7):

$$H_x = -\partial\varphi/\partial x, \quad H_y = -\partial\varphi/\partial y \qquad (23\text{-}9)$$

23-5 Effective Length of the Core

Figure 23-5 shows the machine of Fig. 23-2 cut lengthwise. One of the cores is divided into several packets of length l_1' each, separated by radial cooling ducts of width b_d. As is seen from the gap field pattern, the air gap field is nearly uniform and constant in the region taken up by the core packets (in fact, within the cross-section passed through this region the field may be regarded as planar); is somewhat weakened in the ducts, and gradually collapses on emerging from the core faces and on leaving the air gap.

All this has a well-defined effect on the distribution of the radial (normal) components of the air gap flux density, B. To simplify further calculations without mistreating energy conversion by the machine, we may replace the field varying along the length of the machine by a uniform field with a maximum flux density B_m in the packets. In doing so, we also assume that this uniform field exists over the design

or effective core length l_δ such that

$$\Phi = \int_{-\infty}^{+\infty} B \, dz = B_m l_\delta$$

Hence,

$$l_\delta = \frac{1}{B_m} \int_{-\infty}^{+\infty} B \, dz$$

It can be shown that

$$l_\delta = l - n_d b'_d + 2\delta \qquad (23\text{-}10)$$

where $b'_d = c_0 c_d \delta$
$c_d = (b_d/c_0\delta)/(5 + b_d/c_0\delta)$
$c_0 = 1$, if ducts are made in the stator (or rotor) only
$c_0 = 0.5$, if ducts are made in both the stator and rotor.

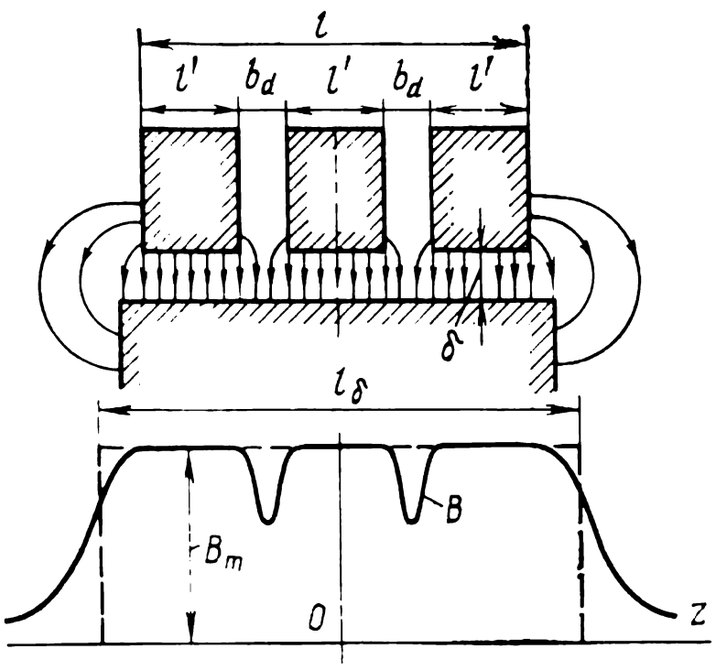

Fig. 23-5 Determining the design length of the core

Also, if the gap is very small ($\delta \ll b_d$), the design or effective width of a duct is $b'_d \approx b_d$. If the gap is very large ($\delta \gg b_d$), the design duct width is $b'_d \approx 0$.

It may be added that, as often as not, l_δ stands for the axial gap length.

24 The Mutual Magnetic Field of a Phase Winding and Its Elements

24-1 The Magnetic Field and MMF Due to a Basic Set of Currents

A basic set of currents periodically alternating in direction every two pole pitches, 2τ, is shown in Fig. 24-1. The currents iw_c and $-iw_c$ are carried in slots on core *C1*. A displacement through a pole pitch, τ, causes the direction of current flow in a slot to reverse. The excited core *C1* is separated

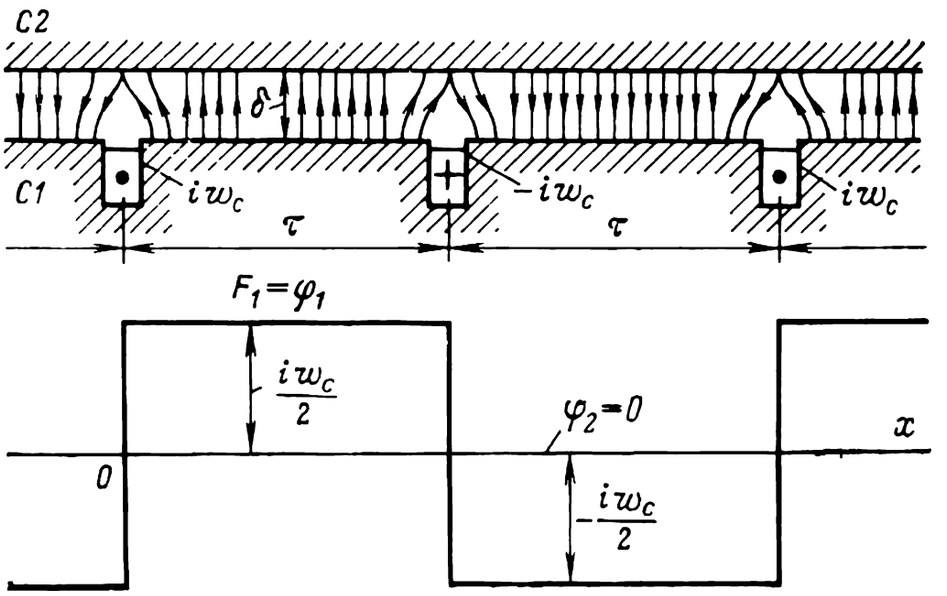

Fig. 24-1 Repeatable pattern of currents

from the unexcited core *C2* by an air gap of width δ. Because it is small in comparison with R, the mean radius of the air gap, we may neglect the effect of the curvature and replace the annular air gap by a "developed" or flattened-out gap (see Fig. 24-1). A reference point in the developed gap can conveniently be located by the distance x from the slot axis, which is connected to the angular coordinate of the point in the annular air gap, γ, by a simple relation

$$x = \gamma R$$

To simplify the analysis, it is advantageous to replace the distributed slot current, as shown in Fig. 24-1, say iw_c, by an equal linear current, $i_s = iw_c$, concentrated at the axis and near the bottom of the slot (Fig. 24-2).

The magnetic potential existing at the boundaries of the air gap, coinciding with the surfaces of the cores *C1* and *C2* can be found by applying Ampere's circuital law to the loop *1'-2'-2-1-1'* which is symmetrical about the slot axis:

$$\oint H_l \, dl = iw_c$$

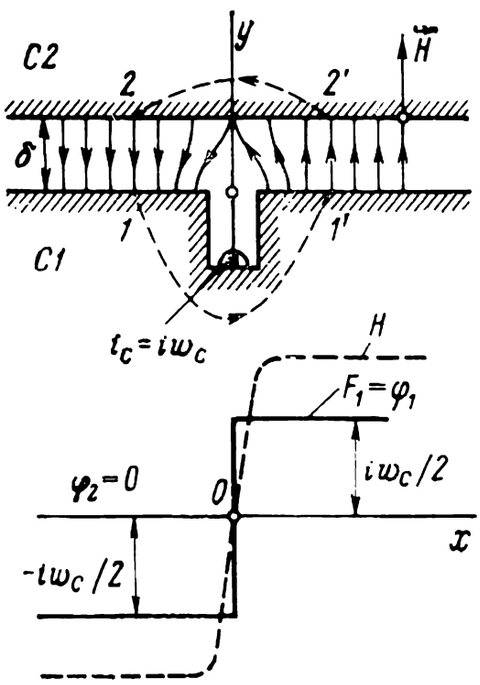

Fig. 24-2 Mutual field and mmf in and around a wound slot (see Fig. 24-1)

Assuming that the permeability of the core is infinite and the magnetic flux density B within the core is finite, we may write

$$H = B/\mu_a = 0$$

so that the magnetic potential experiences no drop within the cores

$$\int_{2}^{2'} H_l \, dl = \int_{1'}^{1} H_l dl = 0 \qquad (24\text{-}1)$$

Therefore, the circulation of the vector **H** may be written as the sum of variations in the air gap potential within portions 1'-2' and 2-1:

$$\oint H_l \, dl = \int_{1'}^{2'} H_l \, dl + \int_{2}^{1} H_l \, dl = \int_{1'2'21} H_l \, dl = iw_c \qquad (24\text{-}2)$$

If we recall that the magnetic field is symmetrical about the slot axis, so that

$$\int_{1'}^{2'} H_l \, dl = \int_{2}^{1} H_l \, dl = iw_c/2 \qquad (24\text{-}3)$$

and set equal to zero the magnetic potential of the unexcited core, $\varphi_2 = 0$, then the magnetic potential of the excited core to the right of the slot axis (with $x > 0$) will be

$$\varphi_1 = \varphi_2 + \int_{1'}^{2'} H_l \, dl = iw_c/2$$

and to the left of the slot axis (at $x < 0$),

$$\varphi_1 = \varphi_2 - \int_2^1 H_l \, dl = -iw_c/2 \qquad (24\text{-}4)$$

It follows from Eq. (24-4) that the potential of the excited core to the left of the slot axis differs from that to the right by the slot current, iw_c. (The current flowing outwards, that is towards the reader, is taken to be positive.)

The air gap field depends on the difference in magnetic potential produced between the surfaces of the two cores by the currents in the respective windings. In the theory of electrical machines, this difference in magnetic potential, equal to the linear integral of the air gap field intensity or the total air gap current, is usually called the *magnetomotive force*, or *mmf* for short.

Choosing as positive for the air gap field and mmf the direction away from the inner core, *C1*, towards the outer core, *C2*, we may define the mmf as

$$F = \varphi_1 - \varphi_2 \qquad (24\text{-}5)$$

In our case, *C1* is excited, *C2* is unexcited, and $\varphi_2 = 0$, so the mmf of *C1* is

$$F_1 = \varphi_1 - \varphi_2 = \varphi_1$$

If *C2* were ecxited and *C1* unexcited, and $\varphi_1 = 0$, the mmf of the excited core would be

$$F_2 = \varphi_1 - \varphi_2 = -\varphi_2$$

With the boundary conditions given by Eqs. (24-3) and (24-4), the magnetic potential in the air gap can be found by Eq. (23-8). If the potential distribution is known, the field intensity can be found by Eq. (23-9). At some distance from a slot, however, the magnetic field strength can be found in a simpler way. As follows from Fig. 24-1, the lines of the magnetic field are complex in shape only near a slot, whereas at some distance from the slot, $|x| > \delta$, the field becomes practically uniform; its lines run normal to the core surface, and its intensity is the same at all the points within the air gap.

Choosing the path of integration (*1'-2'* or *1-2*) to run along a field line (where the field is uniform) and noting that

$$H_l = H_y = H = \text{constant}$$

we get

$$F_1 = \varphi_{m1} - \varphi_{m2} = \int_1^2 H_l \, \mathrm{d}l = \int_0^\delta H_y \, \mathrm{d}_y = H\delta$$

The magnetic field strength in the gap is

$$H = F_1/\delta = F_1\lambda$$

where $\lambda = 1/\delta$ is the permeance of the air gap within a region containing a uniform magnetic field.

The magnetic flux density in the air gap is given by

$$B = \mu_0 H = \mu_0 F_1/\delta = \mu_0 F_1 \lambda \qquad (24\text{-}6)$$

In an electrical machine with a saturated core, the mmf is a sum of several components each of which balances the magnetic-potential difference within a certain portion of the magnetic circuit. These component mmfs are found by calculation.

24-2 The Effect of Core Saliency. The Carter Coefficient

Figure 24-3 shows the magnetic field set up by a basic periodically repeatable set of currents, iw_c and $-iw_c$, carried in some of the slots of core *C1*. The figure shows one slot carrying iw_c (a wound core) and several slots carrying no current (unwound cores). The slot width b_s is assumed to be comparable with the gap width δ. Then the field in the region of the unwound slots is markedly reduced, and its strength is substantially smaller than it is in the teeth.

The magnetic flux across the air gap can be expressed in terms of the normal component of the air gap field intensity, $H_n = H_y$. For example, the flux across the area bounded by tooth pitch *3-4* is

$$\Phi_{34} = \int_{A_{34}} \mu_0 H_n \, \mathrm{d}A = \int_3^4 \mu_0 H_y l_\delta \, \mathrm{d}x$$

where l_δ is the effective core (or axial gap) length.

In many cases, however, one need not know the exact distribution of the normal field component over each tooth pitch. Instead, one may limit oneself to the distribution of

the mean normal component, H_0, which is taken to be such that the magnetic flux across the area bounded by a tooth pitch (unwound) remains unaffected:

$$H_0 = \Phi_{34}/\mu_0 t_Z l_\delta = \int_3^4 H_y \, dx/t_Z \qquad (24\text{-}7)$$

A detailed study into the air gap field will show that when the toothed core *C1* is replaced by a smooth surface

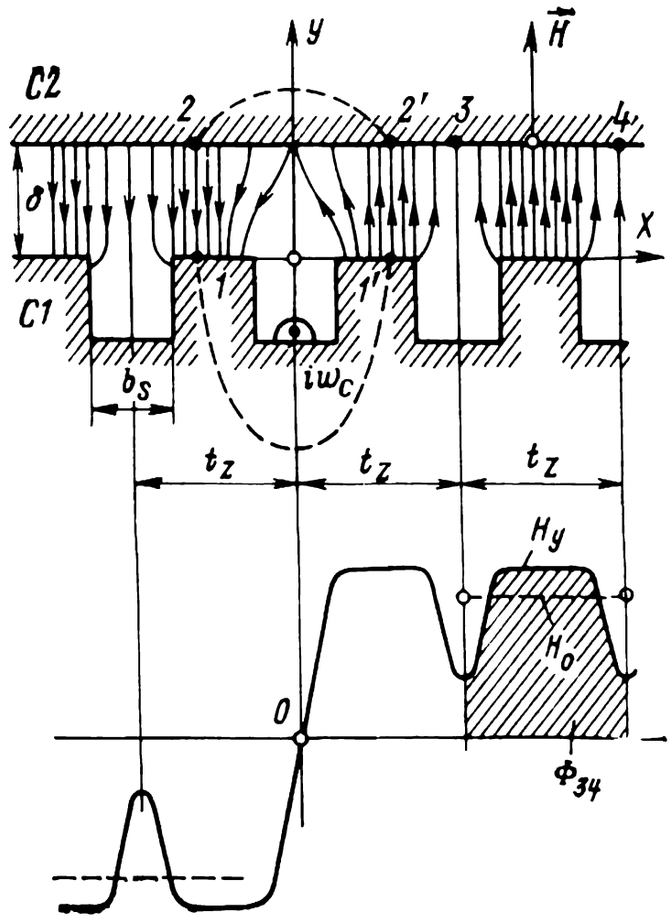

Fig. 24-3 The effect of core saliency on the magnetic field near an unwound slot

separated from *C2* by a distance $\delta_0 > \delta$, the mean normal component of the air gap field, H_0, will remain the same as it was with a toothed core, provided

$$\delta_0 = \delta k_\delta \qquad (24\text{-}8)$$

Here, k_δ is the *Carter coefficient*, named the *airgap factor* in the USSR. When the actual air gap δ is multiplied by k_δ, the product gives the effective gap width, δ_0. The air gap factor is given by

$$k_\delta = t_Z/(t_Z - c_s\delta) \qquad (24\text{-}9)$$

where

$$c_s = (b_s/\delta)^2/(5 + b_s/\delta)$$

In cases where both *C1* and *C2* are toothed, the effect of their teeth can be accounted for by applying the compound air gap factor

$$k_\delta = k_{\delta 1} k_{\delta 2} \tag{24-10}$$

where $k_{\delta 1}$ and $k_{\delta 2}$ are the air gap factors of *C1* and *C2*, respectively. Each is found by Eq. (24-9), assuming that the other core has a smooth surface:

$$k_{\delta 1} = t_{Z1}/(t_{Z1} - c_{s1}\delta)$$
$$c_{s1} = (b_{s1}/\delta)^2/(5 + b_{s1}/\delta)$$
$$k_{\delta 2} = t_{Z2}/(t_{Z2} - c_{s2}\delta)$$
$$c_{s2} = (b_{s2}/\delta)^2/(5 + b_{s2}/\delta)$$

24-3 The MMF Due to a Basic Coil Set

A basic coil set is the simplest repeatable element of a phase winding (see Sec. 23-2). Therefore, prior to determining the magnetic field of a phase, we should find the mmf due to a basic coil set carrying the phase path (circuit) current, i_a.

The instantaneous current in a phase path (circuit) is given by

$$i_a = i/a = \sqrt{2}\, I_a \cos(\omega t) \tag{24-11}$$

where i is the instantaneous phase current, I is the rms phase current, and $I_a = I/a$ is the rms path current.

The pattern of currents carried by the coils in a basic set is repeated every two poles. Therefore, it will suffice to consider the mmf and field due to this set over two pole pitches, as shown in Fig. 24-4. Each pole pitch is seen to contain one coil of the basic set. The instantaneous phase current is assumed to be flowing in the positive direction (that is, from its finish to its start). Its direction at the coil sections is shown in the figure.

The mmf due to a basic coil set can be visualized as the sum of the mmfs due to two periodically recurring sets of currents, namely F' due to the currents in the odd-numbered slots (*1*, *3*, *5*, etc.), and F'' due to the currents in the even-numbered slots (*2*, *4*, *6*, etc.). The mmfs due to periodically

recurring sets of currents have been defined in Sec. 24-1. Graphically, they are combined in Fig. 24-4. Inside a coil pitch, y_c,

$$F = F' + F'' = \pm i_a w_c$$

Between coils, $F = 0$.

On moving in the positive direction, the mmf at the slot axis is incremented by the slot current $i_a w_c$ if the current is

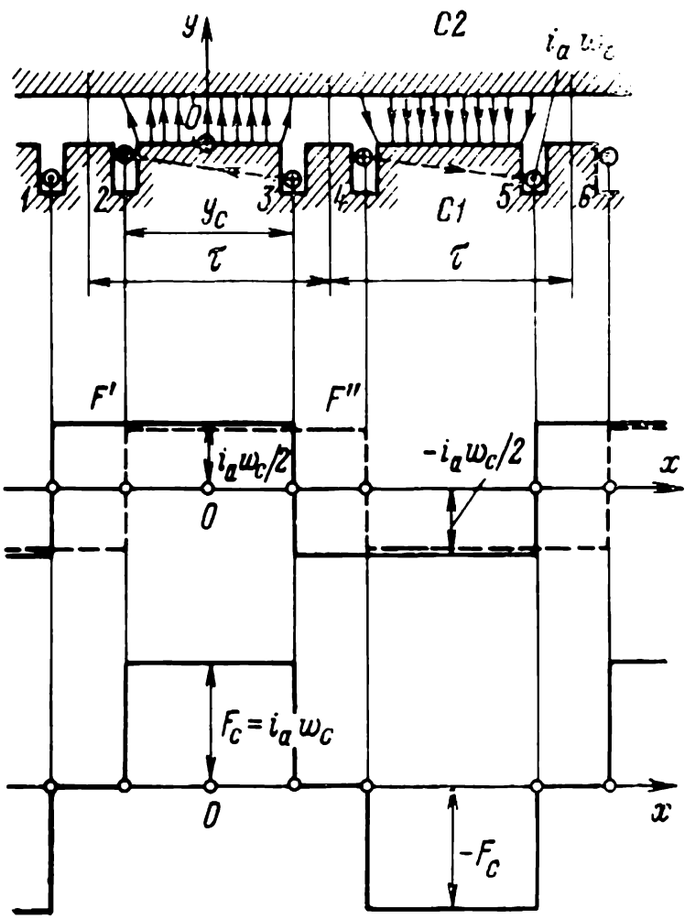

Fig. 24-4 MMF due to a basic coil set

flowing towards the reader, or decremented by the same amount if the current is flowing away from the reader. The mmf is thus seen to vary periodically with a period equal to two pole pitches, 2τ. Therefore, a displacement of 2τ leaves the mmf with its original sign

$$F(x \pm 2\tau) = F(x) \qquad (24\text{-}12)$$

whereas a displacement of τ causes it to change sign

$$F(x \pm \tau) = -F(x) \qquad (24\text{-}13)$$

Assuming that the positive direction for the field and the mmf is from the excited to the unexcited core and taking

as the origin the axis of the coil setting up a positive phase mmf when the current is flowing in the positive direction, we may write the following equation for the mmf over one pole pitch:

$$F = \begin{cases} F_c = i_a w_c = F_{cm} \cos \omega t & \text{for } -y_c/2 < x < y_c/2 \\ 0 \quad \text{for } -\tau/2 < x < -y_c/2 \text{ and} \\ \quad \text{for } \tau/2 > x > y_c/2 \end{cases} \tag{24-14}$$

where $F_{cm} = \sqrt{2} I_a w_c$ is the peak mmf due to the basic coil set.

Thus, when the basic coil set is carrying a sinusoidally varying current i_a, the resultant mmf is a wave stationary

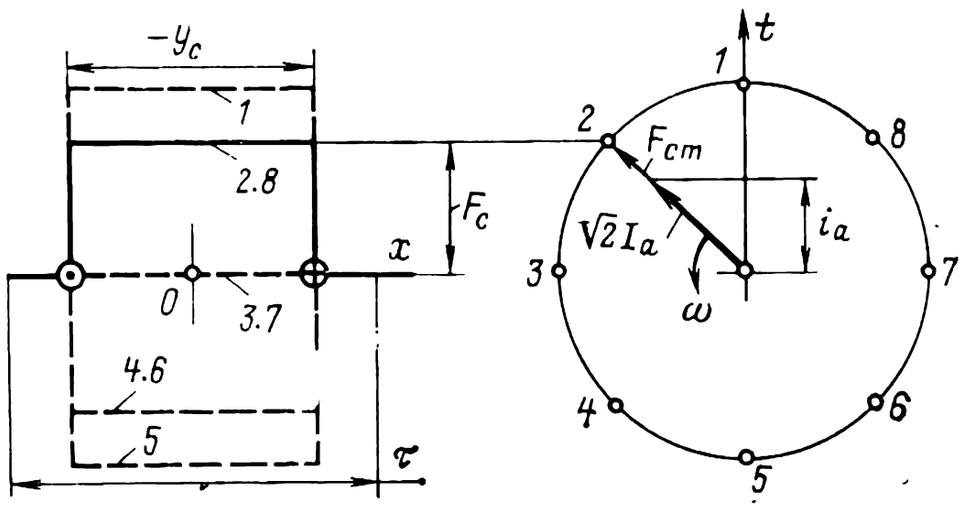

Fig. 24-5 Breathing mmf waveform

in space and pulsating at an angular frequency $\omega = 2\pi f$. The position of the wave in space depends on the arrangement of the coils, and the magnitude of the mmf is determined by the value of i_a.

Figure 24-5 shows the "breathing" mmf waveform during one cycle of change in the current. Equations (24-12) through (24-14) completely describe the mmf all the way round the periphery of the air gap having p pole pairs. For the machine of Fig. 22-3 in which $p = 2$, the distribution of the mmf along the periphery of the air gap is shown in Fig. 24-6*a*.

The position of an arbitrary point in the air gap can be specified by giving either the distance x from the origin along the periphery of the air gap, as indicated on the developed ("unfolded") view of the annular gap (see Fig. 24-4 and elsewhere), or the angle γ from the origin to the point

in question:

$$\gamma = x/R = x\pi/\tau p \qquad (24\text{-}15)$$

where $R = \tau p/\pi$ is the mean radius of the air gap circumference.

Because the mmf pattern is repeated every two poles, all that is necessary to know about the mutual field in a machine can be gleaned from its two-pole model. This model should retain the winding arrangement, as does the

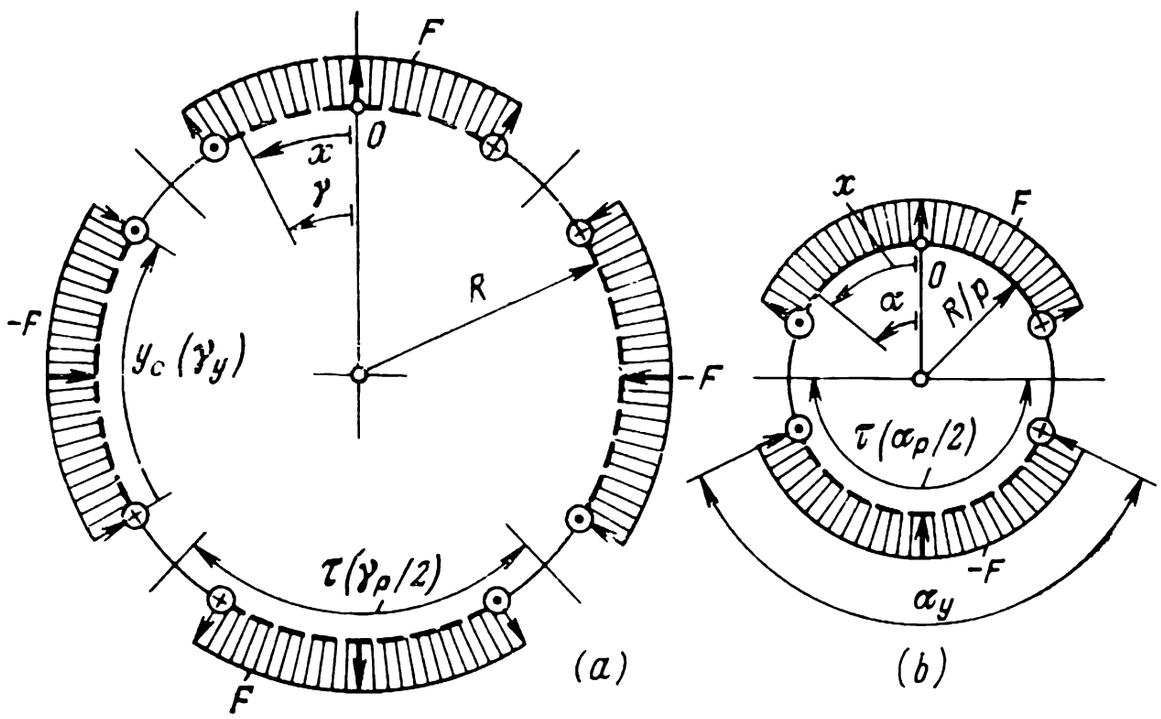

Fig. 24-6 Distribution of the mmf along the periphery of the air gap in (*a*) a $2p$-pole machine and (*b*) its two-pole model

two-pole model of the winding (see Sec. 22-6), the slot and tooth dimensions along the periphery of the air gap (b_s, t_z, τ, and y_c), and also the radial gap length δ and the effective axial gap length l_δ.

The length of the gap circumference in a two-pole model of the machine is 2τ. As compared with the length of the air gap circumference in the prototype machine, it is reduced by a factor of p. Therefore, the radius of the air gap in the model is likewise $1/p$ of that of the actual gap, that is, R/p. In the model, as in the prototype machine, a given point within a pole pitch takes up a position defined by the same distance x from the origin 0. The angle α specifying the position of the similar point in the model, called the *electrical angle*, is p times the mechanical angle in the prototype

machine. Since

$$x = \gamma R = \alpha R/p$$

and subject to Eq. (24-15), it follows that

$$\alpha = p\gamma = (x/\tau)\,\pi \qquad (24\text{-}16)$$

In going from a prototype machine to its model, the angles between any characteristic machine elements within a pole pitch are multiplied by the same factor:

$$\alpha_p = p\gamma_p = 2\pi$$

$$\alpha_y = p\gamma_y = y\pi/\tau$$

To sum up, the electrical angle α between any two machine elements within a pole pitch is thought of as the angle between the same elements in the two-pole model of the machine in which a cycle of change in the field is completed within an angle of 2π.

24-4 Expansion of the Periodic MMF due to a Basic Coil Set into a Fourier Series. The Pitch Factor

Let us expand the mmf due to a repeatable coil set into a Fourier series for $t = 0$, when the current in a parallel path is a positive maximum

$$i_a = \sqrt{2}\, I_a$$

Then the mmf in the coil region $(-y_c/2 < x < y_c/2)$ will be

$$F_{cm} = \sqrt{2}\, I_a w_c$$

The mmf waveform for $t = 0$ is shown in Fig. 24-7. As is seen, the mmf is an even function about the axis passing through the middle of the coil; therefore, the Fourier series will only consist of cosine terms. Also, during the next half-cycle of change the waveform repeats itself, but with its sign reversed. For this reason, the series can only contain odd harmonics [14]. Figure 24-7 shows the fundamental mmf of peak value F_{c1} which completes a half-cycle of change in a time equal to τ_1, and the νth harmonic mmf of peak value $F_{c\nu}$ which completes a half-cycle of change in a time equal to $\tau_\nu = \tau/\nu$.

The mmf can be represented as a sum of harmonic terms

$$F_{t=0} = \sum_{\nu=1}^{\infty} F_{c\nu m} \cos(\nu x/\tau)\,\pi \qquad (24\text{-}17)$$

where $\nu = 1 + 2c = 1, 3, 5, 7$, etc., and $c = 0, 1, 2, 3$, etc.

By comparing the arguments of the cosines with Eq. (24-16), it is seen that they are the electrical angles locating

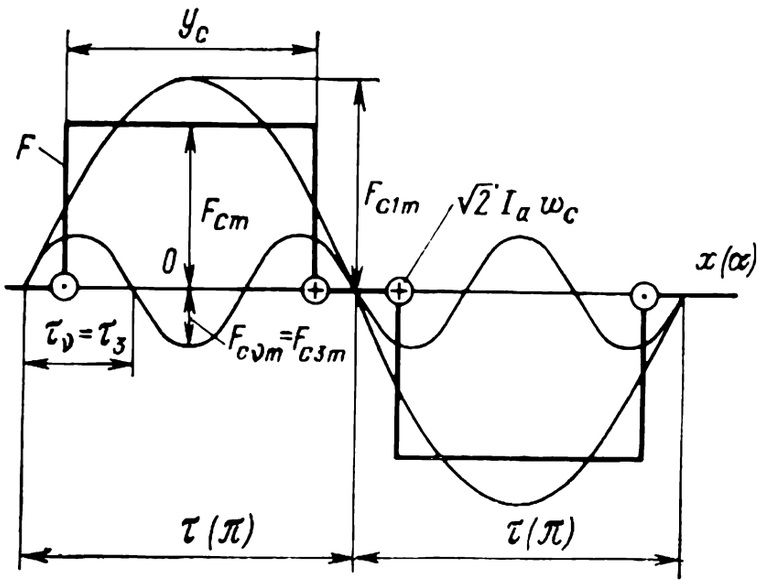

Fig. 24-7 Expansion of the mmf due to the basic coil set into a Fourier series ($t = 0$, $i_a = \sqrt{2}I_a$)

the position of the point x multiplied by ν

$$(\nu x/\tau)\,\pi = \nu\alpha = \alpha_\nu$$

In other words, the arguments of the cosines are equal to the electrical angles α_ν for the νth harmonic with a period taken equal to 2π:

$$(\nu x/\tau)\,\pi = (x/\tau_\nu)\,\pi = \alpha_\nu$$

Subject to the qualifications made as regards the mmf, the coefficients, or the amplitudes, of the various harmonics are given by

$$F_{c\nu m} = \frac{2}{\tau}\int_{-\tau/2}^{+\tau/2} F_{t=0}\cos(\nu x/\tau)\,\pi\,dx = \frac{4}{\pi\nu}F_{cm}k_{p\nu} \qquad (24\text{-}18)$$

where

$$F_{t=0} = F_{cm} \quad \text{for} \quad -y_c/2 < x < y_c/2$$
$$F_{t=0} = 0 \quad \text{for} \quad \tau/2 > |x| > y_c/2$$

Equation (24-18) contains what is known as the *pitch factor*, k_p, defined by

$$k_{pv} = \sin(v y_c \pi/2\tau) = \sin(v\alpha_y/2)$$

It characterizes the effect that the coil pitch y_c and the chording angle α_y have on the peak value of a harmonic mmf.

For the fundamental, that is, for $v = 1$,

$$k_{p1} = \sin(y_c \pi/2\tau) = \sin(\alpha_y/2) \leqslant 1 \qquad (24\text{-}20)$$

With a full pitch, that is, when $y_c = \tau$, the pitch factor for the fundamental is equal to unity

$$k_{p1} = k_p = 1$$

For the higher harmonics ($v > 1$), it may take values

$$k_{pv} = \sin(v\pi/2) = \pm 1 \qquad (24\text{-}21)$$

The sign of the pitch factor gives the sign of the harmonic mmf at the coil axis where $x = 0$ (in Fig. 24-7, k_{p1} and F_{c1m} are positive, whereas k_{p3} and F_{c3m} are negative).

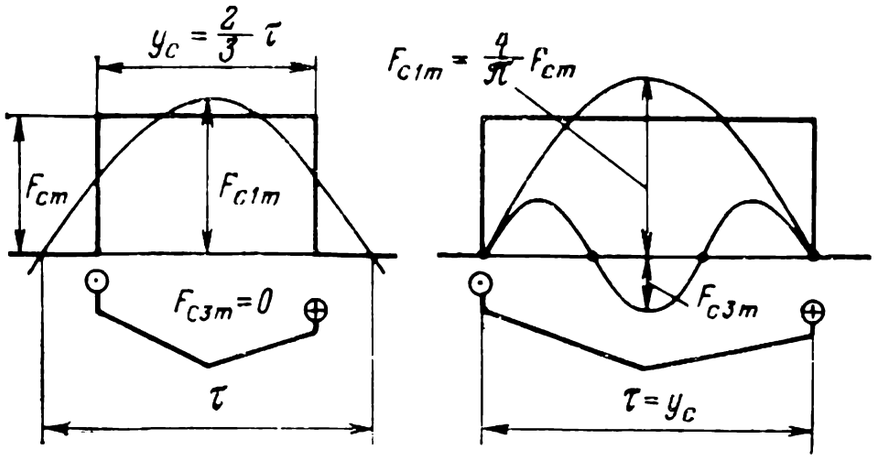

Fig. 24-8 The effect of pitch-shortening (chording) on the mmf harmonics

In the light of the foregoing, the pitch factor may be construed as the ratio of the peak value of a harmonic mmf in a given coil to the peak value of the same harmonic in the case of a full coil pitch, that is, when $y_c = \tau$.

It follows from Eq. (24-19) that the effect of the pitch factor on the mmf varies with the electrical angle spanned by the coil and the order (or number) of the harmonic. This effect is a maximum for the fundamental whose peak

value is

$$F_{c1m} = 4F_{cm}k_{p1}/\pi \qquad (24\text{-}22)$$

The higher harmonic mmfs have substantially lower peak values (their absolute values are meant)

$$|F_{c\nu m}|/|F_{c1m}| = |k_{p\nu}|/\nu|k_{p1}|$$

If we choose the coil pitch such that

$$y_c = (\nu - 1)\tau/\nu$$

the νth harmonic mmf will be nonexistent. This can be proved from Eq. (24-19) on recalling that ν is an odd number and, as a consequence, $\nu - 1$ is always an even number. With the coil pitch thus chosen, the pitch factor for the νth harmonic will be zero

$$k_{p\nu} = \sin \nu\tau \frac{(\nu-1)\pi}{\nu 2\tau} = \sin k\pi = 0$$

where k is an integer.

As an example, when

$$y_c = \frac{\nu-1}{\nu}\tau = 2\tau/3$$

the third harmonic mmf will, as is seen in Fig. 24-8, be nonexistent ($F_{c3m} = k_{p3} = 0$).

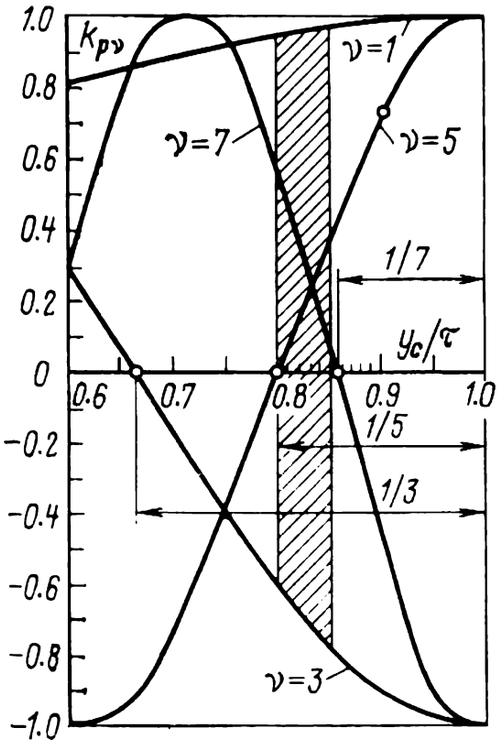

Fig. 24-9 Plots of $k_{p\nu}$ as a function of y_c

For a better performance of the machine, it is desired that the mmf should be sinusoidally or cosinusoidally distributed in space. Therefore, the pitch factor should preferably be chosen such that the higher harmonic mmfs are minimized. This cannot, however, be done for all the higher harmonic mmfs at the same time, because in order to eliminate any particular harmonic, the pitch factor must have a particular value. The best that can be done is to strike a balance by choosing y_c ranging between 0.82τ and 0.85τ. Then, as is seen from Fig. 24-9, the fundamental mmf will remain about the same as with a full pitch ($k_{p1} = 0.96$ to 0.98), whereas the fifth and seventh harmonics will be substanti-

ally attenuated ($k_{p5} = 0.16$ to 0.35, and $k_{p7} = 0.35$ to 0.08). Unfortunately, the third harmonic still retains a marked value, but it can be eliminated from the resultant mmf by other means (see Sec. 25-4). As regards the still higher harmonics (the 11th, 13th, 15th, etc.), they are substantially lower in peak value than the fundamental. Even with high values of the pitch factor,

$$F_{c\nu m} = \frac{4F_{cm}}{\pi\nu} k_{p\nu} \ll F_{c1m} = 4F_{cm}k_{p1}/\pi \qquad (24\text{-}23)$$

24-5 The Phase MMF. The Distribution Factor

With an arbitrary number q of coils per group, a phase of a winding may be imagined consisting of q basic coil sets (elementary phases) in which there is only one coil per pole pitch (see Sec. 24-3). Such a basic coil set (an elementary phase) has $q = 1$. For example, phase A in the winding of Fig. 22-3 consists of $q = 3$ basic coil sets (elementary phases), namely: the basic set of coils *1*, *10*, *19*, and *28* (shown by heavy lines), the basic set of coils *2*, *11*, *20*, and *29*, and the basic set of coils *3*, *12*, *21*, and *30*. Therefore, with an arbitrary q, the phase mmf can be found as the sum of the mmfs due to the various basic coil sets.

For this sum to be taken analytically, it is convenient first to find the various harmonic components of the phase mmf as the sums of the respective harmonic components of mmfs due to the basic coil sets. Let us take this sum, beginning with the fundamental component, then for the higher order harmonic components of the phase mmf on the assumption, as before, that the phase current is a maximum

$$i_a = \sqrt{2}\, I_a$$

The fundamental mmfs for q basic coil sets with peak values F_{c1m} are shown in Fig. 24-10. The basic coil set labelled "1" is made up of the first coils within each pole pitch. The basic coil set numbered "2" consists of the second coils, and so on. Neighbouring basic coil sets are displaced from one another by a tooth (or slot) pitch t_Z along the periphery of the air gap, and the fundamental mmfs in the elementary phases are displaced from one another by the electrical slot (or tooth) angle $\alpha_Z = t_Z\pi/\tau = (2\pi/Z)/p$.

To simplify the matters, the figure shows full-pitch (unchorded) coils. In taking the sum of the fundamental components of mmf set up by the basic coil sets, it should be remembered that they are displaced from each other by the tooth angle α_Z, and their axes *1*, *2*, *3*, and *4* passed through

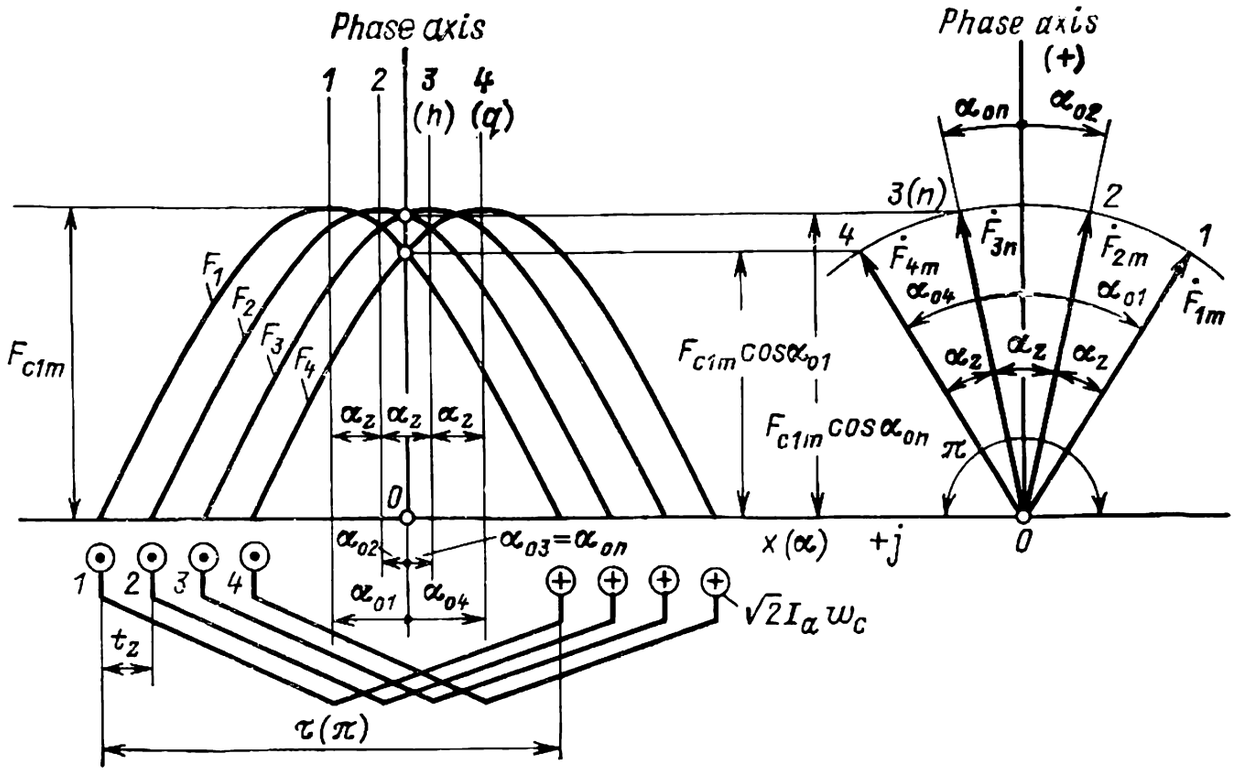

Fig. 24-10 The fundamental mmfs due to the basic coil sets making up a phase with $q = 4$

the peaks of the cosinusoidally distributed mmf are displaced by the angles α_{01}, α_{02}, $\alpha_{03} = \alpha_{0n}$ and $\alpha_{04} = \alpha_{0q}$ from the phase axis (the latter being the axis of symmetry of the coil group within a given pole pitch).

The electrical angle between the axis of the nth basic coil set and the phase axis is

$$\alpha_{0n} = \alpha_Z (n - 1) - \alpha_Z (q - 1)/2 \qquad (24\text{-}24)$$

that is,

$$\alpha_{01} = -3\alpha_Z/2 \quad \alpha_{03} = \alpha_Z/2$$
$$\alpha_{02} = -\alpha_Z/2 \quad \alpha_{04} = 3\alpha_Z/2$$

The phase mmf equal to the sum of the mmfs due to the basic coil sets is cosinusoidally distributed over a pole pitch

$$F = F_{\text{ph}1m} \cos \alpha$$

The phase mmf has a peak value, $F_{\text{ph}1m}$, at the phase axis

and can be found as the sum of the mmfs produced by the various basic coil sets at the phase axis:

$$F_{\text{ph1}m} = \sum_{n=1}^{q} F_{\text{c1}m} \cos \alpha_{0n} \tag{24-25}$$

In developing an analytical expression for the peak value of the phase mmf, it is convenient to write the mmfs due to the basic coil sets as complex amplitudes

$$\dot{F}_{nm} = F_{\text{c1}m} \exp (j\alpha_{0n}) \tag{24-26}$$

shown for $n = 1, 2, 3, 4, \ldots, q$ in Fig. 24-10. If we align the phase axis with the real axis of the complex plane, the mmf due to the nth basic coil set at the phase axis will be equal to the real part of the complex amplitude, $\dot{F}_{nm}$:

$$F_{\text{c1}m} \cos \alpha_{0n} = \text{Re} \{\dot{F}_{nm}\} \tag{24-27}$$

because

$$\exp (j\alpha_{0n}) = \cos \alpha_{0n} + j \sin \alpha_{0n}$$

Hence the peak value of the phase mmf will be

$$F_{\text{ph1}m} = \sum_{n=1}^{q} \text{Re} \{\dot{F}_{nm}\} = \text{Re} \left\{ \sum_{n=1}^{q} \dot{F}_{nm} \right\} = \text{Re} \{\dot{F}_{\text{ph1}m}\}$$

As is seen, the complex amplitude of the phase mmf

$$\dot{F}_{\text{ph1}m} = \sum_{n=1}^{q} \dot{F}_{nm}$$

is the phasor sum of the component mmfs due to the basic coil sets. In Fig. 24-11, their sum is taken on a reduced scale.

Noting that the polygon formed by the complex amplitudes of mmfs being summed can be inscribed in a circle of radius

$$OA = OB + F_{\text{c1}m}/2 \sin (\alpha_Z/2)$$

we can find the peak value of the phase mmf, $F_{\text{ph1}m}$, from the right-angled triangle ODA

$$F_{\text{ph1}m} = 2 (OA) \sin (q\alpha_Z/2) = qF_{\text{c1}m}k_{\text{d1}} = 2\sqrt{2} Iwk_{01}/\pi p \tag{24-28}$$

where $I = aI_a$ = rms phase current
$w = 2pw_c q/a$ = turns per phase path
$k_{w1} = k_{\text{p1}}k_{\text{d1}}$ = winding factor for the fundamental component of mmf.

Equation (24-28) contains what is known as the *distribution factor* for the fundamental component of phase mmf:

$$k_{d1} = \sin(q\alpha_z/2)/q \sin(\alpha_z/2) \qquad (24\text{-}29)$$

It is the ratio of the peak value of the fundamental mmf of a phase to the arithmetic sum of the peak fundamental mmfs

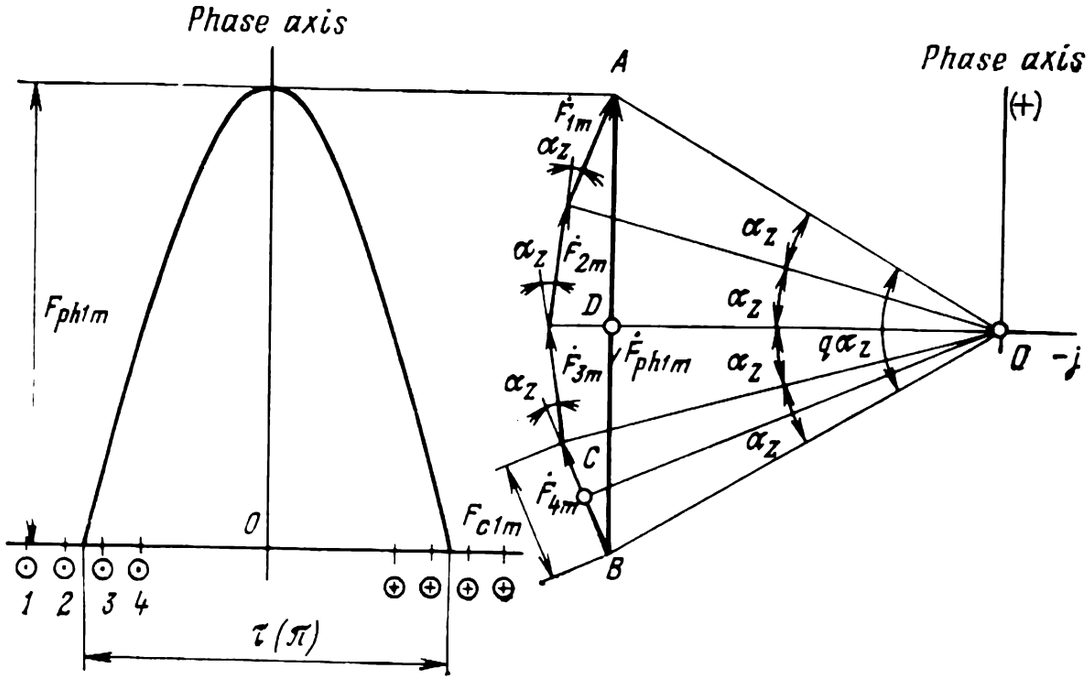

Fig. 24-11 Combining the mmfs due to the basic coil sets in Fig. 24-10, making up a phase

due to the basic coil sets in that phase

$$k_{d1} = F_{ph1m}/qF_{c1m}$$

In finding the peak value of the νth harmonic component of the phase mmf, it should be remembered that the respective angles, $\alpha_{z\nu}$, are ν times as great as for the fundamental:

$$\alpha_{z\nu} + \pi t_z/\tau_\nu = \pi\nu t_z/\tau = \nu\alpha_z \qquad (24\text{-}30)$$

Therefore, the peak value of the νth harmonic of the phase mmf will be

$$F_{ph\nu m} = qF_{c\nu m}k_{d\nu} = \frac{2\sqrt{2}Iwk_{p\nu}k_{d\nu}}{\pi p\nu} \qquad (24\text{-}31)$$

where

$$k_{d\nu} = \frac{\sin(\nu q\alpha_z/2)}{q\sin(\nu\alpha_z/2)} \qquad (24\text{-}32)$$

is known as the *distribution factor for the* νth *harmonic.*

In an m-phase symmetrical winding, a coil group spans $1/m$th fraction of a pole pitch or the electrical angle $\pi/m = q\alpha_Z$ determined for the fundamental. Therefore,

$$k_{d\nu} = \frac{\sin(\nu\pi/2m)}{q \sin(\nu\pi/2mq)} \tag{24-33}$$

Thus, for a three-phase winding, where $m = 3$,

$$k_{d\nu} = \sin(\nu\pi/6)/q \sin(\nu\pi/6q)$$

Using Eqs. (24-31) and (24-33), it is an easy matter to trace how an increase in q, the number of coils per group,

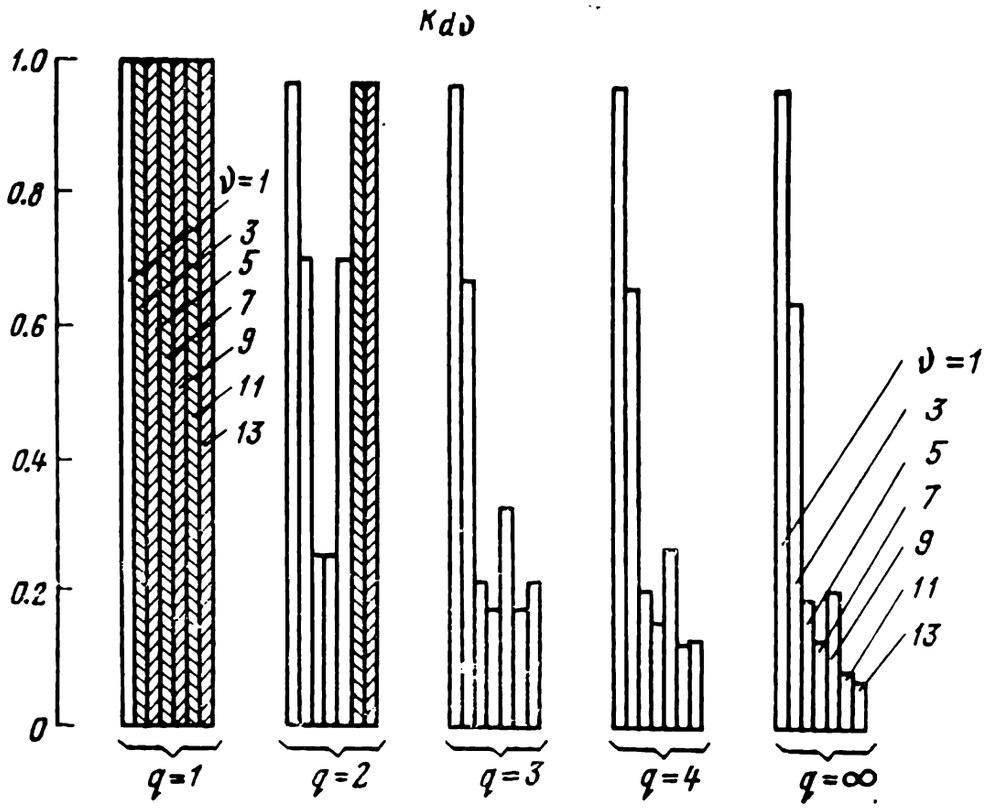

Fig. 24-12 Diagrams of $k_{d\nu}$ as a function of q (for a three-phase winding)

can affect the phase mmf waveform. Figure 24-12 gives the distribution factors for the fundamental and higher-order harmonic components of phase mmf for several values of q. As is seen, when $q = 1$, all distribution factors are unity. As q is increased, k_{d1} decreases insignificantly (when $q = 2$, it is 0.969, and when $q = \infty$, $k_{d1} = 0.955$). In contrast, the distribution factors for the higher harmonics go down abruptly as q is increased, so that when $q = \infty$, the distribution factors for the triplen harmonics become

$$|k_{d\nu}| = 2k_{d1}/\nu$$

and for all the other harmonics,

$$|k_{d\nu}| = k_{d1}/\nu$$

As is seen, even with moderate values of q (say, 3 or 4), the distribution factors are about the same as they are for $q = \infty$. The only exception is the so-called slot harmonics (slot ripple) whose order (number) is given by

$$\nu = kZ/p \pm 1 = 2mqk \pm 1 \qquad (24\text{-}34)$$

where k is any integer. For them, the distribution factor is equal to that for the fundamental component, $k_{d\nu} = k_{d1}$*. For example, when $q = 2$, this property is manifested by the harmonics of order $\nu = 2mqk \pm 1 = 2 \times 3 \times 2k \pm 1 = 11$, 13, 23, and 25. This can readily be verified by reference to Fig. 24-12 where the distribution factors for slot harmonics are shown shaded.

As q goes up, the higher harmonic components contribute progressively less to the phase mmf (the only exception being the slot harmonics). Importantly, in the phase mmf their effect is less noticeable than in the mmf due to a basic coil set [see Eqs. (24-29) and (24-31)],

$$F_{ph\nu m}/F_{ph1m} = F_{c\nu m}k_{d\nu}/F_{c1m}k_{d1} < F_{c\nu m}/F_{c1m}$$

In the limit, for a uniformly distributed winding (with ν other than a multiple of three, and also for other than slot harmonics)

$$F_{ph\nu m}/F_{ph1m} = k_{p\nu}/k_{p1}\nu^2$$

Because in the phase mmf the slot harmonics are present to the same extent as in the mmf due to the basic coil set [see Eqs. (24-26) and (24-31)],

$$F_{ph\nu m}/F_{ph1m} = k_{p\nu}k_{d\nu}/\nu k_{p1}k_{d1} = 1/\nu$$

To minimize their effect, it will be a good plan to avoid the values of q that are less than three. However, already at $q = 3$ the order of slot harmonics,

$$\nu = 2mq \pm 1 = 2 \times 3 \times 3 \pm 1 = 17 \text{ or } 19$$

---

* For slot harmonics (slot ripple), the pitch factor, too, is the same as for the fundamental, that is $k_{p\nu} = k_{p1}$.

is so high that even with $k_{dv} = k_{d1}$ and $k_{pv} = k_{p1}$ these harmonics are only slightly present in the phase mmf

$$F_{ph17m} = F_{ph1m}/17$$

$$F_{ph19m} = F_{ph1m}/19$$

With an appropriately chosen value of y_c and a sufficiently large number of coils per pole per phase, the phase mmf can be made sinusoidal very nearly. When the degree of chording (short-pitching) is taken equal to its recommended value, $y_c/\tau \approx 0.8$, the phase mmf may contain a fairly noticeable third harmonic. This is, however, of minor importance

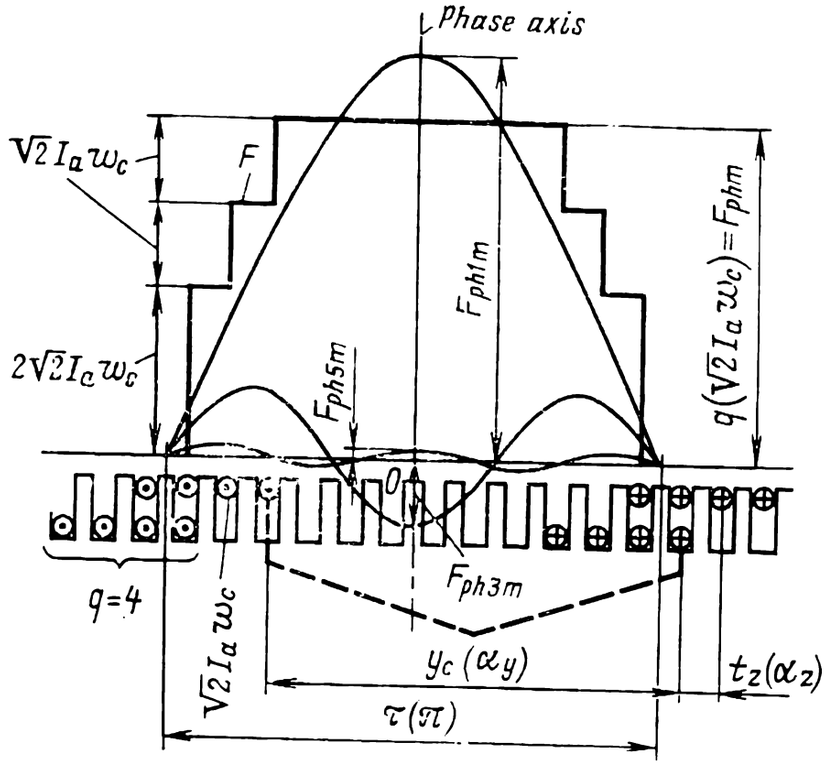

Fig. 24-13 The phase mmf of a three-phase winding ($m = 3$, $q = 4$, $y_c/\tau = 0.835$)

because the resultant mmf of a three-phase winding contains no third harmonic. Figure 24-13 shows the phase mmf and its harmonics for a three-phase winding with $q = 4$ and $y_c/\tau = 0.835$.

Using Eq. (24-31), the peak value of the phase mmf and of its harmonics may be expressed in terms of the peak value of the coil-side current, $\sqrt{2}I_a w_c$, that is,

$$F_{phm} = q\sqrt{2}I_a w_c$$

as

$$F_{phvm} = \frac{4qk_{pv}k_{dv}}{\pi v}\sqrt{2}I_a w_c \qquad (24\text{-}35)$$

The peak values of the mmfs found for the conditions specified in Fig. 24-13 are as follows:

$$F_{\text{ph}m} = 4\sqrt{2}\, I_a w_c$$

$$F_{\text{ph}1m} = 4.74\sqrt{2}\, I_a w_c$$

$$F_{\text{ph}3m} = -0.805\sqrt{2}\, I_a w_c$$

$$F_{\text{ph}5m} = +0.05\sqrt{2}\, I_a w_c$$

$$F_{\text{ph}7m} = -0.028\sqrt{2}\, I_a w_c$$

24-6 Pulsating Harmonics of the Phase MMF

In the previous section, we have seen how the phase mmf is distributed in space at time $t = 0$, when the phase current is a maximum, $i = \sqrt{2}\, I$. Because the phase current varies cosinusoidally

$$i = \sqrt{2}\, I \cos \omega t$$

it is clear that at any other point x (α) in the air gap the phase mmf will be proportional to the instantaneous phase current. Obviously the spatial distribution pattern of the phase mmf will be the same as at $t = 0$ (see above). The solid line in Fig. 24-14 shows the fundamental component of the phase mmf at time $t = 0$. For time t_1, it is shown by a dashed line. Spatial variations in the fundamental component of the phase mmf can be described by the following equation

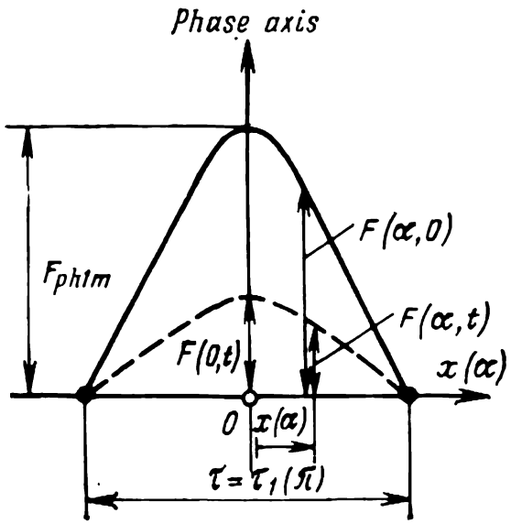

Fig. 24-14 Ripple in the fundamental component of the phase mmf

$$F(\alpha, t) = F(0, t) \cos \alpha = F_{\text{ph}1m} \cos \omega t \cos \alpha \qquad (24\text{-}36)$$

Here, $\alpha = x\pi/\tau$ [see Eq. (24-16)] is the electrical angle defining the position of a given point relative to the phase axis, $F(0, t)$ is the mmf on the phase axis at $\alpha = 0$ and at time t:

$$F(0, t) = F_{\text{ph}1m} \cos \omega t$$

Equation (24-36) is the equation of a pulsating wave; it enables us to determine the fundamental component of the mmf at any point along the air gap and at any time. For the νth harmonic of the mmf, this equation is written similarly

$$F(\alpha, t) = F_{\text{ph}\nu m} \cos \omega t \cos \alpha_\nu \qquad (24\text{-}37)$$

where $\alpha_\nu = x\pi/\tau_\nu$.

The axis of the pulsating mmf remains stationary in space and coincides with the phase axis (see Fig. 25-3).

25 The Mutual Magnetic Field of a Polyphase Winding

25-1 Presentation of the Pulsating Harmonics of the Phase MMF as the Sum of Rotating MMFs

The mutual magnetic field of an m-phase winding is produced by the sum of the phase mmfs. The pulsating harmonics of the phase mmfs can be presented as the sum of revolving mmf waves.

If we write the product of cosines in Eq. (24-36) as the sum of cosines, we get

$$\begin{aligned} F(\alpha, t) &= {}^1/_2 F_{\text{ph}1m} \cos(\omega t - \alpha) + {}^1/_2 F_{\text{ph}1m} \cos(\omega t + \alpha) \\ &= F'_{\text{ph}1m} \cos(\omega t - \alpha) + F''_{\text{ph}1m} \cos(\omega t + \alpha) \\ &= F'(\alpha, t) + F''(\alpha, t) \end{aligned} \qquad (25\text{-}1)$$

The first term in Eq. (25-1) is a forward revolving mmf wave, and the second term is a backward revolving mmf wave. The revolving mmf waves are written with reference to the phase axis which is assumed to be stationary in space. To get insight into the basic properties of these waves, let us re-write Eq. (25-1) in a rotating system of coordinates. The state of the forward rotating mmf wave relative to its axis, which also rotates at angular velocity ω and coincides at time $t = 0$ with the phase axis (Fig. 25-1*a*), is defined by the angle $\alpha_0 = \alpha - \omega t$, and its equation may be written as

$$F'(\alpha, t) = F'_{\text{ph}1m} \cos(-\alpha_0) = F'_{\text{ph}1m} \cos \alpha_0 \qquad (25\text{-}2)$$

At time t, the forward rotating mmf wave is shown in Fig. 25-1*a*. From Eq. (25-2) it follows that the forward rotating mmf is a maximum at $\alpha_0 = 0$, that is

$$F'(\alpha, t) = F'_{\text{ph}1m}$$

It will remain unchanged at any point displaced by an angle α_0 from the mmf axis. In other words, the forward rotating mmf wave remains stationary relative to the mmf

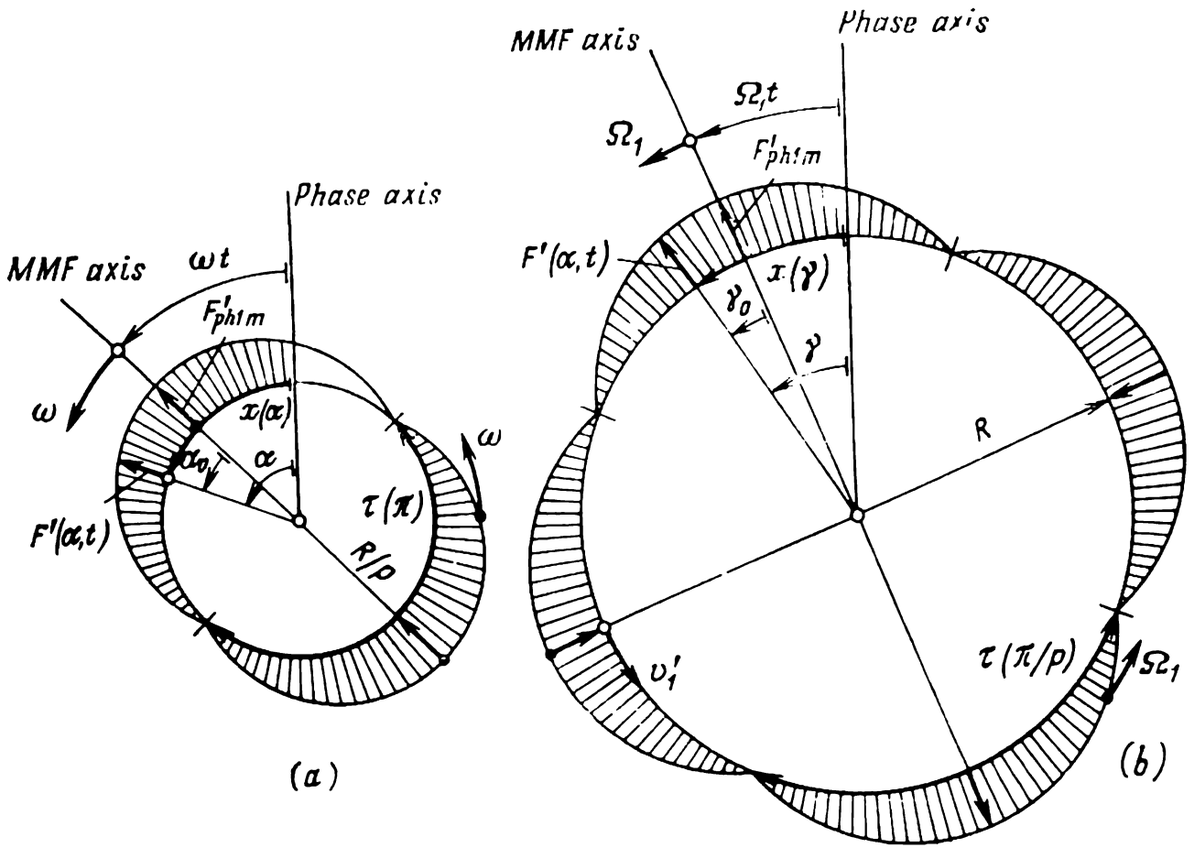

Fig. 25-1 Forward rotating component of the phase mmf in (*a*) the model of a machine and (*b*) in the machine itself for $p = 2$

axis and rotates together with this axis at an angular velocity ω in the positive direction (which is counterclockwise). At $t = 0$, the positive maximum of the mmf wave occurs at the phase axis, $\omega t = 0$.

Figure 25-1*b* shows a rotating mmf wave in a four-pole machine. Therefore, all the angles are halved, that is, reduced, by a factor of p, and the angular velocity of the mmf is

$$\Omega'_1 = \Omega = \omega/p \qquad (25\text{-}3)$$

Or, in words, the angular velocity of the mmf is $1/p$ of its electrical angular velocity which is equal to the angular frequency of the phase current.

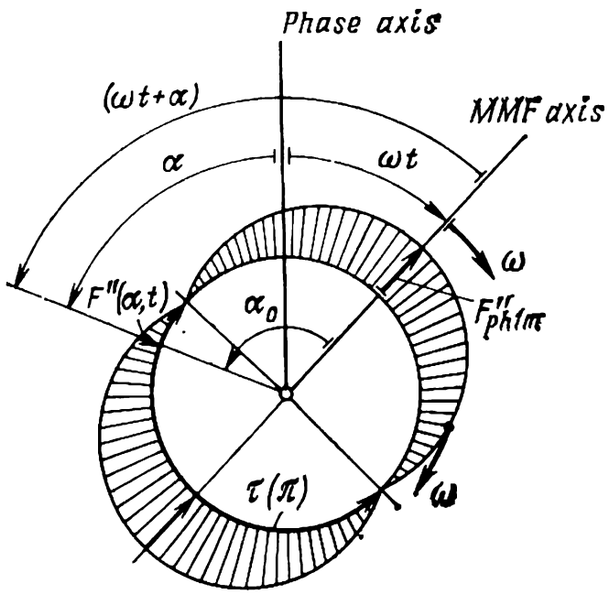

Fig. 25-2 Backward rotating mmf in the model of a machine

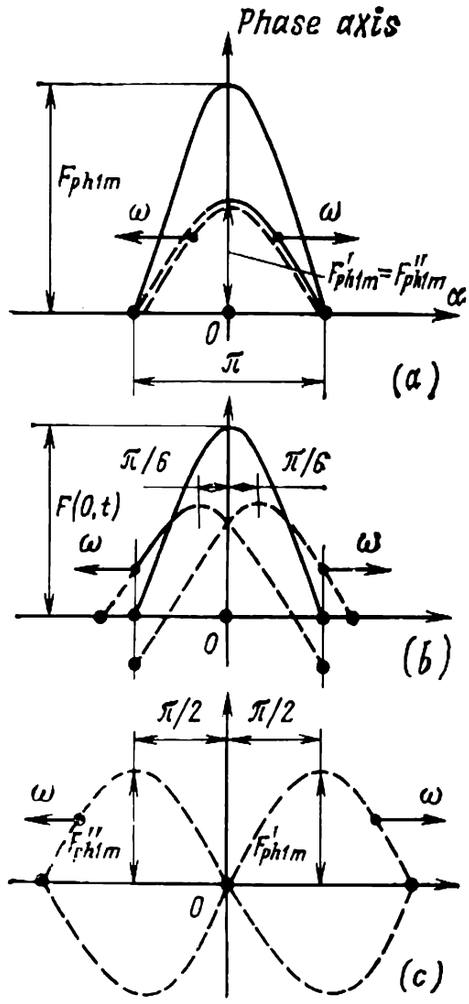

Fig. 25-3 Pulsating harmonic of the phase mmf as the sum of the forward and backward rotating mmf waves

The rotating mmf completes one cycle of change in the time span equal to the circumferential period of the winding

$$2\tau = 2\pi R/p$$

The circumferential linear velocity of the forward rotating mmf wave is

$$u = u_1' = \Omega R = 2f\tau \tag{25-4}$$

where f is the frequency of the current.

The electrical angle is given by

$$\alpha = \gamma p = (x/\tau)\,\pi$$

where x (γ) is the distance from the phase axis.

Reasoning as above and writing an equation for the backward mmf, $F''(\alpha, t)$ rotating about its axis which in turn rotates in the negative direction (which is clockwise) at a velocity ω and is displaced from the phase axis by an angle ωt, it can be shown that $F''(\alpha, t)$ is a backward mmf wave which has properties similar to those of the forward mmf wave (Fig. 25-2). To be more specific, both waves have the same peak value

$$F'_{ph\,1m} = F''_{ph\,1m} = F_{ph\,1m}/2$$

and rotate at angular velocities $\Omega_1' = \omega/p$ and $\Omega_1'' = -\omega/p$.

Their electrical angular velocities are likewise the same in magnitude and are equal to the angular frequency of the phase current

$$\omega_1' = \Omega_1' p = \omega$$
$$\omega_1'' = \Omega_1'' p = -\omega$$

At time $t = 0$, both waves are coincident in space with the phase axis (Fig. 25-3*a*). From that instant on, the forward wave travels in the positive direction, and the backward wave in the negative direction. Figure 25-3*b* and *c* shows the positions of the two waves for $\omega t = \pi/6$ and $\omega t = \pi/2$, respectively.

25-2 Presentation of Phase MMF Harmonics as Complex Time-Space Functions

The mmf at point α and time t, that is, $F(\alpha, t)$, may be treated as the real part of the sum of some complex time-space functions

$$\begin{aligned} F(\alpha, t) &= F'(\alpha, t) + F''(\alpha, t) \\ &= \mathrm{Re}\,[F'_{\mathrm{ph}1m} \exp(j\omega t) \exp(-j\alpha)] \\ &\quad + \mathrm{Re}\,[F''_{\mathrm{ph}1m} \exp(-j\omega t) \exp(-j\alpha)] \end{aligned} \qquad (25\text{-}5)$$

The complex time-space function

$$\tilde{F}'_{\mathrm{ph}1} = F'_{\mathrm{ph}1m} \exp(j\omega t)$$

describes the forward wave of the phase mmf. The complex time-space function

$$\tilde{F}''_{\mathrm{ph}1} = F''_{\mathrm{ph}1m} \exp(-j\omega t)$$

describes the backward wave of the phase mmf. Therefore, Eq. (25-5) may alternatively be written as

$$\begin{aligned} F(\alpha, t) &= F'(\alpha, t) + F''(\alpha, t) \\ &= \mathrm{Re}\,[\tilde{F}'_{\mathrm{ph}1m} \exp(-j\alpha)] + \mathrm{Re}\,[\tilde{F}''_{\mathrm{ph}1m} \exp(-j\alpha)] \end{aligned}$$

If we plot the complex functions $\tilde{F}'_{\mathrm{ph}1m}$ and $\tilde{F}''_{\mathrm{ph}1m}$ on the space-time plane of a two-pole model, in which the real axis runs along the phase axis in Fig. 25-4, and the imaginary axis is turned through $\pi/2$ counterclockwise, we shall see that the angle between the point at the angle α and $\tilde{F}'_{\mathrm{ph}1m}$ is $(\omega t - \alpha)$. Likewise, the angle between the point at the

angle α and $\tilde{F}''_{\mathrm{ph}1m}$ is $(-\omega t - \alpha)$. Therefore, as stems from Eq. (25-1), a projection of $\tilde{F}'_{\mathrm{ph}1m}$ or $\tilde{F}''_{\mathrm{ph}1m}$ on a direction at the angle α will, respectively, give the forward mmf, $F'(\alpha, t)$, or the backward mmf, $F''(\alpha, t)$, at the point in question.

The complex function $\tilde{F}'_{\mathrm{ph}1m}$ rotates in the forward direction (in the direction of positive angles) at angular velocity

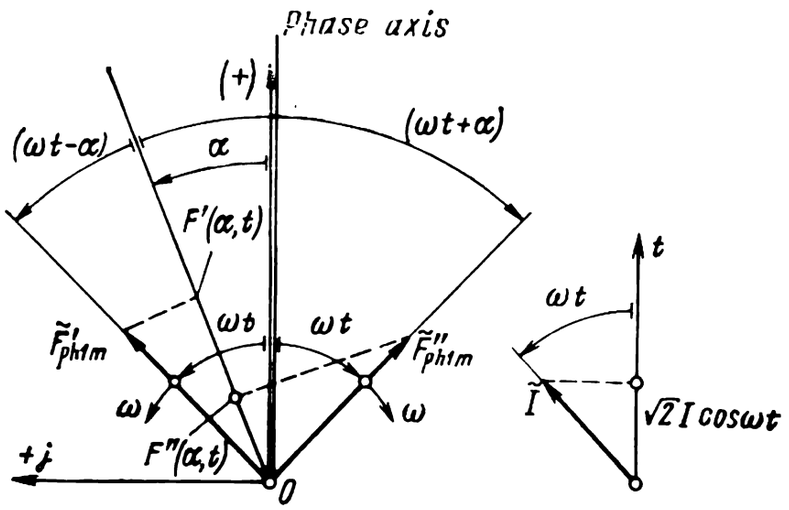

Fig. 25-4 Representation of the phase mmf on the complex plane of a two-pole model

ω, whereas the complex function $\tilde{F}''_{\mathrm{ph}1m}$ does so in the backward direction at the same angular velocity ω. This form of presentation applies when the angle α is reckoned from the phase axis aligned with the real axis of the complex plane, and time is counted from $t = 0$ when the phase current is a maximum, $i = \sqrt{2}I$. In the final analysis, however, we are interested in the mmf of a polyphase winding, and it can be found by adding together the mmfs of the individual phases.

To tackle this problem, we should learn to write the equation of the mmf for an arbitrary phase whose axis makes an angle α_{ph} with the real axis of the complex plane (Fig. 25-5), and whose current is given by

$$i = \sqrt{2}\, I \cos(\omega t - \varphi_{\mathrm{ph}})$$

so that at $t = 0$, the current is

$$i = \sqrt{2} \cos(-\varphi_{\mathrm{ph}})$$

The equation for an arbitrary phase mmf can be written in trigonometric or complex form by analogy with Eq. (25-1) or Eq. (25-5), noting that the angle ωt is now replaced by

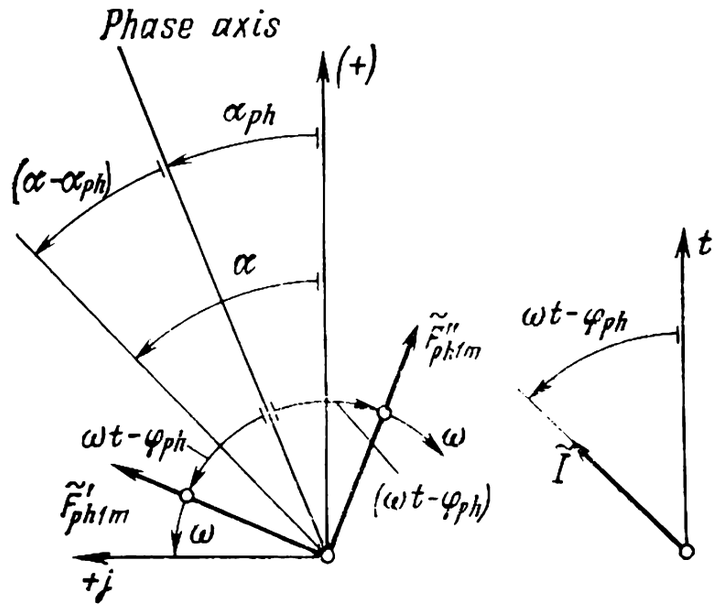

Fig. 25-5 Representation of an arbitrary phase mmf with an arbitrary phase current on the complex plane of a two-pole model

$(\omega t - \varphi_{ph})$, and the angle α by $(\alpha - \alpha_{ph})$ reckoned from the phase axis,

$$F(\alpha, t) = F'_{ph\,1m} \cos[(\omega t - \varphi_{ph}) - (\alpha - \alpha_{ph})] + F''_{ph\,1m} \cos[-(\omega t - \varphi_{ph}) - (\alpha - \alpha_{ph})]$$

or

$$F(\alpha, t) = \mathrm{Re}\{F'_{ph1m} \exp[j(\omega t - \varphi_{ph})] \exp(j\alpha_{ph}) \times \exp(-j\alpha)\} + \mathrm{Re}\{F''_{ph1m} \exp[-j(\omega t - \varphi_{ph})] \exp(j\alpha_{ph}) \times \exp(-j\alpha)\}$$

$$F(\alpha, t) = \mathrm{Re}[\tilde{F}'_{ph1m} \exp(-j\alpha)] = \mathrm{Re}[\hat{\tilde{F}}'_{ph1m} \exp(-j\alpha)] + \mathrm{Re}[\tilde{F}''_{ph1m} \exp(-j\alpha)] \quad (25\text{-}6)$$

A plot of an arbitrary phase mmf on the complex plane of the model is shown in Fig. 25-5. The complex function

$$\tilde{F}_{ph1m} = \hat{\tilde{F}}'_{ph1m} + \tilde{F}''_{ph1m}$$

describes the phase mmf, the complex function

$$\tilde{F}'_{ph1m} = F'_{ph1m} \exp[j(\omega t - \varphi_{ph}) \exp(j\alpha_{ph})]$$

describes the forward rotating wave of the phase mmf, and the complex function

$$F''_{\text{ph}1m} = F''_{\text{ph}1m} \exp\left[-j\left(\omega t - \varphi_{\text{ph}}\right) \exp\left(j\alpha_{\text{ph}}\right)\right]$$

describes the backward rotating wave of the phase mmf.

25-3 Time and Space-Time Complex Quantities * and Functions of the Quantities Involved in Operation of a Polyphase Machine

Scalars sinusoidally varying in time (currents, voltages, emfs, and flux linkages) are customarily represented as complex functions whose projections on the time axis give

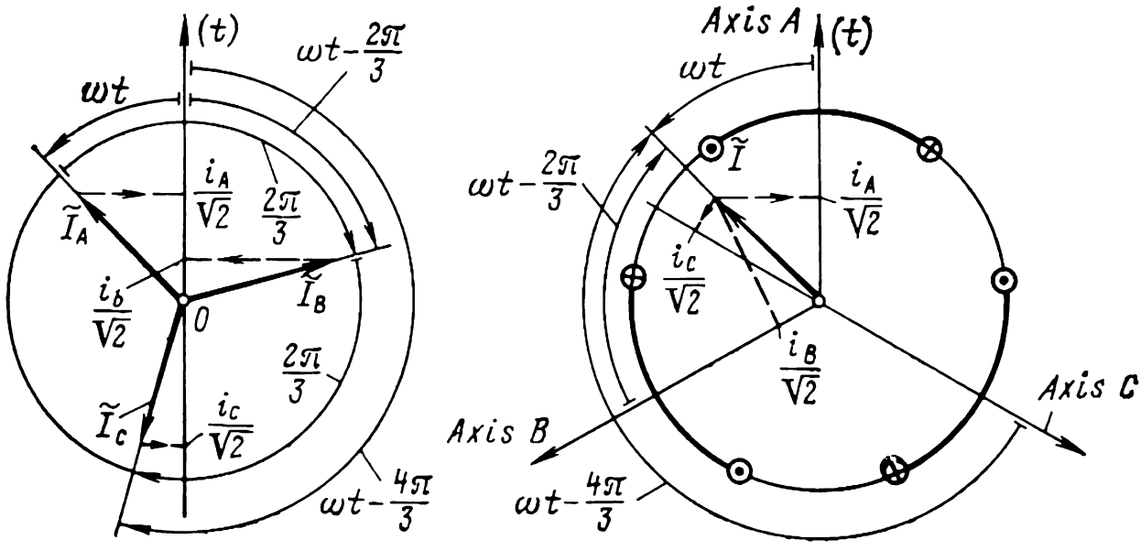

Fig. 25-6 Representation of currents in a three-phase machine on the time complex plane (on the left) and on the space complex plane (on the right) of a two-pole model

instantaneous values of those quantities. For example, on the left of Fig. 25-6, the instantaneous value of the phase A current, reduced by a factor of $\sqrt{2}$, is equal to the projection of the complex harmonic function of the phase A current, $\tilde{I}_A = \tilde{I}_A \exp(j\omega t)$, on the time ($t$) axis aligned with the real axis of the time complex plane or, to state this differently, to the real part of the complex current

* Time varying quantities are usually called phasors. Spatially distributed quantities are true vectors. Frequently, they are plotted together on combined phasor-vector diagram.—*Translator's note.*

function

$$i_A/\sqrt{2} = \text{Re}\,[\tilde{I}_A] = I_A \cos \omega t$$

where $\dot{I}_A = I_A \exp(j0)$ = rms current in phase A in complex notation

I_A = rms current in phase A

Under balanced conditions, the quantities in the other phases of a three-phase machine can be described by complex functions displaced by $-2\pi/3$ (for phase B) and $-4\pi/3$ (for phase C) from those associated with phase A. For example, the currents in phases B and C are written in complex-function notation as

$$\tilde{I}_B = \dot{I}_B \exp(j\omega t)$$

$$\tilde{I}_C = \dot{I}_C \exp(j\omega t)$$

where $\dot{I}_B = I_B \exp(-j2\pi/3)$ and $\dot{I}_C = I_C \exp(-j4\pi/3)$ are the complex rms currents in phase B and C, respectively.

Since the rms phase currents are the same, the magnitudes of the complex currents are likewise the same

$$I_A = I_B = I_C = I$$

The instantaneous phase currents can be found from the following equations:

$$\begin{aligned} i_A/\sqrt{2} &= \text{Re}\,[\tilde{I}_A] = \text{Re}\,[\dot{I} \exp(j\omega t)] \\ i_B/\sqrt{2} &= \text{Re}\,[\tilde{I}_B] = \text{Re}\,\{\dot{I} \exp[j(\omega t - 2\pi/3)]\} \\ i_C/\sqrt{2} &= \text{Re}\,[\tilde{I}_C] = \text{Re}\,\{\dot{I} \exp[j(\omega t - 4\pi/3)]\} \end{aligned} \qquad (25\text{-}7)$$

where $\dot{I} = \dot{I}_A$, and are each a projection of the respective complex current function on the real axis of the time complex plane (Fig. 25-6).

The theory of electrical machines uses another form of representation for the quantities existing in polyphase systems under balanced conditions. More specifically, scalars (currents, voltages, and so on) associated with the various phases are depicted on the space complex plane of a two-pole model as a complex function common to all the phases.

For the phase currents defined by Eq. (25-7) and shown on the left of Fig. 25-6, such a complex function has the

form

$$\tilde{I} = \dot{I} \exp(j\omega t)$$

where $\dot{I} = \dot{I}_A$, and is plotted on the space complex plane of a two-pole model as shown on the right of Fig. 25-6.

In a two-pole model, the phase windings are shown each as a coil traversed by a positive current. The axes of phases A, B, and C are drawn through the centres of the coil groups represented by a single coil. Because the events in phase B lag behind those in phase A, the axis of phase B is displaced from that of phase A by an electrical angle equal to $2\pi/3$ in the positive direction (counterclockwise), and that of phase C by an angle equal to $4\pi/3$ in the same direction. The instantaneous phase current (reduced by a factor of $\sqrt{2}$) is given by a projection of the complex function $\tilde{I}$ on the respective phase axis.

Because the complex current function $\tilde{I}$ takes up the same position relative to the axis of a given phase as the complex current function of the same phase relative to the real axis of the time complex plane (on the left of Fig. 25-6), either form of representation gives the same instantaneous phase current. To demonstrate, projections of the complex current function on the respective phase axes on the space complex plane

$$\begin{aligned} i_A/\sqrt{2} &= \mathrm{Re}\,[\tilde{I}] = \mathrm{Re}\,[\dot{I} \exp(j\omega t)] \\ i_B/\sqrt{2} &= \mathrm{Re}\,[\tilde{I} \exp(-j2\pi/3] \\ &= \mathrm{Re}\,\{\dot{I} \exp[j(\omega t - 2\pi/3)]\} \qquad (25\text{-}8) \\ i_C/\sqrt{2} &= \mathrm{Re}\,[\tilde{I} \exp(-j4\pi/3)] = \mathrm{Re}\,\{\dot{I} \exp[j(\omega t - 4\pi/3)]\} \end{aligned}$$

are the same as projections of the complex functions $\tilde{I}_A$, $\tilde{I}_B$, and $\tilde{I}_C$ on the time axis (see Eq. (25-7) and the plot on the left of Fig. 25-6). Similarly, we can depict on the space complex plane of the model the emfs, voltages and flux linkages associated with the various phases. These quantities, too, will be represented by the respective complex functions common to all the phases.

Earlier, we discussed the representation of spatially distributed, time-varying scalars in the form of space-time complex functions on the space complex plane of a model.

We did this for the rotating mmf wave which is a scalar quantity sinusoidally varying with time and space. The value of the mmf at a given point in the air gap, say, $F'(\alpha, t)$, displaced by an angle α from the origin, was found for each instant of time as a projection of the rotating complex function $F'_{\text{phl}m}$ on the direction at the angle α (see Figs. 25-4 and 25-5).

Now we have depicted phase scalar quantities as complex functions on the same space complex plane. In contrast to the complex functions depicting spatially distributed scalars (mmfs, and, as we shall see later, the normal component of the air-gap magnetic flux density), however, the complex functions representing phase quantities can only be projected on the phase axes. Their projections on an arbitrary reference direction have no physical meaning.

To stress this difference, the complex functions of spatially distributed, time-varying quantities (mmfs and the normal component of the airgap magnetic flux density) will be called *time-space complex functions.* The complex functions of the phase quantities which only vary with time (currents, voltages, emfs, and flux linkages) will be referred to as time complex functions.

25-4 The MMF of a Polyphase Winding. Its Rotating Harmonics

Consider a symmetrical m-phase winding. To simplify the matter, let m be equal to 3. We set out to find the mmf of this three-phase winding as the sum of the mmfs in the individual phases. In doing so, we shall remember that the phase axes are displaced from one another in space by an electrical angle $2\pi/m = 2\pi/3$, and that the phase currents are displaced from one another by the same angle in time.

Suppose that the phases carry a balanced set of PPS currents. Such currents are shown in Fig. 25-6 and can be found by Eq. (25-7) or (25-8). As will be recalled, in a balanced set of PPS currents, the phase B current lags behind the phase A current by $2\pi/3$, and the index "B" is assigned to the phase whose axis is displaced from that of axis A by an electrical angle $\alpha_{AB} = 2\pi/3$ in the positive direction, (see Fig. 25-7).

To combine the phase mmfs in complex form, the axis of phase A must be aligned with the real axis of the complex

plane, and the positive angles α must be counted counterclockwise. Resolving the phase mmfs into the forward and backward components and noting the phase shift φ_{ph} between the currents and the spatial shift α_{ph} between the

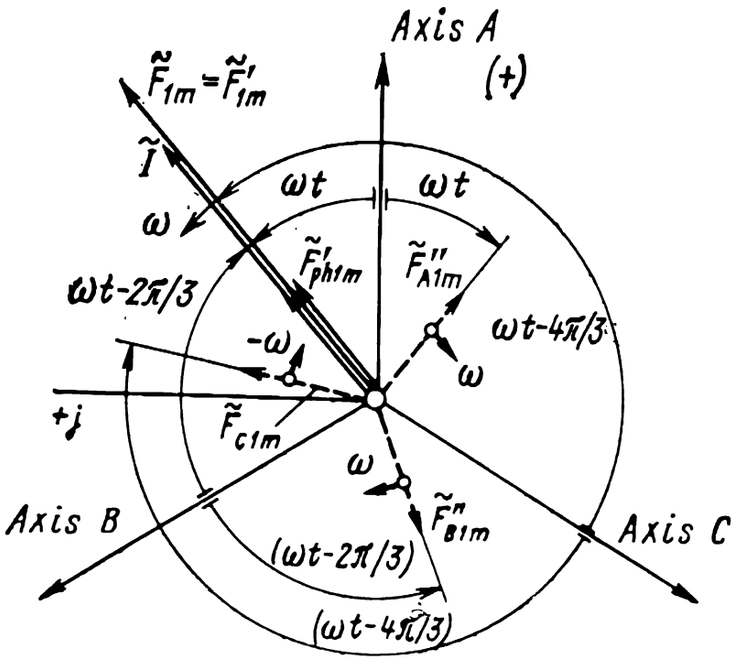

Fig. 25-7 Production of a rotating mmf by a three-phase winding carrying PPS currents

phase axes from Eq. (25-6), we obtain the total forward mmf for a three-phase winding as

$$\begin{aligned}\tilde{F}_{1m} &= \tilde{F}'_{1m} = \tilde{F}'_{A1m} + \tilde{F}'_{B1m} + \tilde{F}'_{C1m} \\ &= F'_{ph1m} \exp [j(\omega t - 0)] \exp (j0) \\ &\quad + F'_{ph1m} \exp [j(\omega t - 2\pi/3)] \exp (j2\pi/3) \\ &\quad + F'_{ph1m} \exp [j(\omega t - 4\pi/3)] \exp (j4\pi/3) \\ &= 3\tilde{F}'_{ph1m} = 3F'_{ph1m} \exp (j\omega t) \\ &= F'_{1m} \exp (j\omega t)\end{aligned}$$

As is seen, all phase mmfs are identical and are depicted graphically by the same complex function. The peak mmf of an m-phase winding is

$$F'_{1m} = F_{1m} = mF'_{ph1m} = mF_{ph1m}/2$$

where F_{ph1m} is the peak value of the pulsating phase mmf wave.

Upon suitable substitutions [see Eq. (24-28)], we get

$$F'_{1m} = F_{1m} = (m\sqrt{2}/\pi)(Iwk_{p1}k_{d1}/p) \qquad (25\text{-}9)$$

The backward phase mmf waves sum to zero [see Fig. 25-7 and Eq. (25-6)]

$$\begin{aligned}\tilde{F}''_{1m} &= \tilde{F}''_{A1m} + \tilde{F}''_{B1m} + \tilde{F}''_{C1m} \\ &= F''_{ph1m} \exp [-j(\omega t - 0)] \exp (j0) \\ &\quad + F''_{ph1m} \exp [-j(\omega t - 2\pi/3)] \exp (j2\pi/3) \\ &\quad + F''_{ph1m} \exp [-j(\omega t - 4\pi/3)] \exp (j4\pi/3) \\ &= 0\end{aligned}$$

To sum up, the fundamental mmf of a three-phase (or, generally, a polyphase) winding carrying a set of PPS currents is the forward rotating mmf with the peak value given by Eq. (25-9). It rotates at an electrical angular velocity ω and a mechanical angular velocity $\Omega_1 = \omega/p$ in the positive direction (counter-clockwise).

On the space complex plane, this mmf runs in the same direction as the complex function $\tilde{I}$ depicting the PPS phase currents (see Fig. 25-7). Recalling that this mmf is proportional to current, $F_{1m} = k_F I$, we may re-write Eq. (25-9) in complex form as

$$\tilde{F}_{1m} = k_F \tilde{I}$$

where

$$k_F = m\sqrt{2}\, wk_1/\pi p$$

The distribution of the fundamental mmf set up by the PPS currents along the periphery of the air gap [see Eqs. (25-1) and (25-5)] can be described by an equation of the form

$$F(\alpha, t) = F_{1m} \cos(\omega t - \alpha) = \text{Re}\,[\tilde{F}_{1m} \exp(-j\alpha)] \quad (25\text{-}10)$$

where

$\alpha = \gamma p = x\pi/\tau$ = the electrical angle defining the position of a given point along the periphery of the air gap

γ = the mechanical angle from the origin (from the axis of the main phase A carrying a current $i_A = \sqrt{2}I \times \cos \omega t$) to the point in question

x = the distance along the periphery of the air gap from the axis of the main phase to the point of interest

τ = the pole pitch for the fundamental component

p = the number of pole pairs along the periphery of air gap for the fundamental component

If a polyphase winding carries NPS currents, the backward phase mmfs will be represented by the same complex function, and the forward mmfs will cancel out. This results in a backward rotating mmf which can be described by an equation of the form

$$F(\alpha, t) = F_{1m} \cos(-\omega t - \alpha)$$
$$= \mathrm{Re}\,[F_{1m} \exp(-j\omega t) \exp(-j\alpha)] \qquad (25\text{-}11)$$

Acting in a similar way, we can combine the higher harmonic components of the forward and backward phase mmfs. In combining, either the forward or the backward νth harmonic waves, or both, may cancel out. Because of this, the resultant mmf may only contain some of the harmonics whose order is given by

$$\nu = 2mc \pm 1$$

where $c = 0, 1, 2, 3, \ldots$ For a three-phase winding, the order of the resultant rotating mmf waves will be $\nu = 1, 5, 7, 11, 13$, etc.

The νth harmonic component of the resultant rotating field will rotate in the forward direction (clockwise), if the "+" sign is adopted in finding the order of the harmonic by the above equation, and in the backward direction, if the "—" sign is adopted.

The peak value of the rotating νth harmonic mmf can be found by an equation similar to Eq. (25-11)

$$F_{\nu m} = \frac{m\sqrt{2}\,Iwk_{d\nu}k_{p\nu}}{\pi\nu p} \qquad (25\text{-}12)$$

where $\nu p = p_\nu$ is the number of pole pairs for the νth harmonic component.

The mechanical angular velocity of the νth harmonic mmf is given by

$$\Omega_\nu = \omega/p_\nu = \omega/\nu p \qquad (25\text{-}13)$$

The angular velocity

$$\omega_\nu = \Omega_\nu p_\nu = \omega \qquad (25\text{-}14)$$

defined as the product of the mechanical speed by the number of pole pairs for the νth harmonic field component (which is also true of the electrical angle for the νth harmonic, $\alpha_\nu = \gamma p_\nu$) may be looked upon as the *electrical angular velocity* of the νth harmonic mmf. It is the velocity at which

the complex function of the ν th harmonic mmf rotates [see Eq. (25-10)]

$$\tilde{F}_{\nu m} = F_{\nu m} \exp(\pm j\omega t)$$

The mechanical angular velocity of the ν th harmonic is 1/ν of that of the fundamental component of the mmf,

$$\Omega_\nu = \Omega_1/\nu$$

The distribution of the ν th harmonic mmf along the periphery of the airgap is described by an equation set up by analogy with Eq. (25-10) (if the harmonic is rotating in the forward direction) or Eq. (25-11) (if the harmonic is rotating in the backward direction):

$$\begin{aligned} F_\nu(\alpha, t) &= F_{\nu m} \cos(\pm\omega t - \alpha_\nu) \\ &= \mathrm{Re}\,[F_{\nu m} \exp(\pm j\omega t) \exp(-j\alpha_\nu)] \end{aligned} \qquad (25\text{-}15)$$

where the "+" sign applies when the harmonics are rotating in the positive (forward) direction, and the "—" sign, when the harmonics are rotating in the negative (backward) direction.

$$\alpha_\nu = p_\nu \gamma = \nu p \gamma = (x/\tau_\nu)\,\pi = \nu x \pi/\tau$$

is the electrical angle defining the position of a given point in the field set up by the ν th harmonic component

$$p_\nu = p\nu$$

is the number of pole pairs along the periphery of the airgap for the ν th harmonic component, and

$$\tau_\nu = \tau/\nu$$

is the pole pitch for the ν th harmonic component.

As a rule, the ν th harmonic is small in peak value, because the winding factor $k_{d\nu}k_{p\nu}$ is only a few hundredths of unity, whereas for the fundamental component it is close to unity. Also, many harmonic components cancel out (for example, this is true of the triplen harmonics in the case of a three-phase winding, that is, those whose order is 3, 9, 15, etc.). Therefore, with a judicious choice of the coil pitch ($y_c = 0.83\tau$) and of the coils per group ($q \geqslant 2$), the mmf of a polyphase (three-phase) winding will differ but little from the fundamental mmf, because the higher harmonics it contains are insignificant in their effect. In fact, it may be treated as the rotating fundamental wave with a peak value

given by Eq. (25-9) and with a mechanical angular velocity $\Omega = \Omega_1 = \omega/p$. If the winding carries PPS currents and the current in phase A is

$$i_A = \sqrt{2}\, I \cos \omega t$$

the peak value of the fundamental mmf at time t will be displaced by a mechanical angle $\gamma = \omega t/p$ from the axis of phase A (or by an electrical angle $\alpha = \omega t$).

The above distinctions of the mmf induced in a three-phase winding are depicted in Fig. 25-8. The phases of the

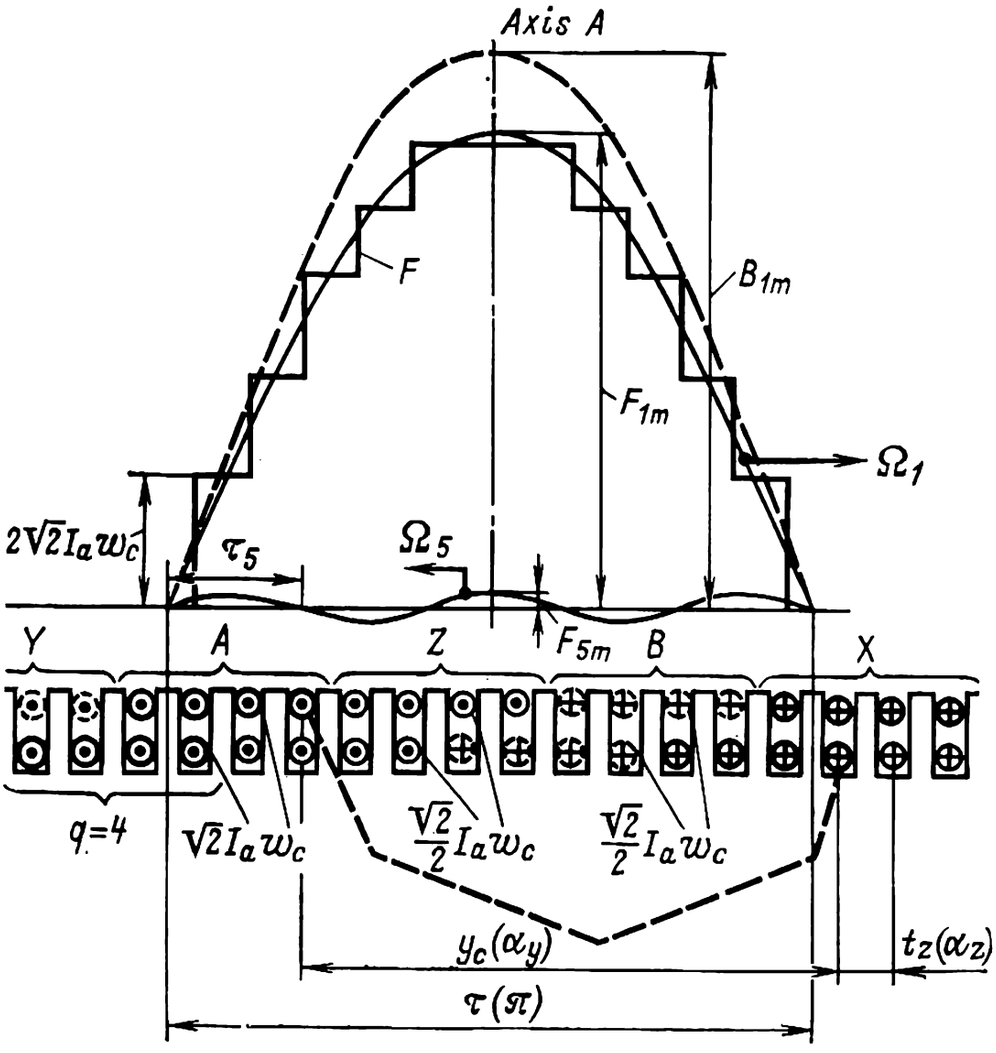

Fig. 25-8 MMF of a three-phase winding ($q = 4$, $y_c/\tau = 0.835$)

winding shown in the figure do not differ from those in Fig. 24-13. From a comparison of the mmf in a three-phase winding with that of any one phase in the same winding (see Fig. 24-13), it is readily seen that the waveform of the mmf is improved appreciably, and it appears sinusoidal very nearly. The third harmonics, rather pronounced in the phase mmfs (see Fig. 24-13), cancel one another upon com-

bining. It is to be noted that in Fig. 25-8 the mmf F is found at $t = 0$, when the current in phase A is a maximum

$$i_A = \sqrt{2}\, I_a \cos \omega t = \sqrt{2}\, I_a$$

and the currents in phases B and C are the same

$$i_B = \sqrt{2}\, I_a \cos (\omega t - 2\pi/3) = -\sqrt{2}\, I_a/2$$

$$i_C = \sqrt{2}\, I_a \cos (\omega t - 4\pi/3) = -\sqrt{2}\, I_a/2$$

As will be recalled, $I_a = I/a$ is the current in a parallel path (circuit) of the winding.

The waveform of the mmf can be plotted as for the mmf of one phase in Fig. 24-13, if we note that the currents in phases B and C are flowing in the reverse direction relative to the positive direction of the phase currents. The peak value of a harmonic mmf can be expressed in terms of the peak values of the coil-side currents, using the equation derived from Eq. (24-35):

$$F_{\nu m} = \frac{m}{2} F_{\mathrm{ph}\nu m} = \frac{2qmk_{\mathrm{p}\nu}k_{\mathrm{d}\nu}}{\pi\nu} (\sqrt{2}\, I_a w_{\mathrm{c}}) \qquad (25\text{-}16)$$

By the above equation, it is an easy matter to get

$$F_{1m} = 7.12\sqrt{2}\, I_a w_{\mathrm{c}}$$

$$F_{5m} = 0.075\sqrt{2}\, I_a w_{\mathrm{c}}$$

$$F_{7m} = -0.042\sqrt{2}\, I_a w_{\mathrm{c}}$$

25-5 The Fundamental Component of the Magnetic Flux Density in a Polyphase Winding (The Rotating Field)

As a rule, the pole pitch for the fundamental mmf of a polyphase winding, $\tau_1 = \tau$, is many times the tooth (or slot) pitch of the cores, t_{Z1} and t_{Z2}:

$$\tau_1/t_{Z1} = q_1 m_1 \gg 1$$

$$\tau_1/t_{Z2} \gg 1$$

Therefore, in calculating the field set up by the fundamental mmf,

$$F(\alpha, t) = F_{1m} \cos (\omega t - \alpha)$$

we are in a position to allow for the effect of saliency on the average by using the air gap factor

$$k_\delta = k_{\delta 1} k_{\delta 2}$$

from Eq. (24-10). Then the mean airgap permeance is the same as in the homopolar case and is given by

$$\lambda_0 = 1/\delta k_\delta \tag{25-17}$$

By definition (see Sec. 24-3), the fundamental radial component of the gap magnetic flux density can be written as

$$B(\alpha, t) = \mu_0 \lambda_0 F(\alpha, t) = B_{1m} \cos(\omega t - \alpha) \tag{25-18}$$

where $B_{1m} = \mu_0 \lambda_0 F_{1m}$ is the peak value of the fundamental component of the magnetic flux density.

In a polyphase machine, the fundamental component of the airgap magnetic flux density is a rotating wave travelling at the same mechanical angular velocity and having the same pole pitch and the same pole-pitch angle as the fundamental mmf (Fig. 25-9):

$$\Omega = \Omega_1 = \omega/p$$

$$\tau = \tau_1$$

$$\gamma_p = 2\pi/p$$

Like the mmf, the magnetic flux density $B(\alpha, t)$ can be depicted on a two-pole model (Fig. 25-10) either as a cosinusoidal rotating wave (Fig. 25-10*a*) or as a space-time complex function

$$\tilde{B}_1 = B_{1m} \exp(j\omega t) \tag{25-19}$$

which is in phase with $\tilde{F}_1$ and $\tilde{I}$. The projection of $\tilde{B}_1$ on an arbitrary direction at an electrical angle $\alpha = p\gamma$ from the origin in the model (Fig. 25-10*b*) is equal to the radial component of the fundamental magnetic flux density at a mechanical angle γ from the origin in the prototype machine (see Fig. 25-9). The origin is usually taken to be the axis of the main phase (phase A) in which the current is a maximum

$$i_A = \sqrt{2}\, I_a \cos \omega t$$

at $t = 0$.

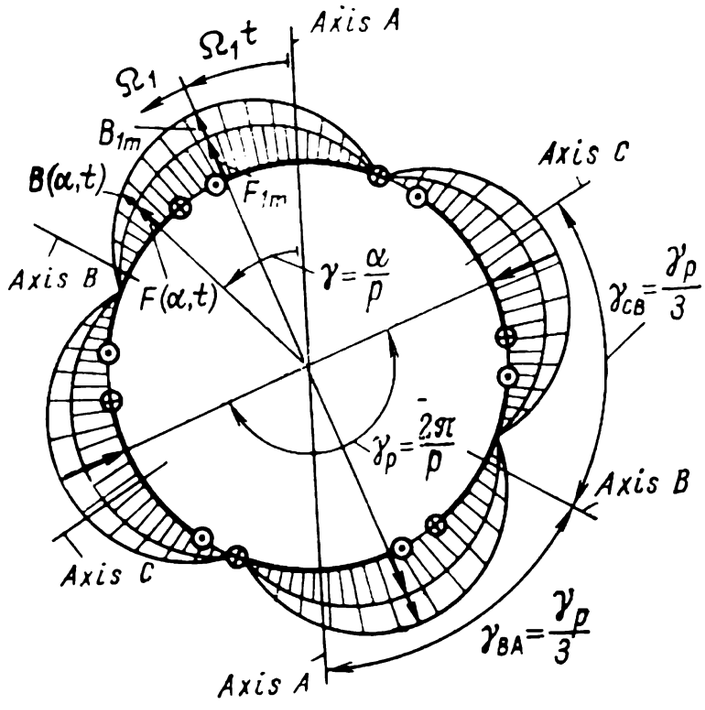

Fig. 25-9 Rotating magnetic field in the airgap of a polyphase $2p$-pole machine

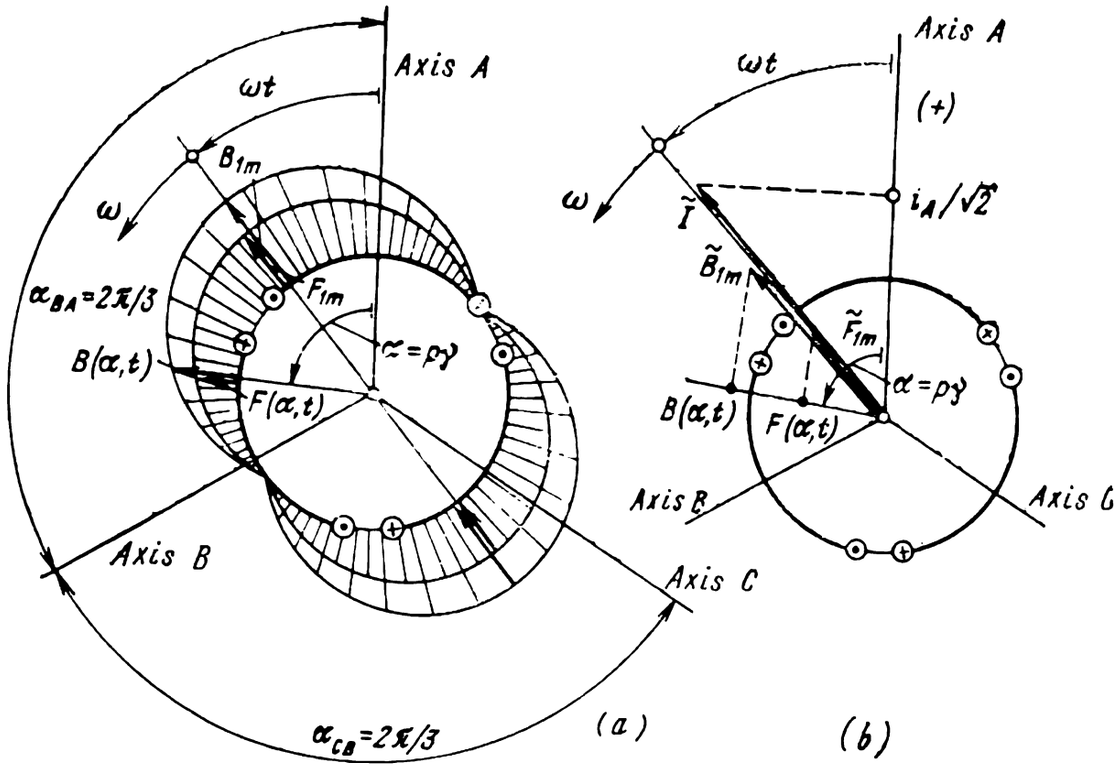

Fig. 25-10 Representation of the rotating magnetic field in the model of Fig. 25-9

25-6 Magnetic Flux Density Harmonics in the Rotating Magnetic Field of a Polyphase Winding

The magnetic flux density harmonics present in the field set up by a polyphase winding are functions of both the spatial distribution of the mmf in the winding and the saliency of the cores. Unfortunately, the saliency affects different harmonics differently, and the air gap factor used in calculating the fundamental component (see Sec. 25-5) does not permit the higher harmonics to be found with sufficient accuracy.

This is the reason why the first step in determining the magnetic field set up by a polyphase winding is to construct a stepped waveform for F, the phase mmf. Prior to that, we must calculate the instantaneous phase currents i_A, i_B, and i_C, the coil-side currents $\pm i_A w_c/a$, $\pm i_B w_c/a$, and $\pm i_C w_c/a$, and the slot currents $i_{s(k-1)}$, $i_{s(k)}$, and $i_{s(k+1)}$. This can readily be done, once the winding circuit is known. The stepped F waveform shown in Fig. 25-8 has been constructed within a pole pitch, τ. In Fig. 25-11, a similar mmf waveform is constructed for a half pole-pitch, $\tau/2$. In this case, we assign an arbitrary magnetic potential, say, $\varphi'_k = 0$, to one of the tooth (or slot) pitches, say, k. Then the potential at the next adjacent tooth pitch, $k + 1$, following the $(k + 1)$th slot with a current $i_{s(k+1)}$ will be

$$\varphi'_{k+1} = \varphi'_k + i_{s(k+1)}$$

(As will be recalled, the current in a slot is assumed to be positive when it is flowing outwards, that is, toward the reader.) Once the potentials in the tooth pitches lying between two adjacent poles, or within two pole pitches, have been found, the next step is to determine the average potential

$$\varphi_{av} = \frac{1}{n} \sum_{k=1}^{n} \varphi'_k$$

and the mmf, F, of the polyphase winding for each of the tooth pitches. It is measured over and above the average potential, φ_{av}, and is equal to

$$\varphi_{k-1} = \varphi'_{k-1} - \varphi_{av}$$

in the $(k-1)$th tooth pitch,

$$\varphi_k = \varphi'_k - \varphi_{av}$$

in the kth tooth pitch, and

$$\varphi_{k+1} = \varphi'_{k+1} - \varphi_{av}$$

in the $(k+1)$th tooth pitch, and so on.

The mmf thus found is shown in Fig. 25-11. It may be taken equal to the sum of tooth-pitch mmfs, $\varphi_k(x)$. Accord-

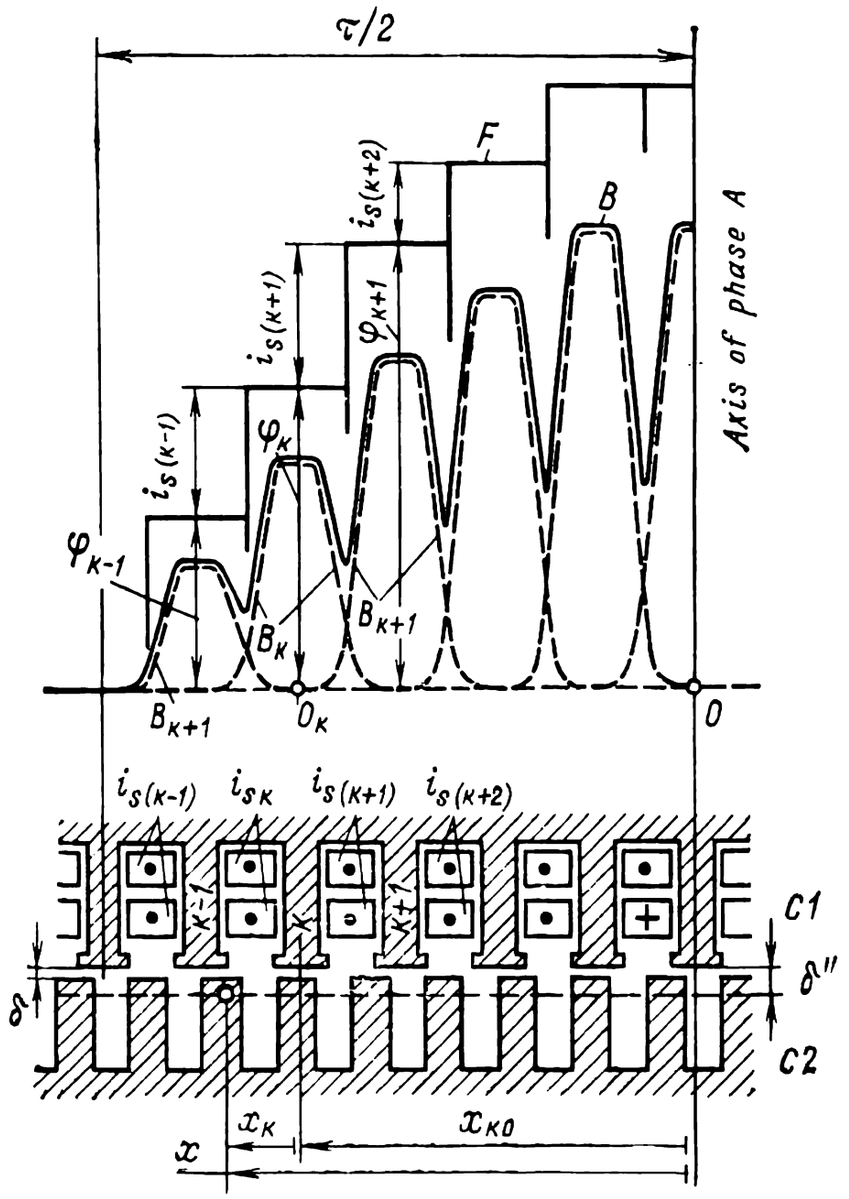

Fig. 25-11 The magnetic field of a polyphase winding and the specified distribution of instantaneous currents among the phases

ingly, the magnetic field set up by a polyphase winding may be defined as the sum of the elementary fields established by the tooth-pitch mmfs $\varphi_k(x)$. The distribution of the mmf for the kth tooth pitch is shown separately in

Fig. 25-12. As is seen, it is rectangular in shape, being $\varphi_k(x) = \varphi_k$ inside the tooth pitch, and

$$\varphi_k(x) = 0$$

outside the tooth pitch. This implies that in calculating the field the following boundary conditions must be assum-

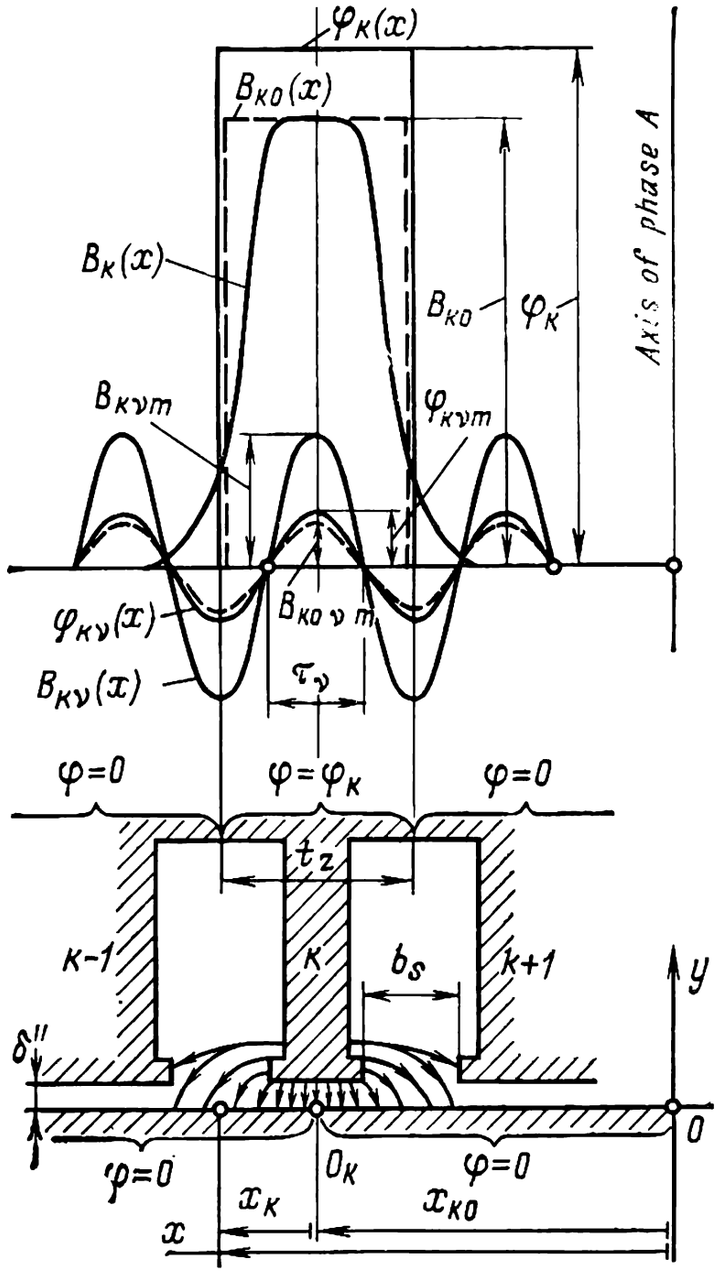

Fig. 25-12 The field set up by the mmf of the kth tooth (slot) pitch

ed: $\varphi = 0$ for core *2*, $\varphi = \varphi_k$ for the kth tooth pitch on core *1* and $\varphi = 0$ for the $(k + 1)$th and $(k - 1)$th and all the other tooth pitches on core *1*.

The field thus obtained is markedly affected by the shape of the slots and air gap. To simplify calculations, only the shape of the excited core, *1*, is accurately reproduced,

because its slots carry the winding in question. The unexcited core, *2*, is replaced by a smooth one, and the effect of its saliency on the air gap permeance is accounted for approximately by introducing an equivalent air gap

$$\delta'' = \delta k_{\delta 2}$$

[see Eq. (24-10)].

The scalar magnetic potential $\varphi(x, y)$ within the field region can be found analytically, using Eq. (23-8). Then the magnetic flux density is found at the surface of the smooth core, *2*, due to the mmf $\varphi_k(x)$:

$$B_k(x) = -\frac{\partial \varphi(x, y)}{\partial y} \mu_0$$

The plot of $B_k(x)$ is shown in Fig. 25-12. Its shape depends on two ratios, namely b_s/δ'' and t_Z/δ''. Because of this, the waveform of magnetic flux density for any other tooth pitch, say, $B_{k+1}(x)$ or $B_{k-1}(x)$, is similar in shape to that of $B_k(x)$. Their ordinates, however, are multiplied by φ_{k+1}/φ_k and φ_{k-1}/φ_k, respectively. Figure 25-11 shows how the resultant B produced by the mmf of a polyphase winding can be found by combining the magnetic flux densities of the individual tooth pitches, $B_k(x)$, $B_{k+1}(x)$, and $B_{k-1}(x)$.

The harmonic components of the resultant magnetic flux density may likewise be found by combining the harmonics of the magnetic flux densities in the individual tooth pitches, $B_k(x)$, $B_{k+1}(x)$, and $B_{k-1}(x)$. Because their respective waveforms are similar in shape, it will suffice to apply Fourier analysis to any one of them, say, $B_k(x)$.

Since the $B_k(x)$ waveform is symmetrical about the centre of the tooth pitch (see Fig. 25-12), its Fourier series contains only a constant component and cosine terms

$$B_k(x) = B_{k,\,\mathrm{av}} + \sum_{\nu=1}^{\infty} B_{k\nu m} \cos(\nu x_k \pi/\tau)$$

where $\nu = 1, 2, 3, \ldots$.

The peak value of the νth harmonic in the Fourier series is given by

$$B_{k\nu m} = \frac{1}{\tau} \int_{-\tau}^{\tau} B_k(x) \cos \frac{\nu x_k \pi}{\tau} \, \mathrm{d}x_k$$

Unfortunately, the analytical expression for $B_k(x)$ is so elaborate that the integral can only be evaluated numerically on a digital computer. To avoid cumbersome computations in engineering applications, Soroker* has proposed to express the peak value of the νth harmonic, $B_{k\nu m}$, in the Fourier expansion of $B_k(x)$ in terms of the νth harmonic, $B_{k0\nu m}$, taken from the Fourier expansion of an idealized rectangular magnetic flux density $B_{k0(x)}$ with a peak value

$$B_{k0} = \mu_0 \varphi_k / \delta''$$

Owing to the symmetry of the $B_{k0}(x)$ waveform about the centre of the tooth pitch (Fig. 25-12), its Fourier expansion likewise contains only a constant and cosine terms

$$B_{k0}(x) = B_{k0,\,\mathrm{av}} + \sum_{\nu=1}^{\infty} B_{k0\nu m} \cos \frac{\nu x_k \pi}{\tau},$$

$$\nu = 1,\ 2,\ 3,\ \ldots$$

The peak values of the expansion terms can readily be found analytically

$$B_{k0\nu m} = \frac{1}{\tau} \int_{x_k=-\tau}^{\tau} B_{k0}(x) \cos \frac{\nu x_k \pi}{\tau}\, \mathrm{d}x_k = (\mu_0/\delta'')\, \varphi_{k\nu m}$$

where

$$\varphi_{k\nu m} = \frac{1}{\tau} \int_{x_k=-0.5t_Z}^{0.5t_Z} \varphi_k \cos \frac{\nu x_k \pi}{\tau}\, \mathrm{d}x_k = \frac{2\varphi_k}{\nu\pi} \sin \frac{\nu t_Z \pi}{2\tau}$$

is the peak value of the νth harmonic mmf in the kth tooth pitch, $\varphi_k(x)$.

The νth harmonics of $B_k(x)$ and $B_{k0}(x)$ are shown in Fig. 25-12. As is seen, they have the same pole pitches, $\tau_\nu = \tau/\nu$, but different peak values, $B_{k\nu m}$ and $B_{k0\nu m}$. The ratio of the values of the magnetic flux density harmonics found with and without allowance for the effect of saliency is termed the slot factor for the νth harmonic

$$C_\nu = B_{k\nu m}/B_{k0\nu m} \qquad (25\text{-}20)$$

* Soroker T.G., Electrotechnicky Obzor, 1972, 10.

It is the same for all tooth pitches of a given core and solely depends on its relative dimensions and the harmonic number

$$C_\nu = f\,(b_s/\delta'',\ b_s/t_Z,\ Z/\nu p)$$

where Z = number of teeth on the core
p = number of pole pairs for the fundamental component
b_s = slot width at the air gap

From statistical analysis of the numerical values of C_ν found for various relative dimensions, the following approximate procedure has been proposed for its calculation.

The slot factor for the νth harmonic is

$$C_\nu = D_\nu - A_\nu/\tan\frac{\pi p\nu}{Z} \qquad (25\text{-}21)$$

where D_ν and A_ν are found, subject to the ratio b_s/δ'' and the value of

$$\varepsilon_\nu = \frac{\pi p\nu}{Z}\,\frac{b_s}{t_Z}$$

(i) For $\varepsilon_\nu \leqslant 2$,

$$A_\nu = \frac{\varepsilon_\nu}{1+5\delta''/b_s}\,(1 - \varphi_{mA}\varepsilon_\nu^2\delta''/b_s)$$

where

$$\varphi_{mA} = 0.4845 - 0.0255\ b_s/\delta'' + 0.0142\ (b_s/\delta'')^2$$

$$D_\nu = 1 - \varphi_{mB}\varepsilon_\nu^2\,(1 - \varphi_{mB}\varepsilon_\nu^2/6)$$

and

$$\varphi_{mB} = 0.5 + \frac{2}{3}\,(\delta''/b_s)^2 - \frac{1}{3\,(1+0.08b_s/\delta'')}$$

(ii) For $\varepsilon_\nu > 2$,

$$A_\nu = \exp\,(-1.46\ \varepsilon_\nu\delta''/b_s)\ \sin\,(0.95\ \varepsilon_\nu - \varphi_{mC})$$

$$D_\nu = \exp\,(-1.46\ \varepsilon_\nu\delta''/b_s)\ \cos\,(0.95\ \varepsilon_\nu - \varphi_{mC})$$

where

$$\varphi_{mC} = 0.7484 - 0.05037\ b_s/\delta'' + 0.001195\ (b_s/\delta'')^2$$

As an example, we shall trace the calculation of C_ν for the cores in Fig. 25-11 or 25-12:

$$\delta = 1\ \text{mm},\ b_s = b_{s1} = 5\ \text{mm},\ b_{s2} = 3.75\ \text{mm}$$

$$t_Z = t_{Z1} = 10\ \text{mm},\ t_{Z2} = 7.5\ \text{mm},\ Z = 24,\ p = 1$$

We shall carry out the calculations for the first tooth (slot) harmonic of order

$$\nu = Z/p - 1 = 24/1 - 1 = 23$$

The airgap factor for the second core [see Eq. (24-10)] is

$$k_{\delta 2} = 7.5/(7.5 - 1.607 \times 1) = 1.272$$

The term "1.607" is given by

$$\gamma = (3.75/1)^2/(5 + 3.75/1) = 1.607$$

The equivalent air gap is

$$\delta'' = \delta k_{\delta 2} = 1 \times 1.272 = 1.272 \text{ mm}$$

The values of the other quantities, as found by the equations given above, are as follows:

$$\begin{aligned} \varepsilon_\nu &= 1.5053 < 2 \\ \tan(\pi p \nu/Z) &= -0.13165 \\ \varphi_{mA} &= 0.60367 \\ \varphi_{mB} &= 0.28955 \\ A_\nu &= 0.43198 \\ D_\nu &= 0.41564 \\ C_\nu &= 3.713 \end{aligned}$$

Once C_ν is found, it is an easy matter to determine the peak value of the νth magnetic flux density harmonic due to the mmf of the kth tooth pitch, $\varphi_k(x)$, with allowance for the saliency of the core

$$B_{k\nu m} = C_\nu B_{k0\nu m} = \frac{\mu_0 C_\nu}{\delta''} \varphi_{k\nu m} \qquad (25\text{-}22)$$

where $\varphi_{k\nu m}$ is the peak value of the νth harmonic mmf over the kth tooth pitch.

Knowing the spatial distribution of the νth harmonic mmf over the kth tooth pitch

$$\varphi_{k\nu}(x) = \varphi_{k\nu m} \cos(\nu x_k \pi/\tau)$$

and using Eq. (25-22), we can readily write an equation for the distribution of the νth harmonic of the magnetic flux density with allowance for saliency

$$B_{k\nu}(x) = B_{k\nu m} \cos(\nu x_k \pi/\tau)$$

So that we could take the sum of the individual magnetic flux densities, we must write the above equation in a coordinate system common to all the loops and having its origin on the axis of phase A (see Figs. 25-11 and 25-12):

$$B_{k\nu}(x) = B_{k\nu m} \cos (x - x_{k0}) (\nu\pi/\tau)$$

Here, $x - x_{k0} = x_k$ is the distance from the axis of the kth tooth to a given point in the air gap, x_{k0} is the distance from the axis of phase A to the axis of the kth tooth, and x is the distance from the axis of phase A to the point in question.

Noting that $x\pi/\tau = \alpha$ is the electrical angle from the axis of phase A to the point in question for the fundamental component, and $x_{k0}\pi/\tau = \alpha_{k0}$ is the electrical angle from the axis of phase A to the axis of the kth tooth, we may rewrite the equations for the spatial disribution of the νth harmonics of the mmf and magnetic flux density as

$$\begin{aligned} \varphi_{k\nu}(\alpha) &= \varphi_{k\nu m} \cos \nu (\alpha - \alpha_{k0}) \\ B_{k\nu}(\alpha) &= B_{k\nu m} \cos \nu (\alpha - \alpha_{k0}) \end{aligned} \qquad (25\text{-}23)$$

Because the currents traversing the phases of the winding have an angular frequency ω, we may argue that the mmf over the kth tooth pitch varies in time with the same frequency

$$\varphi_k = \varphi_{km} \cos (\omega t - \beta_k)$$

where φ_{km} is the time peak value of the mmf over the kth tooth pitch, and β_k is the time phase of the mmf over the kth tooth pitch.

The peak values of the space harmonics of the mmf and magnetic flux density in the kth tooth pitch will vary in time in the same manner:

$$B_{k\nu m} = \frac{\mu_0 C_\nu}{\delta''} \varphi_{k\nu m}$$

where $\varphi_{k\nu m} = (2\varphi_k/\nu\pi) \sin (\nu t_Z \pi/2\tau)$ is the peak value of the νth harmonic mmf at time t, and

$\varphi_{k\nu mm} = (2\varphi_{km}/\nu\pi) \sin (\nu t_Z \pi/2\tau)$ is the peak value of the νth harmonic mmf at the time when

$$\varphi_k(t) = \varphi_{km}$$

Noting that in Eq. (25-23) both $\varphi_{k\nu m}$ and $B_{k\nu m}$ are functions of time, we may write the following equations for the νth harmonics of the mmf and magnetic flux density at any

point in the air gap at an angle α to the phase axis at any instant of time t:

$$\varphi_{k\nu}(\alpha, t) = \varphi_{k\nu mm} \cos(\omega t - \beta_k) \cos \nu (\alpha - \alpha_{k0}) \quad (25\text{-}24)$$

$$B_{k\nu}(\alpha, t) = (\mu_0 C_\nu/\delta'')\varphi_{k\nu mm} \cos(\omega t - \beta_k) \cos \nu (\alpha - \alpha_{k0})$$

On comparing the above equations with Eq.(24-37), it can be seen that they describe pulsating waves.

The resultant νth harmonic of the magnetic flux density in a polyphase winding is obtained by combining the magnetic flux densities due to the mmfs over the tooth pitches:

$$B_\nu(\alpha, t) = \sum_{k=1}^{Z} B_{k\nu}(\alpha, t) = \frac{\mu_0 C_\nu}{\delta''} \sum_{k=1}^{Z} \varphi_{k\nu}(\alpha, t)$$

The sum of the νth harmonic mmfs of all the tooth pitches $\sum_{k=1}^{Z} \varphi_{k\nu}(\alpha, t)$, is equal to the νth harmonic mmf of the polyphase winding, $F_\nu(\alpha, t)$.

Earlier (see Sec. 25-4), it has been shown that if $\nu = 2mc \pm 1$ (where $c = 0, 1, 2, 3, \ldots$), an m-phase winding will generate the νth harmonic mmf as a rotating wave which can be described by Eq. (25-15). Therefore,

$$\sum_{k=1}^{Z} \varphi_{k\nu}(\alpha, t) = F_\nu(\alpha, t) = F_{\nu m} \cos(\pm \omega t - \nu\alpha)$$

As a consequence, the νth harmonic of the magnetic flux density in a polyphase winding is given by

$$B_\nu(\alpha, t) = B_{\nu m} \cos(\pm \omega t - \nu\alpha) \quad (25\text{-}25)$$

where $B_{\nu m} = \mu_0 C_\nu F_{\nu m}/\delta''$ is the peak value of the rotating wave of the νth harmonic magnetic flux density in a polyphase winding.

To sum up, the magnetic flux density in a polyphase winding, as found with allowance for the effect of slots, contains the harmonics of the same order as that of the mmf harmonics. The effect of slots on the peak value of the magnetic flux density harmonics is accounted for by the factor C_ν calculated by Eq. (25-21).

The slot factor may be positive or negative. Accordingly, the magnetic flux density wave may be in phase or in antiphase with the mmf wave. For harmonics with large pole

pitches and satisfying the condition $\tau_\nu = \tau/\nu \gg t_{Z1}$. $C_\nu \approx 1/k_{\delta 1}$. Since for the fundamental component this condition is usually satisfied

$$\tau_1 \gg t_Z = \tau_1/m_1 q_1$$

the peak value of the associated magnetic flux density as given by Eq. (25-25) is

$$B_1 = F_{1m}\mu_0 C_1/\delta'' = F_{1m}\mu_0/\delta k_{\delta 1} k_{\sigma 2}$$

which checks with Eq. (25-18).

The νth harmonics of the magnetic flux density in the case of a rotating field have the same number of pole

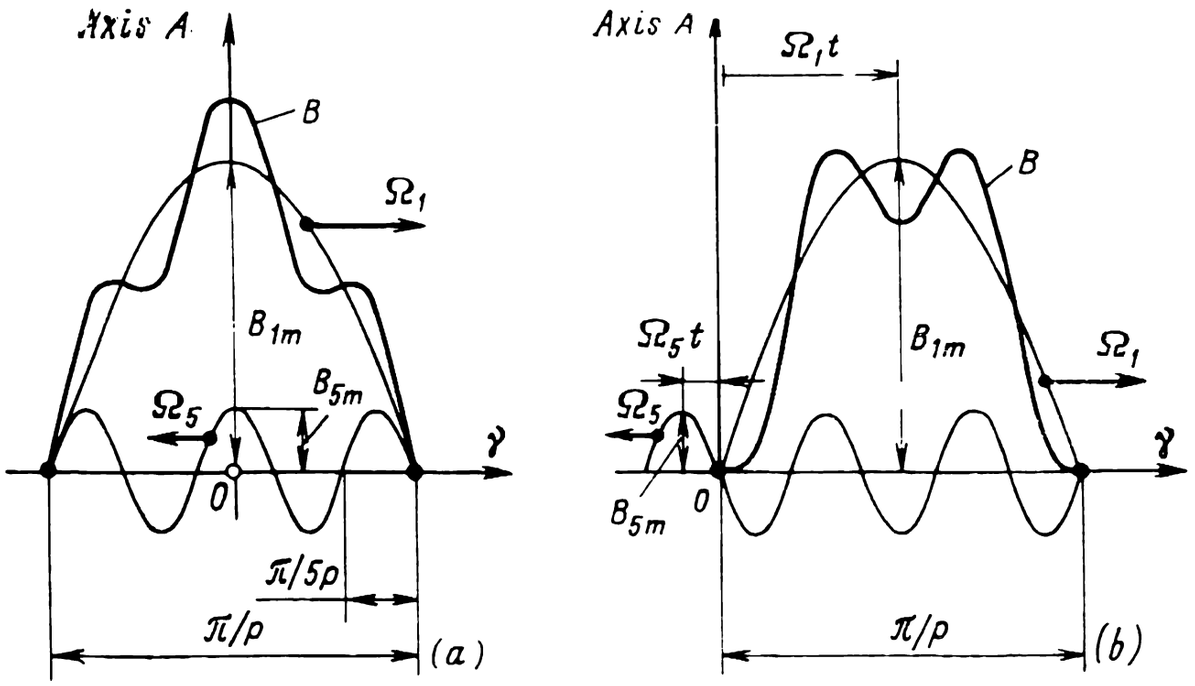

Fig. 25-13 The effect of higher harmonics on the waveform of the rotating **field set up by a polyphase** winding:
(*a*) field at $t = 0$, (*b*) field at $t = \pi/2\omega$

pairs, the same pole pitch, the same sense of rotation, and the same electrical angular frequency as the νth harmonic mmfs [see Eq. (25-13)]. From the fundamental flux density they only differ in the much smaller peak values, the number of pole pairs, and the mechanical frequency of rotation.

Because each harmonic component of the field travels at its own mechanical angular velocity Ω_ν, their relative position is changing all the time, and the resultant field pattern goes through a cycle of change periodically. This property of the field is illustrated in Fig. 25-13 where the magnetic flux density is shown as the sum of the fundamental

and the fifth harmonic. The magnetic flux density is given for two instants, namely $t = 0$, when the current in phase A of the three-phase winding is a maximum (see Fig. 25-13*a*), and $t = \pi/2\omega$, when the phase A current is zero (see Fig. 25-13*b*). At $t = 0$, the peak values of the harmonics occur on the phase axis. During the time $t = \pi/2\omega$ the fundamental wave travels in the positive direction through a mechanical angle

$$\Omega_1 t = (\omega/p)\,(\pi/2\omega) = \pi/2p$$

or an electrical angle $\pi/2$, whereas the 5th harmonic wave travels in the opposite direction through a mechanical angle

$$\Omega_5 t = (\omega/5p)\,(\pi/2\omega) = \pi/2\,(5p)$$

or an electrical angle

$$(5p)\,(\Omega_5 t) = \pi/2$$

Referring to the figure, the magnetic flux density waveform at $t = 0$ differs from that at $t = \pi/2\omega$ because the relative position of the harmonics is changing all the time. (For convenience, the fifth harmonic is shown enlarged fivefold.) When the contribution from the higher harmonics is insignificant, this change in shape is negligible.

The properties of the higher harmonics listed above are typical of the rotating fields produced by polyphase windings carrying balanced sets of PPS or NPS currents with a circular frequency ω.

To sum up, the harmonic components of the field set up by a polyphase winding rotate all at the same electrical velocity $\omega_v = \omega$ which is the same as the circular frequency of the currents, but with different mechanical angular velocities, $\Omega_v = \omega/vp$.

26 The Magnetic Field of a Rotating Field Winding

26-1 The Magnetic Field of a Concentrated Field Winding

Another way of producing a rotating field is to place the field winding on the rotor of a machine. When this winding is energized with d.c., it establishes a magnetic field statio-

nary relative to the rotor, with a radial component of magnetic flux density B (Fig. 26-1). If, now, the rotor is made to rotate at mechanical angular velocity Ω, the magnetic field set up by the rotor winding will likewise rotate with the same angular velocity.

The mmf F produced by a concentrated field winding can be depicted by a rectangular waveform (see Sec. 24-1). It remains constant and equal to $F_m = iw_c$ over a pole pitch. At the slot axis, it changes abruptly by an amount equal to the slot current, $2iw_c$, and reverses in polarity, turning to $-F_m$. The peak value of the mmf can be found as for a single-phase, double-layer, full-pitched winding for which $q = 1$ and $y_c = \tau$ and which carries a direct current, $i = \sqrt{2}\, I_a$:

$$F_m = q(\sqrt{2}\, I_a)\, w_c = iw_c$$

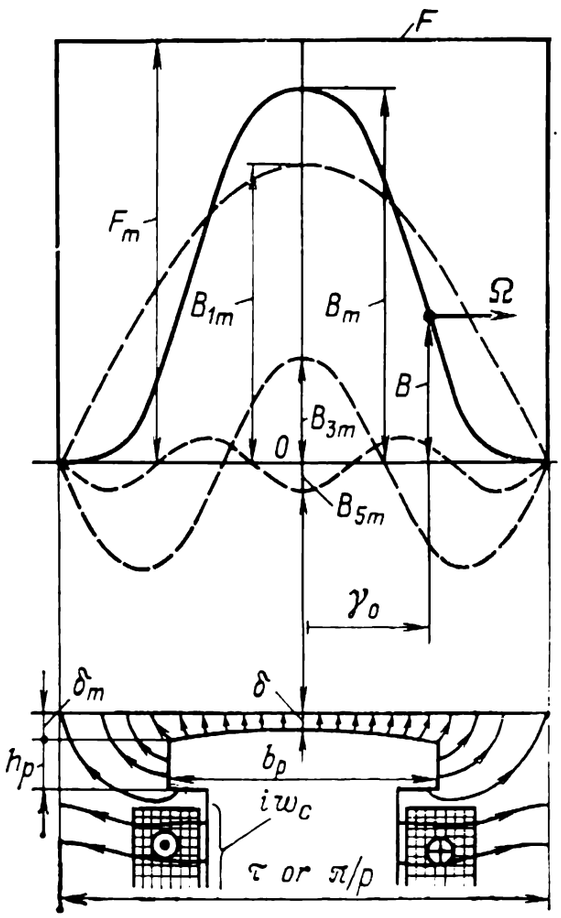

Fig. 26-1 The magnetic field of a concentrated field winding

The air gap field set up by F is calculated over a half-pole pitch by the Laplace equation, (23-8), for a scalar magnetic potential under the following boundary conditions: the potential at the surface of the pole-shoe is φ; the potential at the surface of the smooth core and at the slot axis is zero.

The shape of the waveform depicting the radial component of magnetic flux density at the surface of a smooth core, B, depends on the pole enclosure $\alpha = b_p/\tau$, the relative air gap at the pole tip $\gamma = \delta_m/\delta$, and the relative air gap at the pole axis, $\varepsilon = \delta/\tau$. The magnetic flux density waveform shown in Fig. 26-1 has been plotted for $\alpha = 0.55$, $\gamma = 2$, and $\varepsilon = 0.01$.

It is usual to generate magnetic flux density waveforms on a computer for various values of α, γ, and ε, and to subject them to Fourier analysis. The peak values of the various

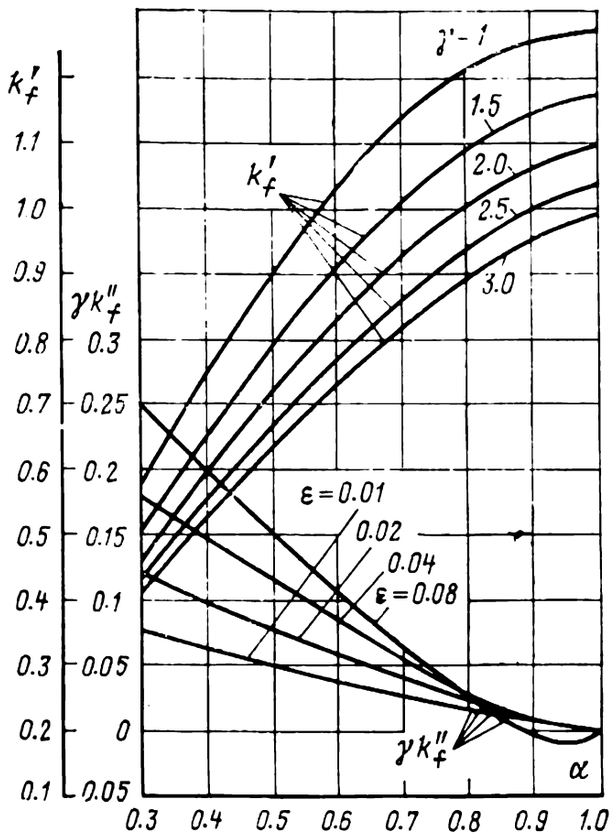

Fig. 26-2 The coefficients of the excitation field determining the mean magnetic flux density: $\alpha_f = \alpha'_f + \alpha''_f = B_{mean}/B_m$, and its fundamental: $k_f = k'_f + k''_f$

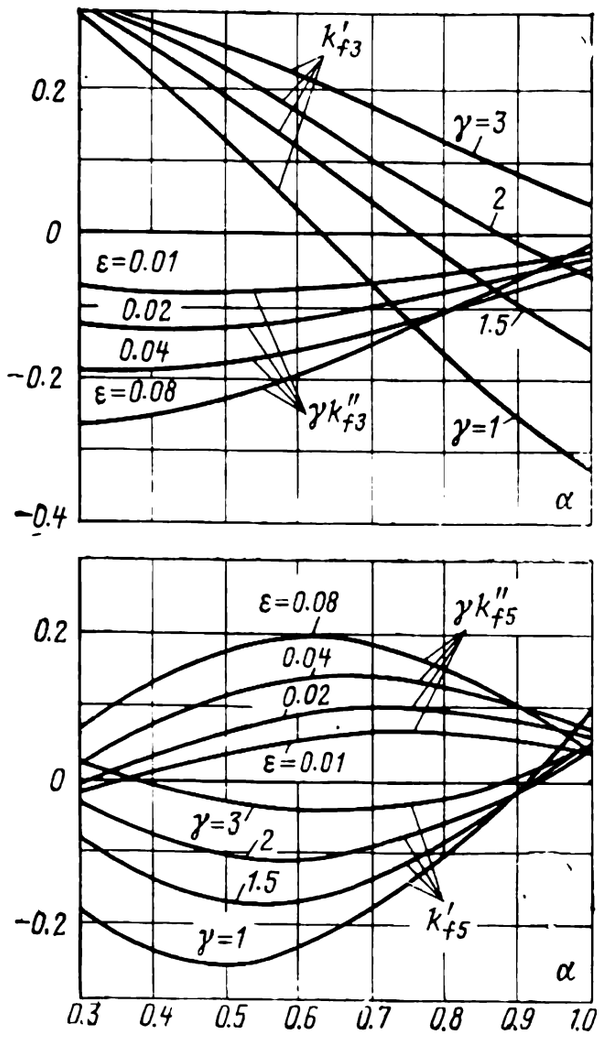

Fig. 26-3 Coefficients of the excitation field determining the higher harmonics of magnetic flux density: $k_{f\nu} = k'_{f\nu} + k''_{f\nu}$

harmonics are then expressed as fractions of the maximum flux density, B_m, called the harmonic coefficients of the excitation field:

$$k_f = B_{1m}/B_m \text{ for the fundamental} \quad (26\text{-}1)$$

$$k_{f\nu} = B_{\nu m}/B_m \text{ for the } \nu\text{th harmonic} \quad (26.2)$$

Here, $B_m = \mu_0 F_m/\delta$ is assumed to be the magnetic flux density set up in a uniform air gap δ by a constant mmf, F_m*.

The most accurate values for k_f and $k_{f\nu}$ for $\nu = 1$, 3, 5, 7, 9, 11, 13, 15, and 17 can be found in [38]. We will only give those required to calculate the harmonic coefficient for the fundamental, k_f (Fig. 26-2) and for the 3rd and 5th harmonics, k_{f3} and k_{f5} (Fig. 26-3). Referring to the figures, we can find the components of the respective harmonic coefficients, namely k'_f and k''_f, k'_{f3} and k''_{f3}, and k'_{f5} and k''_{f5}. (As is seen, the figures give $\gamma k''_f$, $\gamma k''_{f3}$, $\gamma k''_{f5}$.) The harmonic coefficients are found by combining their components for the specified values of α, γ, and ε:

$$k_f = k'_f + k''_f, \quad k_{f\nu} = k'_{f\nu} + k''_{f\nu}$$

The B waveform differs in shape from the mmf waveform and, with a judicious choice of the relative air-gap dimensions, it can be made sinusoidal very nearly. The magnetic flux density waveform can be expanded into a Fourier series where the equation for the νth harmonic about the winding axis is

$$B(\alpha) = B_{\nu m} \cos \alpha_{0\nu} \quad (26\text{-}3)$$

where $\alpha_{0\nu} = \nu\alpha_0 = \nu p\gamma_0$

α_0 = electrical angle defining the position of a given point relative to the winding axis, and

γ_0 = mechanical angle defining the position of the same point relative to the winding axis

26-2 The Magnetic Field of a Distributed Field Winding

The mmf produced by a distributed winding can be depicted by a stepped waveform (Fig. 26-4) similar to that for the phase mmf of a double-layer winding. For a single-layer distributed winding with a slot current iw_c and with q

* In this case, the scalar magnetic potential is $\varphi = F_m$.

wound slots per pole, the peak values of the harmonic mmfs can be found by Eq. (24-35) derived for a phase of a double-layer winding, assuming that the winding is full-pitched ($y_c = \tau$)* and that the maximum coil current in a double-

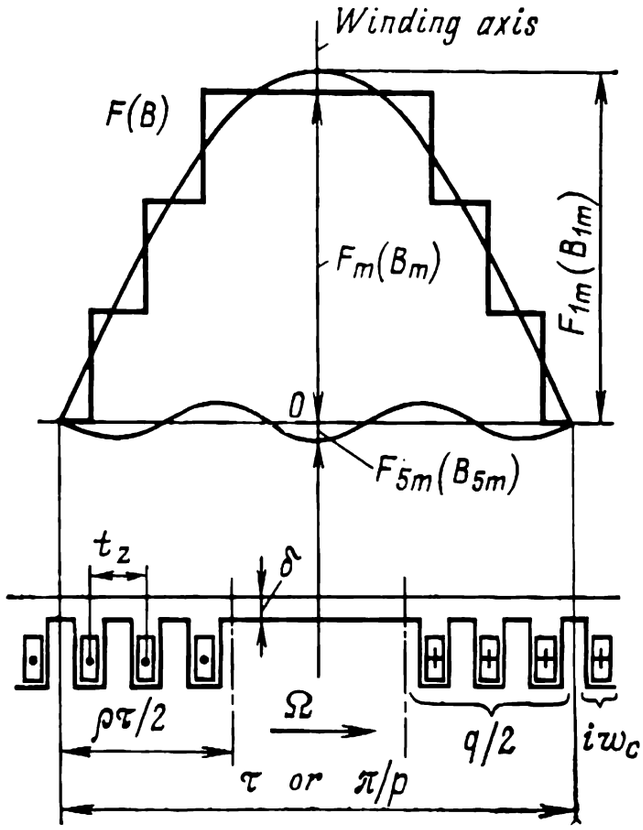

Fig. 26-4 The magnetic field set up by a distributed field winding ($q = 6$, $b/\tau = 2/3$)

layer winding, $\sqrt{2}I_a w_c$, is equal to half the slot current in the field winding, iw_c.

Noting that for $y_c = \tau$, the harmonic pitch factor is unity, $k_{p\nu} = 1$, Eq. (24-35) can be re-written to give the following expression for the peak value of the νth harmonic mmf:

$$F_\nu = \frac{2qk_{d\nu}}{\pi\nu} iw_c = \frac{4k_{d\nu}}{\pi\nu} iw \qquad (26\text{-}4)$$

where

$w = w_c q/2$ = turns per pole of the field winding

$k_{d\nu} = \dfrac{\sin(q\nu\gamma_Z/2)}{q\sin(\nu\gamma_Z/2)}$ = distribution factor for the νth harmonic

$\gamma_Z = t_Z\pi/\tau = \rho\pi/q$ = electrical angle between adjacent wound slots

* As regards the generation of a magnetic field, the field winding may be treated as a full-pitched winding, because the distance between adjacent groups of wound slots is equal to the pole pitch.

t_Z = tooth (slot) pitch
$\rho = b/\tau$ = enclosure of the wound part of a pole
b = length of the wound part of a pole pitch

In this case, the air gap permeance may be deemed constant and equal to

$$\lambda_0 = 1.\delta$$

over the entire length of the pole pitch. Therefore, the magnetic flux density waveform, $B = \mu_0 F \lambda_0$, is the same in shape as the mmf waveform, and the peak values of the harmonic flux densities are proportional to those of the harmonic mmfs

$$B_\nu = \mu_0 F_\nu \lambda_0$$

The equation for the νth magnetic flux density harmonic, referred to the winding axis, does not differ from that for a concentrated winding, Eq. (26-3).

26-3 The Rotating Harmonics of the Excitation Field

As the rotor rotates at mechanical angular velocity Ω, the excitation field and its harmonics (Fig. 26-5 shows only the fundamental and the 5th harmonic) rotate all at the same mechanical angular velocity Ω. This is the reason why, in contrast to the rotating field set up by a polyphase winding, the field established by the field winding remains unchanged in shape as it rotates.

In contrast, the electrical angular velocities of the various harmonics are all different

$$\omega_\nu = p_\nu \Omega_\nu = \nu p \Omega$$

As is seen, it increases with the harmonic order. (Compare it with the field set up by a polyphase winding, where the electrical angular velocities are the same, but the mechanical angular velocities are different.)

An equation for the νth harmonic of the rotating magnetic flux density wave produced by the field winding, referred to a stationary reference axis, may be derived from Eq. (26-3) for the same harmonic. Assume that at $t = 0$ the axis of the winding rotating at mechanical angular velocity Ω runs along the reference axis (see Fig. 26-5*a*). On this

assumption, the angular coordinates of an arbitrary point relative to the winding axis, γ_0, and relative to the reference axis, γ, at an arbitrary instant of time will be connected by an equation of the form

$$\gamma = \gamma_0 + \Omega t$$

Considering the above equation together with Eq. (26-3),

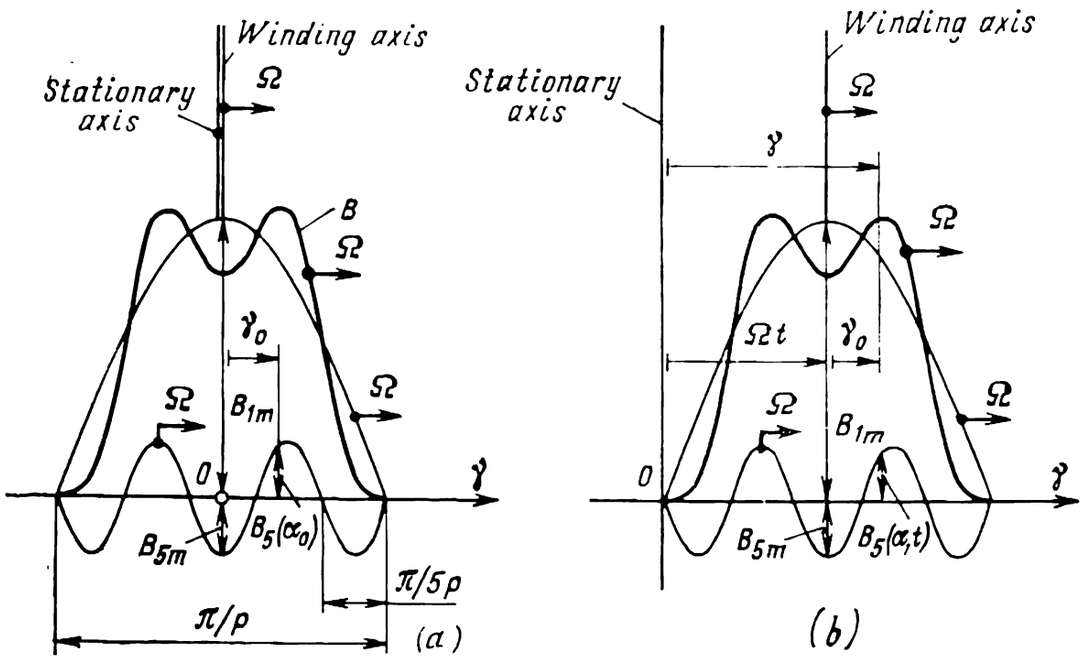

Fig. 26-5 Higher harmonics of the excitation field (*a*) at $t = 0$, (*b*) at an arbitrary time t

we obtain the equation for the νth harmonic of the rotating flux density wave

$$B_\nu(\alpha, t) = B_{\nu m} \cos(\nu p \Omega t - \nu p \gamma) = \\ = B_{\nu m} \cos(\omega_\nu t - \nu \alpha) \qquad (26\text{-}5)$$

Outwardly, Eq. (26-5) is the same as Eq. (25-10) or (25-20) for the νth harmonic of the flux density wave produced by a polyphase winding. The coefficient of γ in this equation is the number of pole pairs for the harmonic in question, $\nu p = p_\nu$. The coefficient of t is the electrical angular velocity of the harmonic, $\nu p \Omega = p_\nu \Omega = \omega_\nu$. The ratio of the two coefficients is the mechanical angular velocity

$$\nu p \Omega / \nu p = \Omega$$

27 Flux Linkages of and EMFs Induced by Rotating Fields

27-1 Introductory Notes

When energized, the windings of an electrical machine set up magnetic fields varying in time and space. As has been shown in Chapters 25 and 26, the air gap magnetic flux density, no matter how it is produced, can be expanded into a Fourier series and presented as the sum of rotating fields differing in the peak value of the radial component, $B_{\nu m}$, the number of pole pairs, p_ν, and the mechanical angular velocity, Ω_ν.

An important problem in the theory of electrical machines is to determine the flux linkages with, and the emfs induced in, the phase winding by the rotating fields. Because polyphase windings and rotating field windings are always designed so that the higher harmonics rapidly diminish in amplitude with increasing order, the winding field can, to a good approximation, be represented by the first term ($\nu = 1$) of the Fourier series. The flux density wave of such a rotating field, with a peak value B_{1m}, is shown, for example, in Figs. 25-9, 25-13, and 26-1.

Relative to a stationary reference axis, the flux density of the forward rotating field is given by Eq. (25-18) as

$$B(\alpha, t) = B_{1m} \cos(\omega t - \alpha) = B_{1m} \cos(p\Omega t - p\gamma) \quad (27\text{-}1)$$

The emf induced in a phase winding by a rotating field can be found as the sum of the emfs in its coils. Therefore, we shall begin by finding the flux linkage and emf for one coil.

27-2 The Flux Linkage and EMF of a Coil

Consider a coil displaced from the origin 0 by a distance x_c along the periphery of the core. The axis of this coil is turned by a mechanical angle $\gamma_c = x_c/R$ from the stationary reference axis. Here, $R = \tau p/\pi$ is the mean radius of the air gap periphery (Fig. 27-1). In the general case, the coil pitch y_c is taken to be shorter than the pole pitch τ. The me-

chanical angle spanned by the coil or the coil pitch angle is

$$\gamma_y = y_c/R$$

The rotating wave of flux density described by Eq. (27-1) travels relative to the coil at mechanical angular velocity Ω. At time t, the axis of the rotating field is displaced from the reference axis by an angle Ωt and takes up the position shown in the figure. The radial component of B at any point

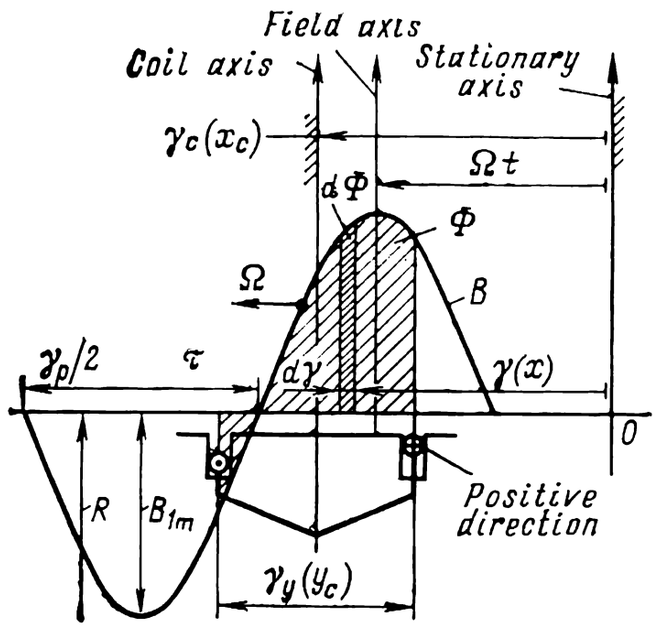

Fig. 27-1 To determining the flux linkage of a coil turn

on the circle, with an angular coordinate γ relative to the reference axis and at time t, can be found by Eq (27-1).

The magnetic flux Φ links with the coil turns through an area A_y of a cylindrical surface of radius R; it spans an arc y_c and extends along the generator of the cylinder for a distance equal to the axial gap length, l_δ (see Sec. 23-5), or mathematically,

$$\Phi = \int_{A_y} B_n \, dA = \int_{A_y} d\Phi$$

Recalling that over the axial gap length the flux density at the axis of the machine remains constant and that in a cylindrical system of coordinates the normal component at a cylindrical surface is equal to the radial component,

$$B_n = B_R = B$$

we may replace integration over a surface by integration over a circle on which the position of a point is defined by the angular coordinate γ.

An elementary area dA may be expressed in terms of an elementary length along the circle, $dx = R d\gamma$, as follows:

$$dA = l_\delta dx = l_\delta R d\gamma$$

Then, an elementary flux will be given by

$$d\Phi = B l_\delta R d\gamma$$

and the integral will have to be taken over the coil pitch, that is, from $\gamma_c' = \gamma_c - \gamma_y/2$ to $\gamma_c'' = \gamma_c + \gamma_y/2$:

$$\Phi_{(t=\text{const})} = \int_{A_y} d\Phi = \int_{\gamma_c'}^{\gamma_c''} B l_\delta R \, d\gamma$$

$$= B_{1m} l_\delta R \int_{\gamma_c'}^{\gamma_c''} \cos(\omega t - p\gamma) \, d\gamma$$

$$= \frac{B_{1m} l_\delta R}{p} \sin(p\gamma - \omega t) \Big|_{\gamma_c'}^{\gamma_c''}$$

Upon substituting the limits of integration and expanding the sines of the sum and difference of angles, namely

$$\sin [(\alpha_c - \omega t) + \alpha_y/2]$$

and

$$\sin [(\alpha_c - \omega t) - \alpha_y/2]$$

we get

$$\Phi = \Phi_{ym} \cos(\omega t - \alpha_c) = k_p \Phi_m \cos(\omega t - \alpha_c) \quad (27\text{-}2)$$

where

$\Phi_{ym} = k_p \Phi_m$ = maximum flux that can link with a given coil of coil pitch y_c

$\Phi_m = \frac{2}{\pi} \tau l_\delta B_{1m}$ = maximum flux linking with a full-pitched coil, $y_c = \tau$

$k_p = \sin(\alpha_y/2) = \sin(y_c \pi/2\tau)$ = pitch factor for the fundamental component of the field

$\alpha_y = p\gamma_y = y_c\pi/\tau$ = electrical angle spanned by the coil

$\alpha_c = p\gamma_c = x_c\pi/\tau$ = electrical angle defining the position of the coil axis relative to the reference axis (origin)

It is seen from Eq. (27-2) that the flux linking the coil turns varies with an angular frequency $\omega = p\Omega$, equal to

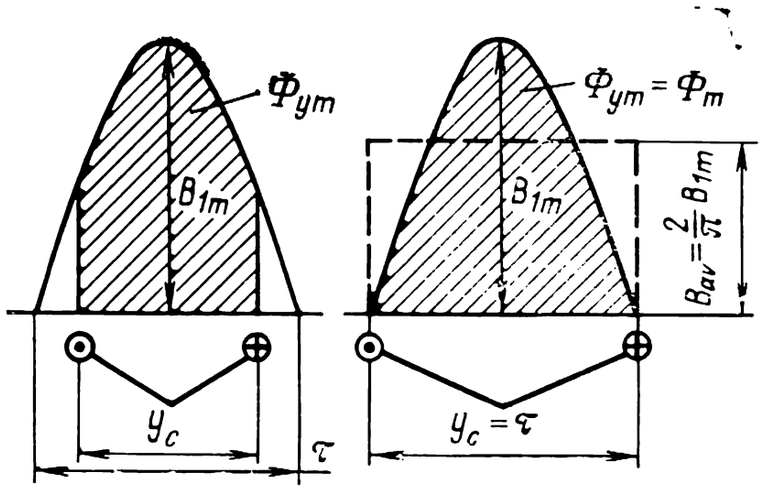

Fig. 27-2 The effect of pitch-shortening (chording) on the maximum flux linking the coil

the electrical angular velocity of the wave. The frequency of the flux is given by

$$f = \omega/2\pi = \Omega p/2\pi$$

Accordingly, the time period of the flux is

$$T = 1/f = 2\pi/\Omega p = \gamma_p/\Omega$$

It is also seen from Eq. (27-2) (see Fig. 27-2 as well) that the flux linking a turn passes through a positive maximum $\Phi = \Phi_{ym}$ when $\omega t - \alpha_c = 0$, that is, at time

$$t = \alpha_c/\omega = p\gamma_c/p\Omega = \gamma_c/\Omega$$

when the axis of the field aligns itself with the coil axis

$$\Omega t = \Omega\,(\gamma_c/\Omega) = \gamma_c$$

The amount by which the flux lags behind depends on the electrical angle $\alpha_c = p\gamma_c$ defining the position of the coil relative to the reference axis.

The maximum coil flux is equal to the shaded area in Fig. 27-2*a*.

The flux linkage of the rotating field with the coil is found by multiplying the flux defined in Eq. (27-2) by the number of coil turns w_c

$$\Psi = w_c\Phi = \Psi_{cm}\cos(\omega t - \alpha_c) \tag{27-3}$$

where

$$\Psi_{cm} = w_c k_p \Phi_m = w_c \Phi_{ym}$$

is the peak or maximum flux linkage with the coil.

The instantaneous emf induced in the coil is given by

$$\begin{aligned} e &= -\mathrm{d}\Psi/\mathrm{d}t = \omega\Psi_{cm}\sin(\omega t - \alpha_c) \\ &= \sqrt{2}\,E_c\sin(\omega t - \alpha_c) \end{aligned} \tag{27-4}$$

The rms value of the coil emf is

$$E_c = \omega\Psi_{cm}/\sqrt{2} = w_c k_p \Phi_m \omega/\sqrt{2} \tag{27-5}$$

Both the flux linkage and the emf can be portrayed on a time vector (phasor) diagram (Fig. 27-3) as complex functions $\tilde{\Psi}_{cm}$ and $\tilde{E}_c$ whose projections on the real axis of the complex plane aligned with the time axis give the respective instantaneous values:

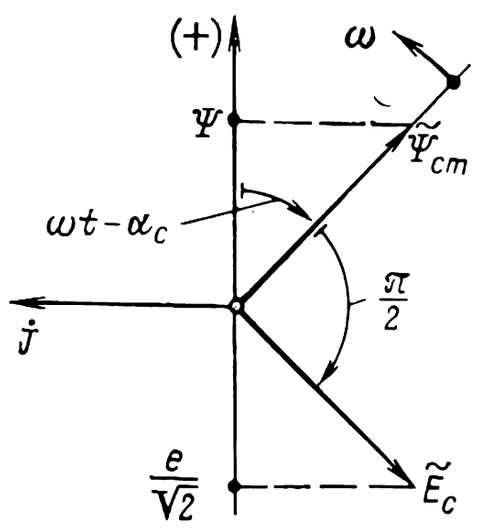

Fig. 27-3 Phasor diagram o the coil flux linkage and emf

$$\begin{aligned} \Psi &= \mathrm{Re}\,(\tilde{\Psi}_c) \\ &= \mathrm{Re}\,\{\Psi_{cm}\exp[j(\omega t - \alpha_c)]\} \\ e &= \mathrm{Re}\,(\sqrt{2}\,\tilde{E}_c) \\ &= \mathrm{Re}\,\{\sqrt{2}\,E_c \\ &\quad \times \exp[j(\omega t - \alpha_c - \pi/2)]\} \end{aligned} \tag{27-6}$$

The positions that the above phasors take up in Fig. 27-3 correspond to the magnetic field shown in Fig. 27-1. Here, $\Psi > 0$, because the flux is directed with the coil axis, whereas $e < 0$ which implies that it is directed against the positive direction in the coil, in accord with the right-hand screw rule.

The coil emf is

$$\tilde{E}_c = -j(\omega/\sqrt{2})\,\tilde{\Psi}_{cm} \tag{27-7}$$

27-3 The Flux Linkage and EMF of a Coil Group

Each pole pitch of a double-layer winding has q coils of a given phase (in Fig. 27-4, $q = 3$).

The waveform of the flux linkages and emfs for the coil group shown in Fig. 27-4, plotted by Eq. (27-3), (27-4) or (27-6), appears in Fig. 27-5. Because the coils in the group are displaced from each other by an electrical angle

$$\alpha_Z = p\gamma_Z = (t_Z/\tau)\,\pi = \alpha_{c2} - \alpha_{c1} = \alpha_{c3} - \alpha_{c2} = \ldots$$

the flux linkage and emf phasors are likewise displaced from each other by the same angle.

The events in the $(k+1)$th (say, second) coil lag behind those in the kth (say, first) coil by the time required for the flux density wave to move through a mechanical angle γ_Z, that is,

$$t = \gamma_Z/\Omega = p\gamma_Z/p\Omega = \alpha_Z/\omega$$

This lag must be allowed for in combining the flux linkages (and emfs) within a given coil group.

The coil-group flux linkage and emf phasors, $\tilde{\Psi}_g$ and $\tilde{E}_g$, are each the phasor sum of the coil linkages and emfs, $\tilde{\Psi}_{c1}$, $\tilde{\Psi}_{c2}$, $\tilde{\Psi}_{c3}$ and $\tilde{E}_{c1}$, $\tilde{E}_{c2}$, $\tilde{E}_{c3}$. Going back to Eq. (24-29) and Figs. 24-10 and 24-11 in Sec. 24-5, it will be recalled that the problem of combining several phasors equal in magnitude,

$$\Psi_{c1m} = \Psi_{c2m} = \Psi_{c3m} = \Psi_{cm}$$

or

$$E_{c1} = E_{c2} = E_{c3} = E_c$$

and displaced from each other by the same angle α_Z has already been solved in determining the mmf of the winding. Therefore, the coil-group flux linkage and emf may be written

$$\begin{aligned} \Psi_{gm} &= q\Psi_{cm}k_d = qw_c k_p k_d \Phi_m \\ E_g &= qE_c k_d \end{aligned} \qquad (27\text{-}8)$$

The coil-group flux linkage phasor is directed along the axis of symmetry of the coil phasors and, as is seen from a comparison of Figs. 27-5 and 27-4, is turned through an angle $(\omega t - \alpha_{ph})$ from the real axis of the complex plane. Here, $\alpha_{ph} = p\gamma_{ph}$ is the electrical

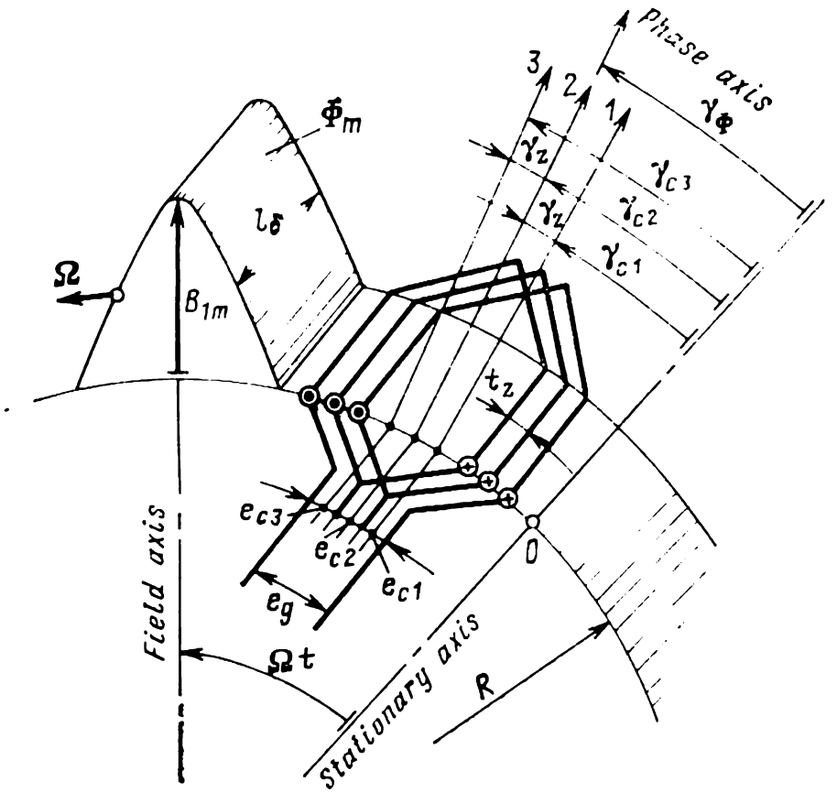

Fig. 27-4 EMF induced in a coil group

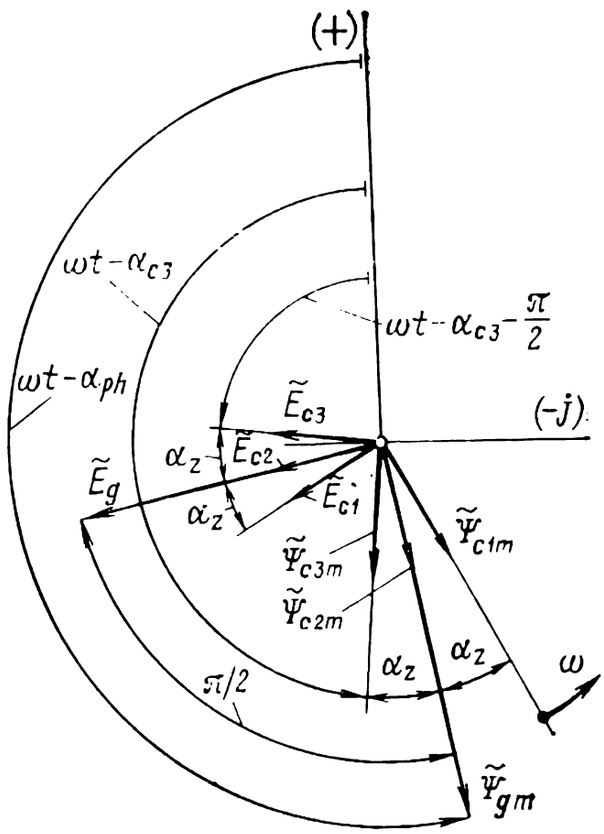

Fig. 27-5 Phasor diagram of flux linkage and emf for a coil group

angle of a coil group or the phase axis. It is to be noted that the axis of a coil group (the phase axis) is the axis of symmetry for the coil group. The angle defining the position of this axis is found as the arithmetic mean of the angles defining the positions of the coils in the group

$$\gamma_{ph} = \frac{\gamma_{c1} + \gamma_{c2} + \ldots + \gamma_{cq}}{q} = \frac{\alpha_{c1} + \alpha_{c2} + \ldots + \alpha_{cq}}{pq} = \alpha_{ph}/p \tag{27-9}$$

The coil-group emf lags behind the coil-group flux linkage by $\pi/2$, and may be written as

$$\tilde{E}_g = -j\tilde{\Psi}_{gm}\omega/\sqrt{2} \tag{27-10}$$

27-4 The Flux Linkage and EMF of a Phase

A phase of a winding is made up of coil groups connected in series-parallel (see Sec. 22-3) A phase of a double-layer winding has $2p$ identical coil groups (one group per pole

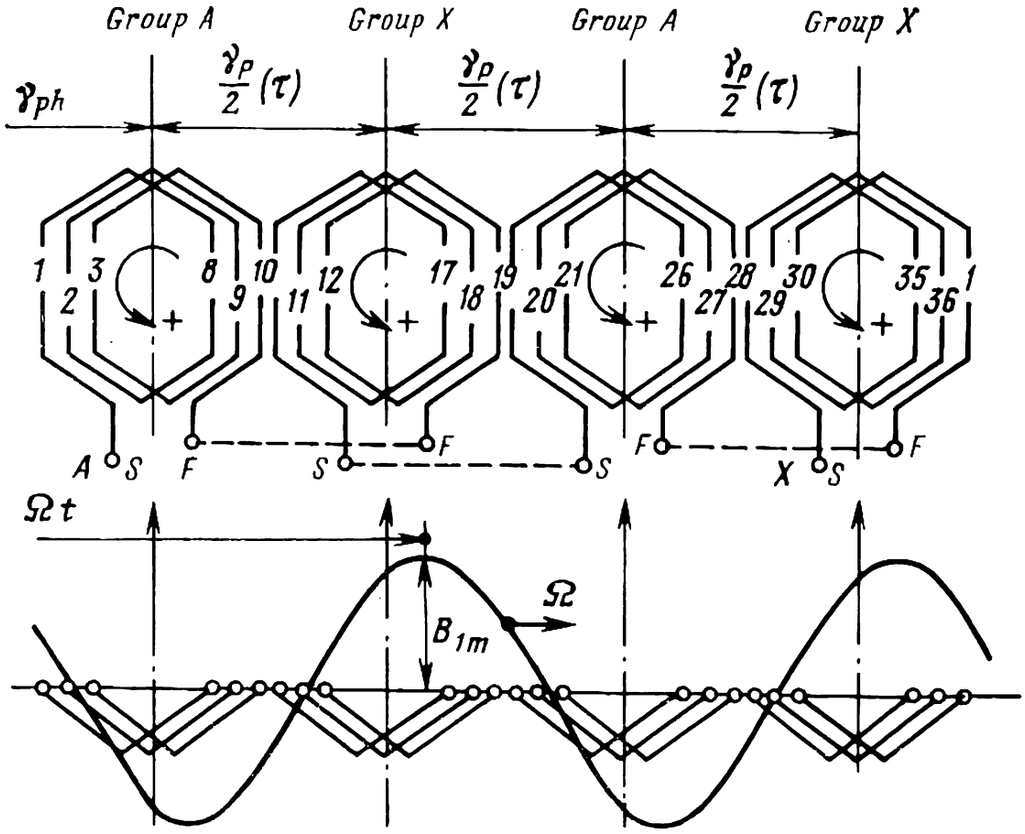

Fig. 27-6 EMF induced in the coil groups of a phase by a rotating field

pitch). As an example, Fig. 27-6 shows the coil groups of phase A in a four-pole, three-phase winding ($2p = 4$). Its complete circuit diagram is shown in Fig. 22-5. Adjacent

coil groups in the phase are displaced from one another by one pole pitch τ or by a half of the pole-pitch angle

$$\gamma_p/2 = 2\pi/2p = \pi/p$$

The respective electrical angle is

$$\alpha_p/2 = p\gamma_p/2 = \pi$$

Therefore, the flux linkages and emfs of the backward coil groups in the same phase, $\tilde{\Psi}_{gXm}$ and $\tilde{E}_{gX}$, are in antiphase with those of the forward coil groups, $\tilde{\Psi}_{gAm}$ and $\tilde{E}_{gA}$. If a phase has a parallel paths (circuits), then each path contains $2p/a$ coil groups. The forward coil groups are connected aiding (with their finishes to the phase finish), whereas the backward coil groups are connected in opposition (with their starts to the phase finish). Exactly this form of connection of coil groups in parallel paths is shown in Figs. 22-5 and 22-6. Now the positive direction around a parallel path (from its finish X towards its start A) is the same as the positive direction around a coil group (from its finish F towards its start S) in all the forward groups connected aiding (A) and is opposite to the positive direction around all the backward coil groups (X).

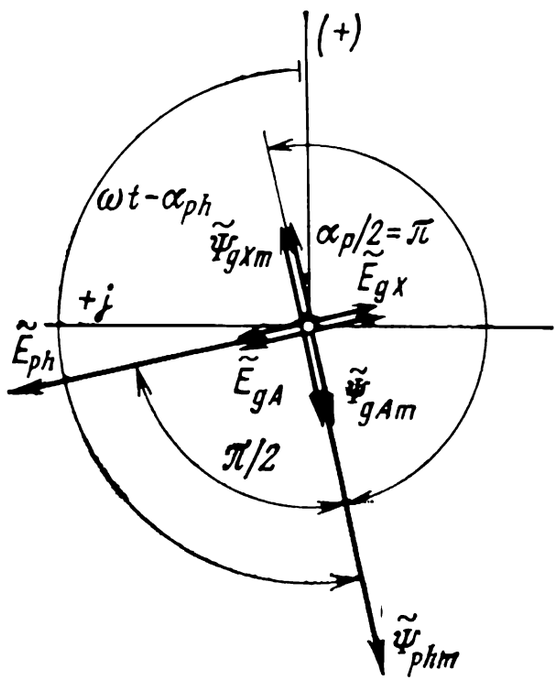

Fig. 27-7 Phasor diagram of flux linkage and emf for a phase in a double-layer winding

With this arrangement, the flux linkages and emfs of the coil groups are combined arithmetically within a particular path, and the flux linkages and emfs in all the paths are the same (Fig. 27-7).

The phase flux linkage and phase emf are respectively equal to the flux linkage and emf of a path

$$\tilde{\Psi}_{phm} = \frac{p\tilde{\Psi}_{gAm} - p\tilde{\Psi}_{gXm}}{a} = 2p\tilde{\Psi}_{gAm}/a \qquad (27\text{-}11)$$

$$\tilde{E}_{ph} = \frac{p\tilde{E}_{gA} - p\tilde{E}_{gX}}{a} = 2p\tilde{E}_{gA}/a \qquad (27\text{-}12)$$

The phase emf can be expressed in terms of the phase flux linkage directly

$$\tilde{E}_{\text{ph}} = 2p\tilde{E}_{gA}/a = -j2p\omega\tilde{\Psi}_{gAm}/a\sqrt{2}$$
$$= -j\omega\tilde{\Psi}_{\text{phm}}/\sqrt{2} \qquad (27\text{-}13)$$

The phase flux linkage (see Figs. 27-6 and 27-7) is in the same direction as the flux linkage of the main coil group whose axis is taken as the phase axis and makes an angle

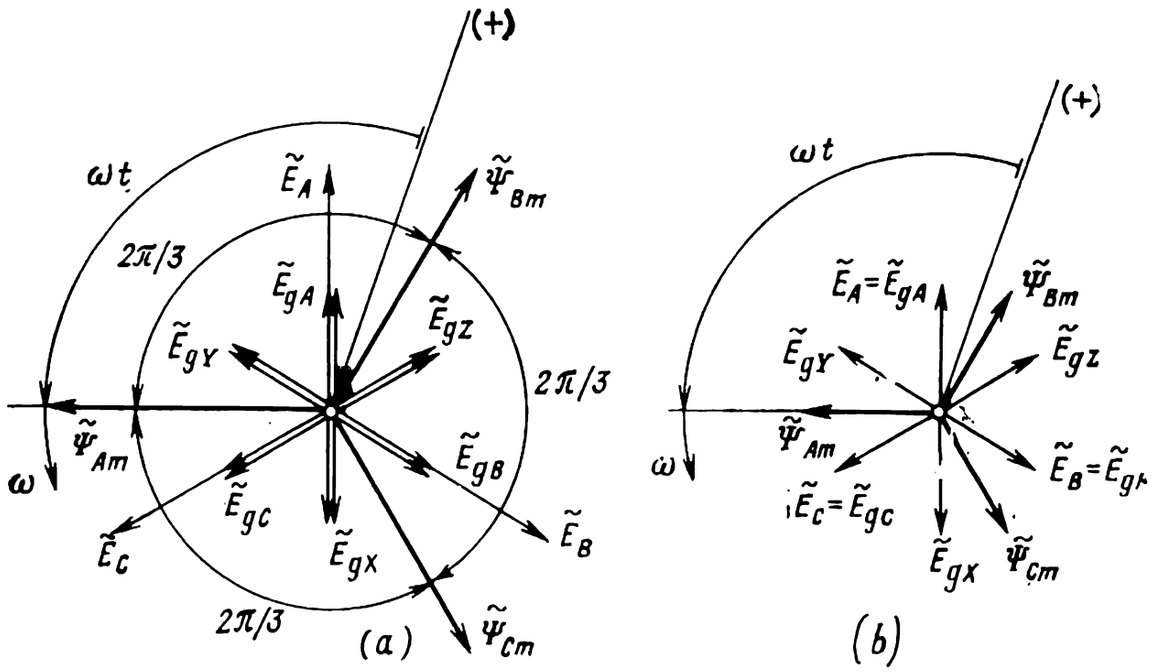

Fig. 27-8 Phasor diagrams of flux linkages and emfs for the phases and coil groups of a three-phase winding:
(*a*) for two paths (circuits) in a phase; (*b*) for four paths (circuits) in a phase

$\alpha_{\text{ph}} = p\gamma_{\text{ph}}$ with the origin. The phase emf lags behind the phase flux linkage by $\pi/2$ (see Figs. 27-7 and 27-8).

The magnitude of the phase flux linkage or phase emf is $2p/a$ times the magnitude of the coil-group flux linkage or emf. The phasor diagrams in Figs. 27-7 and 27-8 are plotted for phase A consisting of the coil groups shown in Fig. 27-6. In Fig. 27-6, the number of paths is $a = 1$, so $2p/a = 4$ (see the dashed connections in Figs. 27-6 and 22-5). In Fig. 27-8*a*, the number of paths is $a = 2$, so $2p/a = 2$. In Fig. 27-8*b*, $a = 4$, so $2p/a = 1$ (see Fig. 22-6*b*).

In accord with Eqs. (27-8) and (27-11), the peak value of the phase flux linkage is

$$\Psi_{\mathrm{ph}m} = 2p\Psi_{gm}/a = wk_{\mathrm{w}}\Phi_m \qquad (27\text{-}14)$$

where

$w = 2pw_{\mathrm{c}}q/a$ = number of series turns per phase
$k_{\mathrm{w}} = k_p/k_{\mathrm{d}}$ = phase winding factor (for the fundamental component of the field)
Φ_m = peak value of the magnetic flux over a pole pitch

The rms value of phase emf given by Eq. (27-13) is

$$E_{\mathrm{ph}} = \omega\Psi_{\mathrm{ph}m}/\sqrt{2} = 2\pi f w k_{\mathrm{w}}\Phi_m/\sqrt{2} \qquad (27\text{-}15)$$

27-5 The Flux Linkages and EMFs of a Polyphase Winding. A Space-Time Diagram of Flux Linkages and EMFs

All the phases in a symmetrical polyphase winding are identical in arrangement. Adjacent phases, say, phases A and B, whose axes make mechanical angles γ_A and γ_B with the stationary reference axis, are displaced from each other by a mechanical angle (see Fig. 22-6)

$$\gamma_{BA} = \gamma_B - \gamma_A = 2\pi/mp = \gamma_{\mathrm{p}}/m$$

or by an electrical angle

$$\alpha_{BA} = \alpha_B - \alpha_A = p\gamma_{BA} = 2\pi/m$$

Therefore, the phase flux linkages and phase emfs are the same in magnitude (Fig. 27-8):

$$\Psi_{Am} = \Psi_{Bm} = \Psi_{Cm} = \Psi_m$$
$$E_A = E_B = E_C = E$$

In the case of a forward rotating field, that is, one moving from phase A to phase B to phase C, the flux linkages and emfs of a polyphase winding form on the complex plane an m-ray star in which the adjacent arms are displaced from each other by an angle $2\pi/m$ (for a three-phase winding, this angle is $2\pi/3$, see Fig. 27-8).

Let the axis of phase A run along the stationary reference axis. Mathematically, this will be written as

$$\alpha_A = p\gamma_A = 0$$

and the instantaneous phase flux linkages will be

$$\Psi_A = \Psi_{Am} \cos(\omega t - \alpha_A) = \Psi_{Am} \cos \omega t$$
$$\Psi_B = \Psi_{Bm} \cos(\omega t - \alpha_{BA}) = \Psi_{Bm} \cos(\omega t - 2\pi/3)$$
$$\Psi_C = \Psi_{Cm} \cos(\omega t - \alpha_{CA}) = \Psi_{Cm} \cos(\omega t - 4\pi/3)$$

Or, in complex notation,

$$\Psi_A = \mathrm{Re}\,[\tilde{\Psi}_{Am}] = \mathrm{Re}\,[\tilde{\Psi}_{Am} \exp(j\omega t)]$$
$$\Psi_B = \mathrm{Re}\,[\tilde{\Psi}_{Bm}] = \mathrm{Re}\,[\tilde{\Psi}_{Am} \exp(-j2\pi/3)]$$
$$\Psi_C = \mathrm{Re}\,[\tilde{\Psi}_{Cm}] = \mathrm{Re}\,[\tilde{\Psi}_{Am} \exp(-j4\pi/3)]$$

The instantaneous phase emfs can be written in a similar way:

$$e_A = \sqrt{2}\,E_A \cos(\omega t - \pi/2)$$
$$e_B = \sqrt{2}\,E_B \cos(\omega t - \pi/2 - \alpha_{BA})$$
$$= \sqrt{2}\,E_B \cos(\omega t - \pi/2 - 2\pi/3)$$

Or, in complex notation,

$$e_A = \mathrm{Re}\,[\sqrt{2}\,\tilde{E}_A] = \mathrm{Re}\,\{\sqrt{2}\,\tilde{E}_A \exp[j(\omega t - \pi/2)]\}$$
$$e_B = \mathrm{Re}\,[\sqrt{2}\,\tilde{E}_B] = \mathrm{Re}\,[\sqrt{2}\,\tilde{E}_B \exp(-j2\pi/3)]$$

By analogy with the phase currents (see Sec. 25-3 and Fig. 25-6), the phase flux linkages (phase emfs) can be depicted on the complex plane of a two-pole model as complex functions common to all the phases.

For the three-phase winding whose flux linkages and emfs are shown on the time complex plane (Fig. 27-8*a*), the flux linkage phasors

$$\tilde{\Psi}_m = \Psi_m \exp(j\omega t)$$

and the emf phasors

$$\tilde{E} = E_{\mathrm{ph}} \exp[j(\omega t - \pi/2)]$$

corresponding to the respective phase quantities are shown on the space complex plane of the model in Fig. 27-9. In the two-pole model, the phase windings are each shown for clarity as a single coil; the positive direction is shown in the sectional view drawn in the same figure. The phase axes are drawn through the centres of the coil groups represented by

one coil. The instantaneous phase flux linkages (or the instantaneous phase emfs reduced by a factor of $\sqrt{2}$) are given by projections of the respective phasors on the axis of the respective phase.

Because the position of the flux linkage or of the emf relative to the axis of a given phase in Fig. 27-9 is the same as that of the flux linkage (or emf) of that phase relative to the real axis of the time complex plane, their instantaneous flux linkage (or the instantaneous emf) is the same in either case.

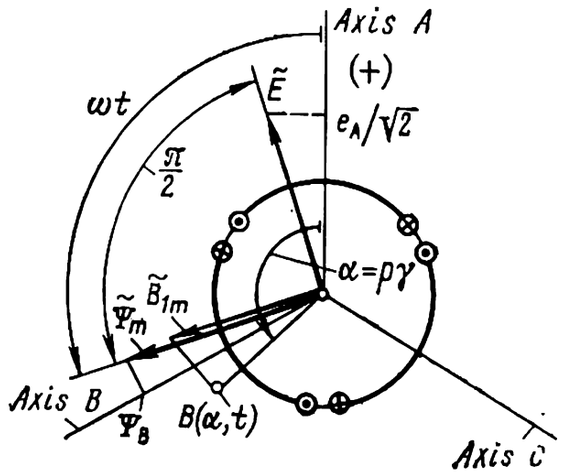

Fig. 27-9 Rotating-field flux density, phase flux linkages and phase emfs shown on the space complex plane of a two-pole model

The space complex plane in Fig. 27-9 also shows the complex function

$$\tilde{B}_{1m} = \dot{B}_{1m} \exp(j\omega t)$$

depicting the magnetic flux density of the rotating field we are considering [see Eq. (27-1)]. It has been plotted in exactly the same way as in Fig. 25-10. (It will be recalled that the axis of phase *A* has been assumed to run along the stationary reference axis.)

As follows from Fig. 27-9 and the applicable equations, the complex functions depicting the magnetic flux density of a rotating field and the flux linkage produced by that field are both in the same direction. This is because the phase flux linkage is a maximum at the instant when the magnetic flux density at the phase axis is a maximum (see above).

27-6 The Flux Linkages and EMFs due to the Harmonics of a Nonsinusoidal Rotating Magnetic Field

As has been explained in Chapters 25 and 26, a rotating field may, in addition to the fundamental component, contain an amount of harmonics.

A rotating field containing harmonics is nonsinusoidal. The flux linkages and emfs produced by the

harmonics can be found by the equations derived for the fundamental component, if they are re-arranged to include the respective harmonic quantities, such as $B_{\nu m}$, τ_ν, and Ω_ν.

From Eq. (27-14) it follows that the νth harmonic component of a rotating field gives rise to a flux linkage with each phase winding, defined (the peak value is meant) by

$$\Psi_{\mathrm{ph}\nu m} = w k_{\mathrm{w}\nu} \Phi_{\nu m} \tag{27-16}$$

where $k_{\mathrm{w}\nu} = k_{\mathrm{p}\nu} k_{\mathrm{d}\nu}$ = phase winding factor for the νth harmonic

$k_{\mathrm{p}\nu}$ = pitch factor for the νth harmonic, Eq. (24-27)

$k_{\mathrm{d}\nu}$ = distribution factor for the νth harmonic, Eqs. (24-32) and (24-33)

$\Phi_{\nu m} = (2/\pi)\tau_\nu l_\delta B_{\nu m}$ = magnetic flux due to the νth harmonic over a pole pitch, Eq. (27-2)

It follows from Eq. (27-15) that the rms value of the phase emf induced by the νth harmonic of the magnetic field is given by

$$E_{\mathrm{ph}\nu} = (\omega_\nu/\sqrt{2})\,\Phi_{\mathrm{ph}\nu m} = (2\pi/\sqrt{2})\, f_\nu w k_{\mathrm{w}\nu} \Phi_{\nu m}$$
$$= 2\sqrt{2}\, f_\nu w k_{\mathrm{w}\nu} (\tau/\nu)\, l_\delta B_{\nu m} \tag{27-17}$$

where $\omega_\nu = \Omega_\nu p_\nu = \Omega_\nu p\nu$ = electrical angular velocity of the harmonic, equal to the circular frequency of the induced emf

$f_\nu = \omega_\nu/2\pi$ = frequency of the induced emf

The emfs induced by the harmonics are superimposed on the emf induced by the fundamental component and affect the resultant phase emf and, in the final analysis, the performance of the machine. This effect varies according as the nonsinusoidal rotating field is produced. Consider two cases which are most typical of all, namely: the magnetic field produced by a polyphase winding (see Chap. 25), and the magnetic field produced by a rotating field winding (see Chap. 26).

1. Typically, the waveform of the nonsinusoidal magnetic field set up by a polyphase winding is continually varying in shape, because its rotating harmonics travel at different mechanical angular velocities (see Fig. 25-13 and Sec. 25-6):

$$\Omega_\nu = \omega/p_\nu = \omega/p\nu$$

where $\omega = 2\pi f$ is the circular frequency of the currents in the polyphase winding.

It is readily seen [see Eq. (27-17)] that the rotating harmonics of this field induce emfs of the same frequency equal to the frequency of the current in the winding

$$\omega_\nu = 2\pi f_\nu = \Omega_\nu p\nu = \omega = 2\pi f$$

A more detailed analysis would show that the emfs due to the harmonics are in phase with the fundamental emf and are added to it arithmetically. The harmonics do not affect the waveform of the fundamental emf, and the resultant emf is sinusoidal.

The effect of the νth harmonic on the rms emf depends on the ratio

$$E_{\mathrm{ph}\nu}/E_{\mathrm{ph}} = k_{\mathrm{w}\nu}B_{\nu m}/\nu k_{\mathrm{w}}B_{1m} = k_{\mathrm{w}\nu}\Phi_{\nu m}/k_{\mathrm{w}}\Phi_m$$

Therefore, even for a concentrated ($q = 1$), full-pitched ($y_{\mathrm{c}} = \tau$) winding, when $k_{\mathrm{w}\nu} = k_{\mathrm{w}} = 1$, this effect is $1/\nu$ of that produced by the νth harmonic of magnetic flux density (with a peak value $B_{\nu m}$) on the fundamental flux density (with a peak value B_{1m}).

Still, the total emf induced by all the harmonics

$$E_{\sigma,\mathrm{rms}} = \sum_{\nu \neq 1} E_{\mathrm{ph}\nu} = 2\sqrt{2} f w \tau l_\delta \sum_{\nu \neq 1} k_{\mathrm{w}\delta}B_{\nu m}/\nu$$

may be fairly large in magnitude, especially in a full-pitched winding and with small values of q.

In practical machines, the ratio

$$E_{\sigma,\mathrm{rms}}/E_{\mathrm{ph}} = \sum_{\nu \neq 1} E_{\mathrm{ph}\nu}/E_{\mathrm{ph}} = \sum_{\nu \neq 1} k_{\mathrm{w}\nu}B_{\nu m}/\nu k_{\mathrm{w}}B_{1m}$$

may range anywhere between 0.005 and 0.05. The smaller values apply to short-pitched windings for which $y_{\mathrm{c}} \approx \approx 0.83\tau$, and $q \gg 1$, so that $k_{\mathrm{w}\nu}/\nu k_{\mathrm{w}} \ll 1$ (see Chap. 24).

Energy conversion by electrical machines mainly utilizes the fundamental component, the sole contributor to the useful field. The fields set up by the harmonics may be classed as leakage field. In Soviet usage, they are referred to as *differential* or *difference leakage fields*, because their sum may be looked upon as the difference between the resultant field of a polyphase winding and the fundamental (or useful) field.

The total harmonic emf

$$E_{\sigma,\mathrm{rms}} = \sum_{\nu \neq 1} E_{\mathrm{ph}\nu}$$

is accordingly called the *differential* (or *difference*) *leakage emf* and treated separately from the emf induced by the fundamental field (see Sec. 28-7).

2. For the nonsinusoidal magnetic field established by a rotating field winding, it is characteristic that the magnetic flux density waveform remains unchanged as the field rotates (see Fig. 26-5 in Sec. 26-3).

Because of this, all of its harmonics rotate at the same mechanical angular velocity equal to the mechanical angular velocity of the field winding

$$\Omega_\nu = \Omega$$

The frequency of the emfs induced by the field harmonics is proportional to the order (number) of the harmonics [see Eq. (27-17)]

$$\omega_\nu = 2\pi f_\nu = \Omega_\nu p\nu = \Omega p\nu = \omega\nu = 2\pi f\nu$$

where $\omega = 2\pi f$ is the circular frequency of the emf induced by the fundamental field.

Thus, the emf induced by the νth space harmonic of the field is the νth time harmonic of the emf. The contribution by the various harmonics depends on the ratio

$$E_{\mathrm{ph}\nu}/E_{\mathrm{ph}} = k_{\mathrm{w}\nu}B_{\nu m}/k_{\mathrm{w}}B_{1m} \qquad (27\text{-}18)$$

where, as will be recalled, $f_\nu = \nu f$. The higher values of the above ratio correspond to a larger departure of the resultant emf from the sinusoidal waveform. On the other hand, for energy conversion by electrical machines and transformers to be most economical (to suffer a minimum of loss), it is essential that the voltages, emfs and currents involved be as close to a sinusoidal waveform as practicable. One of the causes of the increased losses associated with a nonsinusoidal voltage waveform is the circulating currents produced by harmonic emfs and flowing between the machines when several of them are connected for parallel operation.

In designing an electrical machine, every effort is made to make the winding voltages as close to sinusoidal as practicable. In Soviet practice, this is assessed in terms of the deviation factor of a voltage (current) wave defined as

$$k\ (\text{per cent}) = \frac{\sqrt{\sum_{\nu \neq 1} E_{\nu m}^2}}{E_{1m}} \times 100$$

where E_{1m} is the peak value of voltage at the fundamental frequency, and $E_{\nu m}$ is the peak value of the νth harmonic voltage.

One way to achieve this goal is to make as sinusoidal as possible the waveform of the magnetic flux density due to the excitation field (we have already shown how this can be done with a concentrated and a distributed field winding in Chap. 26). Still, for all the measures taken, the distortion factor of the excitation field may exceed the limit. In fact, if the time waveform of the emf were allowed to follow that of magnetic flux density in space, the machine would not be able to perform its designated function. Fortunately, this only happens (compare Figs. 27-10*a* and *b*) in a concentrated phase winding with one coil per group ($q = 1$) and wound with a full pitch ($y_c = \tau$). In the circumstances, $k_w = k_{w\nu} = 1$ and, as follows from Eq. (27-18), the ratio of the harmonic emfs to the fundamental is the same as the ratio of the harmonic flux density to the fundamental component, or mathematically

$$E_{ph\nu}/E_{ph} = B_{\nu m}/B_{1m}$$

When the phases of a three-phase winding are star-connected, the line voltage is free from triplen harmonics of emf, that is, those for which $\nu = 3k = 3, 9, 15$, etc., where $k = 1, 3, 5$, etc. This is so because (see Part One of this text) the harmonic emfs of such an order are the same in all the phases ($e_{A\nu} = e_{B\nu} = e_{C\nu}$), and cancel one another in the line emfs found as the difference of the phase emfs:

$$e_{AB\nu} = e_{A\nu} - e_{B\nu} = 0$$

When a three-phase winding is delta-connected, the line voltage is again free from the triplen harmonics but for a different reason (see Part I of the text). The point is that around a delta circuit the triplen harmonics are added together arithmetically, giving rise to a circulating current

$$\dot{I}_\nu = 3\dot{E}_{A\nu}/3Z_{ph}$$

so that the respective harmonics of line voltage add to zero:

$$\dot{V}_{A\nu} = \dot{E}_{A\nu} - Z_{ph}\dot{I}_\nu = 0$$

Thus, as we have seen, the waveform of line voltage in a three-phase winding is improved as compared with the

waveform of magnetic flux density (see Fig. 27-10*c*) even in the case of the least perfect winding configuration ($y_c = \tau$, $q = 1$). A further improvement in the waveform of both phase and line voltage in three-phase windings can be obtained

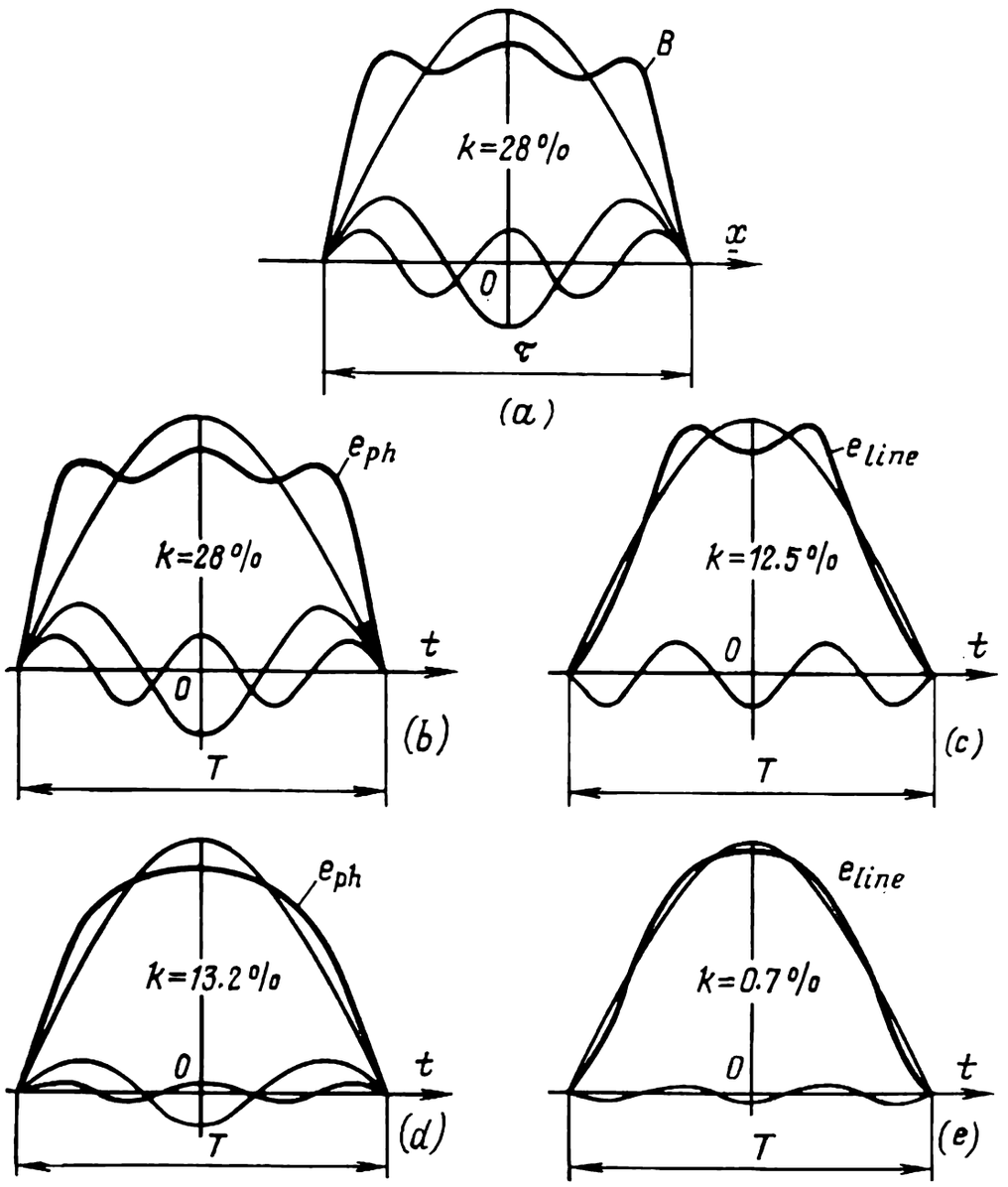

Fig. 27-10 Effect of three-phase winding arrangement on the waveform of phase and line emfs:
(*a*) waveform of the excitation-field flux density; (*b*) phase emf for $y_c = \tau$, $q = 1$; (*c*) line emf for $y_c = \tau$ and $q = 1$; (*d*) phase emf for $y_c = 0.83\tau$, $q = 2$; (*e*) line emf for $y_c = 0.83\tau$, $q = 2$

by using distributed windings ($q > 1$) wound with a short pitch ($y_c \approx 0.83\tau$). In such windings, for all harmonics, except the tooth harmonics (slot ripple), as has been shown in Figs. 24-9 and 24-12, we get

$$k_{wv}/k_w = (k_{pv}k_{dv}/k_pk_d) \ll 1$$

Hence,

$$E_{\text{ph}\nu}/E_{\text{ph}} = k_{\text{w}\nu}B_{\nu m}/k_{\text{w}}B_{1m} \ll B_{\nu m}/B_{1m}$$

This implies that the waveform of emf is more sinusoidal than that of magnetic flux density (see Fig. 27-10*d* and *e*). As is seen, when $y_c \approx 83\tau$ and $q \geqslant 2$, the emf is practically sinusoidal, even though the waveform of magnetic flux density due to the excitation field is substantially nonsinusoidal.

It should be added that in such windings the rms value of phase or line emf does not practically differ from the rms value of the fundamental emf

$$E_{\text{ph}\,\Sigma} = \sqrt{E_{\text{ph}}^2 + E_{\text{ph3}}^2 + E_{\text{ph5}}^2 + E_{\text{ph7}}^2 + \ldots} \approx E_{\text{ph}}$$

28 The Inductances of Polyphase Windings

28-1 The Useful Field and the Leakage Field

Let us consider the magnetic field in an electrical machine with two polyphase windings one of which is wound on the stator, and the other on the rotor.

Assuming that the relative permeability of the stator and rotor cores is infinitely large ($\mu_r = \infty$), the steady-state magnetic field of such a machine can be visualized as consisting of two components, namely the useful field and the leakage field.

As will be recalled the *useful magnetic field* is that which is associated with the fundamental component of the radial magnetic flux density in the air gap. This field plays the decisive part in energy conversion. When $\mu_r = \infty$, the useful field may be imagined as formed by two fields which are stationary relative to each other, namely the useful stator field set up by the currents in the stator winding, and the useful rotor field set up by the currents in the rotor winding. Of course, the air gap flux density due to each of these fields contains only the fundamental component. In turn, the useful stator (rotor) field may be visualized as the sum of the useful fields established by the various phases of the stator (rotor) winding.

The *leakage field* is that which is established by the sets of currents in the stator and rotor windings that do not contribute to the useful field. In other words, when the fundamental fluxes of the stator and rotor fields cancel out, the leakage field only exists in the machine.

The total flux linkage of a polyphase winding may be visualized as the sum of the useful flux linkage and the leakage flux linkage. The former is associated with the useful field whose lines close via the air gap and link both windings of the machine. For this reason, it is called the mutual field. The leakage flux linkage is associated with that part of the leakage field which links only one (stator or rotor) winding.

28-2 The Main Self-Inductance of a Phase

The main phase self-inductance is associated with the mutual flux linkage produced by the respective phase current. Let us find the main self-inductance of phase A in the stator winding. Suppose that the phase winding carries by a positive current whose peak value is

$$i_A = \sqrt{2}\, I_A$$

In Fig. 28-1, phase A is shown for clarity as a single coil. The fundamental component of the phase mmf with the peak value given by Eq. (24-28) is

$$F_{\text{ph}1m} = 2\sqrt{2}\, I_A w_1 k_{\text{w}1}/\pi p$$

In the air gap, it gives rise to a cosinusoidally distributed mutual magnetic field whose flux density at the phase axis, according to Eq. (25-18), is

$$B_{1m} = \mu_0 F_{\text{ph}1m} \lambda_0 = \frac{2\sqrt{2}\, I_A w_1 k_{\text{w}1} \mu_0}{\pi p \delta k_\delta}$$

The fundamental component of the phase mmf and the normal component of the air gap flux density are shown in Fig. 28-1*a*, and the phase magnetic field pattern in Fig. 28-1*b*. Recalling that the axis of the magnetic field runs along the phase axis, its flux linkage with the phase winding [see Eqs. (27-2), (27-13), and (27-14)] can be written as

$$\Psi_{AAm} = w_1 k_{\text{w}1} \Phi_m = \frac{2}{\pi} \tau l_\delta w_1 k_{\text{w}1} B_{1m}$$

This flux linkage is proportional to the number of mutual field lines that cut the surface which spans the contour of coil AX representing phase A actually consisting of many coils.

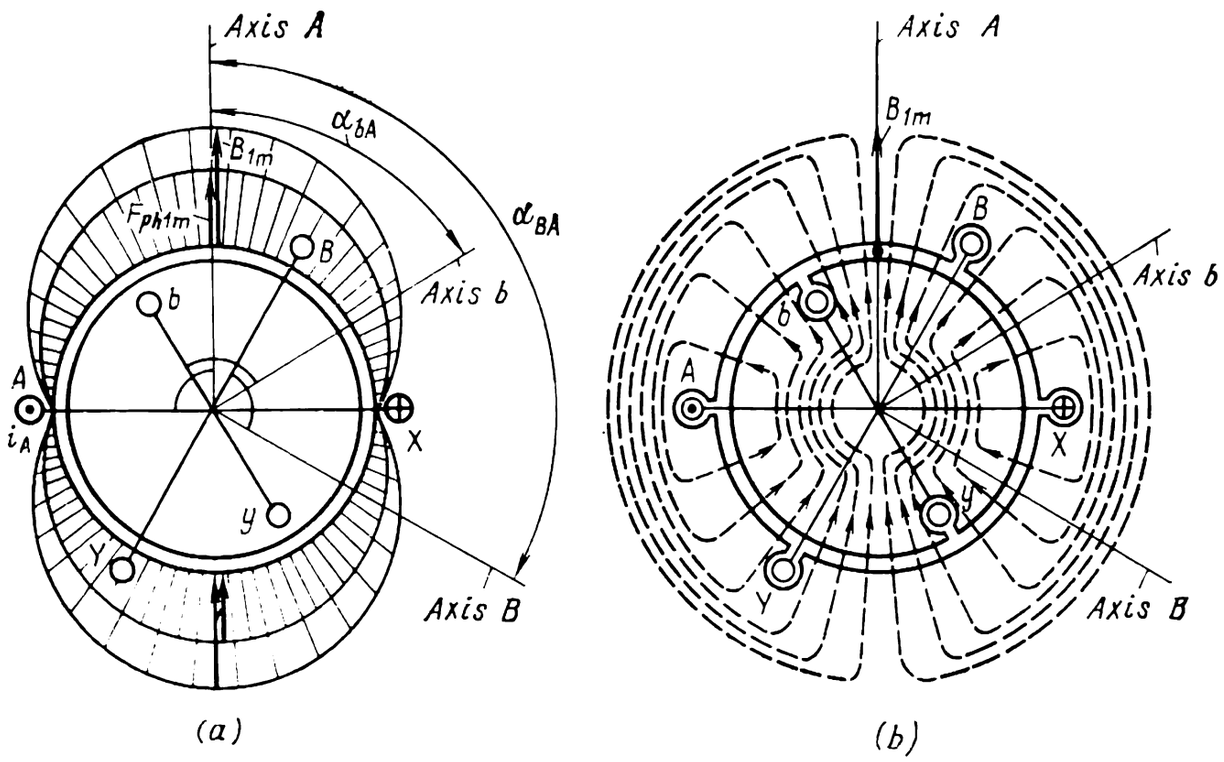

Fig. 28-1 The mutual magnetic field of phase A in a two-pole model: (a) distribution of the normal component of the phase flux density; (b) magnetic field pattern for phase A

By definition, the main self-inductance of a phase A is

$$L_{AA} = \Psi_{AAm}/i_A = \frac{4\mu_0}{p\pi^2}(w_1 k_{w1})^2 \frac{\tau l_\delta}{\delta k_\delta} \qquad (28\text{-}1)$$

It is seen from Eq. (28-1) that the main self-inductance of a phase depends on the air gap dimensions (l_δ, τ, δ, k_δ), the magnetic properties of the air gap (μ_0), and the characteristics of the stator winding (p, w, k_{w1}). In our example, the air gap is uniform, so the main self-inductance is independent of the relative position of the rotor and stator.

28-3 The Main Mutual Inductance between the Phases

The main mutual inductance between the phases varies with the electrical angle between the phase axes. To find the main mutual inductance between phases A and B of a polyphase winding, with their axes displaced from each other by

an electrical angle $\alpha_{BA} = p\gamma_{BA}$, we should first find the flux linkage between the useful field of phase A (shown in Fig. 28-1*a* and *b*) and that of phase B. It has been shown in Sec. 27-2 that the flux linkage of a rotating field with a phase is proportional to the cosine of the electrical angle between the field axis and the phase axis. (In Eq. (27-13) and in Fig. 27-7, this angle is $\omega t - \alpha_{ph}$.) Therefore, the flux linkage of the phase A field (for $i_A = \sqrt{2}\, I_A$) with that of phase B is

$$\Psi_{BAm} = \Psi_{AAm} \cos \alpha_{BA}$$

By definition, the main mutual inductance between phases A and B is

$$\begin{aligned} L_{BA} &= \Psi_{BAm}/i_A = (\Psi_{AAm}/i_A) \cos \alpha_{BA} \\ &= L_{AA} \cos \alpha_{BA} \end{aligned} \tag{28-2}$$

For the three-phase winding in Fig. 28-1,

$$\alpha_{BA} = 2\pi/3, \quad \alpha_{CA} = 4\pi/3$$

Therefore,

$$\cos \alpha_{BA} = \cos \alpha_{CA} = -1/2$$

and the main mutual inductances between the phases are negative

$$L_{BA} = L_{CA} = -L_{AA}/2$$

It is seen from Fig. 28-1*b* that the plane of the phase B coil is cut by half as many field lines as the plane of the phase A coil. Also, whereas the plane of the phase A coil is cut by field lines in the positive direction (with the axis of phase A), the plane of the phase B coil is cut by field lines in the negative direction (against the axis of phase B). This difference in flux linkages controls the magnitude and sign of the mutual inductance.

28-4 The Main Mutual Inductance Between a Stator Phase and a Rotor Phase

As in the previous section, this mutual inductance is a function of the cosine of the electrical angle between the axes of the stator and rotor phases considered. Also, in finding the flux linkage of primary (say, stator) phase A (the primary phases have upper-case letters in their indexes) with, say, secondary (say, rotor) phase b (the secondary phases have lower-case letters in their indexes), it is important to re-

member that a secondary phase has a different number of turns, w_2, and a different winding factor, k_{w2}.

If the electrical angle between the axes of phases A and b (see Fig. 28-1) at a given instant is equal to α_{bA}, then the flux linkage with phase b is given by

$$\Psi_{bAm} = w_2 k_{w2} \Phi_m \cos \alpha_{bA} = \Psi_{aA0} \cos \alpha_{bA}$$

Accordingly, the main mutual inductance between phases A and b is

$$L_{bA} = \Psi_{bAm}/i_A = L_m \cos \alpha_{bA} \qquad (28\text{-}3)$$

where

$$L_m = \frac{4\mu_0}{p\pi^2} (w_1 k_{w1} k_{w2}) \frac{\tau l_\delta}{\delta k_\delta}$$

is the peak value of mutual inductance between a primary phase and a secondary phase (say, phases A and a, when their axes coincide and the electrical angle between them is zero). As is seen from Eq. (28-3), when the rotor rotates at a mechanical angular velocity Ω, the angle $\alpha_{bA} = \Omega pt$ increases in a linear fashion, and L_{bA} is varying harmonically. In Fig. 28-1*b*, the mutual inductance is positive, because the field lines cut the coil plane *by* in the positive direction (along its axis).

28-5 The Main Self-Inductance of the Complete Winding

In addition to the self and mutual inductances examined in the previous sections, which are found by definition, it is convenient in the theory of electrical machines to introduce the concept of the self-inductance of the complete winding.

It can be defined as the self-inductance of a phase (say, phase A) which is in turn defined as the ratio between the maximum flux linkage due to all the primary phases with phase A, and the peak value of the phase A current*. For a three-phase winding,

$$L_{11} = \tilde{\Psi}_{Am}/\sqrt{2}\,\tilde{I}_A = \frac{\tilde{\Psi}_{AAm} + \tilde{\Psi}_{ABm} + \tilde{\Psi}_{ACm}}{\sqrt{2}\,\tilde{I}_A}$$

* This self-inductance is the same for balanced sets of PPS and NPS currents, but is different for ZPS currents.

On expressing the flux linkages in terms of currents, main self- and mutual inductances,

$$\tilde{\Psi}_{AAm} = \sqrt{2}\,\tilde{I}_A L_{AA},\quad \tilde{\Psi}_{ABm} = \sqrt{2}\,\tilde{I}_B L_{AB},\quad \tilde{\Psi}_{ACm} = \sqrt{2}\,\tilde{I}_C L_{AC}$$

and recalling that, in accord with Eq. (28-2),

$$L_{AB} = L_{AC} = -L_{AA}/2$$

and also noting that for balanced sets of PPS and NPS currents

$$\tilde{I}_B + \tilde{I}_C = -\tilde{I}_A$$

we can see that the main self-inductance of the complete winding can be written in terms of the main self-inductance of a phase as

$$L_{11} = \frac{3}{2} L_{AA} = (6\mu_0/p\pi^2)\,(w_1 k_{w1})^2\,(\tau l_\delta/\delta k_\delta)$$

In the general case, for an m_1-phase winding, the main self-inductance is

$$L_{11} = (m_1/2)\,L_{AA} = (2m_1\mu_0/p\pi^2)\,(w_1 k_{w1})^2\,(\tau l_\delta/\delta k_\delta) \quad (28\text{-}4)$$

As an alternative, the main self-inductance of the complete winding can be found from the peak flux linkage of the fundamental rotating field set up by all the phases, with one of the phases. In accord with Eq. (25-9), the peak value of the fundamental mmf of the m_1-phase primary winding that sets up the field is

$$F_{1(1)m} = \frac{m_1 \sqrt{2}\, I_A w_1 k_{w1}}{\pi p}$$

and, in accord with Eq. (24-17), the peak value of magnetic flux density is

$$B_{1(1)m} = \mu_0 F_{1m}/\delta k_\delta$$

As follows from the above equations, the peak flux linkage of a rotating field with a phase is

$$\Psi_{Am} = (2/\pi)\,\tau l_\delta w_1 k_{w1} B_{1(1)m}$$

and the main self-inductance of the primary winding is

$$L_{11} = \Psi_{Am}/\sqrt{2}\, I_A$$

Naturally, the result is the same as that given by Eq. (28-4).

28-6 The Main Mutual Inductance between a Primary Phase and the Secondary Winding

The main mutual inductance between phases of different windings is likewise found from the peak flux linkage of all the secondary phases (or, in other words, due to the rotating secondary field) with a primary phase. It is equal to the ratio of this flux linkage to the peak value of secondary current. The flux linkage with phase A is a maximum when the axis of this phase is aligned with that of phase a, the axis of the rotating field is aligned with the axis of phase A, and the current in phase a is at its peak value.

The peak fundamental mmf of the m_2-phase secondary winding which sets up the field is given by Eq. (25-9)

$$F_{1(2)m} = (m_2 \sqrt{2}/\pi)(I_a w_2 k_{w2}/p)$$

The peak value of the associated fundamental flux density is

$$B_{1(2)m} = \mu_0 F_{1(2)m}/\delta k_\delta$$

The peak flux linkage of the rotating field with the primary phase A is

$$\Psi_{Am} = (2/\pi)\tau l_\delta w_1 k_{w1} B_{1(2)m}$$

and the main mutual inductance between a primary phase and a secondary phase is

$$L_{12m} = \Psi_{Am}/\sqrt{2}\, I_a = (2m_2\mu_0/p\pi^2)(w_1 k_{w1} w_2 k_{w2})(\tau l_\delta/\delta k_\delta) \tag{28-5}$$

It is an easy matter to see that this parameter is connected to the peak mutual inductance between a primary phase and a secondary phase by a simple relation of the form

$$L_{12m} = m_2 L_m/2$$

which is similar to Eq. (28-4).

The main mutual inductance between a secondary phase and the primary winding is given by

$$L_{21m} = m_1 L_m/2$$

and, if $m_1 \neq m_2$, it differs from the mutual inductance between a primary phase and the secondary winding, L_{12m}.

28-7 The Leakage Inductance of the Complete Winding

By definition (see Sec. 28-2), a leakage field exists when the fundamental components of the air gap magnetic fields due to the currents in the stator and rotor windings cancel out:

$$\mathbf{B}_{1(1)m} = \mathbf{B}_{1(2)m}$$

If, to simplify the argument, we assume that the rotor winding is stationary relative to the stator winding, that the axis of phase A is aligned with that of phase a (see Fig. 28-2),

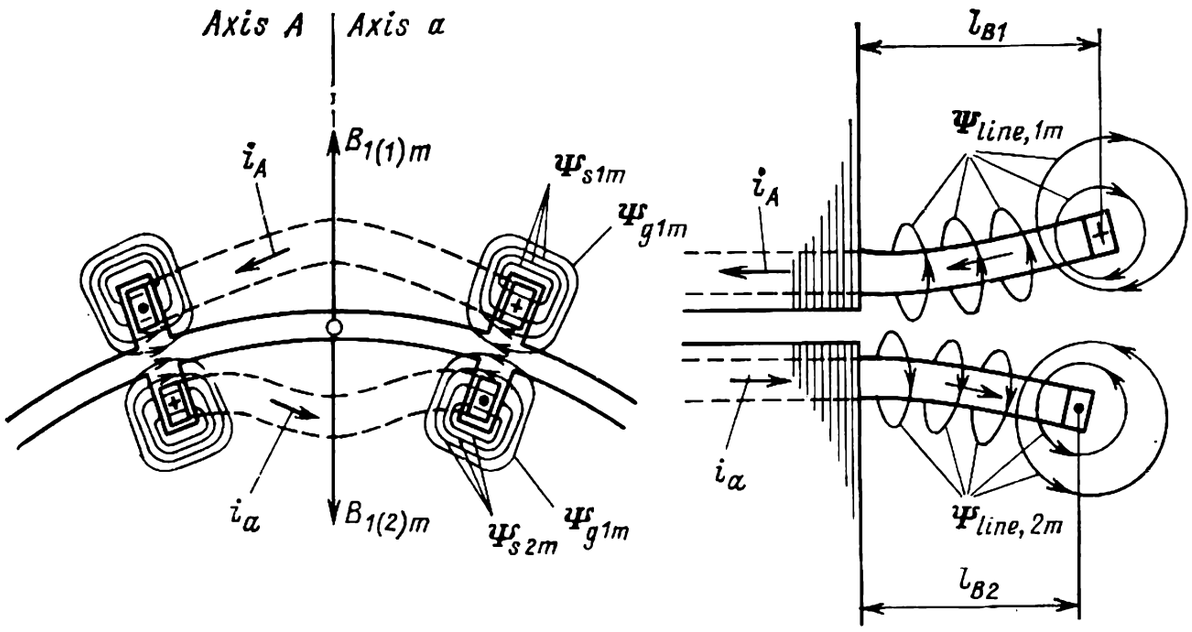

Fig. 28-2 Leakage magnetic field due to the polyphase windings on the stator and rotor (Ψ_g stands for Ψ_t, and Ψ_{line} for Ψ_e)

and that the air gap is uniform, then the fundamental component of the air gap magnetic field will vanish when the fundamental mmfs of the two windings are equal and opposite in peak value. Mathematically, this condition may be written as

$$\dot{F}_{1(1)m} = \frac{m_1\sqrt{2}}{\pi}\frac{\dot{I}_A w_1 k_{w1}}{p} = -\dot{F}_{1(2)m} = -\frac{m_2\sqrt{2}\,\dot{I}_a w_2 k_{w2}}{p}$$

This condition will be satisfied if the secondary phase currents are appropriately related to the primary phase currents

$$\dot{I}_a = -\frac{m_1 w_1 k_{w1}}{m_2 w_2 k_{w2}}\dot{I}_A$$

The other primary (or secondary) phase currents and the phase A (or a) current form between them a balanced set of PPS or NPS currents.

The flux linkage of the leakage field with primary phase A s a maximum when the current in that phase is a maximum, $i_A = \sqrt{2}\, I_A$, whereas the current in secondary phase a must be such that

$$i_a = -i_A\,(m_1 w_1 k_{w1}/m_2 w_2 k_{w2}) = -\sqrt{2}\, I_a$$

Precisely such currents in phases A and a, and appropriate currents in the other primary and secondary phases set up the magnetic field shown in Fig. 28-2.

Given a set of currents, the leakage field can be found by electrical-field equations (see Chap. 23). Then one finds the leakage flux linkage with phase A in the various parts (Ψ_{s1m}, Ψ_{t1m}, Ψ_{e1m}, and Ψ_{d1m}), the total leakage flux linkage with a phase

$$\Psi_{\sigma 1m} = \Psi_{s1m} + \Psi_{t1m} + \Psi_{e1m} + \Psi_{d1m}$$

and the leakage self-inductance of a phase

$$L_{\sigma 1} = \Psi_{\sigma 1m}/\sqrt{2}\, I_A \qquad (28\text{-}6)$$

In this way, the leakage flux linkage of a phase is found with allowance for the effect of the other phases on the stator and rotor. The leakage flux linkage of the secondary winding is calculated in a similar way

$$L_{\sigma 2} = \Psi_{\sigma 2m}/\sqrt{2}\, I_a = \frac{\Psi_{s2m} + \Psi_{t2m} + \Psi_{e2m} + \Psi_{d2m}}{\sqrt{2}\, I_a}$$

The field lines contributing to the slot leakage flux linkage (Ψ_{s1m} and Ψ_{s2m}), the tooth leakage flux linkage (Ψ_{t1m} and Ψ_{t2m}), and the coil-end leakage flux linkage (Ψ_{e1m} and Ψ_{e2m}) are shown in Fig. 28-2 (see also Chap. 23). The differential leakage flux linkage (Ψ_{d1m} and Ψ_{d2m}) is also taken into consideration.

The stator and rotor (primary and secondary) windings always differ in the number of phases, the number of slots per pole per phase, and so on. As a result, the stator and rotor winding factors are different even for the harmonic mmfs of the same order, and the harmonics themselves rotate at different angular velocities. This is the reason why the harmonic mmfs do not cancel one another, although the fundamental mmfs do.

The differential leakage emf, $E_{\sigma d}$, induced by the higher harmonics has been discussed in Sec. 27-6. In its terms, the differential leakage flux linkage for the primary winding may be written

$$\Psi_{\sigma dm} = \sqrt{2}\, E_{\sigma d}/2\pi f = \sqrt{2} \sum_{\nu \neq 1} E_{ph\nu}/2\pi f$$

$$= (2/\pi)\, w_1 \tau l_\delta \sum k_{w1\nu} B_{\nu(1)m}/\nu$$

where $B_{\nu m} = E_{\nu(1)m}\mu_0/\delta k_\delta$.

Omitting the details, we shall only give an equation for the leakage self-inductance of a primary phase, stemming from Eq. (28-6)

$$L_{\sigma 1} = 2\mu_0 w_1^2\, (l_\delta/pq_1)\, \lambda_{\delta 1} \qquad (28\text{-}7)$$

where $\lambda_{\delta 1} = \lambda_{s1} + \lambda_{t1} + \lambda_{e1} + \lambda_{d1}$ is the permeance for the leakage flux linkage (a dimensionless quantity).

The terms of the sum above are the permeances of the various leakage fields, defined per unit of coil-side design length. The higher a given permeance, the larger the associated leakage inductance. The magnitude of a permeance depends on the dimensions governing the respective leakage field. To facilitate computation, equations giving the various permeances have been developed on making certain assumptions as regards the leakage field pattern and taking the permeability of the ferromagnetic parts of a machine to be infinitely large.

For a three-phase, double-layer winding, the various permeances can, in a first approximation, be found by the following equations.

(i) The slot leakage permeance (for the rectangular slot of Fig. 23-4)

$$\lambda_{s1} = (h_c/b_o + h_r/3b_s)\, (3\beta + 1)/4$$

where

h_r = radial depth taken up by conductors in a slot
h_c = clearance between conductors and airgap
b_s = slot width
b_o = width of opening towards the airgap
$\beta = y_c/\tau$ = chording (pitch-shortening) factor

(ii) The tooth leakage permeance (see Fig. 23-4)

$$\lambda_{t1} = [1.1\,(\delta'/b_o) - 0.35\,(\delta'/b_c)^2 - 0.26] \left(\frac{3\beta+1}{4}\right)$$

where $\delta' = k_\delta \delta$ = effective radial length air gap

(iii) The coil-end leakage permeance (see Fig. 28-2)

$$\lambda_{e1} = 0.34 \sqrt{\beta_{r0,1}} + 0.1 (\beta_1 \tau q_1 / l_\delta) \approx 0.3 \beta_1 \tau q_1 / l_\delta$$

where $\beta_{r0,1} = l_{r0,1}/y_{c1} = l_{r0,1}/\beta_1 \tau$ = relative coil-end overhang

$\beta_1 = y_{c1}/\tau$ = chording (pitch-shortening) factor

(iv) The differential leakage permeance (see Fig. 24-3)

$$\lambda_{d1} = (0.7 \text{ to } 1.0) (t_Z / 12\delta k_\delta)$$

where t_Z = tooth (slot) pitch

δ = radial air gap length

The factor 0.7 to 1.0 in the equation for λ_{d1} depends on the degree of pitch shortening (chording), relative slot opening (b_0/t_Z and b_0/δ), the damping effect of currents induced in the secondary winding, etc.

For the secondary three-phase winding, the above permeances can be found by the same equations on replacing the index "1" with "2".

29 The Electromagnetic Torque

29-1 The Torque Expressed in Terms of Variations in the Energy of the Magnetic Field

Let us consider an induction or a synchronous a.c. machine with a uniform air gap. We shall replace the toothed cores by smooth ones and introduce an equivalent air gap length

$$\delta_0 = k_\delta \delta$$

where k_δ is the slot factor accounting for the effect of core saliency on the permeability of the air gap [see Eq. (24-10)].

Suppose that the stator is wound with a symmetrical polyphase winding with $m_1 \geqslant 2$, and that the rotor carries either a symmetrical polyphase winding with $m_2 \geqslant 2$, or a single-phase field winding (this applies to a synchronous machine). Let the stator winding carry a set of PPS currents, I_1, varying with an angular frequency ω_1, and the rotor carry either a set of PPS currents I_2 (in the case of a polyphase winding) varying with an angular frequency ω_2, or a direct

current I_{2m} (in the case of a single-phase field winding), for which $\omega_2 = 0$.

As has been shown in Sec. 21-2, such a machine will be capable of unidirectional energy conversion only if the frequency of stator currents, ω_1, of rotor currents, ω_2, and of mutual inductance, $\omega = p\Omega$, satisfy a certain condition. More specifically, it is required that

$$\omega_1 \pm \omega_2 = \omega = p\Omega$$

If this condition is met (to make the matter more specific, let $\omega < \omega_1$ and $\omega_2 = \omega_1 - \omega$), then, as can readily be shown, the fundamental components of mmfs (or of the rotating fields) due to the balanced sets of currents in the primary and secondary windings will be rotating relative to the stator at the same mechanical angular frequency

$$\Omega_1 = \omega_1/p$$

Referring to the two-pole model of a machine (Fig. 29-1) whose polyphase (three-phase) windings carry PPS currents, it can be seen that the fundamental mmf of the primary winding

$$\tilde{F}_{1m} = \sqrt{2}\, m_1 \tilde{I}_1 k_{w1} w_1/\pi p$$

or the fundamental component of the air gap magnetic flux density

$$\tilde{B}_{1m} = \mu_0 \tilde{F}_{1m}/\delta_0 = \sqrt{2}\, m_1 \mu_0 \tilde{I}_1 k_{w1} w_1/\delta_0 \pi p$$

rotates at an electrical angular velocity $\omega_1 = p\Omega_1$ [see Eq. (25-3)] in the positive direction (this is, from phase A towards phase B).

The fundamental mmf of the secondary winding

$$\tilde{F}_{2m} = \sqrt{2}\, m_2 \tilde{I}_2 k_{w2} w_2/\pi p$$

or the fundamental component of the air gap magnetic flux density

$$\tilde{B}_{2m} = \mu_0 \tilde{F}_{2m}/\delta_0 = \sqrt{2}\, m_2 \mu_0 k_{w2} w_2/\delta_0 \pi p$$

rotates relative to the rotor at an electrical angular velocity ω_2 equal to the angular frequency of the current in the rotor winding, and does so likewise in the positive direc-

tion, that is, from phase a to phase b. (In Fig. 29-1, the velocity of the mmf relative to the rotor, ω_2, is shown relative to the rotor). To find the angular velocity of the secondary mmf F_2 relative to the stator, ω_2', it should be recalled that

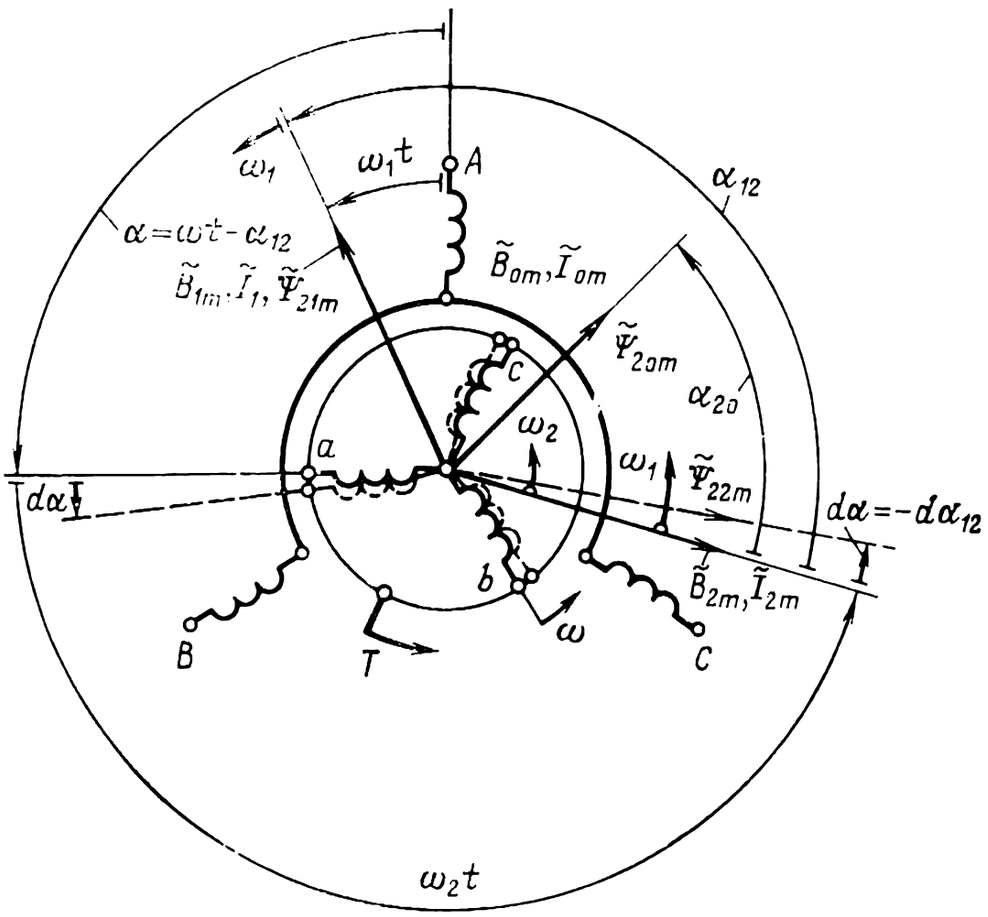

Fig. 29-1 Relative position of the fundamental mmfs and flux linkages in the primary and secondary windings

in the model the rotor rotates at an electrical angular velocity $\omega = \Omega p$ in the positive direction, so this velocity must be added to that of F_2 relative to the rotor

$$\omega_2' = \omega_2 + \omega$$

(In Fig. 29-1, ω_2 is shown likewise relative to the rotor).

Since the condition for the velocity of rotor current is satisfied, we may write

$$\omega_2' = \omega_1 - \omega + \omega = \omega_1 = \Omega_1 p$$

To sum up, unidirectional energy conversion can be performed only if the rotor mmf rotates with the same electrical angular velocity $\omega_1 = \Omega_1 p$ in the model and with the same mechanical angular velocity Ω_1 in the prototype machi-

ne as the stator mmf does. (In Fig. 29-1, $\omega_2' = \omega_1$ is shown relative to the stator.)

The converted energy and the period-averaged electromagnetic torque depend, as will be shown later, on the electrical angle α_{12} between the axes of the stator and rotor fields stationary relative to each other. This angle is connected to the mechanical angle γ_{12} between the same axes in the prototype machine by a known relation, $\alpha_{12} = p\gamma_{12}$. The positive direction for α_{12} (or γ_{12}) and for the torque acting on the rotor is counterclockwise from the axis of the rotor field.

Because under steady-state conditions α_{12} is constant, the torque will likewise remain constant over a revolution, and the period-averaged electromagnetic torque can be found by Eq. (18-6)

$$T_{em} = \partial W/\partial\gamma \,|_{in=\text{constant}}$$

for the arbitrary relative position of the stator and rotor shown in Fig. 29-1. (The angle α between the axes of the main rotor and stator phases is arbitrary.)

In order to find the electromagnetic torque, we should first determine the energy of the air gap magnetic field as a function of B_{1m}, B_{2m}, and α_{12}. The energy of the magnetic field in an elementary volume dV of the air gap is

$$dW = (B_0^2/2\mu_0)\, dV$$

where $B_0 = B_{0m}\cos(p\varphi)$ = magnetic flux density in the elementary volume $dV = l_\delta \delta_0 R d\varphi$

$B_{0m} = \sqrt{B_{1m}^2 + B_{2m}^2 + 2B_{1m}B_{2m}\cos\alpha_{12}}$ = peak flux density of the resultant air gap field

φ = angle defining the position of the elementary volume relative to the resultant field

R = mean air gap radius

The energy of the air gap magnetic field is found by taking the integral over the volume, $V = 2\pi R l_\delta \delta_0$. It is

$$W = \int_V (B_0^2/2\mu_0)\, dV = \int_0^{2\pi} (B_{0m}^2/2\mu_0)\, l_\delta \delta_0 R \cos^2(p\varphi)\, d\varphi$$

$$= \frac{p\tau\delta_0 l_\delta}{2\mu_0}(B_{1m}^2 + B_{2m}^2 + 2B_{1m}B_{2m}\cos\alpha_{12})$$

where $\tau = \pi R/p$ is the pole pitch.

Now we turn the rotor through a small angle $\partial\gamma$, deeming the current constant, and find $dW/d\gamma$. As will be recalled, the mechanical angle γ (or the corresponding electrical angle $\alpha = \gamma p$) is the angle, say, between the axis of the stator phase A and the rotor phase a (as reckoned from the stator phase A in the positive direction, that is, counterclockwise). As the rotor turns through a small angle $d\gamma = d\alpha/p$ in the positive direction (with the phase currents held constant) the rotor mmf and field move along with the rotor, whereas the stator mmf and field remain stationary (see Fig. 29-1). In the process, the angle $\gamma_{12} = \alpha_{12}/p$ between the rotor and stator mmfs decreases in the same proportion as the angle γ increases. (We have assumed that the angle γ_{12} is reckoned from a rotor phase to a stator phase, that is, in the reverse direction from that for the angle γ or α.) As a consequence, the changes in γ and γ_{12} only differ in sign

$$d\gamma = d\alpha/p = -d\gamma_{12} = -d\alpha_{12}/p$$

$$d\alpha = -d\alpha_{12}$$

Hence, it is legitimate to write the derivative as follows:

$$T_{em} = \frac{dW}{d\gamma} = -p\frac{dW}{d\alpha_{12}} = \frac{p^2\tau\delta_0 l_\delta B_{1m}B_{2m}}{\mu_0}\sin\alpha_{12} \qquad (29\text{-}1)$$

$$B_{1m} = \text{const}, \quad B_{2m} = \text{const}$$

Expressing the magnetic flux densities in terms of currents and recalling Eq. (28-3), we get

$$T_{em} = \frac{m_1 m_2 p}{2} I_1 I_2 L_m \sin\alpha_{12}$$

where L_m is the maximum mutual inductance between the stator and rotor phases as defined by Eq. (28-3).

The electromagnetic torque acting on the rotor is positive (that is, is directed counterclockwise) when $0 < \alpha_{12} < \pi$, and negative when $\pi < \alpha_{12} < 2\pi$ (or $0 > \alpha_{12} > -\pi$). On expressing B_2 in terms of I_2 and noting that

$$\Psi_{21m} = 2B_{1m}\tau l_\delta w_2 k_{w2}/\pi$$

is the peak flux linkage of the stator field with a rotor phase, we may write the electromagnetic torque in terms of current and flux linkage as

$$T_{em} = \frac{m_2 p}{\sqrt{2}} I_2 \Psi_{21m} \sin\alpha_{12} \qquad (29\text{-}2)$$

or, in complex notation,

$$T_{em} = \frac{m_2 p}{\sqrt{2}} \operatorname{Im} [\tilde{\Psi}_{21} \tilde{I}_2^*]$$

where $\tilde{I}_2^*$ is the complex conjugate of the secondary (rotor) current.

Using the above equations, it is an easy matter to show that the interaction of I_2 with its own field or flux linkage Ψ_{22} produces no electromagnetic torque. To demonstrate, by Eq. (29-2), this torque is zero:

$$\frac{m_2 p}{\sqrt{2}} I_2 \Psi_{22m} \sin \alpha_{22} = 0$$

where $\Psi_{22m} = 2B_{2m} \tau l_\delta w_2 k_{w2}/\pi$ is the peak flux linkage of the useful self-field with the rotor turns, and $\alpha_{22} = 0$ is the angle between Ψ_{22m} and I_2.

Now we are in a position to express the electromagnetic torque in terms of the total flux linkage with a given winding, Ψ_{20m}, that is, in terms of the flux linkage produced by both the external field, Ψ_{21m}, and the self-field, Ψ_{22m}. For this purpose, we add to the right-hand side of Eq. (29-2) the zero torque associated with the self-flux linkage

$$\begin{aligned} T_{em} &= \frac{m_2 p}{\sqrt{2}} \operatorname{Im} [\tilde{\Psi}_{21m} \tilde{I}_2^*] + \frac{m_2 p}{\sqrt{2}} \operatorname{Im} [\tilde{\Psi}_{22m} \tilde{I}_2^*] \\ &= \frac{m_2 p}{\sqrt{2}} \operatorname{Im} [(\tilde{\Psi}_{21m} + \tilde{\Psi}_{22m}) \tilde{I}_2^*] \\ &= \frac{m_2 p}{\sqrt{2}} \operatorname{Im} [\tilde{\Psi}_{20m} \tilde{I}_2^*] \\ &= \frac{m_2 p}{\sqrt{2}} \Psi_{20m} I_2 \sin \alpha_{20} \end{aligned} \qquad (29\text{-}3)$$

where $\tilde{\Psi}_{20m} = \tilde{\Psi}_{22m} + \tilde{\Psi}_{21m}$ = peak total flux linkage of the main field with the rotor winding

α_{20} = angle between $\tilde{I}_2$ (or $\tilde{B}_2$) and $\tilde{\Psi}_{20m}$ (see Fig. 29-1)

A torque, equal in magnitude but opposite in direction, is also acting on the stator. It can be found by Eq. (29-1) or Eq. (29-2), recalling that the torque at the stator is deemed positive when it is acting clockwise (that is, against the sense of rotation). Alternatively, the electromagnetic torque at the stator may be expressed in terms of stator

quantities. To this end we write B_1 in Eq. (29-1) in terms of I_1 and recall that

$$\Psi_{12m} = 2B_{2m}\tau l_\delta w_1 k_{w1}/\pi$$

Then,

$$T_{em} = \frac{m_1 p}{\sqrt{2}} \Psi_{12m} I_1 \sin \alpha_{12} = \frac{m_1 p}{\sqrt{2}} \operatorname{Im} [\tilde{\Psi}^*_{12} \tilde{I}_1] \qquad (29\text{-}4)$$

where Ψ_{12m} is the peak flux linkage of the rotor field with a stator phase.

Since the interaction of I_1 with the self-field or self-flux linkage

$$\Psi_{11m} = 2B_{1m}\tau l_\delta w_1 k_{w1}/\pi$$

produces no electromagnetic torque, i.e.

$$m_1 p I_1 \Psi_{11m} \sin 0 = 0$$

it is an easy matter to express the electromagnetic torque at the stator in terms of the total flux linkage of the useful field with a stator phase

$$T_{em} = \frac{m_1 p}{\sqrt{2}} \Psi_{10m} I_1 \sin \alpha_{10} = \frac{m_1 p}{\sqrt{2}} \operatorname{Im} [\tilde{\Psi}^*_{10m} \tilde{I}_1] \qquad (29\text{-}5)$$

where $\tilde{\Psi}_{10m} = \tilde{\Psi}_{12m} + \tilde{\Psi}_{11m}$ = peak total flux linkage of the useful field with a stator phase

α_{10} = angle between $\tilde{\Psi}_{10m}$ (which is in phase with $\tilde{\Psi}_{20m}$) and $\tilde{I}_1$ (as reckoned counterclockwise from flux linkage towards current).

Equations (29-4) and (29-5) are equally applicable to a polyphase rotor winding and a d.c.-energized single-phase rotor winding such as used in synchronous machines.

Equations (29-3) and (29-5) where the electromagnetic torque is expressed in terms of Ψ_{20m} or Ψ_{10m} also hold for saturable machines with nonlinear cores. Deriving them subject to the remarks made in Sec. 18-2, it will be seen that to find the electromagnetic torque in such a case it will suffice to substitute into Eq. (29-3) or (29-5) the peak values of the fundamental flux linkages found with allowance for the nonlinearity of the magnetic circuit.

29-2 The Electromagnetic Torque Expressed in Terms of Electromagnetic Forces

In the previous section, we have found the electromagnetic torque from the law of conservation of energy. It can be determined in other ways as well. For example, we could combine the torques due to the electromagnetic forces which arise when a rotating magnetic field interacts with the elementary currents and elementary surfaces of the magnetized cores. We could then have obtained a more detailed picture about the distribution of electromagnetic forces throughout the active parts, the flows of energy converted by a given machine, and their directions. Unfortunately, the mathematics involved would be prohibitive out of any proportion. Therefore, if we are only interested in the main electromagnetic torque associated with the fundamental mmf and airgap magnetic flux density, it is convenient to use the concept of the surface current which replaces the currents in the core slots.

(i) Surface Current and Its Fourier Expansion

We obtain the surface current on replacing the toothed core by a smooth one and spreading each slot currents i_{sk}, over the core surface as a thin sheet with a linear density given by

$$A_{sk} = i_{sk}/b_s$$

The replacement of slot currents by a surface current is illustrated in Fig. 29-2 which repeats the winding and current patterns shown in Fig. 25-8 for $i_A = \sqrt{2}\, I_a$ and $i_B = i_C = -\sqrt{2}\, I_a/2$. Shown below the sectional view of a slot layer in a toothed core is an equivalent smooth core. The air gap is enlarged k_δ times, and the currents are shown spread outside the slots but within the slot boundaries as thin sheets of density A_{sk}.

The slot current i_{sk} is the sum of alternating currents in the conductors laid out in the kth slot. For example, the current in slot *2* of Fig. 29-2 enclosing the forward conductors of phase A and the reverse conductors of phase C is

$$i_{s2} = i_A w_c - i_C w_c$$

At the instant of time shown in Fig. 29-2, when

$$i_A = i_{A\max} = \sqrt{2}\, I_a$$
$$i_B = i_C = -\sqrt{2}\, I_a/2$$

the current in the second slot will be

$$i_{s2} = \sqrt{2}\, I_a w_c + \sqrt{2}\, I_a w_c/2 = (3/2)\sqrt{2}\, I_a w_c$$

The current i_{sk} and the corresponding surface current density for the kth slot, $A_{sk} = i_{sk}/b_s$, are taken to be negative if the current is shown flowing "inwards" (away from the reader),

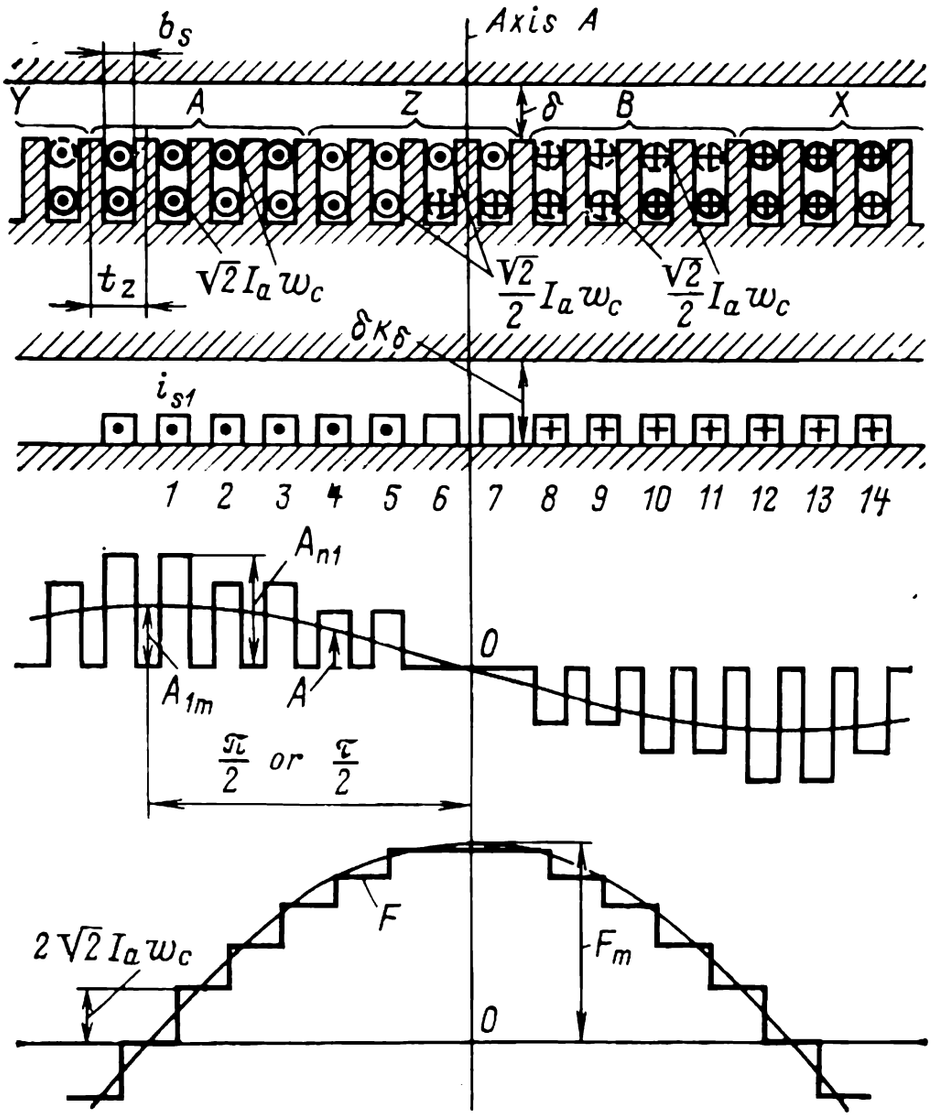

Fig. 29-2 Surface current density and mmfs of a polyphase winding ($m = 3$, $q = 4$, $i_A = \sqrt{2} I_a$, $i_B = i_C = -\sqrt{2} I_a/2$)

that is, with the Z-axis. Therefore in, say, slot *9* the current at the instant of time in question is negative

$$i_{s9} = i_B w_c + i_B w_c = -\sqrt{2}\, I_a w_c$$

Between slots, the surface current density is zero. The cycle of change in the surface current density is the same as for slot currents. Round the periphery of the air gap, it changes p times (where p is the number of pole pairs). As

slot currents vary, the waveform of surface current density also varies in a continuous fashion. On expressing slot currents as functions of time and expanding the spatial distribution of surface current density into a Fourier series, we could find the fundamental surface current density with $2p$ poles round the periphery and with peak value A_{1m}, as shown in Fig. 29-2.

Unfortunately, the above procedure is too time- and effort consuming. A far simpler approach is to express the surface

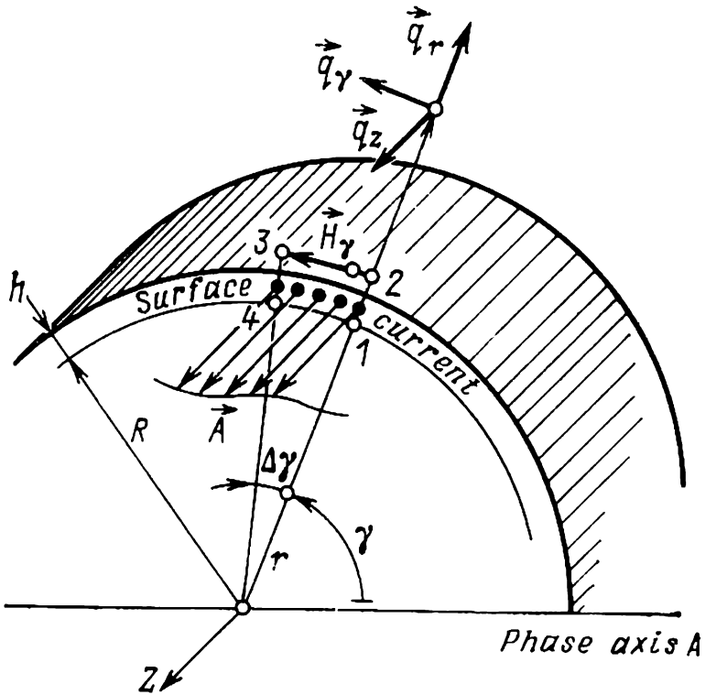

Fig. 29-3 Relationship between the tangential field intensity and surface current density (axial component) in polar coordinates

current density in terms of the mmf or of its harmonic components. Prior to that, it is necessary to find the tangential component, H_γ, of the airgap magnetic intensity on the smooth core surface where the surface current is distributed as an infinite thin sheet of thickness $\Delta = 0$ and of a linear density A (Fig. 29-3). In polar coordinates, the surface current density A, and also the slot currents, are directed along the Z-axis, and $A = A_z$. Let us find the current Δi for a surface element of length $R\,\Delta\gamma$

$$\Delta i = A \times R\,\Delta\gamma$$

Enclose this current by a rectangular loop labelled *1-2-3-4* and having a radial dimension h and a tangential dimension R $(\Delta\gamma)$. Applying Ampere's circuital law to the circulation of the magnetic intensity round the loop *1-2-3-4* where $h \to 0$

and noting that the magnetic intensity on side *1-4* lying within the core of an infinite permeability is zero, we get

$$\oint H_l \, dl = H_\gamma R \Delta\gamma = \Delta i$$

On passing to the limit with $\Delta\gamma \to 0$, we obtain

$$H_\gamma = H_t = \lim (\Delta i / R \, \Delta\gamma) = A$$

This is the expression for H_γ, the magnetic intensity on the surface of the inner core. Applying the same procedure, we can obtain an expression for the magnetic intensity on the surface of the outer core, $H_\gamma = -A$.

To sum up, the tangential component of the magnetic intensity, $H_\gamma = H_t$, on the surface of the core with $\mu_a = \infty$ is equal in absolute value to the current density on that surface, $|A|$.

Proceeding from Eq. (23-9) and setting $dx = R d\gamma$ in polar coordinates, we can write the tangential magnetic intensity as a derivative of the scalar potential on the core surface

$$H_\gamma = -d\varphi / R \, d\gamma$$

Finally, using Eq. (24-5) and the accompanying relations between the mmf and the distribution of φ on the excited core surface ($F = \varphi$ when the inner core is excited, and $F = -\varphi$ when the outer core is excited), we can express the surface current density on the inner or outer core as a derivative of the mmf

$$A = -dF / R \, d\gamma \qquad (29\text{-}6)$$

This relation can be applied not only to the surface current density as a whole, but to its harmonics as well, so that for each harmonic mmf there will be a surface current density harmonic of its own.

Now we set out to find the fundamental surface current density when a polyphase winding carries PPS currents of frequency ω. The fundamental mmf is a rotating wave described by Eq. (25-10). Proceeding from Eqs. (29-6) and (25-10), we have

$$A = -dF / R \, d\gamma = A_{1m} \cos (\omega t + \pi/2 - \alpha) \qquad (29\text{-}7)$$

In terms of the peak value of the fundamental mmf, the peak value of the fundamental surface current density, A_{1m},

can be written

$$A_{1m} = F_{1m}\pi/\tau \tag{29-8}$$

If we use Eq. (25-16) for F_{1m}, then A_{1m} can be expressed in terms of the sum of rms slot currents, $2w_c I_a = I_s$ as

$$A_{1m} = \sqrt{2}\, A_0 k_p k_d \tag{29-9}$$

where $A_0 = 2w_c I_a/t_Z = I_s/t_Z$ is the line load current found from the sum of slot currents.

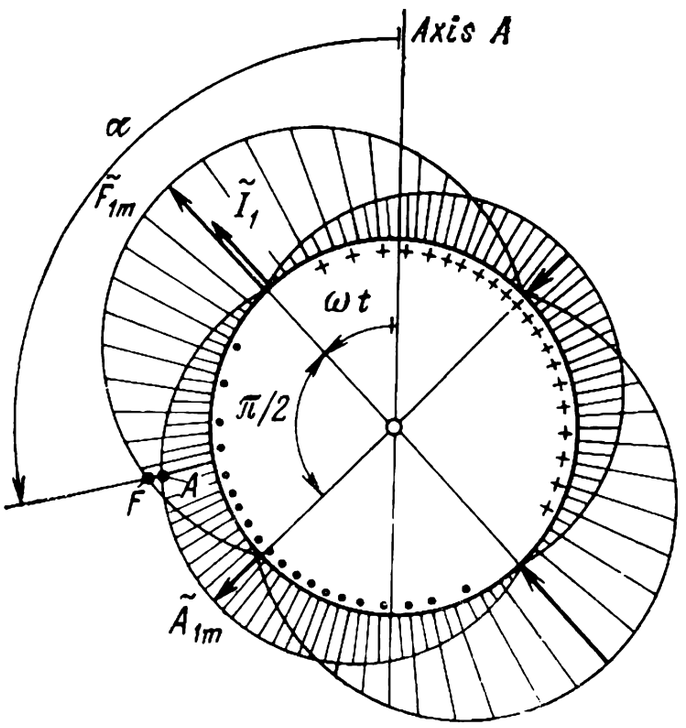

Fig. 29-4 Fundamental component of surface current density (in a two-pole model)

At a point at an angle α to the origin, the surface current density can be presented as the projection of the complex surface current density

$$\tilde{A}_{1m} = j\tilde{F}_{1m}(\pi/\tau) = A_{1m} \exp[j(\omega t + \pi/2)]$$

on the axis at an angle α, that is,

$$A = \mathrm{Re}\,[A_{1m} \exp(-j\alpha)]$$

Using Eqs. (29-7) and (29-9), it is an easy matter to plot the fundamental component of surface current density on the same scale as the slot current densities. This plot is shown in Figs. 29-2 and 29-4. Figure 29-4 also shows the surface current density phasor $\tilde{A}_{1m}$.

From the foregoing, we may conclude that the fundamental component of linear surface current density is a rotating wave with period 2τ and amplitude A_{1m}, travelling at the same mechanical angular velocity Ω (or an electrical angular velocity ω in the model) as the fundamental mmf. Irrespective of the direction in which the mmf is rotating, the

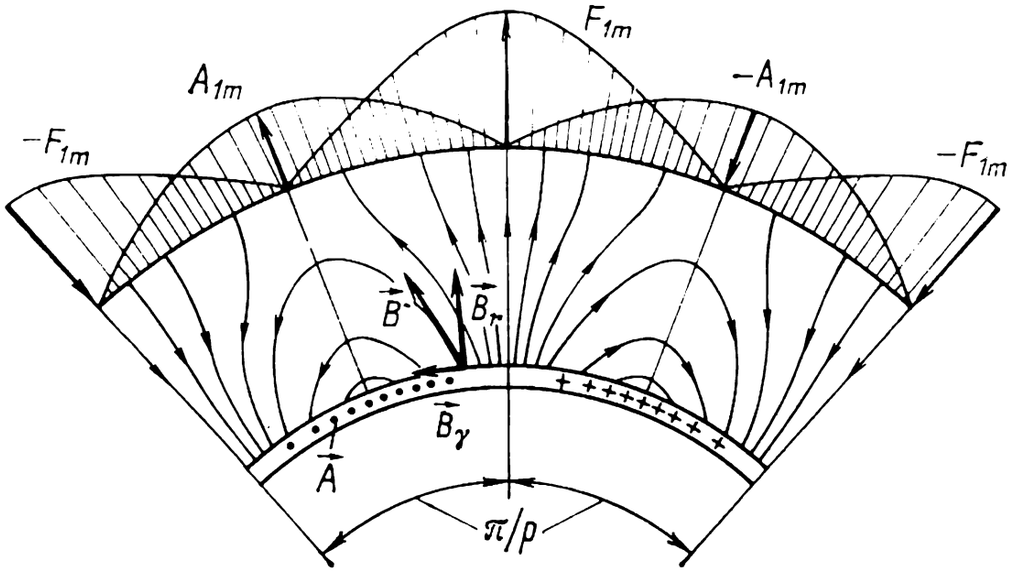

Fig. 29-5 Pattern of the magnetic field set up by currents in the inner core of a machine

surface current density wave always makes an angle of $\pi/2$ with the mmf wave or is displaced through $\tau/2$ counterclockwise.

The above relation between the tangential magnetic intensity and the surface current density, $H_t = H_\gamma = \pm A$, also holds for their fundamental components. Therefore, the air gap magnetic field set up by the slot currents (or by the fundamental component of the equivalent surface current density) always has the tangential as well as the radial component. The radial component of the magnetic flux density can be written in terms of the mmf using Eq. (25-18) as

$$B_r = \mu_0 F / k_\delta \delta \qquad (29\text{-}10)$$

The tangential magnetic flux density on the surface of the excited core may be written directly in terms of the surface current as

$$B_t = B_\gamma = \mu_0 H_\gamma = \pm \mu_0 A \qquad (29\text{-}11)$$

Since no tangential magnetic flux density exists on the surface of the unexcited core, the air gap field set up by the fundamental component has the pattern shown in Fig. 29-5.

It should be noted, though, that the figure shows the field for a very large relative gap, δ/τ, when the radial component is comparable with the tangential component; compare Eqs. (29-10) and (29-11). For the small values of δ/τ usually encountered in practice, the radial component is substantially larger than the tangential component, so the field is essentially a radial one. If, however, we neglected the tangential components, H_y, due to the surface current of

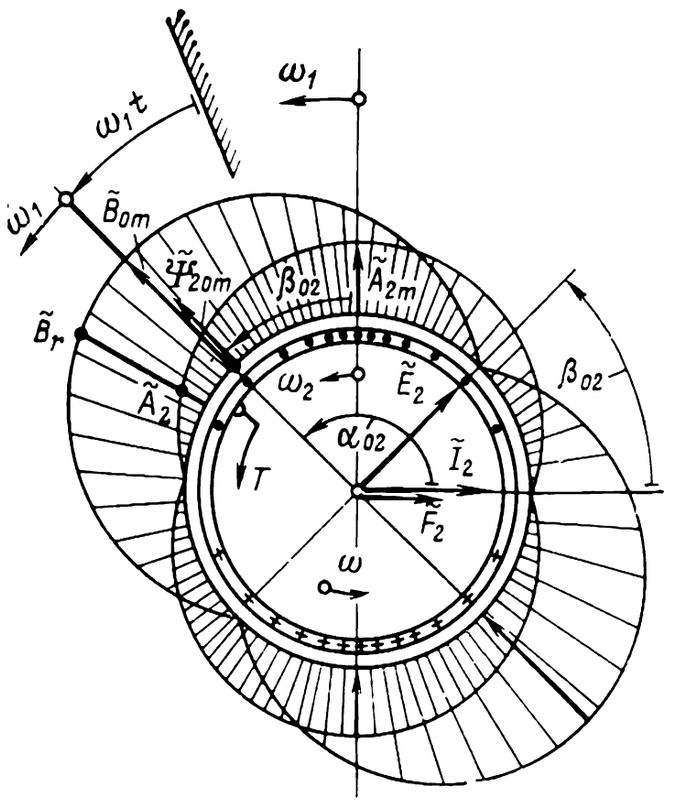

Fig. 29-6 Relative position of rotating waves of radial magnetic flux density B_r and surface current density A

density A, we would be unable to get proper insight into the generation of electromagnetic forces and transfer of energy across the air gap when an electrical machine is running.

(ii) Electromagnetic Torque

Let us find the electromagnetic torque acting on the rotor rotating at a mechanical angular velocity Ω (or at an electrical angular velocity ω in the model of Fig. 29-6). Suppose that the polyphase rotor winding carries a current I_2 with angular frequency ω_2, which gives rise to the fundamental surface current density wave of peak value A_{2m}. The mechanical angular velocity of the surface current density wave relative to the rotor is proportional to the frequency of the

current

$$\Omega_2 = \omega_2/p$$

The electrical angular velocity of this wave relative to the rotor in the model is the same as that of the current and is equal to ω_2.

Relative to the stationary frame of reference, the surface current wave rotates at a mechanical angular velocity $\Omega_1 = \Omega + \Omega_2$. The electrical angular velocity of the wave relative to the stator in the model, $\omega_1 = \omega + \omega_2$, in the case of unidirectional energy conversion (see Sec. 29-1) is always the same as the angular frequency ω_1 of currents in the polyphase stator winding. Therefore, the fundamental stator mmf rotates at a mechanical angular velocity $\Omega_1 = \omega_1/p$ and produces, together with the fundamental component of the rotor surface current rotating at the same mechanical angular velocity, the useful rotating magnetic field in which the radial magnetic flux density has a peak value given by $B_{1\,(0)m} = B_{0m}$. Let the angle between B_0 and A_2 (or between $\tilde{B}_{0m}$ and $\tilde{A}_{2m}$) be denoted by β_{02} and counted from $\tilde{A}_{2m}$ towards $\tilde{B}_{0m}$.

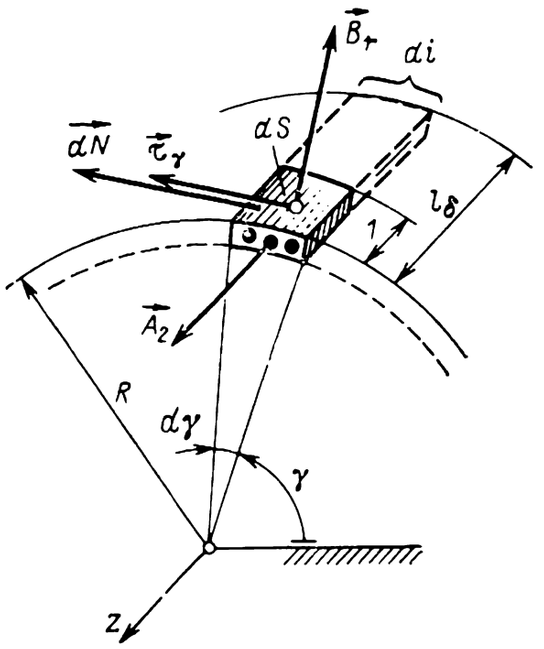

Fig. 29-7 Electromagnetic forces acting on an element of surface current

The electromagnetic torque can be defined as the sum of the torques developed by the electromagnetic forces dN acting on elementary surface currents $di = A_2\,(R\,d\gamma)$. Assume that each elementary current extends along the machine axis for a distance equal to a unit of length and is lying in a magnetic field in which the radial magnetic flux density is B_r. Then the electromagnetic force that is acting on that elementary current in a tangential direction may be written as

$$dN = B_r\,di = B_r A_2 R\,d\gamma$$

The direction of dN can be found by the left-hand rule. An elementary surface current at an angle γ to the origin and the force acting on it are shown in Fig. 29-7.

The electromagnetic torque acting on the surface current and transmitted to the shaft by the mechanically stressed rotor core can be found by adding together the torques produced by the elementary forces

$$dT_{em} = R\, dN$$

over the entire rotor surface facing the air gap (from $\gamma = 0$ to $\gamma = 2\pi$ along the effective core length l_δ)

$$T_{em} = l_\delta \int_0^{2\pi} R\, dN = l_\delta R^2 \int_0^{2\pi} B_r A_2\, d\gamma$$

Using Eq. (25-18) for a rotating magnetic flux density wave

$$B_r = B_{0m} \cos(\omega_1 t - \alpha)$$

and Eq. (29-7) for a rotating surface current wave

$$A_2 = A_{2m} \cos(\omega_1 t - \alpha - \beta_{02})$$

where $\alpha = p\gamma$, and on setting for simplicity $\omega_1 t = 0$, because the integration yields the same result for any instant of time, we obtain

$$T_{em} = \pi R^2 l_\delta B_{0m} A_{2m} \cos\beta_{02} = \frac{p^2\tau^2}{\pi} l_\delta B_{0m} A_{2m} \cos\beta_{02} \qquad (29\text{-}12)$$

Noting that the peak value of the linear surface current density can be expressed in terms of I_2 [see Eqs. (29-8) and (25-9)],

$$A_{2m} = \pi F_{2m}/\tau = (\sqrt{2}\, m_2/\tau)(I_2 w_2 k_{w2}/p)$$

and the peak value of the magnetic flux density defined by Eq. (27-2) can be expressed in terms of magnetic flux

$$B_{0m} = \pi\Phi_m/2\tau l_\delta$$

the electromagnetic torque can be written as a function of the magnetic flux and winding current

$$T_{em} = (pm_2/\sqrt{2})(w_2 k_{w2}\Phi_m) I_2 \cos\beta_{02} \qquad (29\text{-}13)$$

If we recall that the peak value of the total flux linkage with a phase given by Eq. (27-14) is

$$\Psi_{20m} = w_2 k_{w2}\Phi_m$$

and replace β_{02} by $\sin\alpha_{02} = \sin(\pi/2 + \beta_{02}) = \cos\beta_{02}$ [see Fig. 29-6 and Eq. (29-7)], the expression for the torque

will be analogous with Eq. (29-3):

$$T_{em} = (pm_2/\sqrt{2})\,\Psi_{20m} I_2 \sin \alpha_{02}$$

where α_{02} is the electrical angle (see Fig. 29-6) between the flux linkage phasor $\dot{\Psi}_{20m}$ and the current phasor $\dot{I}_2$ (or the mmf phasor $\dot{F}_2$).

As already noted in Sec. 29-1, the torque equation, Eq. (29-3), also holds for saturated machines with a nonlinear magnetic circuit. A further proof of that statement is the fact that it is analogous to the equation derived here for a saturated machine.

29-3 Electromagnetic Force Distribution in a Wound Slot

In finding the electromagnetic torque acting on the rotor, we replaced the toothed rotor whose slots carried certain currents i_s by a smooth core, moved the currents i_s to the surface, and distributed them in the slot regions as an infinite thin sheet of linear density $A_s = i_s/b_s$ (see Fig. 24-2).

The replacement of a toothed by a smooth core will leave unchanged the tangential electromagnetic force N acting on a slot, if the mean air gap magnetic flux density due to the external magnetic field is as found with allowance for the saliency of the stator by the equation

$$B_{\delta,\text{mean}} = \mu_0 F/\delta\, k_{\delta 1} k_{\delta 2}$$

where F = external mmf produced by the stator currents at the axis of the slot in question
$k_{\delta 1}$ = stator air gap factor
$k_{\delta 2}$ = rotor air gap factor
δ = radial gap length.

The total tangential electromagnetic force per unit length of air gap can be found as the sum of the forces

$$dN = B_{\delta,\text{mean}}\, A_s dx$$

applied to the elementary surface currents

$$N = \int_{-b_s/2}^{+b_s/2} B_{\delta,\text{mean}} A_s\, dx = B_{\delta,\text{mean}} A_s b_s = B_{\delta,\text{mean}} i_s$$

Let us now see how this force is distributed in the slot region. The resultant magnetic field in the slot region may be visualized as the sum of the external field (Fig. 29-8*a*) and the self-field set up by the slot current (Fig. 29-8*b*). To determine the tangential forces acting on the slot sides and the slot current, it will suffice to find the respective flux densities in the slot sides and at the centre of a current-carrying conductor. As has been found for real slots and an infinite core permeability ($\mu_{rc} = \infty$). nearly all field lines entering a slot terminate in the slot sides and only a small fraction of the lines reaches the current-carrying conductor. If the flux per unit slot length (see Fig. 29-8*a*) is

$$\Phi = \int_{-b_s/2}^{+b_s/2} B_{y(y=0)}\,dx = B_{\delta,\,\mathrm{mean}} b_s$$

then the flux passing through the slot section at the level of the current-carrying conductor ($y = h_i$) will be

$$c\Phi = \int_{-b_s/2}^{+b_s/2} B_{y(y=h_i)}\,dx = B_s b_s$$

where c ranges from 0.002 to 0.001.

Because the magnetic field is symmetrical and continuous, the flux entering the slot side

$$\Phi_0 = (\Phi - c\Phi)/2$$

differs but little from $\Phi/2$.

On moving away from the air gap, the external magnetic flux density on the slot sides, B_{01} and B_{02}, rapidly diminishes so that level with the conductor top ($y = h$) it is zero very nearly. Therefore, the external flux enters the slot sides within the depth h

$$\Phi_0 = \Phi(1-c)/2 = \int_0^h B_{01}\,dy = \int_0^h B_{02}\,dy$$

From a comparison of the expressions for Φ and $c\Phi$ the external flux density in the conductor region can be written

$$B = cB_{\delta,\,\mathrm{mean}}$$

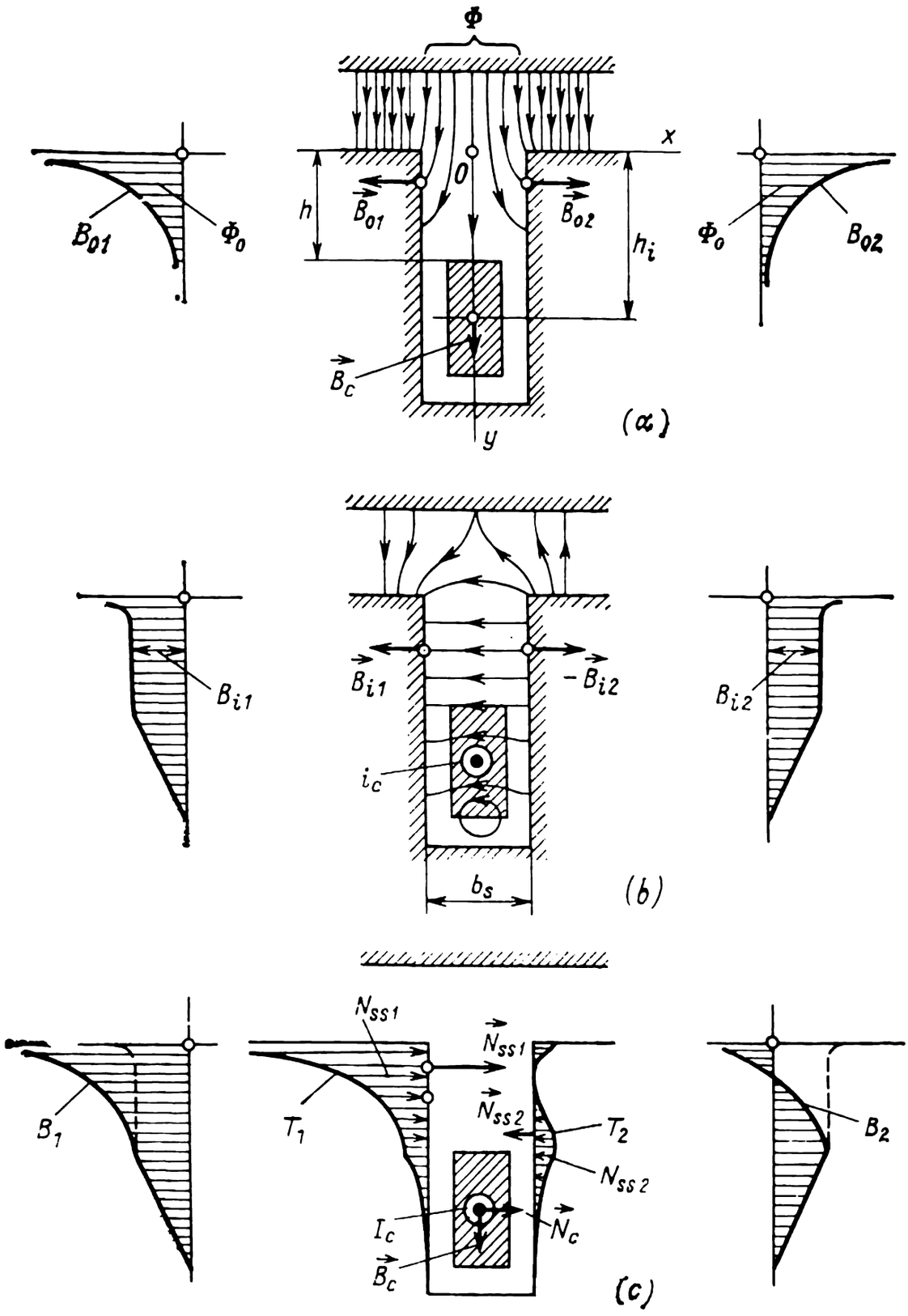

Fig. 29-8 Distribution of electromagnetic forces in the region of a wound slot:
(*a*) external magnetic field due to currents on the other core, $I_s = 0$, $B_{\delta.mean} = 0$; (*b*) magnetic field due to slot current, $B_{\delta.mean} = 0$, $I_s = 0$; (*c*) electromagnetic forces in and around a slot, $I_s \neq 0$, $B_{\delta.mean} = 0$

The pattern of the field set up by the slot current and the distribution of the magnetic flux density in the slot sides are shown in Fig. 29-8*b*.

Within the larger part of the space above the conductor ($0 < y < h$), the magnetic flux density in the slot sides is nearly constant. Applying Ampere's circuital law to the loop enclosing the current and coincident with a field line over the slot width, the respective magnetic flux density can aproximately be written as

$$B_{i1} = B_{i2} = \mu_0 i_c / b_s$$

Now we are in a position to find the tangential electromagnetic forces associated with the resultant magnetic field in the slot region (see Fig. 29-8*c*). The current-carrying conductor is acted upon by a tangential electromagnetic force given by

$$N_c = B_c i_c = c B_{\delta,\text{mean}}\, i_c = cN$$

which is a small fraction of the total force

$$N = B_{\delta,\text{mean}} i_c$$

acting in the wound-slot region.

The greater part of the total electromagnetic force is applied to the slot sides as a magnetic pull. Let us first find the specific magnetic pull, T (in pascals), that is the force per unit area of a ferromagnetic surface ($\mu_{r,\text{Fe}} = \infty$) in a magnetic field. It can be expressed in terms of the normal component of magnetic flux density, B_n, which acts at the surface of a ferromagnetic body in the same direction as the total magnetic flux density, and in terms of the permeability μ_0 of the nonmagnetic medium surrounding that body:

$$T = B^2/2\mu_0$$

The specific magnetic pull vector is always aligned with the normal $\vec{n}$ to the surface of the ferromagnetic body, directed towards the medium having the lower permeability

$$T = \vec{n}\,(B^2/2\mu_0)$$

The specific magnetic pulls T_1 and T_2 acting on the slot sides are normal to the sides. The distribution of

T_1 and T_2

$$T_1 = B_1^2/2\mu_0, \quad T_2 = B_2^2/2\mu_0$$

over the slot depth is a function of

$$B_1 = B_{01} - B_{i1}$$

on the left-hand side, and of

$$B_2 = B_{02} - B_{i1}$$

on the right-hand side. Because they are unbalanced only over the interval $0 < y < h$, the resultant tangential force

$$N_{ss} = N_{ss1} - N_{ss2}$$

applied to the slot sides can be found by combining the elementary forces on each side within the limits specified:

$$N_{ss} = N_{ss1} - N_{ss2} = \int_0^h T_1 \, dy - \int_0^h T_2 \, dy = \int_0^h (T_1 - T_2) \, dy$$

Noting that

$$B_{01} = B_{02} \text{ and } B_{i1} = B_{i2}$$

we get

$$T_1 - T_2 = (2/\mu_0) B_{01} B_{i1}$$

In taking the integral, it should be recalled that

$$B_{i1} \approx \mu_0 i_c / b_s = \text{constant}$$

for $0 < y < h$ (see above). So, on expressing the flux through a slot side

$$\int_0^h B_{01} \, dy$$

in terms of the external flux, $\Phi = b_s B_{\delta,\text{mean}}$, we get

$$N_{ss} = \int_0^h (T_1 - T_2) \, dy = (2/\mu_0) B i_1 \int_0^h B_{01} \, dy$$

$$= (B_{i1}/\mu_0)(1 - c) \Phi = (1 - c) i_c B_{\delta,\text{mean}} = (1 - c) N$$

The total tangential force N acting on the wound-slot region is the sum of N_{ss}, the force applied to the slot sides, and

N_c, the force applied to the current-carrying conductor,

$$N = N_{ss} + N_c = (1 - c)B_{\delta,mean}i_c + cB_{\delta,mean}i_c$$
$$= B_{\delta,mean}i_c$$

This force is equal to the force acting on i_c, the slot current shifted to the core surface. As we have learned, however, the greater proportion of this force acts on the slot sides rather than on the conductor in a slot ($c = 0.001$ to 0.002).

Our reasoning has been based on certain simplifying assumptions as regards the distribution of the external flux density in the air gap and of the flux density due to the slot current in the slot sides. However, the rigorous approach would lead to the same solution — a fact of important practical significance. Because electromagnetic forces largely act on the slot sides (or the core teeth), the conductor insulation may be designed as mechanically strong as may be necessary to transfer $N_c = cN$ which is a very small quantity.

To sum up, owing to the shielding action of teeth on a toothed core, the external field in the region taken up by current-carrying conductors is substantially reduced, and the requirements for the mechanical strength of insulation may be less stringent.

30 Energy Conversion by a Rotating Magnetic Field

30-1 Electromagnetic, Electric and Magnetic Power

The electromagnetic power entering a rotor surface element $dS = 1 \times R d\gamma$ from the air gap is a function of the power developed by an element of torque as an element of current rotates at a mechanical angular velocity Ω_1 (see Sec. 29-2)

$$dP_{em} = \Omega_1 dT = B_r R \Omega_1 A_2 (R\, d\gamma) \qquad (30\text{-}1)$$

Let us write the mechanical angular velocity of a surface current element as the sum of Ω, the rotational angular velocity due to the rotation of the rotor, and Ω_2, the angular velocity of the current sheet relative to the rotor body,

associated with periodic variations in the currents of the rotor winding:

$$\Omega_1 = \Omega + \Omega_2$$

Then the electromagnetic power entering a rotor surface element can be written as the sum of the mechanical power

$$dP_m = \Omega\, dT$$

transferred via this surface element to the shaft, and the electrical power

$$dP_e = \Omega_2\, dT$$

entering the surface current element or the winding to which it is equivalent:

$$\begin{aligned} dP_{em} &= \Omega_1\, dT \\ &= \Omega\, dT + \Omega_2\, dT \\ &= dP_m + dP_e \end{aligned} \quad (30\text{-}2)$$

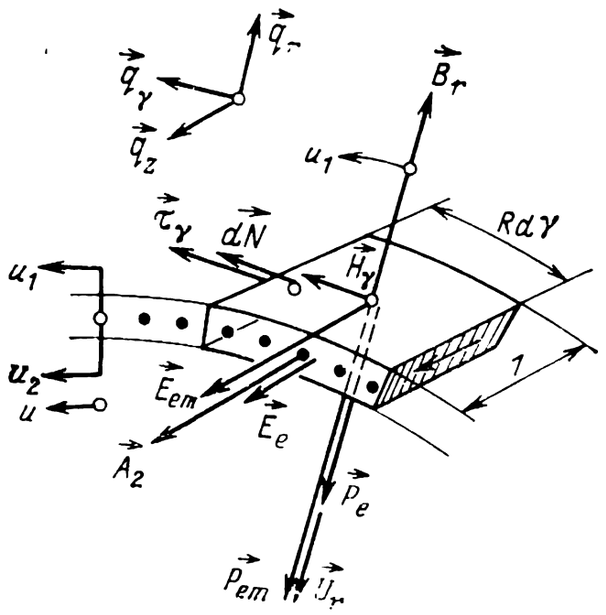

Fig. 30-1 Flux density: electromagnetic power (P_{em}), electric power (P_e), and mechanical power (P_m) (on the surface of the rotor core)

The electromagnetic power flow per unit area (power flux density) and the direction of this flow may be defined in terms of the radial component, $\vec{\mathcal{P}}_{em}$, of the *Poynting vector* [24]

$$\begin{aligned} \vec{\mathcal{P}}_{em} &= \mathbf{E}_{em} \times \mathbf{H}_\gamma \\ &= \mathbf{q}_z \mathbf{q}_\gamma E_{em} H_\gamma \\ &= -\mathbf{q}_r E_{em} H_\gamma \end{aligned}$$

which is seen (Fig. 30-1) to be the product of the axial component of the electric intensity vector, $\mathbf{E}_{em} = \mathbf{q}_z E_{em}$, and the tangential component of the magnetic intensity vector, $\mathbf{H}_\gamma = \mathbf{q}_\gamma H_\gamma$. Here, $\mathbf{q}_\gamma$, $\mathbf{q}_z$, and $\mathbf{q}_r$ are the unit vectors along the respective axes of a cylindrical coordinate system.

If we recall that the tangential magnetic intensity on the rotor surface is equal to the surface current density (see Sec. 29-2)

$$H_\gamma = A_2$$

and also that in defining the total energy entering a surface element we should take into account the electric intensity

found from the total linear velocity of a surface current wave

$$\mathbf{u}_1 = \mathbf{q}_\gamma u_1 = \mathbf{q}_\gamma R\Omega_1$$

that is,

$$\mathbf{E}_{em} = \mathbf{B}_r \times \mathbf{u}_1 = \mathbf{q}_r \times \mathbf{q}_\gamma B_r u_1 = \mathbf{q}_z B_r R\Omega_1$$

then the radial component of the Poynting vector may be written

$$\vec{\mathcal{P}}_{em} = + \mathbf{q}_r \mathcal{P}_{em} \tag{30-3}$$

where

$$\mathcal{P}_{em} = - E_{em} H_\gamma = - B_r R\Omega_1 A_2$$

Naturally, the electromagnetic power entering a rotor surface element, $1 \times R\, d\gamma$, and expressed in terms of the radial component of the Poynting vector

$$dP_{em} = \vec{\mathcal{P}}_{em} R\, d\gamma = - B_r R\Omega_1 A_2 (R\, d\gamma) = - \Omega_1\, dT$$

is the same as given by Eq. (30-1). The "—" sign implies that the power flow is directed inside the rotor, that is, opposite to the radial unit vector $\mathbf{q}_r$. In a similar manner, we can represent the electric power entering a surface current element. In this case, however, the electric intensity must be deduced from the velocity of the surface current wave, solely related to variations in the winding currents:

$$\mathbf{u}_2 = \mathbf{q}_\gamma u_2 = \mathbf{q}_\gamma R\Omega_2$$

$$dP_e = \mathcal{P}_e R\, d\gamma = - (B_r R\Omega_2) A_2 R\, d\gamma = - \Omega_2 dT \tag{30-4}$$

where $\vec{\mathcal{P}}_e = \mathbf{E}_e \times \mathbf{H}_\gamma = \mathbf{q}_r \mathcal{P}_e$, and $\mathcal{P}_e = - E_e \mathbf{H}_\gamma = - B_r R\Omega_2$. Here, the "—" sign likewise indicates the direction of the power flow (see Fig. 30-1).

By the same token, the mechanical power

$$dP_m = \Omega\, dT$$

may be expressed in terms of the radial component of the *Umov vector*, U, defined as the mechanical power flux entering a surface element of a mechanically strained body.

The radial component of the Umov vector for a rotating body is determined as the product of the tangential mechanical stress τ_γ by the tangential linear displacement velocity of a surface element, $u_\gamma = u = R\Omega$

$$\mathbf{U}_r = \mathbf{q}_r U_r$$

$$U_r = - \tau_\gamma u_\gamma = - A_2 B_r R\Omega \tag{30-5}$$

The tangential mechanical stress τ_γ arises on the outer surface of the rotor because it carries surface current elements and the tangential forces dN acting on them

$$\tau_\gamma = dN/R\,d\gamma = \frac{(q_z A_2 R\,d\gamma) \times q_r B_r}{R\,d\gamma} = q_\gamma \tau_\gamma \qquad (30\text{-}6)$$

where $\tau_\gamma = A_2 B_r$ [N m^{-2}].

The mechanical power entering a rotor surface element

$$dP_m = U_r R\,d\gamma = -A_2 B_r R\,\Omega R d\gamma = -\Omega\,dT \qquad (30\text{-}7)$$

is the same as given by Eq. (30-2) where it is expressed in terms of the electromagnetic torque.

By taking an integral over the rotor surface, we can find the electromagnetic and electric powers that enter the rotor in the process of energy conversion:

$$\begin{aligned} P_{em} &= l_\delta \int_0^{2\pi} dP_{em} = \Omega_1 l_\delta \int_0^2 dT = \Omega_1 T \\ P_e &= l_\delta \int_0^{2\pi} dP_e = \Omega_2 l_\delta \int_0^2 dT = \Omega_2 T \\ P_m &= l_\delta \int_0^{2\pi} dP_m = \Omega l_\delta \int_0^{2\pi} dT = \Omega T \end{aligned} \qquad (30\text{-}8)$$

Obviously, as follows from Eq. (30-2),

$$P_{em} = P_e + P_m$$

The electromagnetic power, P_{em}, is the total power transferred by the rotating field to the rotor (Fig. 30-2). Some of this power, P_e, is dissipated as heat in the rotor winding or in the line connected to that winding. This can be proved by re-arranging Eq. (30-8) with the aid of Eqs. (29-3) and (27-15) and also recalling that $\beta_{02} = \alpha_{02} - \pi/2$ is, at the same time, the angle between I_2 and E_2 in the rotor winding. Therefore,

$$P_e = \Omega_2 T = m_2 (P\Omega_2 \Psi_{20}/\sqrt{2})\, I_2 \sin \alpha_{02} = m_2 E_2 I_2 \cos \beta_{02}$$

where $p\Omega_2 = \omega_2$ is the electrical angular frequency of E_2 induced in the rotor winding by the rotating field.

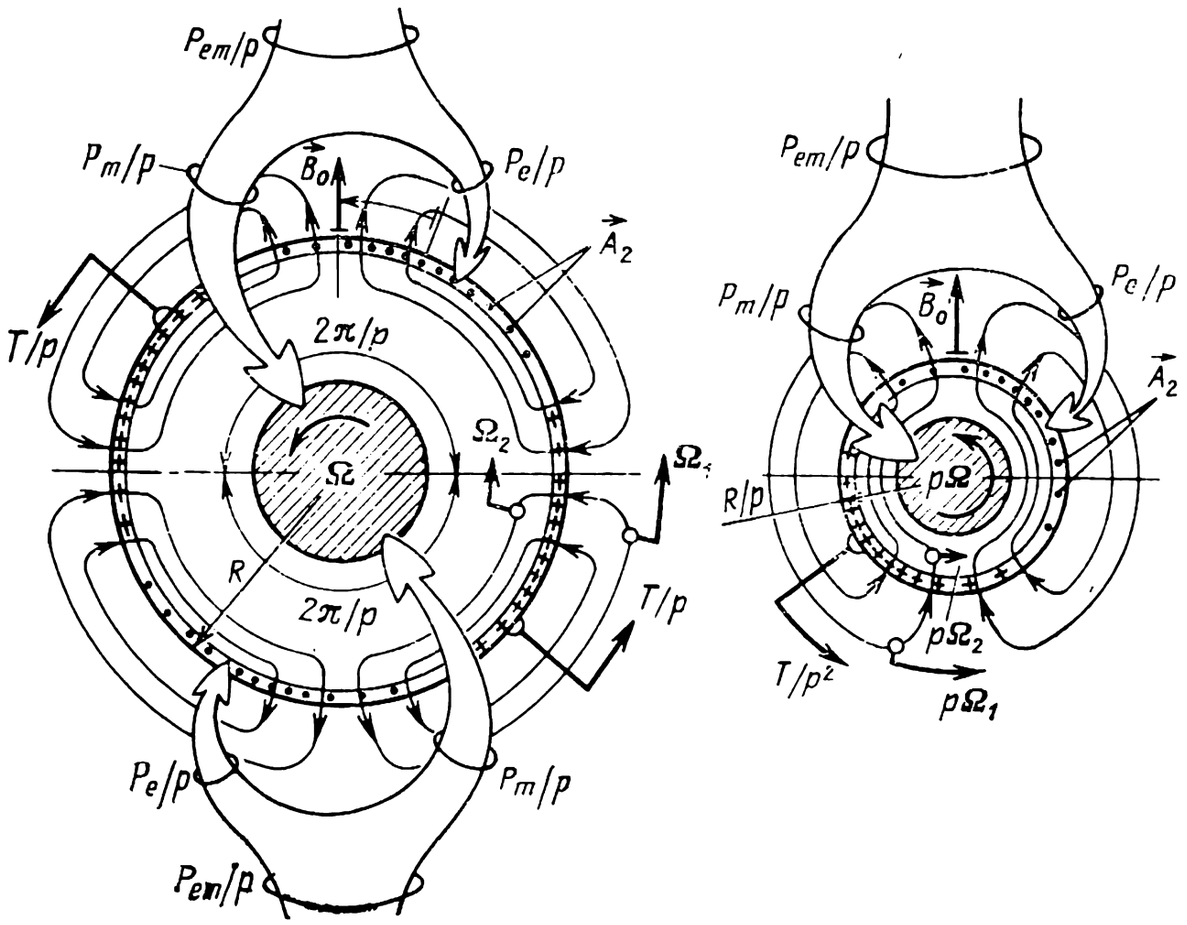

Fig. 30-2 Electromechanical energy conversion by a machine (on the left) and in its model (on the right)

Finally, the remainder of input power is converted to mechanical power

$$P_m = \Omega T$$

transmitted by a mechanically loaded shaft (as the power flow defined by the Umov vector).

* 30-2 Energy Conversion in an Electrical Machine and Its Model

As we have seen in the previous chapters, the two-pole model of an electrical machine is a convenient and instructive tool with which to study what goes on in the machine itself. This is also true of the events involved in energy conversion. In the model shown in Fig. 30-2, we retain the prototype's pole pitch τ, fundamental amplitudes of magnetic flux

density and surface current waves, B_{0m} and A_2, and also phase displacement between these waves in fractions of a pole pitch. Therefore, in the model the waves travel through an angle β_{02} which is p times as great as the angle between these waves, β_{02}/p, in the machine itself. (On the left of Fig. 30-2, the machine's field has four poles.)

Also, we retain in the model the prototype's linear peripheral velocities of the waves and of the core element, u_1, u_2 and u, on the outer surface of the rotor. This is done because in the model the radius of this surface is $1/p$ of its value in the prototype, whereas the angular velocities are p times as high:

$$u_1 = (R/p)\,\Omega_1 p = \Omega_1 R$$
$$u_2 = (R/p)\,\Omega_2 p = \Omega_2 R$$
$$u = (R/p)\,\Omega p = \Omega R$$

The tangential electromagnetic force acting on the surface current in the model's rotor is the same force as operates on the surface current over a pole pitch in the prototype, that is N/p, which is $1/p$ as large as the total tangential force (see above)

$$N = l_\delta \int_0^{2\pi} dN$$

The electromagnetic torque in the model is $1/p^2$ of its magnitude in the prototype, because it is given by the product of the tangential force in the model, N/p, by the radius of its rotor, R/p:

$$(N/p)\,(R/p) = NR/p^2 = T/p^2$$

However, the powers entering the rotor of the model do not differ from the respective powers existing over a pole pitch in the prototype machine. This can be demonstrated by applying Eq. (30-8) to the model:

$$(\Omega_1 p)\,(T/p^2) = \Omega_1 T/p = P_{em}/p$$
$$(\Omega_2 p)\,(T/p^2) = \Omega_2 T/p = P_e/p$$
$$(\Omega p)\,(T/p^2) = \Omega T/p = P_m/p$$

The same relations can be obtained, if we recall that at the similar points over a pole pitch in the prototype and in its model (that is, the points which are at angles γ and

$\alpha = p\gamma$, respectively), the radial magnetic flux density B_r, the linear surface current density A, and all the velocities are respectively the same. Accordingly, P_{em}, P_e and P_m, definable in terms of the radial components of the Poynting and Umov vectors, Eqs. (30-3) through (30-5), are likewise the same at the similar points in the machine and its model.

As is seen, the model is convenient not only in calculating the air gap field, mmf, emf, and flux linkage, and in plotting

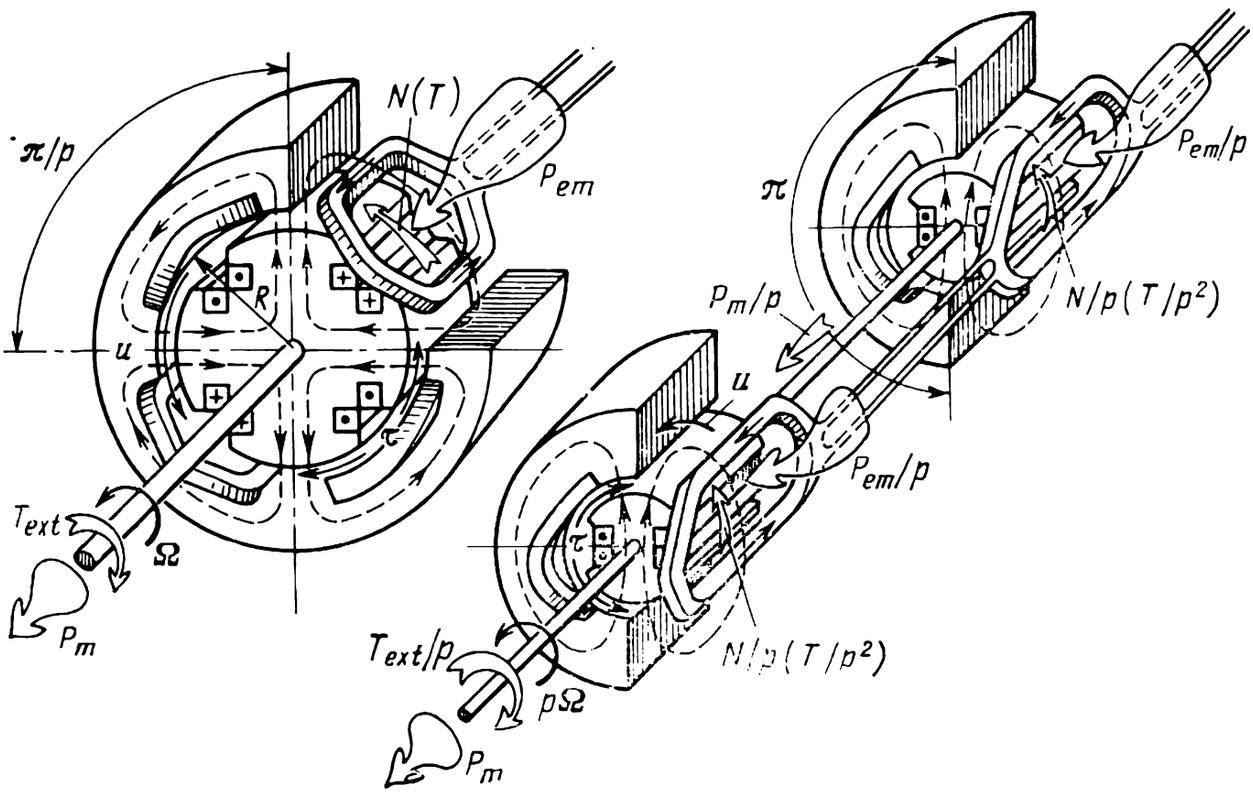

Fig. 30-3 Electrical machine and an equivalent system of p two-pole models

their respective phasor and vector diagrams where these quantities appear as phasors and/or vectors, but also in analyzing power flows. In doing so, it is important to bear in mind that the powers in the model are $1/p$ of their magnitudes in the prototype machine. Therefore, as regards energy conversion, a $2p$-pole machine may be replaced by a system of p models having a common shaft and connected to the same lines and rotating at a speed multiplied p times*. Obviously, such a model system will handle the same powers. A four-pole machine and an equivalent system consisting of two models are shown in Fig. 30-3. The prototype is a syn-

* Instead of combining p models with the same core length l_δ as in the prototype machine, we may use one two-pole machine in which the core length is p times as large.

chronous motor (see Part 5) in which the rotor winding is energized with direct current ($\omega_2 = 0$) and the mechanical angular velocity of the field, Ω_1, is the same as the mechanical angular velocity of the rotor, Ω. Therefore, all of the electromagnetic power, $P_{em} = \Omega_1 T$, applied to the rotor is converted to mechanical power, $P_m = \Omega T$, and the electric power, P_e, entering the rotor winding is zero

$$P_e = \Omega_2 T = 0$$

The directions of the power fluxes, electromagnetic forces and torques hold for the motor mode of operation. The external torque acting on the motor shaft is denoted by T_{ext}.

31 Energy Conversion Losses and Efficiency

31-1 Introductory Notes

As has been shown in Chap. 21, for electric energy, P_e, to be converted into mechanical energy, P_m, or back by a rotating electrical machine, the following conditions must be satisfied.

(i) The rotor whose shaft transmits mechanical energy must be rotating continuously.

(ii) The windings must carry currents whose frequencies are related to one another and to the mechanical angular velocity of the rotor in a certain definite manner.

(iii) The magnetic fluxes linking the windings that are responsible for energy conversion must vary periodically.

As a consequence, some of the energy handled by an electrical machine is inevitably dissipated owing to friction between the rotating parts; this is what is known as *mechanical losses*. Another fraction of the total energy is lost as currents traverse the winding conductors; this is *electrical losses*. Still another fraction of the total energy is lost as the cores undergo cyclic magnetization; this is *magnetic losses*.

All kinds of losses are customarily expressed in terms of the equivalent thermal energy dissipated per unit time or the time rate of energy loss, ΣP. In our subsequent discussion, it will be collectively called the *power losses*.

From the law of conservation of energy, it follows that the useful output power from a machine is always smaller than its input power by an amount equal to the power losses. The ratio of output power to input power gives what is known as the efficiency of an electrical machine, defined as

$$\eta = P_e/P_m = 1 - \Sigma P/(P_e + \Sigma P)$$

in the generator mode of operation, and as (31-1)

$$\eta = P_m/P_e = 1 - \Sigma P/(P_m + \Sigma P)$$

for the motor mode of operation.

It will have been noticed that the efficiency is expressed as a fraction, that is, on a per-unit basis. It may as well be expressed on a percentage basis.

The efficiency of an electrical machine is less than unity on a per-unit basis, or less than 100% on a percentage basis. Obviously, as the losses decrease the efficiency approaches unity (or 100%).

To prevent overheating, the heat dissipated in a machine must be withdrawn and discharged to the surroundings by a cooling system using a gas (most frequently, air) or a liquid as the cooling agent.

31-2 Electrical Losses

The electrical losses in a machine can effectively be reduced by making its conductors of a material having a low resistivity, ρ_t. The best choice is soft copper wire of circular or rectangular cross-section with a low impurity content. Accordingly, this kind of loss is traditionally called the copper loss. The second best choice is aluminium which is currently used on a limited, but an ever increasing scale. Its resistivity is, however, much higher than that of copper.

Because the windings carry alternating current, we have to reckon with the skin effect. It gives rise to variations in the inductive impedance and, as a consequence, in the distribution of current density over the cross-section of conductors. These variations are more noticeable in the conductors laid out in slots than when they are surrounded by a nonmagnetic medium, say, air.

This loss is well known I^2R loss, but R must be the effective resistance. The measured d.c. resistance is only the effective resistance at low frequencies, when the current

distribution may be assumed to be uniform

$$R_0 = \rho_t \frac{2wl_{\text{mean}}}{S_a} \tag{31-2}$$

where $2wl_{\text{mean}}$ = length of series-connected winding (or phase) conductors

l_{mean} = mean length of a half-turn

$S = (a_s b_s) c_a c_b$ = cross-sectional area of the effective conductor

a_s, b_s = dimensions of a rectangular strand in the slot height and width, respectively (see Fig. 31-1)

c_a, c_b = number of strands in the slot height and width, respectively

a = number of circuits in the winding

$\rho_t = \rho_{20} [(1 + \alpha (t - 20^\circ)]$ = resistivity of the conductor at the design operating temperature t

$\alpha = 0.004^\circ\text{C}^{-1}$ = temperature coefficient of resistance for copper (or aluminium)

For a.c. the copper loss has to be computed in terms of $R = k_R R_0$, the resistance of the winding with allowance for a nonuniform current distribution over the cross-section of the conductors.

The extent of variations in the a.c. distribution over the conductor cross-section depends on the magnitude of the slot leakage field. Because the lines of that field are at right angles to the slot axis and are nearly straight lines in a rectangular slot (see Fig. 31-1), the slot leakage flux has just about the same linkage with any strands lying at the same level in the slot height (say, strands *1* and *2*). Accordingly, the inductive impedances of such strands are the same, too.

In contrast, the strands taking up different positions in the slot height differ in inductive impedance as well. As is seen from Fig. 31-1*a* where the slot is shown to contain only one conductor, the inductive impedance (or flux linkage) of strand *1* which is nearer to the air gap is smaller than that of strand *3* lying closer to the slot bottom. This also explains why the current is distributed almost uniformly across the

conductor width and less uniformly along the conductor height. When a slot contains only one conductor, the current density is higher in the strands that are nearer to the air gap (see the current distribution curve in Fig. 31-1*a*). In that part of the cross-section, the current density may substantially exceed the average current density in the conductor

$$J_0 = I/S = I/a_s b_s$$

The part of the conductor section lying deeper in a slot carries only an insignificant fraction of the total conductor

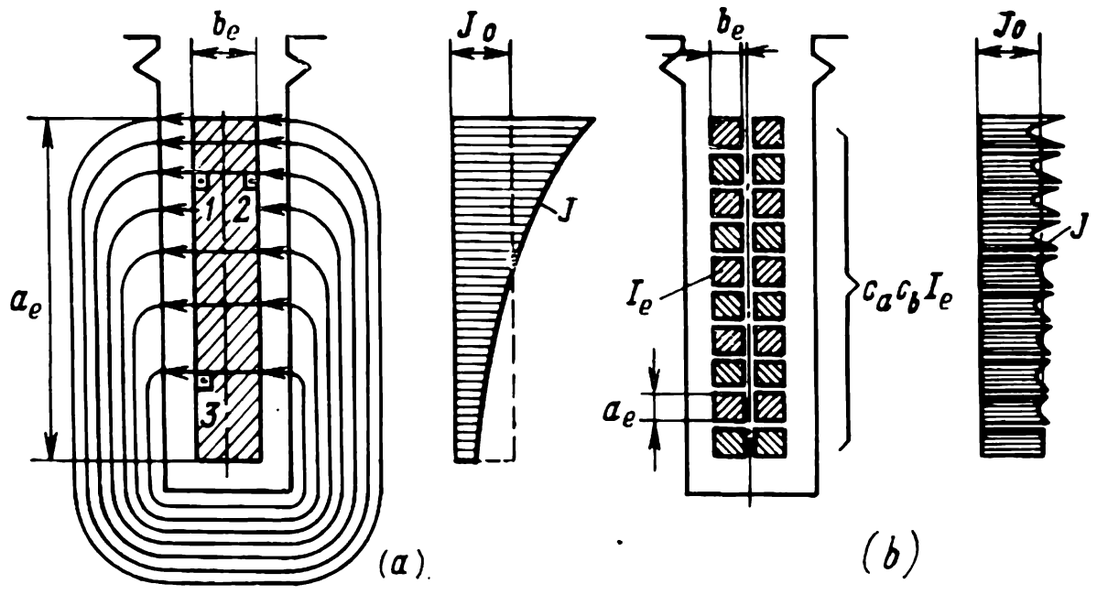

Fig. 31-1 Alternating current density (J) distribution over the cross-section of an effective conductor
(a) one-piece effective conductor, $c_a = c_b = 1$, $u_c = 1$; (b) effective conductor subdivided into strands transposed in the slot depth, $c_a = 10$, $c_b = 2$, $u_c = 1$

current. As a result, the useful cross-section of the conductor decreases, and its resistance goes up. This property is accounted for by what is known as the Field coefficient defined as

$$k_R = R/R_0$$

As is seen from the foregoing, it is a function of the height and number of unstranded effective conductors per slot, and is independent of their width.

Consider the most common forms of slot conductors.

1. Unstranded effective conductors. A slot with a single effective conductor which consists of only one strand occupying the entire slot depth ($c_a = 1$) is shown in Fig. 31-1*a*. The height of the effective conductor is the same as that

of the strand a_s. The number of effective conductors in the slot depth is the same as that of strands $u_c = m_s = 1$. The number of strands in the slot width, c_b, may be taken such that the total width of strands in the slot is $b_1 = c_b b_s$. (What is important is that the effective conductor is not stranded in the slot depth.) With this arrangement the magnitude of the skin effect is a function of the relative height of a strand

$$\xi = a_s/\Delta \tag{31-3}$$

which is defined as the ratio of the height of a strand a_s, to the skin depth* defined as

$$\Delta = \sqrt{2\rho_t b_s/\omega\mu_0 b_1} \tag{31-4}$$

where b_s = slot width
$b_1 = c_b b_s$ = conductor width in the slot
$\omega = 2\pi f$ = angular frequency of the current
μ_0 = permeability of the conductor material (copper or aluminium).

Assuming that the skin effect is only observable within the active length of a half-turn (the part enclosed in a slot), that is, over the length l_δ, and is non-existent in the overhang, that is, over the length $l_{mean} - l_\delta$, we may write for k_R

$$k_R = 1 + (l_\delta/l_{mean})(k_{Ra} - 1) \tag{31-5}$$

where

$$k_{Ra} = \varphi(\xi) + \frac{1}{3}\psi(\xi)(k'_\beta m_c^2 - 1) \tag{31-6}$$

where $k'_\beta = (9\beta + 7)/16$ is the chording (pitch-shortening) factor ($\beta = y_c/\tau$) for double-layer windings (for single-layer windings, $k'_\beta = 1$), and $\varphi(\xi)$ and $\psi(\xi)$ are the Emde functions (see Fig. 31-2). For $\xi \leqslant 1$,

$$\varphi(\xi) = 1 + \frac{4}{45}\xi^4$$

$$\psi(\xi) = \xi^4/3$$

For $\xi > 2$,

$$\varphi(\xi) = \xi$$

$$\psi(\xi) = 2\xi$$

* For a conductor carrying currents at a given frequency as a result of the electromagnetic waves incident on its surface this is the depth below the surface at which the current density has decreased one neper below that at the surface.—*Translator's note.*

As is seen, the value of k_R (and the winding loss) increases with an increase in the relative conductor height and the number of effective conductors in a slot. As a consequence, when the effective conductor in a slot is unstranded ($c_a = 1$), the loss may be prohibitively heavy. A way out is to strand

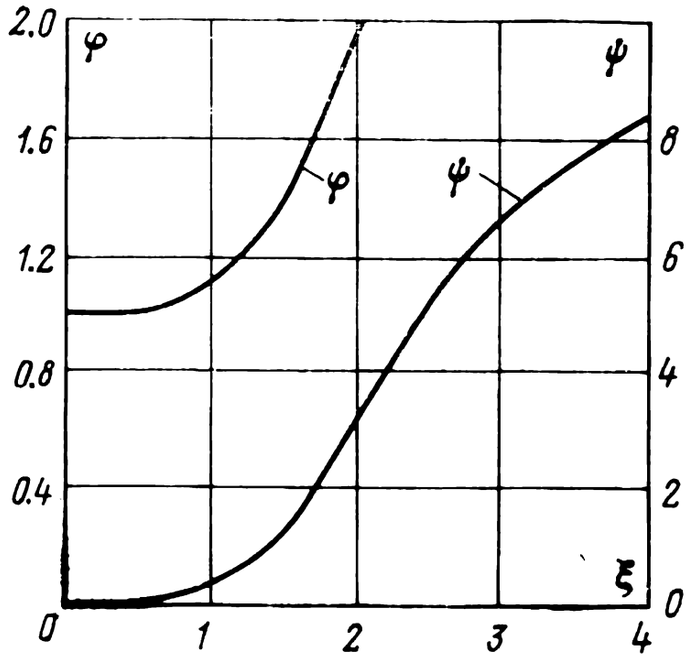

Fig. 31-2 Emde functions

it (in the slot depth) and to transpose the strands within the slot (case 2 below) or within the overhang (as in case 3 below)*.

2. Stranded effective conductors transposed within the slot. Referring to Fig. 31-1*b*, each turn of the effective conductor is made up of two bars joined (by soldering, brazing or welding) at the ends and completely transposed within the slot. The construction of the bar is clear from Fig. 31-3. Owing to the transposition, each strand successively takes up all the likely positions (or levels) in a bar. As a result, the strands in the effective bar have the same inductive impedance, and the current in the effective bar is equally shared among all the strands

$$I_s = I/c_a c_b$$

The current distribution may be other than uniform only within a given strand (see the J curve for strands). The non-uniformity is noticeable in the strand sections lying nearer to the air gap where the leakage field is stronger. Even then,

* Stranding without transposition would not reduce the losses.

the distribution in such sections is more uniform than it is in an unstranded effective conductor (compare Figs. 31-1*a* and *b*). The current density at the periphery of a strand differs but little from the average current density

$$J_0 = I_s/a_s b_s$$

Therefore, the losses in a transposed stranded effective conductor are substantially smaller than they are in an

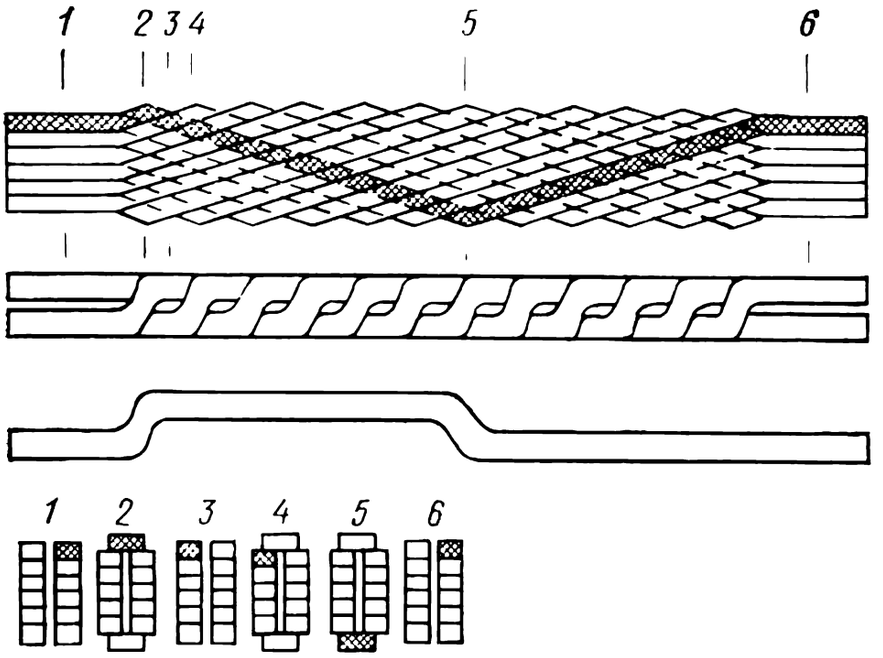

Fig. 31-3 Bar conductor in which the strands are transposed within the slot

unstranded conductor of the same cross-sectional area. In such a case, k_R can be found from Eqs. (31-3) through (31-6). The number of strands in the slot depth is

$$m_s = u_e c_a$$

where u_e is the number of transposed effective conductors in the slot depth (as a rule, $u_e = 2$).

3. Stranded effective conductors with strands transposed within the overhangs. The strands are transposed by twisting some of the effective conductors. Figure 31-4 shows a double-turn coil with two strands per effective conductor ($c_a = 2$, $u_c = 2$). The strands are electrically joined (by soldering, brazing or welding) at the coil ends. Within the coil, they are insulated from each other. The inductive impedance of the strands (say, *1* or *2*) depends on the position they take up in the depth of the slot where the coil is laid. In an "untwist-

ed" coil (shown at the upper left of Fig. 31-4) and in a "twisted" coil (shown at the bottom right of Fig. 31-4) where the effective conductor is turned 180° every turn, the strands take up different combinations of positions.

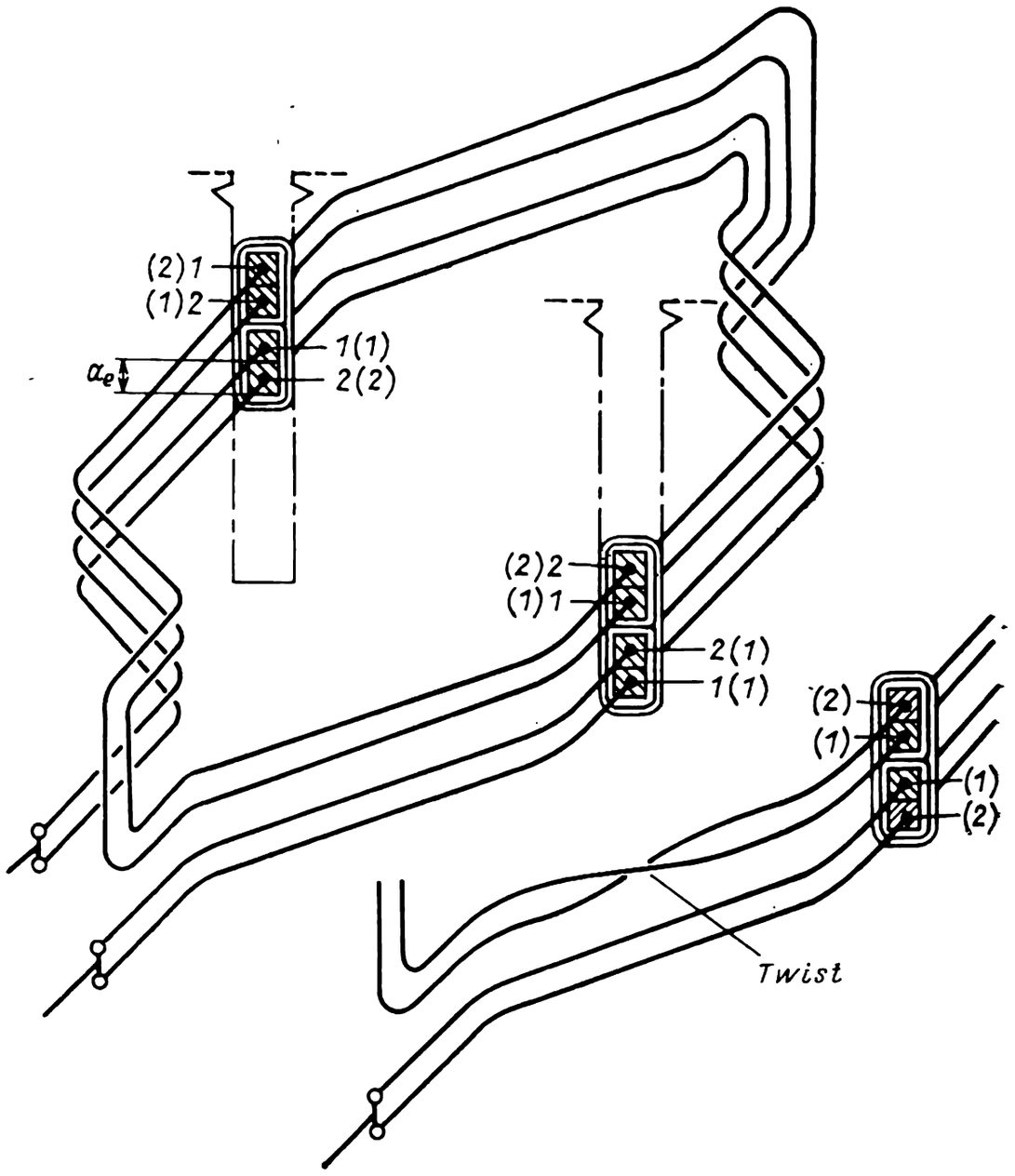

Fig. 31-4 Arrangement of strands in the effective conductors of a coil. The sketch at the bottom right shows a part of a coil overhang with some of the strand twisted (transposed). The numerals in parentheses refer to the corresponding strands in the twisted coil after each turn

In a "twisted" coil, the difference in inductive impedance between the strands is less noticeable than in an "untwisted" coil, and the current distribution among the strands is more uniform. For such a coil, k_R is given by

$$k_R = \varphi(\xi_c) + I\psi(\xi_c)/2 + L_S(\xi^4/6c_a^2)(l_{mean}/l_\delta)(a_s/a_i)^2 \quad (31\text{-}7)$$

where $\xi_e = c_a \xi \sqrt{\frac{a_i l_\delta}{a_s l_{mean}}}$ = relative height of the effective conductor

$\varphi(\xi_e)$, $\varphi'(\xi_e)$ = the Emde functions for ξ_e in Fig. 31-3

a_s = height of a bare strand

a_i = height of an insulated strand

L, L_S = coefficients to be taken from the table according to type of transposition.

Coefficients L and L_S

Coil type	L	L_S
Untwisted	$\frac{1}{2}\left(\frac{u_e^2}{4}-1\right)$	$\frac{u_e^2}{6}\left(4k'_\beta-\frac{3}{4}\right)+\frac{1}{6}$
Twisted every turn	0	$\frac{2}{3}\left(u_e^2 k'_\beta-1\right)$

31-3 Magnetic Losses

Magnetic losses in the cores, or the core loss of electrical machines occur owing to periodic variations in the magnetic field with time.

Here, too, the core loss can be minimized by subdividing the core into electrically insulated elementary magnetic circuits. The required effective cross-sectional area of the core is obtained as the sum of the cross-sectional areas of the elementary magnetic circuits which take the form of ferromagnetic laminations insulated from one another and made in certain thicknesses. The material and thickness of the laminations are chosen according to the frequency of cyclic magnetization.

As has been shown is Sec. 21-2, the frequency of cyclic magnetization for the stator is different from that for the rotor in the general case ($\omega_1 \neq \omega_2$*), each frequency being

* The reference is to the most typical a.c. machine in which one of the windings is laid in slots on the stator core and the other in slots on the rotor core. If the windings are carried by the same core, two magnetic fields will exist within it, each varying at a frequency of its own, ω_1 and ω_2.

the same as that of the current in the respective winding. In induction machines, the relation between the two frequencies depends on the rotational speed, and the lamination thickness must be chosen to suit the nominal speed of rotation. To obtain a uniform distribution of the magnetic flux over the cross-section of each lamination and to keep the core loss to an acceptable level as the frequency is increased, the laminations are made progressively thinner and from suitably alloyed electrical-sheet steels. The cores to be cyclically magnetized at about 50 Hz (which is true of, say, the stators of synchronous and induction machines) are assembled with laminations punched from hot-rolled electrical-sheet steel, usually 0.5 mm thick. The more recent trend has been towards cold-rolled, nonoriented-grain electrical-sheet steels which show a reduced specific iron loss. In large machines, the poles are fabricated from cold-rolled, grain-oriented steels having still better properties (specific loss and permeability) when magnetized in the direction of rolling; such punchings are made also 0.5 mm thick. For higher frequencies (400 to 1 000 Hz), use is made of high-alloy electrical-sheet steels in thicknesses of 0.35 mm, 0.2 mm, 0.1 mm, and 0.05 mm. For machines where the frequency of cyclic magnetization is several hertz or a fraction of a hertz (such as in the rotors of induction machines), or is zero (such as in the rotors of synchronous machines where the magnetic field remains constant in magnitude and direction) the cores may be assembled from structural-steel laminations. The thickness for such laminations is usually chosen from manufacturing considerations (ease of stamping) and may be 1.0 mm, 1.5 mm, 2.0 mm, 4.0 mm, 6.0 mm, and more.

As often as not, especially in mechanically strained rotors, the cores are made in one piece from steel forgings or steel (sometimes cast-iron) castings. In more detail, the properties of electrical-sheet and structural steels are discussed in [13].

(i) Cyclic Magnetization of the Core of an Electrical Machine

Figure 31-5 shows the rotating magnetic field set up by the currents in the three-phase winding of an electrical machine. If we compare the field patterns spaced a quarter-cycle apart, we shall see that the field changes differently in the differ-

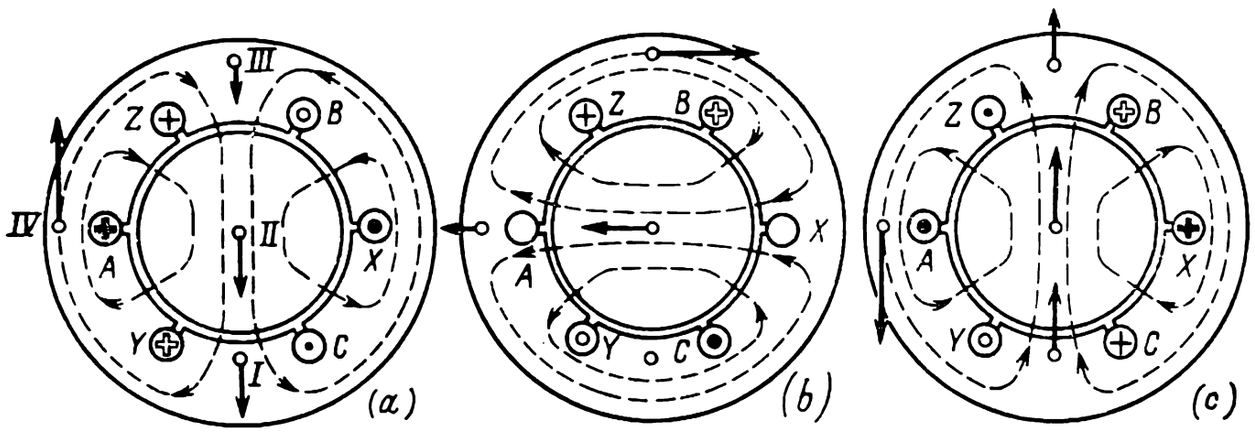

Fig. 31-5 Magnetic field in the teeth and yokes of the cores in a three-phase machine:
(*a*) $t = 0$, (*b*) $t = T/4$, (*c*) $t = T/2$

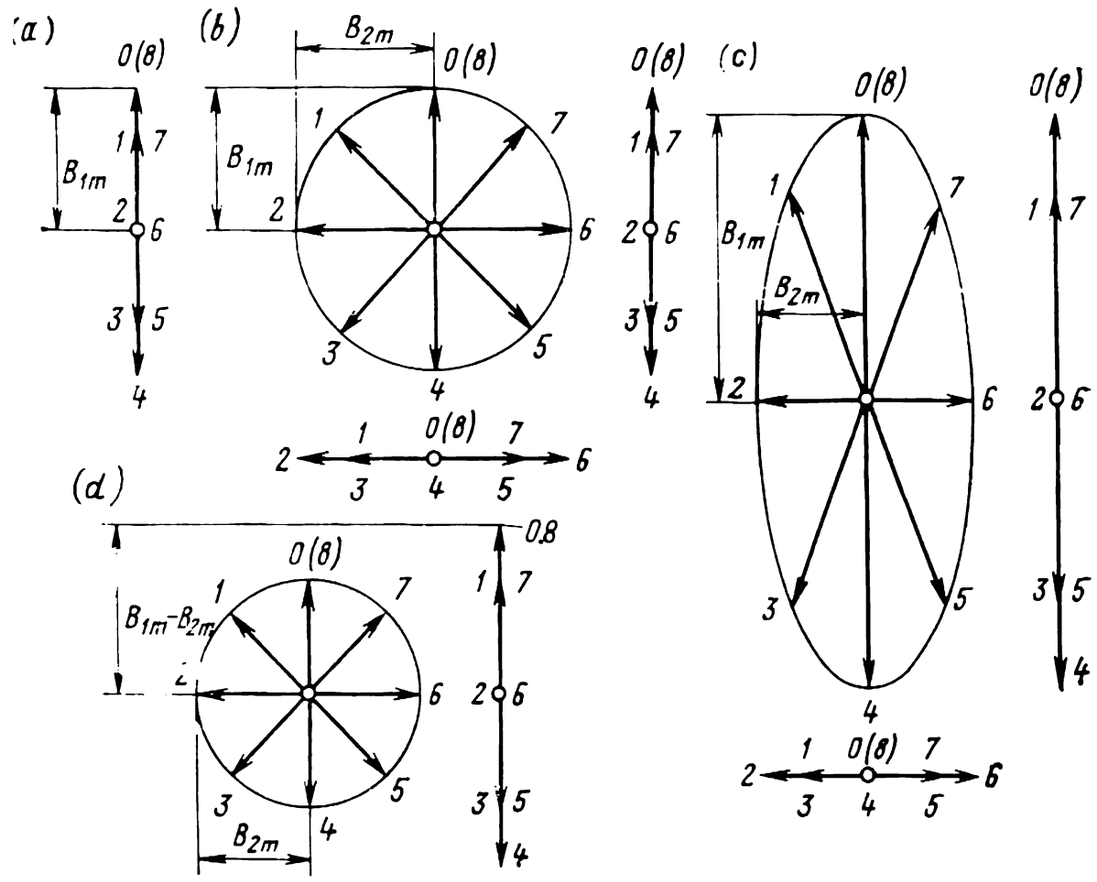

Fig. 31-6 Magnetic flux density for various forms of cyclic magnetization:
(*a*) pulsational magnetization; (*b*) rotational magnetization; (*c*) mixed or elliptical magnetization (with the magnetic flux density vector represented by the sum of two pulsational vectors); (*d*) mixed or elliptical magnetization (with the magnetic flux density vector represented by the sum of a rotational and a pulsational vector)

ent parts of the magnetic circuit. In the teeth (say, at point *I*), the field lines are always directed radially, and the field only changes periodically in magnitude as in a transformer. Accordingly, we may call it pulsational or transformer magnetization. In Fig. 31-6*a*, the magnetic flux density vector with a peak value B_{1m} for pulsational magnetization is shown at instants 0, 1, 2, . . ., 8 spaced $T/8$ apart.

In the yoke of the inner core, the magnetic field changes in a different manner. At point, say, *II* in Fig. 31-5, it remains unchanged in magnitude and only changes in direction. For this field, the magnetic flux density vector rotates at an angular velocity $\omega = 2\pi f$ relative to the yoke, while retaining its value. Accordingly, we may call it rotational magnetization*.

In the case of rotational magnetization, changes in the magnetic flux density vector are shown in Fig. 31-6*b*. Now the vector **B** can be depicted as the sum of two pulsational magnetic flux density vectors equal in peak value to the magnitude of the rotating **B** vector, that is, $|\mathbf{B}|$. To this end, it will suffice to displace the vector axes by $\pi/2$ and to cause one of them to lag behind the other by a quarter of a cycle or an angle $\pi/2$ (so that one of the pulsational vectors is a maximum and the other vanishes).

In the outer yoke, the magnetic flux density has both a radial and a tangential component, such that at points where at a given instant the tangential component is a maximum (at say, point *IV* in Fig. 31-5*a*, where $B_y = B_{1m}$), the radial component is nonexistent ($B_r = 0$). Conversely, at points where at a given instant the radial component is a maximum (at, say, point *III* in Fig. 31-5*a*, where $B_r = B_{2m}$), the tangential component is nonexistent ($B_y = 0$). A quarter of a cycle later (see Fig. 31-5*b*), the radial component becomes a maximum at point *IV* ($B_r = B_{2m}$), and the tangential component vanishes ($B_y = 0$). The reverse change occurs at point *III* ($B_y = B_{1m}$, and $B_r = 0$).

The relative magnitudes of the radial and tangential components, B_{1m} and B_{2m}, vary from point to point round the outer periphery of the yoke. The peak values of both are maximal ($B_{1m} = B_{1\max}$ and $B_{2m} = B_{2\max}$) on the inner

* Rotational magnetization occurs in the yoke of the inner core only in the case of a two-pole field ($p = 1$). When $p > 1$, elliptical magnetization takes place in the inner core (see below).

periphery of the yoke. As the radius of the yoke is increased, both components decrease in peak value, but B_{1m} is reduced insignificantly, whereas B_{2m} on the outer periphery of the yoke vanishes (if we assume that the field is confined within the limits of the yoke). Thus, on the outer periphery of the yoke, where only the tangential time-varying component exists, with a peak value B_{1m}, the magnetization is pulsational. On the inner periphery of the yoke, where two pulsational components unequal in peak value exist, displaced from each other in time and space by an angle $\pi/2$, the magnetization is elliptical. Now the magnetic flux density vector not only rotates at a frequency whose mean value is $\omega = 2\pi f$, but also changes in value from B_{1m} to B_{2m}. It is seen from Fig. 31-6*c* that the tip of the magnetic flux density describes an ellipse in this form of magnetization.

In the case of elliptical magnetization, the magnetic flux density vector may be written as the sum of two pulsational vectors

$$\mathbf{B} = \mathbf{q}_x B_{1m} \cos\omega t + \mathbf{q}_y B_{2m} \sin\omega t \qquad (31\text{-}8)$$

where B_{1m} is the peak value of the vector pulsating along the x-axis and B_{2m} is the peak value of the vector pulsating along the y-axis.

As already noted, the locus of the **B** vector in the general case (for $B_{1m} \neq B_{2m}$) is an ellipse. In vector form, the ellipse is described by Eq. (31-8) where the parameter is time, t. For rotational magnetization, which is a special case, with $B_{1m} = B_{2m}$, the locus of the B vector is a circle. This form of magnetization is quite aptly called circular. For pulsational magnetization, which is another special case where $B_{2m} = 0$ or $B_{1m} = 0$, the locus of the B vector degenerates to a straight line which is aligned with the x- (or y-) axis.

Elliptical magnetization may be treated as a hybrid form because it can be visualized as the superposition of rotational and pulsational magnetization. On re-writing Eq. (31-8) as

$$\mathbf{B} = \mathbf{q}_x (B_{1m} - B_{2m}) \cos\omega t + [\mathbf{q}_x B_{2m} \cos \omega t + \mathbf{q}_y B_{2m} \sin \omega t]$$

we can see that the magnetic flux density vector is obtained as the sum of a rotating vector whose magnitude is B_{2m} and a pulsational vector whose peak value is $B_{1m} - B_{2m}$. Exactly this form is given to the field in Fig. 31-6*d*.

(ii) Core Loss with Pulsational and Rotational Magnetization

The core loss associated with pulsational magnetization was considered in connection with transformers (see Sec. 2-7). The core loss associated with rotational magnetization differs from that of pulsational magnetization. A comparison of hysteresis loss for rotational and pulsational magnetization is given in Fig. 31-7. For rotational magnetization, the loss is plotted as a function of the magnitude of the **B** vector, and for pulsational magnetization, as a function of the peak value of the **B** vector.

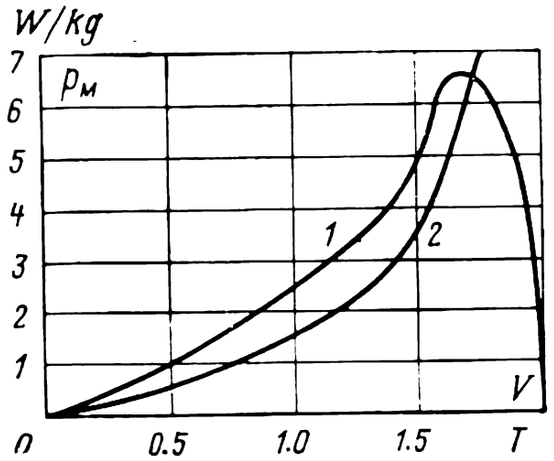

Fig. 31-7 Hysteresis loss in (*1*) rotational magnetization and (*2*) pulsational magnetization (for electrical-sheet steel with 1.91% Si)

At $B < 0.7$ T, the core is slightly saturated (the permeability is nearly constant), and we may treat rotational magnetization as the superposition of two independent pulsational magnetizations along two mutually perpendicular axes. For the value of B given above, the hysteresis loss associated with rotational magnetization is about twice as great as that for pulsational magnetization. As the value of B is increased, the core is saturated progressively more, and the principle of superposition is no longer applicable owing to a substantial nonlinearity of cyclic magnetization.

As is seen from Fig. 31-7, the nonlinearity of the function $B = f(H)$ at $B > 0.7$ T manifests itself in that the ratio of hysteresis loss in rotational magnetization to that in pulsational loss gradually decreases so that at $B = 1.0$ or 1.5 T it is from 1.45-to-1 to 1.65-to-1. When B is about 1.7 T, hysteresis loss is the same in either case, whereas a further increase in B leads to a sudden decrease in hysteresis loss associated with rotational magnetization, so that it is a fraction of that in pulsational magnetization.

Eddy-current loss is solely a function of the magnetic flux density in the laminations and is independent of the field intensity. If we write the magnetic flux density in the case of rotational magnetization as the sum of two pulsation-

al components, we shall see that the eddy-current loss in this case is twice as great as the eddy-current loss in pulsational magnetization for the same peak value of magnetic flux density (that is, irrespective of the magnetic flux density).

(iii) Magnetic Loss in the Magnetic Circuit Elements

In calculating the core loss in the cyclically magnetized electrical-machine components assembled with elecrical-sheet steel laminations insulated from one another, it is important to consider the form of magnetization (pulsational or rotational), the increase in the loss due to manufacturing factors, and also various additional losses.

The point of departure in determining the magnetic loss in magnetic-circuit elements is the total loss in 1 kg of laminations, assuming pulsational magnetization at 50 Hz and a magnetic flux density of 1 T. The total loss is measured by what is known as the *Epstein apparatus* and referred to as the specific loss designated by $p_{1.0/50}$. The values of $p_{1.0/50}$ for various steels are given in [13].

For other values of frequency and magnetic flux density ($B \leqslant 1.6$ T), the specific loss can be found by the equation

$$p_m = p_{1.0/50} \, (f/50)^{1.3} B^2 \qquad (31\text{-}9)$$

if f ranges anywhere between 40 and 60 Hz. If, however, f varies over a broader range, the specific loss is found by an equation in which the hysteresis loss and the eddy-current loss are separated. This is usually accomplished by taking advantage of the fact that for a given value of B_m, the hysteresis loss varies directly with the frequency and the eddy-current loss with the square of the frequency. This equation is

$$p_m = \varepsilon \, (f/50) \, B^2 + \sigma \, (f/50)^2 B^2 \qquad (31\text{-}10)$$

where ε = specific hysteresis loss, W/kg, at $B = 1$ T and $f = 50$ Hz

σ = specific eddy-current loss, W/kg, at $B = 1$ T and $f = 50$ Hz.

The specific core loss is measured under carefully controlled conditions. Among other things, it is required that the individual core laminations should be ideally insulated from one another and annealled after cutting or punching, and

subjected to a sinusoidally varying magnetic flux density. In commercial machines, however, the workmanship is not so perfect. In most cases, the laminations are not annealled after cutting and punching and this leads to an increased hysteresis loss. The insulation between the laminations is often damaged by the heavy pressure used in the assembly of cores. Nor is it always possible to avoid electrical contact between the laminations and the frame (or shaft) and also through burrs on the core teeth. Because of this, additional short-circuited paths are formed for eddy currents. This increase in core loss owing to manufacturing factors is accounted for by applying suitable correction factors.

In calculating the loss in the various elements of the magnetic circuit, one has also to reckon with the fact that the magnetic flux density in the case of pulsational magnetization varies nonsinusoidally (whereas in core-loss measurements by the Epstein apparatus, it is made to vary sinusoidally).

If we expand the magnetic flux density into a Fourier series, we shall see that, in addition to the fundamental component, the series also contains higher harmonics. The losses due to the higher harmonics are added to those associated with the fundamental component, and may quite aptly be called *additional core losses*. If they are not calculated separately, the additional core losses are accounted for by applying additional-loss coefficients.

It should be noted that the additional magnetic losses can be caused even in the cores whose windings carry currents at zero frequency (that is, direct current). The fundamental magnetic flux density in such cores (for example, in the poles of synchronous machines) varies at zero frequency and, as a consequence, the basic core loss is non-existent. In contrast, the additional losses associated with the higher harmonics of magnetic flux density, varying at a high frequency, may be considerable. This is especially so when one core is assembled of heavy-gauge laminations or even made one-piece (because there is no cyclic magnetization at the fundamental frequency), and the other core (on the other side of the air gap) has an appreciable saliency which gives rise to noticeable pulsations in the magnetic flux density on its surface. For such cores, the additional magnetic losses should be calculated separately and added to the total loss.

(iv) Magnetic Loss in the Core Yoke

In calculating this loss, remember that the manner of magnetization is elliptical at the boundary with the toothed layer, and pulsational on the periphery. For the yoke, the overall coefficient allowing for the increase in loss due to inaccuracy in manufacture is taken as $k_{\text{ad},a} = 1.3$ to 1.6, and the yoke loss is given by

$$P_{ma} = k_{\text{ad},\,a}\, p_{ma} m_a \qquad (31\text{-}11)$$

where m_a = mass of the yoke iron; p_{ma} = specific yoke loss by Eq. (31-9) or Eq. (31-10) as measured at B_a and the fundamental frequency f; B_a = peak value of the tangential magnetic flux density in the yoke as found for the fundamental magnetic flux density by calculation of the magnetic circuit for a given type of electrical machine (see Parts 4 and 5).

(v) Magnetic Loss in Core Teeth

The cyclic magnetization of core teeth is pulsational. Therefore, account needs to be taken only of the increase in losses owing to manufacturing factors and of the higher time harmonics. As compared with the yoke, the teeth are smaller in size, and the effect of cutting or stamping is noticeable over a larger tooth area. So, the coefficient taking care of the increase in loss due to manufacturing factors is larger than it is for the yoke. In addition to the fundamental component of peak value B_Z, the magnetic flux density in a tooth has substantial harmonics. Therefore, the additional loss coefficient for teeth is $k_{\text{ad},Z} = 1.7$ to 1.8. The tooth loss is given by

$$P_{m,Z} = k_{\text{ad},Z}\, p_{m,Z} m_Z \qquad (31\text{-}12)$$

where m_Z = mass of the tooth iron; $p_{m,Z}$ = specific tooth loss as given by Eq. (31-9) or (31-10) at B_Z and f; B_Z = peak value of magnetic flux density in the mean tooth section for the fundamental component, as found by calculation of the magnetic circuit for a given machine (see Parts 4 and 5); f = frequency of cyclic magnetization for the fundamental magnetic flux density.

As in transformers, the core loss is mainly a function of the mutual flux. As is seen from Eqs. (31-9), (31-11) and

(31-12). the core loss is proportional to the voltage squared and remains nearly constant as the winding currents vary. The losses associated with the cyclic magnetization by winding leakage fields are poportional to the square of current. These losses are lumped with the additional load loss which is a function of the load current.

31-4 Mechanical Losses

These consist of bearing-friction loss, brush-gear loss, windage loss, and cooling loss.

Bearing-friction loss. Its magnitude varies with bearing design and the lubricant used. In small machines, the bearing-friction loss is kept to a tolerable level by using grease-packed ball and roller bearings. In larger machines, preference is given to sleeve bearings and thin lubricating oils. With all other conditions being equal, the bearing-friction loss builds up with increasing rpm, rotor mass, and shaft diameter at the bearings.

Windage loss. Its amount increases with increasing density and viscosity of the medium inside the machine. The loss is a maximum when the rotor rotates in a liquid medium, and falls to a fraction when the rotor rotates in air. A further decrease by a factor of about ten is obtained when hydrogen is used to fill the insides of a machine.

To minimize the windage loss, the outer surface of the rotor must be made as smooth as practicable. For a given power rating and a given rpm, the windage loss is larger in machines with a larger rotor diameter (with a larger ratio of rotor diameter to design length).

Cooling loss. This loss is the power spent to drive fans or pumps supplying a circulating coolant in the cooling system of a machine. It is proportional to Q, the flow rate of coolant, and H, the head developed by the fan or pump, and increases with decreasing efficiency of the fan or pump.

It can be reduced by making the hydraulic system as perfect as possible and by choosing an appropriate coolant. For liquid coolants it is lower than for gases because a liquid coolant has a higher specific heat capacity, and its flow rate may be kept at a lower level.

The cooling loss is found as explained in Part. 3.

Bibliography

General

1. Петров Г. Н. *Электрические машины.* Энергия, Москва; Ч. I, 1974; Ч. 2, 1963; Ч. 3, 1968.
2. Костенко М. П. *Электрические машины. Часть специальная.* Госэнергоиздат, Москва-Ленинград, 1949.
3. Kostenko M. P., Piotrovsky L. M., *Electrical Machines.* Mir Publishers, Moscow, 1973.
4. Вольдек А. И. *Электрические машины.* Энергия, Ленинград, 1974.
5. Важнов А. И. *Электрические машины.* Энергия, Ленинград, 1974.
6. Сергеев П. С. *Электрические машины.* Госэнергоиздат, Москва-Ленинград, 1962.
7. Алексеев А. Е. *Конструкция электрических машин.* Госэнергоиздат, 1958.
8. Виноградов Н. В. *Производство электрических машин*, Энергия, Москва, 1970.
9. Бертинов А. И. *Электрические машины авиационной автоматики.* Оборонгиз, Москва, 1961.
10. Хрущев В. В. *Электрические микромашины автоматических устройств.* Энергия, Ленинград, 1976.
11. Юферов Ф.М. *Электрические машины автоматических устройств.* Высшая школа, Москва, 1976.
12. Брускин Д. Э., Зороховнч А. Е., Хвостов В. С. *Электрические машины и микромашины.* Высшая школа, Москва, 1971.
13. Грудинский П. Г. (ред.) *Электротехнический справочник*, Т. 1, Энергия, Москва, 1974.
14. Korn, G. A., Korn, T. M., *Mathematical Handbook for Scientists and Engineers*, McGraw-Hill Book Company, New York, 1968.

To Part One

15. Петров Г. Н. *Трансформаторы.* ОНТИ, Москва, 1934.
16. Тихомиров П. М. *Расчет трансформаторов.* Энергия, Москва, 1976.
17. Сапожников А. В. *Конструирование трансформаторов.* Госэнергоиздат, Москва-Ленинград, 1959.
18. Алексеенко Г. В., Ашрятов А. К., Веремей Е. В., Фрид Е. С. *Испытания мощных трансформаторов и реакторов.* Энергия, Москва, 1978.
19. Каганович Е. А. *Испытание трансформаторов малой и средней мощности на напряжение до 35 кВ включительно.* Энергия, Москва, 1969.

20. Фарбман С. А., Бун А. Ю., Райхлин И. М. *Ремонт и модернизация трансформаторов.* Москва, Энергия, 1974
21. Васютинский С. Б. *Вопросы теории и расчета трансформаторов.* Ленинград, Энергия, 1970.

To Part Two

22. Поливанов К. М. *Теоретические основы электротехники.* Ч. 1. Линейные электрические цепи с сосредоточенными постоянными. Энергия, Москва, 1972.
23. Жуховицкий Б. Я., Негневицкий И. Б. *Теоретические основы электротехники.* Ч. 2. Линейные электрические цепи (продолжение). Нелинейные электрические цепи. Энергия, Москва, 1972.
24. Поливанов К. М. *Теоретические основы электротехники* Ч. 3. Теория электромагнитного поля. Энергия, Москва, 1975.
25. Adkins, B. *The General Theory of Electrical Machines*, Chapman and Hall, London, 1959.
26. White, C., Woodson, H. *Electromechanical Energy Conversion.* J. Wiley and Son., Inc., New. York, 1969.
27. Копылов И. П. *Электромеханическое преобразование энергии.* Энергия, Москва, 1973.
28. Иванов-Смоленский А. В. *Электромагнитные поля и процессы в электрических машинах и их физическое моделирование.* Энергия, Москва, 1969.
29. Schuisky, W. *Berechnung electrischer Maschinen*, Springer, Wien. 1960.
30. Сергеев П. С., Виноградов Н. В., Горянинов Ф. И. *Проектирование электрических машин.* Энергия, Москва, 1969.
31. Постников И. М. *Проектирование электрических машин.* Гостехиздат УССР, Киев, 1960.
32. Liwschitz-Garik, M. *Winding Alternating-Current Machines.*
33. Кучера Я., Гапл И. *Обмотки электрических машин.* Перев. с чешск. Изд-во Академии наук, Прага, 1963.
34. Зимин В. И., Каплан М. Я., Палей А. М. и др. *Обмотки электрических машин.* Энергия, Ленинград, 1970.
35. Данилевич Я. Б., Кашарский Э. Г. *Добавочные потери в электрических машинах.* Госэнергоиздат, Москва-Ленинград, 1963.
36. Данилевич Я. Б., Кулик Ю. А. *Теория и расчет демпферных обмоток синхронных машин.* Изд-во АН СССР, Москва, 1962.
37. Данилевич Я. Б., Домбровский В. В., Казовский Е. Я. *Параметры электрических машин переменного тока.* Наука, Москва, 1965.
38. Талалов И. И. *Параметры и характеристики явнополюсных синхронных машин.* Энергия, Москва, 1978.

Index

Many subjects are not included in the Index because they are listed separately in the Contents. Therefore, the reader will be well-advised first to consult the various sections under the individual chapter headings there.

In the Index, each topic has its own section, but subjects common to several topics may be found separately listed.

Airgap factor, 270
Asynchronous machine, 233
Autotransformer, 125, 133
Axial gap length, 266

Breathing mmf wave, 274

Carter coefficient, 270
Coil pitch, 238
Cooling systems for transformers, 186
Conductors,
  stranded, 384
  transposed, 384
  unstranded, 382
Core
  cyclic magnetization of, 388
  salient-pole, 202
Core length, 265
Cyclic magnetization, 388

Distribution factor, 280

Effective core length, 265
Electrical machines,
  asynchronous, 233
  basic arrangement, 18
  basic definitions, 13
  basic designs, 207
  classification, 15, 192
  disc-type, 193
  geared, 195
  general theory, 192
  heteropolar, 207
  homopolar, 207
  induction, 234
  inductor, 218
  linear flat, 193
  linear tubular, 194
  reluctance, 214
  synchronous, 233
Electromagnetic forces, 367
Electromagnetic torque, 351, 364
EMF,
  rotational, 197
  transformer, 197
Energy conversion,
  by electrical machines, 18
  by rotating magnetic field, 372
  by transformer, 15, 75
  conditions for, 201, 227
  efficiency, 379
  losses, 379

Field windings, 255
Flux,
  leakage, 45
  mutual, 45
Flux linkage, 323
  coil, 323
  coil group, 328
  harmonic, 335
  phase, 330
  winding, 333

Generator, def., 13

Impedance,
  mutual in transformer, 117
  short-circuit, 119
Inductance,
  leakage for complete winding, 348
  mutual between phases, 343
  mutual between stator and phase, 344
  mutual in transformer, 51
  polyphase winding, 341
Induction machine, 234

Load unbalance, 145
Losses,
  bearing-friction, 396
  cooling, 396
  copper in transformer, 53
  core, 392
    in transformer, 53
  electrical, 379-80
  magnetic, 379, 387
  mechanical, 379, 396
  no-load in transformer, 53
  power, 379
  windage, 396

Magnetic field,
  calculation of, 257
  from concentrated field winding, 316
  from distributed field winding, 319
  leakage, 341
  mutual, 342
    of phase, 267
    of polyphase winding, 288
  periodic, 201
  from rotating field winding, 316
  spatial pattern of, 262
  useful, 341

Magnetization,
cyclic, 388
pulsational, 392
rotational, 392
Magnetizing current, 58
Measurement, transformer quantities, 99
MMF, 269
phase, 280
MMF equation for transformer, 58
Motor, def., 13

Per-unit notation, 69
Phase belt, 205
Phase sequence
negative, 91
positive, 91
zero, 99
Phasor diagram, 65
Pitch factor, 276
Pole pairs, 202
Pole pitch, 238
Power,
electric, 372
electromagnetic, 372
magnetic, 372

Rotary converter, def., 14
Rotor, def., 18

Self-inductance,
complete winding, 345
phase, 342
Slots per pole, 205
Stator, def., 18
Surface current, 358
Synchronous machine, 233

Temperature limits, transformer, 186
Temperature rise, transformer, 185
Test,
open-circuit, 99
short-circuit, 102
Transformation, three-phase, 79
Transformation ratio, 46
Transformer, def., 14
arc-welding, 180
at no load, 43
auto-, 125, 133
basic arrangement, 15, 27
butt-joint, 34
construction, 31
cooling systems of, 186
copper loss, 53
core and coil unit, 31
core-and-shell type, 34
core type, 33
current, 183
five-leg core-type, 34
imbricated-joint, 34
instrument, 182
phase-angle error, 183
ratio error, 183
insulation-testing, 181
interleaved-joint, 34
magnetization curve, 47
magnetizing current, 58
mitred-joint, 36
multiwinding, 125
no-load current, 49, 117
no-load losses, 52
no-load test, 99
on load, 56, 107
open-circuit current, 117
open-circuit test, 99
overvoltages in, 171
paralleled, 138
parameter calculation, 117
peaking, 182
phase displacement reference numbers, 82
phasor diagram, 65
shell-type, 33
short-circuit impedance, 119
short-circuit test, 102
size relations, 121
special-purpose, 177
strip-wound, 38
structural parts, 38
tap-changing, 112
off load, 113
on load, 114
three-phase, 83, 89, 145
transferring the secondary quantities, 62
transients in, 164
turns ratio, 46
variable-voltage, 179
voltage, 182
Transformer core loss, 53
Transformer emf equation, 46
Transformer equivalent circuit, 68
Transformer fittings, 41
Transformer frame, 37
Transformer leads, 41
Transformer load unbalance, 145
Transformer mmf equation, 58
Transformer mutual impedance, 117
Transformer mutual inductance, 51
Transformer tank accessories, 41
Transformer terminal bushings, 41
Transformer voltage equations, 45, 60
Transformer voltage regulation, 107
Transformer winding connections, 79
Transformer winding insulation, 39
Transformer windings, 32
Transformer yoke clamping, 36
Triplen harmonics, 91

Windings,
a.c. machines, 236
chorded, 238
concentrated, 205
cylindrical, 202
distributed, 205
double-layer, 203
drum, 202
field, 255
fractional-slot, 250
full-pitched, 238
lap, 238, 240
polyphase, 205
selection of, 246
short-pitched, 238
single-layer, 203
two-layer, 236
wave, 238, 244

Printed in the Union of Soviet Socialist Republics